Vol. 16. No 1, 2014

ISSN 1507-2711
Cena: 25 zł (w tym 5% VAT)

EKSPLOATACJA I NIEZAWODNOŚĆ
MAINTENANCE AND RELIABILITY

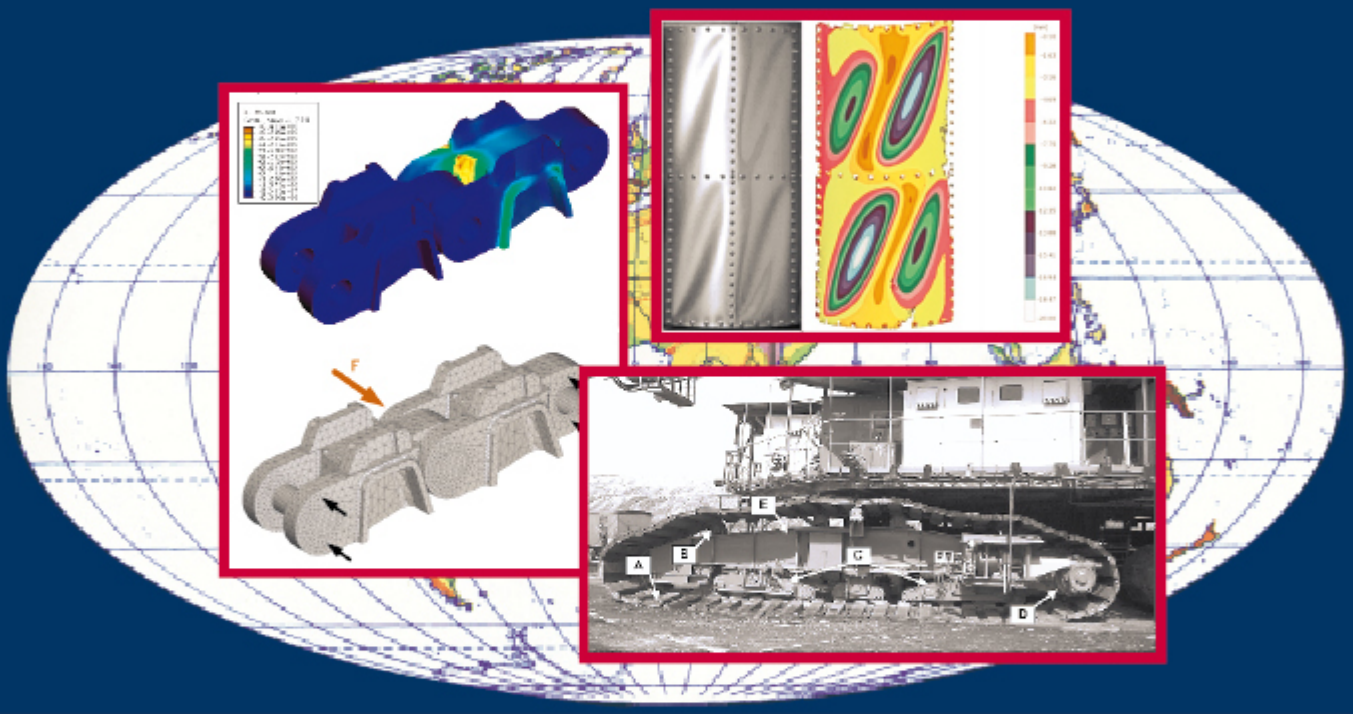

Polskie Naukowo Techniczne Towarzystwo Eksploatacyjne
Warszawa

Polish Maintenance Society
Warsaw

Co-financed by the Minister of Science and Higher Education

The Journal is indexed and abstracted in the Journal Citation Reports (JCR Science Edition), Scopus, Science Citation Index Expanded (SciSearch®) and Index Copernicus International.

The Quarterly appears on the list of journals credited with a high impact factor by the Polish Ministry of Science and Higher Education and is indexed in the Polish Technical Journal Contents database – BAZTECH and the database of the Digital Library Federation.

All the scientific articles have received two positive reviews from independent reviewers.

Our IF is 0.293

Editorial staff:	Dariusz Mazurkiewicz, PhD, DSc (Eng), Associate Professor (Editor-in-Chief, Secretary of the Scientific Board) Tomasz Klepka, PhD, DSc (Eng) (Deputy Editor-in-Chief) Teresa Błachnio-Krolopp, MSc (Eng) (Editorial secretary) Andrzej Koma (Typesetting and text makeup) Krzysztof Olszewski, PhD (Eng) (Webmaster)
Publisher:	Polish Maintenance Society, Warsaw
Scientific patronage:	Polish Academy of Sciences Branch in Lublin
Address for correspondence:	"Eksploatacja i Niezawodność" – Editorial Office 20-618 Lublin, ul. Nadbystrzycka 36, Poland e-mail: office@ein.org.pl http://www.ein.org.pl/
Circulation:	550 copies

Science and Technology

NEW MEMBER OF THE SCIENTIFIC BOARD

ASSOC. PROF. DR GINTAUTAS BUREIKA

Professor Gintautas Bureika has been working at Vilnius Gediminas Technical University (VGTU) since 1990. His teaching subjects include Theory of Rail Traction and Rail Vehicle Dynamics; while the research fields that interest him include Transport Technologies, Rail Vehicle Operation, Rail Vehicle Energy Efficiency, Alternative Fuels for Internal Combustion Engines, Railway and Environment, Railway Safety and Security. He is an author or co-author of more than 80 scientific publications, 12 normative documents of State Company "Lithuanian Railways" and study manuals in Railway Engineering. He is a member of International Rail Researchers Association "EURNEX", member of the Lithuanian Railway Engineers Union; member of the Editorial Board of Journal "TRANSPORT" (*Web of Sciences*, IF) and member of the Editorial Board of Scientific Journal "KONES. Powertrain and Transport". He is also a fellow of Transport Means Safety Committee of Lithuanian Republic Standard Board and a member of VGTU Senate. His homepage can be found at: http://www.gtk.ti.vgtu.lt/en/staff/

SU C, FU YQ. **Reliability assessment for wind turbines considering the influence of wind speed using Bayesian network**. Eksploatacja i Niezawodnosc – Maintenance and Reliability 2014; 16 (1): 1–8.

The reliability of wind turbine is of great importance for the availability and economical efficiency of wind power system. In this article, a reliability model for wind turbine is built with Bayesian network (BN), in which the influence of wind speed is considered. Causal logic method (CLM) is presented for qualitative modeling, which combines the merits of fault tree in handling technical aspects and the strength of BN in dealing with environmental factors and uncertainty. A novel adjustment method based on expectation is proposed for quantitative calculation, by which historical data and expert judgment are integrated to describe the uncertainty in the prior probability distributions. An approximate inference algorithm combining with dynamic discretization of continuous variables is adopted to obtain the reliability index of wind turbine and its elements. A case study is given to illustrate the proposed method, and the results indicate that wind speed is an important factor for the reliability of wind turbine.

SU C, FU YQ. **Ocena niezawodności turbin wiatrowych za pomocą sieci Bayesa z uwzględnieniem wpływu prędkości wiatru**. Eksploatacja i Niezawodnosc – Maintenance and Reliability 2014; 16 (1): 1–8.

Niezawodność turbiny wiatrowej ma ogromne znaczenie dla gotowości i efektywności ekonomicznej instalacji wiatrowej. W niniejszym artykule zbudowano, w oparciu o sieci Bayesa (BN), model niezawodności turbiny wiatrowej uwzględniający wpływ prędkości wiatru. Przedstawiono Metodę Logiki Przyczynowości (Causal Logic Method, CLM), służącą do modelowania jakościowego, która łączy zalety drzewa błędów w odniesieniu do aspektów technicznych z atutami BN w odniesieniu do czynników środowiskowych i niepewności. Do kalkulacji ilościowych zaproponowano nową metodę dopasowania opartą na oczekiwaniach, w której dane z eksploatacji i opinie ekspertów łącznie pozwalają opisać niepewność rozkładów prawdopodobieństwa a priori. Wskaźnik niezawodności turbiny wiatrowej i jej elementów otrzymano posługując się algorytmem wnioskowania przybliżonego w połączeniu z dynamiczną dyskretyzacją zmiennych ciągłych. Dla zilustrowania proponowanej metody przedstawiono studium przypadku, którego wyniki wskazują, że prędkość wiatru jest ważnym czynnikiem niezawodności turbiny wiatrowej.

OSTAPKOWICZ P. **Leakage detection from liquid transmission pipelines using improved pressure wave technique**. Eksploatacja i Niezawodnosc – Maintenance and Reliability 2014; 16 (1): 9–16.

This paper deals with leak detection in liquid transmission pipelines. It focuses on improving the efficiency of a method based on negative pressure wave detection. A new algorithm for pressure wave monitoring has been proposed. The algorithm is aimed to precisely capture the corresponding characteristic points in the signal sequence of negative pressure waves caused by leakage. It uses median filtering of the calculating deviations of pressure signals measured along the pipeline. Adaptive alarm thresholds with reduced margins, based on statistical analysis of the calculating deviations of pressure signals, were used. Additionally, the algorithm is supported by a set of functions base on the calculation of the cross-correlation of the deviations which represent pressure signals from neighboring transducers. The developed technique has been tested on a physical model of pipeline. The pipeline is 380 meters long and 34 mm in internal diameter, and is made of polyethylene (PEHD) pipes. The medium pumped through the pipeline was water. Tests proved, that the proposed solution is sensitive to small leaks and resistant for false alarm (occurring disturbances). It is also capable of localizing the leak point with satisfactory accuracy, without significant delay.

OSTAPKOWICZ P. **Diagnozowanie nieszczelności w rurociągach przesyłowych cieczy z wykorzystaniem zmodyfikowanej metody opartej na detekcji fal ciśnienia**. Eksploatacja i Niezawodnosc – Maintenance and Reliability 2014; 16 (1): 9–16.

Artykuł dotyczy zagadnień diagnozowania wycieków z rurociągów przesyłowych cieczy. Skupia się na polepszaniu skuteczności metody opartej na detekcji fal ciśnienia. Zaproponowano nowy algorytm do monitorowania fal ciśnienia. Algorytm jest ukierunkowany na precyzyjną identyfikację charakterystycznych punktów na przebiegach sygnałów ciśnienia reprezentujących fale wywołane przez zaistniały wyciek. Działanie algorytmu jest oparte o filtrację medianową residuów wyznaczanych dla sygnałów ciśnienia mierzonych wzdłuż rurociągu. Zastosowano adaptacyjne progi alarmowe, obliczane na podstawie analizy statystycznej. Dodatkowo, algorytm wspomagany jest przez wykorzystanie zbioru funkcji korelacji wzajemnej pomiędzy obliczanymi residuami reprezentującymi sygnały ciśnienia z sąsiednich przetworników pomiarowych. Zaproponowane rozwiązanie zostało przetestowane na fizycznym modelu rurociągu, którym tłoczono wodę. Rurociąg ma 380 m długości, średnicę wewnętrzną 34 mm i został wykonany z rur z polietylenu (PEHD). Wyniki badań udowodniły, że proponowane rozwiązanie jest wrażliwe na małe wycieki i odporne na fałszywe alarmy (występujące zakłócenia). Pozwala na zadawalająco dokładną lokalizację wycieku, bez znaczących opóźnień czasowych.

HALIMI D, HAFAIFA A, BOUALI E. **Maintenance actions planning in industrial centrifugal compressor based on failure analysis**. Eksploatacja i Niezawodnosc – Maintenance and Reliability 2014; 16 (1): 17–21.

The industrial maintenance implementation requires to the behaviour system analysis and their components. In this work, we optimize the maintenance actions to eliminate failures in the inspected industrial process. Our purpose in this work is to improve the components reliability in gas compression system, by the planning of the maintenance actions based on failure analysis using the intervention optimization in industrial centrifugal compressor plant. The finality of this proposed approach is proved by the improvement of the reliability performances and by the availability of this oil installation.

HALIMI D, HAFAIFA A, BOUALI E. **Planowanie czynności konserwacyjnych dla przemysłowej sprężarki odśrodkowej w oparciu o analizę uszkodzeń**. Eksploatacja i Niezawodnosc – Maintenance and Reliability 2014; 16 (1): 17–21.

Obsługa urządzeń przemysłowych wymaga analizy zachowań układów i ich części składowych. W niniejszej pracy zoptymalizowano czynności konserwacyjne tak, aby wyeliminować występowanie uszkodzeń w kontrolowanym procesie przemysłowym. Celem prezentowanej pracy było poprawienie niezawodności elementów układu sprężania gazu poprzez zaplanowanie czynności konserwacyjnych w oparciu o analizę uszkodzeń z wykorzystaniem optymalizacji interwencji w przemysłowej sprężarce odśrodkowej. O skuteczności proponowanego podejścia świadczy poprawa parametrów niezawodności oraz gotowość omawianej instalacji olejowej.

OSIPOWICZ T, ABRAMEK KF. **Catalytic treatment in Diesel engine injectors**. Eksploatacja i Niezawodnosc – Maintenance and Reliability 2014; 16 (1): 22–28.

The aim of the study proposed and carried out by the authors was to assess the impact of using platinum as a catalyst carrier in the fuel injector diesel engine with the direct fuel injection for emissions of toxic substances in the exhaust gases into the atmosphere and specific fuel consumption. Experimental studies were carried out on a test bench equipped with a 359 engine and a hydraulic brake with complete measurement apparatus. During the tests the engine worked by external speed characteristics. The analysis of the study showed that it is possible to reduce emissions of toxic compounds into the environment and to reduce specific fuel consumption through the use of catalytic coatings in the diesel engine fuel injector.

OSIPOWICZ T, ABRAMEK KF. **Katalityczna obróbka paliwa we wtryskiwaczach silnika o zapłonie samoczynnym**. Eksploatacja i Niezawodnosc – Maintenance and Reliability 2014; 16 (1): 22–28.

Celem zaproponowanych i przeprowadzonych przez autorów badań była ocena wpływu zastosowania nośnika katalitycznego w postaci platyny we wtryskiwaczu paliwowym silnika z zapłonem samoczynnym z bezpośrednim wtryskiem paliwa na emisję substancji toksycznych w gazach wylotowych do atmosfery oraz jednostkowe zużycie paliwa. Badania eksperymentalne zostały przeprowadzone na stanowisku hamownianym wyposażonym w silnik 359 oraz hamulec hydrauliczny z kompletną aparaturą pomiarową. Podczas badań silnik pracował według zewnętrznej charakterystyki prędkościowej. Analiza przeprowadzonych badań wykazała, że istnieje możliwość ograniczenia emisji związków toksycznych do otoczenia oraz zmniejszenie jednostkowego zużycia paliwa poprzez zastosowanie powłoki katalitycznej we wtryskiwaczu paliwowym silnika ZS.

WANG Y, ZHAO J, JIA X, TIAN Y. **Spare parts allocation optimization in a multi-echelon support system based on multi-objective particle swarm optimization method**. Eksploatacja i Niezawodnosc – Maintenance and Reliability 2014; 16 (1): 29–36.

Spare parts allocation optimization in a multi-echelon support system presents a difficult problem which involves non-linear objective function and integer variables to be optimized. In this paper, a multi-objective optimization model was developed, which maximizes support probability and minimizes support costs. In order to solve the optimization problem, an improved multi-objective particle swarm optimization (MOPSO) method was utilized. In this method, techniques of dimensions reduction and rules-based multi-objective optimization were employed, which can improve the efficiency of MOPSO method. A numerical example was given to show the performance of proposed method.

WANG Y, ZHAO J, JIA X, TIAN Y. **Optymalizacja alokacji części zamiennych w wieloszczeblowym systemie wsparcia na podstawie metody wielokryterialnej optymalizacji rojem cząstek**. Eksploatacja i Niezawodnosc – Maintenance and Reliability 2014; 16 (1): 29–36.

Optymalizacja alokacji części zamiennych w wieloszczeblowym systemie wspomagania stanowi trudne zagadnienie, które wymaga optymalizacji nieliniowej funkcji celu oraz zmiennych całkowitych. W niniejszej pracy, opracowano wielokryterialny model optymalizacyjny, który maksymalizuje prawdopodobieństwo wsparcia i minimalizuje jego koszty. W celu rozwiązania problemu optymalizacyjnego, wykorzystano ulepszoną metodę wielokryterialnej optymalizacji rojem cząstek (MOPSO). W metodzie tej wykorzystano techniki redukcji wymiarów oraz wielokryterialnej optymalizacji algorytmowej, które mogą poprawić efektywność metody MOPSO. Zasady proponowanej metody zilustrowano przykładem numerycznym.

KUCZMASZEWSKI J, PIEŚKO P. **Wear of milling cutters resulting from high silicon aluminium alloy cast AlSi21CuNi machining**. Eksploatacja i Niezawodnosc – Maintenance and Reliability 2014; 16 (1): 37–41.

This paper presents results of tests on the wear of milling cutters resulting from high silicon silumins machining. As a representative for this group of materials EN AC-AlSi21CuNi alloy was chosen. Aluminium alloys containing less than 12 % of Si are classified as difficult-to-cut due to increased abrasive wear of the cutters caused by the influence of silicon precipitates. This affects the cutting process by damaging the quality and accuracy of the manufactured elements. Therefore, it is so significant to determine the durability of the teeth and stop the cutting process when it is being excessively worn.

KUCZMASZEWSKI J, PIEŚKO P. **Zużycie ostrzy frezów podczas obróbki wysokokrzemowego, odlewniczego stopu aluminium AlSi21CuNi**. Eksploatacja i Niezawodnosc – Maintenance and Reliability 2014; 16 (1): 37–41.

W artykule przedstawiono wyniki badań zużycia ostrzy narzędzi frezarskich podczas obróbki wysokokrzemowych siluminów. Jako przedstawiciela tego rodzaju materiałów wybrano stop EN AC-AlSi21CuNi. Stopy aluminium o zawartości Si > 12% określane są jako trudnoskrawalne, ze względu na zwiększone zużycie ścierne ostrzy, wywołane oddziaływaniem wydzieleń krzemu.Ma to niekorzystny wpływ na proces skrawania, pogarsza jakość i dokładność wykonywanych elementów. Istotne jest więc aby określić trwałość ostrza narzędzi i w momencie jego nadmiernego zużycia przerwać proces skrawania.

ROJEK I, STUDZIŃSKI J. **Comparison of different types of neuronal nets for failures location within water-supply networks**. Eksploatacja i Niezawodnosc – Maintenance and Reliability 2014; 16 (1): 42–47.

The different types of neuronal nets for failures location within a water-supply network are presented in the paper. The present utilization of the monitoring systems does not exhaust their possibilities. The monitoring systems operated as autonomic programs gather the information about flows and pressures of water in the source pumping stations, in the zones of hydrophore stations and also in some selected pipes of water network, giving general knowledge about state of its work, when simultaneously they could and should be used as elements of IT systems for network management, and particularly regarding detection and location of hidden water leaks. The models of network failures location are created by means of neuronal nets in the form of MLP and Kohonen nets.

ROJEK I, STUDZIŃSKI J. **Comparison of different types of neuronal nets for failures location within water-supply networks**. Eksploatacja i Niezawodnosc – Maintenance and Reliability 2014; 16 (1): 42–47.

W artykule prezentowane są różne typy sieci neuronowych do lokalizacji awarii w sieci wodociągowej. Obecne wykorzystanie systemów monitorowania nie odpowiada ich możliwościom. Współcześnie systemy monitoringu służą jako autonomiczne programy do zbierania informacji o przepływach i ciśnieniach wody w pompowniach źródłowych, hydroforniach strefowych i końcówkach sieci wodociągowej, dając ogólną wiedzę o stanie jej pracy, gdy jednocześnie mogą i powinny być wykorzystane jako elementy IT systemów zarządzania siecią, w tym w szczególności w zakresie wykrywania i lokalizacji wycieków wody. Modele lokalizacji awarii sieci zostały utworzone przy wykorzystaniu jednokierunkowych sieci neuronowych ze wsteczną propagacją błędu typu MLP i sieci Kohonena.

VALIS D, PIETRUCHA-URBANIK K. **Utilization of diffusion processes and fuzzy logic for vulnerability assessment**. Eksploatacja i Niezawodnosc – Maintenance and Reliability 2014; 16 (1): 48–55.

Assessing the vulnerability of critical infrastructure objects is of major concern when dealing with the process of dependability and risk management. Special attention is paid to the objects of higher interest, such as nuclear power plants. In spite of the protection of these objects, there is still a certain level of a potential threat. The aim of the paper is to describe a possible way of attacking on the object in order to get into a particular part of it. Several characteristics of an adversary´s attempt were obtained. For this reason as well as for modelling adversary´s behaviour diffusion processes have been used.

VALIS D, PIETRUCHA-URBANIK K. **Wykorzystanie procesów dyfuzyjnych i logiki rozmytej do oceny podatności na zagrożenie**. Eksploatacja i Niezawodnosc – Maintenance and Reliability 2014; 16 (1): 48–55.

Ocena podatności na zagrożenie kluczowych obiektów infrastruktury jest głównym problemem rozpatrywanym w kontekście procesu niezawodności oraz zarządzania ryzykiem. Szczególną uwagę przywiązuje się do obiektów wysokiej rangi, takich jak elektrownie jądrowe. Pomimo ochrony tych obiektów, nadal istnieje pewien poziom potencjalnego ich zagrożenia. Celem artykułu jest opisanie możliwego sposobu zaatakowania obiektu z zamiarem dostania się do konkretnej jego części. Otrzymano kilka charakterystyk próby ataku ze strony przeciwnika. Do tego celu, jak również do zamodelowania zachowania przeciwnika, wykorzystano procesy dyfuzyjne.

MACHNIK R, NOCUŃ M. **Effect of anti-corrosion coatings of corona electrodes on selected operating parameters of industrial electrostatic precipitators**. Eksploatacja i Niezawodnosc – Maintenance and Reliability 2014; 16 (1): 56–60.

The problem of corrosion protection of electrostatic precipitators used in the energy industry, during its construction or modernization is of vital importance. Several months construction period and the period of time elapsed from the end of construction to operation promotes corrosion of its components. Significant impact on the electrical parameters of an electrostatic precipitator performance has the corrosion phenomena of its emission components, which are the corona electrodes. Manufacturers do not apply any corrosion protection coating on electrostatic corona electrode for fear of worsening their emissivity. This paper presents the results of comparison of emission properties of corona electrodes with and without corrosion protection coatings. Rode and mast type electrodes were studied. The analysis of the results was performed using a statistical method based on the time-series model. The obtained results clearly show that the use of anti-corrosion coating does not impair the electrical parameters of corona electrodes. Corrosion protection can be used both during the modernization as well as during the construction of new electrostatic precipitators.

MACHNIK R, NOCUŃ M. **Wpływ powłok antykorozyjnych elektrod ulotowych na wybrane parametry eksploatacyjne elektrofiltrów przemysłowych**. Eksploatacja i Niezawodnosc – Maintenance and Reliability 2014; 16 (1): 56–60.

Problem ochrony antykorozyjnej ma istotne znaczenie w okresie budowy lub modernizacji urządzeń odpylających stosowanych w przemyśle energetycznym. Wielomiesięczny okres budowy elektrofiltru oraz okres czasu upływający od zakończeniu montażu do momentu uruchomienia instalacji odpylającej powoduje nieuniknioną korozję jego elementów. Istotny wpływ na elektryczne parametry eksploatacyjne elektrofiltru ma, występujące w tym okresie, zjawisko korozji jego elementów emisyjnych – elektrod ulotowych. Producenci elektrofiltrów nie stosują ochrony antykorozyjnej elektrod ulotowych w obawie przed pogorszeniem emisyjności elektrod. W artykule przedstawiono wyniki badań emisyjności elektrod ulotowych bez zabezpieczeń oraz zabezpieczonych powłokami antykorozyjnymi, dla elektrody prętowej oraz wybranej elektrody przemysłowej typu masztowego. Analizę wyników przeprowadzono z zastosowaniem metod statystycznych opartych na modelu szeregów czasowych. Uzyskane wyniki badań jednoznacznie wykazały, że stosowanie powłok antykorozyjnych nie pogarsza parametrów elektrycznych elektrod ulotowych. Ochrona antykorozyjna może być stosowana zarówno podczas prac modernizacyjnych elektrofiltrów, jak i na etapie budowy nowych urządzeń.

ZUBER N, BAJRIĆ R, ŠOSTAKOV R. **Gearbox faults identification using vibration signal analysis and artificial intelligence methods**. Eksploatacja i Niezawodnosc – Maintenance and Reliability 2014; 16 (1): 61–65.

The paper addresses the implementation of feature based artificial neural networks and vibration analysis for the purpose of automated gearbox faults identification. Experimental work has been conducted on a specially designed test rig and the obtained results are validated on a belt conveyor gearbox from a mine strip bucket wheel excavator SRs 1300. Frequency and time domain vibration features are used as inputs to fault classifiers. A complete set of proposed vibration features are used as inputs for self-organized feature maps and based on the results a reduced set of vibration features are used as inputs for supervised artificial neural networks. Two typical gear failures were tested: worn gears and missing teeth. The achieved results show that proposed set of vibration features enables reliable identification of developing faults in power transmission systems with toothed gears.

ZUBER N, BAJRIĆ R, ŠOSTAKOV R. **Identyfikacja uszkodzeń skrzyni biegów za pomocą analizy sygnału drgań oraz metod sztucznej inteligencji**. Eksploatacja i Niezawodnosc – Maintenance and Reliability 2014; 16 (1): 61–65.

Artykuł omawia zastosowanie sztucznych sieci neuronowych opartych na cechach oraz analizy drgań do celów automatycznej identyfikacji uszkodzeń skrzyni biegów. Prace eksperymentalne przeprowadzono na specjalnie zaprojektowanym stanowisku badawczym, a uzyskane wyniki zweryfikowano na przykładzie przekładni przenośnika taśmowego koparki wielonaczyniowej SRs 1300 wykorzystywanej w kopalni odkrywkowej. Cechy drgań w dziedzinie czasu i częstotliwości są wykorzystywane jako wejścia klasyfikatorów uszkodzeń. Kompletny zbiór proponowanych cech drgań wykorzystano jako wejścia samoorganizujących się map cech, a na podstawie wyników opracowano zredukowany zbiór cech drgań, które wykorzystano jako wejścia do nadzorowanych sztucznych sieci neuronowych. Zbadano dwa typowe uszkodzenia przekładni: zużycie przekładni oraz brakujące zęby przekładni. Uzyskane wyniki wskazują, że proponowany zbiór cech drgań umożliwia niezawodną identyfikację rozwijających się uszkodzeń w układach przenoszenia napędu z kołami zębatymi.

KULIKOWSKI K, SZPICA D. **Determination of directional stiffnesses of vehicles' tires under a static load operation**. Eksploatacja i Niezawodnosc – Maintenance and Reliability 2014; 16 (1): 66–72.

This paper presents the stand test results on the different tires under static conditions. The tests were conducted on a stand that allows registering the force and deflection of the tested tires. The results were used to determinate directional tire stiffness, by using self-made software identification. In the next stage, tread prints were made, which were used to determine the surface area of the tire contact with the ground, depending on the pressure inside the tire and the load. The results showed correlations of stiffness growth with increasing tire pressure at radial, longitudinal and torsional evaluation, the contrary conclusions were put forward in the evaluation of circumferential stiffness. The tires, which the characteristics were significantly different from the study group, were also presented. The received results can be the input data for dynamic tests.

KULIKOWSKI K, SZPICA D. **Wyznaczanie sztywności kierunkowych opon pojazdów samochodowych w warunkach statycznego działania obciążenia**. Eksploatacja i Niezawodnosc – Maintenance and Reliability 2014; 16 (1): 66–72.

W artykule przedstawiono wyniki badań stanowiskowych różnego rodzaju opon samochodowych w warunkach statycznych. Próby przeprowadzono na stanowisku umożliwiającym rejestrację siły i odkształcenia badanej opony. Uzyskane wyniki posłużyły wyznaczeniu sztywności kierunkowych opon, wykorzystując własne oprogramowanie identyfikujące. W kolejnym etapie wykonano odciski bieżnika, które posłużyły do wyznaczenia pola powierzchni styku opony z podłożem w zależności od ciśnienia wewnątrz opony oraz obciążenia. Wyniki wykazały korelacje dotyczące wzrostu sztywności w miarę zwiększania ciśnienia w oponie przy ocenie promieniowej, wzdłużnej, skrętnej, przeciwne wnioski wysunięto w przypadku oceny obwodowej. Zaprezentowano również opony odstające o charakterystykach znacznie odbiegających od badanej grupy. Otrzymane wyniki mogą być danymi wejściowymi do badań dynamicznych.

LINGAITIS LP, LEBEDEVAS S, LIUDVINAVIČIUS L. **Evaluation of the operational reliability and forecasting of the operating life of the power train of the freight diesel locomotive fleet**. Eksploatacja i Niezawodnosc – Maintenance and Reliability 2014; 16 (1): 73–79.

The article provides analysis of the passivity of various options for the rational use of the fleet of diesel locomotives with the purpose of improving the operational reliability indicators of diesel engines installed on freight diesel locomotives. The rationality of the use of mathematical statistical methods, with their application to in-service diesel engines installed on diesel locomotives, was assessed with the use of the accumulated statistical data on breakdowns/disorders of main-line diesel locomotives of State Company "Lietuvos geležinkeliai" (Lithuanian Railways). On the basis of technical documentation, with the use of the results of comparative tests and practically approbated indirect diesel engine reliability criteria, the comparative assessment of the operating life of in-service diesel engines installed on freight diesel locomotives has been performed. In order to substantiate the adequacy of tests, the adaptation of the programme modules of mathematical computer simulation of the parameters of diesel engines of the fleet operated by Lithuanian Railways. The differences between the results established by the experiment and simulated by the computer do not exceed 5–7 %. The indirect criteria of evaluating the mechanical and thermal load of parts of diesel engines installed on diesel locomotives have been selected and adapted. An algorithm of the methodology for the evaluation of the reliability criteria of diesel engines installed on diesel locomotives and forecasting of the operating life has been developed. It has been implemented in the form of a mathematical simulation programming complex.

LINGAITIS LP, LEBEDEVAS S, LIUDVINAVIČIUS L. **Ocena niezawodności eksploatacyjnej i prognozowanie żywotności układu przeniesienia napędu we flocie spalinowych lokomotyw towarowych**. Eksploatacja i Niezawodnosc – Maintenance and Reliability 2014; 16 (1): 73–79.

Artykuł przedstawia analizę pasywności różnych opcji racjonalnego wykorzystania floty lokomotyw spalinowych mającą na celu poprawę wskaźników niezawodności eksploatacyjnej silników wysokoprężnych użytkowanych w towarowych lokomotywach spalinowych. Zasadność stosowania matematycznych metod statystycznych do analizy eksploatacji silników wysokoprężnych użytkowanych w lokomotywach spalinowych oceniano z wykorzystaniem zgromadzonych danych statystycznych dotyczących awarii / nieprawidłowego działania lokomotyw spalinowych jeżdżących na głównych liniach kolejowych Firmy Państwowej„Lietuvosgeležinkeliai" (Koleje Litewskie). Na podstawie dokumentacji technicznej, z wykorzystaniem wyników testów porównawczych i sprawdzonych w praktyce pośrednich kryteriów niezawodności silników wysokoprężnych, dokonano oceny porównawczej żywotności silników wysokoprężnych zamontowanych w towarowych lokomotywach spalinowych. W celu potwierdzenia trafności badań, zastosowano moduły programowe matematycznej symulacji komputerowej parametrów silników wysokoprężnych floty eksploatowanej przez Koleje Litewskie. Różnice pomiędzy wynikami otrzymanymi na drodze doświadczalnej a wynikami symulowanymi komputerowo nie były większe niż 5–7%. Wybrano i przyjęto pośrednie kryteria oceny mechanicznych i termicznych obciążeń części silników wysokoprężnych zamontowanych w lokomotywach spalinowych. Opracowano algorytm metodyki oceny kryteriów niezawodności silników wysokoprężnych użytkowanych w lokomotywach spalinowych oraz prognozowania ich żywotności. Został on wdrożony w postaci kompleksu do programowania symulacji matematycznych.

SOKOLSKI P, SOKOLSKI M. **Evaluation of resistance to catastrophic failures of large-size caterpillar chain links of open-pit mining machinery**. Eksploatacja i Niezawodnosc – Maintenance and Reliability 2014; 16 (1): 80–84.

Large-size caterpillar undercarriages of basic mining machines are operated in extremely harsh conditions: they are subjected to high workloads and aggressive environmental influence. Under these conditions, the degradation can develop intensively and results in wear and tear of parts and subassemblies of these undercarriages. Especially dangerous are the catastrophic failures of components of the caterpillar chain: links or connecting pins (plastic deformations or brittle fractures), which generally exclude further work of the undercarriage. Because of that, a study on the structure of the damaged parts was carried out. Basing on numerical models of typical large–size chain links an assessment of effort of these parts was done, critical areas in their build were localized and proposals of modifications of their geometrical parameters were formulated as well. The main result of implementation of these modifications is a significant increase in links' resistance to catastrophic failure, which is particularly important in terms of operational safety and reliability of basic machines.

SOKOLSKI P, SOKOLSKI M. **Ocena odporności na uszkodzenia katastroficzne wielkogabarytowych ogniw gąsienicowych podwozi maszyn podstawowych górnictwa odkrywkowego**. Eksploatacja i Niezawodnosc – Maintenance and Reliability 2014; 16 (1): 80–84.

Wielkogabarytowe podwozia gąsienicowe maszyn podstawowych górnictwa odkrywkowego pracują w wyjątkowo trudnych warunkach eksploatacyjnych: są poddawane ekstremalnie dużym obciążeniom roboczym oraz agresywnemu oddziaływaniu środowiska. W takich warunkach procesy degradacji mogą rozwijać się szczególnie intensywnie, a ich efektem są zużycie lub uszkodzenia elementów i podzespołów tych podwozi. Szczególnie groźne są uszkodzenia katastroficzne elementów łańcucha gąsienicy: ogniw lub sworzni łączących (odkształcenia plastyczne lub kruche pęknięcia), które wykluczają na ogół dalszą eksploatację podwozia. Mając to na uwadze, przeprowadzono studium struktury uszkodzeń elementów wielkogabarytowych podwozi gąsienicowych. Na podstawie modeli numerycznych dokonano oceny wytężenia typowych wielkogabarytowych ogniw gąsienicowych, wyznaczono obszary krytyczne i zaproponowano modyfikacje ich cech geometrycznych. Wynikiem tych modyfikacji jest znaczące zwiększenie odporności ogniw na uszkodzenia katastroficzne, co jest szczególnie istotne w aspekcie bezpieczeństwa eksploatacji maszyn podstawowych.

GUO YM, WANG XT, LIU C, ZHENG YF, CAI XB. **Electronic system fault diagnosis with optimized multi-kernel svm by improved CPSO**. Eksploatacja i Niezawodnosc – Maintenance and Reliability 2014; 16 (1): 85–91.

Electronic systems' safety operation has become a key issue to complex and high reliability systems. Now more emphasis has been laid on the accuracy of electronic system fault diagnosis. Based on the characteristics of the electronic system fault diagnosis, we design a multi-classification SVMs model to attain better fault diagnosis accuracy, which utilizes multi-kernel function consisting of several basis kernel functions to enhance the interpretability of the classification model. In order to optimize the performance of multi-classification SVMs with multi-kernel, we improve the Chaos Particles swarm Optimization (CPSO) algorithm to achieve the optimum parameters of SVMs and the multi-kernel function. For the improved CPSO algorithm, a modified Tent Map chaotic sequence is used to strengthen the search diversity, and an effective method is embedded to the stander PSO algorithm which can ensure to avoid premature stagnation and obtain the global optimization values. The fault diagnosis simulation results of an electronic system show the proposed optimization

GUO YM, WANG XT, LIU C, ZHENG YF, CAI XB. **Diagnoza uszkodzeń układu elektronicznego z wykorzystaniem Wielojądrowej Maszyny Wektorów Nośnych (SVM) zoptymalizowanej przy pomocy poprawionego algorytmu CPSO**. Eksploatacja i Niezawodnosc – Maintenance and Reliability 2014; 16 (1): 85–91.

Bezpieczeństwopracy układów elektronicznych stało się kluczowym zagadnieniem w odniesieniu do złożonych układów o wysokiej niezawodności. Obecnie coraz większy nacisk kładzie się na trafność diagnozy uszkodzeń układów elektronicznych. Na podstawie charakterystyki diagnozy uszkodzeń układów elektronicznych, opracowaliśmy model wielokryterialnej klasyfikacji SVM pozwalający osiągnąć lepszą trafność diagnozy uszkodzeń. Model wykorzystuje funkcję wielojądrową składającą się z kilku bazowych funkcji jądrowych pozwalającą na zwiększenie interpretowalności modelu klasyfikacyjnego. Aby zoptymalizować działanie modelu wielokryterialnej klasyfikacji SVM wykorzystującego funkcję wielojądrową, udoskonaliliśmy algorytm Optymalizacji Metodą Chaosu-Roju Cząstek (CPSO), co pozwoliło osiągnąć optymalne parametry SVM i funkcji wielojądrowej. W poprawionym algorytmie CPSO wzmocniono różnorodność wyszukiwania poprzez wykorzystanie chaotycznej sekwencji generowanej przez zmodyfikowaną mapę

scheme is a feasible and effective method and it can significantly improve the fault diagnosis accuracy of the multi-kernel SVM.

GLOWACZ A, GLOWACZ A, GLOWACZ Z. **Recognition of monochrome thermal images of synchronous motor with the application of quadtree decomposition and backpropagation neural network**. Eksploatacja i Niezawodnosc – Maintenance and Reliability 2014; 16 (1): 92–96.

Technological progress and decreasing prices of thermographic cameras make their application to monitoring and assessing a technical state of machines is profitable. In article is described the recognition method of imminent failure conditions of synchronous motor. The proposed approach is based on a study of thermal images of the rotor. Extraction of relevant diagnostic information coded in thermal images is important for diagnosing of machine. It can be performed with the use of selected methods of analysis and recognition of images. Studies were carried out for two conditions of motor with the application of quadtree decomposition and backpropagation neural network. The experiments show that the method can be useful for protection of synchronous motor. Moreover, this method can be used to diagnose equipments in steelworks and other industrial plants.

LIU Y, FAN J, LI Y. **One system reliability assessment method for CNC grinder**. Eksploatacja i Niezawodnosc – Maintenance and Reliability 2014; 16 (1): 97–104.

The reliability level of CNC (Computer Numerical Control) grinder is usually assessed by fault data counted in laboratory or in field, which needs the grinder to be assembled and it is one afterwards estimation method. To evaluate the reliability level of CNC grinder in design phrase, one system reliability assessment method and algorithm was put forward by subsystem's reliability in this article, which needs subsystem classification, reliability test, distribution function fitting, parameters estimation and reliability assessment. The calculation result showed that the method was feasible and accurate compared with the traditional way. The method is one contribution to reliability design for CNC grinder and is one reference to other mechatronic products.

JAROSIŃSKI W. **Periodic technical inspections of vehicles and road traffic safety with the number of road accidents involving fatalities**. Eksploatacja i Niezawodnosc – Maintenance and Reliability 2014; 16 (1): 105–111.

The article is an attempt to find relationship between the implemented system of periodic technical inspections of vehicles and the number of road accidents, reliability of vehicles and road safety. The study utilises results of comparative tests, where the relationships and parameters could be directly observed for the cases with the system implemented and some without periodic technical inspections at all (for example: between the states of the USA, Australia and the research work conducted in Norway in the 90's). The analysis of results leads to unexpected conclusion that system of periodic technical inspections of vehicles does not have statistically significant effect on the number of accidents, including the number of road accidents involving fatalities.

ANTOSZ K, STADNICKA D. **The results of the study concerning the identification of the activities realized in the management of the technical infrastructure in large enterprises**. Eksploatacja i Niezawodnosc – Maintenance and Reliability 2014; 16 (1): 112–119.

The activities realized within the technical infrastructure supervision are particularly important for large enterprises. It's commonly believed that in large enterprises there is a wide range of tasks realized within the technical infrastructure supervision. The studies done so far indicate only the machine supervision strategies used in enterprises, yet it doesn't indicate what activities are specifically realized. In fact, in spite of the rules adopted for each strategy, they are not used entirely in practice. The aim of the survey, of which the results are presented in this paper, was to identify the real activities conducted in enterprises within the technical infrastructure supervision in large enterprises. The survey concerned production enterprises functioning in different industries on a specified area. The results were drawn up and presented graphically. The results indicate both the activities which are commonly realized and those which are rare in this group of enterprises.

GALAR D, BERGES L, SANDBORN P, KUMAR U. **The need for aggregated indicators in performance asset management**. Eksploatacja i Niezawodnosc – Maintenance and Reliability 2014; 16 (1): 120–127.

Composite indicators formed when individual Indicators are compiled into a single index. A composite indicator should ideally measure multidimensional concepts that cannot be captured by a single index. Since asset management is multidisciplinary, composite indicators would be helpful. This paper describes a method of monitoring

tent, a także włączono do standardowego algorytmu PSO efektywną metodę pozwalającą uniknąć przedwczesnej stagnacji oraz uzyskać globalne wartości optymalizacji. Wyniki symulacji diagnozy uszkodzeń systemu elektronicznego pokazują, że proponowany system optymalizacji może być wykorzystywany jako skuteczna metoda umożliwiająca znaczne zwiększenie trafności diagnozy uszkodzeń z wykorzystaniem wielojądrowej SVM.

GLOWACZ A, GLOWACZ A, GLOWACZ Z. **Rozpoznawanie monochromatycznych obrazów cieplnych silnika synchronicznego z zastosowaniem kwadratowo-drzewowej dekompozycji i sieci neuronowej**. Eksploatacja i Niezawodnosc – Maintenance and Reliability 2014; 16 (1): 92–96.

Postęp techniczny i malejące ceny kamer termowizyjnych sprawiają, że ich zastosowanie do monitorowania i oceny stanu technicznego maszyn jest opłacalne. W artykule opisano metodę rozpoznawania stanów przedawaryjnych silnika synchronicznego. Proponowane podejście jest oparte na badaniu obrazów cieplnych wirnika. Ekstrakcja istotnej informacji diagnostycznej zakodowanej w obrazach cieplnych jest ważna dla diagnozowania maszyny. Zabieg taki może być wykonany z użyciem wybranych metod analizy i rozpoznawania obrazów. Przeprowadzono badania dla dwóch stanów silnika z zastosowaniem kwadratowo-drzewowej dekompozycji i sieci neuronowej z algorytmem wstecznej propagacji błędów. Eksperymenty pokazują, że metoda może być przydatna do zabezpieczania silników synchronicznych. Ponadto metoda może być stosowana do diagnozowania urządzeń w hutach i innych zakładach przemysłowych.

LIU Y, FAN J, LI Y. **Metoda oceny niezawodności systemuszlifierki CNC**. Eksploatacja i Niezawodnosc – Maintenance and Reliability 2014; 16 (1): 97–104.

Poziom niezawodności szlifierki CNC (sterowanej numerycznie) zazwyczaj ocenia się na podstawie danych o uszkodzeniach liczonych w laboratorium lub w terenie, co wymaga zmontowania szlifierki i jest metodą oceny post-factum. Aby umożliwić ocenę poziomu niezawodności szlifierki CNC na etapie projektowania, w niniejszym artykule zaproponowano metodę oceny niezawodności systemu oraz odpowiedni algorytm wykorzystujące dane dotyczące niezawodności podsystemów. Model ten wymaga klasyfikacji podsystemów, badań niezawodności, dopasowania funkcji rozkładu, oceny parametrów oraz oceny niezawodności. Wyniki obliczeń wykazały, że omawiana metoda sprawdza się i jest dokładna w porównaniu z metodą tradycyjną. Przedstawiona metoda stanowi wkład do procesu projektowania niezawodności szlifierki CNC i znajduje odniesienie do innych produktów mechatronicznych.

JAROSIŃSKI W. **System okresowych badań technicznych pojazdów a bezpieczeństwo ruchu drogowego i liczba zdarzeń drogowych z udziałem ofiar śmiertelnych**. Eksploatacja i Niezawodnosc – Maintenance and Reliability 2014; 16 (1): 105–111.

Artykuł jest próbą znalezienia relacji pomiędzy wdrożonym systemem okresowych badań technicznych pojazdów, a liczbą zdarzeń drogowych i szerzej niezawodnością pojazdów i bezpieczeństwem ruchu drogowego. W pracy między innymi wykorzystano wyniki badań porównawczych, dla których można było wprost obserwować zależność i parametry dla przypadków z wdrożonym systemem okresowych badań technicznych i bez niego (na przykładzie Stanów Zjednoczonych, Australii i Norwegii). Analiza wyników prowadzi do zaskakującego wniosku, że wyżej wymieniony system nie ma statystycznie istotnego wpływu na liczbę wypadków, w tym liczbę zdarzeń drogowych z udziałem ofiar śmiertelnych.

ANTOSZ K, STADNICKA D. **Wyniki badań dotyczących identyfikacji działań realizowanych w zarządzaniu infrastrukturą techniczną w dużych przedsiębiorstwach**. Eksploatacja i Niezawodnosc – Maintenance and Reliability 2014; 16 (1): 112–119.

Działania realizowane w zakresie nadzoru nad infrastrukturą techniczną są szczególnie istotne dla dużych przedsiębiorstw. Powszechnie panuje przekonanie, że w dużych przedsiębiorstwach istnieje duży zakres zadań realizowanych w ramach nadzoru nad infrastrukturą techniczną. Dotychczas przeprowadzone badania wskazują jedynie na stosowane w przedsiębiorstwach strategie nadzoru nad maszynami, jednakże nie wskazuje się, jakie działania są konkretnie realizowane. W rzeczywistości mimo zasad przyjętych dla każdej strategii w praktyce nie są one tak do końca stosowane. Celem badań, których wyniki przedstawiono w niniejszej pracy, było zidentyfikowanie rzeczywistych działań, które są prowadzone w przedsiębiorstwach w zakresie nadzoru nad infrastrukturą techniczną w dużych przedsiębiorstwach. Badania dotyczyły przedsiębiorstw produkcyjnych funkcjonujących w różnych branżach przemysłu na określonym obszarze. Wyniki badań opracowano i przedstawiono w postaci graficznej. Wyniki badań wskazują zarówno na te działania, które są powszechnie realizowane, jak i na te, które rzadko występują w tej grupie przedsiębiorstw.

GALAR D, BERGES L, SANDBORN P, KUMAR U. **Potrzeba zagregowanych wskaźnikówwydajności w zarządzaniuaktywami**. Eksploatacja i Niezawodnosc – Maintenance and Reliability 2014; 16 (1): 120–127.

Wskaźniki złożone tworzy się poprzez zebranie pojedynczych wskaźników w jeden indeks. Idealnie, wskaźnik złożony powinien mierzyć pojęcia wielowymiarowe, których nie da się uchwycić przy pomocy pojedynczego indeksu. Ponieważzarządzanie aktywami jest dziedziną wielodyscyplinarną, przydatne byłoby wykorzystanie w niejwskaźników złożonych.

a complex entity in a processing plant. In this scenario, a composite use index from a combination of lower level use indices and weighting values. Each use index contains status information on one aspect of the lower level entities, and each weighting value corresponds to one lower level entity. The resulting composite indicator can be a decision-making tool for asset managers.

TAO J, YU Z, REN Z, YI X. **Study of an adaptive accelerated model and a data transfer method based on a reliability enhancement test**. Eksploatacja i Niezawodnosc – Maintenance and Reliability 2014; 16 (1): 128–132.

To assess the reliability of a product using a Reliability Enhancement Test (RET), this study first considers the change process of the Arrhenius model parameters by combining the Arrhenius model with the Duane model and gives an adaptive accelerated model and a parameter estimation method. Then, the data transfer method from the RET to normal test stress are described based on the adaptive accelerated model. Finally, the differences observed when the RET is used for a reliability identity test or a reliability growth test are discussed, and an engineering case demonstrates a method for obtaining the reliability index of a product using the RET.

KOSZAŁKA G. **Model of operational changes in the combustion chamber tightness of a diesel engine**. Eksploatacja i Niezawodnosc – Maintenance and Reliability 2014; 16 (1): 133–139.

The paper presents the results of tightness testing of an internal combustion engine combustion chamber during long-term operation. The tests were conducted on 5 six-cylinder diesel engines used in motor trucks. Changes in tightness for the distance range 0–500,000 km were determined based on the measurement results of the following: pressure drop measured using a cylinder leak-down tester, maximum compression pressure in the cylinders, and the blow-by flow rate at different engine operating conditions. The obtained test results were analyzed statistically. Stochastic models of changes in engine combustion chamber tightness versus distance traveled were developed. Each model describes the time history of the mean value of a selected diagnostic parameter and the limits of probable changes in this parameter. The test results have shown that both the rate and character of changes as a function of engine operation time differed depending on a parameter. The maximum compression pressure was characterized by the lowest dynamics of changes (a decrease by less than 20% for the distance range 0–500,000 km), the cylinder leakage was characterized by a moderate change dynamics, while the blow-by flow rate exhibited the highest dynamics of changes (a threefold increase at 2200 rpm). It should also be mentioned that in the case of the first two parameters, the rate of changes increased with the distance traveled, whereas in the case of the blow-by the observed changes were linear. Also, dispersion fields (i.e. changes in standard deviations) were calculated for the tested diagnostic parameters.

GAN S, SHI J. **Maintenance optimization for a production system with intermediate buffer and replacement part order considered**. Eksploatacja i Niezawodnosc – Maintenance and Reliability 2014; 16 (1): 140–149.

Existing research on maintenance is mostly devoted to maintenance planning without considering other related issues. However, optimizing maintenance separately may lead to unexpected system cost, due to the interaction between maintenance, buffer, and replacement parts. In this paper, a production system consisting of two serial machines and an intermediate buffer is studied. The upstream machine deteriorates with time, and the deterioration degrees are classified into different working conditions and represented by ascendant states. During the maintenance optimization for the upstream machine, the replacement part order and buffer inventory are both considered. Therefore, the system state is complex with the buffer level, machine working condition, and replacement parts taken into account together. One type of control-limit policy is applied based on system state, and then the system and decision process are modeled by discrete Markov method. Through policy-iteration algorithm, the control-limit policy is optimized for the minimal long-term expected cost rate. Numerical examples are delivered to illustrate the proposed method and for the parameter sensitivity analysis.

SOWA A. **Formal models of generating checkup sets for the technical condition evaluation of compound objects**. Eksploatacja i Niezawodnosc – Maintenance and Reliability 2014; 16 (1): 150–157.

The paper refers to problems connected with building systems of computer-aided generation of evaluation sets of features necessary for the evaluation of compound objects' ability, and also the localization of imperfections of their component elements. In order to solve these problems, the usefulness of both the matrix method of determining sets of checkups and the cross-out method was analyzed. Binary and three-valued models of technical condition evaluation of the object's elements as well as the object's input and output features were formed. It allows then for the creation of the object matrix model which is used in both analyzed methods. For the matrix method, binary and three-valued evaluation models of distinguishing of the object technical condition were also defined. The binary models were used in a program which generates sets of features of the ability and localizing test. This program was

W przedstawionej pracyopisano metodęmonitorowania złożonej jednostki w zakładzie przetwórczym. W podanym scenariuszu, złożony wskaźnik wykorzystania powstał z połączenia wskaźników wykorzystania niższego rzędu z wartościami ważonymi. Każdy wskaźnik wykorzystania zawiera informacje na temat statusu jednego aspektu jednostek niższego rzędu, a każda wartość ważona odpowiada jednej jednostce niższego rzędu.

TAO J, YU Z, REN Z, YI X. **Badania adaptacyjnego modelu przyspieszonego oraz metody transferu danych w oparciu o test poprawy niezawodności**. Eksploatacja i Niezawodnosc – Maintenance and Reliability 2014; 16 (1): 128–132.

Aby ocenić niezawodność produktu za pomocą testu poprawy niezawodności (Reliability Enhancement Test, RET), w badaniach najpierw rozważano proces zmiany parametrów modelu Arrheniusa poprzez połączenie modelu Arrheniusa z modelem Duane'a oraz przedstawiono adaptacyjny model przyspieszony i metodę oceny parametrów. Następnie, na podstawie adaptacyjnego modelu przyspieszonego opisano metodę transferu danych z RET do badań przy normalnym oddziaływaniu czynników zewnętrznych. Wreszcie, omówiono różnice obserwowane przy zastosowaniu RET do badań identyfikacyjnych niezawodności i badań wzrostu niezawodności. Na przykładzie zagadnienia inżynierskiego przedstawiono także metodę obliczania wskaźnika niezawodności produktu za pomocą RET.

KOSZAŁKA G. **Model eksploatacyjnych zmian szczelności przestrzeni nadtłokowej silnika o zapłonie samoczynnym**. Eksploatacja i Niezawodnosc – Maintenance and Reliability 2014; 16 (1): 133–139.

W artykule przedstawiono wyniki badań szczelności komory spalania silnika o zapłonie samoczynnym w czasie długotrwałej eksploatacji. Badania przeprowadzono na 5 egzemplarzach sześciocylindrowego silnika wykorzystywanego do napędu samochodów ciężarowych. Zmiany szczelności w zakresie przebiegów 0–500 tys. km określono na podstawie wyników pomiarów: spadku ciśnienia z wykorzystaniem próbnika szczelności komory spalania, maksymalnego ciśnienie sprężania w cylindrach oraz natężenia przedmuchów spalin do skrzyni korbowej w różnych warunkach pracy silnika. Wyniki badań poddano analizie statystycznej. Opracowano stochastyczne modele zmian szczelności komory spalania silnika w funkcji przebiegu samochodu. Model opisuje przebieg wartości średniej wybranego parametru diagnostycznego w czasie oraz granic obszaru prawdopodobnych zmian tego parametru.Wyniki badań wykazały, że zarówno prędkość jak i charakter zmian w funkcji czasu eksploatacji były różne dla różnych parametrów. Najmniejszą dynamiką zmian wyróżniało się maksymalne ciśnienie sprężania (spadek o mniej niż 20% w zakresie przebiegów samochodu: 0–500 tys. km), średnią dynamiką – wskaźnik szczelności, a największą – natężenie przedmuchów spalin (3-krotny wzrost przy 2200 obr/min), przy czym dla dwóch pierwszych parametrów szybkość zmian zwiększała się wraz z przebiegiem samochodu, natomiast w przypadku przedmuchów spalin zmiany miały charakter liniowy. Wyznaczono również pola rozproszeń (zmian odchyleń standardowych) dla badanych parametrów diagnostycznych.

GAN S, SHI J. **Optymalizacja konserwacji systemu produkcyjnego uwzględniająca bufor pośredni i zamówienia części zamiennych**. Eksploatacja i Niezawodnosc – Maintenance and Reliability 2014; 16 (1): 140–149.

Prowadzone dotychczas badania nad konserwacją poświęcone są głównie harmonogramowi konserwacji, nie przywiązując uwagi do innych wiążących się z nią zagadnień. Jednakże, prowadzona niezależnie optymalizacja konserwacji może prowadzić do nieplanowanych kosztów z uwagi na powiązania między konserwacją, buforem i częściami zamiennymi. Niniejszy artykuł analizuje system produkcyjny składający się z dwóch urządzeń szeregowych oraz bufora pośredniego. Urządzenie na początku linii z czasem się zużywa, a stopień zużycia sklasyfikowano z uwagi na różne warunki pracy i przedstawiono za pomocą stanów wstępujących. W ramach optymalizacji konserwacji urządzenia na początku linii, rozważono zarówno zamówienia części zamiennych jak i zapasy bufora. Tak więc, na kompletny obraz stanu systemu składają się poziom bufora, warunki pracy urządzenia, oraz części zamienne. Jeden z rodzajów strategii poziomu kontroli oparty jest o stan systemu, następnie system i proces decyzyjny są modelowane przy wykorzystaniu ukrytych modeli Markowa. Strategia poziomu kontroli została zoptymalizowana dla minimalnego długofalowego i prognozowanego poziomu kosztu za pomocą algorytmu iteracji strategii. Przedstawiono również przykłady liczbowe aby zilustrować proponowaną metodę a także przeprowadzić analizę wrażliwości na zmiany parametrów.

SOWA A. **Modele formalne generowania zbiorów sprawdzeń dla oceny stanu technicznego obiektów złożonych**. Eksploatacja i Niezawodnosc – Maintenance and Reliability 2014; 16 (1): 150–157.

Praca dotyczy problemów związanych z budową systemów wspomaganego komputerowo generowania zbiorów sprawdzeń cech niezbędnych do oceny zdatności obiektów złożonych, a także lokalizacji niezdatności ich elementów składowych. Analizowano przydatność do tego celu macierzowej metody określania zbiorów sprawdzeń oraz metody skreśleń. Sformułowano binarne i trójwartościowe modele ocen stanu technicznego elementów obiektu oraz jego cech wejściowych i wyjściowych. Pozwala to wtedy na utworzenie macierzowego modelu obiektu, wykorzystywanego w obu analizowanych metodach. Dla metody macierzowej zdefiniowano także binarne i trójwartościowe modele oceny rozróżnialności stanów technicznych obiektu. Binarne modele wykorzystano w programie generującym zbiory cech testu zdatności i lokalizującego, napisanym przy użyciu pakietu Mathematica. Przy trójwartościowym modelu ocen do generowania zbiorów

written with the use of a Mathematica package. For a three-valued evaluation model for generating the feature checkup sets, the use of the cross-out method was proposed for both tests, with the technical state distinguishing conditions formed for this method. There was also presented an example of using this method to determine checkup sets of features which allow for the evaluation of the technical condition of part of the carriage brake pneumatic system.

BAJRIĆ R, ZUBER N, ŠOSTAKOV R. **Relations between pulverizing process parameters and beater wheel mill vibration for predictive maintenance program setup**. Eksploatacja i Niezawodnosc – Maintenance and Reliability 2014; 16 (1): 158–163.

Beater wheel mills are designed to prepare a coal powder air fuel mixture for combustion in furnace chambers of coal-fired power plants by coal drying, pulverizing, classifying and transport. Their multipurpose function usually results in operation instability accompanied by unacceptable vibration. This usually is a significant problem due to unplanned shutdowns. Beater wheel mill maintenance program requires special attention due to operation under non-stationary conditions. The purpose of this paper was to identify pulverizing process parameter that affect the beater wheel mill vibration level and severity at the same time by using statistical principles under a wide range of operating conditions. This paper intends to establish the foundations to investigate correlation of pulverizing process parameter with beater wheel mill vibration in order to setup a better predictive maintenance program. To achieve this goal, the beater wheel mill vibration under different combinations of selected pulverizing process parameters are analyzed using statistical tools. Experiments were carried out under different conditions for two identical but separated beater wheel mills. The influence of pulverizing process parameter, such as electrical current of the driving motor, mill capacity, boiler production, coal types on mill vibration are investigated to identify the potential malfunction of beater wheel mills and their associated components for predictive maintenance purposes. The results have demonstrated that the selected pulverizing process parameters do not have significant influence on beater wheel mill vibration severity. Unlike most coal mills where pulverizing process parameters must take into account, here with beater wheel impact mills it is not the case and condition monitoring of these mills could be conducted offline or online using standard vibration condition monitoring methods.

KOPECKI T, MAZUREK P. **Numerical representation of post-critical deformations in the processes of determining stress distributions in closed multi-segment thin-walled aircraft load-bearing structures**. Eksploatacja i Niezawodnosc – Maintenance and Reliability 2014; 16 (1): 163–169.

The study presents results of a research work on the problem of obtaining reliable results of nonlinear FEM analyses of thin-walled load-bearing structures subjected to post-critical loads. Consistency of numerical simulations results and actual stress distribution states depends on the correct numerical reproduction of bifurcations that occur during advanced deformations processes.

sprawdzeń cech dla obu testów zaproponowano użycie metody skreśleń i sformułowano dla niej warunki rozróżnialności stanów technicznych. Przedstawiono także przykład użycia tej metody do określenia zbiorów sprawdzeń cech pozwalających na ocenę stanu technicznego części układu pneumatycznego hamulca wagonu.

BAJRIĆ R, ZUBER N, ŠOSTAKOV R. **Relacje między parametrami procesów rozdrabniania i drganiami młyna wentylatorowego a ustawienia programu konserwacji predykcyjnej**. Eksploatacja i Niezawodnosc – Maintenance and Reliability 2014; 16 (1): 158–163.

Młyny wentylatorowe są urządzeniami, które poprzez suszenie, rozdrabnianie, odsiewanie i transport węgla przygotowują mieszankę pyłowo-gazową przeznaczoną do spalania w komorach paleniskowych elektrowni węglowych. Ich uniwersalność zwykle wiąże się z niestabilną pracą połączoną z niepożądanymi drganiami. Jest to zwykle znaczący problem z uwagi na niezaplanowane przerwy w pracy. Program konserwacji młyna wentylatorowego wymaga szczególnej uwagi ze względu na działanie w niestacjonarnych warunkach pracy. Celem artykułu jest wyznaczenie parametrów procesów rozdrabniania wpływających jednocześnie na poziom i natężenie drgań młyna wentylatorowego przy użyciu reguł statystycznych w zróżnicowanych warunkach pracy. Zamierzeniem pracy jest stworzenie podstaw dla badań nad zależnościami między parametrami procesu rozdrabniania a drganiami młyna wentylatorowego w celu ulepszenia programu konserwacji predykcyjnej. Aby osiągnąć założony cel, przeanalizowano przy użyciu narzędzi statystycznych drgania młyna wentylatorowego przy różnych kombinacjach wybranych parametrów procesu rozdrabniania. Badania przeprowadzono w różnych warunkach na dwóch identycznych, lecz odrębnych młynach wentylatorowych. Wpływ parametrów procesu rozdrabniania, takich jak prąd elektryczny silnika napędowego, pojemność młyna, kotły, czy typ węgla, na drgania młyna zbadano w celu określenia potencjalnych awarii młyna i jego części składowych na potrzeby jego konserwacji predykcyjnej. Wyniki badań pokazały, iż wybrane parametry procesu rozdrabniania nie mają znaczącego wpływu na natężenie drgań młyna wentylatorowego. W przeciwieństwie do większości młynów węglowych, w przypadku których należy brać pod uwagę parametry procesu rozdrabniania, kontrola stanu młynów wentylatorowych może być prowadzona w trybie offline lub online za pomocą standardowych metod monitorowania warunków drgania.

KOPECKI T, MAZUREK P. **Numerical representation of post-critical deformations in the processes of determining stress distributions in closed multi-segment thin-walled aircraft load-bearing structures**. Eksploatacja i Niezawodnosc – Maintenance and Reliability 2014; 16 (1): 163–169.

Opracowanie przedstawia wyniki badań związanych z problemem uzyskiwania wiarygodnych wyników nieliniowych analiz numerycznych, w ujęciu metody elementów skończonych, cienkościennych struktur nośnych poddawanych obciążeniom zakrytycznym. Zgodność wyników numerycznych symulacji z rzeczywistymi dystrybucjami naprężeń uzależniona jest od poprawnego numerycznego odwzorowania bifurkacji zachodzących w procesach zaawansowanych deformacji.

Article citation info:
SU C, FU YQ. Reliability assessment for wind turbines considering the influence of wind speed using Bayesian network. Eksploatacja i Niezawodnosc – Maintenance and Reliability 2014; 16 (1): 1–8.

Chun SU
Ye-qun FU

RELIABILITY ASSESSMENT FOR WIND TURBINES CONSIDERING THE INFLUENCE OF WIND SPEED USING BAYESIAN NETWORK

OCENA NIEZAWODNOŚCI TURBIN WIATROWYCH ZA POMOCĄ SIECI BAYESA Z UWZGLĘDNIENIEM WPŁYWU PRĘDKOŚCI WIATRU

The reliability of wind turbine is of great importance for the availability and economical efficiency of wind power system. In this article, a reliability model for wind turbine is built with Bayesian network (BN), in which the influence of wind speed is considered. Causal logic method (CLM) is presented for qualitative modeling, which combines the merits of fault tree in handling technical aspects and the strength of BN in dealing with environmental factors and uncertainty. A novel adjustment method based on expectation is proposed for quantitative calculation, by which historical data and expert judgment are integrated to describe the uncertainty in the prior probability distributions. An approximate inference algorithm combining with dynamic discretization of continuous variables is adopted to obtain the reliability index of wind turbine and its elements. A case study is given to illustrate the proposed method, and the results indicate that wind speed is an important factor for the reliability of wind turbine.

Keywords*: Bayesian network, wind turbine, reliability assessment, wind speed.*

Niezawodność turbiny wiatrowej ma ogromne znaczenie dla gotowości i efektywności ekonomicznej instalacji wiatrowej. W niniejszym artykule zbudowano, w oparciu o sieci Bayesa (BN), model niezawodności turbiny wiatrowej uwzględniający wpływ prędkości wiatru. Przedstawiono Metodę Logiki Przyczynowości (Causal Logic Method, CLM), służącą do modelowania jakościowego, która łączy zalety drzewa błędów w odniesieniu do aspektów technicznych z atutami BN w odniesieniu do czynników środowiskowych i niepewności. Do kalkulacji ilościowych zaproponowano nową metodę dopasowania opartą na oczekiwaniach, w której dane z eksploatacji i opinie ekspertów łącznie pozwalają opisać niepewność rozkładów prawdopodobieństwa a priori. Wskaźnik niezawodności turbiny wiatrowej i jej elementów otrzymano posługując się algorytmem wnioskowania przybliżonego w połączeniu z dynamiczną dyskretyzacją zmiennych ciągłych. Dla zilustrowania proponowanej metody przedstawiono studium przypadku, którego wyniki wskazują, że prędkość wiatru jest ważnym czynnikiem niezawodności turbiny wiatrowej.

Słowa kluczowe*: Sieć Bayesa, turbina wiatrowa, ocena niezawodności, szybkość wiatru*

1. Introduction

Wind energy is a kind of clean and renewable energy. Its installed capacity has grown rapidly around the world in recent years [7]. In China, for instance, it has shown a booming growth in wind power since 2005, and the installed capacity has increased from 503MW in 2005 to around 60GM by the end of 2012 [14]. Due to the variability of wind, shifting loads and fluctuating energy demands, components of wind turbines are susceptible to damage, including gearboxes, blades, generators and electrical components, etc [13]. Since wind power projects are long-term and capital-intensive, spanning about 20–25 years, the failures of components will cause excess repair and maintenance costs, thereby reducing the power generation [12]. For instance, for a variety of reasons, the average utilization time of wind turbines with full capacity in China is only 1920 hours in 2011, which is significantly lower than 2200 hours as planned.

With the increasing number of wind turbines and wind farms, the importance of their reliability and availability has attracted great attention. Negra et al. [20] summarized the factors that affect the reliability of wind power system, including wind turbine performance, and some reliability evaluation indices were also presented. Considering wind turbine as a two-state system, Manco et al. [16] proposed a reliability model with Markovian approach. Fazio et al. [8] adopted universal generating function (UGF) to build the reliability model of wind turbine, in which wind speed, energy conversion and failure characteristics were considered. Guo et al. [10] applied three-parameter Weibull distribution to describe the reliability growth of wind turbines with incomplete failure data. But up to now, the research on reliability assessment for wind turbines is still very limited [9].

Wind turbine is a kind of multi-component complicated system. The behaviors of the components in such a system include failure priority, dependent failures and interactions, etc [15]. In practice, the interactions among the assemblies of wind turbines are quite complicated, thus it can not simply be regarded as a series blocks of assemblies [2]. Furthermore, the reliability of wind turbine is also affected

by various environmental factors, such as wind speed, temperature, humidity, location of wind farm [30]. By analyzing failure data and wind speed data, Tavner et al. [27] concluded that high wind speeds reduce wind turbine reliability. Su et al. [25] analyzed the correlation between failure rate of wind turbine and wind speed by time series approach. They ascribed a periodicity in failure rates of wind turbines to the effect of wind speed, but didn't go further to investigate how to take wind speed into consideration when evaluating the reliability. The interaction among the components and the influence of wind speed greatly increase the difficulties in system reliability assessment with traditional reliability methods.

Bayesian network (BN) has the ability to depict the uncertainty and interactions among the assemblies. It also provides the possibility to combine different sources of information together, such as expert knowledge, environmental and human factors. Most associated literatures focused on the learning and inference algorithms related with BN. Nonetheless, the application of BN in reliability has aroused great interest among researchers in the past few years [28]. Bobbio et al [3] showed how to map fault trees into BN, and reliability analysis for a multiprocessor system was also completed with BN. Compared with fault tree method, some restrictive assumptions in BN can be removed, and various dependencies among components can also be expressed efficiently. Marquez et al. [17] proposed a hybrid BN framework to analyze dynamic fault tree, meanwhile, the failure distributions of static and dynamic logic gates were obtained by using an approximate inference algorithm involving dynamic discretization of continuous variables. Boudali et al. [5] presented a discrete-time BN framework to fulfill the reliability analysis for a dynamic system. They also proposed a continuous BN framework, which considered not only the combination of failure events, but also the sequence ordering of the failure [4]. Sørensen [23] described the degradation process before failure by pre-posterior Bayesian, and the influence of uncertainty on degradation, maintenance cost and whole life cycle cost were analyzed in order to optimize the operation and maintenance.

In this paper, BN is adopted to build reliability model of wind turbine, and wind speed and the uncertainty in reliability parameters are also taken into consideration. A casual logic method (CLM) is proposed to build the qualitative model, and a novel method is presented to handle the uncertainty of parameters. The case study indicated that by considering the influence of wind speed, the reliability assessment results of wind turbine are more practical.

The remainder of this paper is organized as follows. Section 2 gives a brief introduction of BN, and the procedure to build a reliability model based on BN is also provided. CLM for qualitative modeling is presented in Section 3. In Section 4, a novel adjustment method based on expectation is proposed to adjust prior probability distribution, and an approximate inference algorithm combining with dynamic discretization is adopted to obtain conditional probability distributions. In Section 5, a case study for wind turbine reliability assessment considering the influence of wind speed is provided to illustrate the feasibility of the proposed approach. In Section 6, conclusions and further studies are offered.

2. Reliability modeling based on Bayesian network

2.1. Introduction to Bayesian network

Bayesian network (BN) is also known as casual network, or probabilistic dependence graph [3]. It is a graphical network established on the basis of well-defined probabilistic reasoning, and it has strong ability to deal with uncertainty and dependence [6]. Based on the observations and other prior information, the probability distribution of random variables can be calculated by BN.

In general, the definition of a BN can be divided into two parts: qualitative and quantitative [18]. The qualitative part is described by a directed acyclic graph (DAG), in which the nodes represent system variables $X=\{x_1, x_2, \ldots, x_n\}$, and directed arcs symbolize the causal or influential relationships between variables. Fig. 1 gives a simple BN with nodes $\{x_1, x_2, x_3, x_4\}$, in which only the qualitative part is shown. Nodes x_1 and x_2 are the parents of node x_3, and node x_3 is the parent of node x_4. The direct arcs between nodes x_1 and x_3 as well as nodes x_2 and x_3 mean that node x_3 is affected by nodes x_1 and x_2, while x_1 and x_2 are independent. Similarly, node x_4 is dependent on node x_3. The quantitative part is conditional probability distributions (CPD), $p(x_i|\mathrm{pa}(x_i))$, which define the probability relationship among the nodes by their parent nodes $\mathrm{pa}(x_i)$. Those nodes without parents are called root nodes, and their CPD can be simply indicated as $p(x_i|\phi)=\mathrm{p}(x_i)$, which is also called prior probability distributions. The main feature of BN is representing a joint probability distribution by factorization of variables based on conditional independence, which can be expressed as

$$p(x_1, x_2, \ldots, x_n) = \prod_{i=1}^{n} p(x_i \mid pa(x_i)) \tag{1}$$

According to the separation of conditional independence, the distribution of joint probability can be divided into some simple prob-

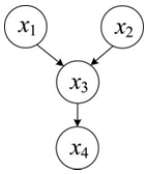

Fig. 1. An example BN with nodes $\{x_1, x_2, x_3, x_4\}$

ability distributions. In this way, the complexity of the model is reduced, and the inference efficiency can be improved obviously. Take Fig. 1 as an example, its joint probability distribution is equivalent to

$$p(x_1, x_2, x_3, x_4) = p(x_1)p(x_2)p(x_3 \mid x_1, x_2)p(x_4 \mid x_3) \tag{1a}$$

The marginal probability distribution of a node can be obtained by joint probability distribution. Assuming that the nodes in Fig. 1 are discrete, the marginal probability distribution of x_4 is denoted as

$$p(x_4) = \sum_{x_1, x_2, x_3} p(x_1, x_2, x_3, x_4) = \sum_{x_1, x_2, x_3} p(x_1)p(x_2)p(x_3 \mid x_1, x_2)p(x_4|x_3) \tag{1b}$$

2.2. Modeling process

In this study, we are interested in the reliability assessment of wind turbines based on BN, and the influence of wind speed is also considered. Roughly, there are four steps involved in the modeling, as seen in Fig. 2.

Step 1: **System definition.** Basic events and logic gates are deter-

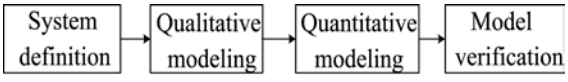

Fig. 2. Flow chart of reliability assessment

mined by classical reliability analysis methods, including FTA and RBD. Afterwards the environmental factors, such as wind speed, are introduced into the model on the basis of the requirement of reliability assessment. Meanwhile, continuous and discrete variables are also defined at this stage.

Step 2: **Qualitative modeling.** CLM is adopted to establish qualitative model, i.e., definition of DAG. In order to make the inference

effective, intermediate nodes are necessary when a node has more than three parents.

Step 3: **Quantitative modeling.** It includes the setting of prior probability distributions and CPD. Prior probability distributions are obtained based on historical data and subjective judgment. The root nodes which correspond to the assemblies or subsystems of wind turbine are characterized by their prior probability density functions. A novel approach is proposed to adjust the parameters of prior distributions. All non-root nodes, i.e. logic gates and dependent components, are characterized by their CPD.

Step 4: **Model verification.** Reliability evaluation and sensitivity analysis are included in this step. In this article, an approximate inference algorithm combining with dynamic discretization of continuous variables is adopted to obtain TTF distribution of wind turbine. The details can be found in Ref. [21]. The result is also compared with the one that doesn't consider the influence of wind speed and the uncertainty of parameters. Sensitivity analysis is conducted to illustrate how the reliability of wind turbine changes with the variations of average wind speed.

3. Qualitative modeling

Ref. [22] presented a hybrid causal logic method (HCLM), in which BN was integrated into event sequence diagrams or fault trees. Inspired by HCLM, we present a casual logic method (CLM) to guide the reliability modeling of wind turbine based on BN. Firstly the logic relation of fault tree is transformed into BN, then wind speed is added into BN regarded as a common environmental factor. Finally, the BN model is adjusted again for considering the uncertainty of parameters in prior probability distribution. Compared with HCLM, CLM guarantees that all the basic events are represented only once, which can reduce the complexity of the model. Meanwhile, a new algorithm of combination of fault trees and BNs is dispensable. An example is showed in Fig. 3 to illustrate CLM in detail.

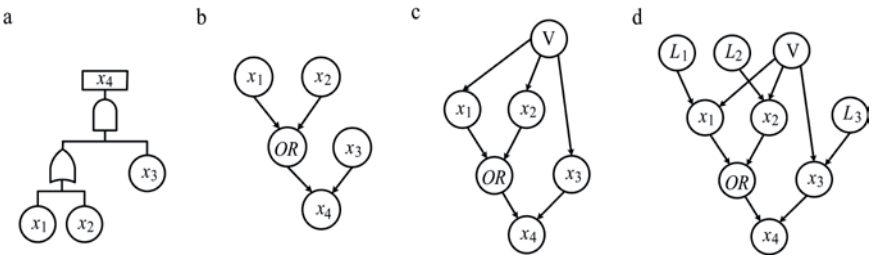

Fig. 3. CLM framework: a) Fault trees of an example; b) Mapping fault trees to BN; c) Components affected by wind speed; d) Uncertainty of prior probability distributions.

As seen in Fig. 3a, it is assumed that a fault tree of wind turbine consists of three basic events x_1, x_2, x_3 with an AND gate and an OR gate respectively. Either event x_1 or x_2 failure will lead to the failure of OR gate's output. As for AND gate, top event x_4 fails only when all of its input events fail. Therefore, the cut sets are $\{x_1, x_3\}$, $\{x_2, x_3\}$, and $\{x_1, x_2, x_3\}$, which are used for defining all the fault modes of the system. The fault tree can be mapped into BN, shown as Fig. 3b. The basic events in fault tree equal to the root nodes in BN. It needs to be pointed out that if the basic events appear more than once, one corresponding node in BN is enough. Similarly, each logic gate can be represented by a corresponding node in BN. Nodes are connected by directed arcs in BN just as corresponding gates in fault tree.

In practical applications, the reliability of wind turbine is also affected by wind speed, which is difficult to be handled quantitatively. In this paper, the influence of wind speed is expressed by the change of components' life-lengths. When wind speed is not taken into consideration, the life-lengths of components are independent. But when components are exposed to some common environment, the correlation among their life-lengths is as follows: a tough environment leads to reduced life-lengths for all components, whereas a gentle environment implies that the life-lengths of the components are increased. Thus, let V represent wind speed, and make links between node V and each component to express the influence of wind speed on them. The qualitative part of BN model considering wind speed influence is built, as illustrated in Fig. 3c.

Furthermore, the uncertainty of parameters is also considered in the BN model. In general, the TTF distributions of basic events are assumed to be probability distributions with constant parameters. But in this study, parameters are considered as random variables, and modeled using probability distributions. Nodes L_1, L_2, L_3 are created to describe the probability distribution of parameters, and are added as the parents of corresponding nodes, as shown in Fig. 3d.

The qualitative reliability model with BN can be built according to the steps above. The corresponding BN model can describe the structure of wind turbine, the interactions among components, and the influence of environmental factors on system reliability.

4. Quantitative calculation

In this study, continuous nodes are used to represent TTF of basic events and logic gates, and discrete nodes are used to describe the states of wind turbine and its subsystems at a particular point in time. Prior probability distributions and CPD are needed to evaluate wind turbine reliability. If sufficient historical data are available, prior probability distributions can be obtained. But in practice, failure data are usually limited. Therefore, the prior probability distributions are usually obtained according to the judgment of experts' knowledge and experience. A novel approach is proposed in Section 4.2 to adjust parameters of prior probability distributions, which can combine historical data and expert judgment. CPD for TTF τ of fault tree logic gates, $f(t|\mathrm{pa}(\tau))$, needs to be calculated, where τ is a function of corresponding input components' TTF, namely $\tau = \rho(\mathrm{pa}(\tau))$.

Considering the reliability model consists of both discrete and continuous nodes, and after adjustment the prior probability distributions are non-Gaussian distributions, an approximate inference algorithm combining with dynamic discretization of all continuous variables are adopted to generate TTF distributions of wind turbine and its subsystems. Thus the reliability of wind turbine at any mission time can be derived.

4.1. Dynamic discretization and approximate inference

Inference is carried out using a standard BN propagation algorithm. Considering the reliability model of wind turbine includes both discrete and continuous nodes with non-Gaussian distributions, exact inference seems troublesome. An approach is applied in this paper, by which the ranges of all continuous variables are dynamically discretized, and CPD at each discretization step is approximated by using a weighted uniform density function [21].

The dynamic discretization consists of two parts: 1) searching an optimal partition set $\Psi=\{w_1, w_2, \ldots, w_n\}$ in range of variables; 2) optimizing the values for the discretized probability density function $\tilde{f}(t)$, which are defined as a piecewise constant function on the partitioning intervals.

Different from the static discretization splitting the range evenly, the dynamic discretization searches the variable range for most accurate specification of high-density regions. At each stage in the iterative process, a candidate discretization, $\Psi=\{w_1, w_2, \ldots, w_n\}$, is judged whether the entropy error is below a given threshold. If not, repeat the process until at an acceptable degree.

The approximate inference algorithm uses a weighted uniform density function to approximate the conditional density functions after each dynamic discretization. Here is a case with only two parents to illustrate the approximate inference algorithm:

1) Assume system S has two parent nodes A and B. The TTF of S, A, B are t_A, t_B, t_S, respectively. t_S can be expressed by its input nodes, namely $t_S = \rho(t_A, t_B)$.
2) Suppose the variables have partition sets Ψ_A, Ψ_B. For each pair of interval in the respective sets Ψ_A and Ψ_B, such as an interval (a_1, a_2) in Ψ_A and (b_1, b_2) in Ψ_B, the maximum m and minimum l for each set of values $\rho(a_1, b_1)$, $\rho(a_1, b_2)$, $\rho(a_2, b_1)$, $\rho(a_2, b_2)$ are calculated with the approach respectively.
3) If the number of such kind of interval is I, then a uniform probability density mass $U(l_i, m_i)$ is generated in interval (l_i, m_i) over the range of t_S, for $i \in$ I. Assuming that partition set $\Psi s=\{w_1, w_2, \ldots, w_n\}$, then the conditional density function of nodes t_S in the partitioning interval w_k can be defined as

$$p(ts \in wk)U(t;li,mi) \tag{2}$$

where $p(ts \in wk)$ represents the fraction of uniform mass $U(t; l_i, m_i)$ corresponding to the interval w_k

$$p(ts \in wk) = \begin{cases} \int_{wk} U(t;li,ui)dt & if \quad wk \cap (li,mi) \neq \phi \\ 0 & otherwise \end{cases} \tag{3}$$

By iteratively updating the partitioning intervals using dynamic discretization, the accurate approximations of CPD are obtained, and the input variables are not limited to exponential or Gaussian families.

4.2. Parameter uncertainty of prior probability distribution

In this section, a novel method called adjustment method based on expectation is proposed to deal with the uncertainty of parameters in prior probability distributions. Generally, the expected values of TTF distributions can show the average life-lengths of components. It is simple and intuitive to judge the fluctuating ranges of average life lengths, while it is hard to decide the parameters of the distribution functions. Therefore, the expected values of TTF distributions together with regulation factors are considered to achieve uncertainty of prior probability distributions.

Suppose the TTF distribution of a node in BN is f with parameters $K=\{K_1, K_2, \ldots, K_n\}$, $i=1, 2, \ldots, n$, which can be expressed as $f(t|K_1, K_2, \ldots, K_n)$ with $t \geq 0$. Its expectation can be calculated by

$$ET = \int t \cdot f(t|K_1, K_2, \ldots K_n)dt = g(K_1, K_2, \ldots K_n) \tag{4}$$

Now the parameters $K=\{K_1, K_2, \ldots, K_n\}$ are obtained based on historical data, namely $K_1=k_1, K_2=k_2, \ldots, K_n=k_n$. The distribution with constant parameters can be written as $f(t|K_1=k_1, K_2=k_2, \ldots, K_n=k_n)$, and its expected value can be calculated by Eq. (4)

$$E(t|K_1 = k_1, K_2 = k_2, \ldots, K_n = k_n) = g(k_1, k_2, \ldots, k_n), \tag{5}$$

Let the regulation factors of parameters $K=\{K_1, K_2, \ldots, K_n\}$ be $\theta=\{\theta_1, \theta_2, \ldots, \theta_n\}$, $i=1, 2, \ldots, n$. The uncertainty of parameter K_i is dependent on regulation factors θ_i, which belongs to [0, 1]. The bigger θ_i is, the less convincible fitting distributions will be. Here, we assume that the expectation obeys triangular distribution as below after expert's adjustment.

$$g(k_1, k_2, \ldots, K_i, \ldots, k_n) \sim Triangle((1-\theta_i)g, (1+\theta_i)g, g), \tag{6}$$

where g is short for the expected value $g(k_1, k_2, \ldots, k_n)$ in Eq. (5); $(1-\theta_i)g$ and $(1+\theta_i)g$ represent the lower limit and upper limit of triangular distribution, respectively.

The distribution for parameters can be generated from Eq. (6), shown as

$$K_i \sim \text{triangular}\ (\min(g^{-1}((1-\theta_i)g), g^{-1}((1+\theta_i)g)), \max(g^{-1}((1-\theta_i)g), g^{-1}((1+\theta_i)g)), g^{-1}(g)), \tag{7}$$

where g^{-1} is the inverse function of $g(k_1, k_2, \ldots, K_i, \ldots, k_n)$ in Eq. (6).

Here is an example to illustrate the method. Suppose the TTF distribution of component A is exponential distribution with $k=1/1000$, i.e. Exp(1/1000). The regulation factor given by expert is 0.2, then we can obtain that $k \sim$ triangular (1/1200, 1/800, 1/1000) according to Eqs. (4) – (7). The prior probability distribution of component A after adjustment is shown as Fig. 4:

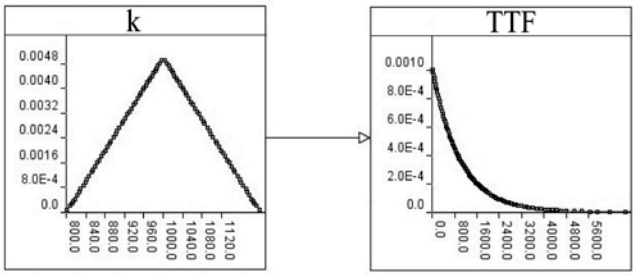

Fig. 4. An example for adjustment of prior probability distribution

4.3. CPD for Boolean constructs

The dynamic discretization algorithm, together with the approximation approach, allows us to estimate the CPD for the fault tree constructs automatically.

The TTF of Boolean constructs in simple fault trees are defined by the input components of the construct, i.e., $\tau=g(pa(\tau))$. Let t_i ($i=1, 2, \ldots, n$) denote the TTF of the ith parent node.

The AND gate means that only if all the input components fail, the output of the AND gate will fail. Suppose TTF of AND gate is t_{AND}, and according to the definition of AND gate, its failure probability in time interval $(0, t]$ can be given by

$$p(t_{\text{AND}} \leq t) = p(t_1 \leq t, \cdots, t_n \leq t) = p(\max_i \{t_i\} \leq t), \tag{8}$$

where the TTF of AND gate, t_{AND}, is a random variable defined by its corresponding input nodes' TTF, namely $t_{\text{AND}} = \max_i \{t_i\}$.

As for OR gate, it means that if at least one input component fails, the output of the OR gate will fail. Similarly, the failure probability of t_{OR}, namely the TTF of OR gate, in time interval $(0, t]$ can be formulated as

$$p(t_{\text{OR}} \leq t) = 1 - p(t_1 > t, \cdots, t_n > t) = p(\min_i \{t_i\} \leq t) \tag{9}$$

where the TTF of OR gate t_{OR} is a random variable defined by its parents, namely $t_{OR} = \min_i \{t_i\}$.

5. Case study

5.1. Description of wind turbine

Wind turbine is a complicated system which is composed of several subassemblies. Fig. 5 shows the main subassemblies in a typical geared generator wind turbine [1]. Although all the subassemblies are indispensable both in function and reliability, for simplification here we only focus on some important subassemblies, including gearbox, blades, generator, electrical subsystem, converter, yaw assembly, pitch assembly, brake assembly, and hydraulic assembly. Brake assembly is parallel connected by air brake and mechanical brake. From the view of reliability, the above assemblies can be considered in series, and the reliability block diagram is shown in Fig. 6. Safety subsystem is composed of yaw assembly, pitch assembly, brake assembly, and hydraulic assembly. It is of great importance for the operation, reliability and safety of wind turbine. Fig. 7 illustrates a fault tree, in which the basic events represent the failure of subsystems or assemblies, and the failure of wind turbine is the top event. The symbols for the basic events are shown in Table 1.

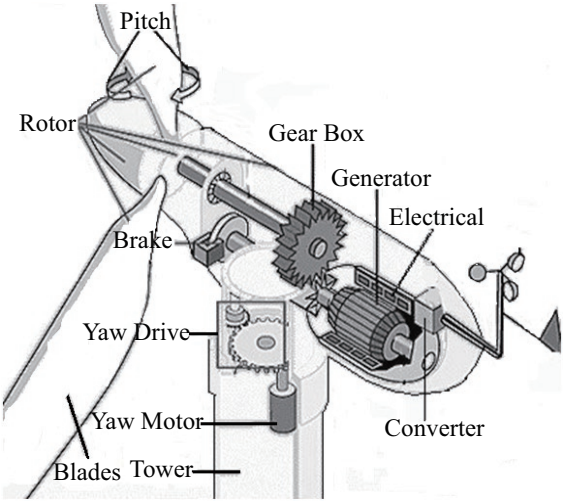

Fig.5. Structure of wind turbine

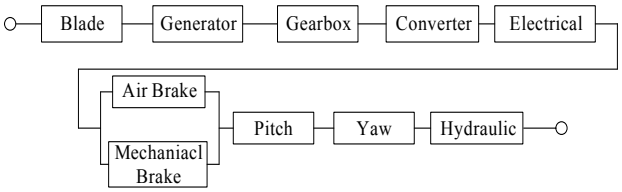

Fig. 6. Reliability block diagram of wind turbine

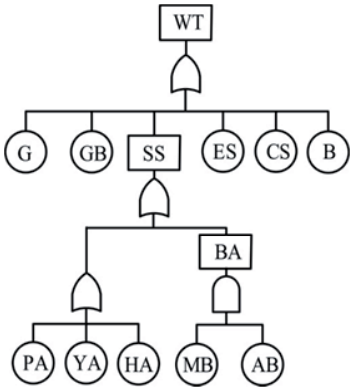

Fig. 7. A fault tree of wind turbine

Table 1. Symbols for basic events

Symbol	Basic event
G	Failure of Generator
GB	Failure of Gear Box
B	Failure of Blade
ES	Failure of Electrical Subsystem
CS	Failure of Converter Subsystem
SS	Failure of Safety Subsystem
PA	Failure of Pitch Assembly
BA	Failure of Brake Assembly
HA	Failure of Hydraulic Assembly
YA	Failure of Yaw Assembly
AB	Failure of Air Brake
MB	Failure of Mechanical Brake

Generally, the wind turbine could continue to work when safety subsystem fails, but in a suboptimal situation [1]. Therefore, it's not always practical to consider safety subsystem as a series relationship. Considering that classical reliability methods are not skillful in dealing with the environmental factor, in this article BN is applied to build the reliability model, and study the influence of wind speed on the reliability.

5.2. Reliability model of wind turbine based on BN

5.2.1. Qualitative modeling for reliability of wind turbine based on BN

On the basis of fault tree in Fig. 7 and the function of safety subsystem, the BN model which ignores the safety subsystem is built, as show in Fig. 8a. The corresponding BN model of the safety subsystem is as shown in Fig. 8b. The influence of safety subsystem on wind turbine reliability is mainly reflected on the protection of blades. The life-lengths of blades are affected by the state of safety subsystem. Hence, Figs. 8a and 8b can be combined by the node "on?" which represents the state of safety subsystem, seen in Fig. 8c.

After mapping the fault tree into BN, the influence of wind speed and the uncertainty of parameter are considered by using CLM. The range of wind speed has diverse influence on life-lengths of subsystems and assemblies. Therefore, node "$v>v_0$" is added to divide wind speed interval, and it is connected to all subsystems and assemblies. As for uncertainty of parameters, only one parameter in each prior probability distribution is adjusted in this study, which can be described by nodes L_i, where i =1 to 10. The qualitative reliability model of wind turbine based on BN is established, as shown in Fig. 9.

5.2.2. Definition of TTF distributions

Based on the failure data recorded in Windstas for the wind farms in Denmark and Germany during 1994 to 2004, some statistic analyses for the life data of wind turbines have been done in Refs. [11, 24, 25]. The TTF distributions of corresponding subsystems and assemblies are extracted, as presented in Tables 2 and 3, respectively. When the wind speed is larger than cut-out speed (in this case it is 20 m/s), the prior probability distributions of subsystems and assemblies are different. Ref. [26] analyzed which subsystem or assembly's reliability is greatly affected by wind speed. The result showed that the generator is the greatest effect, with yaw assembly and pitch assembly closely behind, whereas mechanical brake, hydraulic assembly, air brake, gearbox, blades are affected not so remarkable. According to

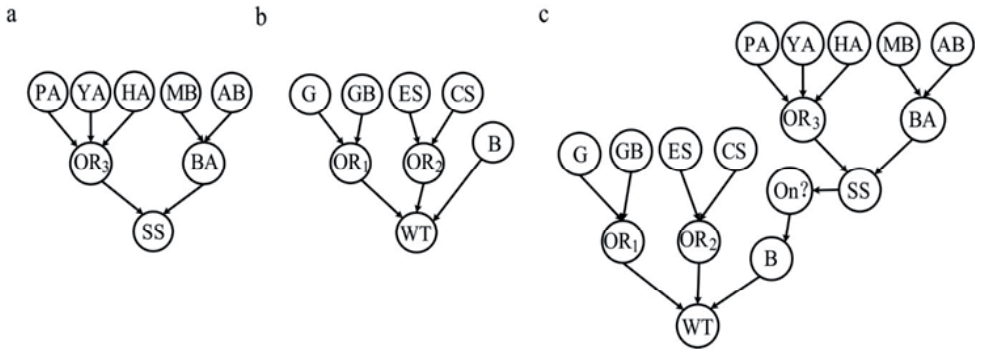

Fig. 8. Mapping fault tree of wind turbine into BN: a) BN model for wind turbine without consideration of safety subsystem; b) BN model for safety subsystem; c) BN model for entire wind turbine system

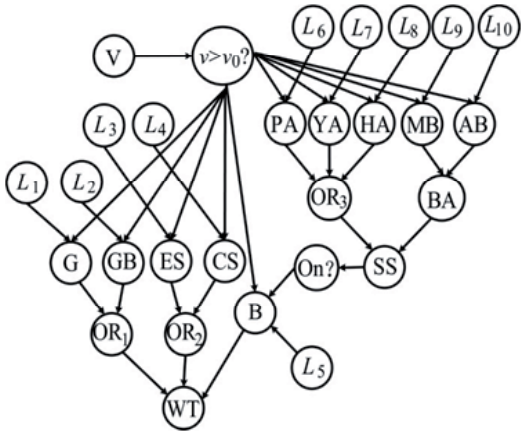

Fig. 9. Qualitative reliability model for wind turbine

Table 2. TTF distributions of subsystems and assemblies

Nodes	TTF distribution when $0<v\leq20(h)$	TTF distribution when $v>20(h)$
Gearbox	Weibull(12300,1.05)	Weibull(12300,1.05)
Generator	Weibull(76000, 1.2)	Weibull(7600, 1.2)
Electrical subsystem	Weibull(35000, 1.5)	Weibull(35000, 1.5)
Converter subsystem	Exp(1/45000)	Exp(1/45000)
Yaw assemble	Exp(1/65000)	Exp(1/8125)
Pitch assemble	N(84534,506)	N(14089,506)
Hydraulic assemble	Weibull(66000, 1.3)	Weibull(33000, 1.3)
Air brake	Exp(1/100000)	Exp(9/500000)
Mechanical brake	Exp(1/120000)	Exp(1/30000)

Table 3. TTF distributions of blades

	TTF distribution (*h*)	State of safety subsystem (Safe or Failure)	Wind speed (*m/s*)
Blade	N(42000, 663)	Safe	$0<v\leq20$
	N(42000, 663)	Safe	>20
	N(42000, 663)	Failure	$0<v\leq20$
	N(28000, 663)	Failure	>20

that conclusion, the prior probability distributions judged by experts are shown in column 3 of Table 2.

From Tables 2 and 3, it can be found that the TTF distributions of the subsystems or assemblies obey Weibull(α, β), Exp($1/\lambda$) and N(μ, σ^2), respectively. To simplify the calculation, we consider uncertainty for only one parameter in each distribution, i.e., α in Weibull distribution, λ in exponential distribution and μ in normal distribution.

5.2.3. Reliability assessment of wind turbine

The reliability model is built with Agenarisk© software, and after running for 25 iterations the TTF distributions of wind turbine and its subsystems are obtained. If the wind speed and the uncertainty of parameters are not considered, the reliability of wind turbine at 1000h turns out to be 96.21%, which is quite closed to the result 96.17% in Ref. [11]. Thus, the modeling method and calculating algorithm proposed in this study is with high accuracy.

Now we consider the influence of wind speed and parameters' uncertainty. Assuming that the wind speed obeys Weibull (14, 1.94) and all the regulation factors are set to 0.1. The TTF distributions of subsystems and wind turbine are shown as Fig. 10. In order to make the figure concise, some nodes are hidden. Fig. 11 presents a clear image of TTF distribution of the wind turbine. From Figs. 10 and 11, we can learn that the reliability of the wind turbine at 1000h is 95.18%, and the mean time to failure (MTTF) is 13944h. Obviously, the wind speed and parameters' uncertainty have greatly decreased the reliability.

Meanwhile, from Fig. 11 we can find that firstly the TTF distribution increases within a relatively short period from 0h to around 3000h, and then it keeps declining, which is consistent with the fact that maintenance is not taken into account in this study. It implies that if maintenance is ignored, the TTF is not long enough to meet high availability requirement for wind turbines. Given the target reliability, the corresponding time can be obtained according to TTF distribution. That provides a theoretical foundation for the decision-making of preventive maintenance. In the engineering practice, the life expectancy of wind turbine is about 20 years, and the required technical availability of wind turbines is quite high [29]. Therefore, good reliability design and maintenance management are of crucial importance to the normal operation and economic benefit of wind turbines.

Based on the TTF distribution of wind turbine, the reliability at different points in time can be calculated, and the reliability-to-time curve is drawn, as shown in Fig. 12. In the same manner, reliability-to-time curve without considering the influence of wind speed is also illustrated. Both the curves have the same changing trends, which decrease over time. Compared with the curve not considering the influence of wind speed, the curve considering the influence of wind speed is less reliable, and the gap between them increases with time. For example, at 0h the reliability is 100% for both curves, the gap increases to 5.85% at 10000h. Therefore, the influence of wind speed on wind turbine reliability should not be ignored.

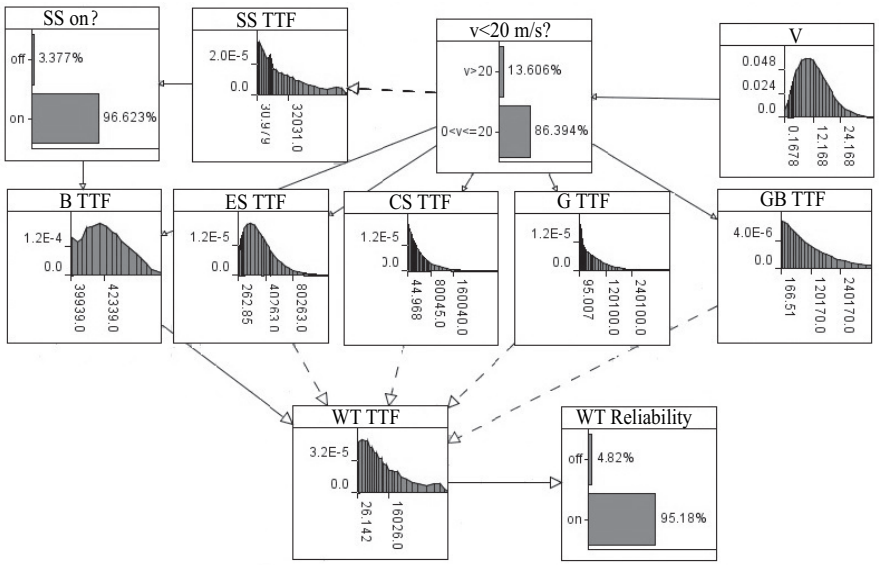

Fig. 10. TTF distributions of wind turbine and its subsystems

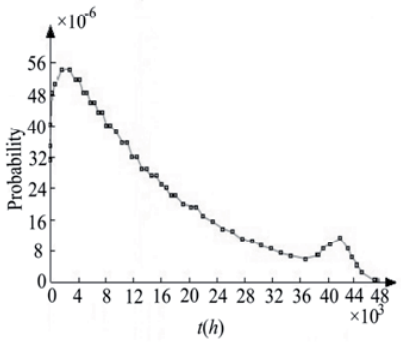

Fig. 11. TTF distribution of wind turbine

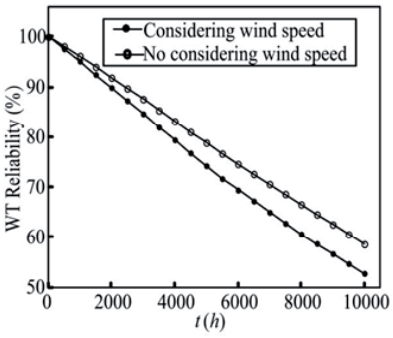

Fig. 12. Reliability-to-time curves of wind turbine

5.3. Reliability over wind speed

In this section, the influence that wind speed acts on the reliability of wind turbine will be further analyzed. Generally, the wind speed is supposed to obey Weibull distribution [19]. The average wind speed $\bar{v}$ can be expressed by the shape parameter α and scale parameter β. Keeping β fixed and by changing α, the relevance between average wind speed and wind turbine's reliability can be analyzed. Running the models under different wind speeds for 25 iterations respectively, the reliabilities at 1000h are evaluated, as shown in Fig. 13. In addition, the corresponding reliabilities under the assumption that the safety subsystem is failed are also calculated, shown also in Fig. 13. Obviously, they have similar variation trends. But if the safety subsystem fails the reliability of wind turbine will be lower, which demonstrates the importance of safety subsystem in protecting the blades and the entire device. Fig. 13 can also show that the gap between the two estimates increases with the values of wind speed. Both Fig. 12 and Fig. 13 illustrate the influence of wind speed on wind turbine's reliability. It's also worth pointing out that this model can be used for wind turbines in different areas with varied wind conditions as long as the prior probability distribution of wind speed is obtained.

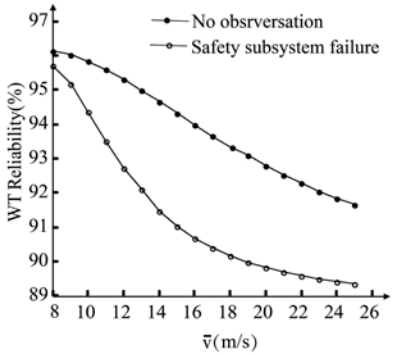

Fig. 13. Reliability of wind turbine varied with wind speed

6. Conclusion and further study

In this article, a reliability model of wind turbine is built based on BN, in which the influence of wind speed is also taken into consideration. The CLM is proposed to direct qualitative modeling. The fault trees are mapped into BN, then the wind speed and parameters' uncertainty are considered. A novel adjustment method based on expectation is presented to modify the prior probability distributions. An approximate inference algorithm involving dynamic discretization is adopted to calculate the TTF distribution of wind turbine. Therefore the reliability of wind turbine can be evaluated. The case study shows that the approach proposed in this article is suitable for reliability assessment of wind turbines. Additionally, the TTF distribution can provide a reasonable guide for the maintenance decision of wind farms.

In this study, we focus only on reliability assessment of wind turbine based on BN. While in practice, maintenance and availability are also very important topics. Hence, we intend to carry out further studies on maintenance decision-making and availability assessment for wind turbines or wind farms based on the theory of Bayesian network in the near future.

References

1. Arabian-Hoseynabadi H, Tavner PJ, Oraee H. Reliability comparison of direct-drive and geared-drive wind turbine concepts. Wind energy 2010; 13(1): 62–73.

2. Bai YS, Jia XS, Cheng ZH. Group optimization models for multi-component system compound maintenance tasks. Eksploatacja i Niezawodnosc – Maintenance and Reliability 2011; 49(1): 42–47.
3. Bobbio A, Portinale L, Minichino M, Ciancamerla E. Improving the analysis of dependable systems by mapping fault trees into Bayesian networks. Reliability Engineering & System Safety 2001; 71(3): 249–260.
4. Boudali H, Dugan JB. A continuous-time Bayesian Network reliability modeling, and analysis framework. IEEE Transactions on Reliability 2006; 55(1): 86–97.
5. Boudali H, Dugan JB. A discrete-time Bayesian network reliability modeling and analysis framework. Reliability Engineering & System Safety. 2005; 87(3): 337–349.
6. Boudali H, Dugan JB. A new Bayesian Network approach to solve dynamic fault trees. Proceedings of Reliability and Maintainability Symposium, Alexandria, Virginia, 2005.
7. Ding FF, Tian ZG. Opportunistic maintenance for wind farms considering multi-level imperfect maintenance thresholds. Renewable Energy 2012; 45:175–182.
8. Fazio AR Di, Russo M. Wind farm modelling for reliability assessment. IET Renewable Power Generation 2008; 2 (4): 239–248.
9. Gao Q, Liu C, Xie B, Cai X. Evaluation of the mainstream wind turbine concepts considering their reliabilities. IET Renewable Power Generation 2012; 6(5): 348–357.
10. Guo HT, Watson S, Tavner P, Xiang JP. Reliability analysis for wind turbines with incomplete failure data collected from after the date of initial installation. Reliability Engineering & System Safety 2009; 94(6): 1057–1063.
11. Guo JY, Sun YQ, Wang MY, Ding XB. System reliability synthesis of wind turbine based on computer simulation. Journal of Mechanical Engineering 2012; 48 (2): 2–8. (In Chinese)
12. Joshi DR, Jangamshetti SH. A novel method to estimate the O&M costs for the financial planning of the wind power projects based on wind speed – A case study. IEEE Transactions on Energy Conversion 2010; 25(2):1–7.
13. Kusiak A, Verma A. Analyzing bearing faults in wind turbines: A data-mining approach. Renewable Energy 2012; 48: 110–116.
14. Li X, Hubacek K, Siu YL. Wind power in China – Dream or reality? Energy 2012; 37 (1): 51–60.
15. Li YF, Huang HZ, Xiao NC, Li HQ. A new fault tree analysis method: fuzzy dynamic fault tree analysis. Eksploatacja i Niezawodnosc – Maintenance and Reliability 2012; 14(3): 208–214.
16. Manco T, Testa A. A Markovian approach to model power availability of a wind turbine. In Power Tech, Lausanne, 2007, 1256–1261.
17. Marquez D, Neil M, Fenton N. Solving Dynamic Fault Trees using a New Hybrid Bayesian Network Inference Algorithm. In 16th Mediterranean Conference on Control and Automation Congress Centre, Ajaccio, France, 2008, 604–609.
18. Nadkarni S, Shenoy PP. A Bayesian network approach to making inferences in causal maps. European Journal of Operational Research 2001; 128 (3): 479–498.
19. Nechval KN, Nechval NA, Berzins G, Purgailis M. Planning inspections in service of fatigue-sensitive aircraft structure components for initial crack detection. Eksploatacja i Niezawodnosc- Maintenance and Reliability 2007; 3(35): 76–80.
20. Negra NB, Holmstrom O, Bak-Jensen B, Sorensen P. Aspects of relevance in offshore wind farm reliability assessment. IEEE Transactions on Energy Conversion 2007; 22 (1): 159–166.
21. Neil M, Tailor M, Marquez D. Inference in hybrid Bayesian networks using dynamic discretization. Statistics and Computing 2007; 17(3): 219–233.
22. Røed W, Mosleh A, Vinnemc JE, Aven T. On the use of the hybrid causal logic method in offshore risk analysis. Reliability Engineering & System Safety 2009; 94 (2): 445–455.
23. Sørensen J D. Framework for risk-based planning of operation and maintenance for offshore wind turbines. Wind Energy 2009; 12(5): 493–506.
24. Spinato F, Tavner PJ, Van Bussel GJW, Koutoulakos E. Reliability of wind turbine subassemblies. IET Renewable Power Generation. 2008; 3(4): 387–401.
25. Su C, Jin Q, Fu YQ. Correlation analysis for wind speed and failure rate of wind turbines using time series approach. Journal of Renewable and Sustainable Energy 2012; 4 (3): 1–13.
26. Tavner PJ, Edwards C, Brinkman A, Spinato F. Influence of Wind Speed on Wind Turbine Reliability. Wind Engineering 2006; 30(1): 55–72.
27. Tavner PJ, Xiang J, Spinato F. Reliability Analysis for Wind Turbines. Wind Energy 2007; 10(1): 1–18.
28. Weber P, Medina-Oliva G, Simon C, Iung B. Overview on Bayesian networks applications for dependability, risk analysis and maintenance areas. Engineering Applications of Artificial Intelligence 2012; 25(4): 671–682.
29. Weisser D. A wind energy analysis of Grenada: an estimation using the 'Weibull' density function. Renewable energy 2003; 28(11): 1803–1812.
30. Xiea KG, Billinton R. Considering wind speed correlation of WECS in reliability evaluation using the time-shifting technique. Electric Power Systems Research 2009; 79 (4): 687–693.

Chun SU
Ye-qun FU
Department of Industrial Engineering
School of Mechanical Engineering, Southeast University,
Jiangning District, Nanjing 211189, Jiangsu Province, China
E-mails: suchun@seu.edu.cn, purple1004@126.com

Article citation info:
OSTAPKOWICZ P. Leakage detection from liquid transmission pipelines using improved pressure wave technique. Eksploatacja i Niezawodnosc – Maintenance and Reliability 2014; 16 (1): 9–16.

Paweł OSTAPKOWICZ

LEAKAGE DETECTION FROM LIQUID TRANSMISSION PIPELINES USING IMPROVED PRESSURE WAVE TECHNIQUE

DIAGNOZOWANIE NIESZCZELNOŚCI W RUROCIĄGACH PRZESYŁOWYCH CIECZY Z WYKORZYSTANIEM ZMODYFIKOWANEJ METODY OPARTEJ NA DETEKCJI FAL CIŚNIENIA*

This paper deals with leak detection in liquid transmission pipelines. It focuses on improving the efficiency of a method based on negative pressure wave detection. A new algorithm for pressure wave monitoring has been proposed. The algorithm is aimed to precisely capture the corresponding characteristic points in the signal sequence of negative pressure waves caused by leakage. It uses median filtering of the calculating deviations of pressure signals measured along the pipeline. Adaptive alarm thresholds with reduced margins, based on statistical analysis of the calculating deviations of pressure signals, were used. Additionally, the algorithm is supported by a set of functions base on the calculation of the cross-correlation of the deviations which represent pressure signals from neighboring transducers. The developed technique has been tested on a physical model of pipeline. The pipeline is 380 meters long and 34 mm in internal diameter, and is made of polyethylene (PEHD) pipes. The medium pumped through the pipeline was water. Tests proved, that the proposed solution is sensitive to small leaks and resistant for false alarm (occurring disturbances). It is also capable of localizing the leak point with satisfactory accuracy, without significant delay.

Keywords*: pipelines, leak detection and location, pressure wave detection.*

Artykuł dotyczy zagadnień diagnozowania wycieków z rurociągów przesyłowych cieczy. Skupia się na polepszaniu skuteczności metody opartej na detekcji fal ciśnienia. Zaproponowano nowy algorytm do monitorowania fal ciśnienia. Algorytm jest ukierunkowany na precyzyjną identyfikację charakterystycznych punktów na przebiegach sygnałów ciśnienia reprezentujących fale wywołane przez zaistniały wyciek. Działanie algorytmu jest oparte o filtrację medianową residuów wyznaczanych dla sygnałów ciśnienia mierzonych wzdłuż rurociągu. Zastosowano adaptacyjne progi alarmowe, obliczane na podstawie analizy statystycznej. Dodatkowo, algorytm wspomagany jest przez wykorzystanie zbioru funkcji korelacji wzajemnej pomiędzy obliczanymi residuami reprezentującymi sygnały ciśnienia z sąsiednich przetworników pomiarowych. Zaproponowane rozwiązanie zostało przetestowane na fizycznym modelu rurociągu, którym tłoczono wodę. Rurociąg ma 380 m długości, średnicę wewnętrzną 34 mm i został wykonany z rur z polietylenu (PEHD). Wyniki badań udowodniły, że proponowane rozwiązanie jest wrażliwe na małe wycieki i odporne na fałszywe alarmy (występujące zakłócenia). Pozwala na zadawalająco dokładną lokalizację wycieku, bez znaczących opóźnień czasowych.

Słowa kluczowe*: rurociągi, wykrywanie i lokalizowanie wycieków, detekcja fal ciśnienia.*

1. Introduction

Even if properly designed, built and serviced a liquid transmission pipeline is exposed to the risk of leakage. In order to minimize the effects and risks caused by leakages, leak detection systems (LDS) are installed in pipelines. The purpose of such systems is to detect, locate, as well as determine the magnitude of leakage. Most popular leak detection systems are developed with the use of diagnostic methods which are based on measurements of internal flow parameters (flow rate, pressure and fluid temperature). In the literature such diagnostic methods are called *indirect (analytical, internal) methods* [1, 3, 9].

The implementation of leakage diagnosis process is a rather complex issue. Existing leak detection methods, whose review can be found in [3, 9], alone do not ensure the execution of all diagnostic tasks. Particular methods are useful only in reference to specified operation state of the pipeline and the characteristics of leakage. Therefore, the elaboration of an effective and reliable leak detection system requires the use of at least several internal methods working concurrently. Such methods are activated by suitable synchronization algorithms which are used to detect a steady or unsteady (transient) state of pipeline operation, as it is mentioned in [9].

In the case of liquid transmission pipelines operating under steady-state conditions, detection and location of leakages can be quite effective with the use of the method based on negative pressure wave detection. At present, thanks to many advantages, it is one of the most widely used methods. However, quite often it proves to be not enough effective. Therefore, a solution to improve the effectiveness of this method has been proposed.

An important element of research into new solutions of leak detection is their verification. The optimal solution would be to conduct such verification using an existing pipeline. In the case of the developed solution, a physical model of a pipeline was used, with water as the pumped medium. An extensive research program with simulated leaks was conducted on the pipeline. The following were taken into account: changes of the operating point of the pipeline, different location and size of simulated leaks, and the way of their increasing (sudden and slow). Carrying out such research program on a real pipeline would be connected with high costs and would suspend its normal exploitation.

The obtained results showed, that the developed solution (algorithm) gives the possibility to improve the effectiveness of the method based on negative pressure wave detection. In particular, it relates to the following elements: improving the level of detecting leakages and

(*) Tekst artykułu w polskiej wersji językowej dostępny w elektronicznym wydaniu kwartalnika na stronie ***www.ein.org.pl***

the accuracy of pressure wave front identification, and thus, the accuracy of leakage location.

The developed solution (algorithm) can be applied to existing pipelines, as one of the elements of LDS system, and will be co-responsible for the detection and location of leakages. Two types of transmission pipelines: liquid (including crude oil and its products) and gas are taken into account.

2. The method based on negative pressure wave detection

2.1. Description of leakage phenomenon

Assuming that a tight pipeline operates under stationary conditions, pressure and flow rate along the pipe have stabilized values, with low levels of fluctuations.

Example signals of pressure and flow rate in the pipeline without and with leakage are shown in Figure 1a and 1b. The signals are measured at the inlet and outlet, and in the case of pressure, additionally at several points along the pipeline. According to Figure 1a, the state without leakage is represented by period "A". Indexes "0" in the marking of individual pressure signals indicate their average values in this period. The end of this interval determines the beginning of leak.

Occurrence of leakage changes pressure in the pipeline. At the beginning, a sudden pressure drop takes place in the leak point. Afterwards the pressure drop propagates in both directions of the pipeline in the form of a negative wave. Such a front of wave can be recognized in the pressure signals as a characteristic impulse. In case of sudden leakages (whose flow rate reaches the nominal value in short time after the moment of their occurrence) negative pressure waves have clearly visible fronts. For slowly increasing leakages where pressure changes are milder, fronts of waves have a smoother shape. Behind the front of a wave, the longer is the distance from the leak point, the smaller is the pressure drop in the pipeline (Fig. 1a). The observed pressure drops depend on the size of leakage, its position, and flow conditions.

Some time after the occurrence of leakage flow conditions in the pipeline are stabilized. As it is shown in Figure 1a, such new steady-state conditions are represented by period "C". Average values for individual pressure signals in this period (marked with "1") are different from those before the leakage.

Apart from changes in the pressure, the occurrence of leakage results also in the changes of flow in the pipeline. Compared to the state before leakage, the flow rate in the section from the inlet to the leak point is increasing, and the flow rate in the section from the leak point to the outlet is decreasing (Fig. 1b).

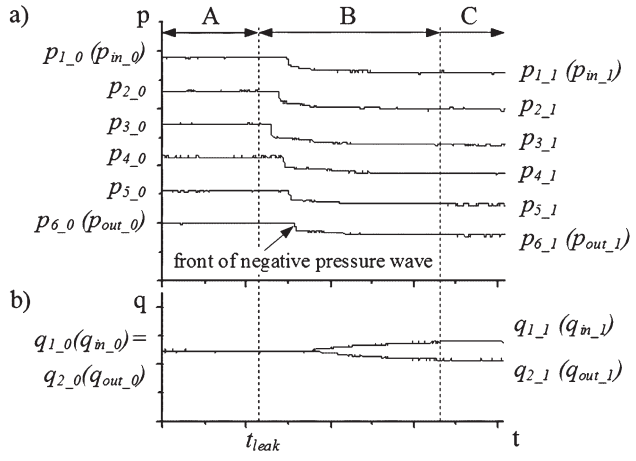

Fig. 1. Signals in the pipeline before and after the occurrence of leakage: a) pressure, b) flow rate; where: t_{leak} – the beginning of leakage

It should be noted that the relationship between changes in the pressure and flow take specific values for various pipelines. Also, one should remember that changes in the pressure and flow can be caused by many other phenomena, not directly related to leak.

2.2. General characteristics of the method

The monitoring of the above described phenomenon of pressure wave propagation is the essence of the method based on pressure wave detection. The method is aimed at detecting and locating leakages. In practice, it is concerned with a single leakage.

The method is based on measurements of pressure signals in pipelines. The analysis of such signals is carried out in order to detect the fronts of propagating pressure waves, considering the fact that such waves at first appear in measuring points located closest to the leakage point and then, with certain delay, in more distant points [8, 9].

The localization of leakage is realized by means of determined moments $t_{wav}(z_n)$. These are moments of detection of pressure wave fronts passing through individual measuring points z_n (see the graph in Figure 2). Knowing the order of the passes of pressure wave fronts through individual measuring points and the distance between the points, it is possible to find the leak point as the intersection of straight lines A-C and C-B, according to the relation (1). The relation is defined as a location formula.

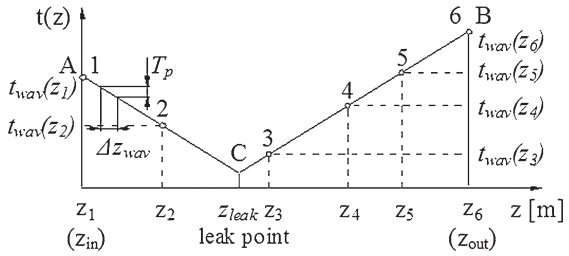

Fig. 2. Detection of pressure waves passing through individual measuring points in relation to time

$$z_{leak} = \frac{a_k}{a_p + a_k} \cdot l + \frac{t_{wav}(z_{in}) - t_{wav}(z_{out})}{a_p + a_k} \tag{1}$$

where: $a_p = 1/c_p$, $a_k = 1/c_k$ – slope coefficients of the straight lines A-C and C-B;

c_p, c_k – average velocities of pressure waves in the sections: $0 < z < z_{leak}$, $z_{leak} < z < l$;

l – length of the pipeline (distance between outermost pressure measurement points z_{in} and z_{out});

$t_{wav}(z_{in})$, $t_{wav}(z_{out})$ – determined moments of pressure wave fronts reaching the points of coordinates $z_{in} = 0$, $z_{out} = l$.

It should be added that in addition to the standard solution offered by the method, techniques of assessing the shape of the pressure wave are used. This way of diagnosis has the additional possibility of estimating the size of the leak. The estimation is based on the analysis of the observed wave amplitude when attenuation on a given section of the pipeline is known. These types of techniques, however, are not of interest to this study.

2.3. Requirements, advantages and disadvantages of the method

The method is relatively inexpensive and easy to use. It can even be applied with the use of only two pressure sensors placed at the inlet and outlet of the pipeline. In this variant, the velocities of pressure waves c_p and c_k, taken into account in the formula (1), respectively in the form of slope coefficients a_p and a_k, must be estimated basing on analytical relationships, i.e. according to (2), given in [4]. A better solution is to use more than two pressure sensors, located at regular intervals along the pipeline. This solution reduces the time of detection and improves the accuracy of location of the leak. In this case pressure waves velocities c_p and c_k, taken into account in the formula (1), are determined empirically, with much greater accuracy. Such assessment is made by measuring the delay of a wave passing between given pressure measurement points on a given section of the pipeline, when the distance between the points is known.

$$c = \frac{1}{\sqrt{\rho\left(\frac{1}{K} + \frac{d}{E \cdot e}\right)}} \tag{2}$$

where: c – velocity of pressure wave,
ρ – liquid density,
K – liquid's modulus of elasticity,
E – modulus of elasticity for pipe material (Young's modulus),
e – pipe wall thickness,
d – inside diameter of pipe.

An important requirement of the method concerning measuring instrumentation and the components of telemetry system is precise time synchronization when measuring pressure at various points along the pipeline. It is also required to use relatively short sampling period of the signals. The sampling period T_p determines the minimum error Δz_{wav} allowed when tracking the location of a pressure wave front (Fig. 2). Depending on the length of the pipeline, the sampling period should be tenths, hundredths or even thousandths of a second.

One should emphasize the speed with which the method works. With non inertial pressure transducers located every few kilometers, detection and location of leaks takes usually a few seconds. Referring to Figure 1, the detection and location of leakage usually does not go beyond the period "B". Such result would be difficult to achieve by means of other methods. For example, the gradient method, which is described in [7], requires the use of measured data related to the period "C", which significantly extends the time of diagnosis.

It must be remembered, however, that if a leak is not immediately detected (e.g. due to a temporary crash or shutdown of the LDS) there will be no other possibility of detection with this method.

Despite undoubted advantages of the method, its effectiveness is often not satisfactory. In practice, it is possible to detect only large leakages (about 1 % of the nominal flow rate – according to information in available studies or even about 3÷5 % – according to information provided by pipeline operators) and locate them not very accurately (ranging from several hundred meters even up to dozens of kilometres).

2.4. Problems to solve

The implementation of the method poses a basic problem with detection of pressure waves propagation as a result of the occurrence of leakage and the exact identification of the front of wave passing through the measuring pressure points z_n.

When detecting pressure waves one should be aware of false alarming and the possibility of miss alarming. The difficulty in identifying the front of negative pressure wave consist in a correct capturing of characteristic points on signal profiles, which mark the beginning of the observed pressure change impulse. These points represent the moments $t_{wav}(z_n)$. The accuracy with which the moments $t_{wav}(z_n)$ are captured, has a major impact on the precision of leak location, according to the formula (1). The level of difficulty in identification of a wave front is essentially determined by its shape and amplitude. These parameters, which characterize the profile of pressure wave propagation, are dependent on the location of the leak, its size and the way it is increasing (which, in turn, depends on the development of damage to the pipeline). The easiest to diagnose are those pressure waves whose fronts are clearly visible and which occur as a result of sudden leakages (whose flow reaches the nominal value in short time after they occur). In leakages increasing slowly, due to the milder character of pressure changes, wave fronts have a smoother shape, which makes their identification difficult and for leakages increasing very slowly the identification may not be possible at all. It is necessary that negative pressure waves on the analyzed signal profiles were characterized by a sufficiently large amplitude in relation to the level of pressure fluctuation, occurring disturbances and measuring noises and the range of sensor accuracy.

Various signal processing methods are used in order to identify the pressure wave front together with moments $t_{wav}(z_n)$. According to [2], the following can be mentioned: fast difference algorithm, Kalman filter, wavelet transform, correlation analysis, and others. An important feature of such methods should be the elimination of noise from the pressure wave signal while retaining its original characteristics. In practice, however, it appears that these techniques show satisfactory performance only for large leaks and with high level of disturbance and noise in the case of small leaks (even less than 2 % of the nominal flow rate), they prove to be rather ineffective [2].

A solution that would improve the effectiveness of the method based on negative pressure wave detection should involve:

- detecting possibly smallest leaks in possibly shortest time,
- locating leaks with high accuracy through more precise determination of moments $t_{wav}(z_n)$,
- extending the applicability of the method to slowly increasing leaks,
- obtaining high level of resistance for false alarms in states with no leakage.

It should be also noted that pressure wave propagation can be also accompanied by other flow phenomena whose impact may change the way it develops. These can include: flow disturbances, multiphase flow, incomplete filling of the pipe, lack of continuity of the stream. Negatively conditioned pressure wave propagation may indicate the presence of changes in the wave velocity, attenuation level and wave front distortion. Thus, when required, the standard solution of the method with the use of the equation (1), should be subjected to an appropriate adjustment.

Additionally it should be also remember that pressure waves caused by a leak may have a strong resemblance to pressure transients, which may be a consequence of technological operations, such as: opening and closing of valves, starting and stopping of pumps, or change of the operating point of the pipeline. It is therefore necessary to use algorithms that reliably differentiate the occurrence of a leak from the other operational cases, as noticed by [9]. These types of algorithms, however, are not of interest to this study.

3. Characteristics of the developed solution

The proposed solution takes into account the previously defined requirements for improving the effectiveness of the method based on negative pressure wave detection. It involves the use of pressure signals p_n from measuring transducers located at the inlet and outlet and a few extra points along the pipeline. The number of all pressure transducers is equal to j. The solution includes a procedure for detecting and locating the leakage. Its key element is an algorithm that is designed to detect the leakage by means of detecting the phenomenon of pressure wave propagation and to provide information about the development of the phenomenon, i.e. to determine moments $t_{wav}(z_n)$. Then, on the basis of the moments $t_{wav}(z_n)$, the leakage is localized according to the formula (1). The algorithm operates in a continuous cycle and generates diagnostic results each time it receives the signals p_n with a sampling period T_p. It is based on the analysis of variables Δp_n that correspond to measured pressure signals p_n. The variables Δp_n represent deviations (residua), calculated as [3, 8]:

$$\Delta p_n{}^k = p_n{}^k - \overline{p}_n{}^k , \tag{3}$$

where: $p_n{}^k$ – the value of the measured pressure signal in the moment k,

$\overline{p}_n{}^k$ – the reference value in the moment k.

The reference value $\overline{p}_n{}^k$ is calculated by applying filtering based on a recursive filter (4) and referred to as *a recursive averaging with fading memory (exponential smoothing)*.

$$\overline{p}_n{}^k = (\alpha \cdot \overline{p}_n{}^{k-1}) + ((1-\alpha)\cdot p_n{}^k) \tag{4}$$

where: $\overline{p}_n{}^{k-1}$ – the reference value in the moment $k-1$ resulting from the applied sampling period T_p,

$p_n{}^k$ – the value of the measured pressure signal in the moment k,

α – filter correction factor $0 < \alpha < 1$.

In the existing approach adopted by the author [8], a wave front was detected through the detection of variables Δp_n exceeding the assumed alarm thresholds Th_n marked as "nom" (Fig. 3a). Due to disturbances and measuring noises the alarm thresholds Th_n were set with quite large margins. On the one hand, it prevented the generation of false alarms in states without leakage. On the other hand, it resulted in delays in the detection of wave fronts, which were detected only in the moment $t_{wav}{}^I(z_n)$. The wrongly determined moments $t_{wav}{}^I(z_n)$ caused, in turn, errors in the location of leakage. With so large alarm threshold margins it was often impossible to detect small leaks, even the sudden ones, not to mention those slowly increasing.

The essence of the proposed solution is an improved way of determining the moments $t_{wav}{}^{II}(z_n)$ (Fig. 3b). For this purpose the algorithm shown in Figure 4 has been elaborated. The algorithm contains the following main elements:

a) median filtering of the variables Δp_n which results in the variables Δpf_n,
b) new way of setting alarm thresholds Thf_n which involves lowering the margins,

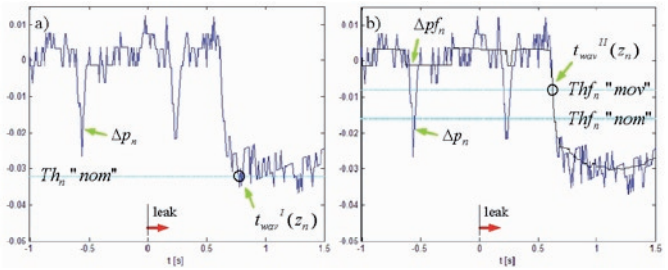

Fig. 3. Way of determining the moments $t_{wav}(z_n)$ corresponding to front of pressure wave: a) existing approach, b) proposed approach

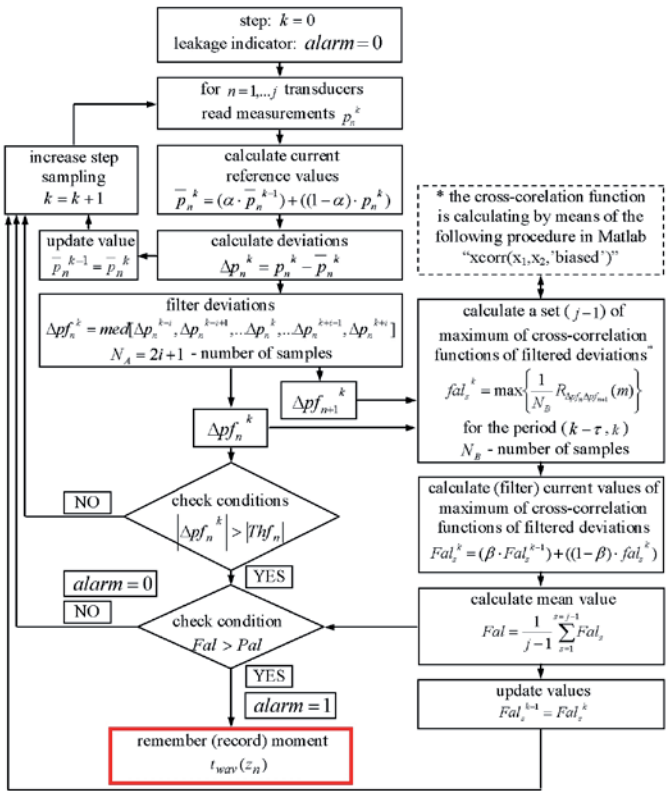

Fig. 4. Algorithm for leakage detection, with determination of moments $t_{wav}(z_n)$

c) the calculation of additional function Fal.

Regarding a) Median filtering is particularly useful when the analyzed signal is used for time synchronization. This type of problem occurs in the case of analysis aimed at detecting pressure wave fronts. Median filter is particularly well suited for the removal of impulse noise or disturbance that is characteristic of pressure measurements. At the same time the filter retains signal slope and properly follows its trend. The median filter is implemented using a movable window with the length of $N_A = 2i+1$ of the input signal samples. The longer is N_A, the longer the impulses which the median filter is able to „delete".

Regarding b) The applied adaptive alarm thresholds Thf_n are calculated on the basis of statistical analysis of variables Δpf_n. In Figure 3b, which shows changes of variable Δpf_n, one can observe a standard alarm threshold marked as "nom". Its value is determined so that it prevents an occurrence of an alarm without leakage. The alarm threshold with lowered margins was marked as "mov". Lowering the margins of alarm thresholds Thf_n helps to improve the accuracy of wave

front detection together with its moments $t_{wav}{}^{II}(z_n)$. In this way it is possible then to enhance the precision of the location of leakage.

Regarding c) The use of lower margins for alarm thresholds can cause false alarms in states without leakage. The possibility of such a situation is taken into account here as a normally occurring state. Therefore, to reliably recognize the states of leakage, the algorithm is further supported by the determination of additional function Fal. This function is the medium value of a set of functions $\{Fal_s\}_{s=1,\ldots,j-1}$ (where j denotes the number of all used pressure transducers) base on the calculation of the cross-correlation of the variables Δpf_n. Particular functions Fal_s in the set are calculated according to a sensitive algorithm presented in [5, 6]. The functions Fal_s are the result of filtration of the functions fal_s, based on a recursive filter, referred to *as recursive averaging with fading memory (exponential smoothing)*. The individual functions fal_s are the maximum values of the cross-correlation function corresponding to the correlation of the variable Δpf_n representing the given measuring point with the variable Δpf_{n+1} which represents the neighbouring measuring point along the pipeline. Cross-correlation functions are calculated with the time shift $k-\tau$. The shift value τ is determined using the velocity of the pressure wave propagation and taking into account the distance between the pressure measuring points that correspond to the variables Δpf_n and Δpf_{n+1}. If the function Fal exceeds its alarm threshold Pal, the occurrence of leakage is confirmed.

4. Verification of the developed solution

4.1. The test stand

The above presented solution has been put through experimental tests. They were conducted on a test stand with a physical model of a pipeline (Fig. 5). The medium pumped through the pipeline was water.

Fig. 5. The pipeline

The pipeline is 380 meters long and is made of polyethylene (PEHD) pipes which are 34 mm in internal diameter and 40 mm in external diameter. It consists of three sections each of which is over one hundred meter long. The sections: 0÷140 m, 140÷280 m and 280÷380 m, are joined with the use of special connectors which have the same diameter as the pipeline. The model pipeline is equipped with standard measuring devices: two electromagnetic flow meters (at the inlet and outlet), six pressure transducers and two thermometers. The pressure transducers are located at 1st, 75th, 141st, 281st, 335th, and 378th meter of the pipeline. They are connected to a PC equipped with a 12 bit A/D converter. In order to simulate leakages, manually operated valves with exchangeable orifices with holes of different diameters were used.

4.2. Test conditions

Before each simulation of leakages the pipeline operated under steady-state conditions. The test simulations included varied leakages: from very fast opening of the valves to slow. The results presented in this work were obtained for the following settings of the operating point of the pipeline: inlet pressure $p_{in\_0} \approx 5.7$ bar, outlet pressure $p_{out\_0} \approx 2.2$ bar, nominal flow rate $q_{in\_0} \approx 95$ l/min, temperature of pumped water ranging from $18°$ C to $22°$ C. Leaks sized 1–10 % of the nominal flow rate q_{in_0} were simulated at selected points, located between the first and the last three pressure sensors, about coordinates: 155, 195 and 235 m. Three experiments were performed for each leakage value. Measured signals were sampled with the frequency of $f_p = 100$ Hz. Such a choice of the frequency value resulted from the velocity of pressure wave propagation in the pipeline, taking also into account the wave front tracking error and the location of the measuring pressure points.

4.3. Results of tests with simulated leaks

An important element of this research was to compare the diagnosis of simulated leaks obtained by means of the existing algorithm, with the results obtained using the developed algorithm.

An appropriate choice of the alarm thresholds Th_n and Thf_n was a crucial element for proper operation of both compared algorithms. The choice was based on the statistical analysis of individual variables Δp_n and Δpf_n in states without leakage. The stabilized values of measured pressure signals with certain levels of fluctuations and noises resulting from the pumping (the flow) of water trough the pipe and the measurement of signals correspond to such steady states of the pipeline operation. Other additional disturbances were not simulated.

The performed analysis consisted of a series of experiments where, for each experiment in the same length of time window, the following statistical parameters were determined: "min" – the minimum value of the variable, "mean" – the average value of the variable and "std" – the standard deviation for the variable. Then the average value "μ" and the standard deviation "σ" of the distributions "mean" and "std" obtained for each experiment were determined. The results of this analysis are presented in the form of Table 1.

The analysis of the results led to the choice of the average values "μ" of the standard deviations "std" for the calculation of the alarm thresholds Th_n and Thf_n. The value of each threshold was determined by the following formulas:

$$Th_n = -b \times \mu(std)\{\Delta p_n\} \quad and \quad Thf_n = -b \times \mu(std)\{\Delta pf_n\} \qquad (5)$$

where: b – a coefficient determined experimentally.

When determining the value of individual alarm thresholds Thf_n it was assumed to use identical values of coefficients b (Table 2). Standard alarm threshold values Thf_n, denoted as "nom", were de-

Table 1. The statistical parameters of the variables Δp_n and Δpf_n

variables		Δp_1	Δp_2	Δp_3	Δp_4	Δp_5	Δp_6
–	min	–0.03682	–0.09311	–0.02935	–0.02645	–0.06246	–0.02769
μ	mean	–0.00004	–0.00004	–0.00002	–0.00003	–0.00003	–0.00003
	std	0.00522	0.00461	0.00427	0.00487	0.00520	0.00597
σ	mean	0.00042	0.00038	0.00035	0.00034	0.00034	0.00035
	std	0.00078	0.00067	0.00056	0.00070	0.00067	0.00066
variables		Δpf_1	Δpf_2	Δpf_3	Δpf_4	Δpf_5	Δpf_6
–	min	–0.01630	–0.01091	–0.01300	–0.01377	–0.01428	–0.01356
μ	mean	0.00044	0.00025	0.00023	0.00011	0.00012	0.00017
	std	0.00253	0.00273	0.00267	0.00317	0.00312	0.00330
σ	mean	0.00051	0.00045	0.00040	0.00040	0.00041	0.00044
	std	0.00037	0.00037	0.00035	0.00047	0.00043	0.00043

Table 2. The values of the alarm thresholds Th_n and Thf_n

alarm thresholds	Th_1	Th_2	Th_3	Th_4	Th_5	Th_6
b=20.5	–0.1069	–0.0946	–0.0875	–0.0999	–0.1067	–0.1224
b=6.5	–0.0339	–0.0300	–0.0277	–0.0317	–0.0338	–0.0388
b=5.0	–0.0261	–0.0231	–0.0213	–0.0244	–0.0260	–0.0298
alarm thresholds	Thf_1	Thf_2	Thf_3	Thf_4	Thf_5	Thf_6
"nom" b=6.5	–0.0165	–0.0177	–0.0174	–0.0206	–0.0203	–0.0214
"mov" b=5.0	–0.0127	–0.0137	–0.0134	–0.0159	–0.0156	–0.0165

termined in such a way that if they exceeded the observed minimum values of the variables Δpf_n they would not trigger the alarm in states without leakage. This situation was obtained for the value of coefficients $b = 6.5$. Then the alarm threshold values Thf_n with reduced margins, marked as "mov", were set with the assumed value of coefficients $b = 5.0$.

Certain problems occurred when determining the value of individual alarm thresholds Th_n. They resulted from large differences between the observed minimum values of individual variables Δp_n. Assuming absence of false alarms in states without leakage and the use of the same values of coefficients b would mean that the value of the coefficients should be as high as $b = 20.5$. This, in turn, could mean that many leaks would not be detected. Hence, in order to compare the accuracy of both algorithms in detecting pressure wave fronts, but ignoring the possibility of false alarms, when determining the alarm thresholds Th_n the same values of coefficients $b = 5.0$ were used as for the alarm thresholds Thf_n.

A similar statistical analysis was carried out in order to determine the alarm threshold Pal. Its value was equal to $Pal = 0.0000115$.

For both algorithms, the following parameter values were used: $\alpha = 0.995$, $\beta = 0.900$, $N_A = 35$, $N_B = 25$ and $\tau = 0.25$ sec. The values were determined experimentally.

When localizing simulated leakages, the velocities of pressure waves c_p and c_k (respectively in the form of slope coefficients a_p and a_k) taken into account in the formula (1) were determined on the basis of two subsets of data: the initial $^{(p)}\{z_n, t_{wav}(z_n)\}_{n=1,2,3}$ – for the first three sensors and the final $^{(k)}\{z_n, t_{wav}(z_n)\}_{n=4,5,6}$ – for the other three sensors, using the least-squares approximation method.

An influence of changes in the density of pumped medium on changes in the velocity of propagation of pressure waves, resulting from changes in temperature, was not taken into account. Such problem was ignored as the range of temperature changes of water pumped through the pipeline was small and did not cause significant changes in its density. For many liquids, such as crude oil and its products, small temperature changes can cause significant changes in density, and therefore in the velocity of pressure waves.

In addition, an algorithm which, basing on the determined order of the passes of pressure wave fronts through individual measuring points z_n (where: $n = 1,..., j \geq 2$ and outermost pressure measuring points z_1 and z_j are located at the inlet and outlet of pipeline, and therefore $z_1 = z_{in}$ and $z_j = z_{out}$) adjusts subsets of

Table 3. Times of detection "RT" and errors of localization "LE" of simulated leakages obtained by means of the existing algorithm "I" and using the developed algorithm "II"

leakages		sudden				slow(1)					slow(2)				
		I		II		valve	I		II		valve	I		II	
z_{leak}	q_{leak} [%]	RT [s]	LE [m]	RT [s]	LE [m]	[s]	RT [s]	LE [m]	RT [s]	LE [m]	[s]	RT [s]	LE [m]	RT [s]	LE [m]
155 [m]	1.0	1.52	47.5	1.94	67.8	3.5	–	–	2.13	26.9	6.3	–	–	2.47	57.7
	1.5	0.98	26.0	1.15	30.2	3.9	1.91	-13.3	2.03	-8.7	5.0	3.06	50.1	3.17	58.8
	2.0	1.09	11.1	1.18	-2.9	5.7	2.58	18.3	2.52	16.0	7.1	2.42	-18.8	2.61	-4.4
	2.5	0.75	0.2	0.91	2.1	3.8	1.51	6.1	1.66	14.9	7.8	2.35	23.7	2.38	10.4
	3.0	0.86	1.7	1.03	-1.1	4.0	1.70	-18.7	1.84	-14.8	7.0	2.42	38.9	2.37	-3.4
	3.5	0.85	-1.3	1.01	-0.2	3.8	1.39	11.9	1.49	16.8	8.7	2.28	31.4	2.42	23.6
	4.0	0.75	2.5	0.90	-3.5	5.6	2.23	2.8	2.35	2.8	8.8	3.04	-14.3	3.15	0.2
195 [m]	1.0	2.54	-27.2	1.04	14.5	3.9	–	–	2.45	41.2	10.0	–	–	3.15	-32.5
	1.5	0.79	4.5	0.94	3.4	4.8	1.64	-1.1	1.76	9.3	8.2	1.77	137.4	1.85	13.3
	2.0	0.76	-1.5	0.92	-3.9	5.1	1.82	-2.6	1.90	5.7	9.1	1.61	54.2	1.71	0.1
	2.5	0.72	-3.8	0.84	-7.0	5.2	1.72	10.1	1.77	-7.6	8.8	2.34	32.0	2.23	16.1
	3.0	0.72	-4.6	0.86	-3.3	5.1	2.21	-14.2	2.26	-14.4	8.2	1.99	-9.1	2.00	-5.6
	3.5	0.69	-0.3	0.84	-3.9	5.2	1.91	20.9	1.94	1.4	7.6	1.97	14.3	1.96	22.1
	4.0	0.65	-1.7	0.81	1.1	3.8	1.21	5.1	1.31	0.8	8.6	1.49	-7.9	1.61	14.7
235 [m]	1.0	2.71	-49.2	1.01	34.1	4.3	–	–	1.74	-7.9	8.3	–	–	1.74	-7.9
	1.5	0.88	-9.7	0.96	-3.2	5.0	2.10	-22.3	2.01	-5.2	8.8	2.53	48.2	2.45	-5.0
	2.0	0.70	33.4	0.94	-5.2	4.3	1.78	34.8	2.13	-22.3	7.6	1.44	-14.3	1.43	-3.6
	2.5	0.66	17.0	0.93	-2.7	5.0	2.04	-19.1	2.01	-17.6	8.6	1.92	4.2	1.98	-3.1
	3.0	0.68	0.4	0.96	-5.8	3.7	1.94	-9.9	2.01	-1.2	8.9	2.32	-11.9	2.27	9.0
	3.5	0.80	-6.0	0.95	-5.3	3.9	2.11	0.9	2.26	1.7	9.9	3.22	-14.0	3.54	9.1
	4.0	0.58	-5.1	0.91	0.9	4.5	1.70	-5.8	1.78	6.3	9.2	2.11	-10.5	2.17	-31.0

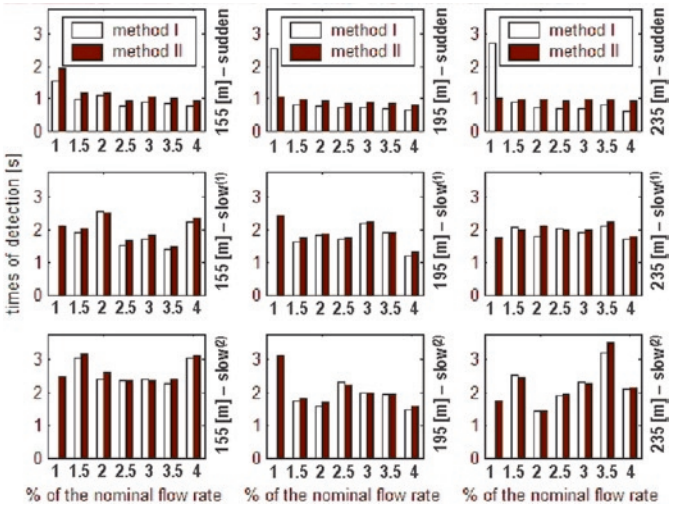

Fig. 6a. Times of detection of simulated leakages obtained by means of the existing algorithm "I" and using the developed algorithm "II"

data: $^{(p)}\{z_n, t_{wav}(z_n)\}_{n=1,\ldots,j-r}$ and $^{(k)}\{z_n, t_{wav}(z_n)\}_{n=j-r+1,\ldots,j}$ which are used for estimation of the velocities of the pressure waves c_p and c_k, taken into account in the formula (1). Otherwise, if a given subset contains only data from a single measuring point z_1 or z_j, it means that the leak place is located only behind a single pressure sensor from the beginning or the end of the pipeline. Then estimation of the pressure wave velocities c_p or c_k is performed analytically using the formula (2).

Table 3 shows the times of detection and the results of location of the simulated leakages, sudden and slow, obtained for the compared algorithms. The results are also shown in the form of diagrams in Figures 6a and 6b. Leakage detection time is defined here as the time from the occurrence of leakage to the moment when the last piece of information necessary to detect and locate the leakage is obtained. The leakage location results are given in the form of errors, i.e. the difference between the determined and the actual place of the leakage. For sudden leakages, which were simulated with the total time of opening the valves from 0.15 to 0.30 seconds, the results refer to average values obtained from three experiments. For slow leakages, the results refer to single experiments, with different total times of opening the valve labelled "slow$^{(1)}$ and "slow$^{(2)}$". The table, additionally, provides the total time of opening the valves for slow leakages, labelled "valve", which ranged from 3.50 to 10.00 seconds.

Additionally, Figure 7 shows profiles of example functions Fal obtained for leakages of 1.5 % of the nominal flow rate which were simulated in the three selected points along the pipeline.

Analyzing the results, one can observe a significant increase in the accuracy of locating sudden leakages when the developed solution is used. Leakage detection and location accuracy in slow leakages was improved, too.

In addition, it can be seen that the developed algorithm is characterized by similar times of leakage detection to the existing algorithm. This was achieved in spite of the application of the median filter which introduces some delay due to the time window containing N_A samples where the current estimate concerns the central sample.

Moreover, the profiles of the functions Fal signal certain possibility concerning further improvement of leakage detection.

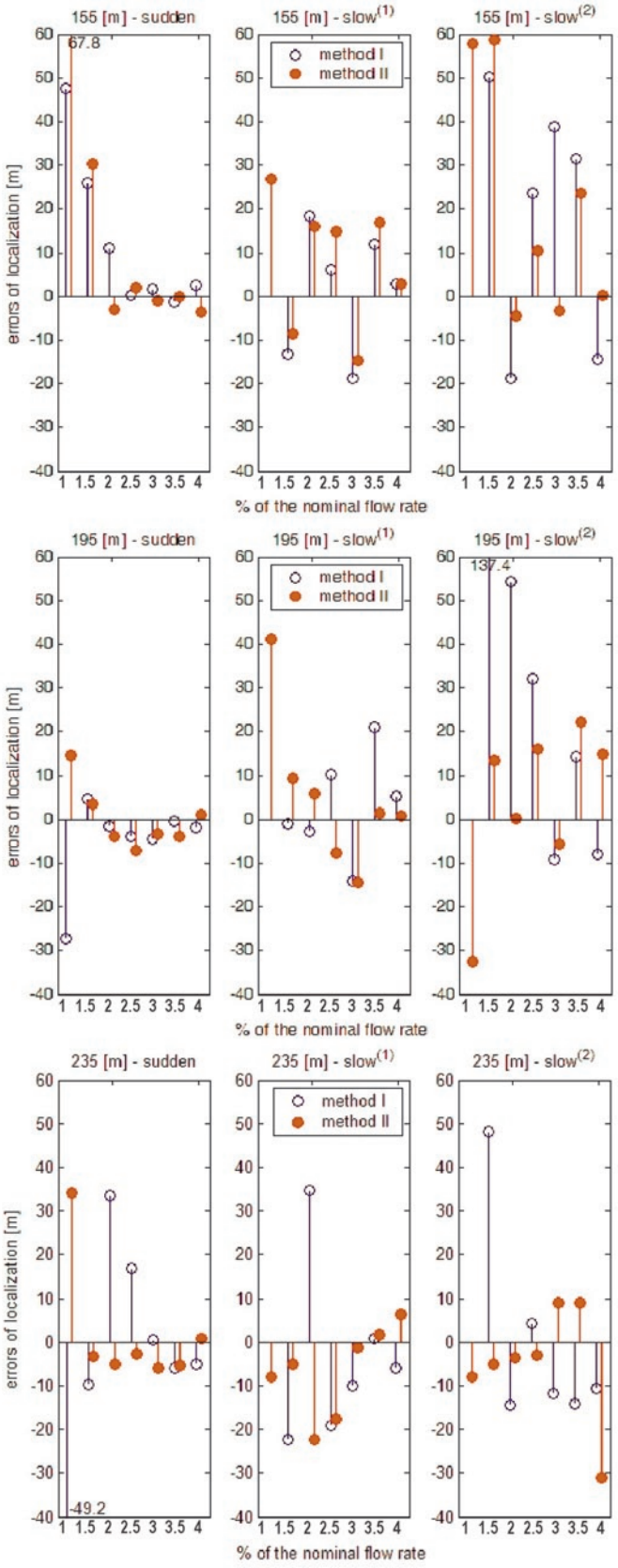

Fig. 6b. Errors of localization (b) of simulated leakages obtained by means of the existing algorithm "I" and using the developed algorithm "II"

5. Conclusion

The solution to improve the effectiveness of the method based on negative pressure wave detection has been developed. It is aimed to

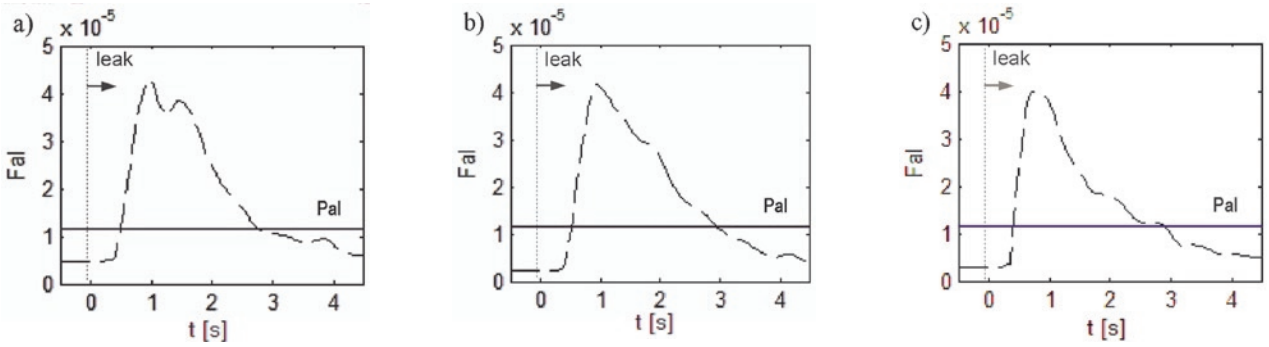

Fig. 7. Functions Fal obtained for sudden leakages of 1.5 % of the nominal flow rate simulated at the points of coordinates: a) 155 m b) 195 m c) 235 m

precisely capture the corresponding characteristic points in the signal sequence of negative pressure waves caused by leakage.

The proposed technique is sensitive to small leaks and resistant to false alarms (occurring disturbances). It is also capable of localizing the leakage point with satisfactory accuracy and without significant delay.

Acknowledgement: *The research work financed with the means of the Ministry of Science and Higher Education (Poland) in the years 2010-2013 as the research project Nr N N504 494439.*

References

1. Billman L, Isermann R. Leak detection methods for pipelines. Automatica 1987; 23: 381–385.
2. Han Li, De-yun Xiao, Xiang Zhao. Morphological filtering assisted field-pipeline small leakage detection. Proceedings of the 2009 IEEE International Conference on Systems, Man, and Cybernetics, San Antonio, TX, USA, October 2009.
3. Kowalczuk Z, Gunawickrama K. Detecting and locating leaks in transmission pipelines, in.: Korbicz KJ, Koscielny JM, Kowalczuk Z, Cholewa W (Eds.). Fault Diagnosis: Models, Artificial Intelligence, Applications. Berlin: Springer-Verlag, 2004; 822–864.
4. Mitosek M. Fluid mechanics in engineering and environmental protection. Warsaw: Publishing House of the Warsaw University of Technology, 2001.
5. Ostapkowicz P. Signals of weak interobject interactions in diagnosing of lekages from pipelines. Eksploatacja i Niezawodnosc – Maintenance and Reliability 2007; 33: 31–45.
6. Ostapkowicz P. Improving the efficiency of diagnosing of leaks from liquid transmission pipelines by using the new diagnostic information – the signals of weak interactions between objects. Solid State Phenomena 2009; 147-149: 492–497.
7. Ostapkowicz P. Leak location for liquid transmission pipelines using gradient-type method - case study. Pomiary Automatyka Kontrola – Measurement Automation and Monitoring 2011; 57: 1311–1316.
8. Sobczak R. The pipeline leakage location method by following the pressure wave front. Przemysl Chemiczny – Chemical Industry 2004; 83: 296–299.
9. Turkowski M, Bratek A, Slowikowski M. Methods and systems of leak detection in long range pipelines. Journal of Automation, Mobile Robotics & Intelligent Systems 2007; 1: 39–46.

Paweł OSTAPKOWICZ
Faculty of Mechanical Engineering
Bialystok University of Technology
ul. Wiejska 45C, 15-351 Białystok, Poland
E-mail: p.ostapkowicz@pb.edu.pl

Article citation info:
HALIMI D, HAFAIFA A, BOUALI E. Maintenance actions planning in industrial centrifugal compressor based on failure analysis. Eksploatacja i Niezawodnosc – Maintenance and Reliability 2014; 16 (1): 17–21.

Djamel HALIMI
Ahmed HAFAIFA
Elahmoune BOUALI

MAINTENANCE ACTIONS PLANNING IN INDUSTRIAL CENTRIFUGAL COMPRESSOR BASED ON FAILURE ANALYSIS

PLANOWANIE CZYNNOŚCI KONSERWACYJNYCH DLA PRZEMYSŁOWEJ SPRĘŻARKI ODŚRODKOWEJ W OPARCIU O ANALIZĘ USZKODZEŃ

The industrial maintenance implementation requires to the behaviour system analysis and their components. In this work, we optimize the maintenance actions to eliminate failures in the inspected industrial process. Our purpose in this work is to improve the components reliability in gas compression system, by the planning of the maintenance actions based on failure analysis using the intervention optimization in industrial centrifugal compressor plant. The finality of this proposed approach is proved by the improvement of the reliability performances and by the availability of this oil installation.

***Keywords**: Maintenance planning, reliability, availability, gas compression system, centrifugal compressor, optimization, failure analysis.*

Obsługa urządzeń przemysłowych wymaga analizy zachowań układów i ich części składowych. W niniejszej pracy zoptymalizowano czynności konserwacyjne tak, aby wyeliminować występowanie uszkodzeń w kontrolowanym procesie przemysłowym. Celem prezentowanej pracy było poprawienie niezawodności elementów układu sprężania gazu poprzez zaplanowanie czynności konserwacyjnych w oparciu o analizę uszkodzeń z wykorzystaniem optymalizacji interwencji w przemysłowej sprężarce odśrodkowej. O skuteczności proponowanego podejścia świadczy poprawa parametrów niezawodności oraz gotowość omawianej instalacji olejowej.

***Słowa kluczowe**: Planowanie obsługi, niezawodność, gotowość, układ sprężania gazu, sprężarka odśrodkowa, optymalizacja, analiza uszkodzeń.*

1. Introduction

Today the availability control in industrial systems, allow the industry to act on the production conformity, its costs of operations, competitiveness and commercial success. For correct exploitation, it is now not only offering a better plant supervision but also to achieve the optimum production with an implementation of fault diagnosis [5, 7, 9, 13, 16 and 21]. Indeed, the technological developments and the implementation of measurement tools of various parameters defining the material state; systematic preventive maintenance remains especially for components, whose failure can cause major problems in reliability terms, maintainability, availability and security [1, 3, 6 and 18]. In the oil and gas industry in the compression stations the turbo compressor provide the main function of the station, which requires these materials and especially during the period of large requests of gas, improved availability can be achieved by the organization of the maintenance actions schedule has made from the real data of site.

In this paper, we propose the use of the optimization techniques based on the number of intervention given by the failure rate, to improve the maintenance actions planning of a gas compression system. This gas pipeline installation, present in their operation a risk to passed in degraded mode and undergoes accidental defects.

In several applications, there are more than a few techniques that can be used for increase maintenance actions [14, 15, 19, 23, 24, 25 and 28]. By the basis of this work, we can confirm that the conditional maintenance optimizes the maintenance and especially to perform at the right time with the right cost. That after the proposed linearization of the failure rates with an objective function, we evaluates the cost summary of maintenance according to the numbers of interventions of the different components responsible for the unavailability of our compression system.

2. Maintenance cost based on failure rate analysis

Today, the race for profitability no longer possible to ignore the search for more efficient operation of its equipment [2, 4]. This is why we must constantly seek the best ways to combine technologies and applications to perfect the tools to make good decisions consistently in terms of maintenance and operations rate optimization with equipment availability [11, 27]. Conditional maintenance optimizes maintenance and especially to perform at the right time at the right cost. Indeed, the costs of a policy of routine maintenance are incompatible with the requirements of industrial business productivity today. In addition, the downsizing of many services, limited capacity to respond to incident, hence the need to anticipate failures using conditional preventive methods [8, 26].

To estimate the maintenance cost based on the estimated number of intervention in $[0,T]$, we use the equation (1), taking the random variable h as the number of failures in the time interval $[0,T]$, the model is as follows [12, 17]:

$$P(T,h)=\frac{a^h}{h!}e^{-\alpha} \tag{1}$$

where $P(T,h)$ is the probability of failure in the interval $[0,T]$ and α is the expected value of the number of failures in the interval $[0,T]$:

$$a=\int_0^T \lambda(t)dt \tag{2}$$

If there is a material composed mainly of sub assemblies whose failure rate rose linearly, we can write:

$$\lambda_i(t)=\lambda_i+k_i t \tag{3}$$

And the failure rate overall, considering the components in series in terms of reliability, can be written as follows:

$$\lambda(t)=\lambda_0+\sum_1^m k_i t \tag{4}$$

With $\lambda_0=\sum_1^m \lambda_i$

Performing a repair at subsets i decreases its failure rate to its initial value $\lambda_i(t)$ during the time λ_i for the scheduled period T .

Using equation (2), the expected number of failures in the interval $[0,T]$ is written as follows:

$$\alpha=\lambda_0 T+\sum_1^m \frac{k_i T^2}{2} \tag{5}$$

We consider the structure and the periodicity of interventions planned maintenance system on a time interval $[0,T]$. Planned periods are designated by $\Delta_1,\Delta_2,\Delta_3,...,et\,\Delta_m$ for a material whose m components require routine maintenance previously scheduled, so we can write:

$$\begin{aligned} &t=t_1+i\Delta_1\\ &t_3=t_1+i\Delta_1+j\Delta_2\\ &.....\\ &t_m=t_1+i\Delta_1+j\Delta+...+p\Delta_m \end{aligned} \tag{6}$$

Where $i,j,..,p$ is the number of planned interventions applied consecutively subsets 1.2 and $m-1$ during the time t_m . In this way the expression of the failure rate can be presented by $\lambda(t_1,t_2,t_3,...,t_m)=\lambda(t_1,i,j,...,p)$. Denote $n_1,n_2,n_3,...,et\,n_m$ the amount of time periods whose durations are respectively $\Delta_1,\Delta_2,\Delta_3,...,et\,\Delta_m$ staggered period $[0,T]$ such as:

$$\begin{aligned} n_1&=\frac{\Delta_2}{\Delta_1}\\ n_2&=\frac{\Delta_3}{\Delta_2}\\ n_3&=\frac{\Delta_4}{\Delta_3}\\ n_m&=\frac{T}{\Delta_{m-1}} \end{aligned} \tag{7}$$

It is not difficult to find the connections between the amount of time periods of duration $\Delta_1,\Delta_2,\Delta_3,...,et\,\Delta_m$ and the amount realized on the $[0,T]$ period of planned repairs respectively [10]:

$$\begin{aligned} n_{p1}&=(n_1-1)\prod_2^m n_i\\ n_{p2}&=(n_2-1)\prod_3^m n_i\\ n_{p3}&=(n_3-1)\prod_4^m n_i\\ n_{pm}&=(n_m-1) \end{aligned} \tag{8}$$

The expected number of failures in the time interval $[0,T]$ for the case of linear variation of failure rates over time and after the division of the time axis into intervals equal to Δ_1, and their summation is calculated as follows:

$$a(t_1,n_1,n_2,n_3,...,n_m)=n_m\sum_{p=0}^{n_m-1}...\sum_{j=0}^{n_2-1}\sum_{i=0}^{n_1-1}\int_0^{\Delta_1}\left[\begin{array}{l}\lambda_0+k_1t_1+k_2(i\Delta_1+t_1)+k_3(i\Delta_1+j\Delta_2+t_2)+\\ ...+k_m(i\Delta_1+j\Delta_2+...+p\Delta_{m-1}+t_1)\end{array}\right] \tag{9}$$

The timing of the implementation of prophylactic repair is falling failure rates corresponding to their initial values λ_i but these jumps do not lower the failure rate to the value λ_0 only when the realization of the general revision.

The failure rate $\lambda(t_1,i,j,...,p)$ is equal to the expected number of failures [20, 22]. We can deduce that in the limiting case when performing an unlimited number of repair: the expected number of approaches to failure $\lambda_0 T$. After the integration of the equation (8), with some transformations we have:

$$a(t_1,n_1,n_2,n_3,...,n_m)=\lambda_0 T+\frac{k_1T^2}{2n_1n_2n_3..n_m}+\frac{k_2T^2}{2n_1n_2n_3..n_m}+\frac{k_3T^2}{2n_3..m}+...+\frac{k_mT^2}{2n_m} \tag{10}$$

Posing

$n_{p1}=0,\ n_{p2}=0,n_{p3}=0....et\,n_{pm}=1$, determining the value of the expected number of failures for the case

$$\begin{aligned} S=&(C_A\lambda_0T+C_{A1}\frac{k_1T^2}{2n_1n_2n_3..n_m}+C_{A2}\frac{k_2T^2}{2n_2n_3..n_m}+C_{A3}\frac{k_3T^2}{2n_3..n_m}+...+C_{Am}\frac{k_mT^2}{2n_m})+\\ &C_1(n_1-1)n_2n_3..n_m+C_2(n_2-1)n_3..n_m+C_3(n_3-1)n_4..n_m+C_m(n_m-1) \end{aligned} \tag{11}$$

The mathematical model based n_i is given by:

$$\min S = C_A \lambda_0 T + \sum_{i=1}^{m} \left[C_{Ai} \frac{k_i T^2}{\prod_{j=i}^{m} n_j} + C_i (n_i - 1) \prod_{j=i+1}^{m} n_j \right] \qquad (12)$$

3. Industrial application

In oil industry, the turbochargers must ensure to increased availability and especially during the large gas demand to meet commitments and contracts accorded with customers. On the maintenance plan and according to the manufacturer these machines require three types of revisions at 8000 h, 16000 h and at 32000 h often scheduled outside the period of wide application in the summer. With the application of schedule revisions, it was found that these machines break down – even during the often-wide demand because some components do not change automatically when revisions and cause excessive maintenance costs high not seen the failure prediction or forecasting the supply of replacement equipments. To minimize the exploitation risk, we address that is to strengthen the planning revisions by a systematic maintenance program based on maintenance cost components that greatly influence the availability of turbochargers. The practice has shown that 70% of the turbochargers defects are due: following

- M1 sheathing β1=1,88
- M2 Tightness ring β2=2,14
- M3 carring bearing β3=3,55
- M4 labyrinth support β4=2,09

To remedy this situation, we propose a maintenance strategy specific to this case and we determine the appropriate maintenance intervals. The figure 1, clearly show the trend on failure rates of components considered in our examined turbochargers.

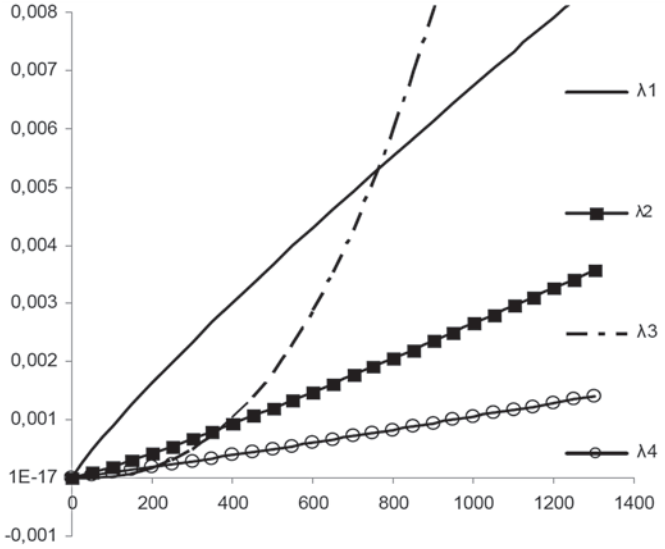

Fig. 1. Failures rates variation of the considered components

For the component 1, it is clear that it ages quickly compared to subset 2 and 4, and that these three elements have shape parameters β between (1.5 and 2.5), which corresponds to a mode of fatigue failure, which justifies their progressions almost linear. Regarding the component 4, at first he ages very slowly, and beyond (200 days), he begins to age more rapidly than the other component which justifies its failure mode is that the wear. It is clear that the failure rates of components 1, 2 and 4 (shown in figures 2, 3 and 4), we have a great linearity and especially during their active lifetimes.

It is clear that the failure rate of the three elements has a little change lointe linear regression, but errors during the active life and compensate (R2 = 0.887), we can say that the linearity can ensure prac-

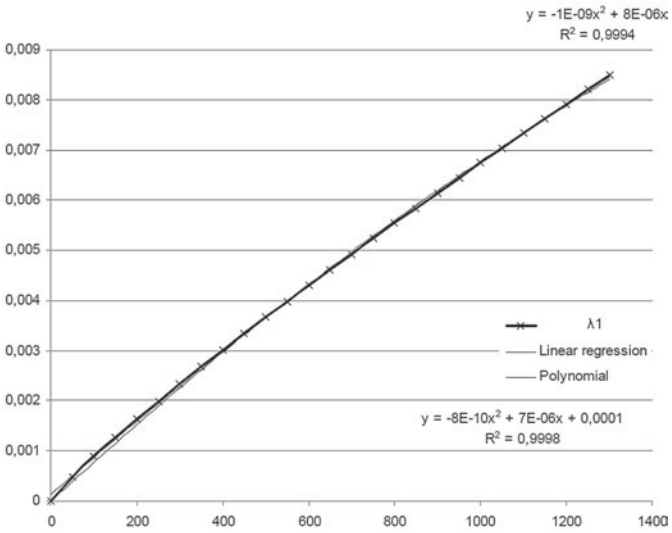

Fig. 2. Failure rate of component 01

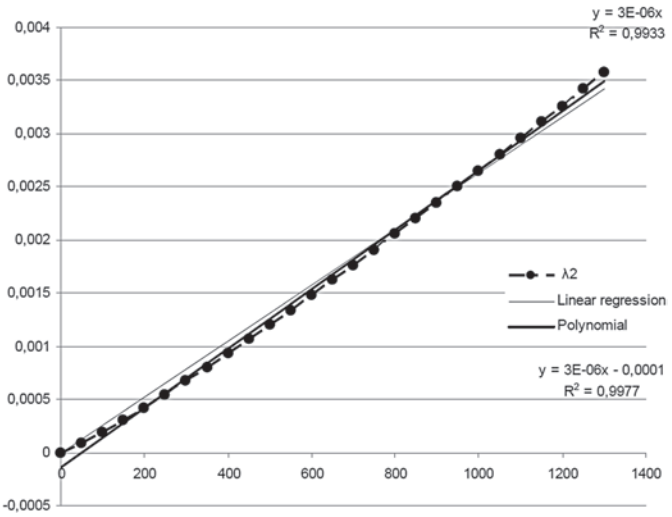

Fig. 3. Failure rate of component 02

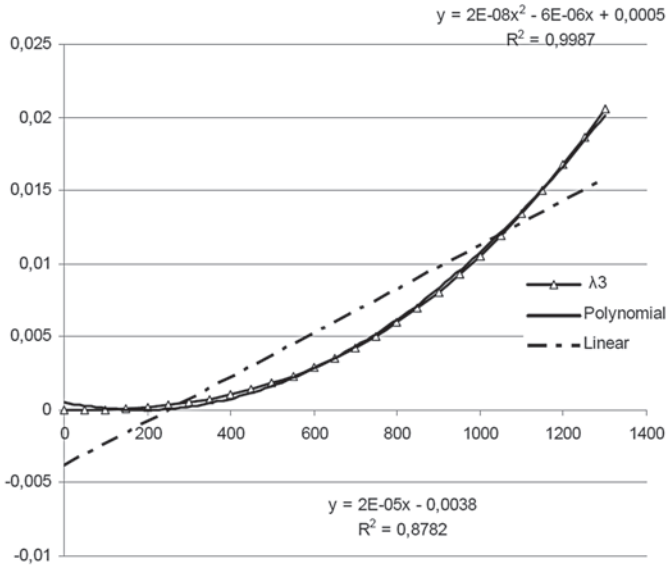

Fig. 4. Failure rate of component 03

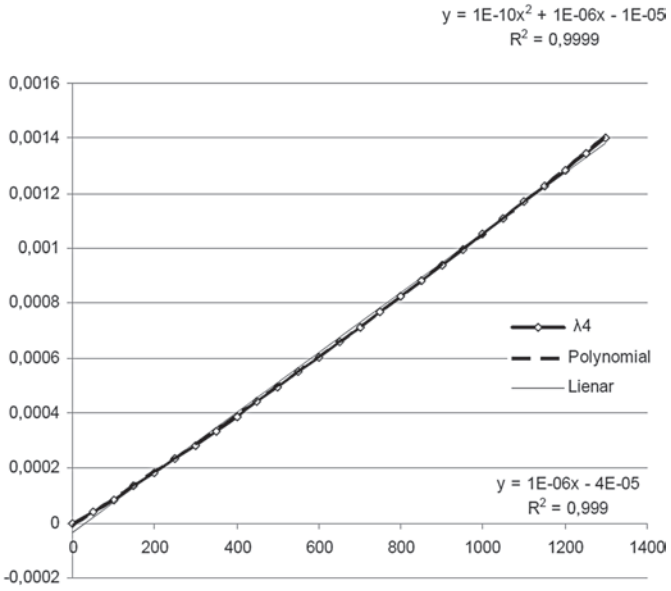

Fig. 5. Failure rate of component 04

tical results satisfactory. We can conclude that the maintenance operations and intervention of the examined turbochargers will be carried according to the flowing action plans, shown in figures 6, 7 and 8:

According to the data sheet 1:

- N4= 1,11 T4= 900 Days
- N3= 1,5 T3= 600 Days
- N2= 1,33 T2= 450 Days
- N1= 1,5 T1= 300 j

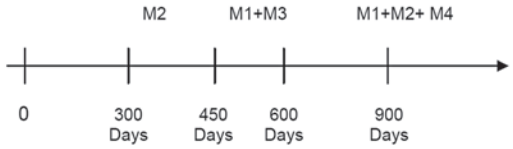

Fig. 6. Maintenance operations action plans according to the data sheet 1

According to the data sheet 2:

- N4= 1,25 T4= 800 Days
- N3= 1,6 T3= 500 Days
- N2= 1,25 T2= 400 Days
- N1= 1,6 T1= 250 Days

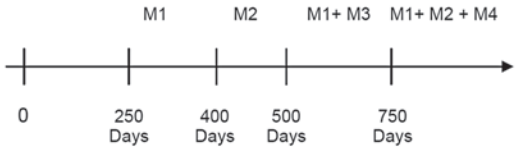

Fig. 7. Maintenance operations action plans according to the data sheet 2

According to the data sheet 3:

- N4= 1 T4= 1000 Days
- N3= 1,33 T3= 750 Days
- N2= 2,3 T2= 325 Days
- N1= 1,3 T1= 250 Days

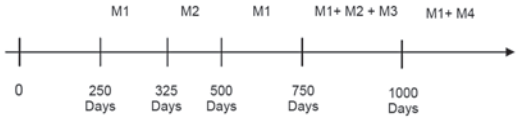

Fig. 8. Maintenance operations action plans according to the data sheet 3

Based on the feedback data, we estimate the laws of aging components of our system examined. Given the results obtained were classified according to their components considered failure modes identified based on estimated values of shape coefficient β:

- Components 1,2 and 4 form the first group for which the mode of failure is the most dominant fatigue according to the estimated values of the parameter β and which are (1.88, 2.14; 2.09) respectively.
- Component 3 is part of the second group, the failure mode is the most dominant wear (β = 3.55).

This has helped to develop approaches to maintenance optimization for each group separately and determine the optimal intervals to include additional repair the structure of the repair cycle recommended by the manufacturer.

4. Conclusion

The maintenance control in industrial plants is based on the knowledge of their behavior, therefore the right choice of the corrective action periodicity of maintenance. Between the good and the malfunction time of the system exploitation, there is a state in which can work as he can at any moment cause unscheduled action whose cost is often too high. In this work, we have determined the optimal timing of repair, to optimize the maintenance actions to eliminate failures in the inspected industrial centrifugal compressor. The finality of this proposed approach is proved by the improvement of the reliability performances and by the availability of this oil installation.

After solving the equation of cost summary based on the linearity of the failure rates of the components of a centrifugal compressor, we have conclude that, the results are very satisfactory with the implementation schedule of routine maintenance, as well as the supply of spare parts. In this paper and after a preset study reliability-one was interested in the most penalizing components in order to control the reliability of the turbo compressor from a few components. Illustrated work shows that the components whose failure mode is wear and from a certain period of normal operation; aging increases its acceleration resulting in a drop in physico mechanical materials and that these components is the result of wear. For parts against deteriorating fatigue have a constant acceleration in their aging which results in a failure rate of linearity.

After the linearization of the failure rates with the proposed objective function, we have evaluates the cost summary of maintenance, according to the optimal timing of repair, in our examined compression system. We result that developed approach of maintenance actions planning makes it possible to increase the working time of the examined compression system. The developed approach of maintenance actions planning allowing better performances in reliability of the examined gas compression system, at the moment of its exploitation for its maintenance.

References

1. Aghezzaf EH, Jamali MA, Ait-Kadi D. An integrated production and preventive maintenance planning model. European Journal of Operational Research 2007; 18(1, 2): 679–685.
2. Anthony Kelly, Maintenance and the industrial organization. Plant Maintenance Management Set 2006 ; 3(1) : 3–8.

3. Carnero MC. Selection of diagnostic techniques and instrumentation in a predictive maintenance program. A case study. Decision Support Systems 2005; 38(4): 539–555.
4. Devarun Ghosh, Sandip Roy, Maintenance optimization using probabilistic cost-benefit analysis. Journal of Loss Prevention in the Process Industries 2009; 22(4): 403–407.
5. Djamel Halimi, Ahmed Hafaifa, Elahmoune Bouali and Mouloud Guemana, Vibrations detection and isolation in centrifugal pump used in petroleum industry using spectral analysis approach. Archive of Sciences Journal 2012; 65(11): 234–245.
6. Eisinger S, Rakowsky UK. Modeling of uncertainties in reliability centered maintenance — a probabilistic approach. Reliability Engineering & System Safety 2001; 71(2): 159–164.
7. Elhaj M, Gu F, Bal AD l, Albarbar A, Al-Qattan M, Naid A. Numerical simulation and experimental study of a two-stage reciprocating compressor for condition monitoring. Mechanical Systems and Signal Processing 2008; 22(2): 374–389.
8. Enrique Castillo, Roberto Mínguez, Carmen Castillo, Sensitivity analysis in optimization and reliability problems. Reliability Engineering & System Safety 2008; 93(12): 1788–1800.
9. Farrahi GH, Tirehdast M, Masoumi Khalil Abad E, Parsa S, M. Motakefpoor. Failure analysis of a gas turbine compressor. Engineering Failure Analysis 2011; 18(1): 474–484.
10. Fazzini PG, Márquez AA, Otegui JL, Barcia P. Cause and effect assessment after a complex failure of a large ethylene compressor. Engineering Failure Analysis 2006; 13(8): 1358–1369.
11. Garcia E, Guyenne H t, Lapayre JC, Zerhouni N. A new industrial cooperative tele-maintenance platform. Computers & Industrial Engineering 2004; 46(4): 851–864.
12. Goel HD, Grievink J, Weijnen MPC. Integrated optimal reliable design, production, and maintenance planning for multipurpose process plants. Computers & Chemical Engineering 2003; 27(11): 1543–1555.
13. Heyen G, Murphy K, Marchio D, Kalata P, Kalitventzeff B. Dynamic simulation and control of gas turbines and compressor systems. Computers & Chemical Engineering 1993; 17(1): 299–304.
14. Jiandong Zhang, Gang Rong, Weifeng Hou, Chenbo Huang, Simulation based approach for optimal scheduling of fuel gas system in refinery. Chemical Engineering Research and Design 2010; 88(1): 87–99.
15. Lebele-Alawa BT, Hart HI, Ogaji SOT, Probert SD. Rotor-blades' profile influence on a gas-turbine's compressor effectiveness. Applied Energy 2008; 85(6): 494–505.
16. Lei You, Jun Hu, Fang Fang and Lintao Duan, Fault Diagnosis System of Rotating Machinery Vibration Signal. Procedia Engineering 2011; 15(1): 671–675.
17. Li YG, Nilkitsaranont P. Gas turbine performance prognostic for condition-based maintenance. Applied Energy 2009; 86(10): 2152–2161.
18. Moore WJ, Starr AG. An intelligent maintenance system for continuous cost-based prioritisation of maintenance activities. Computers in Industry 2006; 57(6): 595–606.
19. Mouloud Guemana, Slimane Aissani and Ahmed Hafaifa, Use a new calibration method for gas pipelines: An advanced method improves calibrating orifice flowmeters while reducing maintenance costs. Hydrocarbon Processing Journal 2011; 90(8): 63–68.
20. Panida Jirutitijaroen, Chanan Singh, The effect of transformer maintenance parameters on reliability and cost: a probabilistic model. Electric Power Systems Research 2004; 72(3): 213–224.
21. Otegui JL, Fazzini PG, Marquez AA, Barcia PL. Failure analysis of packing plate in a hyper compressor at a petrochemical plant. Engineering Failure Analysis 2008; 15(5): 531–542.
22. Radouane Laggoune, Alaa Chateauneuf, Djamil Aissani, Impact of few failure data on the opportunistic replacement policy for multi-component systems. Reliability Engineering & System Safety 2010; 95(2): 108–119.
23. Radouane Laggoune, Alaa Chateauneuf, Djamil Aissani, Opportunistic policy for optimal preventive maintenance of a multi-component system in continuous operating units. Computers & Chemical Engineering 2009; 33(9): 1499–1510.
24. Vassiliadis CG, Arvela J, Pistikopoulos EN, Papageorgiou LG. Planning and maintenance optimization for multipurpose plants. Computer Aided Chemical Engineering 2000; 8(1): 1105–1110.
25. Wang Hongzhou and Pham Hoang, Reliability and optimal maintenance: Series: Springer Series in Reliability Engineering 2006; ISBN 978-1-84628-324-6.
26. Xuan Hai-jun, Song Jian, Failure analysis and optimization design of a centrifuge rotor. Engineering Failure Analysis 2007; 14(1): 101–109.
27. Yuan Mao Huang, Sheng-An Yang, A measurement method for air pressures in compressor vane segments. Measurement 2008; 41(8): 835–841.
28. Zouakia Rochdi, Bouami Driss, Tkiouat Mohamed, Industrial systems maintenance modelling using Petri nets. Reliability Engineering & System Safety 1999; 65(2): 119–124.

Djamel HALIMI
Elahmoune BOUALI
Laboratory Reliability of Hydrocarbons Equipment and Materials (LFEPM)
University of Boumerdes
35000, Algeria
Emails: halimi_fhc@yahoo.fr, e_bouali@umbb.dz

Ahmed HAFAIFA
Applied Automation and Industrial Diagnostic Laboratory, Faculty of Science and Technology
University of Djelfa
17000 DZ, Algeria
E-mail: hafaifa@univ-djelfa.dz

Article citation info:
OSIPOWICZ T, ABRAMEK KF. Catalytic treatment in Diesel engine injectors. Eksploatacja i Niezawodnosc – Maintenance and Reliability 2014; 16 (1): 22–28.

Tomasz OSIPOWICZ
Karol Franciszek ABRAMEK

CATALYTIC TREATMENT IN DIESEL ENGINE INJECTORS

KATALITYCZNA OBRÓBKA PALIWA WE WTRYSKIWACZACH SILNIKA O ZAPŁONIE SAMOCZYNNYM*

The aim of the study proposed and carried out by the authors was to assess the impact of using platinum as a catalyst carrier in the fuel injector diesel engine with the direct fuel injection for emissions of toxic substances in the exhaust gases into the atmosphere and specific fuel consumption. Experimental studies were carried out on a test bench equipped with a 359 engine and a hydraulic brake with complete measurement apparatus. During the tests the engine worked by external speed characteristics. The analysis of the study showed that it is possible to reduce emissions of toxic compounds into the environment and to reduce specific fuel consumption through the use of catalytic coatings in the diesel engine fuel injector.

***Keywords**: combustion engine, toxin emission, fuel treatment, injectors, fuel injection modeling.*

Celem zaproponowanych i przeprowadzonych przez autorów badań była ocena wpływu zastosowania nośnika katalitycznego w postaci platyny we wtryskiwaczu paliwowym silnika z zapłonem samoczynnym z bezpośrednim wtryskiem paliwa na emisję substancji toksycznych w gazach wylotowych do atmosfery oraz jednostkowe zużycie paliwa. Badania eksperymentalne zostały przeprowadzone na stanowisku hamownianym wyposażonym w silnik 359 oraz hamulec hydrauliczny z kompletną aparaturą pomiarową. Podczas badań silnik pracował według zewnętrznej charakterystyki prędkościowej. Analiza przeprowadzonych badań wykazała, że istnieje możliwość ograniczenia emisji związków toksycznych do otoczenia oraz zmniejszenie jednostkowego zużycia paliwa poprzez zastosowanie powłoki katalitycznej we wtryskiwaczu paliwowym silnika ZS.

***Słowa kluczowe**: silnik spalinowy, emisja substancji toksycznych, obróbka paliwa, wtryskiwacze, modelowanie wtrysku paliwa.*

1. Introduction

Development of internal combustion engines in recent years has been directed at improving the environmental and economic operating parameters. Environmental parameters of the engine are related to the emission of toxic substances into the atmosphere in the exhaust gases, whereas economic ones are connected with fuel consumption. Requirements related to reducing emissions of toxic substances into the atmosphere and a reduction in fuel consumption become more stringent each year [1]. In order to fulfill them, electronics systems that control the course of fuel injection characteristics and devices for emission control in the form of catalytic converters in exhaust systems were used. Research on the use of catalysts in the engines combustion chambers has been also conducted. These solutions are used in engine parts, which are directly related to the combustion and the reduction of toxic compounds produced, that is in the injection apparatus, combustion chamber and exhaust systems [2, 5]. Engine working process is associated with the process of combustion of a mixture of fuel and air. This cycle consists of: preparing a mixture for combustion, combustion and emission control. The key step in this chain of events refers to the preparation of the mixture for combustion.

The combustion process of a mixture of fuel and air in the combustion chamber of the diesel engine consists of several stages. The analysis undertaken in this work concerns the first and also the most important phase, which is the ignition delay period. This is the time which includes the moment of appearance of the first drops of fuel in the combustion chamber until their self-ignition. It has a direct influence on the kinetic combustion, which is the second stage. The objective is to ensure that the ignition delay period was as short as possible. The longer it takes, the more fuel is accumulated in the cylinder, and it causes the combustion in the second period takes place rapidly, causing a high rate of pressure build [25].

The main physical parameters of the fuel in diesel engines are: density, viscosity and surface tension. They have a direct impact on the droplet diameter, the shape and the scope of jet fuel spray and they are related to the ignition delay period. Whereas, chemical parameters of the fuel depend on the structural composition of the hydrocarbons, where the most numerous group represent paraffin hydrocarbons C_nH_{2n+2}.

Chemical properties of the fuel can be changed by the paraffin dehydrogenation, that is some reactions may occur in the presence of catalyst, as a result of which the paraffins are converted into hydrocarbons of the C_nH_{2n} olefin group with the hydrogen molecule emission. In turn, hydrogen, due to the high diffusion coefficient in the air, a large capacity to the ignition and the high combustion rate as well as wide flammability limits of the mixture, reduces the ignition delay period under the conditions in the combustion chamber. Taking these facts into account, it can be concluded that the proper preparation of fuel in the form of changes in its physical and chemical parameters can improve both economic and ecological indicators of diesel engine work [9].

The favorable change of physical and chemical parameters of the fuel is possible by pretreatment of the fuel, conducted immediately before its injection to the combustion chamber in its contact with the material of the catalytic action in the nozzle holder. Thus, the authors made an attempt to assess the impact of a catalytic carrier, that is platinum used in the fuel system, on the combustion process in a diesel

(*) Tekst artykułu w polskiej wersji językowej dostępny w elektronicznym wydaniu kwartalnika na stronie ***www.ein.org.pl***

engine, which has a direct impact on fuel consumption and emissions of toxic substances. This issue is currently not being used in engines.

2. Analysis of the literature on the subject of the paper

Currently, catalysts have not found their applications in the injection apparatus of diesel engines . However, the analysis for combustion and the use of materials for catalytic action in the combustion chamber and the exhaust system provide a powerful application of catalysts in fuel injection systems. [3, 4, 6, 7, 10, 14, 15, 16, 17, 19, 21, 22, 24].

Analysis of the available research literature indicates that one of the possible ways to change the physical parameters of the fuel before its atomization into the combustion chamber is the thermal method. Combustion of the heated fuel enables to control the initial period of combustion, and thus lets to reduce the maximum pressure in the combustion chamber and the speed of their growth. Moreover, it leads to reducing further noise and increasing durability of the engine. As the study results show, heating the fuel to 230°C (503 K) helps to achieve a marked reduction in the rate of pressure rise in the cylinder, in addition there is the decrease in smoke and the reduction of specific fuel consumption [12]. Increase in fuel temperature accelerates the reaction of fuel cracking in the combustion chamber and due to the shortening the fuel heating time it causes shortening the ignition delay period [9].

Different method was heating the fuel in the tank due to the installation of electric heaters [9]. In this way of the thermal impact on fuel (heating fuel in the tank) it is possible to obtain almost any temperature, however, it should be considered that the steam conveying the injection pump will be working under different conditions by changing the viscosity and density of the fuel. The elimination of this problem is possible using the heating system in the high pressure, but in this case the possibility of pressure changes in the pipes and the fuel injection characteristics (other operating conditions in the injector) should be taken into account [11]. This is confirmed by the results conducted so far, in which the desired effect is not achieved throughout the whole range of engine load [6]. It should be noted that while the engine is powered with fuel, heated in front of the injection pump or fuel injector, a partial improvement in the engine was achieved, but it concerned only certain working conditions, and the results did not indicate the stability of their achievements. In addition, the registration of the indicator diagram and the characteristics of the fuel injection showed a marked change in relation to the graphs of a conventional engine. That fact can explain the failure to apply the thermal pretreatment of the fuel in engines, although many authors emphasize possibilities to improve their work with this way of impact on the physical parameters of the fuel. Other method of increasing the temperature of injection fuel is he annular channel located at the bottom of the jet block. The fuel flowing this way receives the heat from the most heated part of the discharge jet and the other thermodynamic state is atomized into the engine combustion chamber. It should be noted that with such a distribution of the heating system, the adverse impact of changes in physical parameters of the fuel on plunger and barrel assembly: nozzle holder – needle is completely eliminated. There is possibility to use catalytic converter in annular channel which activities could change chemical fuel parameters due to dehydrogenetion of hydrocarbons [13].

The catalytic treatment of the fuel in the combination with the heat treatment may be carried out in pintle injectors with the location of the catalyst in the discharge jet cooling system, whereas in the multi-hole injectors – on the imprecise part of the needle.

3. Research objectives

The aim of the study was to determine the impact of the catalytic coating in the diesel engine injector with the direct fuel injection on emissions of toxic substances into the air and the specific fuel consumption. This article is about the testing the emissions of nitrogen oxides, carbon monoxide, smoke and carbon dioxide emissions of the diesel engine by introduction of a platinum catalyst on the part of non-working injector needle. The tests were carried out on the engine test bench. During the tests the engine worked according to external speed characteristics in the revolutions frequency of 1200 – 2700 min^{-1}. Engine test bench have been carried out with the following engine configuration: injection timing of 18.5°, ejaculation pressure of 22 MPa (factory pressure setting).

The measurements were made in steady state conditions at selected points on the external characteristics of the velocity. Test items were factory fuel injectors and fuel injectors imposed on the catalyst imposed on non-working part of the needle.

4. Analysis of the temperature in the multi-hole injector nozzle

In order to determine the fuel temperature during its flow in the multi-hole injector (Fig. 1) the equations of the heat transfer and fluid flow through the tubular channel were used and the heat exchange by transmissivity was established [18, 23].

Fuel characteristics:

- Fuel absolute weight $\gamma = 840$ kg/m^3
- Specific heat $c = 2140$ J/kg·K
- Thermal conductivity $k = 0{,}1433$ J/m·s·K
- Heat transfer coefficient $\lambda = 165$ W/m^2·K

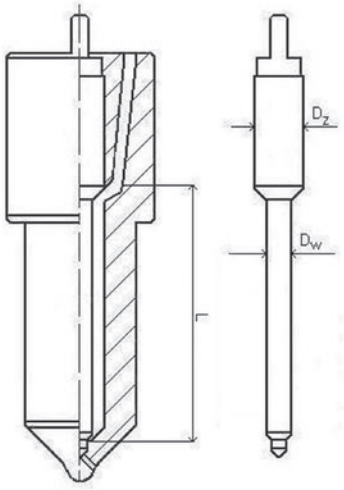

Fig. 1. Schematic of multi-hole injector

Injector characteristics:

$D_z = 0{,}005$ [m]
$D_w = 0{,}0045$ [m]
$L = 0{,}0\ 275$ [m]
$g_v = 0{,}0000094$ [m^3/s]

Mathematical model of the multi-hole fuel injector proposed by the authors:

The duration of one cycle of the fuel injection:

$$T_w = \frac{120}{n} \text{ [s]} \tag{1}$$

The volume of the fuel injected within one injection:

$$V_0 = T_w \cdot g_v \ [\mathrm{m}^3] \tag{2}$$

The fuel which flows around the injector needle forms a ring around it (in cross section). In order to facilitate the calculation of the heat exchange between the walls of the injector nozzle and the fuel, the conversion of the ring cross-section into a circular cross-section is necessary.
Cross-sectional area of the fuel pillar:

$$P_1 = \frac{\pi}{4}(D_z^2 - D_w^2) \ \ [\mathrm{m}^2] \tag{3}$$

Equivalent channel diameter:

$$D_1 = \sqrt{\frac{\pi}{4}} P_1 \ [\mathrm{m}] \tag{4}$$

Equivalent channel volume:

$$V_1 = P_1 \cdot L \ [\mathrm{m}^3] \tag{5}$$

The number of fuel doses per volume of the fuel injector nozzle channel:

$$j = \frac{V_0}{V_1} \tag{6}$$

Fuel injection time:

$$\tau = \frac{\phi}{720} T_w \ [\mathrm{s}] \tag{7}$$

where φ – rotation angle of crankshaft
Length of the segment corresponding to a dose of a specific fuel volume *l*:

$$l = \frac{L}{j} \ [\mathrm{m}] \tag{8}$$

Lateral surface area of the liquid column of the length *l filling the* channel *f :*

$$f = \pi \cdot D_1 \cdot l \ [\mathrm{m}^2] \tag{9}$$

The volume of the fuel pillar on the length *l*:

$$V_s = l \cdot P_1 \ [\mathrm{m}^3] \tag{10}$$

Fuel charge mass relating to the length *l*:

$$m = V_s \cdot \gamma \ [\mathrm{kg}] \tag{11}$$

Fuel rate in the channel:

$$u = \frac{l}{\tau} \ [\mathrm{m/s}] \tag{12}$$

Reynolds number:

$$\mathrm{Re} = \frac{2 D_1 u}{\nu} \tag{13}$$

To read the value of the kinematic viscosity in the graph (Fig. 2) the temperature of the fuel T_0 is needed:

$$T_0 = \frac{T_{pi} + T_{sci}}{2} \ [\mathrm{K}] \tag{14}$$

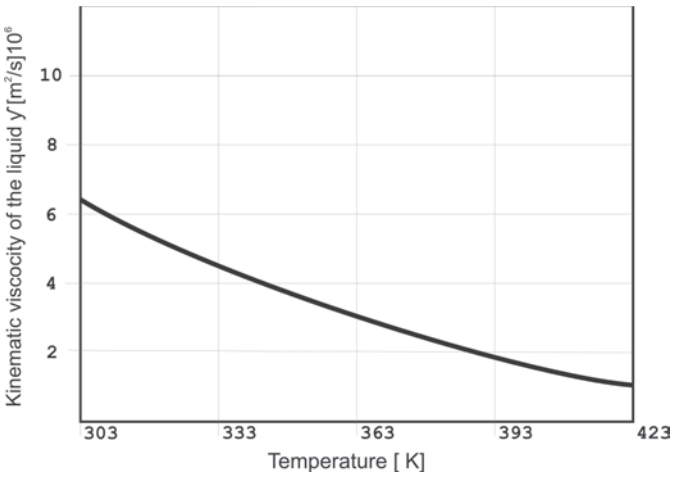

Fig. 2. Changing the viscosity of the fuel according to the temperature

Prandtl number for the fuel flowing into the channel section calculated by the arithmetic average of the temperature of the wall and fluid:

$$\mathrm{Pr} = \frac{\nu \cdot c \cdot \gamma}{\lambda} \tag{15}$$

Heat transfer coefficient of the flow through the channel:

$$\alpha_i = 0,023 \frac{\lambda}{2 D_1} \mathrm{Re}^{0,8} \mathrm{Pr}^{0,4} \tag{16}$$

Factor related to the geometry of the channel:

$$\eta = \frac{2}{D_1} \tag{17}$$

Factor related to the physical properties of the fuel flow:

$$\beta_i = \frac{\alpha_i}{c \cdot \lambda \cdot u} \tag{18}$$

Factor related to the heat transfer coefficient between the wall of the atomizer and the fuel flowing into the channel:

$$\Theta = 0,9993 \cdot e^{-2\eta\beta_i} \tag{19}$$

The fuel temperature after the flow through the selected channel segment:

$$T_{dyni} = T_{sci} - \Theta \cdot (T_{sci} - T_{pi}) \ [\mathrm{K}] \tag{20}$$

The amount of heat supplied to the fuel during its stay in the atomizer channel:

$$Q = k \cdot f \cdot (T_{sci} - T_{pi}) \cdot (T_w - \tau_w) \ [\mathrm{J}] \tag{21}$$

Increase in fuel temperature during the downtime on the selected section of the channel:

$$\Delta T_i = \frac{Q_i}{m \cdot c} \ [\mathrm{K}] \tag{22}$$

The final temperature of the fuel at the outlet from the selected section of the channel t_{ki}:

$$T_{ki} = T_{dyni} + \Delta T_i \ [\mathrm{K}] \tag{23}$$

Growth of the fuel temperature over the entire length of the channel:

$$\Delta T_k = T_{ki} - T_{pi} \ [\mathrm{K}] \tag{24}$$

The aim of the analytical researches was determining the temperature inside fuel injector, because one should to make a perfect match equivalent catalytic converter. The calculation shown that the fuel temperature in the injector nozzle is about 343 K. The analysis for the literature there is the possibility of using platinum as the catalytic converter in temperature condition in the Diesel injector [20].

5. Research characteristics

The object of the research was multi-hole injectors of the 359 diesel engine and the direct fuel injection shown in Fig. 3 and 4 [7].

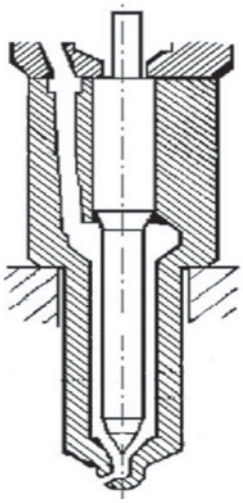

Fig. 3. Schematic of the multi-hole injector cup of the 359 engine

On the non-working part of the needle in the injector the catalytic coating in the form of platinum was applied, as it is shown in Fig. 4 [9]. Based on analysis of the literature it was found that the most appropriate catalyst due to the temperature in the injector cup is platinum [8].

Fig. 4. Needle with the catalytic coating applied on the non-working part [8]

6. Methods for testing

Researches has been made by using schema:

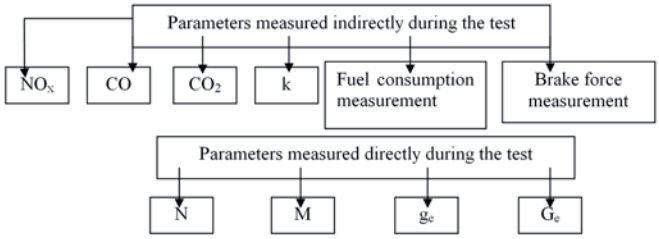

Engine power was calculated from the formula:

$$N = \frac{n \cdot P}{1160} [kW] \tag{23}$$

The engine torque was calculated from the relationship:

$$M = 8,231 \cdot P[Nm] \tag{24}$$

Specific fuel consumption was calculated from the formula:

$$g_e = \frac{3600 \cdot 103}{t \cdot N} [\frac{g}{kWh}] \tag{26}$$

Where:

- NO_x – nitric oxides,
- CO – carbon monoxide,
- k – opacity factor,
- N – engine power,
- M – engine torque,
- g_e – specific fuel consumption,
- n – engine speed,
- P – brake force,
- t – time of the fuel flow in the meter,
- 103 – fuel weight in metrology device [g].

Engine researches have been made in the laboratory with 359 engine. The toxins measurements have been carried out by using MDO opacimeter and IMR 1500 fumes analyser.

7. Description of the studies

The research was carried out on laboratory by using Bosch Common Rail CRIN injectors 0445120219. The aim of laboratory researches was fuel injection stream observation with the use of stroboscope. Fig. 5 and 6 put forward the injection fuel stream to the combustion chamber.

Fig. 5. Stream of the fuel injected in the factory injector

Fig. 6. Stream of the fuel injected in the injector with the catalytic coating applied

The laboratory researches enabled the observation of injection fuel stream. It is noticed on fig. 6 that injection fuel stream on injector with catalytic converter is dispersed. Catalytic fuel treatment interfere in chemical not physical. The injector has been used by 135 MPa injection pressure and 1000 μs injection time. Fuel dosage for conventional injector is 364,12 mm^3/H and for injector with a fuel pretreatment is 366,24 mm^3/H. The range of correct injector parameters for 135 MPa injection pressure and 1000 μs injection time is 370,5 +/− 11,5 mm^3/H. There is possibility to improve the process of coming into combustible mixture through better mix fuel and air.

The aim of this study was to analyze the engine workflow and its economic and environmental operating parameters using conventional injectors and the injectors with the catalytic coating applied on the non-working part of the needle.

Fig. 7 and 8 shows the results of 359 engine running on two types of the injectors.

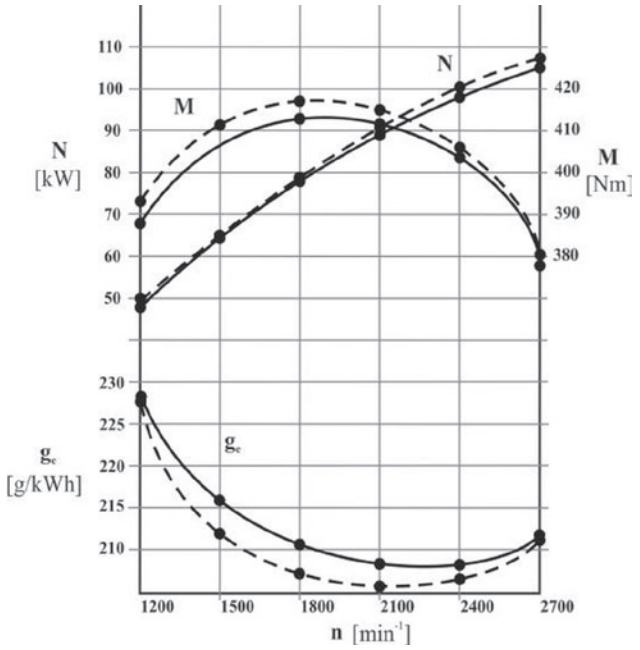

Fig. 7. Comparison of the basic parameters of the 359 engine work on two types of the injectors with the factory set engine: continual line – conventional injector, dotted line – injector with the fuel pretreatment

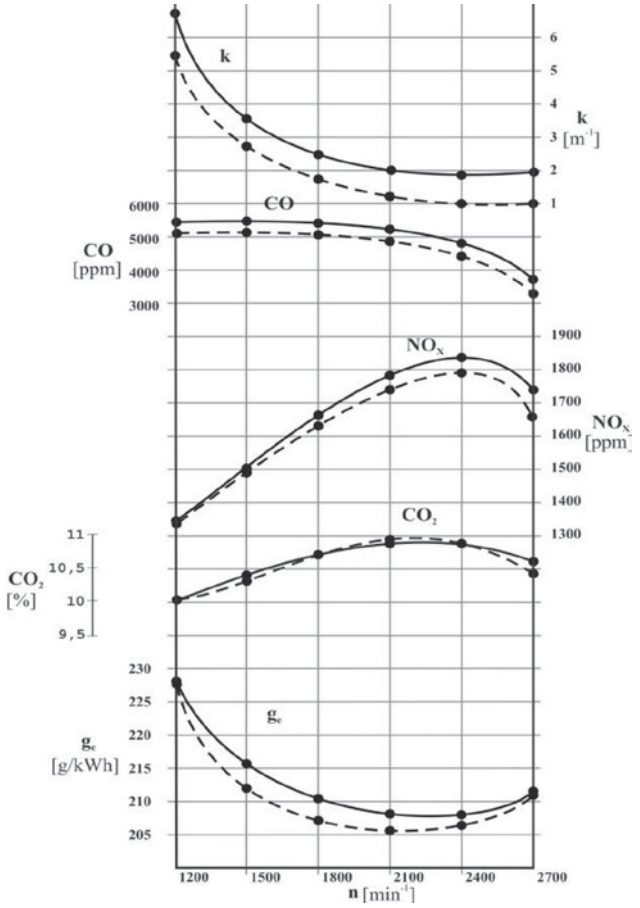

Fig. 8. Comparison of ecological and economic parameters of the 359 engine on two types of injectors with the factory set engine: continual line – conventional injector, dotted line – injector with the fuel pretreatment

Fig. 7 shows the results of the 359 engine in the form of external speed characteristics. During the study the engine power (N), engine torque (M) and the specific fuel consumption (g_e) were recorded.

It is noticed using platinum catalytic converter improved torque in whole range of engine speed. The power increase begins from 2100 min^{-1} engine speed. Catalytic converter influence on reducing individual fuel consumption and for engine speed 1800 min^{-1} was 205 g/kWh.

Fig. 8 shows the results of the 359 engine in the form of external speed characteristics. During the study the smoke (k), carbon monoxide (CO), nitrogen oxides (NO_x), carbon dioxide (CO_2) emissions and the specific fuel consumption (g_e) were recorded.

8. Conclusions

The analysis of the literature research, as well as the analytical and experimental studies for the application of the fuel pretreatment in diesel engines allow to formulate the following conclusions:

- beneficial reduction of the ignition time can be achieved by reducing the energy activation, using the phenomenon of catalysis, which implies the use of materials having a catalyst in the injection system;
- based on mathematical model the Best catalytic converter working by 343 K temperature is platinum;
- so far, the use of catalysts in combustion piston engines have taken place in the exhaust systems in the form of catalytic converters, there are a few research studies on the use of catalysts in the combustion chamber, there are not any works on the use of catalysts in the fuel injection system;
- an innovative fuel injection system in diesel engines has been proposed in which catalytic fuel processing takes place directly before the spraying, it could be used in all multiholes Diesel injectors as well in Common Rail system;
- a type of catalysts and methods of their application to the fuel injector components have been chosen;
- o the concept and the physical models of multi – hole injections with the system of the catalytic fuel pretreatment have been developed;
- experimental studies on the structural solutions of the fuel injectors equipped with the system for catalytic and thermal fuel pretreatment on the test bench and test stands have been carried out;
- the results of conducted researches show that it has been obtained the improvement of economical and ecological engine work parameters;
- in order to do additional researches of phenomenon in Diesel combustion chamber one should make indication Diesel engine with injectors with the fuel pretreatment;

The aim of the study was to determine the effect of the use of a catalytic coating in the cup of the multi-hole injector in the diesel engine with the direct fuel injection.

Before the selection of a suitable catalyst, the temperature in the cup of the multi-hole injector has been calculated. Then, on the basis of the literature analysis the appropriate catalyst has been selected and its correct operation corresponds with the surrounding in the engine injector. After the test preparation the laboratory and motor tests have been conducted.

During the laboratory analysis, the change in the structure of the injected fuel stream has been observed, using the injectors with the catalytic coating applied on the non-working part of the needle. Engine tests have shown that the specific fuel consumption decreased by about 10%, the smoke decreased by approximately 15% and the carbon monoxide emissions decreased by about 10% across the whole range of the engine speed while the nitrogen oxide emissions decreased by about 8% in the range of 1500 – 2700 rev/min.

To sum up, the studies carried out have shown that the use of the fuel pretreatment system in the form of coating applied on the non-working part of the injector needle in the 359 engine improves its environmental and economic operating parameters.

References

1. Czarnigowski J, Droździel P, Kordos P. Charakterystyczne zakresy prędkości obrotowych wału korbowego podczas pracy silnika spalinowego w warunkach eksploatacji samochodu. Eksploatacja i Niezawodnosc – Maintenance and Reliability 2012; 2: 55–62.
2. Heywood JB. Internal combustion engines fundamentals. New York: McCraw – Hill Book Co., 1988.
3. Hossam A, El A, Yiguang J. Direct numerical simulations of exhaust gas recirculation effect on multistage autoignition in the negative temperature combustion regime for stratified HCCI flow conditions by using H2O2 addition. Combustion Theory and Modelling 2013; 17: 316–334.
4. Hsin-Kan W, Chia-Yu Ch, Kang-Shin Ch, Yuan-Chung L, Chung-Bang Ch: Effect of regulated harmful matters from a heavy – duty diesel engine by H2/O2 addition to the combustion chamber. Fuel 2012; 93: 524–527.
5. Janiszewski H, Falkowski T, Sławski Cz. Krajowe silniki wysokoprężne. Obsługa i naprawa. Warszawa: Wydawnictwa Komunikacji i Łączności, 1987.
6. Yamamoto K, Fujikake F, Matsui K. Non – catalytic after – treatment for Diesel particulate carbon – fiber filter and experimental validation. Proceedings for the Combustion Institute 2013; 34: 2865–2875.
7. Klyus O. Zastosowanie wstępnej termicznej i katalitycznej obróbki paliwa w aspekcie poprawy ekologicznych i ekonomicznych wskaźników pracy silników z zapłonem samoczynnym. Szczecin: Wydawnictwo Akademii Morskiej w Szczecinie, 2007.
8. Klyus O, Mysłowski J, Osipowicz T. Wtryskiwacz paliwa, Patent, RP, P-381413, 2006.
9. Klyus O. Analiza zastosowania katalizatorów w aparaturze paliwowej silników z zapłonem samoczynnym. Szczecin: Zeszyty Naukowe Akademii Morskiej w Szczecinie 2009; 18: 54–58.
10. Klyus O, Wierzbicki S. Wpływ temperatury paliwa na tworzenie mieszaniny paliwowo – powietrznej w silnikach z zapłonem samoczynnym, III Międzynarodowa Konferencja Naukowa: Rozwój Teorii i Technologii w Technicznej Modernizacji Rolnictwa. Olsztyn, 2000: 47–55.
11. Knefel T. Ocena techniczna wtryskiwaczy Common Rail na podstawie doświadczalnych badań przelewów. Eksploatacja i Niezawodnosc – Maintenance and Reliability 2012; 1: 42–53.
12. Kowalczyk M. Studium problemów dymienia silników wysokoprężnych z wtryskiem bezpośrednim. Zeszyt Rozpraw nr 139. Poznań: Wydawnictwo Politechniki Poznańskiej, 1982.
13. Kubiak M, Perlicki J. Metale nieżelazne. Warszawa: Państwowe Wydawnictwo Ekonomiczne, 1980.

14. Murali Krishna MVS, Kishor K, Murthy PVK, Gupta AVSSKS, Narasimha Kumar S. Comparative studies on Performance evaluation of a two stroke coated spark ignition engine with alcohols with catalytic converter. Renewable and Sustainable Energy Reviews; 2012; 16: 6333–6339.
15. Mingming Z, Yu M, Dongke Z. Effect of a homogeneous combustion catalyst on the combustion characteristics and fuel efficiency in a diesel engine. Applied Energy; 2012; 91: 166–172.
16. Chakraborty N, Swaminathan N. Reynolds Number Effects on Scalar Dissipation Rate Transport and Its Modelling in Turbulent Premixed Combustion. Combustion Science and Technology 2013; 185: 676–709.
17. Niewczas A, Rychter M. Rozpływ cząstek metalicznych i innych twardych zanieczyszczeń w układzie olejenia i układzie wydechowym silnika spalinowego. Eksploatacja i Niezawodnosc – Maintenance and Reliability 2000; 1: 24–35.
18. Osipowicz T. Przyrost temperatury w kanale grzewczym we wtryskiwaczu silnika z zapłonem samoczynnym. Kaliningrad: Wyd. KGTU, 2007: 64–73.
19. Payri R, Salvador F J, Martí-Aldaraví P, Martínez-López J. Using one-dimensional modeling to analyse the influence of the use of biodiesels on the dynamic behavior of solenoid-operated injectors in common rail systems, Detailed injection system model. Energy Conversion and Management 2012; 54: 90–99.
20. Prace naukowe instytutu chemii i technologii nafty i węgla Politechniki Wrocławskiej: Właściwości powierzchniowe modyfikowanych rafineryjnych katalizatorów platynowych. Monografie nr 54/27, 1996.
21. Heck RM, Farrauto RJ. Automobile exhaust catalyst. Applied Catalysis, A: General 221, 2001: 443–457.
22. Rychlik A. Metoda pomiaru zużycia paliwa tłokowych silników spalinowych z wykorzystaniem zindywidualizowanych parametrów elektromagnetycznych wtrysku. Eksploatacja i Niezawodnosc – Maintenance and Reliability 2007; 2: 28–36.
23. Szargut J. Termodynamika. Gliwice: Wydawnictwo Politechniki Śląskiej, 2000.
24. Mittal V, Pitsch H, Egolfopoulos F. Assessment of counterflow to measure laminar burning velocities using direct numerical simulations. Combustion Theory and Modelling 2012; 16: 419–433.
25. Wajand JA, Wajand JT. Tłokowe silniki spalinowe średnio i szybkoobrotrowe. Warszawa: Wydawnictwa Naukowo – Techniczne, 2005.

Tomasz OSIPOWICZ
Karol Franciszek ABRAMEK
Zachodniopomorski Uniwersytet Technologiczny w Szczecinie
Katedra Eksploatacji Pojazdów Samochodowych
Al. Piastów 19, 70-310 Szczecin, Polska
E-mails: Tomasz.Osipowicz@zut.edu.pl , Karol.Abramek@zut.edu.pl

Article citation info:
WANG Y, ZHAO J, JIA X, TIAN Y. Spare parts allocation optimization in a multi-echelon support system based on multi-objective particle swarm optimization method. Eksploatacja i Niezawodnosc – Maintenance and Reliability 2014; 16 (1): 29–36.

Yabin WANG
Jianmin ZHAO
Xisheng JIA
Yan TIAN

SPARE PARTS ALLOCATION OPTIMIZATION IN A MULTI-ECHELON SUPPORT SYSTEM BASED ON MULTI-OBJECTIVE PARTICLE SWARM OPTIMIZATION METHOD

OPTYMALIZACJA ALOKACJI CZĘŚCI ZAMIENNYCH W WIELOSZCZEBLOWYM SYSTEMIE WSPARCIA NA PODSTAWIE METODY WIELOKRYTERIALNEJ OPTYMALIZACJI ROJEM CZĄSTEK

Spare parts allocation optimization in a multi-echelon support system presents a difficult problem which involves non-linear objective function and integer variables to be optimized. In this paper, a multi-objective optimization model was developed, which maximizes support probability and minimizes support costs. In order to solve the optimization problem, an improved multi-objective particle swarm optimization (MOPSO) method was utilized. In this method, techniques of dimensions reduction and rules-based multi-objective optimization were employed, which can improve the efficiency of MOPSO method. A numerical example was given to show the performance of proposed method.

Keywords*: MOPSO; spare parts; allocation; optimization; support probability.*

Optymalizacja alokacji części zamiennych w wieloszczeblowym systemie wspomagania stanowi trudne zagadnienie, które wymaga optymalizacji nieliniowej funkcji celu oraz zmiennych całkowitych. W niniejszej pracy, opracowano wielokryterialny model optymalizacyjny, który maksymalizuje prawdopodobieństwo wsparcia i minimalizuje jego koszty. W celu rozwiązania problemu optymalizacyjnego, wykorzystano ulepszoną metodę wielokryterialnej optymalizacji rojem cząstek (MOPSO). W metodzie tej wykorzystano techniki redukcji wymiarów oraz wielokryterialnej optymalizacji algorytmowej, które mogą poprawić efektywność metody MOPSO. Zasady proponowanej metody zilustrowano przykładem numerycznym.

Słowa kluczowe*: MOPSO; części zamienne; alokacja; optymalizacja; prawdopodobieństwo wsparcia.*

1. Introduction

The importance of spare parts management has increased in the past decades. The reason may be the increasing value of spare part inventory investment, and higher requirement of system availability and support level for technically advanced systems. Spare parts allocation is to allocate spare parts over different echelons of inventories to grantee a high efficiency of support system. Therefore, the purpose of spare parts optimal allocation is to achieve the maximal integrated economic benefit and spare part supportability. This presents a NP hard problem and efforts have been made by using methodologies of system decision-making, operational research and engineering economics theory [14, 21]. For example, DuyQuang Nguyen [9], Dubi [7] studied spare parts allocation and optimization questions in preventive maintenance by Monte Carlo simulation method; CAO Huizhi [12] set up a spare parts optimization model by fuzziness theory. Samuel L. Dreyer [19] and Doc Palmer [6] researched on spare parts management and optimization through enterprise resources plan (ERP); Derek T. Dwyer [5] and Ilgin M. Ali [13] studied spare parts stock quantity based on genetic arithmetic, and developed an optimization model; Faisal I. Khan [10] studied on spare parts allocation and optimization based on risk analysis within spares costs restriction. Although the above studies have obtained some productions, most of them took single equipment as the objective and optimized only for single objective. In fact, spare parts allocation should think about different kinds of equipments in a whole and think over more objectives such as spare parts support probability, support costs etc. The spare parts allocation and optimization for multi-objects are more difficult for the complex relations among every objective, which may be conflict or supplement one another.

Particle swarm optimization (PSO) is a kind of evolutionary calculation technology based on colony aptitude theory, which was brought forward by American Doctor Eberhart and Kennedy in 1995. The idea of PSO came from birds' preying behavior. In the method, it was assumed that a group of birds were searching for foods at random, and there was only one piece of food in a certain area. All those birds didn't know where the food was, while they knew the distance between the food and their current positions. Then the optimal strategy of finding food was to get the area where is nearest to the food from every bird's current position. In PSO, each unity was taken as a particle with certain position and speed. The particle's position presents the solution of the question.

By comparing with PSO, MOPSO needs to take into account of a number of objectives and make a choice from a set of feasible solutions. Therefore, the key problem is that

how to confirm a proper fitness function, which is used to measure the quality of a solution scheme for multi-objective case. According to fitness function, the solution methods for PSO can be classified as objective polymerization method, Pareto dominated based method and rule-based method. Objective polymerization method [4, 17] takes multi-objective function polymerized by power adding and converts the multi objectives to a single objective. In Pareto dominated based method [1, 3, 16], the best isolated none-inferior solution was endowed with global minimum, which can induct MOPSO method to find a none-inferior solution with a symmetrical distribution. About rule based method [2, 8], not all objectives were considered at one time. According to different circs in optimization process, the fitness function was converted from different objective.

A multi-objective optimization model of spare parts allocation was developed by using an improved MOPSO method, which takes the maximum support probability of spare parts and the minimal support costs as the objective functions. The solution techniques, such as dimensions reduction and rules-based multi-objective optimization, were utilized in order to improve the solving efficiency of MOPSO method.

2. Modeling of spare parts allocation and optimization

2.1. Problem description and model assumptions

Most inventory control problems in the real world involve multiple echelons. For example, in many military logistics areas, support systems are operated in echeloned manner. In the paper, a two-echelon spare support system is considered, where there are a number of maintenance facilities and spare parts inventories in the first echelon, and only one maintenance facility and one warehouse in the second echelon. Each maintenance facility has a spare inventory correspondingly, which stores certain types of spare parts. When a repairable unit in an equipment fails, the failed unit will be replaced if there is a spare in the first echelon of inventory. Otherwise, a spare part is back-ordered from the second echelon of inventory. The local repair facility tries to repair the failed units which are repairable at the facility; otherwise, the units will be sent to the second facility for repair. The units which have been repaired will be stored in local inventories as spare parts. Besides, we have following assumptions.

(1) The demand for each type of spare part is independent, and each unit's failure obeys exponential distribution;
(2) All the replaceable units are significant components, and lack of any one will lead to equipment down;
(3) It is assumed that some failure modes of a unit are repairable, and the repair rate is constant;
(4) Only corrective maintenance is considered and related spare parts demand is assumed to follow Poisson distribution;
(5) The maintenance capability is infinite, and repair of failed units may be conducted once they are replaced from equipment;
(6) Continuing examine strategy (*S*-1, S) is adopted for the first echelon of spare inventory;
(7) The lateral supply in the same maintenance facilities is not considered.

The spare part allocation relation is shown as Figure 1. Where, k denotes the sequence of specific type of equipment, and N_j denotes the equipment number of this type.

2.2. Notations

The notations used to develop the model are listed below:

i – types of spare parts, which can be 1,2,…,I;
I – total number of spare parts types;
J – the number of maintenance facilities in the first echelon;

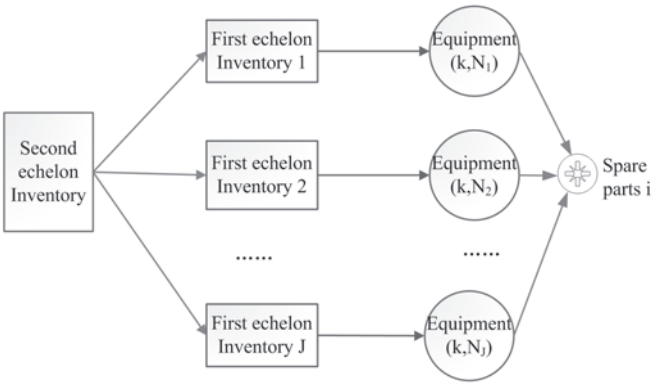

Fig.1. Relation of the spare parts allocation

K – the number of equipment with certain type;
T – equipment working time;
E_{ji} – the demand of spare part i at jth inventory in the first echelon in a period of equipment working time;
E_i – the average demand of spare part i in the first echelon in a period of equipment working time;
$E[B(S_i)]$ – the expected shortage of spare i for the first echelon when the stock level in local inventory is S_i;
$E[D(S_i, S_{oi})]$ – the expected shortage of spare i in the second echelon, when stock level in the first echelon is S_i, and the second echelon is $S_{o,i}$;
t_o – the average lead time in the first echelon to backorder spare parts;
t_m – the average lead time in the second echelon inventory to acquire spare parts;
S_{ji} – the stock level of spare part i at the jth inventory of the first echelon;
S_{oi} – the stock level of spare part i at the inventory of the second echelon;
$P(x_{ji})$ – the probability of ith spare part demand for jth inventory in the first echelon j, and x_{ji} is demand value of spare part i;
x'_{ji} – the amount of shortage for spare i at the jth inventory of the first echelon;
$P_o(x'_{ji})$ – the probability of ith spare demand at jth inventory of the first echelon;
ξ_i – the shortage probability of spare parts i in the second echelon;
η_i – the shortage probability of spare parts i in the first echelon;
R_i – the probability of repair for ith replaceable unit in the first echelon;
E_i^v – the maximum inventory for spare parts i in the first echelon;
E_{oi} – the average demand quantity of spare parts i in the second echelon;
E_{oi}^v – the maximum inventory for spare parts i in the second echelon;
C_i – the cost of a spare part i;

T_{bfi} – the mean-time between failures of spare parts *i*.

2.3. Development of the model

(1) Demand of spare parts in the first echelon

Because $P(x_{ji})$ denotes probability of spare parts demand for the first echelon *j*, and the number of demand is x_{ji}. The expected demand of spare part *i* in the first echelon can be expressed as:

$$E_{ji} = \sum_{x_{ji}=0}^{\infty} x_{ji} P(x_{ji}) \tag{1}$$

(2) Shortage ratio of spare parts in the first echelon

Denote $E[B(S_{ji})]$ as the inventory shortage of spare *i* for the first echelon. It is the expectation of spare parts demand, which exceeds the stock level, S_{ji}, in the first echelon. Hence, it can be expressed as:

$$E[B(S_{ji})] = \sum_{x_{ji}=S_{ji}+1}^{\infty} (x_{ji} - S_{ji}) P(x_{ji}) \tag{2}$$

The average demand of spare parts in the first echelon can be given by:

$$E_i = \sum_{j=1}^{J} E_{ji} \tag{3}$$

As there are J inventories in the first echelon, the expected shortage of spare *i* can be obtained through summing the shortage over the J inventories. That is,

$$E[B(S_i)] = \sum_{j=1}^{J} E[B(S_{ji})] \tag{4}$$

From Eqs.(3) and (4), we can have that the shortage ratio of spare *i* in the first echelon:

$$\eta_i = \frac{E[B(S_i)]}{E_i} \tag{5}$$

(3) The spare parts demand ratio in the second echelon

It is noted that when the demand for spare parts exceeds the stock level of the first echelon of inventory, a spare backorder for the second echelon of inventory will be conducted. Therefore, the probability of *i*th spare part demand for the second echelon $P_0(x'_{ji})$ can be expressed as:

$$\begin{cases} P_o(x'_{ji}) = P_j(x'_{ji} + S_{ji}) & x'_{ji} > 0 \\ P_o(x'_{ji}) = \sum_{x_{ji}=0}^{S_{ji}} P_j(x_{ji}) & x'_{ji} = 0 \end{cases} \tag{6}$$

The demand probability $P_o(y_i)$ of spare *i* can be calculated using the $P(x'_{ji})$ dispersed k-fold discrete convolution, that is:

$$P_o(y_i) = \sum_{x'_{1i}+x'_{2i}+\cdots x'_{Ji}=y_i} P_o(x'_{1i}) P_o(x'_{2i}) \cdots P_o(x'_{Ji}) \tag{7}$$

Actually, the right part of the above equation is a calculation of the *k*-fold discrete convolution, which can be solved by the Conv function in Matlab [11].

In the following, we will show that the demands of spare parts still follow Poisson distribution for the second echelon.

Consider the interval $[0,t]$. Let $N(t)$ denote the number of spare part demands within the interval $[0,t]$ and $X(t)$ denote the number of failures in the interval, and then $X(t)$ can be represented by:

$$X(t) = \sum_{n=1}^{N(t)} W_n(t) \tag{8}$$

Here, $W_n(t)$ is a binary variable defined by:

$$W_n(t) = \begin{cases} 1 & \mathrm{i} \in \theta \\ 0 & otherwise \end{cases} \tag{9}$$

Where θ is the set of failure modes of replaceable units which are repairable. And according to the previous assumption that $P[W_n(t)=1] = 1-R$.

For any real number *u*, the characteristic function, $\phi_{X(t)}(u)$ of $X(t)$ can be given by:

$$\phi_{X(t)}(u) = E\{\exp[iuX(t)]\} \tag{10}$$

Where *i* is an imaginary number, i.e. $i = \sqrt{-1}$, and $E(Y)$ is the expectation of *Y*.

It can be shown that:

$$E\{\exp[iuX(t)]\} = \sum_{k=0}^{\infty} E\{[\exp(iuX(t))] | N(t)=k\} P[N(t)=k] \tag{11}$$

When *k* failures have occurred in $(0,t]$, i.e. $N(t)=k$, $X(t)$ is the sum of *k* independent and identical random variables of $W_n(t)$, then:

$$E\{[\exp(iuX(t))] | N(t)=k\} = (E\{\exp[iuW_n(t)]\})^k \tag{12}$$

As assumed above, $N(t)$ is a NHPP, and then the probability of *k* demands occurring in the interval $(0,t]$ is given by:

$$P[N(t)=k] = (\int_0^t \lambda(\tau)d\tau)^k \exp[-\int_0^t \lambda(\tau)d\tau] / k! \tag{13}$$

Where $\lambda(\tau)$ is the rate of failure occurrence at time τ.

Substituting equations (12) and (13) into Equation (11), and using equation (10), the characteristic function can be rewritten as:

$$\phi_{X(t)}(u)=\sum_{k=0}^{\infty}(E\{\exp[iuW_n(t)]\})^k(\int_0^t\lambda(\tau)d\tau)^k\exp[-\int_0^t\lambda(\tau)d\tau]/k!$$

$$=\exp\{[E(e^{iuW_n(t,)}-1)]\int_0^t\lambda(\tau)d\tau\}$$

$$=\exp\{(e^{iu}-1)P[W_n(t)=1]\int_0^t\lambda(\tau)d\tau\} \quad (14)$$

From equations (14) it follows that:

$$\phi_{X(t)}(u)=\exp\{(e^{iu}-1)(1-R)\int_0^t\lambda(\tau)d\tau\} \quad (15)$$

This is a characteristic function of a random variable with a Poisson distribution. This implies that $X(t)$ is a NHPP, and the expected number of failures in $(0,t]$ is given by:

$$\Lambda(0,t)=(1-R)\int_0^t\lambda(\tau)d\tau \quad (16)$$

For the case of constant failure rate of replaceable unit, the demand rate of spare in the second echelon of system can be expressed as: $\lambda_{oi}=(1-R_i)J\lambda_i$.

When the demands of unit i obey Poisson distribution, we have:

$$P_o(y_i)=\sum_{k=0}^{y_i}\frac{(\lambda t)^k}{k!}e^{-\lambda t} \quad (17)$$

On the basis of demand probability of spare i in the second echelon, we can obtain the expected demand of spare parts for the second echelon of inventory:

$$E_{oi}=\sum_{y_i=0}^{\infty}y_iP_o(y_i) \quad (18)$$

The expected shortage of spare i for the second echelon can be expressed as:

$$E[D(S_i,S_{oi})]=\sum_{y_i=S_{oi}+1}^{\infty}(y_i-S_{oi})P_o(y_i) \quad (19)$$

Then the shortage probability of spare parts i for the second echelon can be denoted as:

$$\xi_i=\frac{E[D(S_i,S_{oi})]}{E_{oi}} \quad (20)$$

(4) The average delay time for spare parts in the first echelon

The supply delay of spare parts in the first echelon can be divided into two cases. Firstly, there is a shortage of spares in first echelon but there are a number of spares in the second echelon. In this case, the delay time can be given by $(1-\xi_i)\eta_i t_o$. Secondly, there is a shortage of spares both in first echelon and second echelon. In this case, the delay time can be expressed as $\eta_i\xi_i(t_o+t_m)$. Therefore, the average delay time of spare i in the first echelon can be given by:

$$T_{Di}=(1-\xi_i)\eta_i t_o+\xi_i\eta_i(t_o+t_m)=\eta_i t_o+\xi_i\eta_i t_m \quad (21)$$

(5) The support probability for spare i

It is assumed that life distribution of component i is known, and the mean time between failures of the component i can be obtained, then the steady-state support probability of spare parts i can be expressed as:

$$P_i=\frac{T_{bf_i}}{T_{bf_i}+T_{Di}} \quad (22)$$

Through the collation, we can obtain:

$$P_i=\frac{T_{bf_i}E_iE_{oi}}{T_{bf_i}E_iE_{oi}+\sum_{j=1}^{J}\sum_{x_{ji}=S_{ji}+1}^{\infty}(x_{ji}-S_{ji})p(x_{ji})\cdot[t_oE_{oi}+t_m\sum_{y_i=S_{oi}+1}^{\infty}(y_i-S_{oi})p_o(y_i)]}$$

$$=\frac{\sum_{j=1}^{J}\sum_{x_{ji}=1}^{\infty}x_{ji}p(x_{ji})\cdot\sum_{y_i=0}^{\infty}y_ip_o(y_i)T_{bf_i}}{\sum_{j=1}^{J}\sum_{x_{ji}=1}^{\infty}x_{ji}p(x_{ji})\cdot\sum_{y_i=0}^{\infty}y_ip_o(y_i)T_{bf_i}+\sum_{j=1}^{J}\sum_{x_{ji}=S_{ji}+1}^{\infty}(x_{ji}-S_{ji})p(x_{ji})\cdot[t_o\sum_{y_i=0}^{\infty}y_ip_o(y_i)+t_m\sum_{y_i=S_{oi}+1}^{\infty}(y_i-S_{oi})p_o(y_i)]} \quad (23)$$

Therefore, the support probability of all spare parts can be given by:

$$P_S=\prod_{i=1}^{I}P_i \quad (24)$$

(6) Multi-objective allocation and optimization model

The allocation and optimization model of spare parts can be expressed as:

$$\max \quad P_S=\prod_{i=1}^{N}\frac{T_{bf_i}E_{oi}\sum_{j=1}^{J}E_{ji}}{T_{bf_i}E_{oi}\sum_{j=1}^{J}E_{ji}+(\sum_{j=1}^{J}(E_{ji}-S_{ji})[t_oE_{oi}+t_m(E_{oi}-S_{oi})]} \quad (25)$$

$$\min \quad C_S=\sum_{i=1}^{N}C_i(\sum_{j=1}^{J}(S_{ji}+S_{oi}) \quad (26)$$

Subject to

$$0\le\frac{\sum_{j=1}^{J}E_{ji}-S_{ji}}{\sum_{j=1}^{J}E_{ji}}\le 1,\forall i=1,2,...,N \quad (27)$$

$$0\le\frac{E_{oi}-S_{oi}}{E_{oi}}\le 1,\forall i=1,2,...,N \quad (28)$$

$$0\le S_{ji}\le E_i^v,S_{ji}\text{is an integer},\forall i=1,2,...,N \quad (29)$$

$$0\le S_{oi}\le E_{oi}^v,S_{oi}\text{is an integer},\forall i=0,1,2,...,N \quad (30)$$

Where, Eqs.(25) and (26) represent the optimization objectives which maximizing support probability of spare parts and minimizing the costs of spare parts.

Constraint (27) means that the shortage rate of spare parts *i* in the first echelon is greater than or equal to 0, and less than or equal to 1.

Constraint (28) means that the shortage rate of spare parts *i* in the second echelon is greater than or equal to 0, and less than or equal to 1.

Constraint (29)means that the stock quantity of spare parts *i* in the first echelon is an integer, which does not exceed the maximum inventory limit.

Constraint (30) means that the stock quantity of spare parts *i* in the second echelon is an integer, which dose not exceed the maximum inventory limit.

3. Solution of spare parts allocation and optimization models

3.1. Characteristic of the optimization model

It can be seen that spare parts allocation and optimization models are high-dimensional, non-linear, multi-objective optimization models from formula (25) to (30). So, the traditional optimization algorithm is ineffective to these models. Therefore, an improved algorithm is presented in order to solve such an optimization problem, which includes the following characteristic of analysis and processing.

(1) In practice, the supportability between various spare parts is independent among them. Therefore, when support probability of each spare parts getting the maximum, the probability of such spare parts will obtain maximum. Similarly, when the costs of each type of spare parts are minimal, the costs of such spare parts are also minimal. So dimensionality reduction can be used. Namely, optimized for each variety of spare parts, and then we can get the optimization solution of all kind of spare parts.

(2) In the spare parts optimization and allocation models, there are two different objective functions. Decision-makers preferences of these two objectives are different at different stages and with different tasks. Therefore, the rule based method for solving the MOPSO is more reasonable.

(3) In the particle swarm optimization, ω is the most important controllable parameter. For the premature of PSO method and late oscillation phenomenon in the near global optimal solution, the PSO method needs to be improved in order to enhance the quality and efficiency of the solution.

3.2. Particle representation

Using vector-based method, particle representations can be shown in Figure 2. Each particle corresponds to a spare part configuration program.

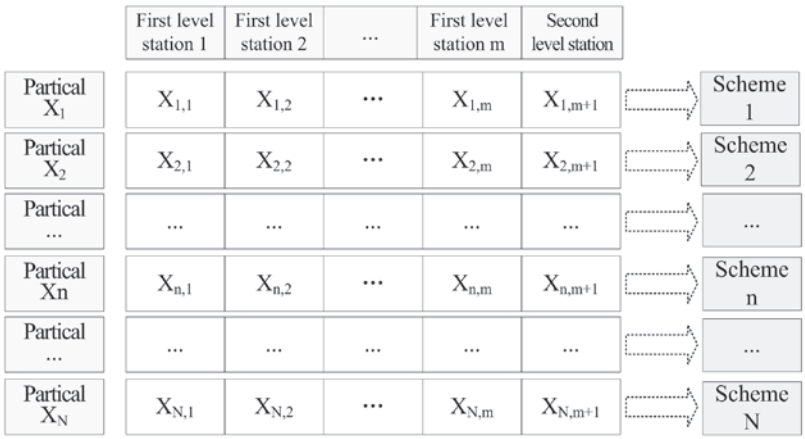

Fig.2. The sketch map of particle's denotation

It is noted that $x_n = [x_{n,1},...x_{n,j},...x_{n,m},x_{n,m+1}]$ $n \in \{1,2,...,N\}$, (*N* presents the number of particles), Particle dimension is m+1; $x_{n,j}$ denotes the allocation number of spares *i* in the first echelon. $j \in \{1,2,...,m\}$,and m is the number of the first echelon institutions; $x_{n,m+1}$ denotes the allocation number of spares *i* in the second echelon.

3.3. Fitness calculation

Fitness function is used to evaluate the pros and cons of the individual groups. The function values guide the movement direction and speed of the particle swarm. A rule-based method was employed to determine the fitness function, which compromises the two goals of optimization problem, that is, maximizing the support probability (Goal 1) and minimizing the support cost (Goal 2) for spare parts *i*. Clearly, when Goal 1 was implemented, we can simply confirm the neighborhood of Goal 2, and then calculate the fitness of each particle.

3.4. Particle update

Particle swarm method takes on a rapid convergence speed, which can easily lead to the loss of population diversity. In order to prevent its fall into local optimal solution, this paper puts forward a dynamic swarm strategy for the selection of the two particle swarms. In this strategy, each particle swarm optimizes a single goal, and the global optimal value of the first particle swarms are used in the rate equation of the second particle swarm. While the global optimal value of the second particle swarm are used to update the first particle swarm. Namely:

$$S_{1\cdot v_{id}}(t+1) = \omega S_{1\cdot v_{id}}(t) + c_1 r_1[S_{1\cdot p_{id}}(t) - S_{1\cdot x_{id}}(t)] + c_2 r_2[S_{2\cdot p_{gd}}(t) - S_{1\cdot x_{id}}(t)] \tag{31}$$

$$S_{2\cdot v_{id}}(t+1) = \omega S_{2\cdot v_{id}}(t) + c_1 r_1[S_{2\cdot p_{id}}(t) - S_{2\cdot x_{id}}(t)] + c_2 r_2[S_{1\cdot p_{gd}}(t) - S_{2\cdot x_{id}}(t)] \tag{32}$$

$$S_{1\cdot x_{id}}(t+1) = S_{1\cdot x_{id}}(t) + v_{id}(t+1), \qquad 1 \le i \le n,\ 1 \le d \le D \tag{33}$$

$$S_{2\cdot x_{id}}(t+1) = S_{2\cdot x_{id}}(t) + v_{id}(t+1), \qquad 1 \le i \le n,\ 1 \le d \le D \tag{34}$$

$$v_{id}(t) = [S_{1\cdot v_{id}}(t) + S_{2\cdot v_{id}}(t)]/2 \tag{35}$$

3.5. Weight improvement

In particle swarm optimization methods, the inertia factor is the most important controllable parameter, which is used to control the influence degree of the current speed on the updating speed. The larger the parameter value, the more beneficial for a wide range of global search. The smaller the parameter value, the more favorable in the current range of local search. A large number of experiments[15, 18, 20] have shown that the effectiveness of the algorithm is larger when the parameter value is between 0.4 and 1.4. In this article, the inertia factor was selected by the following formula:

$$\omega_g = \omega_{\max} - g\frac{\omega_{\max} - \omega_{\min}}{G_{\max}} \tag{36}$$

In this formula, ω_{max} denotes the maximum inertia weight, ω_{min} denotes the minimum inertia weight, g denotes the iteration steps, and G_{max} represents the maximum number of iteration steps.

3.6. Procedure of solution algorithm

The procedure of MOPSO solution algorithm is shown in Figure 3.

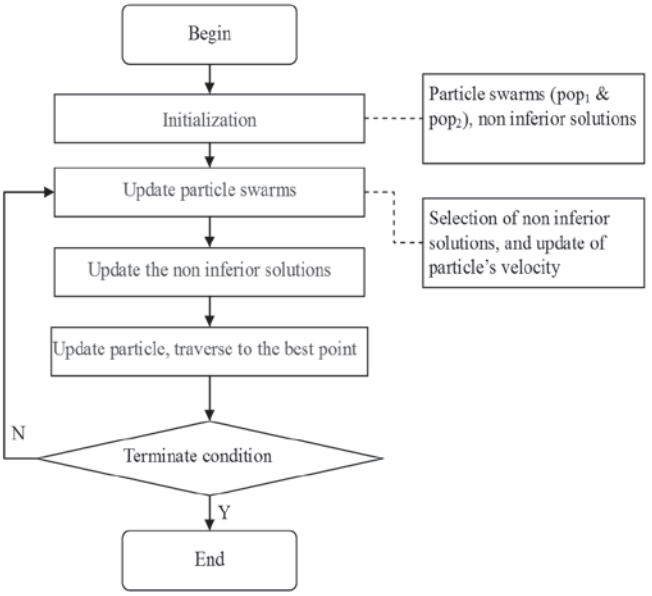

Fig. 3. Procedure of rules based MOPSO solution algorithm

Step 1: Initialization. The non-inferior solution and particle swarm POP_1, POP_2 were initialized randomly. In the mean time, the objectives and constraints of each particle in particle swarm was computed. While, each particle's velocity as well as the best point of each particle have traversed were initialized in the particle group.

Step 2: Update the particle swarms. The particle velocity can be updated by equations (31) and (32), while the position of the particle can be updated according to equations (33) to (35).

Step 3: Update the non-inferior solutions.

Step 4: Update the optimal solution, which was found by each particle.

Step 5: Terminate the condition judgment. If the condition was satisfied, the procedure will be terminated, otherwise will go to step 2.

4. Numerical example

4.1. Description of the problem

It was supposed that in workshops X and Y both there are18 sets of production equipment. Spare parts A and B are two critical spare parts of the equipment. The mean time needed for backordering spares from the second echelon is 480 h, while the mean time for acquiring spares in the second echelon is 720 h. P_{ji}, S_{ji}, S_{oi} and T_{bf} were listed in Table 1. In order to complete annual production tasks (at 1600 h), how to allocate such spare parts which can get the maximum support probability of the spare parts system, while the guaranteeing costs is minimum.

4.2. Problem solving and analysis

The basic data such as E_{ji} E_{oi} and the highest reserves E^v_i, $E_{oi}{}^v$ in different institutions can be calculated, which are shown in the Table 2.

Table 1. Input data of the example

Workshop	Number of Equipment	Types of Spare parts	P_{ji}	T_{bf}(h)	S_{ji}	S_{oi}
X	18	A	0.8	3500	5	2
		B	0.75	2500	5	3
Y	18	A	0.9	3500	8	2
		B	0.95	2500	8	3

Table 2. Basic data of the numerical example

Sequence number	Spare name	T_{bf}(h)	E_{1i}	E_{2i}	E_{oi}	E^v_i	$E_{oi}{}^v$	C_i (RMB YUAN)
1	A	3500	7	8	2	10	3	1200
2	B	2500	9	11	7	12	8	500

In this paper, Matlab was used to program the MOPSO algorithm. The computer configuration is the Intel (R) Core (TM) i5, CPU 2.27 GHz and Memory 2G. The size of the two particle swarms are all 40 particles, and the number of iterations is 100 generations, ω_{max} is 1.2, ω_{min} is 0.5, C_1 is 0.5, and C_2 is 0.5. As a result, the average computation time is 6 sec. The results of the optimization of spare parts are shown in Table 3. The individual fitness values are shown in Figure 4, and the non-inferior solutions distribution in the objective space is shown in Figure 5.

Table 3. Optimization results of the spare parts allocation

Scheme	Allocation for spare A			Allocation for spare B			Support probability P	C_A(RMB YUAN)
	S_{11}	S_{21}	S_{o1}	S_{21}	S_{22}	S_{o2}		
1	0	0	2	0	0	9	0.792	6900
2	0	0	2	0	0	10	0.823	7400
3	0	0	2	0	0	11	0.856	7900
4	0	0	3	0	0	9	0.871	8100
5	0	0	3	0	0	10	0.905	8600
6	0	0	3	0	0	11	0.941	9100
7	0	0	3	1	1	11	0.944	10100
8	1	1	3	0	1	11	0.946	12000
9	0	1	3	2	2	11	0.948	12300
10	1	1	3	2	2	11	0.950	13500
11	2	2	3	1	2	11	0.953	14200
12	2	2	3	2	2	11	0.955	15900

As can be seen from Table 3, when the support cost is ¥6900, the optimal allocation scheme is that 2 of spare part A are allocated in the second echelon and none in other echelons; and stock level of spare parts B is 9 in the second echelon. With this scheme, the spare support probability is 0.792. With the increasing support costs, the spare support probability is also increased. Decision-makers can select the suitable spare parts allocation scheme from the different optimization schemes according to the needs and actual conditions, which can meet the demands of the support probability and limit of spare parts costs.

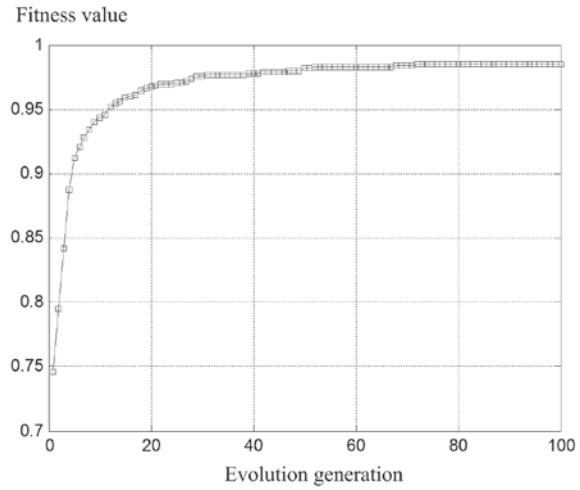

Fig. 4. The changing of best fitness in MOPSO for spare parts

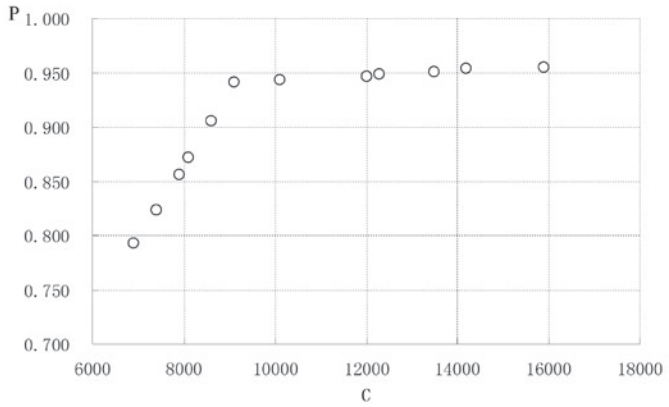

Fig. 5. The distribution of Pareto solutions in the objective space for spare parts

Figure 4 shows the relation between optimal individual fitness and evolution generation. It is seen that the best individual fitness value basically turns to stabilization when the evolution generation is beyond 50.

The distribution of the non-inferior solutions in the objective space is shown in Figure 5. It can be seen that with the increasing of support costs with in a certain range, the support probability of spare is also rising. However, when the support probability of spare reached 0.95, even with increasing the number of spare parts support costs, the changes in the probability is very small. Therefore, decision-makers can determine a suitable solution by the tradeoff between the two goals of the spare parts support probability and support costs. As a result, we can select a allocation scheme of spare parts from non-inferior solutions.

In addition, the collections of non-inferior solutions in the target space are corresponding to the 12 different schemes in Table 3 respectively. Policy-makers can make a tradeoff from the two goals of the probability of spare supportability and support costs to determine a suitable solution from the non-inferior solutions for the spare parts allocation. For example, if the spare support probability is not less than 0.90, and with a minimum cost, one can select the target space of the fifth non-inferior solutions (P=0.905, C=8600RMB¥). In this scheme, 3 of spare part A are allocated in the second echelon and none in other echelons; and stock level of spare part B is 10 in the second echelon.

5. Conclusions

This paper develops an improved MOPSO method of spare parts allocation and optimization, which takes into account of multiple objectives such as support probability of spare parts and support costs, and focuses on the whole system of maintenance support. Compared with other methods, such as GA, and ANN, this method is more efficient to solve the non-linear, multi-objective and high-dimensional problems of the allocation and optimization models. At last, a numerical example has verified the feasibility and effectiveness of the models and algorithm for the spare parts. In this paper, we have assumed that the failure rate of a replaceable unit is constant, and there is no lateral supply between the inventories at the same echelon. However, it can be extended to consider lateral supply and other distributions of unit failures. This topic will be studied in our following research.

Reference

1. Abido MA. Multi-objective particle swarm optimization for optimal power flow problem. 2008 12th International Middle East Power System Conference, 2008: 392–396.
2. Andries P. Engelbrecht write, Ying Tan translate. Basic of computer swarm intelligence. Beijing: Qinghua University Press, 2009.
3. Baltar Alexandre M, Fontane Darrell G. Use of multi-objective particle swarm optimization in water resources management. Journal of Water Resources Planning and Management 2008: 257–265.
4. Deb K. Genetic algorithms in multimodal function approximation. Master's thesis, University of Alabama, 1989.
5. Derek T. Dwyer. Heuristic algorithm for U.S. naval mission resource allocation. ADA488672, 2008.
6. Doc Palmer. Maintenance planning and scheduling handbook. New York: McGraw Hill Press, 2006.
7. Dubi A. The Monte Carlo method and optimization of spare parts in complex realistic scenarios. 2006 Annual Reliability and Maintainability Symposium, 2006: 37–44.
8. Dunwei Gong, Yong Zhang, Jianhua Zhang. Multi-objective particle swarm optimization based on minimal particle angle. Lecture Notes in Computer Science 2005, 3644(1): 571–576.
9. DuyQuang Nguyen, Bagajewicz Miguel. Optimization of preventive maintenance scheduling in processing plants. Computer Aided Chemical Engineering 2008; (25): 319–324.
10. Faisal I. Khan, Mahmoud M. Haddara. Risk-based maintenance (RBM): A quantitative approach for maintenance/inspection scheduling and planning. Journal of Loss Prevention in the Process Industries 2003, 16(6): 561–573.
11. Gang Li. Handbook for quickly check of MATLAB function. Beijing: Qinghua University Press, 2011.
12. Huizhi Cao, Chunjie Wang. Optimized resources configuration of vehicle equipment maintenance support for military operation other than war based on rough set theory. Journal of Academy of Military Transportation 2010; 12(3): 38–41.
13. Ilgin M. Ali, Tunali Semra. Joint optimization of spare parts inventory and maintenance policies using genetic algorithms. International Journal of Advanced Manufacturing Technology 2007; 30(5): 594–604.
14. Jeremy A. Lifsey. Optimization of maintenance resources. European Journal of Operational Research 1965; 13(6): 1007–1019.

15. Jingxuan Wei. Evolutionary Algorithms for single-objective and mufti-objective optimization problems. Xi'an University In Candidacy for Degree of Doctor of Philosophy, 2009.
16. Leong, Wen-Fung Yen, Gary G. Dynamic swarms in PSO-based multi-objective optimization. 2007 IEEE Congress on Evolutionary Computation, 2007: 3172–3179.
17. Parsopoulos KE, Vrahatis MN. Recent approaches to global optimization problems through particle swarm optimization. Natural computing 2002; 1(2–3): 235–306.
18. Ran He. An improved particle swarm optimization based on self-adaptive escape velocity. Journal of Software 2005; 16(72): 2036–2044.
19. Samuel L. Dreyer, CPL. PMP. Advance Maintenance Planning and Schedule. Proceedings of IEEE Autotestcon, 2006: 341–347.
20. Sicrra M R, Coello CAC. Multi-objective particle swarm optimizers: A survey of the state-of-the-art. International Journal of Computational Intelligence Research 2006; 2(3): 287–308.
21. Wenbin Wang. A joint spare part and maintenance inspection optimisation model using the delay-time concept. Reliability Engineering and System Safety 2011; (96): 1535–1541.

Yabin WANG
Jianmin ZHAO
Xisheng JIA
Yan TIAN
Department of Management Engineering
Shijiazhuang Mechanical Engineering College
Shijiazhuang, P. R. China
E-mail: wangyabin123@163.com

Article citation info:
KUCZMASZEWSKI J, PIEŚKO P. Wear of milling cutters resulting from high silicon aluminium alloy cast AlSi21CuNi machining. Eksploatacja i Niezawodnosc – Maintenance and Reliability 2014; 16 (1): 37–41.

Józef KUCZMASZEWSKI
Paweł PIEŚKO

WEAR OF MILLING CUTTERS RESULTING FROM HIGH SILICON ALUMINIUM ALLOY CAST AlSi21CuNi MACHINING

ZUŻYCIE OSTRZY FREZÓW PODCZAS OBRÓBKI WYSOKOKRZEMOWEGO, ODLEWNICZEGO STOPU ALUMINIUM AlSi21CuNi*

This paper presents results of tests on the wear of milling cutters resulting from high silicon silumins machining. As a representative for this group of materials EN AC-AlSi21CuNi alloy was chosen. Aluminium alloys containing less than 12 % of Si are classified as difficult-to-cut due to increased abrasive wear of the cutters caused by the influence of silicon precipitates. This affects the cutting process by damaging the quality and accuracy of the manufactured elements. Therefore, it is so significant to determine the durability of the teeth and stop the cutting process when it is being excessively worn.

***Keywords**: silumins, wear of tools, tools durability, cutting forces, surface roughness.*

W artykule przedstawiono wyniki badań zużycia ostrzy narzędzi frezarskich podczas obróbki wysokokrzemowych siluminów. Jako przedstawiciela tego rodzaju materiałów wybrano stop EN AC-AlSi21CuNi. Stopy aluminium o zawartości Si > 12% określane są jako trudnoskrawalne, ze względu na zwiększone zużycie ścierne ostrzy, wywołane oddziaływaniem wydzieleń krzemu.Ma to niekorzystny wpływ na proces skrawania, pogarsza jakość i dokładność wykonywanych elementów. Istotne jest więc aby określić trwałość ostrza narzędzi i w momencie jego nadmiernego zużycia przerwać proces skrawania.

***Słowa kluczowe**: siluminy, zużycie narzędzi, trwałość narzędzi, siły skrawania, chropowatość.*

1. Introduction

Aluminium alloys can be characterized as free machining, however, it is difficult to compare with machinabilty of other metals. This is induced by the properties of aluminium alloys, such as high linear expansion coefficients and relatively low linear elasticity coefficients [6, 11].

There are many grades of aluminium alloys and due to that fact, to facilitate the choice of machining conditions, they were grouped into categories according to three major criteria: silicon content, method of the performed heat treatment (heat treating and cold working) and their purpose (for plastic working and for casting) [6, 11, 12]. Aluminium alloys are grouped as follows:

- group 1 — alloys with Si ≤ 2 %,
- group 2 — alloys with 2% < Si ≤ 12 %,
- group 3 — alloys with Si > 12 %.

Alloys from the 2nd group are free machining, ergo they are not problematic for the process. The machinability of the alloys from groups 1 and 3, however, can be characterized as more difficult to work with. In group 1 this feature is caused by high plasticity and tendency to form built-up edges or even "clogging" the flutes of rotary tools. Yet, when machining the alloys from group 3 exceeded tool use occurs due to highly abrasive in their nature silicon precipitates [2, 9, 11]. Nonetheless, these alloys posses many beneficial operating properties, such as high strength, resistance to corrosion and abrasive wear, as well as low thermal expansion and excellent castability. All that contributes to their having application in manufacturing of spare parts for combustion engines, compressors, pumps and components of braking systems [5, 7, 9, 11].

To determine the value of wear, the so-called wear indices are used. With geometric quantities they define the wear of flank face and rake face (Fig. 1). The following are the wear indexes of the flank face wear [3, 13]:

VB_B – average flank face wear bandwidth;
VB_{Bmax} – maximum flank face wear bandwidth;
VB_C – nose wear bandwidth;
VB_A – wear bandwidth in A zone;
VB_N – notch wear width;

Rake face wear indices are the following [3, 13]:

KT – crater depth (maximum crater depth on the rake face);
KB – crater width (the distance between primary cutting edge and the most distant crater edge on the rake face);
KE – retreat of tool nose (radius wear) depicted on the tool reference plane as P_r on the intersection point with the tool back plane P_p;
KM – crater center distance defined as the distance between primary cutting edge and its maximum depth, perpendicular to the cutting edge;
KF – the distance between the crater and the primary cutting edge;
K – crater index $K = KT/KM$.

Apart from the aforementioned indices the so-called indirect indices are used, which can be divided into physical and technological. Physical indices are the following [3]:

- vibrations, including acoustic emission (amplitude, frequency),
- components of cutting forces, torque and power,
- cutting temperature,
- chip colour,
- chip form and shape.
- Technological indices are the following [3]:
- dimensional and shape accuracy,
- quality of the surface layer, including mostly surface roughness etc.

(*) Tekst artykułu w polskiej wersji językowej dostępny w elektronicznym wydaniu kwartalnika na stronie ***www.ein.org.pl***

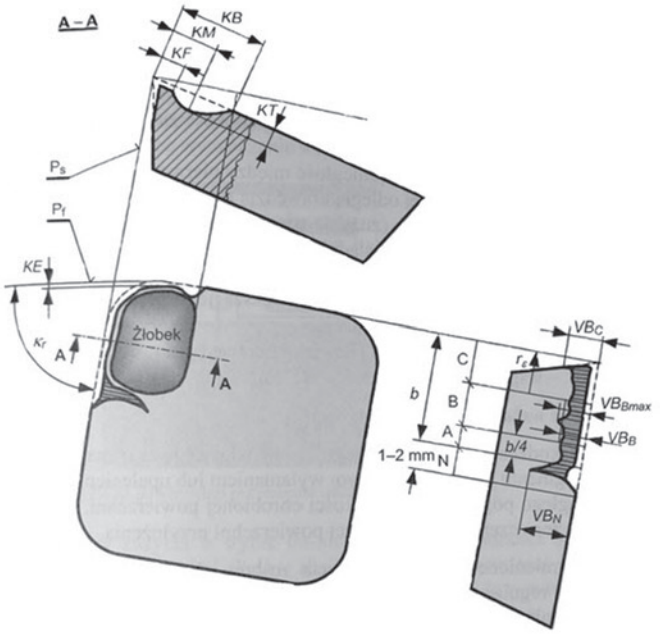

Fig. 1. Wear indices [1]

This paper presents the results of the test concerning wear on cutters of the chosen milling tools resulting from high silicon casting aluminium alloys machining. The criteria for the tool wear identification, except for geometric wear indices, indirect indices were applied, that is cutting forces and machine surface roughness measurements. Excessive usage of tools that occurs when machining these type of alloys increases cutting forces, which affects the machine tool operating conditions [1, 4, 8, 9]. Surface quality deterioration [1], which is also present, affects the utilization qualities of the manufactured elements – surface defects result in lower endurance as the majority of cracks are generated in the surface layer.

To machine hypereutectoid Al-Si alloys machine tools with carbonado teeth or made of carbonado coating sintered carbides are recommended. Such tools are durable and using them, beside decreasing cutting forces, improves the quality of the surface manufactured [1, 2, 8, 10, 16, 18]. However, they are very expensive, which increases manufacturing costs, therefore for the purpose of this paper tests were made with HSS, uncoated carbide machine tools and milling cutters with replaceable inserts, for which the biggest obstacle in high silicon alloys Al-Si machining is their durability.

2. Description and results of the research

As an representative of high silicon silumins EN AC-AlSi21CuNi alloy was used for the purpose of this research. Its chemical composition as well as physical and mechanical properties are presented in Table 1. This alloy is employed mostly for casting of highly loaded pistons in combustion engines and it proves good durability in elevated temperature, low friction factor, high resistance to corrosion and abrasion plus good castability.

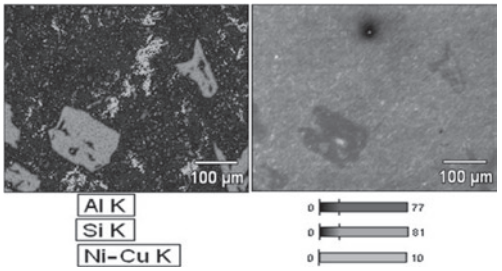

Fig. 2. Depiction of AlSi21CuNi surface from SEM microscope and a map of chemical elements distribution for this alloy

Figure 2 depicts alloy's surface seen through an SEM microscope and a map of chemical elements distribution developed with use of an EDS probe. On the map colour green represents silicon precipitates, light blue shows Ni-Cu phase and red stands for aluminium. Silicon precipitates, which demonstrate high hardness and abrasibility properties causing excessive use of cutters, are clearly visible here.

Three milling cutters, each 20 mm in diameter and made from a different type of material, were used (Fig. 3):

- monolithic HSS milling cutter NFPa Φ20 Z=4,
- folding milling cutter R390-020B20-11L with R390-11 T308E-ML tips,
- monolithic carbide milling cutter without coating E5423200.

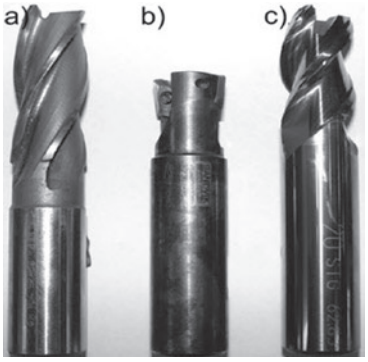

Fig. 3. Tools that were used for machining: a) NFPa, b) R390-020B20-11L, c) E5423200

For each tool different cutting parameters were applied (Table 2), chosen according to the specialist literature or producer's guidelines [14, 15, 17].

Cutting tests consisted of milling a groove (with full diameter of a tool), 20 mm wide and 6 mm deep. Altogether there was 3.6 mm of groove to mill for each tool.

Machining parameters for the milling cutters NFPa φ20, R390-020B20-11L and E5423200 were tagged in Table 2 as P1, P2, P3 accordingly. They differ for each tool in cutting speed, which was assigned depending on the material of a tool.

2.1. Wear of teeth

Most of all, when cutting aluminium alloys, teeth wear occurs in the flank face [3]. Consequently the following two indices were applied to evaluate the wear:

Table 1. Chemical content and properties of the alloy AlSi21CuNi [5, 13]

Designation and chemical content	PN-EN1780-2	Feature	Si	Cu	Ni	Mg	Mn	Cr	Fe	Ti	Zn
	EN AC-AlSi21CuNi	AK20	20-22	1.4-1.5	1.4-1.6	0.4-0.6	0.4-0.6	≤0.7	≤0.7	≤0.2	≤0.2
Physical and chemical properties	Density	Hardness		Abrasability in reference to Al-Cu		Durability R_m		Young's modulus		Poisson ratio	
	2700 kg/m^3	85-110 HB		0.65		150-190 MPa		82000 MPa		0.26	

Table 2. A set of parameters for each tool [14, 15, 17]

The tool	Slot and end mill	Folding slot and end mill	Carbide slot and end mill without coating
Parameter number	P1	P2	P3
Tool designation	NFPa φ20	R390-020B20-11L	E5423200
Working part material	HSS	R390-11 T308E-ML	H10F
Number of teeth	4	2	3
Cutting speed v_c	75 m/min	300 m/min	500 m/min
Rotational speed n	1194 rev/min	4777 rev/min	7962 rev/min
Rate of feed f_z	0,1 mm/tooth	0,1 mm/tooth	0,1 mm/tooth
Rate of travel v_f	478 mm/min	955 mm/min	2389 mm/min
Depth of cut a_p	6 mm	6 mm	6 mm
Width of cut a_e	20 mm	20 mm	20 mm

- maximum wear bandwidth VB_B,
- nose wear bandwidth VB_C.

When performing each test, the course of wear process of each tool was being analyzed, both as a function of the machining time (Fig. 4) and milling path (Fig. 5).

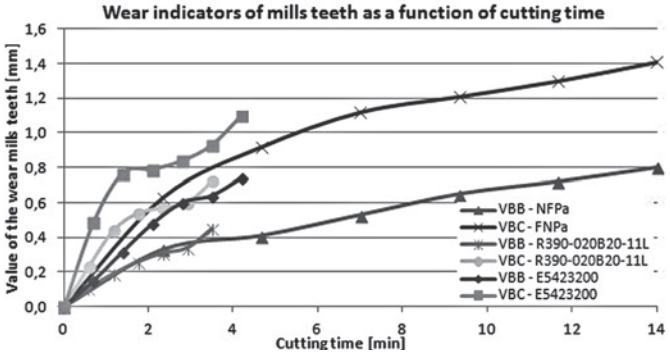

Fig. 4. Wear of the cutter as a function of cutting time (machining parameters for mills: NFPa – P1; R390-020B20-11L – P2; E5423200 – P3 according to Table 2)

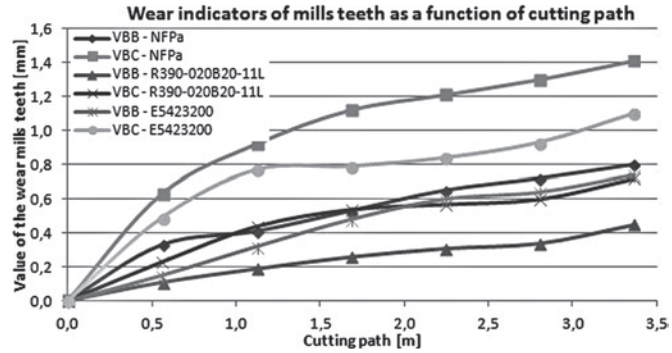

Fig. 5. Wear of the cutter as a function of cutting path (machining parameters for mills: NFPa – P1; R390-020B20-11L – P2; E5423200 – P3 according to Table 2)

The most substantial wear was detected in NFPa mill and a smaller in size but also considerable in carbide tool E5423200. The reason for that is high cutting speed and lack of coating. For R390-020B20-11L mill cutting speed was lower than for the carbide mill and the wear was the smallest. Less sizable wear is also a result of applying indexable tool insert with coating, which reduces abrasion. It is particularly significant in case of hypereutectic silumins machining. When milling them silicon precipitates which appear increase this kind of wear. This research confirms high "abrasibility" of this alloy making it difficult machining.

2.2. Surface quality

There are many factors which influence the roughness of the surface, such as material, quality of workmanship, tool contour and angles, milled material properties, technological parameters applied and other. Among technological parameters the one of the highest influence for the surface quality is rate of feed per tooth f_z. Cutting speed v_c has lower impact on it. When carrying out the research, roughness of the milled groove bottom (Fig. 6a) and its lateral surface (Fig. 6b) were measured. Surface quality, as predicted, deteriorates along with the increased wear of tools. The worst surface quality was observed for NFPa mill made of HSS. Similar surface condition measured on the bottom was detected when the folding and carbide milling cutters were used. These tests proved the lowest roughness of the lateral surface of the groove when carbide mill was applied.

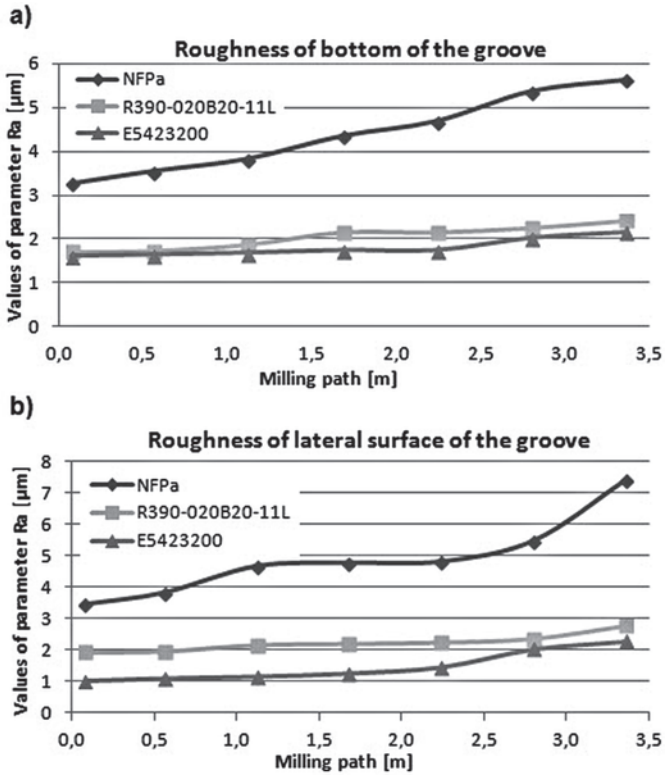

Fig. 6. Surface roughness of: a) bottom of the groove, b) lateral surface of the groove (machining parameters for mills: NFPa – P1; R390-020B20-11L – P2; E5423200 – P3 according to Table 2)

It is worth emphasizing that in spite of substantial wear of the milling cutters, defined with VB_B i VB_C indices, surface roughness as a function of cutting path for mills R390-020B20-11L andE5423200, changes only slightly. These alterations are calculated around 1µm. Yet, the R_a parameter change for NFPa mill circulates around 3µm.

2.3. Cutting forces

Values and amplitudes of cutting forces influence the accuracy and quality of the elements manufactured. High cutting forces cause increased wear of the tools and tool-in-use machines systems. The highest values of cutting forces was observed for the folding tool (mill R390-020B20-11L) and the lowest for the mill E5423200 (Fig. 7).

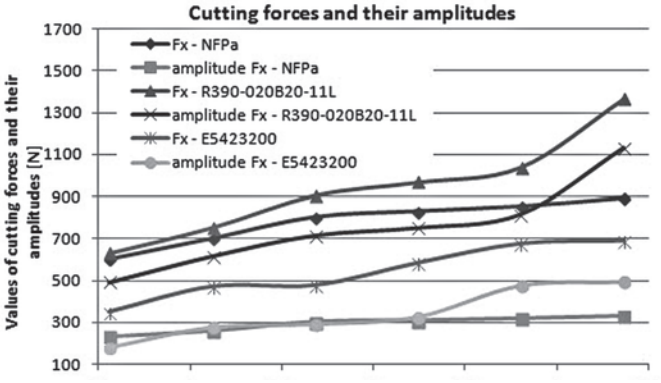

Fig. 7. Maximum values and amplitudes of cutting forces components for different tools (machining parameters for mills: NFPa – P1; R390-020-B20-11L – P2; E5423200 – P3 according to Table 2)

Decreased cutting forces for the carbide tool result from lower cutting resistance which can be contributed to "sharp" tool geometry and high cutting speed (after exceeding certain value v_c, increase in cutting speed causes the cutting forces to decrease). These forces in case of the folding tool are similar to the forces for HSS mill. The forces amplitudes, however, which are the process stability indicators, are the highest for this tool and they exceed to a high degree the values for the two other mills (for the forces components: Fx i Fy ca. 40%). The key factor here is the geometry of the teeth, especially less teeth than in case of the two other tools (Table 2), lower tool rake and helix angles λ_s=5°. Such parameters affect the operating stability of a tool, which results in the increase of cutting forces amplitudes [12].

3. Summary and conclusions

The conducted study and experimental research triggered the following conclusions:

- HSS tools should not be used when machining high silicon silumins.
- The highest increase in cutting forces occurred when machining with folding tool, which is unprofitable due to mill durability, machining tools and quality of the machined surfaces.
- The study shows that among the tools analyzed the most satisfactory results were observed for the carbide mill.
- Ra parameter value is comparable for the carbide mill and the folding mill, thus the choice of the most appropriate tool should be based on economic analysis for each technological situation.
- Cutting forces amplitudes, being a meaningful indicator of the cutting process dynamics, are the highest for the folding mill, which ought to be considered when choosing tools for particular purposes.
- Regardless of significant wear of the tools during the machining, the change of the Ra parameter is relatively small, comparing the beginning and the end of the process. It is of high importance regarding the machining quality.

The experimental study indicate that the tools durability is significant when machining high silicon silumins. This concerns especially automated machining on numerically controlled machine tools. Frequent exchange of tools due to their wear can result in problems both with technological machines control and quality of the elements machined.

Financial support of Structural Funds in the Operational Program – Innovative Economy (IE OP) financed from the European Regional Development Fund, IE OP No. 01.01.02-00-015/08-00 is gratefully acknowledged.

Bibliography

1. Arumugam P U, Malshe A P, Batzer S A. Dry machining of aluminum–silicon alloy using polished CVD diamond-coated cutting tools inserts. Surface and Coatings Technology 2006; 11: 3399–3403.
2. Burek J, Płodzień M. Wysokowydajna obróbka części ze stopów aluminium o złożonych kształtach. Mechanik 2012; 7: 542–549.
3. Cichosz P. Narzędzia skrawające. Wydawnictwa Naukowo-Techniczne 2007.
4. Davima J P, Baptista A M. Relationship between cutting force and PCD cutting tool wear in machining silicon carbide reinforced aluminum. Journal of Materials Processing Technology 2000; 103: 417–423.
5. Dobrzański L A. Podstawy nauki o materiałach i metaloznawstwo. Wydawnictwa Naukowo-Techniczne 2007.
6. Feld M. Obróbka skrawaniem stopów aluminium. Wydawnictwa Naukowo-Techniczne 1984.
7. Haque M M, Khan A A, Ismail A A. Investigation on tool wear rate for modified and unmodified aluminum-silicon casting alloy. International Journal of Modern Physics 2009; Vol. 23, Nos. 6 & 7: 826–831.
8. Hu J, Chou Y K, Thompson R G. Nanocrystalline diamond coating tools for machininghigh - strength Al alloys. International Journal of Refractory Metals & Hard Materials 2008; 26: 135–144.
9. Liu J, Chou K Y. On temperatures and tool wear in machining hypereutectic Al–Si alloys with vortex-tube cooling. International Journal of Machine Tools and Manufacture 2007; 3–4: 635–645.
10. Martini C, Morri A. Face milling of the EN AB-43300 aluminum alloy by PVD- and CVD-coated cemented carbide inserts. International Journal of Refractory Metals and Hard Materials 2011; 29: 662–673.
11. Oczoś K E, Kawalec A. Kształtowanie metali lekkich. Wydawnictwo Naukowe PWN 2012.
12. Pieśko P, Kuczmaszewski J. Obróbka skrawaniem współczesne problemy. Analiza wpływu czynnej długości krawędzi skrawającej na wartość i przebieg sił skrawania. Agencja MAGA 2010; IV Szkoła Obróbki Skrawaniem: 309–316.
13. Polskie Normy: PN-EN 573:3 2005; PN-EN 1780-2:2004; PN-ISO 3685:1996.
14. Poradnik CoroGuide. AB Sandvik Coromant 2007.

15. Poradnik Obróbki Skrawaniem. AB Sandvik Coromant 2010.
16. Roy P, Sarangi S K, Ghosh A, Chattopadhyay A K. Machinability study of pure aluminium and Al–12% Si alloys against uncoated and coated carbide inserts. International Journal of Refractory Metals & Hard Materials 2009; 27: 535–544.
17. Wołk R. Normowanie obróbki skrawaniem. Państwowe Wydawnictwa Techniczne 1972.
18. Yoshikawa H, Nishiyama A. CVD diamond coated insert for machining high silicon aluminum alloys. Diamond and Related Materials 1999; 8: 1527–1530.

Józef KUCZMASZEWSKI
Paweł PIEŚKO
Department of Production Technology
Lublin University of Technology
ul. Nadbystrzycka 36D, 20-618 Lublin, Poland
E-mails: j.kuczmaszewski@pollub.pl; p.piesko@pollub.pl

Article citation info:
ROJEK I, STUDZIŃSKI J. Comparison of different types of neuronal nets for failures location within water-supply networks. Eksploatacja i Niezawodnosc – Maintenance and Reliability 2014; 16 (1): 42–47.

Izabela ROJEK
Jan STUDZIŃSKI

COMPARISON OF DIFFERENT TYPES OF NEURONAL NETS FOR FAILURES LOCATION WITHIN WATER-SUPPLY NETWORKS

PORÓWNANIE RÓŻNYCH TYPÓW SIECI NEURONOWYCH DO LOKALIZACJI AWARII W SIECIACH WODOCIĄGOWYCH*

The different types of neuronal nets for failures location within a water-supply network are presented in the paper. The present utilization of the monitoring systems does not exhaust their possibilities. The monitoring systems operated as autonomic programs gather the information about flows and pressures of water in the source pumping stations, in the zones of hydrophore stations and also in some selected pipes of water network, giving general knowledge about state of its work, when simultaneously they could and should be used as elements of IT systems for network management, and particularly regarding detection and location of hidden water leaks. The models of network failures location are created by means of neuronal nets in the form of MLP and Kohonen nets.

***Keywords**: water-supply networks, network hydraulic models, detection and location of water leaks, MLP and Kohonen neuronal nets.*

W artykule prezentowane są różne typy sieci neuronowych do lokalizacji awarii w sieci wodociągowej. Obecne wykorzystanie systemów monitorowania nie odpowiada ich możliwościom. Współcześnie systemy monitoringu służą jako autonomiczne programy do zbierania informacji o przepływach i ciśnieniach wody w pompowniach źródłowych, hydroforniach strefowych i końcówkach sieci wodociągowej, dając ogólną wiedzę o stanie jej pracy, gdy jednocześnie mogą i powinny być wykorzystane jako elementy IT systemów zarządzania siecią, w tym w szczególności w zakresie wykrywania i lokalizacji wycieków wody. Modele lokalizacji awarii sieci zostały utworzone przy wykorzystaniu jednokierunkowych sieci neuronowych ze wsteczną propagacją błędu typu MLP i sieci Kohonena.

***Słowa kluczowe**: sieci wodociągowe, modele hydrauliczne sieci, wykrywanie i lokalizacja wycieków wody, sieci neuronowe MLP i Kohonena.*

1. Introduction

At the Systems Research Institute of Polish Academy of Sciences (IBS PAN) an IT system for computer aided management of communal water networks has been developed and one of its tasks is the water net failures localization [9]. To do it the water net hydraulic model and a SCADA system installed on the water net are used. In the paper a new algorithms for the water net failures localization using the water net hydraulic model, a SCADA system and the MLP (multilayer network with error back propagation) or Kohonen neuronal nets is described.

The waterworks enterprise regarding the water network management deals with the water distribution of appropriate quality and in quantity guaranteeing satisfaction of the recipient's needs, with correct exploitation of water-supply network assuring the proper pressure in receiving units, with the efficient removing of failures and with planning and executing the works connected with conservation, modernization and extension of the network [2]. One can say that there are generally 3 main tasks of water net management: water supply in desired amounts to the water net end users [6], production of water of desired quality [6, 14] and reduction of water net operational costs; in the latter case the reduction of water losses resulted through the water net failures is one of the most essential management problems [3, 4, 8, 13, 15]. The water leaks can cause the losses of water in pipelines coming sometimes even to 30% of the whole water production what influences negatively the financial results of waterworks enterprises. Therefore the fast location and elimination of hidden leaks of water from leaky pipelines brings the measurable economic advantages both for the supplier, that is the water-supply enterprise, and for the users of the water network.

2. Algorithms of failure location in water-supply networks

Different approaches and the computational algorithms to aid detection and location of water leaks in water networks have been already described by many authors. In each case the measurements of water flow and pressures in the water net and sometimes also the water network hydraulic model are the basis of investigation. An appropriate computer infrastructure installed and exploited in the waterworks is needed for practical realization of these algorithms. Different stages of the water net failures localization can be presented in the following way:

- failure detection – a failure state on a water net is determined through observation of a higher water reception, but its location is not known,
- failure location – failure state and its exact or approximate location are determined by means of some suitably worked algorithms, with the use of a monitoring system, hydraulic models of water network and potentially of neural networks,
- failure counteraction – prognoses of coming failures basing on historical data concerning the previous failure cases are calcu-

(*) Tekst artykułu w polskiej wersji językowej dostępny w elektronicznym wydaniu kwartalnika na stronie ***www.ein.org.pl***

lated and using them the development of plans of water net revitalization is occurred.

On the first stage of investigation only appropriate densely monitoring and diagnostic systems (SCADA) installed on the water nets can be used whose tasks are to find out and to localize the arisen leaks. The diagnostic methods implemented in these systems exploit in their calculations the measurements of water flows in the water net pipes like pressure, velocity, flow rate and temperature [1, 3, 13] and the only disadvantage of them is the necessity of installation of many measurement devices on the pipelines. This induces high costs of the whole installation which mostly are not to cover by the waterworks. On the second stage beside the technical infrastructure as SCADA also several software applications are in use for failure location in the water networks what makes the problem more sophisticated. In a more simple version of investigation the additional items being the complement of the monitoring system are mathematical models of the water network and these models are mostly a water net hydraulic model to simulate the network and a parametrical model for modeling the hydraulic one [15, 16]; in the latter case often neuronal nets or fuzzy sets or time series models are used. By more complex versions of investigation integrated IT systems are used that consist not only of SCADA and water net mathematical models but also of a GIS system and of different algorithms of optimization. Such the technical and information infrastructure permits not only to detect and locate the water net failures but also to manage the network, executing such the tasks like the water net control, analysis of water quality, optimization and design of the network etc. [8, 11]. This marks that the high developed computer technologies can become in future an useful and indispensable tool for the water net operators and the waterworks decision makers helping the rational operation and exploitation of the network and the whole enterprise. So far such the complex and integrated IT systems because of their very high costs are under development mostly in academic units but not in use in Polish waterworks [10]. On the third stage of investigation the problem to be solved concerns not the finding out the water net failures that have been already occurred but it consists in recognition of the potential failure risk and in eliminating it by appropriate technical counteractions.

The analysis presented in the paper belongs to the second stage of investigation and it consists on detection and localization of water net failures by means of an IT system consisting of GIS, SCADA, a water net hydraulic model and of neuronal nets simulating the network by means of its hydraulic model. The goal of the investigation is to confirm the usefulness of neuronal nets by modeling the water networks and detecting their failures. A positive result will allow to include this modeling tool into the IT system developed as an integral system module. The exemplary calculations have been made with the real data coming from the communal waterworks in Rzeszow [5] and the neuronal nets applied were MLP and Kohonen ones [12]. The investigation has been made using the following algorithm:

1. Planning the monitoring system to be installed on the water net investigated. The system shall consist of specially selected measurement points which are most sensitive against the flow and pressure changes arisen in the water net.
2. Calibration of the water net hydraulic model by using the monitoring system planed.
3. Hydraulic calculations of the water networks by its standard load to determine the standard distributions of flows and pressures in the selected monitoring points.
4. Successive simulation of water leaks in all nodes of the water net by use of the hydraulic model to determine the distributions of flows and pressures in the monitoring points resulted from the failures simulated.
5. Creation of the neuronal classifier locating the failures in form of different type of neural nets and choice of the best classifier according to criterion of the largest sensibility.

2.1. Planning the monitoring system regarding the most sensitive water net points

While planning a monitoring system the number and location of the measurement points must be defined carefully. It means that regarding the high installation costs the number of points shall be minimized and their location shall be chosen in the way assuring the winning of possibly most information concerning the water flow changes in the water net. Such the sensitive points reacting on the flow changes not only in their closest neighborhood but also in farther surroundings are called characteristic points and their choice is not a trivial problem. Usually while planning monitoring systems for water nets the goal to maximize recorded information will be achieved by maximizing the number of monitoring points what raises the monitoring costs and discourages the decision makers to develop the sufficient densely systems. As a result the systems installed are not suited to calibrate the water net hydraulic models neither to find out the water leaks. To solve this problem properly an algorithm of multi-criterion optimization can be used with 2 criteria regarding the number of measuring points and the quantity of gaining information [8]. The minimized number of measuring points concerns the water net characteristic points and the choice of them can be performed for example by means of the algorithm proposed by Straubel and Holznagel in [7]. In our investigation the rang list of sensitive points of the water network in Rzeszow has been made using the algorithm of Straubel and Holznagel and for the farther calculations two sets of points were choosen for the planed monitoring system: one set with 10 most sensitive points and the second set with 20 measuring points.

2.2. Hydraulic calculation of the water network by use of the calibrated hydraulic model

After the monitoring system has been already planed the calibration of the water net hydraulic model can be automatically executed. To do this a multi-criterion optimization can be also used with two criteria regarding the differences between the measured and calculated values of water flows and pressures in the monitoring points [8]. With the hydraulic model calibrated the simulation runs for the water net with its standard load (normal state) and with the simulated water leaks in different net nodes (failure states) can be performed. The recorded values of flows and pressures in the monitoring points for normal and failure states of the water net can be used for the preparation of learning files for the neural networks that will serve in turn as models to detect and locate the failures in the water network. In our investigation for its simplification only the water flow values have been regarded and recorded.

The simulation of water leaks in the water net has been made as follows:

- the values of water flow in chosen network nodes have been enlarged for several times,
- each time the hydraulics of the water net has been calculated using the hydraulic model,
- the differences in flow values between the normal and failure states of the water net observed in the monitoring points have been recorded,
- the monitoring point with strongest reaction on the simulated failure has been registered.

2.3. Creation of the neuronal classifier locating the failures using the MLP networks

The models for failure detection and location are created by use of neural networks of MLP type [12]. These networks are currently most widespread and used in the practice. In a multi-layer network with error backpropagation (MLP) the selection of number of neurons in input layer is conditioned by the dimension of data vector *x*. The neu-

ral model consists of the sum of input signals x_1, x_2, ..., x_N multiplied by weight coefficients w_{i1}, w_{i2}, ..., w_{iN} and of an additional value w_{i0}. The output signal of the model marked u_i has got the form:

$$u_i = \sum w_{ij} x_j + w_{i0} \tag{1}$$

and it is subsequently given to a non-linear activation sigmoidal function $f(u_i)$:

$$f_u(u_i) = \frac{1}{1+\exp(-\beta u_i)} \tag{2}$$

In the calculations performed the experiments with neuronal networks of different structure and with 1 hidden layer have been executed. The water net investigated consists of 390 nodes. On the first step of calculations 10 monitoring points have been considered and in 36 selected nodes the water leaks have been simulated. On the second step the number of monitoring points raised to 20 and the number of nodes with water leaks raised to 44. The neuronal classifier was created according to the methodology described in [4]. While calculating the MLP models 2 parameters were changed in the network structure: the number of neurons in the hidden layer that changed from 5 to 25 and the number of learning epochs that has taken the values 200, 500 and 1000. The inputs of the neural nets calculated are the flow values in the water net nodes with simulated leaks and the output of the neural nets shows the monitoring point with strongest reaction on the water leak (Fig. 1).

27	28	29	30	31	32	33	34	35	36	37
2740	2779	3028	6144	3587	3596	4138	4181	4250	4411	Monitoring point
-5,04	-94,46	-2,71	-2,79	-3,1	-8,43	-6,31	-2,2	-1,69	-4,76	0
-5,04	-94,46	-2,71	-2,79	-3,1	-8,43	-6,31	-2,2	-1,69	-4,76	4
-5,04	-94,46	-2,71	-2,79	-3,1	-8,43	-6,31	-2,2	-1,69	-4,76	6
-5,04	-94,46	-2,71	-2,79	-3,1	-8,43	-6,31	-2,2	-1,69	-4,76	6
-25,04	-94,46	-2,71	-2,79	-3,1	-8,43	-6,31	-2,2	-1,69	-4,76	7
-5,04	-470,46	-2,71	-2,79	-3,1	-8,43	-6,31	-2,2	-1,69	-4,76	10
-5,04	-94,46	-10,71	-2,79	-3,1	-8,43	-6,31	-2,2	-1,69	-4,76	4

Fig. 1. The structure of teaching set for MLP nets; columns 27 till 36 are the inputs and column 37 is the output

Table 1. The parameters of MLP nets for 10 monitoring points

No	Network name	Teaching quality	Testing quality	Validation quality
1	MLP 36-8-11	88,31776	95,55556	88,88889
2	MLP 36-15-11	97,66355	97,77778	95,55556
3	MLP 36-22-11	94,39252	97,77778	93,33333
4	MLP 36-19-11	97,66355	97,77778	95,55556
5	MLP 36-21-11	94,39252	97,77778	93,33333
6	**MLP 36-24-11**	**97,19626**	**97,77778**	**97,77778**
7	MLP 36-23-11	97,66355	97,77778	95,55556

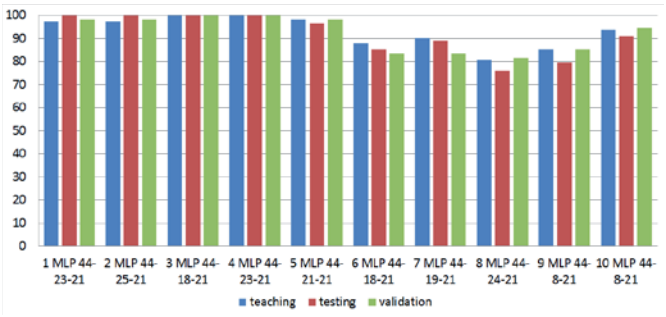

Fig. 2. Calculation results of the MLP nets obtained for 20 monitoring points [%]

Table 2. The parameters of MLP nets for 20 monitoring points; the qualities are given in %.

No	Network name	Teaching quality	Testing quality	Validation quality
1	MLP 44-23-21	97,2222	100,0000	98,1481
2	MLP 44-25-21	97,2222	100,0000	98,1481
3	**MLP 44-18-21**	**100,0000**	**100,0000**	**100,0000**
4	**MLP 44-23-21**	**100,0000**	**100,0000**	**100,0000**
5	MLP 44-21-21	98,0159	96,2963	98,1481
6	MLP 44-18-21	87,6984	85,1852	83,3333
7	MLP 44-19-21	90,0794	88,8889	83,3333
8	MLP 44-24-21	80,5556	75,9259	81,4815
9	MLP 44-8-21	85,3175	79,6296	85,1852
10	MLP 44-8-21	93,6508	90,7407	94,4444

Table 3. Calculation results of MLP nets for new data files (20 monitoring points)

Results of MLP net for new data on input											
No.	1 MLP 44-23-21	2 MLP 44-25-21	**3 MLP 44-18-21**	**4 MLP 44-23-21**	5 MLP 44-21-21	6 MLP 44-18-21	7 MLP 44-19-21	8 MLP 44-24-21	9 MLP 44-8-21	10 MLP 44-8-21	**Pattern**
1	4	4	**0**	**0**	0	0	11	0	0	0	**0**
2	3	3	**3**	**3**	3	3	3	3	3	3	**3**
3	8	8	**8**	**8**	8	8	8	8	8	8	**8**
4	15	15	**15**	**15**	15	19	15	15	15	15	**15**
5	11	11	**11**	**11**	11	11	11	11	11	11	**11**
6	13	13	**13**	**13**	13	13	13	13	13	20	**13**
7	4	4	**4**	**4**	4	4	4	4	4	20	**4**
8	16	16	**16**	**16**	16	16	16	16	16	16	**16**
9	12	12	**12**	**12**	12	2	12	12	12	12	**12**
10	7	7	**7**	**7**	7	15	7	13	1	7	**7**
11	9	9	**9**	**9**	9	9	7	13	6	9	**9**
12	20	20	**20**	**20**	20	20	20	0	20	20	**20**
13	1	1	**1**	**1**	1	2	1	13	1	13	**1**
14	2	2	**2**	**2**	0	2	2	15	0	2	**2**
15	17	17	**17**	**17**	17	15	5	13	17	17	**17**
16	5	5	**5**	**5**	5	10	5	15	16	5	**5**
17	6	6	**6**	**6**	6	19	6	13	6	14	**6**
18	14	14	**14**	**14**	14	2	10	13	6	14	**14**
19	18	18	**18**	**18**	18	2	19	15	18	14	**18**
20	19	19	**19**	**19**	19	19	19	13	7	19	**19**
21	10	10	**10**	**10**	0	10	10	13	0	10	**10**
22	13	13	**13**	**13**	13	13	13	13	0	1	**13**
Number of correct classifications	21	21	**22**	**22**	20	13	17	10	14	16	
Number of incorrect classifications	1	1	**0**	**0**	2	9	5	12	8	6	
Number of correct classifications in %	98,46	98,46	**100,00**	**100,00**	97,49	85,41	87,43	79,32	83,38	92,95	

The number of examples for determining the neural nets is 304 for the first step of calculation with 10 monitoring points and 360 for the second step with 20 monitoring points. The teaching, testing and validation files contained every time 70%, 15% and 15% of examples.

In Tables 1 and 2 and in Fig. 2 one can see the results of calculation got for the cases with 10 and 20 monitoring points. Model MLP 36-24-11 with 24 neurons on the hidden layer is best for 10 monitoring points (medium quality equals to 97,58%) and models MLP 44-18-21 and MLP 44-23-21 are equally best for 20 monitoring points (with medium quality of 100%).

Table 3 shows the results of calculation with the MLP models determined for 20 monitoring points and with new data files prepared for checking the models correctness under new conditions of computation. One can see that the best models MLP 44-18-21 and MLP 44-23-21 that have been received with the old data confirm also their efficiency by means of these checking runs.

2.4. Creation of the neuronal classifier locating the failures using the Kohonen networks

The models for failure location in the water net are presently created by use of the neural networks of Kohonen type. Kohonen nets are one of the basic types of self-organizing nets. Just thanks to ability of self-organization they open completely new possibilities and one of them is the adaptation to the input data which were previously not known [12]. Kohonen nets are usually one-way nets in which each neuron is connected with all components of N-dimensional input vector x. The weight coefficients of neurons connections create the vector $w_i=[w_{i1}, w_{i2}, ..., w_{iN}]^T$. The input signals are on the begin of computation normalized, i.e. $||x||=1$, what could be written down as follows:

$$x_i = \frac{x_i}{\sqrt{\sum_{v-1}^{N}(x_v)^2}} \tag{3}$$

After stimulating the network by the input vector x a kind of competition occurs between the neurons and the winner w_w fulfills the relation:

$$d(x, w_w) = \min_{l \le i \le n} d(x, w_i) \tag{4}$$

where $d(x, w_i)$ means the distance between vector x and vector w in Euclidean space. Each neuron is enclosed with a topological neighborhood $G(i,x)$ and in the classic Kohonen algorithm function $G(i,x)$ is defined as follows:

$$G(i,x) = \begin{cases} 1 & \text{dla } d(i,w) \le R \\ 0 & \text{dla } d(i,w) > R \end{cases} \tag{5}$$

where R means the neighborhood radius. While calculating a Kohonen net the radius R shall diminish to 0.

By the calculation of Kohonen models the nets were parameterized by two parameters: the number of neurons in the so called topological layer and the number of teaching epochs. The first parameter has taken the values 2x8, 5x5, 10x10 and the second parameter has taken the values from 1000 to 20000. Similarly to the previous investigation the network inputs are the flow values for normal and failure states of the water net in the nodes selected for the water leaks simulation and additionally the number of the most sensitive monitoring point is also considered as the input signal. In a Kohonen network does not exist an output. Two investigation steps have been performed regarding 10 and 20 monitoring points and 36 and 44 water net nodes have been selected for the water leak simulations in respective steps.

In Fig. 3 the structure of the teaching file for the first step of investigation is shown in which all columns mean the input data for the neural nets calculated. In the calculations 304 examples were used for the investigation step with 10 monitoring points and 360 examples were used for the second step. The teaching, testing and validation files contain in the following 70%, 15% and 15% examples. In Tables 4 and 5 and in Fig. 4 the calculation results obtaining for the Kohonen nets while performing the first and second steps of investigation are shown. In the first case the model SOFM 37-100/100 and in the second case the model SOFM 45-225/1000 are the best.

24	25	26	27	28	29	30	31	32	33	34	35	36	37
2158	2186	2447	2740	2779	3028	6144	3587	3596	4138	4181	4250	4411	Monitoring point
-25,7	-4,2	-4,83	-5,04	-94,46	-2,71	-2,79	-3,1	-8,43	-6,31	-2,2	-1,69	-4,76	4
-5,74	-20,2	-4,83	-5,04	-94,46	-2,71	-2,79	-3,1	-8,43	-6,31	-2,2	-1,69	-4,76	6
-5,74	-4,2	-20,8	-5,04	-94,46	-2,71	-2,79	-3,1	-8,43	-6,31	-2,2	-1,69	-4,76	6
-5,74	-4,2	-4,83	-25	-94,46	-2,71	-2,79	-3,1	-8,43	-6,31	-2,2	-1,69	-4,76	7
-5,74	-4,2	-4,83	-5,04	-470,5	-2,71	-2,79	-3,1	-8,43	-6,31	-2,2	-1,69	-4,76	10
-5,74	-4,2	-4,83	-5,04	-94,46	-10,7	-2,79	-3,1	-8,43	-6,31	-2,2	-1,69	-4,76	4
-5,74	-4,2	-4,83	-5,04	-94,46	-2,71	-2,79	-3,1	-8,43	-6,31	-2,2	-1,69	-20,8	2
-5,74	-4,2	-4,83	-5,04	-94,46	-2,71	-2,79	-3,1	-8,43	-6,31	-2,2	-1,69	-4,76	0

Fig. 3. The structure of teaching set for Kohonen nets

Table 4. The parameters of Kohonen nets for 10 monitoring points

No	Network name	Teaching quality	Testing quality	Validation quality
1	SOFT 37-16/1000	81,9384	14,3036	7,4902
2	SOFT 37-16/20000	20,0225	20,9363	11,9975
3	SOFT 37-25/1000	20,3248	17,1003	12,9749
4	**SOFT 37-100/1000**	**80,8903**	**79,7651**	**83,4712**
5	SOFT 37-100/10000	82,7746	76,2847	78,0958
6	SOFT 37-100/20000	83,1150	73,5965	79,7852

Table 5. The parameters of Kohonen nets for 20 monitoring points

No	Network name	Teaching quality	Testing quality	Validation quality
1	SOFT 45-25/15000	9,7870	4,7473	4,7570
2	SOFT 45-100/1000	71,1903	66,3754	70,7134
3	SOFT 45-100/10000	61,7010	61,5446	59,4152
4	SOFT 45-100/15000	69,1089	68,1126	62,5354
5	SOFT 45-100/20000	69,4488	67,6256	61,6244
6	**SOFT 45-225/1000**	**97,3839**	**99,1899**	**97,9011**

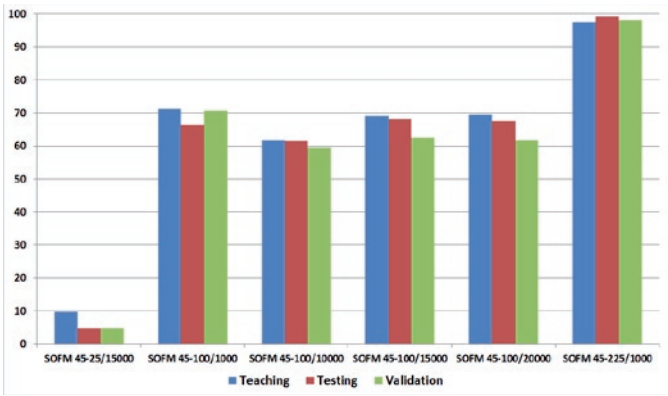

Fig. 4. Calculation results of the Kohonen nets obtained for 20 measurement points [%]

Table 6. Calculation results of Kohonen net for new data files (20 measurement points)

Results of Kohonen net for new data on input							
No.	1 SOFT 45-25/15000	2 SOFT 45-100/1000	3 SOFT 45-100/10000	4 SOFT 45-100/15000	5 SOFT 45-100/20000	**6SOFT 45-225/1000**	**Pattern**
1	15	0	0	0	0	**0**	**0**
2	3	3	3	3	3	**3**	**3**
3	8	8	8	8	8	**8**	**8**
4	0	15	7	15	9	**7**	**15**
5	11	11	11	11	11	**11**	**11**
6	16	13	13	13	13	**13**	**13**
7	4	4	4	4	4	**4**	**4**
8	13	16	16	16	16	**16**	**16**
9	7	12	12	12	12	**12**	**12**
10	12	7	15	7	7	**15**	**7**
11	1	9	20	9	15	**9**	**9**
12	20	20	9	20	20	**20**	**20**
13	9	2	1	1	1	**1**	**1**
14	17	1	2	2	2	**2**	**2**
15	2	17	5	17	5	**17**	**17**
16	6	6	17	6	17	**5**	**5**
17	5	5	14	5	18	**6**	**6**
18	18	14	6	19	14	**14**	**14**
19	14	19	19	18	6	**18**	**18**
20	10	18	18	14	10	**19**	**19**
21	19	9	8	9	19	**10**	**10**
22	11	13	13	13	13	**13**	**13**
Number of correct classifications	5	15	11	17	14	**21**	
Number of incorrect classifications	17	7	11	5	8	1	
Number of correct classifications in %	22,73	68,18	50,00	77,27	63,64	**98,16**	

Table 6 shows the results of calculation with the Kohonen models received for 20 monitoring points and with the new data files prepared for checking the models correctness under new conditions of computation. The results confirm once again that model SOFM 45-225/1000 is the best and its quality equal to 98,16% is similar to this one from earlier calculations.

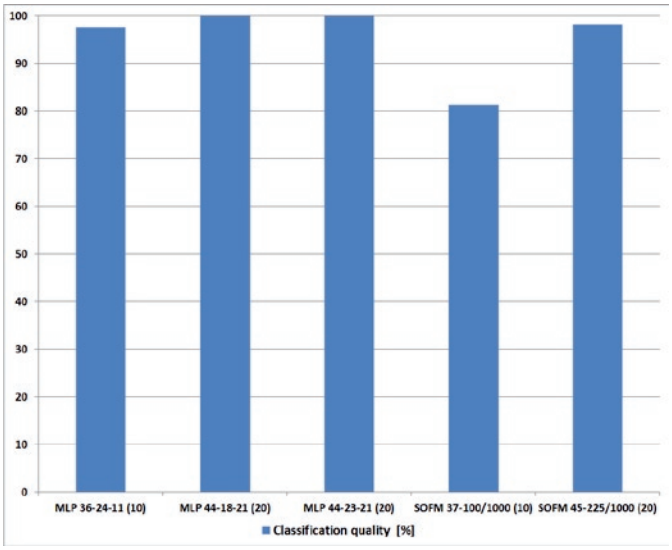

Fig. 5. Comparison of MLP and Kohonen nets.

Table 7. Comparison of MLP and Kohonen nets

No	Net name	Number of measurement points	Classification quality [%]
1	MLP 36-24-11	10	97,58
2	MLP 44-18-21	20	100,00
3	MLP 44-23-21	20	100,00
4	SOFM 37-100/1000	10	81,38
5	SOFM 45-225/1000	20	98,16

2.5. Comparison of MLP and Kohonen nets and choice of the best classifier

In Table 7 and in Fig. 5 the results of comparison between MLP and Kohonen nets is presented. The results show a supriority of MLP models in relation to the Kohonen ones while detecting and locating the water network failures. MLP nets have got in general shorter times of teaching and they give the better classification nof the water leaks.

3. Conclusions

The received results of computation show the usefulness of neural networks by the solution of such complicated problems as detection of water net failures and their localization. This means that the neuronal models can be used as efficient tools included as integral elements into computer aided IT systems applied for management of waterworks.

Acknowledgement:
The paper is issued in frame of the project No NR14-0011-10/2010 financed by the Polish Ministry of Sciences and Higher Education.

References

1. Billman L, Isermann R. Leak detection methods for pipelines. Automatica 1987; 23: 381–385.
2. Farmani R, Ingeduld P, Savic D, Walters G, Svitak Z, Berka J. Real-time modeling of a major water supply system. International Conference on Computing and Control for the Water Industry 2007; 160(2): 103–108.
3. Kowalczuk Z, Gunawickrama K. Detecting and locating leaks in transmission pipelines. Fault Diagnosis: Models, Artificial Intelligence, Applications. Berlin: Springer-Verlag, 2004; 822–864.

4. Rojek I. Study of failure location algorithms in form of neuronal nets for water-supply networks. The report to the research project No. 14-0011-10/2010. Warsaw: IBS PAN, 2012 (in Polish).
5. Rojek I, Studziński J. Failures location algorithms for water-supply network by use the neural networks. Studies & Proceedings of Polish Association for Knowledge Management 2011; 8: 146–156 (in Polish).
6. Smarter Water Management. IBM, 2009; http://www.ibm.com/ibm/ideasfromibm/us/smartplanet/ topics/water-management/.
7. Straubel R, Holznagel B. Mehrkriteriale Optimierung für Planung und Steuerung von Trink- und Abwasser-Verbundsystemen. Wasser Abwasser 1999; 140(3): 191–196.
8. Studziński J. Rechnerunterstützte Endscheidungshilfe für kommunale Wasserwerke mittels mathematischer Modelle. Krigingsapproximation und Optimierung. Modellierung und Simulation von Ökosystemen. Workshop Kölpinsee 2011.
9. Studziński J. Decisions making systems for communal water networks and wastewater treatment plants. Modeling Concepts and Decision Support in Environmental Systems. Warsaw: IBS PAN, 2006; 49.
10. Studziński J. The innovations of XXI age – the modern information techniques for the management in network enterprises. Innovative Mazovia. Płock: Publishing House of SWPW, 2010 (in Polish).
11. Rojek I. Support of decision making processes and control in systems with different scale of complexity using artificial intelligence methods. Bydgoszcz: Publishing House of Kazimierz Wielki University, 2010 (in Polish).
12. Tadeusiewicz R. Discovery of neural networks properties using programs in C + + . Cracow: Polish Academy of Arts and Sciences, 2007 (in Polish).
13. Turkowski M, Bratek A, Słowikowski M. Methods and systems of leak detection in long range pipelines. Journal of Automation, Mobile Robotics & Intelligent Systems 2007; 1: 39–46.
14. Wei S, Gnauck A. Game Theory Based Water Quality Models for Reservoir Management. Environmental Informatics and Systems Research. 21st Conference on Informatics for Environmental Protection ENVIROINFO. Aachen: Shaker Verlag, 2007; 1: 363–370.
15. Wyczółkowski R, Moczulski W. Concept of intelligent monitoring of local water supply system. Artificial Intelligence Methods AI-METH. Gliwice: Silesian University of Technology, 2005; 147–148.
16. Wyczółkowski R, Wysogląd B. An optimization of heuristic model of water supply network. Computer Assisted Mechanics and Engineering Science CAMES 2007; 14: 767–776.

Izabela ROJEK
Institute of Mechanics and Applied Computer Science
Kazimierz Wielki University
ul. Chodkiewicza 30, 85-064 Bydgoszcz, Poland
E-mail: izarojek@ukw.edu.pl

Jan STUDZIŃSKI
Systems Research Institute Polish Academy of Sciences
ul. Newelska 6, 01-447 Warsaw, Poland
E-mail: studzins@ibspan.waw.pl

Article citation info:
VALIS D, PIETRUCHA-URBANIK K. Utilization of diffusion processes and fuzzy logic for vulnerability assessment. Eksploatacja i Niezawodnosc – Maintenance and Reliability 2014; 16 (1): 48–55.

David VALIS
Katarzyna PIETRUCHA-URBANIK

UTILIZATION OF DIFFUSION PROCESSES AND FUZZY LOGIC FOR VULNERABILITY ASSESSMENT

WYKORZYSTANIE PROCESÓW DYFUZYJNYCH I LOGIKI ROZMYTEJ DO OCENY PODATNOŚCI NA ZAGROŻENIE*

Assessing the vulnerability of critical infrastructure objects is of major concern when dealing with the process of dependability and risk management. Special attention is paid to the objects of higher interest, such as nuclear power plants. In spite of the protection of these objects, there is still a certain level of a potential threat. The aim of the paper is to describe a possible way of attacking on the object in order to get into a particular part of it. Several characteristics of an adversary´s attempt were obtained. For this reason as well as for modelling adversary´s behaviour diffusion processes have been used.

***Keywords**: vulnerability, critical infrastructure, diffusion processes.*

Ocena podatności na zagrożenie kluczowych obiektów infrastruktury jest głównym problemem rozpatrywanym w kontekście procesu niezawodności oraz zarządzania ryzykiem. Szczególną uwagę przywiązuje się do obiektów wysokiej rangi, takich jak elektrownie jądrowe. Pomimo ochrony tych obiektów, nadal istnieje pewien poziom potencjalnego ich zagrożenia. Celem artykułu jest opisanie możliwego sposobu zaatakowania obiektu z zamiarem dostania się do konkretnej jego części. Otrzymano kilka charakterystyk próby ataku ze strony przeciwnika. Do tego celu, jak również do zamodelowania zachowania przeciwnika, wykorzystano procesy dyfuzyjne.

***Słowa kluczowe**: podatność na zagrożenie, kluczowa infrastruktura, procesy dyfuzyjne.*

1. Introduction – motivation

Modern history is rich with examples of various terrorist attacks against structures, transportation systems, etc. worldwide. In the aftermath of the September 11th tragedies, the vulnerability of the whole infrastructure to terrorist attack has gained national attention. In light of this vulnerability, various governmental agencies are looking into ways to improve the design of structures to better withstand extreme loadings. Tens of per cent of the homeland security outlays are devoted by countries to making potential targets less vulnerable to potential terrorist attacks. This is to protect what we usually call "Critical Infrastructure", "Key Asset" and/or "Key Resources". The objective of this article is to assess the behaviour of a potential adversary whose intention is either to damage the object/system, or steal nuclear material. Since the behaviour of an adversary is highly unpredictable (at least at the beginning) and the result is rather uncertain (although we expect he needs to reach the goal), the way of describing his behaviour will be tackled in more detail. The process of breaking into the building is continuous in time. However, its development is dynamic and changeable, and, as we have mentioned before, the result is quite indeterminate [2, 23, 24, 32, 37, 38, 42]. But the adversary makes an effort to achieve the goal to a certain time. A proper tool used for assessing such process might be the diffusion Wiener process which was applied several times also in technical area see e.g. [1, 3, 4, 6, 7, 8, 9, 13, 25, 26 etc.]. In this case we presume that the attack time is a random variable.

System vulnerability is described in several ways and indicates many characteristics of system condition. The vulnerability term and its meaning are more developed in section 2. However, the main idea of the paper is to describe selected aspects of observed system vulnerability. We assume the vulnerability is compounded both from probability of successfully completed attack and from conditional consequences of this attack when completed successfully.

Therefore the paper describes expected adversarys behaviour in the secured area. The principles presented in the paper are subdivided into two parts.

Modelling the FPT (First Passage Time) using specific diffusion process – which is represented by the adversary's respective trajectory length and time to reach the goal. When an adversary is detected at the same time the security unit is alerted and gets into motion. We model here just the probability that the attacker will reach the goal – this is modelled by time elapsed or/and distance competed.

Modelling the consequences after successful attack is completed. Fuzzy approach seems to be suitable as the whole process includes humans. Therefore we assume the level of uncertainty is quite high plus consequences modelling are vague and conditional. Therefore the fuzzy logic seems to be appropriate.

The paper introduces the possibility of applying the Wiener process while modelling an expected movement trajectory (distance from a beginning – both time and physical distance). Provided an adversary really breaks into the building, the results of the work might serve to model not critical, but presumed path of adversary movement. In view of the stochastic way of the process, we have taken into consideration factors relating to time, morphology, area, shape and nature of an agglomeration, including adversary skills.

From the experience the terrorist attacks are unpredictable for two main reasons [22]:

Terrorists have many more categories of legitimate targets, as well as worldwide scope, compared to traditional security concerns (which

(*) Tekst artykułu w polskiej wersji językowej dostępny w elektronicznym wydaniu kwartalnika na stronie ***www.ein.org.pl***

used to have the comparable luxury of protecting obvious military assets, or home territory).

Terrorist attack can have different objectives like harming people, damaging infrastructure, causing panic, etc.

Although such objectives may often overlap, these varying objectives lead to varying types or location targets. However, we have to keep in mind that detection and prevention must always remain to be the first line of defence [39, 40].

In our case it is always about an attempt to damage the building, or steal interesting (e.g. nuclear) material. Several experiments have been performed very recently in this area and all models presented below are based on real data. Unfortunately the data are classified and quite sensitive. Before presenting the results here data were de-sensitised and the results correspond with the reality in modified way.

Outcomes of this paper might be used for adjustment of physical protection systems in secured area. We have proved in this particular case that the reaction time of security unit is acceptable in terms of adversary's behaviour when attempting to reach the goal. For other instances the outcomes of this paper might be of use and inspirational when setting up the physical protection system.

2. Vulnerability and different ways of its assessment

We would like to turn our attention to some selected information sources since there are many of them and many options how to describe vulnerability. Department of Homeland Security (DHS) in the USA defines vulnerability as "physical feature or operational attribute that renders an entity, asset, system, network, or geographical area to exploitation or susceptible to a given hazard" (2010) [12]. The key of assessing vulnerability properly is in the last phrase of that definition. Although vulnerability assessments can be standalone documents, vulnerability is best understood within a risk context, specifically the interaction between the threat and the consequence. This interaction is the reason that vulnerability V is sometimes defined as the probability of success (of an attack) P_S given an attack A or probability of the consequence occurring given an event. Mathematical expression is then:

$$V = P_S(\mathrm{A}) \tag{1}$$

In either case vulnerability is the collective influence of physical features or operations that reduce the effectiveness (alternatively success) of the adversary's attack or that make the target better able to sustain the attack. Analysis is highly dependent, therefore, on the method of attack and strength of the attack expected. A building's vulnerability to an improvised explosive device (IED) will differ from the vulnerability to a vehicle-born IED (VBIED), for example, depending on the assumption in the definition of those attacks, such as amount or type of explosives, entry points, and stand-off distance. Even within the category of VBIED, vulnerability will differ based on terrorist tactics, such as leaving the vehicle on the street adjacent to the building or ramming the vehicle into a building or its defensive perimeter. The more specific the context, the more accurate the vulnerability assessment for particular target can be [41, 43].

For security risk, vulnerability is also influenced by the terrorist adversary. Terrorist groups have different levels of competence and expertise. This can affect not only target selection, but also their knowledge of countermeasures and their determination to overcome those countermeasures through technology or effort. For this reason we have to accept kind of conceptual approach to vulnerability assessment of structures as mentioned for instance in [12]:

1. Characteristics of the asset itself.
2. The protective measures that prevent the attack.
3. Access allowed to outsiders and insiders.
4. The functional dependencies on internal and external entries.
5. Generating scenarios.
6. Attack methods filtering.
7. Event/fault tree analysis (recognisability, countermeasures effectiveness, robustness/resistance).
8. Combining the components.

If we speak about vulnerability, we cannot forget to emphasise also the structural robustness. It might be expressed by "Protection categories" as said in [43], "Robustness Index" as mentioned in [14] and has several degrees on scale – usually 1-10. Some retrofit recommendations for increasing the structure robustness are for instance listed in [11]. Considering the further statements in [14], there are three most important structural properties which increase a structure's/building's ability to survive catastrophic overload or damage:

- Structural redundancy (A structure that will perform well in catastrophic situation will permit gravity loads that must be supported during the event to be carried to the foundations using multiple load paths).
- Fireproofing toughness (A structure's ability to resist fire is an important contribution to its robustness, since fire is often a part of a catastrophic event).
- Connection robustness (Structural connections are very important and are critical in holding a building together during the large movements that occur in a fire or another catastrophic event).

There are several ways of assessing the severity of a possible terrorist attack. Many of them are based on conventional standards like [e.g. 15, 17, 19, 21, 31]. In [29] there are also mentioned some possible tools for risk assessment either software-based (e.g. RAMPART – Risk Assessment Method-Property Analysis and Ranking Tool; CONTAMW – software for vulnerability assessment; HVAC – software for heating, ventilation, and air condition in buildings assessment) or classical (standards and books).

Referring to the application of mathematical tools applied and to the materials presented above, the vulnerability is associated with the probability the adversary achieves the goal plus consequences from such act – meaning successful goal approach. Both of these components might be modelled differently.

3. Diffusion processes and attacks on the objects of critical infrastructure

Diffusion processes are part of mathematics in the area of stochastic processes [such as 6, 7, 8, 9, 13, 25, 26, 27, 34, 35, 36]. Generally, the Brownian motion ranks among the simplest stochastic processes with continuous time. In fact it is understood as a limit process for both simpler and more complex types of stochastic processes. Due to normal distribution of random variable and its application capabilities, the Brown motion might be used universally. The application of the Brown motion can be found in many areas. Among others we suppose it can be also used when assessing the vulnerability of critical infrastructure objects. Standard use is related to modelling with the use of differential equations. We pick up one specific example of diffusion processes which is Wiener process.

Rules of the general Wiener process might be specified as follows:

A real stochastic process $\{W(t)\ t\in\langle 0; +\infty)\}$ in a probability space (Ω, A, P) is called *the Brown motion* or the *Wiener process*, if the following applies:

1. $W(0) = 0$ almost everywhere,
2. $W(t) - W(s)$ has $N(0, t - s)$ distribution for $t > s \geq 0$,
3. For arbitrary $0 < t_1 < t_2 < \cdots < t_n$ growths $W(t_1), W(t_2) - W(t_1), W(t_3) - W(t_2), \ldots, W(t_n) - W(t_n - 1)$ are mutually independent random variables. $W(t)$ is in fact a physical movement trajectory of an adversary in a building – it can represent the travelled distance or time – in a very specific manner.

Next, it applies that

1. $E[W(t)] = 0$ for $t > 0$
2. $E[W_2(t)] = t$ *for* $t > 0$

The Wiener process represents one possible form of diffusion processes. It is actually the integral of what is in practical applications called a white noise. The Wiener process with drift will be used in our application.

In view of simplified and generally hypothetical theoretical adversary's behaviour and the nature of diffusion processes the Wiener process – meaning Brownian motion without drift – model might be shown e.g. in the graph below – figure 1, where "mu" is mean value and "sigma" is standard deviation. This process in practice however is not much likely.

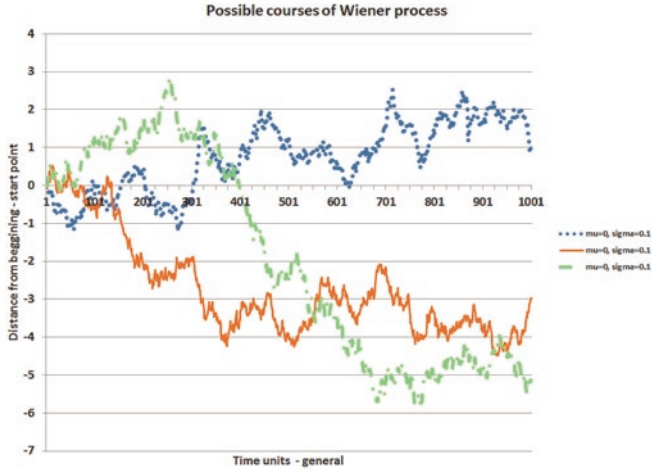

Fig. 1. Graphical model of general Wiener process

The attacker may use basically two principles/ways for reaching the goal – either brutal force or smart strategy as presented in figure 2. We assume a weighted stochastic proportional combination of both will apply while the equipment of the attacker is always the same. The weight of proportion for both brutal force and strategy is based on empirical experience. These input boundary conditions are to be justified at the beginning of the process. It is assumed that the time of passing obstacles (Level of Protection – LOP) will be the same when having the same equipment. The next assumption is that the likelihood of adversary detection at single LOPs will be also the same, or may equal to 0.

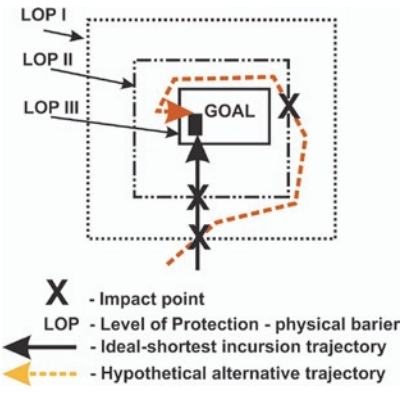

Fig. 2. Possible way of incursion of an adversary into a building

First Passage Time (FPT) – meaning the moment when attacker reaches the goal or some front layers of protection (LOP) – is presented in figure 3. This is just generalised way of the attacker's approach to the understanding the mean values of passage as they are linear for us. Real data were recorded while performing live experiments.

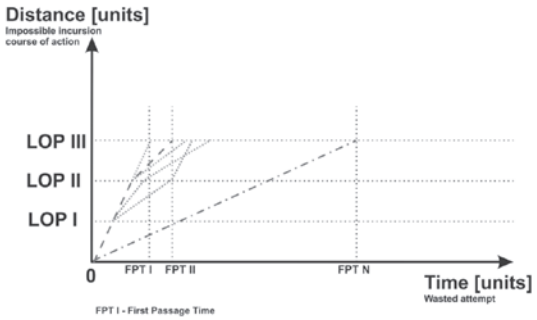

Fig. 3. Possible way of incursion into a building by an adversary

4. Example of a possible adversary's attack on an object of interest

The adversary's incursion into a building might be crippled by time and distance limits. The adversary wants to achieve his goal as soon as possible (it does not always mean the shortest way and fastest motion and neither that the goal could not be achieved more quickly). His main effort is to complete his mission (as fast/smoothly as possible) and if possible not to be detected due to security systems during his incursion. If he were detected, he could try to abandon his plan, or could keep achieving the objective. However, according to Wiener process assumptions, adversary's movement in the area of concern is expected in any way but always consist of combination of brutal force and smart strategy. FPT (First Passage Time) is the moment when the adversary achieves his final goal. While the way forward might have two typical boundary conditions 1. „the sooner the better" or 2. „Rome was not built in a day…". Let's assume that both previously mentioned strategies have their actual and effective limits.

The experimental data were used as inputs to above mentioned Wiener process. These data were collected for individual attackers therefore the linear course of a mean time of the goal approach was calculated using linear regression and including confidence interval for an individual attempt. The experiments were performed on various surfaces. Generalised and publically accessible outcomes are shown in figure 4. This figure has been constructed based on many consulta-

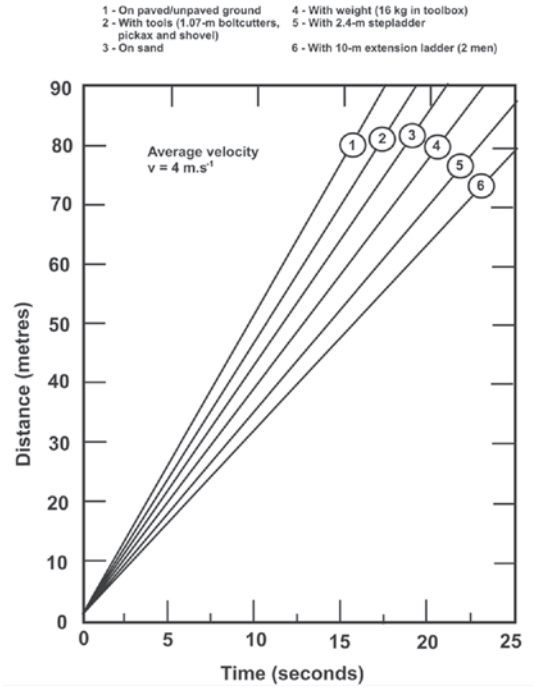

Fig. 4. Basic regression parameters as inputs to Wiener process

tions with experts in this area, based on searching several literature sources and based on personal experience of the authors. It may have similar origin in other publications. Detailed analytical results from tests can unfortunately not be presented in open form but were available and used for further modelling and simulation process.

Graphical representation of de-sensitised characteristics is mentioned in figure 5 bellow. Confidence level is 95%. The positive shift on y-axis means that in time "0" – when detected on some LOP – the attacker has already managed to reach some trajectory.

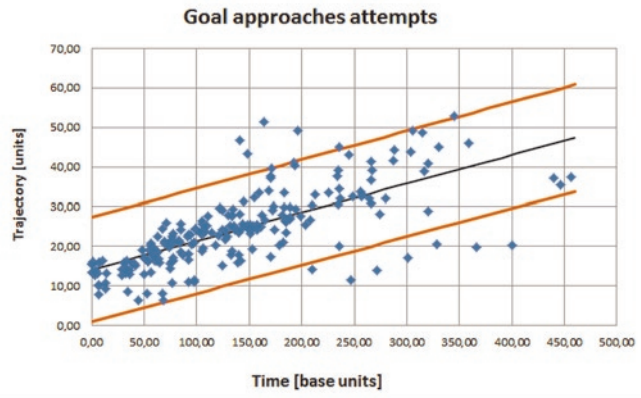

Fig. 5. Basic regression parameters as inputs to Wiener process

For our particular practical application we use a Wiener process with positive drift where mu is higher than 0. Which means the adversary is approaching the intended final goal. The principle of such approach is presented by function in equation (2):

$$f(x) = \frac{W(t) \cdot \sigma}{\sqrt{t}} + \mu \qquad (2)$$

where W(t) – is standard randomly generated Wiener process depending on time of attempt, σ is standard deviation for individual value calculated for each time increment, μ is calculated mean value of an attacker's trajectory increment in time (t).

There are two possibilities when an adversary behaves inside the area. As previously said we always assume positive drift which means the attacker will approach the final goal. Negative drift means that the attacker will never reach the goal and will be caught and pacified by action of security service. First of this options is modelled, simulated and presented in figure 6 while the second one in figure 7. The Wiener process simulation courses were performed 10e6 times which are assumed to be almost near the reality.

On "y – axis" there is line in value number 50 (always the modified value). Where the value actually means the critical length of the estimated physical/ideal/air-line or ground plot trajectory needed to reach the goal successfully. The other threshold both in figure 6 and 7 (on x-axis 260) means in our case experimentally recorded first time point where security unit comes to the scene and act. The adversary's behaviour behind this point will be modelled using probability distribution with expected goodness-of-fit.

Let us presume the way of breaking an adversary into a building could be demonstrated by the Wiener process with positive drift as presented above. We assume that the random variable – the time trajectory parameter – has either Gamma Distribution, Inverse Gaussian Distribution or LogNormal Distribution.

The FPT distribution was modelled based on the real test data and above mentioned principles. The outcome in form of boundary conditions and FPT probability distribution is presented in figure 8. Where full line presents Gamma Distribution, dash line presents LogNorm

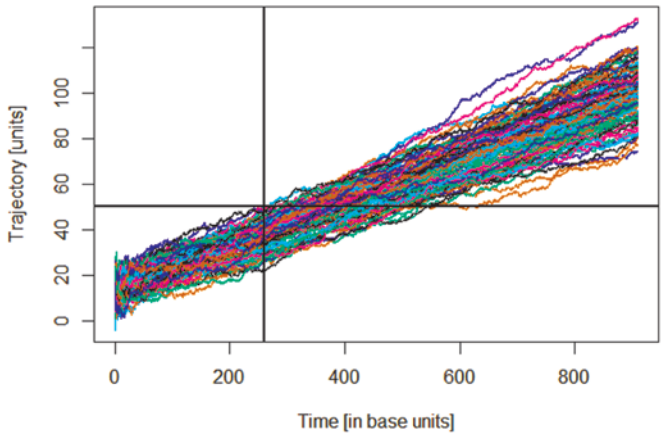

Fig. 6. Model of attacker behaviour when reaching the goal in positive attempt

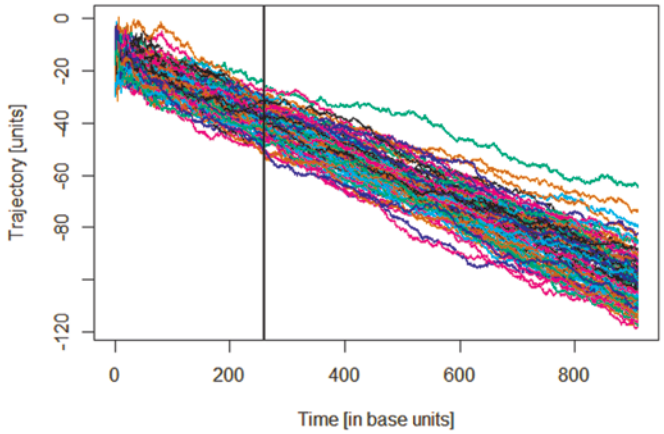

Fig. 7. Model of attacker behaviour when reaching the goal but with negative attempt

Distribution and dash and dot line presents the Inverse Gaussian Distribution (IGD).

Basic characteristics of the FHT histogram are: Min Value: 134.00 [Time units]; 1st Qu: 336,40 [Time units]; Median: 377.70 [Time units]; Mean Value: 382.00 [Time units]; 3rd Qu: 422.80 [Time units]; Maximum Value: 886.60 [Time units]; 2.5%: 265.05 [Time units]; 97.5%: 523.65 [Time units]; Variance: 4333.44 [Time units]; Standard Deviation: 65.62887 [Time units].

The Kolmogorov-Smirnoff tests for goodness-of-fit were performed at the same time in R-Studio for foreseen types of distri-

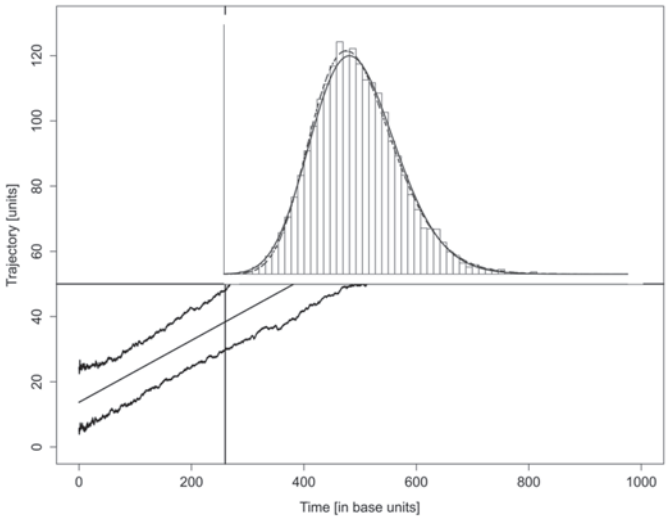

Fig. 8. FHT model of an adversary when reaching the goal

butions. The outcomes showed and confirmed our expectations. The "p-value" for LogNorm Distribution was 0.7453, for IGD was 0.3957 and for Gamma 0.2733. So in terms of FPT distribution we can more likely rely on the Log Norm distribution in this case. The Comparisons of probability density functions with empirical cumulative distribution function (Ecdf) for IGD and LogNorm Distribution is presented in figure 9 where LogNorm (left) is green and IGD (right) is red.

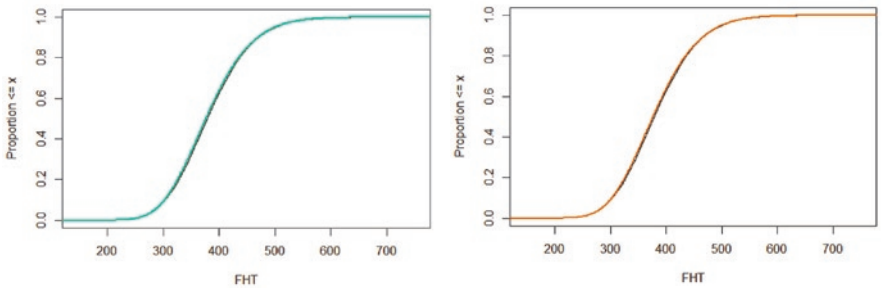

Fig. 9. Comparison of cdf of LogNorm (left) and of IGD (right) with Ecdf

Based on these outcomes we can see that an adversary's attempt will be most likely not successful if the security unit reacts by 260 [Time units]. Everything behind this time point onwards may create potential for an adversary's success when reaching the goal.

It would be very useful – based on an attacker position, target location and distance of both an attacker to the target and the security unit to the attacker – utilization of multidimensional Brownian motion for this whole procedure assessment.

Therefore we have also to assess next situation when the attacker's success can generate variable consequences. The level of uncertainty and vagueness in terms of effects assessment is quite high since human element is present. Therefore classical risk approach combined with fuzzy approach is presented further to assess the level of consequent risk.

5. Proposal of risk assessment of an adversary's attack

Risk assessment is a key phase of the system safety management process and shall introduce some risk reduction activities [see e.g. 18, 19, 20, 33]. Safety and protection of the system performance plus critical infrastructure objects is associated with the relation to hazard analysis – especially an event frequency, case of and event occurrence, identification of an event causes and reducing negative effects of an event occurrence.

The following method of risk assessment is proposed while estimating the risk of nuclear power plant fault. The discussed risk assessment is associated with an adversary's attack. We consider the probability of reaching and destruction a goal/target (e.g. generator, first circle, and reactor) (P), consequences of reaching and destruction the target (C), and the possible threat detection (D). The idea for this approach was inspired by principles of addressing the risk priority number (RPN) – as we consider as total risk level [see e.g. 15]:

$$RPN = R = P \times C \times D \tag{3}$$

For every situation we have assessed a score which is assigned to the parameters P, C and D. Total risk number may vary in the range of [1÷75].

Probability (P) estimates that a particular system target (e.g. generator, first circle, and reactor) will be chosen by an adversary's for attack, and then it might be reached in respective time based on his intent and capability as described in previous section.

Point weights associated with P – probability of choice a target – are based on common expert estimates and are as follows:

- remote; it would be very unlikely to be observed, $P < 10^{-6}$ 1/year; point scale 1,
- moderate; likely to occur more than once, $10^{-6} < P < 10^{-3}$ 1/year; point scale 2,
- very high; near certain to occur several times, $P < 10^{-3}$ 1/year; point scale 3.

The values for C, D parameters can be obtained as follows:

The criteria for evaluating the threat consequences:

– minor: point scale 1; performance of system is affected with minor effect,

– low: point scale 2; system performance is affected with small effect; the maintenance may not be needed; renewal costs will be up to 10e3 EUR,

– moderate: point scale 3; performance of system is affected seriously and the maintenance is needed, renewal costs will be up to 10e5 EUR,

– high: point scale 4; operation of system is broken down without compromising safe, renewal costs will be up to 10e7 EUR,

– very high: point scale 5; highest consequences ranking of a failure mode, hazardous consequences, renewal costs will exceed 10e9 EUR.

Consequences (C) can be divided into the following groups in the case of a nuclear power plant might be chosen for terrorist attack:

- economic and financial (energy network disorganization of the country or region, the need to repair the damage and launch control systems, the removal of radioactive contamination, the need of the population evacuation from the contaminated sites, the impact on the local economy and the national capital losses),
- environmental (associated with environmental pollution),
- health (birth defects caused by radiation, increased mortality, illness absences and medical expenses),
- social, governance and the psychological (impact on the ability to maintain order and to deliver minimum services by the state),
- other (legal, cost of land interdiction and litigation, payment of compensation adjudicated).

Basically all consequences might be also expressed in monetary values. However the criteria of the consequences assessing suggested in this work should be based on the information from entrepreneurs of the nuclear power plant and can be derived from incident data.

Point weights associated with D are as follows:

- point scale 1: almost certain likelihood that the potential of occurring such failure mode will be detected,
- point scale 2: high likelihood of detecting the potential of occurring such failure mode,
- point scale 3: moderate likelihood of detecting the potential of occurring such failure mode,
- point scale 4: remote likelihood of detecting the potential of occurring such failure mode,
- point scale 5: absolute uncertain likelihood that the process controls will not detect a potential adversary's attack and subsequent failure mode.

It is needed to apply specific approach as all these components – P; D; C – are of various natures in terms of their assessment and description. Therefore subsequent fuzzy sets scaling is applied. Such approach with fuzzy logic implementation would be useful when we deal with incomplete, imprecise, unclear data.

The final step is to define the risk level and to determine limits of its fragmental levels: tolerable (further reduce if practicable), [1÷9]; undesirable (risk reduction as much and promptly as possible),

Table 1. Three-parametric risk matrix

Detection (D)	Consequences (C)														
	Minor			Low			Moderate			High			Very high		
	Probability (P)														
	Unlikely	Moderate	High	Unlikely	Moderate	High	Unlikely	Moderate	High	Unlikely	Moderate	High	Unlikely	Moderate	High
Almost certain possibility	(1) T	(2) T	(3) T	(2) T	(4) T	(6) T	(3) T	(6) T	(9) T	(4) T	(8) T	(12) UN	(5) T	(10) UD	(15) UD
High possibility	(2) T	(4) T	(6) T	(4) T	(8) T	(12) UD	(6) T	(12) UD	(18) UD	(8) T	(16) UD	(24) UD	(10) UD	(20) UD	(30) UA
Moderate possibility	(3) T	(6) T	(9) T	(6) T	(12) UD	(18) UD	(9) T	(18) UD	(27) UD	(12) UD	(24) UD	(36) UA	(15) UD	(30) UA	(45) UA
Low possibility	(4) T	(9) T	(12) UD	(9) T	(16) UD	(24) UD	(12) UD	(24) UD	(36) UA	(16) UD	(32) UA	(48) UA	(20) UD	(40) UA	(60) UA
Absolute uncertain possibility	(5) T	(12) UD	(15) UD	(12) UD	(20) UD	(30) UD	(15) UD	(30) UA	(45) UA	(20) UD	(40) UA	(60) UA	(25) UA	(50) UA	(75) UA

where: T– tolerable risk, UD – undesirable risk; UA – unacceptable risk

[10÷27]; unacceptable (immediate action required), [30÷75]. In table 1 there are presented the three-parameter risk matrix.

The calculated risk can be presented in form of fuzzy risk priority numbers which are shown on figure 10 and for membership function F_T, F_{UD}, F_{UA} can be determined by the formulas 4–6. On the *x*-axis there is the Total Risk Number following the principles above.

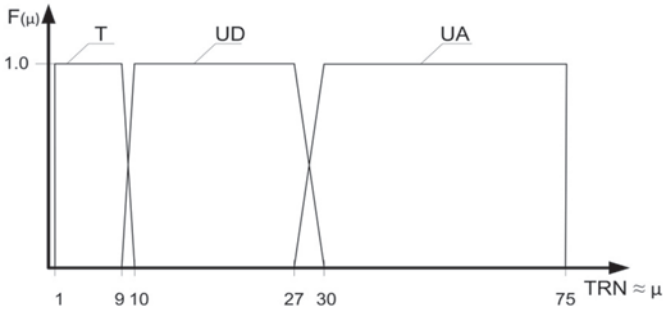

Fig. 10. Membership function of risk

$$F_T(\mu)=\left\{0\ for\ TRN\in\left(-\infty;1>@1\ for\ TRN\in<1;9>@\frac{TRN-10}{9-10}\ for\ TRN\in<9;10>@0\ for\ TRN\in<10;\infty\right)\right.$$

$$F_{UD}(\mu)=\left\{0\ for\ TRN\in\left(-\infty;9>@\frac{TRN-9}{10-9}\ for\ TRN\in<9;10>@1\ for\ TRN\in<10;27>@\frac{TRN-30}{30-27}\ for\ TRN\in<27;30>@0\ for\ TRN\in<30;\infty\right)\right.$$

$$F_{UA}(\mu)=\left\{0\ for\ TRN\in\left(-\infty;27>@\frac{TRN-27}{30-27}\ for\ TRN\in<27;30>@1\ for\ TRN\in<30;75>@0\ for\ TRN\in<75;\infty\right)\right.$$

The fuzzy approach has been used as initial idea description, proposal and determination of possible risk resulting from adversary's attack. This field is just open and not completed yet. Deeper studies on this issue will continue.

6. Discussion

Following the suggested way of using the Wiener process, some adversary's behavioural patterns can be modelled. As stated above and assumed before the Wiener process parameters shall be in special form – namely the drift. Mainly, we are not going to focus on a critical trajectory – ideal for achieving the goal. We are going to concentrate on adversary's possible movement between single layers of protection. These layers are the same in terms of detection probability and the time necessary for overcoming them. The result of the solution is the time of the first achievement of the goal. This result is compared with an ideal time of detection – the sum of times from the detection to the reaction of protections systems. If the result is for a potential intruder more beneficial, then it will be necessary to take measures.

Next, we follow the assumption that we know all weak points of a protected building. However, we suppose a potential adversary does not know them and we do not know his attack plan. Therefore the adversary's movement between protection layers could be stochastic, although he is motivated by not being detected at all and by achieving his goal as soon as possible. The reasons for his stochastic behaviour have been stated above. This model does not take into consideration different levels of difficulty when overcoming obstacles on an adversary's trajectory. It is rather obvious

and not unambiguous that different wall fillings in a building (or potential paths to the building) have effect on the speed of the advance. This situation could affect the Wiener process development for this application. Therefore we have not included the difficulties of overcoming obstacles this time.

This approach can very well fit while modelling an attacker's movement for low risk targets as well as higher level risks. On these assumptions – based on our practical experiences and real examples – the fuzzy model was created.

7. Conclusion

This paper is to bring one of possible alternatives for using diffusion processes in technical applications. Because the attack on the objects of interest is a fact, we are made to look for adequate ways of expressing such processes. The presumed movement of an adversary and his behaviour in time is believed to be diffusion stochastic processes. Admittedly we do not know where exactly the attack will take place, but we could be able to predict how it might develop, how long it might take and how successful it could be. Using all these characteristics, the vulnerability of critical infrastructure objects can be described directly and indirectly. It is widely supposed that the Wiener processes are going to be used in this area in much greater extent.

For further development we expect combining of two-dimensional diffusion stochastic processes. One motion of the trajectory will represent attacker's behaviour while the other one – at the same time – will represent the RFT (Response Force Time). It is expected that while combining these two processes together it will be possible to obtain precise picture of the physical protection system efficiency and facility vulnerability.

***Acknowledgement**: This paper has been prepared with the great support of the project for the institutional development of K-202 University of Defence, Brno and by the Ministry of Interior of the Czech Republic (project "The Evaluation of Physical Protection System Effectiveness Based on its Modelling ", No. VG20112015040).*

Bibliography

1. Bibbona E, Panfilo G, Tavella P. The Ornstein-Uhlenbeck process as a model of a low pass filtered white noise. Metrologia 2008; 45: 117–126. doi:10.1088/0026-1394/45/6/S17.
2. Blais RA, Henry MD, Lilley SR, Pan JA, Grimes M, Haimes YY. Risk-based methodology for assessing and managing the severity of a terrorist attack. 2009 IEEE Systems and Information Engineering Design Symposium, SIEDS '09, art. no. 5166175: 171–176.
3. Bohner M, Peterson A. Dynamic Equations on Time Scales: An Introduction with Applications. Boston: Birkhäuser, 2001.
4. Bohner M, Sanyal S. The Stochastic Dynamic Exponential and Geometric Brownian Motion on Isolated Time Scale. Community Mathematical Anals 2010; 8: 120–135.
5. Coffey WT, Kalmykov YP, Waldron JT. The Langevin Equation. With Application in Physics, Chemistry and Electrical Engineering, World Scientific Series in Contemporary Chemical Physics, World Scientific, Singapore 1996; 10: 428.
6. Csörgö M. Random Walk and Brownian Local Times in Wiener Sheets. Periodica Mathematica Hungarica 2010; 61: 1–21.
7. Desmond AF, Chapman GR. Modelling Task Completion Data with Inverse Gaussian Mixtures. Applied Statistics 1993; 4(42): 603–613.
8. Doksum KA, Hóyland A. Models for Variable-Stress Accelerated Life Testing Experiments Based on Wiener Processes and the Inverse Gaussian Distribution. Technometrics 1992; 1(34): 74–82.
9. Doob JL. The Brownian movement and stochastic equations. Annals of Mathematics, 1942; 43: 351–369.
10. ECSS (European Cooperation for Space Standardization)-Q-ST-40-02C Space product assurance – Hazard analysis.
11. Eytan R. Cost effective retrofit of structures against the effects of terrorist attacks – the Israeli experience. Proceedings of the Structures Congress and Exposition 2005; 2161–2172.
12. French GS, Gootzit D. Defining and assessing vulnerability of infrastructure to terrorist attack, Vulnerability, Uncertainty, and Risk: Analysis, Modelling, and Management. Proceedings of the ICVRAM 2011 and ISUMA 2011 Conferences 2011; 782–789.
13. Grow D, Sanyal S. Brownian Motion Indexed by a Time Scale. Stochastic Analysis and Applications 2011; 29: 457–472.
14. Iding RH. A methodology to evaluate robustness in steel buildings – Surviving extreme fires or terrorist attack using a robustness index, Proceedings of the Structures Congress and Exposition 2005; 511–515.
15. IEC 60812:2006 Ed. 2.0 Analysis techniques for system reliability – Procedure for failure mode and effects analysis (FMEA).
16. IEC 61508-(1-7)/:2008 Ed. 2.0 Functional Safety of Electrical/ Electronic/ Programmable Electronic safety-Related Systems.
17. ISO 13824:2009 Ed. 1.0 – General principles on risk assessment of systems involving structures.
18. ISO 31 000:2009 Ed.1.0 – Risk management – Principles and guidelines on implementation.
19. ISO/IEC 31010:2009 Ed. 1.0 – Risk Management – Risk Assessment Techniques.
20. ISO/IEC Guide 73:2009 Ed. 2.0 – Risk management – Vocabulary – Guidelines for use in standards.
21. JCSS (Joint Committee on Structural Safety) – Principles, System Representation & Risk Criteria 2008.
22. Jordán F. Predicting target selection by terrorists: A network analysis of the 2005 London underground attacks. International Journal of Critical Infrastructures 2008; 4(1–2), 206–214.
23. Kelly TJ, Hofacre K C, Derringer T L, Riggs K B, Koglin E N. Testing of safe buildings detection technologies and other homeland security technologies in EPA's Environmental Technology Verification (ETV) program, Proceedings of the Air and Waste Management Association's Annual Meeting and Exhibition 2004; 3449–3457.
24. Kemp RL. Assessing the vulnerability of buildings, Journal of Applied Fire Science 2007; 14 (1): 53–61.
25. Kolárová E. Stochastic differential equations in electro-technic. Dissertation thesis. Brno: VUT, 2005.
26. Kolárová E. The Brownian Bridge Process. In XXVII International Colloquium, Brno, 2009.
27. Lefebre M, Perotto S. A semi-Markov Process with Inverse Gaussian Distribution as Sojourn Time. Applied Mathematical Modelling 2011; 35: 4603–4610.
28. Linden M. Modelling Strike Duration Distribution: a Controlled Wiener Process Approach. Applied Stochastic Models in Bussiness and Industry 2000; 16: 35–45.
29. Marshall HE, Chapman RE, Leng CJ. Risk mitigation plan for optimizing protection of constructed facilities. Cost Engineering 2004; 46(8): 26–33.

30. Merritt D, Berczik P, Laun F. Brownian motion of black holes in dense nuclei. The Astronomical Journal 2007; 2(133): 553–563, doi:10.1086/510294.
31. MIL-STD-882D Standard Practice for System Safety.
32. Mueller J. Assessing Measures Designed to Protect the Homeland, Policy Studies Journal 2010; 1(38): 1–21.
33. Pietrucha-Urbanik K, Studziński A. Analysis of water pipe breakage in Krosno, Poland. Environmental Engineering IV, Pawłowski A., Dudzińska MR, Pawłowski L. (eds), London: Taylor & Francis Group, 2013, 59–62.
34. Promislow D, Young V. Minimizing the Probability of Ruin when Claims Follow Brownian Motion with Drift. North America Actuarial Journal 2005; 9: 109–128.
35. Sherif YS. and Smith ML. First-Passage Time Distribution of Brownian Motion as a Reliability Model. IEEE Transaction on Reliability 1980; 5(R-29): 425–426.
36. Smith ChE, Lánský P. A reliability application of a mixture of inverse Gaussian distributions. Applied Stochastic Models and Data Analysis 1994; (10) 61–69.
37. Stewart MG. Cost effectiveness of risk mitigation strategies for protection of buildings against terrorist attack. Journal of Performance of Constructed Facilities 2008; 2(22): 115–120.
38. Stewart MG. Life-safety risks and optimisation of protective measures against terrorist threats to infrastructure. Structure and Infrastructure Engineering 2011; 6(7): 431–440.
39. Valis D, Koucky M, Zak L. On approaches for non-direct determination of system deterioration. Eksploatacja i Niezawodnosc – Maintenance and Reliability 2012; 14(1): 33–41.
40. Valis D, Vintr Z, Koucky M. Contribution to highly reliable items' reliability assessment. Reliability, Risk and Safety: Theory and Applications, Proceedings of the European Safety and Reliability Conference, ESREL 2009, Prague, Czech Republic, 2010; 1–3: 1321–1326.
41. Valis D, Vintr Z, Malach J. Selected aspects of physical structures vulnerability – state-of-the-art. Eksploatacja i Niezawodnosc – Maintenance and Reliability 2012; 14(3): 189–194.
42. Williamson EB, Winget DG, Risk management and design of critical bridges for terrorist attacks. Journal of Bridge Engineering 2005; 10 (1): 96–106.
43. Zehrt Jr WH, Acosta PF. Analysis and design of structures to withstand terrorist attack, Proceedings of the Structures Congress and Exposition 2003; 585–592.

David VALIS
Faculty of Military Technologies
University of Defence
Kounicova 65, 662 10 Brno, Czech Republic
E-mail: david.valis@unob.cz

Katarzyna PIETRUCHA-URBANIK
Faculty of Civil and Environmental Engineering
Rzeszów University of Technology
Al. Powstańców Warszawy 6, 35-959 Rzeszów, Poland
E-mail: kpiet@prz.edu.pl

Article citation info:
MACHNIK R, NOCUŃ M. Effect of anti-corrosion coatings of corona electrodes on selected operating parameters of industrial electrostatic precipitators. Eksploatacja i Niezawodnosc – Maintenance and Reliability 2014; 16 (1): 56–60.

Ryszard MACHNIK
Marek NOCUŃ

EFFECT OF ANTI-CORROSION COATINGS OF CORONA ELECTRODES ON SELECTED OPERATING PARAMETERS OF INDUSTRIAL ELECTROSTATIC PRECIPITATORS

WPŁYW POWŁOK ANTYKOROZYJNYCH ELEKTROD ULOTOWYCH NA WYBRANE PARAMETRY EKSPLOATACYJNE ELEKTROFILTRÓW PRZEMYSŁOWYCH*

The problem of corrosion protection of electrostatic precipitators used in the energy industry, during its construction or modernization is of vital importance. Several months construction period and the period of time elapsed from the end of construction to operation promotes corrosion of its components. Significant impact on the electrical parameters of an electrostatic precipitator performance has the corrosion phenomena of its emission components, which are the corona electrodes. Manufacturers do not apply any corrosion protection coating on electrostatic corona electrode for fear of worsening their emissivity. This paper presents the results of comparison of emission properties of corona electrodes with and without corrosion protection coatings. Rode and mast type electrodes were studied. The analysis of the results was performed using a statistical method based on the time-series model. The obtained results clearly show that the use of anti-corrosion coating does not impair the electrical parameters of corona electrodes. Corrosion protection can be used both during the modernization as well as during the construction of new electrostatic precipitators.

***Keywords**: anti-corrosion coatings; electrostatic precipitators; corona electrodes.*

Problem ochrony antykorozyjnej ma istotne znaczenie w okresie budowy lub modernizacji urządzeń odpylających stosowanych w przemyśle energetycznym. Wielomiesięczny okres budowy elektrofiltru oraz okres czasu upływający od zakończeniu montażu do momentu uruchomienia instalacji odpylającej powoduje nieuniknioną korozję jego elementów. Istotny wpływ na elektryczne parametry eksploatacyjne elektrofiltru ma, występujące w tym okresie, zjawisko korozji jego elementów emisyjnych – elektrod ulotowych. Producenci elektrofiltrów nie stosują ochrony antykorozyjnej elektrod ulotowych w obawie przed pogorszeniem emisyjności elektrod. W artykule przedstawiono wyniki badań emisyjności elektrod ulotowych bez zabezpieczeń oraz zabezpieczonych powłokami antykorozyjnymi, dla elektrody prętowej oraz wybranej elektrody przemysłowej typu masztowego. Analizę wyników przeprowadzono z zastosowaniem metod statystycznych opartych na modelu szeregów czasowych. Uzyskane wyniki badań jednoznacznie wykazały, że stosowanie powłok antykorozyjnych nie pogarsza parametrów elektrycznych elektrod ulotowych. Ochrona antykorozyjna może być stosowana zarówno podczas prac modernizacyjnych elektrofiltrów, jak i na etapie budowy nowych urządzeń.

***Słowa kluczowe**: powłoki antykorozyjne; elektrofiltr; elektrody ulotowe.*

1. Introduction

Electrostatic purification methods of gases generated during the combustion of fuels in energy production are currently the only economically justified way to protect the air. The main part of the line of extraction of dust aerosols, resulting from combustion of fuel in the boiler energy, is electrostatic precipitator (ESP). Electrostatic precipitators are large-size devices. The volume of the chamber of currently used industrial electrostatic precipitators may be up to 40 thousand of m^3, with a total working area of collecting electrodes of up to 160 thousand m^2. The number of emission electrodes is up to 14 thousand.

Electrostatic precipitators are unique devices, designed for the purification of exhaust gas of a specific power boiler. Fuel type and its physical and chemical properties are set up on the stage of the implementation of the project both power boiler, as well as cooperating with it dust extraction system. Implementation of the investment, such as a gas extraction line usually takes several months, and naext few months elapses after the completion of the construction to begin the operation. The reason for this is the need for the supplier to accomplish a numerous tests of the finished device, as required by the investor. Studies, carried out by the manufacturer, include both the determination of electrical parameters, the distribution of exhaust gas velocity in selected sections of ESP, as well as issues related to the security service. Such a long period of time, when the electrostatic precipitator is not in operation causes corrosion of its construction components. The most important is corrosion of the corona electrodes, as the basic parameters of an electrostatic precipitator performance like corona starting voltage and current density on the surface of the collecting electrodes depend on their condition.

Currently built electrostatic corona electrodes are made of general purpose construction steel. The use of steel with high corrosion resistance is not desirable due to financial reasons. Despite the problems arising from the corona electrode corrosion, producers do not protect them by appling antycorrosion coatings containing a rust inhibitor. This is due to the fear of the danger of electrostatic precipitator working disturbance caused by changes in the electrical parameters of corona electrodes coated with high resistivity coating. This study aimed to determine the influence of corrosion protection coatings of the corona electrode on their electrical parameters. Consequently, they should give the ansever whether the effect of the corrosion protection is so unfavorable that prevent its use.

(*) Tekst artykułu w polskiej wersji językowej dostępny w elektronicznym wydaniu kwartalnika na stronie ***www.ein.org.pl***

2. Research methodology

The most important parameters characterizing the electrical corona electrodes are [4, 15, 16]:

– Current-voltage characteristics, and initial corona voltage determined on its basis,
– Current density at the surface of collecting electrode

The first parameter, defined as the emissivity of the electrode, provides the intensity of the electric field produced by the corona electrode. Electric field strength influences the time of obtaining the charge by the dust grains allowing the migration and deposition on the collecting electrode. The second parameter affects the mechanical properties of the deposited dust layer on the surface of the electrode. The current density on the surface of collecting electrode is affected by the emissivity of corona electrode and conductance of a medium (gas-dust aerosols) present in the space between electrodes [18], at the given configuration of the electrodes. In the process of operation, both electrostatic parameters are set at the required level by selecting the corona electrode voltages and operation regime of high voltage power supplier to prevent the phenomenon of migration of dust grains separated from the collecting electrode to the further zones of electrostatic precipitator.

Research equipment constructed by the authors to study the electrical parameters of corona electrode (Fig. 1.) depending on its configuration, allows the determination of current-voltage characteristics or the current density on the surface of the collecting electrode.

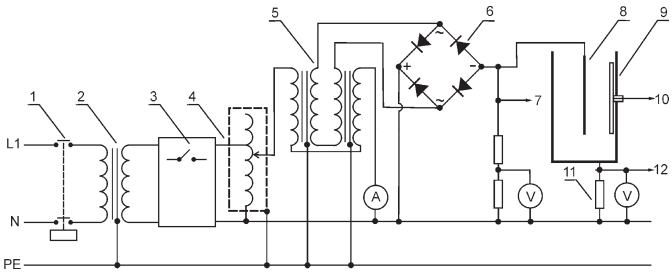

Fig. 1. Scheme of the equipment to test corona electrode parameters 1– circuit of power supply switch, 2– isolation transformer, 3– circuit for overcurrent protection, 4– high voltage control loop, 5– set of high voltage transformers, , 6– set of HV rectifiers, 7– circuit for measuring HV, 8– corona electrode, 9– colleting electrode, 10– current measuring circuit (current density at the surface of collecting electrode), 11– decade resistor, 12– current measuring circuit (I–U characteristic)

The measuring station have an active collecting electrode h = 1.0 m hight and with a maximum division of collecting electrodes H = 0.6 m allows the study of industrial corona electrodes up to 0.8 m. The measuring station consists of a supporting frame to which the collecting electrodes with the total area of 4 m^2. Tested corona electrode (8) is attached to the support frame and supplied with a DC high voltage (6). Power supply voltage allows the continuous adjustment in the range from 0 to 75 kV. The collecting electrodes (9) are connected to ground via a resistors decade box (11). The tolerance of the resistors value is 0.05%. Measuring the voltage present on the resistor and measuring the voltage on the corona electrode allows to determine the current-voltage characteristics of the collecting electrode.

During the measurement of the current–voltage characteristic of corona electrode, signal voltage of corona electrode (7) and the current flowing between the collecting electrodes and groung electrode (12) are applied to the analog inputs of 16-bit measurement card NI USB-6039 connected to the computer. The data acquisition is performed by software specially developed for this purpose in LabView programme. Measurement is carried out for the corona electrode voltages in the range of 0 to 65 kV. Each data points were measured in increment of ΔU = 500 V by the card working with a sampling rate 2KS/s. The average value of measured value was recorded and written to a file to be subjected to further analysis.

Measurement of the current density distribution on the surface of the collecting electrode is realized with 16 fields spread over the length of the measuring electrode (along the x–axis) with a constant space Δx = 0.05 m. Due to the relatively low value of the current flowing between measureing fields (10) and ground electrode of the system, the signals were sent to the, specially designed for the purpose, high stability amplifier circuit realized on INA 114 Burr–Brown using multiplexer 1 of 16. The amplified voltage signal was recorded by the data acquisition NI USB–6039 using a computer. Specially developed software enables data acquisition and control the operation of the multiplexer. Recorded value of the voltage is obtained by averaging 2000 measurements for each measurement field. The measurement data are recorded in a series of five measurements, which means that the measured value corresponding to the current value of the current flowing through each of the fields is the average of 10 thousand measurements. Such a high number of measurements are taken to minimize the influence of AC component of the high voltage transformer. The measured data are stored in the form of ASCII files to enable further analysis.

The study involved 5 cylindrical electrodes, in the form of rods of Ø = 6 mm made of steel S275 and four mast type electrodes. Carrying mast of the electrodes on the study, was made of steel pipe with a diameter of Ø = 10 mm. Emission elements made of steel strip were welded at equal intervals. The essence of this type of electrode structures is the presence of tips with a small radius of curvature being the source of the corona. Different manufacturers use similar electrostatic electrodes design solution, but the diameters of the mast and shape of the carrier emission elements (such as nail, elements in a shape Δ or U made of a wire with a diameter of 3 to 5 mm) are different. The geometry of the blades are selected depending on the desired emissivity of the electrode [11]. An example of the mast type electrode is shown in Figure 2.

Fig. 2. Mast type discharge electrode

Current-voltage characteristics and current density distribution on the collecting electrode was carried out for the electrodes without corrosion protection and with anti–corrosion coating. Anti–corrosion coating has a thickness of 50 to 65 μm, and was applied by pneumatic spraying technique. Tests were performed for three anti-corrosion agents: "Unikor C" with filler containing iron oxide (III), water-soluble polydispersion of acrylic resin with an organic filler and a polyurethane varnish without filler. The condition of the measurements were as follow: the temperature t = 22°C, the relative air humidity w = 53%, atm pressure p = 987.9 hPa.

3. Methodology for the statistical analysis of the current density distribution on the collecting electrode

Analysis of recorded value of the current flowing in the space between electrodes of electrostatic precipitator is difficult due to possible deviations from classical assumptions of normal population distribution of the results and the lack of correlation of the random sample results. Therefore, for the analysis of this phenomenon, the methodology belonging to the group of non–classical statistical methods was applied [8]. For the analysis of the distribution of current density on the surface of collecting electrode a method based on time–series model formalism was used [3]. This method is widly applied to the

analysis of acoustical phenomena [7, 13], and is increasingly used in other fields such as genetics [5, 6]. In the analysis process the measurement data *{x1, x2, ..., xn}* are the time series of random value of variable *X* representing a further observations *{x1, x2, ..., xn}* describing the current density at the collecting electrode. It is assumed that the probabilistic structureot the measured data can be described by the equation:

$$X_t = \mu_t + \varphi_t + \xi_t \,;\; t = 1,2,...,n \tag{1}$$

It was father assumed that the structure of the analyzed phenomenon is created by: trend μ_t associated with factor enforcing the level of the analyzed values, cyclic component φ_t corresponding to the periodically recurring changes and residual component ξt, satisfying the conditions of the normal distribution of noise and resulting from random noise. The classic model of a random sample probe assumes the conditions of a normal distribution for the next observation. Model applied to the analysis of the phenomenon, differs from the classical model by the assumption of the presence of a enforce mechanism changing the results, the recorded signal is subjected to random disturbances (noise signal), satisfying the conditions of the normal distribution with zero expected value and variance σ_ξ^2. In this case, the estimation problem of expected value and variance of the measured data comes down to identification of the structure of the time series.

Analysis of the distribution of current density on the collecting electrode surface were done using a program, for this purpose developed, and containing advanced statistical functions TSA (Time Series Analysis) of LabView programme. This program allows after preprocessing of the measured data (resampling, smoothing), calculate the following values for the analyzed quantity:

– The average value $\mu = \frac{1}{n}\sum_{i=0}^{n-1} X_t(i)$ after elimination of extreme values
where: μ - arithmetic mean value, n – the number of elements of the time series *Xt*,

– Value of mean RMS (Root Mean Square) $\psi = \sqrt{\frac{1}{n}\sum_{i=1}^{n}|x_i|^2}$
where ψ_x – RMS value, n – the number of elements of *X*,

– Magnitude of power spectrum PS (Power Spectrum) FFT (Fast Fourier Transform) of the current density at the collecting electrode (in the form of squares RMS)

– Power spectrum density PSD (Power Spectrum Density) FFT of the time series *Xt* (in the form of squares of the RMS per unit of x-axis of collecting electrode).

PDS describes the frequency distribution of a registered signal (or time series). and is defined as: $P(t) = f(t)^2$ for the signal *f(t)*. Average (or expected) value of *P(t)* is the sum of power spectral density calculated for all values of frequency or time. Using the Fourier transform:

$$\hat{f}_T(\omega) = \frac{1}{\sqrt{T}}\int_0^T f(t)\exp(-i\omega t)dt \tag{2}$$

where:

$\hat{f}_T(\omega)$ – Fourier transform in the frequency domain,
ω – circular frequency (2πf)
i – the imaginary unit ($i^2 = -1$),

power spectral density can be defined as [1, 2]:

$$PSD\ (\omega) = \lim_{T\to\infty} E\left[\ \left|\hat{f}_T(\omega)\right|^2\right] \tag{3}$$

where:

PSD (ω) – power spectral density,
E – the expected value of a random variable.

Alternatively, assuming a stationary nature of the studied phenomenon, which takes place in this case, according to the theorem of Wiener-Chinczyn, the power spectral density of such a process is the Fourier transform of the autocorrelation function $R(\tau) = \langle f(t)\cdot f(t+\tau)\rangle$ [15]:

$$PSD\ (f) = \hat{f}_T(R(\tau)) \tag{4}$$

where:

R(τ) – autocorelation function,
τ – signal delay time.

The procedures for the calculation of the power spectrum and power spectral density are included in the LabVIEW function libraries.
To analyse electrical parameters of electrodes tools for time series analysis available in the Advanced Signal Processing module – Time Series Analysis Tools of the LabVIEW was used [14].

The tested electrodes satisfy the condition of similarity in terms of geometry and material characteristics [9, 12]. They are objects whose properties can be determined by comparing the magnitudes: the power spectrum and power spectral density analysis of the measured values. The use of statistical methods for the analysis of time series simplifies the analysis of the results obtained by measuring electrical parameters of tested electrodes. It also provides information about the object uner test, which can not be obtained by other methods. This allows the construction of mathematical models of the phenomena occurring in the space between electrodes of electrostatic precipitator depending on the shape of the applied corona electrode. This information can be used for utilitarian purposes.

4. The results

Based on measured data recorded for each of the tested electrodes the current-voltage characteristics was determined and based on then specific initial voltage corona was calculate[4, 16]. The results for the mast type electrode are shown in Figure 3.
The initial corona voltage of corona electrode without coating and with anti-corrosion coatings, determined on the basis of current-voltage characteristics, are provided in Table 1.

The results confirm that the initial corona voltage and current-voltage characteristics of the corona electrode made of steel, are affected only by their geometrical parameters and the presence of anti-corrosion coating does not affect their electrical parameters.

Table 1. Initial corona voltage of corona electrode

Anti–corrosion coating type	Initial corona voltage [kV]	
	mast type electrode	cylindrical electrode Ø=6 mm
without coating	17,0	48,0
acrylic resin	16,8	51,4
Unikor C	17,4	48,0
polyurethane varnish	17,0	48,0

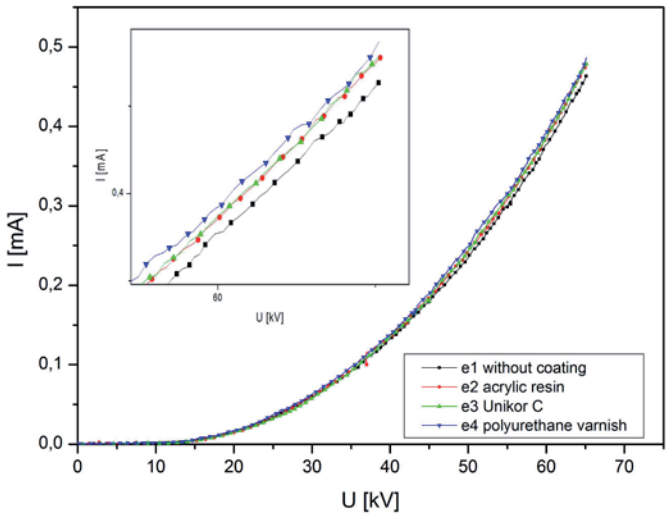

Fig. 3. Current-voltage characteristics of the mast type spike corona electrode

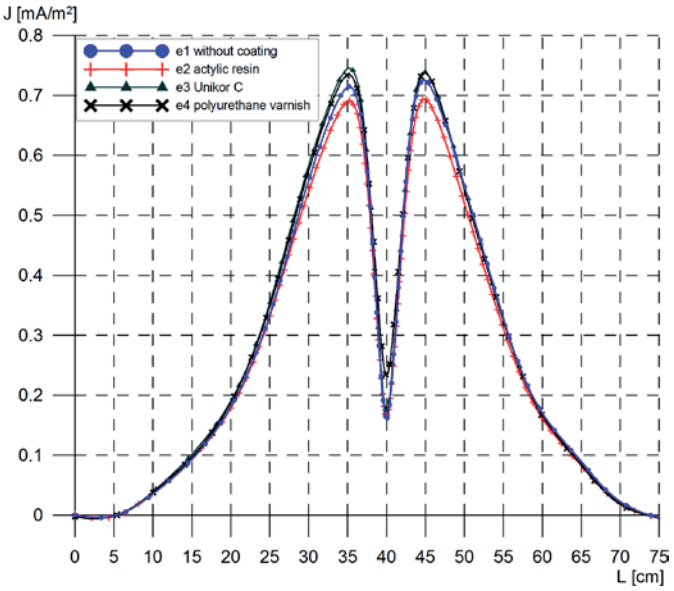

Fig. 4. Current density distribution of on the surface of the collecting electrode for a mast type spike corona elektrode

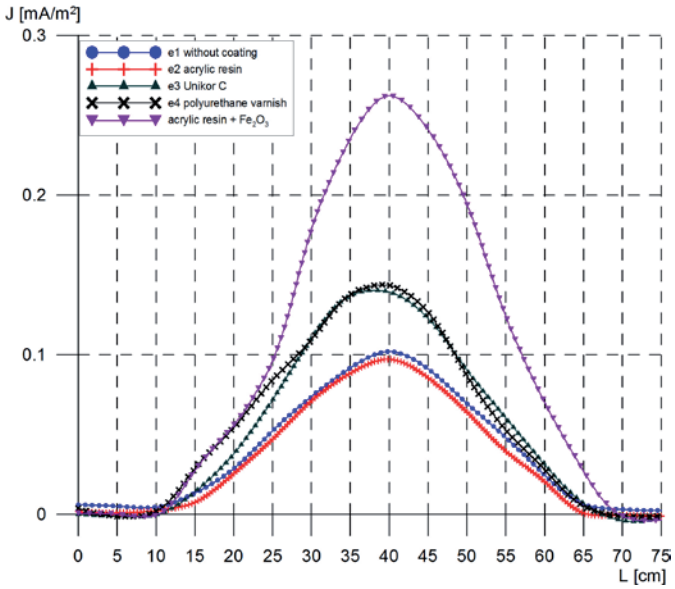

Fig. 5. Current density distribution of on the surface of the collecting electrode for a cylindrical corona electrode

The results of measurements of the current density distribution on the collecting electrode in case of spike electrode without coating and with anti–corrosion coatings are shown in Figure 4.

The results of analogous measurements corresponding to a cylindrical electrode (having a diameter of Ø = 6 mm), are shown in Figure 5. For these electrodes, the differences in a current density depending on the presence and the type of anti-corrosion coating are much more visible than in the case of a spike electrodes.

Influence of the coating with filler in the form of iron dioxide (III) on the electrical parameters of the discharge electrode, it was confirmed by introducing into the waterborne anticorrosive formulation, 15% by weight of Fe_2O_3. The measurement results confirmed that the presence of iron dioxide (III) in the coating, applied to the surface of the discharge electrode, significantly changes its electrical characteristics by increasing the emissivity.

Effect of the presence of the iron oxide (III) as a filler in the coating on the electrical parameters of corona electrode was studied by applying water-based anti-corrosion paint filled with 15 wt.% Fe_2O_3. The results confirmed that the presence of iron oxide (III) in the coating applied to the corona electrode significantly changes its electrical characteristic by increasing the emissivity.

Table 2. The results of the statistical analysis of the current density distribution on the surface of collecting electrode

Electrode	Anti–corrosion coating type	Mean Value	Root Mean Square (RMS) Value	Magnitude	
				Power Spectrum (PS)	Power Spectral Density (PSD)
mast type	without coating	0,2047	0,3469	0,3440	16,949
mast type	acrylic resin	0,1990	0,3343	0,3208	15,8545
mast type	Unikor C	0,2106	0,3568	0,3652	18,057
mast type	polyurethane varnish	0,2136	0,3561	0,3722	18,667
cylindrical Ø = 6 mm	without coating	0,0341	0,0525	0,0090	0,46689
cylindrical Ø = 6 mm	acrylic resin	0,0295	0,0491	0,0080	0,4210
cylindrical Ø = 6 mm	Unikor C	0,0441	0,0728	0,0176	0,9183
cylindrical Ø = 6 mm	polyurethane varnish	0,0471	0,0746	0,0182	0,9427
cylindrical Ø = 6 mm	acrylic resin + 15 wt.% iron oxide (III)	0,0817	0,1338	0,0596	3,0957

Table 2 presents the summary of the statistical analysis results using TSA model.

The test results show that the use of anticorrosion coating with the filler in the form of dioxide of iron (III), does not worsen of the emissivity parameters of corona electrodes protected from corrosion, but even increases it. One can assume that this is due to the physicochemical properties of the compound, but the cause of this phenomenon has not been determined. A different situation occurs in the case of rod electrodes secured by a polymer coating (polyurethane resin). The intensity of the corona discharge of rode type electrode dependents on the radius of curvature of the electrode. It is believed that the thin layer (~ 50 μm), applied by spraying has local discontinuities or areas with a lower thickness, which are the source of the corona. This increases the emissivity of the rod electrode similar to the spike electrodes, having blades with a small radius of curvature. That interpretation is borne on the electrical properties of polyurethane polymers such as high value of the resistivity [19].

5. Conclusions

The results of emissivity tests of corona electrodes used in the electrostatic precipitators showed that the use of anti-corrosive coatings does not adversely affect their electrical parameters. The presence of anti-corrosion coating does not infuence the current-voltage characteristics of the respondents corona electrode. Analysis of the results of the current density distribution on the surface of collecting electrode using TSA indicates that the corrosion protection in the form of coatings deposited on the electrode surface does not decrease in corona current density. Research has also shown that the anti-corrosion filler in the form of iron oxide (III), commonly used due to their low price, have a positive influence on the electrical characteristics of corona electrode. This responds to the concerns of electrostatic manufacturers if corrosion protection used during manufacturing and testing, will not adversely affects the operational performance of dust extraction system. The study showed that the corona electrode corrosion protection can and should be used at the assembly stage, prior to entry into service. It was also found that the anti-corrosion coating containing iron oxide as a filler (III) is the best choice for corona electrode protection against corrosion.

Acknowledgement: *The research work financed with the means of Polish National Science Center grant nr 7041/B/T02/2011/40 as a research project.*

References

1. Aboutanios E, Mulgrew B. Iterative frequency estimation by interpolation on Fourier coefficients. IEEE Transactions on Signal Processing, 2005; 53: 1237–1242.
2. Abramowitz M, Stegun IA, eds. Handbook of Mathematical Functions, New York, Dover, 1965.
3. Box GEP, Jenkins GM. Time Series Analysis. San Francisco: Holden Day, 1976.
4. Böhm J Electrostatic precipitators. Elsevier, Chemical Engineering Monographs, 1982.
5. Ceccarelli M, Maratea A. Virtual genetic coding and time series analysis for alternative splicing prediction in C. elegans. Elsevier, Artificial Intelligence in Medicine, 2009; 45: 109–115.
6. Chen-Hsiang Yeang, Jaakkola T. Time Series Analysis of Gene Expression and Location Data. IEEE International Symposium on BioInformatics and BioEngineering, IEEE Computer Society 2003: 305–312.
7. Deller Jr. JR, Hansen JHL, Proakis JG. Discrete-Time Processing of Speech Signals, New York: John Wiley and Sons, Inc., 2001.
8. Domański C, Pruska K. Nieklasyczne metody statystyczne. PWE, Warszawa 2000.
9. Jech T. Set Theory. Springer Monographs in Mathematics, Berlin, New York: Springer-Verlag, 2003.
10. Jędrusik M, Świerczok A. The correlation between corona current distribution and collection of fine particles in a laboratory-scale electrostatic precipitator. Journal of Electrostatics 2013; 71, 3: 199–203.
11. Jędrusik M, Świerczok A,Teisseyre R. Experimental study of fly ash precipitation in a model electrostatic precipitator with discharge electrodes of different design. Powder Technology 2003; 135/136: 295–301.
12. Levy A. Basic Set Theory. Berlin, New York: Springer-Verlag, 1979.
13. Mueller M, Ellis D P W, Klapuri A, Richard G. Signal processing for music analysis. IEEE Journal of Selected Topics in Signal Processing 2011; 5: 1088–1110.
14. National Instruments LabView Advanced Signal Processing, Time Series Analysis Tools User Manual 2005.
15. Parker KR. Applied Electrostatic precipitation. Blackie Academic & Profesional, London, 1997.
16. Parker K. Electrical operation of electrostatic precipitators. The Institution of Electrical Engeneers, London, 2003.
17. Ricker DW. Echo Signal Processing. Berlin, New York: Springer-Verlag, 2003.
18. Thomson JJ. Conduction of Electricity through Gases, Cambridge University Press, New York, 1945.
19. Yasar Razzaq M, Anhalt M, Frormann L, Weidenfeller B. Thermal, electrical and magnetic studies of magnetite filled polyurethane shape memory polymers. Elsevier, Materials Science and Engineering 2007: 227–235.

Ryszard MACHNIK
Faculty of Mechanical Engineering and Robotics
AGH University of Science and Technology
Mickiewicza 30, 30-059 Cracow, Poland

Marek NOCUŃ
Faculty of Materials Science and Ceramics
AGH University of Science and Technology
Mickiewicza 30, 30-059 Cracow, Poland
E-mails: machnik@agh.edu.pl, nocun@agh.edu.pl

Article citation info:
ZUBER N, BAJRIĆ R, ŠOSTAKOV R. Gearbox faults identification using vibration signal analysis and artificial intelligence methods. Eksploatacja i Niezawodnosc – Maintenance and Reliability 2014; 16 (1): 61–65.

Ninoslav ZUBER
Rusmir BAJRIĆ
Rastislav ŠOSTAKOV

GEARBOX FAULTS IDENTIFICATION USING VIBRATION SIGNAL ANALYSIS AND ARTIFICIAL INTELLIGENCE METHODS

IDENTYFIKACJA USZKODZEŃ SKRZYNI BIEGÓW ZA POMOCĄ ANALIZY SYGNAŁU DRGAŃ ORAZ METOD SZTUCZNEJ INTELIGENCJI

The paper addresses the implementation of feature based artificial neural networks and vibration analysis for the purpose of automated gearbox faults identification. Experimental work has been conducted on a specially designed test rig and the obtained results are validated on a belt conveyor gearbox from a mine strip bucket wheel excavator SRs 1300. Frequency and time domain vibration features are used as inputs to fault classifiers. A complete set of proposed vibration features are used as inputs for self-organized feature maps and based on the results a reduced set of vibration features are used as inputs for supervised artificial neural networks. Two typical gear failures were tested: worn gears and missing teeth. The achieved results show that proposed set of vibration features enables reliable identification of developing faults in power transmission systems with toothed gears.

***Keywords**: gearbox vibration, gear fault, artificial neural network, self-organized feature map.*

Artykuł omawia zastosowanie sztucznych sieci neuronowych opartych na cechach oraz analizy drgań do celów automatycznej identyfikacji uszkodzeń skrzyni biegów. Prace eksperymentalne przeprowadzono na specjalnie zaprojektowanym stanowisku badawczym, a uzyskane wyniki zweryfikowano na przykładzie przekładni przenośnika taśmowego koparki wielonaczyniowej SRs 1300 wykorzystywanej w kopalni odkrywkowej. Cechy drgań w dziedzinie czasu i częstotliwości są wykorzystywane jako wejścia klasyfikatorów uszkodzeń. Kompletny zbiór proponowanych cech drgań wykorzystano jako wejścia samoorganizujących się map cech, a na podstawie wyników opracowano zredukowany zbiór cech drgań, które wykorzystano jako wejścia do nadzorowanych sztucznych sieci neuronowych. Zbadano dwa typowe uszkodzenia przekładni : zużycie przekładni oraz brakujące zęby przekładni. Uzyskane wyniki wskazują, że proponowany zbiór cech drgań umożliwia niezawodną identyfikację rozwijających się uszkodzeń w układach przenoszenia napędu z kołami zębatymi.

***Słowa kluczowe**: drgania skrzyni biegów, uszkodzenie skrzyni biegów, sztuczna sieć neuronowa, samoorganizująca się mapa cech.*

1. Introduction

Rotating machines are the most common type of machines found in different industry fields and they have to work with high performances. An unscheduled stop due to the machine's failure leads to high maintenance and production costs risks. High costs are initiated through the production stops, losses, and urgent procurements of spare parts. High risks are associated with the possibilities of workers' injuries and secondary damages of neighboring machines. To avoid such a scenario, several maintenance strategies have been developed, from the breakdown maintenance to condition based and proactive maintenance. The implementation of condition-based maintenance implies monitoring of machine operating condition based on the physical parameter that is sensitive to machine degradation. Among many possible parameters, mechanical vibration acquired at the bearing's housing is one of the best parameter for early detection of a developing fault inside a machine. Methods of vibration signal analysis enable the extraction of type and severity of a fault. Despite the fact that the information on type and severity of a fault is contained in the vibration signal, due to the:

a. existence of multiple faults on a machine,
b. dependence of vibration signal content on operating conditions,
c. existence of vibration components from neighboring machines,

derivation of incorrect vibrodiagnostical conclusions and wrong estimation of machine criticality in the plant, is a very common situation. To avoid this, there are two approaches:

a. engagement of highly skilled and trained vibration analysts or
b. application of artificial intelligence (AI) methods for reliable extraction of an existing fault.

Engagement of certified vibration analysts can be a problematic issue due to the following reasons: there are not many of them, in many cases they don't have a substitution when absent and they are often engaged in other maintenance tasks so they cannot be fully focused on the analysis of acquired data from the machine. In such an environment, implementation of AI methods through previously developed and validated fault identification algorithm has a huge potential.

There are several methods of AI, which can be used for automatic fault identification of rotating machine: artificial neural networks (ANN), fuzzy logic, expert systems and hybrid intelligence systems. The most applied are ANN [22, 1]. One of the reasons for that is due to their ability to learn i.e. to adopt novelties. This adaptability of ANN results in a possibility for detection of an existence of a new condition (fault) based on the existing data [21, 9]. In addition, ANN

are efficient in modeling of complex nonlinear phenomena that are present in several types of rotating machinery faults.

A review of existing literature [10, 6, 20] shows that several types of ANN are successfully implemented in automatic fault identification: back propagation feed forward network (BPFF), multiple layer perceptron network (MLP), back propagation multiple layer perceptron (BPMLP), radial basis function network (RBF), self-organized feature map (SOFM) and principal component's analysis (PCA). An excellent review of different types of ANN and training algorithms implementation for different types of rotating machinery can be found in [17]. From the data presented, the increasing trend of implementation of MLP with back propagation training algorithm, with the number of neurons in hidden layers taken as a variable, is evident.

A successful implementation of BPMLP and SOFM for the identification of gearbox faults can be found in [2, 3, 8, 12, 14, 16, 19, 7]. The authors used different scalar features obtained from vibration data as inputs for neuron classifiers.

In this paper, the authors used vibration scalar features obtained in both, frequency and time domains. Definition of vibration features is done based on an assumption that these parameters are sensitive to gearbox failures tested in this paper: worn gears and missing teeth.

2. Vibration analysis techniques for gearbox failures identification

The main origin of vibrations in gearboxes is a tooth meshing which is transient by its nature. According to [15] there are several components of gear vibrations: components at the gear mesh frequencies (GM) due to the tooth profile deviation from an ideal profile, components of amplitude modulation due to the gearbox load variation, components of the frequency modulation due to the uneven space between individual teeth and transients due to the surface irregularities on the tooth surface. Along with these components from the gears, the vibration signal acquired from the gearbox housing can contain components due to the existing unbalance, misalignment, defective bearings, bent and cracked shafts, looseness etc. Gearbox GM components are calculated for every transmission stage as:

$$GM = T_{in} * f_{in} = T_{out} * f_{out} \quad (1)$$

where T_{in} and T_{out} are number of teeth on input and output gear, respectively, while f_{in} and f_{out} are rotating frequencies of the input and output shaft, respectively.

The most exploited vibration signal analysis techniques for gearbox defect identification are: time domain techniques, frequency domain techniques, cepstrum analysis and time –frequency techniques.

Time domain techniques are focused on extracting the statistical indices of time wave in order to quantify the transient phenomena that originates from the defective gear. Time domain techniques for gearbox diagnostics can be performed on several types of time waveform: raw time waveform, time waveform obtained through synchronized time averaging technique (TSA), residual time waveform, differential time waveform and band pass filtered time waveform. Residual time waveform is obtained from TSA waveform by removal of harmonic families of shaft speed and gear mesh components, while the band pass filtered time waveform is a result of a band pass filtering of TSA time waveform around a gear mesh component and its modulation sidebands. Differential signal is obtained by removal of sidebands from a residual signal. Scalar features that can be extracted on these time waveforms are classic features from higher order statistics, such as root mean square (RMS), peak values (P), standard deviation (StDev), kurtosis parameter (Kurt), skewness (Sk) and also special features developed for gearbox monitoring [18].

Frequency domain techniques refer mainly to the representation of the time signal in frequency domain using the algorithm of Fast Fourier transformation (FFT). The main advantage in using cepstrum analysis is the ability to detect periodicity in frequency domain i.e. repeated patterns in a spectrum, which is common in cases with defective gears. Time - frequency methods founded their role in gearbox diagnostics since, due to the presence of transients generated by the gear mesh activity, the signal is non-stationary. As a result, time-frequency methods provide a simultaneous view in both domains (time and frequency). The main time-frequency methods used are short time Fourier transformation (STFT), Wigner-Ville distribution (WVD) and Wavelet analysis (WA).

3. Experimental set up and results

The test rig, designed for the purpose of dataset collection, is shown on the Figure 1. The test rig consists of a 0.37kW variable frequency drive connected over the universal joint shaft to the single stage gearbox with spur gears. In reality and especially in mining industry, gearboxes often operate under the conditions of unsteady load and speed. As a result, their behavior and acquired vibration signals are very dependent on the current operating regime [4, 5, 23, 24]. For the purpose of load detection and control, the output shaft is connected to the friction brake. The resulting torque is measured through the bending force registered with a platform type load cell. For the purpose of load control, the stranded wire is connected to the friction pads and over the pulley; the other end is loaded by the mounted weight. This assures a constant torque for different level of brake pads wornness.

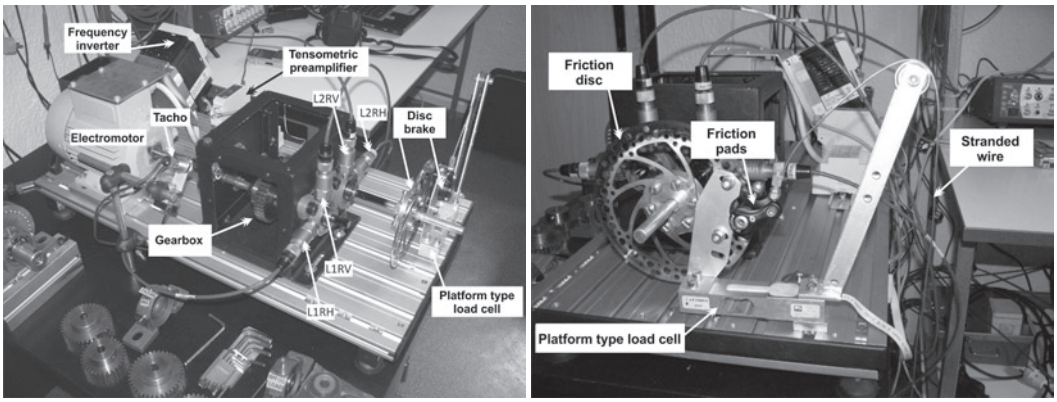

Fig. 1. Test rig used for vibration acquisition on faulty gearbox

Gearbox vibrations are measured in radial directions, using an industrial type IEPE accelerometers mounted at the roller element bearing housings using mounting studs. Input shaft speed is measured using a non-contacting laser sensor and a reflective mark. Also equivalent noise levels with A weighting were measured using an IEPE based microphone. Three sets of gears were tested: gears in a new condition, worn gears and gears with two missing teeth on the input gear, labeled as "OKOK", "PZOK" and "NZOK", respectively. All the tests were performed at the 22Hz of input speed; the input gear has 37 teeth so the five harmonics of GM frequencies are 814 Hz, 1628 Hz, 2442 Hz and 4070 Hz, respectively.

Vibration, force and tacho signals were acquired simultaneously using a multichannel vibration analyzers NetdB and MVX and dbFA and XPR software from 01db-Metravib.

Vibration acquisition included the measurement of[1]: raw time waveforms, narrow band FFT in different frequency ranges with 3200 lines of resolution (2 Hz–2 kHz, 2 Hz–5 kHz, 2 Hz–20 kHz), envelope spectra, time waveform obtained by TSA technique with 100 averages, Cepstrum and autocorrelation functions of the raw and TSA time waveforms. Based on these measurements 58 scalar features were extracted: RMS values of vibration velocity, RMS values of acceleration in several frequency bands (10 Hz – 20 kHz, 2 Hz – 300 Hz, 2 Hz – 2 kHz, 1 kHz – 2 kHz, 2 kHz – 6 kHz, 6 kHz – 10 kHz, 10 kHz – 20 kHz), 01dB bearing defect factor[2], Kurtosis values obtained from raw, band pass filtered (700 Hz – 1400 Hz) and TSA time waveforms, peak to peak values obtained from raw and TSA time waveforms, amplitudes of first five harmonics of GM, overall accelerations obtained from narrow bands around first five harmonics of GM (with bandwidth equals to five sidebands from each side of the central frequency – GM as shown on Figure 2.), amplitude extractions for first four harmonics of the roller elements bearing defect frequencies obtained from FFT and envelope spectra and equivalent A weighted noise levels.

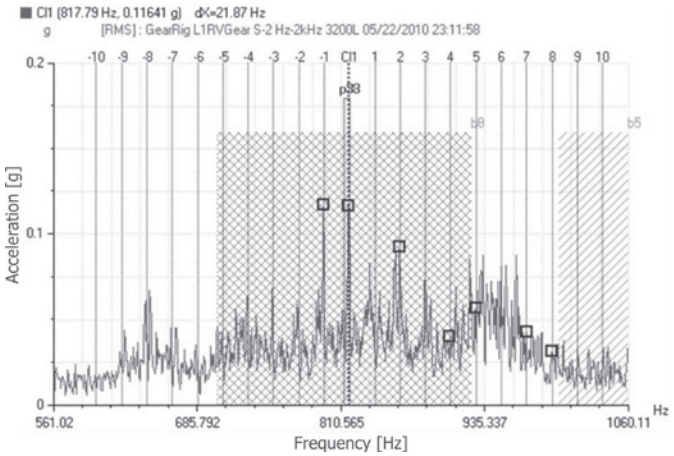

Fig. 2. 1xGM extraction and width for overall energy calculation in the frequency band

SOFM [11] is an excellent tool for the visualization of high dimensional data. In this paper, the idea of using SOFM is the selection of most suitable input features for ANN, since the success of ANN pattern recognition is highly dependent on the choice of input features. SOFM consists of neurons organized in a low dimensional grid where each neuron has a dimension that equals to the number of the input features. The map topology is dictated through neighboring relations between the adjacent neurons. During the SOFM training, the weight vectors move across the data, the map gets organized and, in result, the neighboring neurons have similar weight vectors. SOFM testing was performed in SOM toolbox for Matlab environment [25]. The quality of clustering is analyzed using distance matrix, which visualizes the distances between adjacent neurons on the map: low values indicate clusters while higher values indicate the borders between existing clusters. On the other hand, component planes for each input feature show the values of that feature for each unit on the map. This makes them convenient for analyzing the influence of each input feature on the clustering.

For every gear pair tested, 100 measurements were acquired with 10 minutes of delay between them. This resulted in the matrix of input features with 300 rows. Input matrix with 58 scalar features was labeled and introduced to SOFM algorithm. As a results, a SOFM with quantization error 1.8512, shown on figure 3, is generated. The quantization error is a measure of map resolution and is defined as an average distance between each data vector and its best matching unit. Figure 4 shows the map topology with the projections of input vectors and color coded labels (OKOK-red, NZOK-green, PZOK-blue).

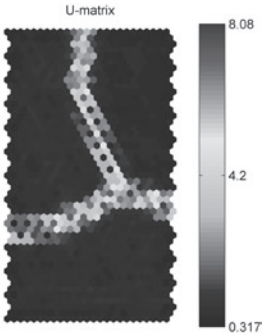

Fig. 3. Distance matrix for SOFM with 58 input features

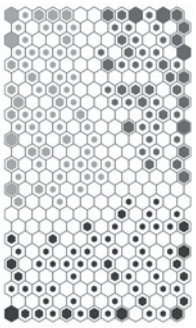

Fig. 4. SOFM topology with color coded labels

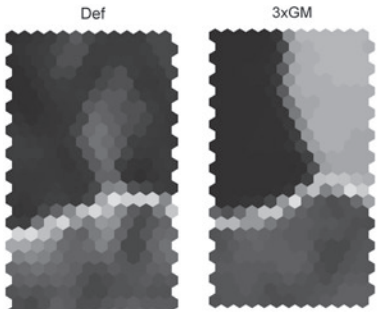

Fig. 5. Component planes for bearing defect factor and 3rd GM harmonic

Figure 5 shows component planes for bearing defect factor and the third harmonic of the GM. It is evident that the GM harmonic amplitude is a much better choice. Therefore, based on the analysis of the component planes, a reduction of the number of the input features is done. As a result from a total of 58 input features, 24 were chosen: overal acceleration in the mentioned frequency bands, Kurtosis parameters of the raw and TSA time waveforms and their autocorrelations, peak to peak values of the raw and TSA timewaveforms, A weighted noise levels, amplitudes of the GM harmonics and overall accelerations from narrow bands around the GM components. As a results of the SOFM training with the dataset that consists 24 input features a SOFM with much smaller quatization error (0.9031) is generated – Figure 6.

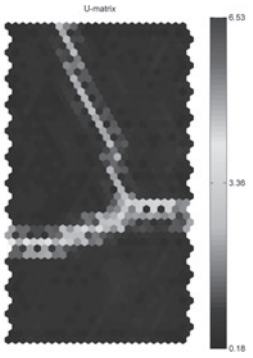

Fig. 6. Distance matrix for SOFM with 24 input features

MLP ANN utilized in this research had a classification task – to detect an exact gearbox defect type. Several architectures of MLP ANN were tested by the means of choosing the optimal network architecture from the point of the number of neurons in the hidden layer,

1 Definition of measurement parameters and frequency ranges was guided by additional tests, performed, but not presented in this paper – analysis of combination of gear and roller element bearing faults and development of automatic alghoritms for multiple faults identification.

2 Linear combination of peak and RMS values of acceleration.

type of activation functions and type of the learning algorithm. For building, testing and training, Statistica Automatic Neural Networks package has been used. 210 input vectors (70% of the dataset) were used for training while 45 input vectors were used for cross verification and testing. The software automatically determined network complexity. 20 networks were tested. The best network with 12 neurons in hidden layer (MLP 24-12-3) and with excellent classification – 100% for each output case.

4. Case study

SOFM and ANN for automatic identification of rotating machinery faults was implemented on the mine strip bucket wheel excavator SRs 1300 [23, 24], where an online system for the excavator surveillance based on strain, stress and vibration measurement has been installed [13]. After the monitoring system was installed, several faults on the excavator were identified (roller element bearings faults on the input stage of the bucket wheel drive gearbox, roller element bearings fault on the motor of the first belt conveyor drive, gear failure at the third transmission stage of the first belt conveyor gearbox etc.). As a case study to be presented in this paper, a pinion failure of the belt conveyor gearbox is chosen. A belt drive is driven through a 450 kW motor working at 955 RPM. A three stage gearbox (shown on Figure 7) is connected to the drive through rigid coupling. The numbers of teeth on gears and GM components in the term of orders of the input frequency are shown on table 1.

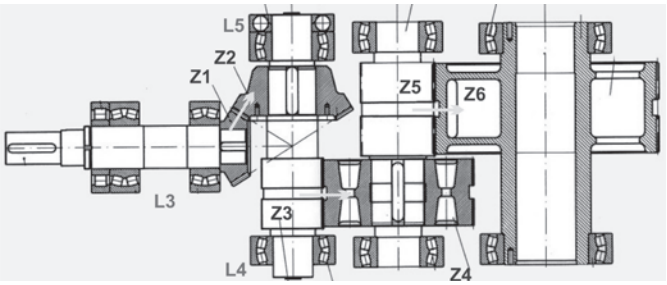

Fig. 7. Belt drive gearbox scheme with the locations of accelerometers (L3, L4, L5)

Table 1. Number of teeth and GM frequencies for the analyzed gearbox

Number of teeth		Transmission ratio	GM [order]
z1	29	0.63043	29
z2	46		
z3	57	0.40141	35.93478261
z4	142		
z5	47	0.31973	11.89390692
z6	147		

Nearly two years after monitoring system installation and data collection, maintenance engineers reported a sudden increase in accelerations coming from the sensors mounted on the gearbox. Analysis of the frequency spectra revealed that the increase in overall accelerations originates from the occurrence of GM of the third transmission stage (Figure 8). Also sidebands from the pinion's drive are visible. Unfortunately, the initial measurement setup did not include accelerometers mounted at the bearings of the third transmission stage. Therefore, measurements from location L5, as the closest to the third stage, were chosen for the analysis.

After the gearbox overhaul, the origin of high GM activity was found – missing teeth on the pinion gear at the third transmission stage. Initial measurement setup defined for this machine included

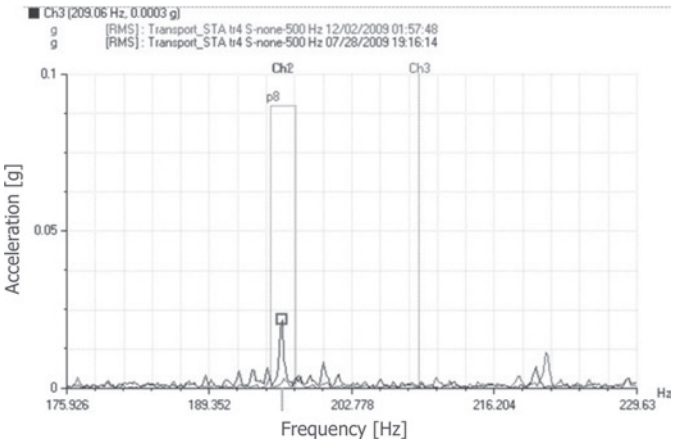

Fig. 8. Comparison of frequency spectra from the measurement point L5

amplitudes from first three harmonics of GM frequencies, overall accelerations in bands around GM and their difference calculated at each GM harmonic. Therefore, these values (for the GM on the third stage) were chosen as input features for SOFM and ANN. The occurrence of a fault was identified on trend plots of the mentioned features so it was easy to assign labels to the input dataset, which was consisted of 1011 individual records. Input matrix was introduced to the SOFM algorithm and a SOFM with quantization error 0.7273 was generated (Figures 9 and 10). As it can be seen from the figures the classification of the map neurons in two distinct clusters are more than satisfactory.

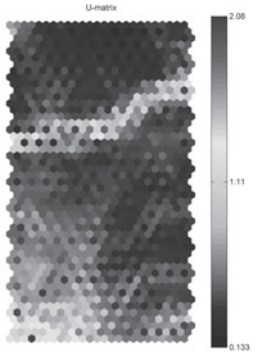

Figure 9. Distance matrix for SOFM with 9 input features

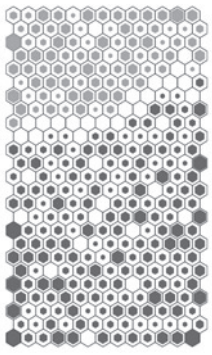

Figure 10. SOFM topology with color coded labels (green-OK, red-NOK)

Result of the unlabeled dataset introduction to ANN algorithm resulted in the ANN with excellent classification – 100% for each case. As in previous cases 70%, 15% and 15% of the total dataset was used for training, cross verification and testing of the ANN. The wining network had 4 neurons in the hidden layer (MLP 9-4-2).

5. Conclusion

Vibration analysis is a proven method for achieving a high reliability of rotating machinery. However, for complex machines, such as gearboxes, evaluation of machine condition based on vibration measurements could be a hard task and implementation of AI can help. In this paper, we demonstrated the use of SOFM and ANN for automatic identification of missing and worn teeth in gearboxes that work under steady loads. It is shown that SOFM can be used for preprocessing phase where a reduced set of vibration features should be defined as inputs in ANN algorithm. Excellent classification of existing faults was obtained by the use of ANN. Results indicated that overall acceleration values defined in frequency bands that cover GM components and amplitudes of GM are satisfactory features that can be used for automatic identification of gear faults.

Acknowledgement: *The research work financed with the means of the State Ministry of science and technological development (Serbia) in the years 2008-2010 as a research project.*

References

1. Baillie D, Mathew J, Diagnosing Rolling Element Bearing Faults with Artificial Neural Networks. Acoustics Australia 1994; 22(3); 79–84.
2. Bartelmus W, Zimroz R, Batra H, Gearbox vibration signal pre-processing and input values choice for neural network training. Conference proceedings - AI-METH 2003 Artificial Intelligence Methods, Gliwice Poland; 2003; 21–14.
3. Bartelmus W, Zimroz R, Application of self-organised network for supporting condition evaluation of gearboxes. Conference proceedings - Methods of Artificial Intelligence AI-METH Series, Gliwice Poland; 2004; 17–20.
4. Bartelmus W, Zimroz R, A new feature for monitoring the condition of gearboxes in nonstationary operating conditions. Mechanical Systems and Signal Processing 2009; 23: 1528–1534.
5. Bartelmus W, Zimroz R. Vibration condition monitoring of planetary gearbox under varying external load. Mechanical Systems and Signal Processing 2009; 23: 246–259.
6. Bishop C. Neural Networks for Pattern Recognition. Oxford University Press 1995.
7. Czech P, Łazarz B, Wilk A. Application of neural networks for detection of gearbox faults. WCEAM CM 2007. Harrogate, United Kingdom, 2007.
8. Guanglan L , Tielin S, Weihua L, Tao H, Feature Selection and Classification of Gear Faults Using SOM. Advances in Neural Networks – ISNN 2005, Springer Berlin / Heidelberg; 2005: 556–560.
9. Hoon S, Worden K, Farrar C, Novelty Detection under Changing Environmental Conditions, LA-UR-01-1894. SPIE's 8th Annual International Symposium on Smart Structures and Materials, Newport Beach, CA; 2001.
10. Jyh-Shing R.J, Chuen-Tsai S, Mizutani E, Neuro-fuzzy and soft computing : a computational approach to learning and machine intelligence. MATLAB curriculum series. Prentice Hall, 1997.
11. Kohonen T. Self-Organizing Maps. Springer, Berlin, 1995.
12. Lazarz B, Wojnar G, Czech P. Early fault detection of toothed gear in exploitation conditions. Eksploatacja i Niezawodnosc – Maintenance and Reliability 2011; 1(49): 68-77.
13. Licen H et all. Continuous remote monitoring of vital parameters of mobile machinery relevant for their operating condition as a part of their total reliability and predictive maintenance. Project 14037 financed by the Serbian Ministry of Science and Technological Development of Republic of Serbia, 2008-2010.
14. Rafiee J, Arvani F, Harifi A, Sadeghi MH. Intelligent condition monitoring of a gearbox using artificial neural network. Mechanical Systems and Signal Processing 2007; 21(4): 1749–1754.
15. Randall RB. A new method of modeling gear faults. ASME J. Mech. Design 1982; 104: 259–267.
16. Sadeghi MH, Rafiee J, Arvani F, Harifi A. A Fault Detection and Identification System for Gearboxes using Neural Networks. Neural Networks and Brain, ICNN&B '05. International Conference. 2005.
17. Sick B. Review On-Line And Indirect Tool Wear Monitoring In Turning With Artificial Neural Networks: A Review Of More Than A Decade Of Research, Mechanical Systems and Signal Processing 2002; 16(4): 487–546.
18. Stewart RM. Some Useful Data Analysis Techniques for Gearbox Diagnostics, Institute of Sound and Vibration Research, Southampton University, Southampton, 1977.
19. Staszewski WJ, Worden K. Classification of faults in gearboxes – pre-processing algorithms and neural networks, Neural Computing and Applications 1997; 5: 160–183.
20. Veelenturf LPJ. Analysis and Applications of Artificial Neural Networks, Prentice Hall, 1995.
21. Worden K, Sohn H, Farrar CR. Novelty Detection in a Changing Environment: Regression and Interpolation Approaches, Journal of Sound and Vibration 2002; 258 (4); 741–761.
22. Zhong B. Developments in intelligent condition monitoring and diagnostics, System Integrity and Maintenance, 2nd Asia-Pacific Conference(ACSIM2000) Brisbane Australia; 2000; 1–6.
23. Zuber N. Automation of rotating machinery failures by the means of vibration analysis. PhD Thesis, Faculty of Technical Sciences – University of Novi Sad, 2012.
24. Zuber N, Ličen H, Bajrić R. An innovative approach to the condition monitoring of excavators in open pits mines, Technics technologies education management-TTEM 2010; 5(3): 841–847.
25. SOM Toolbox for Matlab, laboratory for information and computer science, University of Helsinki, http://www.cis.hut.fi/projects/somtoolbox.

Ninoslav ZUBER
Faculty of Technical Sciences
University of Novi Sad
Trg Dositeja Obradovica 6, Serbia
Rusmir BAJRIĆ
Public enterprise Elektroprivreda BIH
Coal Mine Kreka, Mije Keroševica 1, Tuzla, Bosnia and Herzegovina
Rastislav ŠOSTAKOV
Faculty of Technical Sciences
University of Novi Sad
Trg Dositeja Obradovica 6, Serbia
E-mails: zuber@uns.ac.rs; rusmir.bajric@kreka.ba; sostakov@uns.ac.rs

Article citation info:
KULIKOWSKI K, SZPICA D. Determination of directional stiffnesses of vehicles' tires under a static load operation. Eksploatacja i Niezawodnosc – Maintenance and Reliability 2014; 16 (1): 66–72.

Krzysztof KULIKOWSKI
Dariusz SZPICA

DETERMINATION OF DIRECTIONAL STIFFNESSES OF VEHICLES' TIRES UNDER A STATIC LOAD OPERATION

WYZNACZANIE SZTYWNOŚCI KIERUNKOWYCH OPON POJAZDÓW SAMOCHODOWYCH W WARUNKACH STATYCZNEGO DZIAŁANIA OBCIĄŻENIA*

This paper presents the stand test results on the different tires under static conditions. The tests were conducted on a stand that allows registering the force and deflection of the tested tires. The results were used to determinate directional tire stiffness, by using self-made software identification. In the next stage, tread prints were made, which were used to determine the surface area of the tire contact with the ground, depending on the pressure inside the tire and the load. The results showed correlations of stiffness growth with increasing tire pressure at radial, longitudinal and torsional evaluation, the contrary conclusions were put forward in the evaluation of circumferential stiffness. The tires, which the characteristics were significantly different from the study group, were also presented. The received results can be the input data for dynamic tests.

***Keywords**: stiffness, pneumatic tire, determination, static tests.*

W artykule przedstawiono wyniki badań stanowiskowych różnego rodzaju opon samochodowych w warunkach statycznych. Próby przeprowadzono na stanowisku umożliwiającym rejestrację siły i odkształcenia badanej opony. Uzyskane wyniki posłużyły wyznaczeniu sztywności kierunkowych opon, wykorzystując własne oprogramowanie identyfikujące. W kolejnym etapie wykonano odciski bieżnika, które posłużyły do wyznaczenia pola powierzchni styku opony z podłożem w zależności od ciśnienia wewnątrz opony oraz obciążenia. Wyniki wykazały korelacje dotyczące wzrostu sztywności w miarę zwiększania ciśnienia w oponie przy ocenie promieniowej, wzdłużnej, skrętnej, przeciwne wnioski wysunięto w przypadku oceny obwodowej. Zaprezentowano również opony odstające o charakterystykach znacznie odbiegających od badanej grupy. Otrzymane wyniki mogą być danymi wejściowymi do badań dynamicznych.

***Słowa kluczowe**: sztywność, opona pneumatyczna, wyznaczanie, badania statyczne.*

1. Introduction

Expectations which puts out for car tires are not limited only to give them the longest life. Table 1 shows a number of other requirements for tires.

Table 1. Requirements for car tires

Requirements for car tires			
Material:	**Economic:**	**Performance:**	**Functional:**
retreadability	available production technologies	ability to roughness	proper stress-strain characteristics
resistance to climate conditions	material availability	resistance to aging	ability to aquaplanning
low mass	low price	resistance to wear	static and dynamic balance
ability to recycle		low noise	optimal adhesive properties
		long life	

Also, the requirements for tires are: high abrasion resistance, optimum stiffness characteristics and low rolling resistance [9]. They were presented in Table 1. The behavior of tires largely depends on its interaction with the ground [7] but the impact to their work have also the speed and loads on vehicle axles [15]. The parameters which determine the ability to control the vehicle, in addition to the geometry of the chassis (steering) axle loads and speed, include designated in this paper stiffness and the contact area of the tire tread with the ground. This determines the slip angle in the tire [5].

Basing on the literature analysis, it should be noticed that a small portion of it, deals with the determination of important parameters of tires which are being in exploitation. In the paper [17], methods of determining the radial stiffness were presented, for example: the static method, in which the tests were carried out at different pressures inside the tire, but it was related to brand new tires. On the other hand, in [2, 16] it was focused on influence of the tire stiffness on vehicle vibrations - in result: on the users comfort (also new tires). In [12], there were presented the results of research on the influence of run-flat inserts only on the radial stiffness of the tire, whereas there should also be expected for the assessment of lateral stiffness. The value of stiffness was the main parameter which in [6] was used to formulate the coefficient of longitudinal slip stiffness.

It should be kept in mind that tire manufacturers have tire parameters that can be used for comparative purposes, but do not provide them with the tire. One of the commonly

(*) Tekst artykułu w polskiej wersji językowej dostępny w elektronicznym wydaniu kwartalnika na stronie ***www.ein.org.pl***

available parameters, included in the markings shown on the sidewall of the tire, is load index [10], the values of other parameters are available for an additional charge.

Concerning the above, it was considered purposeful to determine directional stiffness of tires of different construction and purpose, which are in various stages of operating capacity, and as a result would be possible to compare their parameters. Thus designated target characteristic values can be used to model the movement of the vehicle, particularly in simulations of collisions where vehicles involved are not always brand new.

Stiffness characteristics are usually determined in static way by mounting a pneumatic wheel on a stand in the position that allows applying a load and measure the tires deflection.

The overall stiffness of the pneumatic tire C [6] is defined as:

$$C = \frac{\Delta x}{\Delta l} \left[\frac{N}{m}\right] \tag{1}$$

where: Δx – increase of the value of the static reaction (radial, longitudinal, lateral, torsional), Δl – increase of tire deformation

Depending on the direction of the force there are distinguished:

- **Radial stiffness** – it`s calculated as the dependence of the radial tire deflection of the vertical force. Since the radial stiffness largely depends on the size of dynamic load chassis components, so as ride comfort [12]. Due to the fact that the pneumatic tire has a multilayer construction, while the tire is loaded there is a hysteresis effect - the generation of energy loss during the loading and unloading tire [3, 6, 8, 12].
- **Circumferential stiffness** – this is the relationship between the longitudinal movement and the longitudinal force, applied to the wheel axis. Circumferential forces (braking, driving) causes circumferential distortion in tire shell. Circumferential stiffness allows to define the properties of the tire in the longitudinal direction and slip stiffness [6].
- **Lateral stiffness** – the dependence of the lateral displacement of the tire side force, applied to the wheel axle. Lateral stiffness is particularly important with tire overdrive phenomenon during the lateral tire slip [11]. Overdrive phenomenon in tire during the lateral slip is the result of changes in shell tire deformation in the transverse direction [15], in other words, the lateral reaction, resulting in a zone of the tread contact with the ground, is transferred to the wheel rim by means of the elastic element (tire). Due to the lateral stiffness, elastic properties of the tire in the transverse direction can be defined [11].
- **Torsional stiffness** – the relationship between the received angle of rotation of the tire and torque. This parameter significantly affects on the lateral slip angle, which is very important for sports vehicles [4, 14, 16].

Studies on the effect of the pressure in the tires to the size of the surface area of the tire tread contact with the road [13] were already run in the 80's. It has been proved that the pressure variation inside the tire has a significant effect on the change of stress distribution on the surface of the contact with the ground [1].

The research are intended to determine the presence of influence of input signal (tire pressure, load and hence the stress distribution) on the output quantities (tire stiffness, the size of the tire contact area with the ground) without specifying the functional dependence.

2. Tires characteristics

Considering the variety of available car tires, the selection of a representative group of tires was motivated by the general criteria, such as availability, dimensional popularity, type of tread or application.

Research subjects were divided into three groups according to their use, as follows:

- group I (summer tires),
- group II (M+S tires),
- group III (group III (other, which include spare tire, off-road, and after regeneration – poured).

Due to the fact that the tires used in the studies were exploited, coming from the dismantling, and long ago excluded from the production, a certain data were not possible to get.

3. Research methodology

The research consisted of three phases:

- phase I – experimental research (with pressure in tire – 1.2 *bar*; 2.2 *bar*; 3.2 *bar*), the registration of load and deformation,
- phase II – stiffness identification of pneumatic tires,
- phase III – the preparation of the tire tread prints.

Characteristics were made on the machine for static testing of car tires located in Vehicle Laboratory on Faculty of Mechanical Engineering in Bialystok University of Technology (Fig. 1).

4. Registration of the measurements

To receive parameters values (force, deformation) in the course of research there were used: force transducer Dir-1-WT1, displacement transducer Cl100 and laptop computer with NI DAQCard-6024E card. Registration of waveforms was made using the original software created in LabVIEW, where it was visible preview of current parameters, as well it was possible to save the results to a text file. 10 repetitions of each measurement were performed.

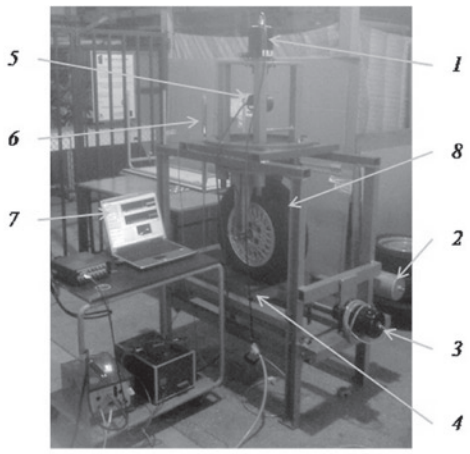

Fig. 1. Research station to determine tire stiffness : 1 - pneumatic cylinder for simulating the radial load , 2 - pneumatic cylinder for simulating torsional load , 3 - pneumatic cylinder for achieving circumferential and lateral load, 4 - sliding plate, 5 - Dir-force transducer 1-WT1, 6 - CL100 displacement transducer, 7 - laptop computer with a NI DAQCard-6024, 8 - tested tire

4.2. Treatment of experimental results

Due to the fact that the electrical equipment (laptop, converters, amplifiers) used in the study were powered by electric site, in addition to the results, disturbances (noise and 'peaks') were also recorded, because test card was very sensitive to the minimum voltage change. These disturbances (from the mains) were the result of, for

Table 2. Brands and models of tires used in research

Nr.	Brand and Model	Size	Load index	Speed index	Year	Internal tire construction		Photo
						Side	Tread	
GROUP I								
1.	Uniroyal Rallye 680	175/65 R13	-	-	-	1 polyester	1 polyester 2 steel	
2.	Kormoran Impulser	155/70 R13	75	T	2000	1 polyester	1 polyester 2 steel	
3.	Debica Passio	135/80 R12	68	T	2004	-	-	
4.	Debica D-164	135/70 R13	68	T	1994	1 rayon	1 rayon 2 steel	
GROUP II								
5.	Marshal Powergrip 749	175/70 R13	82	T	2002	1 polyester	1 polyester 2 steel	
6.	Pirelli Iceplus	155/65 R13	73	Q	2009	1 nylon	1 nylon 2 steel	
7.	Berlin-tyre	155/70 R13	-	-	1995	-	-	
8.	Pirelli P400 Aquamile	155/70 R13	75	T	2006	1 polyester	1 nylon 2 steel 1 polyester	
GROUP III								
9.	USSR ИВ – 167	5,90-13	-	-	-	-	-	
10.	Continental CST 14	105/70 R14	84	M	1991	-	1 rayon 2 steel	
11.	Stomil D-90	165 R13	-	-	-	-	-	

example, other applications requiring switching on and off of electrical equipment near to research station. Interference frequency pointed to the 50 *Hz*, which results from the supply voltage frequency and the amplitude did not exceed 5% of the test range. The transitional recorded peaks did not exceed 20% of the test range. Measurements had static character, so in the registered range of data momentary peaks accounted for 5% of the total results. In order to remove interference, the recorded results were subjected to processing (filtering). Filtration is the process of extinguishing the signal spectrum in the selected frequency ranges. To remove noise from the recorded measurements, Butteworth low-pass filter was used [18].

4.3. Stiffness identification

For identification of the stiffness, the linear regression and the method of least squares were used. Procedures were written in the code of the MATLAB - SIMULINK, Guide addition. FPE_1 (2) index minimalisation was performed numerically using gradientlessness Nelder - Mead simplex method [18], until the desired accuracy of the calculations was achieved, adopted at the $1e^{-6}$ (Fig. 2).

$$FPE_1 = \frac{m+l}{m(m+l)}\sum_{i=1}^{m}\left(F_d - F_m\right)^2 \quad (2)$$

where: m, l –numbers, F_d – measured force values, F_m – model force values

Using the recorded waveforms, force changes in the course of the next iteration the F_m model were sought.

To determine the average error, the FPE_2 index was defined as follows:

$$FPE_2 = \frac{1}{m}\sum_{i=1}^{m}\left(F_d - F_m\right) \quad (3)$$

and the FPE_3 index which is the maximum value of the error

$$FPE_3 = MIN\left(F_d - F_m\right) \quad (4)$$

A qualitative assessment of the experimental F_d and model F_m force fit was based on values of the linear regression coefficient adjusted for degrees of freedom:

$$R^2 = 1 - \frac{m-l}{m-1}\frac{\sum_{i=1}^{m}\left(F_d - F_m\right)^2}{\sum_{i=1}^{m}\left(F_d - \overline{F_m}\right)^2} \quad (5)$$

The dialog box of stiffness identification program (Fig. 3) contains: the function buttons by which the source files are determined, the objective function and procedures (pre-load, pre-deflection) (1), the area that indicates the result of identifying and assumed deflection and pre-load, power – torque coefficient and displacement - the angle (2), the area showing FPE_1, FPE_2, FPE_3 and $R2$ (3), a window showing the course of the force and deflection at the time (4), a window showing the dependence of the strength of the deflection (5) and the search button (6). Block diagram of the program is shown in Figure 2.

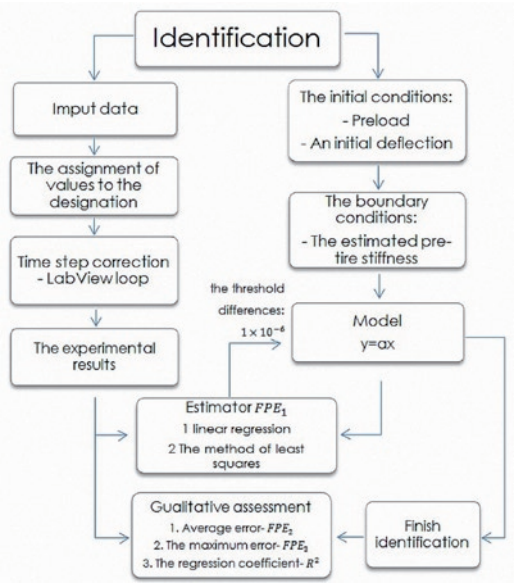

Fig. 2. Block diagram of the stiffness identification program ,,Tire" in Matlab - Simulink Guide

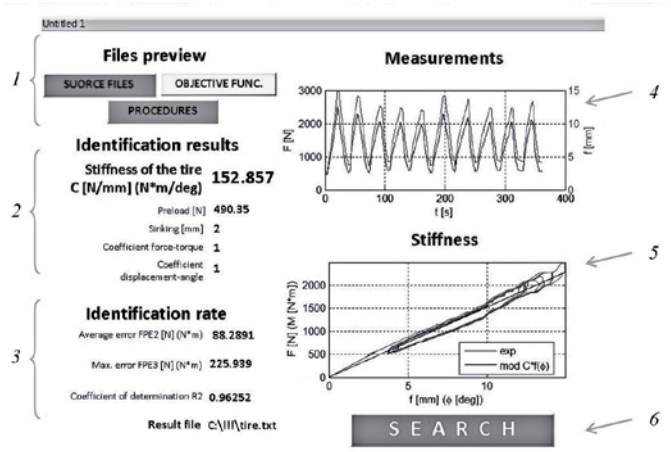

Fig. 3. The dialog box to stiffness identification program (Matlab-Simulink, Guide addition)

4.4. The maximum error of estimate of at the assumed number of repetitions

In order to determine the accuracy of the results (maximum error of estimation) at a predetermined minimum number of measurements, preliminary studies were carried out. The study consisted of a vertical load the tire mounted on the rim and the registration of the deflection as a function of the loading force with the nominal tire pressure of 2,2 *bar*. Tests were repeated 10 times. From the measurements was determined tire radial stiffness, and is shown on a bar graph (Fig. 4). Determined values were adopted for statistical analysis, and to determine the maximum estimation error in the relevant studies.

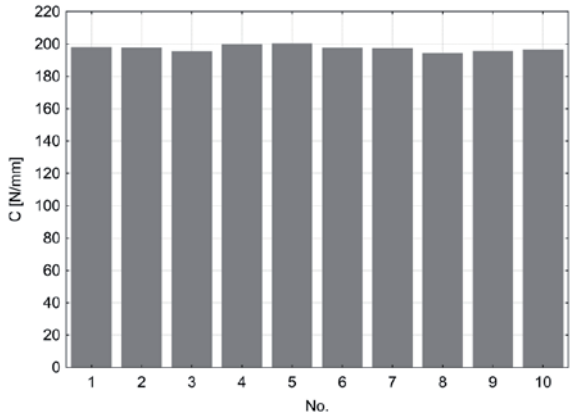

Fig. 4. Bar graph showing the designated values of radial tire stiffness from 10 repetitions

An important parameter that had to be determined in order to calculate the maximum error of estimation is the number of degrees of freedom, comprising as the number of independent observations minus the number of relations that combine these results together. Assuming the number of repetitions of measurements n = 10, and the variance, the maximum error of estimation was specified:

$$D = \sqrt{\frac{S^2 \cdot t_\alpha}{n}} = 0{,}95\left[\frac{N}{mm}\right] \quad (6)$$

where: S – standard deviation from sample, n – number of repetitions, t_α – statistics.

5. Determination of torsional stiffness

Determination of torsional stiffness consisted on the use of a device that allows the "twist" of the tire. It was implemented by using the swivel plate (Fig. 5) mounted movably on thrust bearings on the table. Torsion angle φ dependence of displacement x is shown in Figure 6.

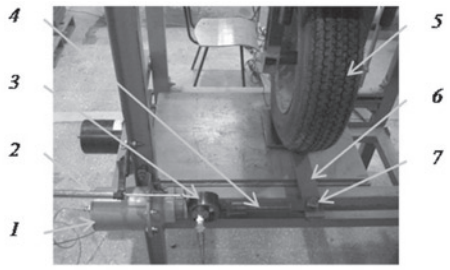

Fig. 5. Mechanism to determine the torsional stiffness: 1 - cylinder, 2 - displacement transducer CL100, 3 - Dir force transducer 1-WT1, 4 - pusher, 5 - tire, 6 - torsion plate, 7 - pin

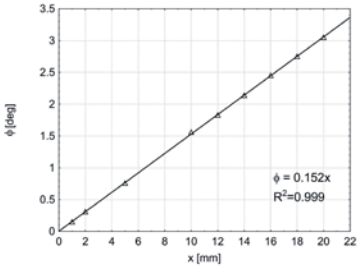

Fig. 6. Dependence of the angle of twist φ [deg] of displacement x [mm]

Knowing arm r at which force F acts, the torque was determined from the formula:

$$M_s = F \cdot r \ \left[N \cdot m\right] \tag{7}$$

where: M_s – torsional torque [Nm], F – force [N], r – radius [m].

The resulting equation was used in the program for the stiffness identification

Table 3. Coding of test tires

Code	Brand	Model
GROUP I		
L-1	Uniroyal	Ralle 680
L-2	Kormoran	Impulser
L-3	Debica	Passio
L-4	Debica	D-164
GROUP II		
M-1	Marshal	Powergrip 749
M-2	Pirelli	Iceplus
M-3	Berlin-Tyre	-
M-4	Pirelli	P400 Aquamile
GROUP III		
I-1	USSR	ИВ – 167
I-2	Continental	CST14
I-3	Stomil	D-90

6. Results and analysis

The results were presented in the bar charts form, that transparently shows the differences between tires stiffness, depending on the pressure in the tire. In order to improve the readability of graphs, names used car tires were encoded. The summary of results is presented in [10].

6.1. Radial stiffness

When examining radial stiffness of the tested tires (Figure 7), in each case there can be noticed that the higher the pressure in the tire, the stiffness increases. The biggest jump was recorded in the I-1 tire, between the tire pressures 2.2 *bar*–3.2 *bar* (60.3%). The smallest difference in stiffness was observed in the case of a L-3 tire tire pressures between 2.2 *bar*–3.2 *bar* equal to 13.7%.

6.2. Circumferential stiffness

Referring to circumferential stiffness some tire of each group (Fig. 8), it was noted that the value of stiffness, with increasing inflation pressure, decreases.

The L-4 tire's circumferential stiffness, with the lowest pressure (1.2 *bar*), was equal 78.2 *N*/*mm*, while the maximum pressure equal to 3.2 *bar* stiffness amounted only 45.9 *N*/*mm* (difference 70%). In the case of M-4 tires, at the lowest pressure (1.2 *bar*) circumferential stiffness was 133.88 *N*/*mm*, at a nominal pressure of 2,2 *bar* only 84.96 *N*/*mm* (a difference of 57.5%). Further pressure increases caused that the stiffness increased

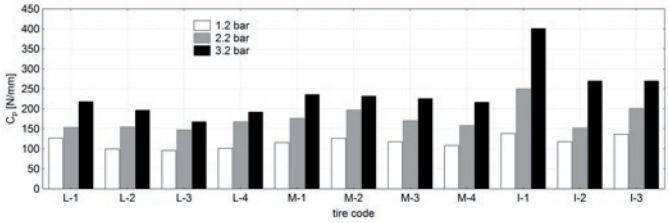

Fig. 7. Tire radial stiffness changes according to the pressure in the tire

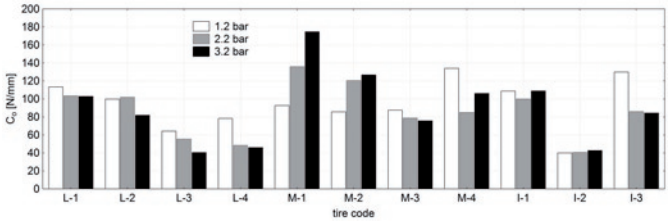

Fig. 8. Changes in the tire of circumferential stiffness depending on the pressure in the tire

of 24.7%. Referring to the circumferential stiffness, tires from group III, it was noted a decrease stiffness with increasing pressure in the I-3 tire. At the lowest pressure (1.2 *bar*) circumferential stiffness was 129.95 *N*/*mm*, at a nominal pressure of 2,2 *bar* – 85.95 *N*/*mm* (a difference of 51.2%). With further pressure increase, it can be noticed a slight decrease in stiffness of 84.25 *N*/*mm*. Changing the tire stiffness as a function of pressure in the tire I-2 is small (about 5%).

6.3. Lateral stiffness

In the case of another determined parameter, which is the lateral stiffness (Fig. 9), as well as the radial stiffness, a bar chart shows an increasing trend in stiffness with the increase of the tire pressure for each tire group, in addition to tire I-2, wherein was noticed stiffness decrease with pressure increase. Also, the tire L-2,where stiffness decreased with increasing inflation pressure from 2.2 *bar* to 3.2 *bar*, up to 18.5%. Relatively high stiffness jump (54.9%) is visible when the pressure is changing from 1.2 *bar* to 2.2 *bar* in the L-2 tire (61.5%) and from 2.2 *bar* pressure to 3.2 *bar* in the L-4 tire (48%).

6.4. Torsional stiffness

In the case of the last designated parameter, which is the torsional stiffness (Fig. 10), as in the case of the circumferential stiffness, there

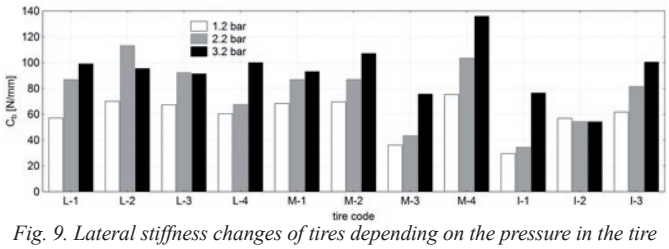

Fig. 9. Lateral stiffness changes of tires depending on the pressure in the tire

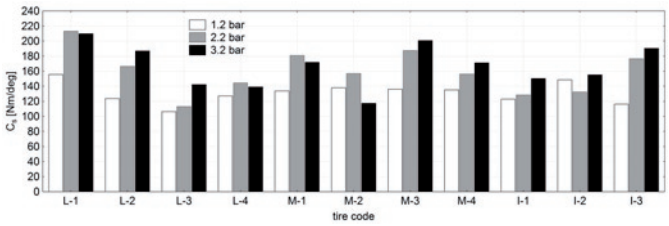

Fig. 10. Changes in torsional stiffness depending on the tire inflation pressure

is a noticeable decrease in stiffness L-1 tire with inflation pressure increase from 2.2 *bar* to 3.2 *bar* of 1.6%.

The relatively large stiffness jump (37%) shows the pressure change from 1.2 *bar* to 2.2 *bar* in the same tire (L-1). A change in pressure from 2.2 *bar* to 3.2 *bar* resulted in as decrease of torsional stiffness in L-4 tire by 3.8%. Another noticeable drop in stiffness with increasing pressure was in the tire M-1 (from 2.2 *bar* to 3.2 *bar* - 5.2%). At I-2 tire pressure change from 1.2 *bar* to 2.2 *bar*, the torsional stiffness decreases by 12%. With further increase of the pressure up to 3.2 *bar*, stiffness increases by 17% compared to the stiffness at a pressure of 2.2 *bar*.

7. Tire deformations

Vertical load applied to the tire in order to determine the radial stiffness, causes deformation of the tire in the manner shown on Figure 11. Force of gravity of the vehicle tire creates a longitudinal force in the area of wheel contact with the ground and results in a deformation shown in Figure 11a. Load tire with braking torque or driving torque results in a longitudinal force in the area of wheel contact with the ground and results in a deformation shown in Figure 11b. However, when determining the lateral stiffness, that is by applying a force in the direction transverse to the longitudinal axis of the tire and recording the movement of the table, there can be seen the deformation of the tire like on the image (Figure 11c).

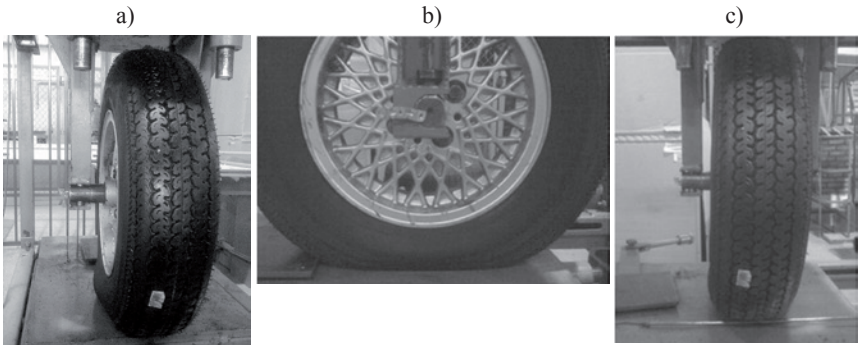

Fig. 11. Deformations of the tire when determining stiffness: a) radial, b) circumferential, c) lateral

8. Tire prints

When turning the wheel on a hard surface, a tire is deformed resulting in the formation of surface contact with the road. All the forces needed for acceleration, braking and steering implementation are carried through the tread with the road contact surface. Changing the tire pressure directly affects the size of the surface area of the tire contact with the road. As it is known, the larger a surface area contact with the ground, the lower the penetration of the tire on soft ground (that is used in off-road vehicles - reducing the pressure during the crossings in difficult terrain). This results in a higher rolling resistance, thus, greater fuel consumption and emitted noise by the tire tread.

In order to see the surface area of the contact patch under various pressures in the tires and different loads, the prints of one of the tire tread have been made (Fig. 12).

On the basis of the results, bar graphs were created, which show dependency of contact area changes as a function of inflation pressure (Fig. 13) and the dependence of the contact area changes as a function of pressure force (Fig. 14).

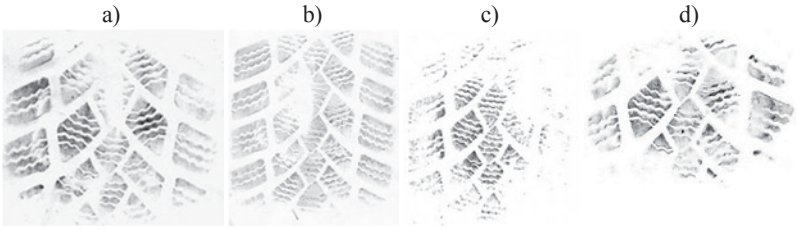

Fig. 12. Uniroyal Rallye 680 tread prints: - tire pressure 2.2 bar - load: a – 1841 N, b – 3682 N; - load 614 N – tire pressure: c – 1.5 bar, d – 3 bar

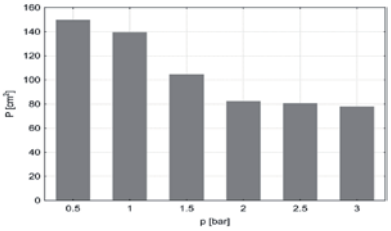

Fig. 13. Changing the area of contact as a function of the pressure in the tire at a constant load.

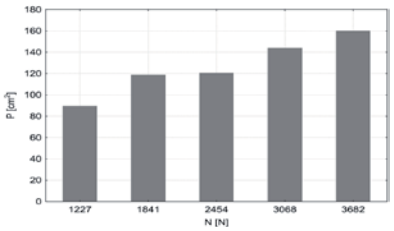

Fig. 14.Changing the contact surface as a function of pressure force at a constant pressure in the tire

With the increase of pressure in the tire, contact area with the ground track decreases. The biggest change in area (about 70%) was observed in the range of pressure from 1 bar to about 2 *bar* (Fig. 13). When increasing tire load at a constant value of 2.2 *bar* nominal pressure in the tire (Fig. 14), the surface area of the tread contact with the road increases. This is most noticeable in the ranges of load changes from 1227 *N* to 1841 *N* (approximately 66%) and from 2454 *N* to 3068 *N* (approximately 80%).

9. Conclusions

The results for the tire stiffness refer to the exploited tire, which are in various stages of utility. The research had comparative character, in which it was tried to find some correlations in static conditions. The research for 11 pieces of various kinds of tires, it was found that the average tire has a radial stiffness of about 180 [*N*/*mm*], circumferential 80 [*N*/*mm*], lateral 65 [*N*/*mm*] and torsional 150 [*Nm*/*deg*]. In the case of radial stiffness, with increasing tire pressure, increased their value, similar to the

lateral stiffness. In some cases a declines and torsional stiffness were occured with increasing pressure in the tire.

With the increase in pressure in the tire, contact area with the ground is reduced. The biggest change in area (about 70%) was observed in the range of pressure from 1 bar to about 2 *bar*. When increasing the tire load with constant nominal value pressure in the tire of 2.2 *bar*, the area of contact with the ground increased to 35%.

The parameters are applicable to the modeling of the vehicle motion, which operates mainly for lateral drift angle of tires, which has an effect on vehicle controllability, especially in sports cars [14]. At a later stage it is planned to construct the experimental tire dynamic research stand, particularly to determine the tire side abolition or damping, where provided to base the identification models on the results of previous work.

References

1. Bris S. S, Ungureanu N, Maican E, Murad E, Vladut V. FEM model to study the influence of tire pressure on agricultural tractor wheel deformations. International Scientific Conference: Engineering for Rural Development 2011; 10: 223-228.
2. Dworecki Z, Fiszer A, Łoboda M, Przybył J. Równania opisujące wpływ sztywności opon na drgania ciągnika rolniczego. Inżynieria Rolnicza 2007; 2(90): 43-48.
3. Fielding-Russell G. S, Pillai P.S. Tire rolling resistance from whole-tire hysteresis ratio. Rubber Chemistry and Technology 1992; 65(2): 444-452.
4. Genta G, Morello L. The Automotive Chassis. Volume 1: Components Design. Torino: Springer, 2009.
5. Gruber P, Sharp R. S, Crocombe A. D. Friction and camber influences on the static stiffness properties of a racing tyre. Faculty of Engineering and Physical Sciences, University of Surrey, 2008.
6. Jackowski J, Luty W, Wieczorek M. Analiza możliwości oszacowania wzdłużnej sztywności poślizgowej opon na podstawie statycznych badań laboratoryjnych. Journal of KONES Powertrain and Transport 2006, 13(1): 94-101.
7. Jackowski J, Prochowski L. Analiza wpływu konstrukcji ogumienia na obciążenia dynamiczne pojazdu i nawierzchni drogi. Biuletyn WAT 10/89.
8. Kasprzyk T, Prochowski L, Szurkowski Z. Optymalizacja własności sprężystych i dobór konstrukcji ogumienia samochodu osobowego dla różnych warunków eksploatacji. Auto-Technika Motoryzacyjna 10/74 i 11/74.
9. Krmela J, Beneš L, Krmelová V. Statical experiments of tire as complex long-fibre composite for obtaining material parameters and deformation characteristics. Materials Engineering - Materiálovéinžinierstvo 2012; 19: 124-135.
10. Kulikowski K. Badania statyczne opon samochodowych. Praca dyplomowa magisterska, pod kierunkiem D. Szpicy, Politechnika Białostocka, Białystok, 2012.
11. Luty W. Wyznaczanie parametrów modelu nadbiegania ogumienia na podstawie wyników badań eksperymentalnych. Postępy Nauki i Techniki 2012; 14: 135-147.
12. Luty W, Simiński P. Analiza sprężystości promieniowej ogumienia 14.00R20 z wkładką typu RUN-FLAT. Czasopismo Techniczne M 2008; 132-138.
13. Marshek KM, Saraf CL, Chen HH, Connell RB, Hudson WR. Experimental Investigation of Truck Tire Inflation Pressure on Pavement-tire Contact Area and Pressure Distribution. n. Report No. 386-1. Center for Transportation Research, University of Texas at Austin, Austin, 1985.
14. Milliken WF, Milliken DL. Race car vehicle dynamics. Warrendale: SAE International, 1995.
15. Mitschke M. Dynamika samochodu, Drgania. tom 2. Warszawa: WKiŁ, 1987.
16. Pacejka HB. Tyre and vehicle dynamics. 2nd edition. Oxford: Butterworth-Heinemann, 2002.
17. Taylor RK, Bashford LL, Schrock MD. Methods for measuring vertical tire stiffness. Transactions of the ASAE 2000; 43(6): 1415-1419.
18. Yang WY, Cao W, Chung TS, and Morris J. Applied numerical methods using MATLAB. Hoboken, New Jersey: John Wiley & Sons, Inc., 2005.

Krzysztof KULIKOWSKI
Dariusz SZPICA
Faculty of Mechanical Engineering
Bialystok University of Technology,
ul. Wiejska 45C, 15-351 Bialystok, Poland
E-mails: k.kulikowski@doktoranci.pb.edu.pl, d.szpica@pb.edu.pl

Article citation info:
LINGAITIS LP, LEBEDEVAS S, LIUDVINAVIČIUS L. Evaluation of the operational reliability and forecasting of the operating life of the power train of the freight diesel locomotive fleet. Eksploatacja i Niezawodnosc – Maintenance and Reliability 2014; 16 (1): 73–79.

Leonas Povilas LINGAITIS
Sergejus LEBEDEVAS
Lionginas LIUDVINAVIČIUS

EVALUATION OF THE OPERATIONAL RELIABILITY AND FORECASTING OF THE OPERATING LIFE OF THE POWER TRAIN OF THE FREIGHT DIESEL LOCOMOTIVE FLEET

OCENA NIEZAWODNOŚCI EKSPLOATACYJNEJ I PROGNOZOWANIE ŻYWOTNOŚCI UKŁADU PRZENIESIENIA NAPĘDU WE FLOCIE SPALINOWYCH LOKOMOTYW TOWAROWYCH

The article provides analysis of the passivity of various options for the rational use of the fleet of diesel locomotives with the purpose of improving the operational reliability indicators of diesel engines installed on freight diesel locomotives. The rationality of the use of mathematical statistical methods, with their application to in-service diesel engines installed on diesel locomotives, was assessed with the use of the accumulated statistical data on breakdowns/disorders of main-line diesel locomotives of State Company "Lietuvos geležinkeliai" (Lithuanian Railways). On the basis of technical documentation, with the use of the results of comparative tests and practically approbated indirect diesel engine reliability criteria, the comparative assessment of the operating life of in-service diesel engines installed on freight diesel locomotives has been performed. In order to substantiate the adequacy of tests, the adaptation of the programme modules of mathematical computer simulation of the parameters of diesel engines of the fleet operated by Lithuanian Railways. The differences between the results established by the experiment and simulated by the computer do not exceed 5–7 %. The indirect criteria of evaluating the mechanical and thermal load of parts of diesel engines installed on diesel locomotives have been selected and adapted. An algorithm of the methodology for the evaluation of the reliability criteria of diesel engines installed on diesel locomotives and forecasting of the operating life has been developed. It has been implemented in the form of a mathematical simulation programming complex.

***Keywords**: diesel engine of locomotive, indirect reliability criteria, operating life.*

Artykuł przedstawia analizę pasywności różnych opcji racjonalnego wykorzystania floty lokomotyw spalinowych mającą na celu poprawę wskaźników niezawodności eksploatacyjnej silników wysokoprężnych użytkowanych w towarowych lokomotywach spalinowych. Zasadność stosowania matematycznych metod statystycznych do analizy eksploatacji silników wysokoprężnych użytkowanych w lokomotywach spalinowych oceniano z wykorzystaniem zgromadzonych danych statystycznych dotyczących awarii / nieprawidłowego działania lokomotyw spalinowych jeżdżących na głównych liniach kolejowych Firmy Państwowej „Lietuvos geležinkeliai" (Koleje Litewskie). Na podstawie dokumentacji technicznej, z wykorzystaniem wyników testów porównawczych i sprawdzonych w praktyce pośrednich kryteriów niezawodności silników wysokoprężnych, dokonano oceny porównawczej żywotności silników wysokoprężnych zamontowanych w towarowych lokomotywach spalinowych. W celu potwierdzenia trafności badań, zastosowano moduły programowe matematycznej symulacji komputerowej parametrów silników wysokoprężnych floty eksploatowanej przez Koleje Litewskie. Różnice pomiędzy wynikami otrzymanymi na drodze doświadczalnej a wynikami symulowanymi komputerowo nie były większe niż 5–7%. Wybrano i przyjęto pośrednie kryteria oceny mechanicznych i termicznych obciążeń części silników wysokoprężnych zamontowanych w lokomotywach spalinowych. Opracowano algorytm metodyki oceny kryteriów niezawodności silników wysokoprężnych użytkowanych w lokomotywach spalinowych oraz prognozowania ich żywotności. Został on wdrożony w postaci kompleksu do programowania symulacji matematycznych.

***Słowa kluczowe**: silnik wysokoprężny lokomotywy,pośrednie kryteria niezawodności, żywotność.*

1. Introduction

In the last decade, Europe is forced to resolve unprecedented problems raised by transportation: traffic flows have increased significantly, and the leading role has been taken by road transport, which appeared to be better adapted to new economic phenomena. The domination of this mode of transport in Europe poses serious problems (traffic congestions, hazardous impact on the environment and human health, and threatening statistics of traffic accidents).

In order to mitigate these problems, the European Council and the European Commission have taken the following actions: increase of taxes on road transport, renewal of alternative means of transport (encouragement of the use of seaborne and inland waterway transport, revitalisation of railways, and development of multimodal transport operations).

In their turn, international railway organisations, such as the International Union of Railways (UIC), the Community of European Railways (CER), the International Union of Public Transport, (UITP), and the Union of European Railway Industries (UNIFE) agreed to increase during the period 2000–2020 the market share to be taken by railways from 6 % to 10 %, and that in the area of freight transportation from 8 % to 15 % as well as to decrease the emission of pollutions by 50 %.

During the last decade, the situation in railway transport in Europe changed in principle. The potential oriented to the growing dependency of the economy on transport, with regard to the dynamics of de-

mand, variety of ownership, service flexibility, and needs of engineering and technology has been created in a systemic and rapid manner. This process has been influenced by qualitative changes introduced by laying fast communication railways and constructing new rolling stock. Railway transport has become competitive owing to high speed, comfort, high service level, traffic safety and environmental friendliness.

Today the railway transport sector is assessed as an especially important segment of economy, which to a great extent determines the movement of goods within the country and their transportation abroad, which has a significant impact on all companies of the country – consignors and consignees as well as related businesses.

It is the establishment of new services and promotion of intermodality which was the purpose of the great changes that took place in the fleet of rolling stock of Lithuanian Railways during the recent five years. According to the requirements set by Directive 2001/12EB of the Parliament and the Council to reform the rolling stock system by separating operational activities from rolling stock repair works, company "Vilniaus Lokomotyvų Remonto Depas" was established in 2003. It was this subsidiary of Lithuanian Railways to which the main goal was set: to restore the existing fleet of traction rolling stock, to find methods to modernise diesel locomotives and to implement the requirements set by the Directive. Therefore, this company became the first in the Baltic region which started a programme for complex and responsible modernisation of rolling stock. Besides, in 2005 the unprecedented agreement of Lithuanian Railways with Siemens AG (Germany) was signed, according to which 34 units of customised ER 20CF series diesel locomotives were to be manufactured.

These changes allowed enhancing the efficiency of the consumption of resources and improving the operational environmental indicators. Both these aspects perfectly meet the requirements specified in the Directive of the Parliament and the Council concerning the control and improvement of energy resources consumption efficiency (COM (2001) 370).

With fleets of diesel locomotives being constantly supplemented with new and modernised traction units, it became a strategic goal of complex studies to investigate, form, and substantiate possible reserves and directions of the improvement of operational reliability as well as energy and environmental indicators and measures for their implementation ensuring more effective functioning of the Lithuanian Railways transport because the reliability of diesel engines determines to a great extent determines not only economic, but also environmental operational indicators of diesel locomotives. This is why this article describes the main accent of the studies performed, which is devoted to the reliability indicators of diesel engines of diesel locomotives.

2. Assessment of the operational reliability of a diesel engine determined by methods of mathematic statistics

The factors characterising the reliability of a diesel engine of a diesel locomotive are divided into structural, technological, and operational.

Analysis of the operation of diesel engines [1–6, 14, 15] shows that breakdowns during their operation occur as a result of infringement of the technical maintenance and repair regulations, improper use of the operational materials regulated in the technical documentation, and long-term operation under overloaded modes.

Referring to the aforementioned, it can be claimed that it would be reasonable to envisage in comparative studies of the operational reliability indicators of diesel engines of different types installed in diesel locomotives, first of all, analysis and comparison of their reliability indicators with regard to environmental and operating conditions.

Practice shows that the main criterion of the enhancement of the durability is the improvement of the resistance of reliability limiting assemblies and parts (the cylinder-piston group, crank-piston rod mechanism, assemblies of inflation and fuel injection systems, etc.) to wear.

Depending on the operating time of the diesel engine, the indicators representing its reliability (breakdown intensity, density distribution $f(t)$, and probability distribution $P(t)$) are described by the different laws of mathematical statistics described below:

1. For newly commissioned diesel engines, for which breakdowns of technological (production) character are inherent during the running-in (assembling, metal processing, etc.), the logarithm density distribution is applied, which is expressed by the following formula:

$$f(t)=\frac{1}{t\sigma\sqrt{2\pi}}\exp\left(-\left(\ln t-a\right)/2\sigma^2\right), \tag{1}$$

where: σ – standard deviation; t – exploitation duration till failure; α – ln$t$ average value.

2. For new diesel engines that have passed the running-in period and are at the beginning of the normal operation period, the characteristic exponential probability distribution law; breakdowns mostly have the character of sudden occurrence as a result of local thermal or mechanical overload of parts, infringement of operating rules, etc. The law of characteristic exponential probability distribution is expressed by the following formula:

$$P(t)=l^{-\frac{t}{T}}. \tag{2}$$

where: T – average working duration without failure; l – fixed interval of duration; t – exploitation duration till failure.

3. For objects that have been in operation for a long period of time (when the operating l approaches the life limit), the processes of part wear and metal aging accelerate; correspondingly, the flow of breakdowns grows intensively and is described in the best manner by the normal probability distribution law:

$$P(t)=1-\frac{1}{\sigma\sqrt{2\pi}}\cdot l^{-\frac{-(t_i-\overline{T})^2}{2\sigma^2}} \tag{3}$$

where σ – standard deviation; T – average working duration without failure; l – fixed interval of duration; t_i – working time till failure of i-th element.

In order to apply one or the other of the aforementioned laws for the establishment of reliability, a certain number of tests (breakdowns), which requires a long period of time under natural operating conditions, is necessary. Collected statistical data according to corresponding locomotive types range from 4 to 12 years of operating period.

From the available collected data, especially for new locomotives, this number is so far insufficient in order to apply the aforementioned probability laws directly. In such cases, Student's coefficient is applied, which is chosen depending on the numbers of tests and the degree of the selected probability.

On the basis of the review and analysis of the mathematical statistics methods, when applying them to study objects, the following is stated:

1) for the determination and forecasting of the reliability indicators of diesel engines, quite a comprehensive array of statisti-

cal data on their breakdowns is necessary: in the case of normal law (distribution probability β = 0,9–0,95; variation factor v = 0,20), the number of the elements of diesel engines under the study (differentials according to characteristic groups of parts: the cylinder-piston group, crank-piston rod mechanism, assemblies of inflation and fuel injection systems, etc.) should be at least 40–60 items; in the case of applying the Weibull law – 50–60 items and more (β = 0,95; relative error 5–10 %);

2) with the application of mathematical statistics methods for studying the reliability indicators of diesel engines installed on diesel locomotives of Lithuanian Railways, attention must be paid to the following:
   - obsolete and newly modernised diesel engines installed on diesel locomotives are in different stages of the operating cycle (normal operation; intensive aging); methodologically, they should be subject to different probability distribution laws and, when comparing calculation results, it should be taken into account [7, 9];
   - data on breakdowns of new/modernised diesel engines, as we mentioned above, are not sufficient; therefore, the Student's adjustment shall apply here.

Upon evaluation of the entire versatility of statistical data, during short operating period (for new locomotives), computer simulation and similarity theory methods were applied in this study for the establishment of the reliability of operating parameters of diesel engines installed on diesel locomotives and forecasting of operating duration, i.e. with the use of the practically proved criteria of the thermal and mechanical load of parts which define the structural and operating process peculiarities of diesel engines [9, 11, 13, 14].

The ongoing energy-mass transfer within the subsystems of the third level is driven by gradients of temperature, stress, chemical potentials and dislocation density. The direction of the energy-mass transfer is opposite to the vector of gradient of chemical potential, so the decrease in its intensity occurs in the course of the development of the process.

3. Selection of indirect criteria for the forecasting of the operating life of a diesel engine

When operating diesel engines of the same series installed on diesel locomotives of the same type, the degree of wear of assemblies and parts may differ remarkably in regard to separate models. This fact is substantiated by a wide spectrum of possible operating modes of diesel engines, which is highly dependent on the relation of the engine with wheel-sets (electrical, hydraulic, and mechanical drive), its intended purpose (main-line, passenger, and shunting transport), and track profile (slopes and turns), etc.

On these grounds, in practice, of relevance is the evaluation of the degree of wear of the cylinder-piston group (CPG) and parts of the slider-crank mechanism (as more limiting the reliability of the diesel engine and life of the assemblies). According to it, both the direct and inverse task can be resolved: the determination of the rational inter-maintenance period and residual life of the engine under a certain degree of diesel engine load when carrying freights (direct task); optimisation of the operating load cycle parameters at lines in order to extend the duration of operation (transport operations) inverse task.

The wear rate of parts under equal conditions (equal design arrangements of engines, manufacturing technologies and materials, types of fuel, and lubricants) are basically defined by the movement speeds of friction surfaces in respect of each other that are exposed to pressure forces and temperature values of friction surfaces. Since the proper evaluation of the thermal condition of parts and assemblies and mechanical load under operating conditions is difficult to implement due to technical and design constraints, various methods and criteria [8], which either reflected the thermal flow directed to walls of cylinder heads and hubs, or temperatures of certain parts of the cylinder-piston group which, in their turn, define the indirect criteria of thermal and mechanical stresses of those parts or the whole engine, started to be proposed [7].

The fact that priority in similar studies is given to the analysis of thermal stresses is substantiated by the statistics of experimental and calculation data. Thermal stresses of CPG parts account for 80–90 % of the aggregate balance of thermal and mechanical stresses [13].

The principal possibility of the application of such criteria is substantiated by temperature changes of similar character in parts of the cylinder-piston group in engines of various types and rapidity depending on the load, rotations of the crankshaft and inflation air pressure.

The performance of research tests of the wear of parts of the cylinder-piston group and processing of the results obtained during those tests allowed determining the main operating indicators of engines that influence the rate of growth of the wear of the cylinder-piston group most of all: mean effective pressure P_{me}, maximum cycle pressure $P_{\max}$, excess air ratio α, exhaust gas temperature T_T, average piston speed C_m, inflation air pressure P_K, and crankshaft rotations n. Increase in these parameters is in one way or another associated with changes in temperatures of all the parts of the cylinder-piston group and the same temperature stresses by almost linear dependencies.

For example, Prof A. K. Kostin [7] proposed the following expression of parameters for the evaluation of thermal stresses of the indirect piston and determination of the average thermal flow through cylinder surfaces being cooled:

$$\zeta = P_{\max} \cdot \left(\frac{1}{\alpha}\right)^{0.88} \cdot \left(P_K \cdot C_m\right)^{0.5} \cdot n \,. \tag{4}$$

Other criteria of complex indirect thermal stresses (of the firm Rikardo, CNIDI, Prof. S. V. Kamkin, Prof. M. I. Fedorov, etc.), which can be used for the evaluation of the thermal condition of the parts of the cylinder-piston group, are also known. However, those are already sophisticated criteria of complex indirect thermal stresses, the determination of which requires parameters obtained during bench tests of the engine.

The following indirect criteria have been selected for the adaption of diesel engines of a diesel locomotive:

- $P_D = \frac{P_e}{D \cdot i}$ – prof Ginzburg criterion (applicable to diesel engines of a wide range of applications; load of parts is evaluated according to the "piston power");
- $q_\Pi = \left(\frac{1}{\alpha}\right)^{0.88} \left(P_K c_m\right)^{0.5}$ – applicable to diesel engines of a wide range of applications and types; specific heat flow to the piston bottom and cylinder head is evaluated according to the operating process parameters;
- $\Pi = \left(P_{me} \cdot t_r\right) / \left(P_{\max} \cdot c_m\right)$ – criterion (applicable to marine diesel engines; the mechanical and thermal load of parts is evaluated according to the general energy indicators and working process parameters of the diesel engine);
- $q_R = \left(\frac{Gf}{F_{stum}}\right)^{0.8} \left(\frac{\varepsilon}{(\varepsilon - 1)} \cdot n \cdot S \cdot \rho_k\right)^{-0.3}$ – Ricard firm criterion (applicable to high-speed automotive diesel engines; specific heat flow to the piston bottom is evaluated according

to general energy and design parameters); here, in addition to the parameters of Formula (3): P_e – diesel engine power, kW; P_{me} – mean effective pressure, MPa; P_K – inflation air pressure, MPa; α – excess air ratio; t_r – exhaust gas temperature, °C; c_m – mean piston speed, m/s; G_f – hourly fuel consumption, kg/h; F_{stum} – piston fuel area, m^2; S – piston stroke, m; ε – compression degree; n – diesel engine rotations, min^{-1}; ρ_K – inflation air density, kg/m^3; i – number of cylinders.

The criterions applicable to marine and high-speed diesel engines and then they completely approved for other types of diesel engines, for loco diesel as well.

The structure of the criteria is adapted according to the diesel fuels of diesel locomotives under study, upon entering the corresponding values of the design parameters (see Table 1).

Table 1. Indirect reliability criteria adapted for Lithuanian Railways diesel locomotive diesel engines

Criteria	Model			
	14D40	2-2D49	Caterpillar 3512B HD-SC	MTU16V4000R41
P_D	$\frac{P_e}{23\cdot 12}$	$\frac{P_e}{26\cdot 12}$	$\frac{P_e}{17\cdot 12}$	$\frac{P_e}{16{,}5\cdot 16}$
ζ	$P_{\max}\cdot 10^{-1}\cdot\alpha^{-0.88}\cdot\left(P_K\cdot 10^{-1}\cdot\frac{0.3}{30}\right)^{0.5}\cdot n^{1.5}$	$P_{\max}\cdot 10^{-1}\cdot\alpha^{-0.88}\cdot\left(P_K\cdot 10^{-1}\cdot\frac{0.26}{30}\right)^{0.5} n^{1.5}$	$P_{\max}\cdot 10^{-1}\cdot\alpha^{-0.88}\cdot\left(P_K\cdot 10^{-1}\cdot\frac{0.215}{30}\right)^{0.5}\cdot n^{1.5}$	$P_{\max}\cdot 10^{-1}\cdot\alpha^{-0.88}\cdot\left(P_K\cdot 10^{-1}\cdot\frac{0.19}{30}\right)^{0.5}\cdot n^{1.5}$
q_Π	$\alpha^{-0.88}\cdot\left(P_K\cdot 10^{-1}\cdot\frac{0.3\cdot n}{30}\right)^{0.5}$	$\alpha^{-0.88}\cdot\left(P_K\cdot 10^{-1}\cdot\frac{0.26\cdot n}{30}\right)^{0.5}$	$\alpha^{-0.88}\cdot\left(P_K\cdot 10^{-1}\cdot\frac{0.215\cdot n}{30}\right)^{0.5}$	$\alpha^{-0.88}\cdot\left(P_K\cdot 10^{-1}\cdot\frac{0.19\cdot n}{30}\right)^{0.5}$
Π	$\frac{P_{me}(T_r-273)}{P_{\max}\left(\frac{0.3\cdot n}{30}\right)}$	$\frac{P_{me}(T_r-273)}{P_{\max}\left(\frac{0.26\cdot n}{30}\right)}$	$\frac{P_{me}(T_r-273)}{P_{\max}\left(\frac{0.215\cdot n}{30}\right)}$	$\frac{P_{me}(T_r-273)}{P_{\max}\left(\frac{0.19\cdot n}{30}\right)}$
q_R	$\left(\frac{Gf}{0.0415}\right)^{0.8}\cdot\left(0.322\cdot n\cdot 348.4\cdot\frac{P_K}{T_K}\right)^{-0.3}$	$\left(\frac{Gf}{0.0531}\right)^{0.8}\cdot\left(0.278\cdot n\cdot 348.4\cdot\frac{P_K}{T_K}\right)^{-0.3}$	$\left(\frac{Gf}{0.0227}\right)^{0.8}\cdot\left(0.23\cdot n\cdot 348.4\cdot\frac{P_K}{T_K}\right)^{-0.3}$	$\left(\frac{Gf}{0.0214}\right)^{0.8}\cdot\left(0.203\cdot n\cdot 348.4\cdot\frac{P_K}{T_K}\right)^{-0.3}$

3.1. Approbation of reliability criteria

The criteria have been approbated with the use of the locomotive diesel engine operating (testing) load cycle structure according to ISO 8178-4(F) (see Table 2).

Table 2. Locomotive diesel engine operating (testing) load cycle structure according to ISO 8178-4(F)

Power (load), %	100 %	50 %	No-load run
Rotations, %		transient	
Relative part of operating duration	0.25	0.15	0.60

The values of the criteria are calculated according to the parameters of the diesel locomotive operating characteristic for the modes of nominal power, 50 % load, and no-load run. For example, the values $\xi_{100\%}$, $\xi_{50\%}$, and $\xi_{no-load}$ are calculated for the criterion ζ.

The integral value of the criterion characteristic to the whole operating (testing) cycle is determined according to the following formula: $\xi = \xi_{100\%}\cdot\tau_{100\%} + \xi_{50\%}\cdot\tau_{50\%} + \xi_{no-load}\cdot\tau_{no-load}$, where $\xi_{100\%}$, $\tau_{50\%}$, $\tau_{no-load}$ – the relative parts of the operating period of the diesel engine equal to 0,25; 0,15; 0,6, correspondingly (see Table 3).

3.2. Reliability evaluation of diesel engines of main-line diesel locomotives according to operating duration (life) indicators

Because of different methodology for the repair cycle rating of diesel engines installed on Lithuanian Railways diesel locomotives that are supplied by manufacturers from various countries, time to overhaul are evaluated by values of different indicators:

- Colomna Energy Service OU (Russia) diesel engines: 14D40 series (M62 and 2M62) – 8 640 000 l of fuel consumed; 2–2D49 series (M62K and 2M62K) – 1 500 000 km diesel locomotive run or 12 years;
- Zeppelin – Cat Power Systems Corporation (Germany – USA), Caterpillar 3512B HD-SC series (2M62M and 2M62UM) diesel engines – 5 840 000 l of fuel consumed;
- MTU Friedrichshafen GmbH (Germany), MTU16V4000R41 series(ER 20CF) diesel engines – 48 000 motor-hour or 18 years.

The data provided by these manufacturers and determined during operation were expressed in operating years on the basis of statistical average values of Lithuanian Railways determined during operation].

As a result (on the basis of the statistical data concerning the consumption of 1 500 000 l by a diesel engine of a diesel locomotive in 15 000 motor-hour), the time to overhaul of M62 and 2M62 type diesel locomotive serial 14D40 type diesel engines is 8 640 motor-hour or 14.8 years.

The operating life of 2–2D49 series diesel engines of the same manufacturer installed on remotorised M62K and 2M62K type diesel locomotives is 78 840 motor-hour or 13.5 years (on the basis of the statistical run operation average value of the diesel engine, t. y. 100 000 km per year).

When performing calculations for the diesel engines of Zeppelin – Cat Power Systems Corporation for modernised 2M62M and 2M62UM type diesel locomotives, different fuel consumption

Table 3. The values of the reliability criteria of diesel engines of Lithuanian Railways freight diesel locomotives calculated in accordance with the operating trial cycle modes (ISO 8178/4)

Model engines	P_d	ζ	q_Π	Π	q_R	Load
MTU16V4000R41	10.1	32230	1.133	5.466	311.2	100 %
	5.06	11980	0.815	7.079	209	50 %
	0.606	655	0.214	6.226	66.5	No-load
	3.65	10245	0.533	6.164	149.1	Average cycle values
Caterpillar 3512B HD-SC	8.33	24738	1.004	5.559	274.3	100 %
	4.1	8300	0.78	6.478	147.1	50 %
	0.49	548	0.203	3.835	55.5	No-load
	2.81	7758	0.489	4.663	123.9	Average cycle values
2-2D49	4.712	6878	0.69	7.392	143.7	100 %
	2.35	2805	0.594	7.208	101.4	50 %
	0.484	308	0.193	6.56	81.2	No-load
	1.82	2325	0.377	7.1380	99.62	Average cycle values
14D40	2.663	4965	0.602	4.8	214.73	100 %
	1.34	1890	0.427	3.83	129.4	50 %
	0.274	484	0.242	3.04	104	No-load
	1.31*	1815	0.360	3.6	135.4	Average cycle values

) In the formula for the value of prof Ginsburg Pd applicable to a two-stroke 14D40 diesel engine a multiplier 0.5 is introduced as compared to four-stroke diesel engines.

efficiency indicators of 14D40 and 3512B HD-SC diesel engines were taken into account. When operating in the nominal mode, the specific effective fuel consumption of Caterpillar 3512B HD-SC diesel engine is by 8 % lower than that of 14D40. However, these parameters do not reveal the real operating comparative diesel consumption levels because diesel engines of diesel locomotives operate at low-load and no-load modes for a major part of the operating cycle duration (up to (up to 50–60 %).

The use of fuel injection and air supply control electronic systems (as in Caterpillar 3512B HD-SC and MTU16V4000R41 diesel engines) in principle improves the fuel consumption efficiency indicators of the diesel engine.

Comparative operating fuel consumption levels of diesel locomotives calculated for 100 000 tkm have been evaluated on the basis of the tests performed by Lithuanian Railways on one of the railway lines (when changing the weight of the train from 5 000 t to 3 000 t, the number of axes from 164 to 284 units, etc.).

The obtained fuel consumption of diesel engines of M62M diesel locomotives were by ~24 % lower compared to 14D40 diesel engine installed on M62 diesel locomotives (5 diesel locomotives of each make were used in the tests). On the other hand, based on the weight and length standards of Lithuanian Railways for freight train units, the capacity of M62M locomotive is by 25–20 % higher than that of M62M (M62). It means that under Lithuanian Railways transportation conditions, higher fuel consumption efficiency of M62M diesel locomotive is "compensated" by higher diesel engine load. The obtained result is 12.4 years or, if recalculated into operating duration, 59 400 motor-hour.

For MTU16V4000R41 series diesel engines of new ER 20CF type diesel locomotives manufactured by MTU Friedrichshafen GmbH, the manufacturers guarantee interpretations of a span of 48 000 motor-hour or 18 years of operation to major overhaul. 18 years of operation is only possible subject to compliance with the condition set by the manufacturer that the diesel engines will operate in accordance with the standard ISO 8178 – 4, F load cycle. Besides, according to the recalculation of the average daily operating time of a locomotive, the obtained proportion of 48000 motor-hour/18 years will be maintained only provided that the diesel engine of the diesel locomotive works for not more than 7 h per day, while the average daily working time of Lithuanian Railways main-line freight locomotives reaches 16 h per day, i.e. double the time stipulated by the manufacturer. For these reasons, as a result of the performed recalculation of the time span to major overhaul under the standard applicable to other diesel engines, it was established that the operating life shortens from the value of 18 years to 8.2 years.

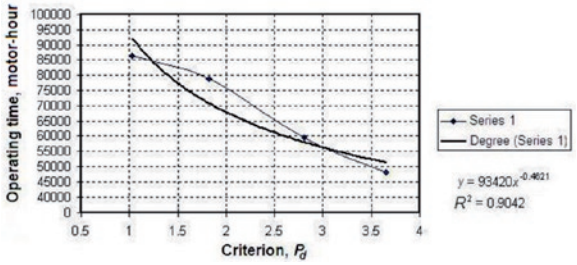

Fig. 1. Result of the adaptation of P_d criterion for diesel engines of Lithuanian Railways freight diesel locomotives

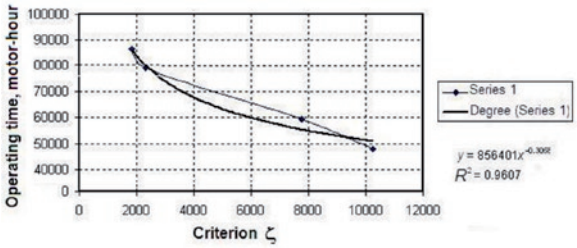

Fig. 2. Result of the adaptation of ζ criterion for diesel engines of Lithuanian Railways freight diesel locomotives

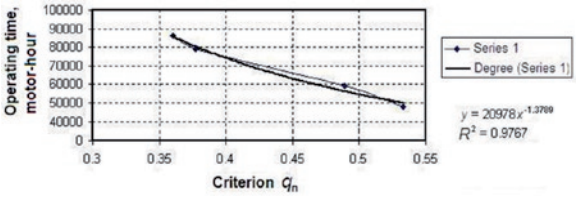

Fig. 3. Result of the adaptation of q_Π criterion for diesel engines of Lithuanian Railways freight diesel locomotives

3.3. Grounds of the methodology for the forecasting of the operating life of diesel engines of freight diesel locomotives

The logical and technological compatibility of the methodology being developed with the train departure planning and scheduling technologies of Lithuanian Railways – computer mathematical simulation, whose functioning algorithm is based on rolling stock traction calculations, was assumed as one of its basic principles [8].

The main aspects of the methodology and components are schematically presented on Fig. 4.

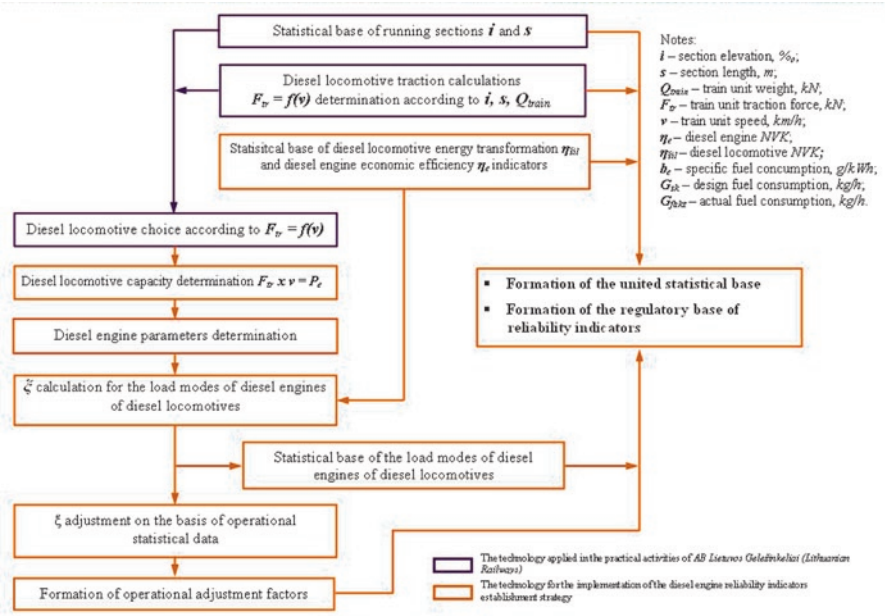

Fig. 4. The principal diagram of the methodology for the establishment of reliability indicators of diesel engines installed on diesel locomotives

Therefore, on the basis of the graphical dependencies of all parameters of indirect criteria of diesel engines installed on diesel locomotives ($x_e = f(P_e, n, Controler\ position)$) values of ξ could be calculated exactly.

Depending on the load modes of the diesel locomotive (which, alternatively, could also be recorded or simulated for statistical purposes by the computer after modifying the PC programme used by Lithuanian Railways for departure planning), the integral ξ criterion for the diesel locomotive for operation at segments of the corresponding section is determined.

Because of the impact of transient operating modes on reliability indicators, adjustment factors are introduced on the basis of operational data.

The implementation of the methodology provides for the following:

1) Mathematical computer simulation of the operating characteristics of diesel engines installed on 14D40, 2-2D49, Caterpillar 3512B HD-SC, and MTU16V4000R41 diesel locomotives and comparison of the obtained results with experimental data;
2) Selection of indirect criteria of diesel engines installed on diesel locomotives and their processing for the models of the fleet of Lithuanian Railways;
3) Development of an algorithm for the calculation of operational reliability indicators of diesel engines installed on diesel locomotives in order to achieve its compatibility with the new information technologies of Lithuanian Railways;
4) Determination of reliability indicators of diesel engines installed on diesel locomotives and the development and testing of a programming mathematical simulation complex for the forecasting of operating life under operating conditions.

Outcome of the investigation will be published in other publications.

4. Conclusions

1. Evaluation of a whole versatility of statistical data, during a relatively short operating period of new diesel locomotives, showed that methods of computer simulation and similarity theory should be applied for the determination of the reliability of operating parameters and forecasting of operating life of diesel engines installed on diesel locomotives, i.e. with the use of practically approbated thermal and mechanical load criteria of parts, which define the design and operating process particularities of diesel engines under conditions similar to those under which diesel engines are operated by Lithuanian Railways. The resistance of the parts of the cylinder-piston group (CPG) and slider-crank mechanism (SCM) to wear is one of the main criteria of their durability preconditioning their operating work time, i.e. operating life. By analysing the indicators of the operating reliability of diesel engines on this basis, the dependency between external environmental and diesel locomotive operating factors and the character of wear of the parts contained in the CPG and SCM of a diesel engine has been studied.
2. The adequacy of applying indirect mechanical and thermal load criteria of parts of diesel engines installed on diesel locomotives for diesel engines installed on diesel locomotives of AB "Lietuvos Geležinkeliai" Lithuanian Railways is proved by the obtained strong correlation dependency (determination coefficient $R^2 \approx 0.95$) between these criteria and the operating life of diesel engines (old modernised and new ones).
3. On the basis of the performed analytical studies, a methodology for the mathematical simulation of operating indicators of diesel engines installed on diesel locomotives, including reliability ones, has been developed on the basis of the classic principals of rolling stock traction calculations.

References

1. Analysis of the technical condition of diesel locomotives and diesel multiple-unit rolling stock of Russia's federal railway transport for 2001 (Анализ технического состояния тепловозов и дизельного моторвагонного подвижного состава федерального железнодорожного транспорта России за 2001 год). Москва: Транспорт, 2002, 64 с.
2. Analysis of the technical condition of diesel locomotives of Russia's federal railway transport for 2002 (Анализ технического состояния тепловозов федерального железнодорожного транспорта России за 2002 год). Москва: Транспорт, 2003, 48 с.
3. Bochkaryov S. Valiullin R. Life of diesel engines installed on diesel locomotives and measures for its determination. Railway transport operating efficiency enhancement (Бочкарев С.; Валиуллин Р. Ресурс тепловозных дизелей и средства его определения. Повышение эффективности работы железнодорожного транспорта). Межвузов сборник научных трудов 2000; 20(1): 142–143.

4. Chetvergov V. Reliability of locomotives (Четвергов В. Надежность локомотивов). Москва: Маршрут, 2003, 415 с.
5. Grachyov V, Valiyev M. Assessment of the technical condition of diesel engines installed on diesel locomotives according to the data of the on-board microprocessor control system (Грачев В., Валиев М. Оценка технического состояния тепловозного дизеля по данным бортовой микропроцессорной системы управления). Известия Петербургского университета путей сообщения 2010; 1: 22–32.
6. Kossov Ye, Sirotenko I. Addressing the issue of the forecasting of a sufficient residual life of diesel generators installed on diesel locomotives (Коссов Е., Сиротенко И. К вопросу прогнозирования остаточного ресурса тепловозного дизель-генератора). Вестник ВНИИЖТа 2000; 7: 38–43.
7. Kostin A, Pugachyov B, Cochinev Y. Operation of diesel engines in exploitation condtions (Костин А., Пугачев Б., Кочинев Ю. Работа дизелей в условиях эксплуатации). Ленинград: Машиностроение, 1989; 120–126.
8. Kuzmich V, Rudnev V, Frenkel S. Theory of locomotive traction (Кузьмич В.; Руднев В.; Френкель С. Теория локомотивной тяги). Москва: Маршрут, 2005, 448 с.
9. Lingaitis LP, Dailydka S, Jevdomacha G. Research on selection of modes of driving heavy trains on main IXB and IXD corridors of JSC "Lietuvos geležinkeliai", Transport problems – Problemy transportu, 2012: 4(7), 39–47.
10. Lingaitis LP, Mjamlin S, Baranovsky D, Jastremskas V. Experimental Investigations on Operational Reliability of Diesel Locomotives Engines Motors, Eksploatacja i Niezawodnosc – Maintenance and Reliability, 2012: 1(14), 6–11.
11. Liudvinavičius L, Lingaitis LP. New locomotive energy management systems, Eksploatacja i Niezawodnosc – Maintenance and Reliability, 2010: 1(45), 35–41.
12. Liudvinavičius L, Lingaitis LP. Management of locomotive tractive energy resources. Energy Management Systems, Rijeka, Croatia: InTech, 2011, 199–222.
13. Mollenhauer K, Tschöke H. Handbook of Diesel Engones. Springer, 2010, 636 p.
14. Prosvirov Yu. Problems of the improvement of diagnostics of diesel engines installed on diesel locomotives (Просвиров Ю. Проблемы совершенствования систем диагностирования тепловозных дизелей). Самара: СамИИТ, 1999б 218 с.
15. Shmoilov A., Nosyrev D. Methodology for the determination of the parameters of diesel engines installed on diesel locomotives (Шмойлов А., Носырев Д. Методика определения параметров рабочего процесса дизеля тепловоза). Вестник транспорта Поволжья 2010; 3: 34–42.
16. Volodina A. Locomotive energy units (Володина А. Локомотивные энергетические установки). Москва: ЖЕЛДОРИЗДАТ, 2002, 718 с.

Leonas Povilas Lingaitis
Department of Railway Transport
Vilnius Gediminas Technical University
J. Basanaivičiaus str., 28-135, LT-03224 Vilnius, Lithuania

Sergejus Lebedevas
Maritime Institute
Klaipėda University
Herkaus Manto str. 84, LT-92294 Klaipėda, Lithuania
E-mail: sergejus.lebedevas@ku.lt

Lionginas Liudvinavičius
Department of Railway Transport
Vilnius Gediminas Technical University
J. Basanaivičiaus str., 28-135, LT-03224 Vilnius, Lithuania
E-mail: llionginas.liudvinavicius@vgtu.lt

Article citation info:
SOKOLSKI P, SOKOLSKI M. Evaluation of resistance to catastrophic failures of large-size caterpillar chain links of open-pit mining machinery. Eksploatacja i Niezawodnosc – Maintenance and Reliability 2014; 16 (1): 80–84.

Piotr SOKOLSKI
Marek SOKOLSKI

EVALUATION OF RESISTANCE TO CATASTROPHIC FAILURES OF LARGE-SIZE CATERPILLAR CHAIN LINKS OF OPEN-PIT MINING MACHINERY

OCENA ODPORNOŚCI NA USZKODZENIA KATASTROFICZNE WIELKOGABARYTOWYCH OGNIW GĄSIENICOWYCH PODWOZI MASZYN PODSTAWOWYCH GÓRNICTWA ODKRYWKOWEGO*

Large-size caterpillar undercarriages of basic mining machines are operated in extremely harsh conditions: they are subjected to high workloads and aggressive environmental influence. Under these conditions, the degradation can develop intensively and results in wear and tear of parts and subassemblies of these undercarriages. Especially dangerous are the catastrophic failures of components of the caterpillar chain: links or connecting pins (plastic deformations or brittle fractures), which generally exclude further work of the undercarriage. Because of that, a study on the structure of the damaged parts was carried out. Basing on numerical models of typical large–size chain links an assessment of effort of these parts was done, critical areas in their build were localized and proposals of modifications of their geometrical parameters were formulated as well. The main result of implementation of these modifications is a significant increase in links' resistance to catastrophic failure, which is particularly important in terms of operational safety and reliability of basic machines.

***Keywords**: Large-size caterpillar undercarriages, degradation, failures of chain links, numerical strength analyses.*

Wielkogabarytowe podwozia gąsienicowe maszyn podstawowych górnictwa odkrywkowego pracują w wyjątkowo trudnych warunkach eksploatacyjnych: są poddawane ekstremalnie dużym obciążeniom roboczym oraz agresywnemu oddziaływaniu środowiska. W takich warunkach procesy degradacji mogą rozwijać się szczególnie intensywnie, a ich efektem są zużycie lub uszkodzenia elementów i podzespołów tych podwozi. Szczególnie groźne są uszkodzenia katastroficzne elementów łańcucha gąsienicy: ogniw lub sworzni łączących (odkształcenia plastyczne lub kruche pęknięcia), które wykluczają na ogół dalszą eksploatację podwozia. Mając to na uwadze, przeprowadzono studium struktury uszkodzeń elementów wielkogabarytowych podwozi gąsienicowych. Na podstawie modeli numerycznych dokonano oceny wytężenia typowych wielkogabarytowych ogniw gąsienicowych, wyznaczono obszary krytyczne i zaproponowano modyfikacje ich cech geometrycznych. Wynikiem tych modyfikacji jest znaczące zwiększenie odporności ogniw na uszkodzenia katastroficzne, co jest szczególnie istotne w aspekcie bezpieczeństwa eksploatacji maszyn podstawowych.

***Słowa kluczowe**: wielkogabarytowe podwozia gąsienicowe, degradacja, uszkodzenia ogniw gąsienicowych, numeryczne analizy wytrzymałościowe.*

1. Introduction

Large-size caterpillar undercarriages of basic mining machines are subjected to extremely high workloads and are exposed to harsh environmental influence (low temperature, rain, dust, mud). In such circumstances, parts and subassemblies of these undercarriages are particularly vulnerable to degradation and damage.

Decisive impact on the scale and intensity of degradation processes of parts of the caterpillar undercarriages have values and character of the acting workloads. In this aspect, particularly dangerous are extremely high loads, unforeseen by the designer. They can result in sudden/catastrophic damages, associated with the destruction of entire elements – such as a plastic deformation and a brittle fracture.

Statistics show that damages of caterpillar chains account for about 15% of all cases of damages of the driving units of multi–bucket excavators (Fig. 2) [12]. Nearly 70% of them arise from operational reasons: due to high dynamic loads (especially during start-up and turning), severe tribological conditions in the chain (limited ability to provide adequate lubrication, which results in faster abrasive wear of the elements) and an aggressive influence of the soil environment (corrosion and aging of materials). Less than 10% of the total damages of the undercarriages' components in basic machines is caused by technological reasons – in particular imperfections of the materials or inadequate chemical-heat treatment.

2. Basic forms of degradation of chain links

The results of the degradation of large–size caterpillar undercarriages are the partial or total failures of their components, wherein approximately 80% of all cases comprise the partial ones, with a further work of the basic machine possible, although to a limited extent (e.g. at reduced speed and movement resistance).

In the context of the possible consequences of the caterpillar chain's damages, its links and connecting pins are particularly important. Almost every failure of one of the links or connecting pins excludes further work of the machine.

The research shows that the degradation of chain links occurs primarily in the following areas (Fig. 3) [12]:

(*) Tekst artykułu w polskiej wersji językowej dostępny w elektronicznym wydaniu kwartalnika na stronie ***www.ein.org.pl***

Fig. 1. Basic subassemblies of a large-size tracked undercarriage: A – caterpillar chain, B – supporting wheels, C – balance lever's units, D – driving wheel, E – caterpillar's girder [authors' archive]

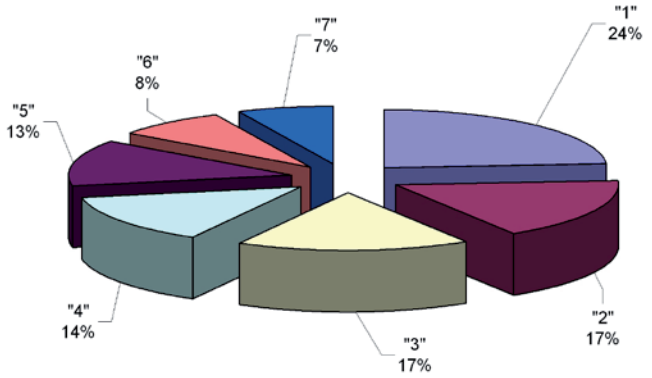

Fig. 2. The structure of failures of caterpillar undercarriages of basic machines in Polish open-pit mines: 1 – unit of upper supporting wheel, 2 – unit of balance lever and carriage, 3 – girder's supporting structure, 4 – caterpillar chain, 5 – unit of driving wheel, 6 – unit of turning wheel, 7 – drive of the caterpillar [12]

- In the area of lugs (zone „1", Figure 3). The degradation in these areas is an effect of extremely high workloads, unexpected in the normal operation. Such situations may occur for example during a turning process with a curve radius too small, especially in case of turning in place. It can result in a plastic deformation or a fracture of lugs and each of these cases is virtually irreparable damage, rated as a so-called catastrophic one.
- At the surfaces of holes in the pin joints in the links' lugs (zone "2", Figure 3). This degradation is an abrasive one and is caused by friction between the pins and bushings with corrosion and mechanical impurities inside the joints.
- At the surface of the raceway of the links (zone "3", Figure 3). This degradation is an effect of rolling out of the upper part of the link by rolling wheels. In addition, impact loading may appear when rolling wheels overrun subsequent links.
- At the front and rear of the upper parts of the links in the contact area with driving wheel (zone "4", Figure 3). The degradation of these areas is a result of the impact of driving system's teeth. Due to the necessity of the combine forward or backward movement, the degradation occurs in both the front and the rear zone of the link.
- At the base of the link's lugs (zone "5", Figure 3). Degradation in this area is caused by friction between subsoil and links under the action of large loads (unit pressure of 100 kPa).

Degradation of pins connecting links is relatively easy to remove by replacing the pin with a new or a remanufactured one. A little more cumbersome is to remove effects of the degradation of the holes in the pin joints. In such cases, the repair consists in replacing the bushing. Degradation of the lugs in the chain links: a plastic deformation and a brittle fracture (Fig. 4), evolving under the influence of overload is usually an irreparable damage and qualifies the entire link to be replaced. Often in such cases it is also necessary to exchange the two mating

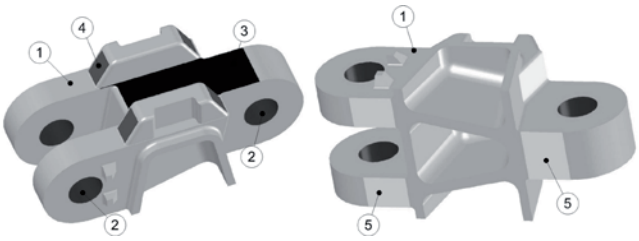

Fig. 3. Areas of basic degradation of large-size chain links [12] (detailed description in the text)

links. This entails significant costs resulting not only from the cost of the links, but also including losses generated from the out–of–order state of the machine.

Small plastic deformation of links' lugs does not always mean a need for instant exchange of the link, but continued usage of such a part could result in damage to other parts of the driving unit.

A typical example of the negative consequences of continued use of links and connecting pins with plastic deformations is a phenomenon called bevelling of crawler treads which causes an uneven distribution of loading on the subsoil. In extreme cases, this can lead to damage to the crawler treads by their mutual overlap.

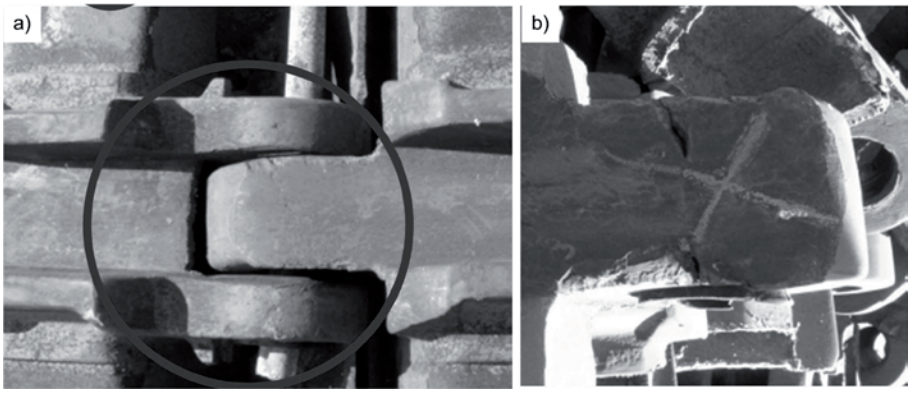

Fig.4. Examples of failures of links' lugs: a) plastic deformation, b) brittle fracture [authors' archive]

A degradation of a pin joint hole which is made directly in a link's lug (e.g. ovalisation or fissure of surface) is an irreparable damage, which qualifies the whole link to be replaced. One way to enable repair of the damaged pin joint's holes is to use a bushing which, after

reaching the wear limit is exchanged for a new one – without the need for replacing the entire link.

The main causes of a gradual degradation of the pin joint holes are unfavourable tribological conditions (high values of unit loading make it difficult to obtain proper lubrication while hard inclusions act as an abrasive) and corrosion (water and mud causing an accelerated destruction of the holes' and pins' surfaces due to an aggressive chemical influence).

3. Short review of state of the art in operational issues of chain links

There are plenty of scientific achievements related to the subject of operation of large-size caterpillar undercarriages of basic mining machinery.

An extensive study on the general problems of long-term degradation of multi–bucket excavators and stackers is given in [5, 7]. A unique position in the literature describing in details the effects of the degradation of basic mining machines in Polish coal mines is a work [1].

Publications relating to specific issues in the field of degradation of caterpillar undercarriages' components are focused on the following main thematic groups:

- identification of workloads,
- issues of strength,
- analysis of the degradation processes,
- designing issues,
- operational issues.

The problem of determining workloads acting on parts of large–size caterpillar undercarriages was analyzed among others in [9, 10]. An empirical method for evaluation of traction forces during the operation of basic mining machinery was presented.

A case of a damage of a driving shaft of an undercarriage of a multi–bucket excavator is the subject of work [8]. Based on a numerical analysis and measurement's results it was showed that the main cause of the failure was the wrong shape of the shaft's end, which led to the formation of the constructional notch in this area. As a result the shaft was twisted through the development of local plastic deformations and stresses surpassed the fatigue strength [8].

The issue of the strength of caterpillar undercarriages' components is presented, inter alia, in works [3, 11, 13]. The case of the degradation of stackers' chain links is analyzed in detail in [3]. It was showed that the main causes of the damage were material defects: microcracks and precipitation of carbides. In [2] damages of elements of a bucket wheel excavator's undercarriage were analyzed: balance levers, links and crawler treads. Basing on numerical simulations it was shown that the cause of the damages was too low strength of these elements on a lateral loading.

Issues related to a rational design of caterpillar chains' parts: links, connecting pins and treads are objects of interest especially by designing centres. In this regard, a particular achievement is a novel solution of friction node "bushing – pin" connecting links. It was developed by the Designing-Technical Office SKW [14]. This node is protected against the rock-soil particles getting inside.

Publications in the field of operational issues of large-size caterpillar undercarriages include issues of new materials, lubricants and lubrication techniques that could be used in nodes connecting links. The usage of conventional lubricants in heavily loaded nodes does not always enables to obtain better tribological characteristics.

Original solutions in this area were developed at the Division of Fundamentals of Machinery Design and Tribology in the Wroclaw University of Technology. One of these solutions is the application of lithium grease mixed with PTFE powder, which significantly increases the efficiency of lubrication, while lowering wear of the friction elements [6]. Another proposal is to use grease with the addition of graphite and molybdenum disulfide in the form of powders, which significantly reduces the shear stress in the lubricant and thus lowers the resistance to motion in the lubricated node [4]. Both of these solutions can be used in caterpillar chains of undercarriages in large-size mining machines.

4. Strength analysis – limiting loading of chain links

Pin joint hole is a notch in the chain links' lugs sections. Therefore, it is one of the most vulnerable areas to damage in the structure of the links, particularly under conditions of high lateral forces. In extreme conditions, regardless of the links' damage, it may inter alia effect in broken drawbar which steers the process of turning of the entire machine. Such a case is described in detail in [1].

In view of the possible consequences of lugs' damage, the authors have developed basic numerical models of large-size links used in excavators' and stacker's undercarriages. One such a model of links type "I" is shown in Figure 5.

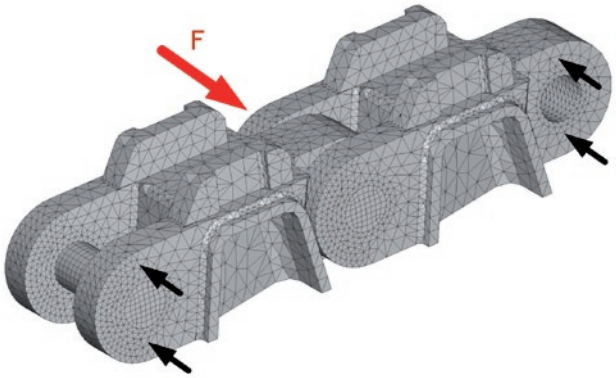

Fig. 5. Discrete model of "link – pin – link" connection [12]

Strength analyses were carried out using finite elements method for lateral loads in the range of F = 10÷10,000 kN, assuming some specific boundary conditions (support of links' connection). In the calculations the strength and ductile properties of cast steel L35GSM (Yield strength R_e = 850 MPa among others) as the material from which the links are made were taken into account. As the main objectives of the numerical simulations the following were assumed:

- To determine critical areas of the links' structure particularly vulnerable to the formation of defects because of a concentration of stresses.
- To estimate the value of the limit load, causing the destruction of the links, such as a plastic deformation and a brittle fracture.

Basing on results of the calculations it was found out that one of the most dangerous areas in the "link – pin – link" connection zone are bases of the narrow lugs. It was also shown that the limit value of lateral load which surpassing results in plasticizing of the links type "I" is about $F_{max} \approx 3000$ kN. Exemplary results of stress analysis for such values of load are shown in Figure 6.

The results of these calculations were verified with the research realised in the Division of Reliability Engineering and Diagnostics from Institute of Machinery Design and Operation at Wroclaw University of Technology. The test were carried out at a laboratory of a manufacturer of these links.

On the basis of the standard PN-G-47000-2: 2005: "Open pit mining. Multi-bucket excavators and stackers. Part 2: Introduction to computing" it was assumed that the required safety factor of links related to the yield stress is X = 1,3. This means that the maximum value of the stress in the links, as defined by Huber – von Mises yield criterion should not exceed 650 MPa.

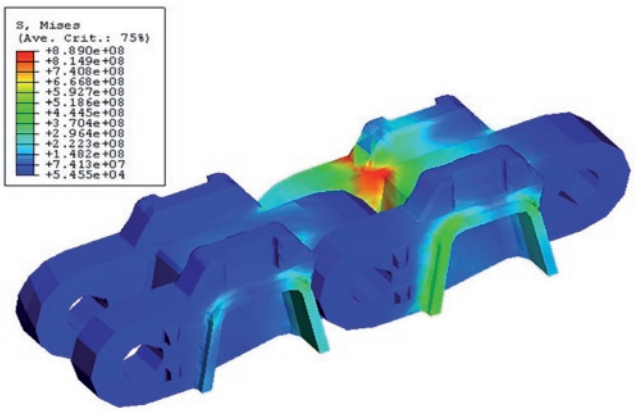

Fig. 6. Exemplary distribution of von Mises stress in the "link – pin – link" connection under the influence of plasticizing lateral loading.

With this in mind, concepts of geometrical modification of the links in their critical areas were developed. It is where the material's plasticization occurred. In particular, changes were introduced in the areas of bases of both the narrow and the broad lugs. Modifications included as well surfaces of the links mating with the driving wheel. These modifications are described in detail in [12]. The results of the simulation of effort of links with modified geometry are shown in Figure 7.

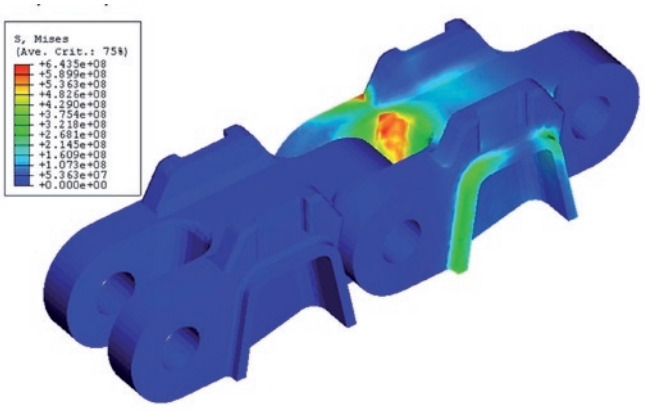

Fig. 7. Exemplary distribution of von Mises stress in the "link – pin – link" connection under the influence of plasticizing lateral loading after applying modifications of the critical areas.

It is noticeable that after the changes in the geometry of the critical sections, as proposed by one of the authors [11, 12], a significant reduction in the maximum values of von Mises stress is achieved (up to the level of 650 MPa).

This also means that the modified chain links are able to carry the load capacity larger by about 30% when compared to currently used links. This can help to increase the safety and reliability of caterpillar undercarriages of basic machinery.

4. Summary

Chain links are among the key elements of undercarriages of large–size basic mining machinery. Their degradation occurs in most of cases, because of operational reasons i.e. due to high workload and adverse environmental conditions (dust, mud, low temperature).

In this context it is important to understand the mechanisms of degradation of these elements, as well as to identify the so-called critical areas which are particularly vulnerable to damage and as well to determine load limits resulting in damage of the links: either plastic deformation or brittle fracture.

With this in mind, basing on a statistical data analysis from repair divisions in Polish coal mines and the authors' own research the structure of typical forms of degradation occurring in large–size chain links was determined. Cases of both gradual degradation (wear, corrosion), and a sudden/catastrophic one (plastic deformation, chipping, cracking) were included.

In order to perform strength analysis geometrical models of typical chain links used in caterpillar undercarriages of basic mining machinery were made. Numerical simulations of effort of the links for different variants of lateral external loads were performed. On this basis, critical areas in the structure of the analyzed links particularly vulnerable to damages were designated and the ultimate values of loading that causes the damage were calculated.

In order to increase the resistance to failure of the chain links, concepts of changes of their geometrical features in critical areas were developed. The effects of these changes are: an increase of about 30% of the limit load and a reduce of the links' effort under current maximum level of workload.

The implementation of these modifications can help to improve the reliability of large–size caterpillar undercarriages, because operation of chain links even partially degraded can initiate the process of destruction of other undercarriage's components – as a kind of a "domino effect". A striking example of this is a damage of crawler treads due to bevelling.

Acknowledgment: *The work has been co–financed with EU funds by European Social Fund (Research no. MK/SN/280/V/2011/U).*

References

1. Babiarz S, Dudek D. Kronika awarii i katastrof maszyn podstawowych w polskim górnictwie odkrywkowym. Wrocław: Oficyna Wydawnicza Politechniki Wrocławskiej 2007 (in Polish).
2. Bosnjak S, Petkovic Z, Zrnic N, Pantelic M, Obradovic A. Failure analysis and redesign of the bucket wheel excavator two-wheel bogie. Engineering Failure Analysis 2010, 17: 473–485.
3. Bosnjak SM, Arsic MA, Zrnic ND, Odanovic ZD, Djordevic MD. Failure Analysis of the Stacker Crawler Chain Link. Procedia Engineering 2010, 10: 2244 2249.
4. Czarny R, Paszkowski M. The influence of graphite solid additives, MoS2 and PTFE on changes in shear stress values in lubricating greases, Journal of Synthetic Lubrication 2007, 24 (1): 19–29.
5. Dudek D, Nowakowski T. Problems of degradation and maintenance of surface mine engineering machines. Proceedings of International Symposium on Materials Ageing and Component Life Extension, Milan, Italy, 10-13 October 1995. Vol. 2. Eds. V. Bicego, A. Nitta, R. Viswanathan Warley: Engineering Materials Advisory Services, 1995: 1285-1294.
6. Krawiec S. The synergistic effect of copper powder with PTFE in a grease lubricant under mixed friction conditions, Archives of Civil and Mechanical Engineering 2011, 11 (2): 379–390.

7. Nowakowski T. Comparative analysis of degradation degree of bucket wheel excavators. Proceedings of ESREL '99 - The Tenth European Conference on Safety and Reliability, Munich-Garching, Germany, 13–17 September 1999. Vol. 1/ Ed. by G. I. Schueller, P. Kafka Rotterdam: A.A.Balkema, 1999: 223-227.
8. Rusiński E, Harnatkiewicz P, Bobyr M, Yakhno B. Caterpillar drive shaft damage causes analysis. Archives of Civil and Mechanical Engineering 2008, 8 (3):117–129.
9. Smolnicki T, Maślak P. Measurement of traction and steering forces of multicaterpilar mechanism of stacker machine drive. 27th Danubia-Adria Symposium on Advances in Experimental Mechanics, September 22nd-25th, Wroclaw 2010, Wrocław University of Technology: 195–196.
10. Smolnicki T, Maślak P. Multicaterpillar track chassis of big machines – identification of loads. Key Engineering Materials 2012, 490: 187–194.
11. Sokolski P. Analiza wpływu cech geometrycznych na wytężenie obszarów krytycznych ogniw gąsienicowych wielkogabarytowych maszyn górniczych. Górnictwo Odkrywkowe 2011, 52 (3/4): 38–41 (in Polish).
12. Sokolski P. Metoda diagnozowania ogniw gąsienic wielkogabarytowych maszyn roboczych. (rozprawa doktorska). Wrocław: Politechnika Wrocławska, Instytut Konstrukcji i Eksploatacji Maszyn, Seria PRE Nr 9/2012 (in Polish).
13. Sokolski P. Poprawa efektywności działania wielkogabarytowych podwozi gąsienicowych poprzez modyfikacje postaci geometrycznej ich elementów. Monografia: Efektywność wykorzystania maszyn roboczych i urządzeń w przemyśle: eksploatacja – niezawodność – bezpieczeństwo. Red. nauk. Adam Idzikowski. Częstochowa: Sekcja Wydawnictw Wydziału Zarządzania Politechniki Częstochowskiej 2013: 108–116 (in Polish).
14. Wocka N, Warcholak A. Działania innowacyjne zwiększające trwałość i niezawodność eksploatacyjna gąsienicowych mechanizmów jazdy koparek i zwałowarek w polskich kopalniach węgla brunatnego. Górnictwo i Geoinżynieria 2011,35 (3/1): 291–307 (in Polish).

Piotr SOKOLSKI
Marek SOKOLSKI
Institute of Machinery Design and Operation
Faculty of Mechanical Engineering, Wroclaw University of Technology
ul. Wybrzeże Wyspiańskiego 27, 50-370 Wrocław, Poland
E-mails: piotr.sokolski@pwr.wroc.pl, marek.sokolski@pwr.wroc.pl

Article citation info:
GUO YM, WANG XT, LIU C, ZHENG YF, CAI XB. Electronic system fault diagnosis with optimized multi-kernel SVM by improved CPSO. Eksploatacja i Niezawodnosc – Maintenance and Reliability 2014; 16 (1): 85–91.

Yang-Ming GUO
Xiang-Tao WANG
Chong LIU
Ya-Fei ZHENG
Xiao-Bin CAI

ELECTRONIC SYSTEM FAULT DIAGNOSIS WITH OPTIMIZED MULTI-KERNEL SVM BY IMPROVED CPSO

DIAGNOZA USZKODZEŃ UKŁADU ELEKTRONICZNEGO Z WYKORZYSTANIEM WIELOJĄDROWEJ MASZYNY WEKTORÓW NOŚNYCH (SVM) ZOPTYMALIZOWANEJ PRZY POMOCY POPRAWIONEGO ALGORYTMU CPSO

Electronic systems' safety operation has become a key issue to complex and high reliability systems. Now more emphasis has been laid on the accuracy of electronic system fault diagnosis. Based on the characteristics of the electronic system fault diagnosis, we design a multi-classification SVMs model to attain better fault diagnosis accuracy, which utilizes multi-kernel function consisting of several basis kernel functions to enhance the interpretability of the classification model. In order to optimize the performance of multi-classification SVMs with multi-kernel, we improve the Chaos Particles swarm Optimization (CPSO) algorithm to achieve the optimum parameters of SVMs and the multi-kernel function. For the improved CPSO algorithm, a modified Tent Map chaotic sequence is used to strengthen the search diversity, and an effective method is embedded to the stander PSO algorithm which can ensure to avoid premature stagnation and obtain the global optimization values. The fault diagnosis simulation results of an electronic system show the proposed optimization scheme is a feasible and effective method and it can significantly improve the fault diagnosis accuracy of the multi-kernel SVM.

***Keywords**: electronic system; fault diagnosis; support vector machine; chaos particles swarm optimization; multi-kernel.*

Bezpieczeństwopracy układów elektronicznych stało się kluczowym zagadnieniem w odniesieniu do złożonych układów o wysokiej niezawodności. Obecnie coraz większy nacisk kładzie się na trafność diagnozy uszkodzeń układów elektronicznych. Na podstawie charakterystyki diagnozy uszkodzeń układów elektronicznych, opracowaliśmy model wielokryterialnej klasyfikacji SVM pozwalający osiągnąć lepszą trafność diagnozy uszkodzeń. Model wykorzystuje funkcję wielojądrową składającą się z kilku bazowych funkcji jądrowych pozwalającą na zwiększenie interpretowalności modelu klasyfikacyjnego. Aby zoptymalizować działanie modelu wielokryterialnej klasyfikacji SVM wykorzystującego funkcję wielojądrową, udoskonaliliśmy algorytm Optymalizacji Metodą Chaosu-Roju Cząstek (CPSO), co pozwoliło osiągnąć optymalne parametry SVM i funkcji wielojądrowej. W poprawionym algorytmie CPSO wzmocniono różnorodność wyszukiwania poprzez wykorzystanie chaotycznej sekwencji generowanej przez zmodyfikowaną mapę tent, a także włączono do standardowego algorytmu PSO efektywną metodę pozwalającą uniknąć przedwczesnej stagnacji oraz uzyskać globalne wartości optymalizacji. Wyniki symulacji diagnozy uszkodzeń systemu elektronicznego pokazują, że proponowany system optymalizacji może być wykorzystywany jako skuteczna metoda umożliwiająca znaczne zwiększenie trafności diagnozy uszkodzeń z wykorzystaniem wielojądrowej SVM.

***Słowa kluczowe**: układ elektroniczny, diagnoza uszkodzeń, maszyna wektorów nośnych, optymalizacja metodą chaosu-roju cząstek; funkcja wielojądrowa.*

1. Introduction

Electronic diagnosis is always an important research field of fault diagnosis. With the rapid development of the electronic technology in recent years, [21] more and more electronic systems become critical components of the whole system, and their safety also become the key issue to the system reliability. Thus, according to the information collected from the test ports, inferring the state condition, determining the fault location, forecasting the future failure and then giving the necessary maintenance tips have great significances to accomplishing the missions successfully.

However, electronic system fault diagnosis is complexity and difficulty in many cases. For example, one fault phenomenon always shows with several fault modes. We need to solve multi-classification fault diagnosis problem. In recent years, some intelligent classification methods, such as artificial neural network (ANN) [10], Support Vector Machine (SVM) [5], etc. have been applied to electronic system fault diagnosis. As a state-of-the-art learning method based on the statistical learning theory, SVM not only characterizes a simple model structure, but also has excellent classification in solving learning problem with small training sample set. [9, 30] It can solve the problems of "over fitting", local optimal solution and low-convergence rate existing in ANN. Moreover, SVM has better generalization performance than ANN due to its risk minimization principle. [15] Thus, SVM has received more extensive attention and achieved superior performance in electronic system fault diagnosis. However, SVM also has two main drawbacks in practical application of multi-classification fault diagnosis.[15, 34]

Firstly, because SVM is originally designed for binary-class classification, we must combine several binary-SVMs for the multi-classification with a suitable structure, such as "one-against-rest", "one-against-one", "decision directed acyclic graph (DDAG)", etc. [4, 16, 34] But the performance does not seem satisfactory as much as the binary classification. This may be due to that, whatever the scheme is, each binary-SVM must train at least two class fault mode data, i.e., we must look at least two different class data as same class. Generally, an appropriate kernel for one class fault mode data does not always conduct to the others. So, it is difficult to attain good results by the reported schemes.

Secondly, it is difficult to select the appropriate parameter values of the SVM model, which have a great impact on the generalization capability and model accuracy. Researchers proposed many optimization methods to solve the problem, such as genetic algorithm, particles swarm optimization (PSO) algorithm, etc. [17]. But these methods involve too many human factors or requirements, for example, the kernel function should be continuously differentiable, and the results of SVM classifier are prone to failing into the local minimum.

In order to overcome above shortcomings, we propose a new scheme to improve the classification performance of electronic system fault diagnosis. This scheme includes two parts: One is to design a appropriate multi-classification SVMs model using several multi-kernel SVMs, which depends on the characteristics of electronic system fault diagnosis and can mine the information in the data more effectively. The other one is to improve the chaotic particles swarm optimization (CPSO) algorithm to optimize the parameters of the classifier, which can avoid the premature stagnation and ensure to obtain the best parameters values combination. The feasibility and efficiency of the proposed scheme for electronic system fault diagnosis are verified via application experiments.

The remainder of the paper will be structured as follows: Section 2 gives a brief introduction of SVM and stander PSO algorithm; Section 3 proposes the scheme of electronic fault diagnosis with multi-kernel SVM and the improved CPSO algorithm; Section 4 shows application experiments of electronic system fault diagnosis; and Section 5 gives the conclusions.

2. Related work review

2.1. Support vector machines

As a machine-learning algorithm, SVM integrates the optimal separating hyper-plane with the kernel method. Its resolution has good generalization capability, and the generalization capability is independence of the particular sample distribution. The performance of SVM is mainly referred to its generalization capability, namely the capability of recognizing the new data, and availability to the situation of small samples.[9, 15, 30] SVM is more suitable for electronic system fault diagnosis, because electronic system always shows nonlinear, complexity and diversity features.

Consider n training data x_i and the corresponding labels y_i ($i = 1, 2, ..., n$). In the simplest form, SVM will yield a hyper-plane that separates the training data by a maximal margin. The data lying on one side of the hyper-plane are labeled as +1, and the other data lying on the other side are labeled as −1. The training data that lie closest to the hyper-plane are called support vectors. In the case of linearly data, it is possible to determine the hyper-plane $w^T x + b = 0$ that separates the given data, where w and b are used to define the position of the separating hyper-plane. It is easy to find that the parameter pair (w, b) corresponding to the optimal hyper-plane is the solution to the following optimization problem:

$$\begin{aligned} &minimize: L(w) = \frac{1}{2}\|w\|^2 \\ &subject\ to: y_i(w^T x_i + b) \geq 1 \qquad i = 1, 2, ..., n \end{aligned} \tag{1}$$

For linearly non-separable cases, there is no such a hyper-plane that is able to classify every training sample correctly. So the optimization idea is generalized via the concept of soft margin. The new optimization problem thus becomes:

$$\begin{aligned} &minimize: L(w, \xi_i) = \frac{1}{2}\|w\|^2 + c\sum_{i=1}^{n}\xi_i \\ &subject\ to: y_i(w^T x_i + b) \geq 1 - \xi_i \qquad i = 1, 2, ..., n \end{aligned} \tag{2}$$

where ξ_i is called slack variables related to the soft margin, and c is the tuning parameter used to balance the margin and training error. Both optimization problems (see Eq. (1) and Eq.(2)) can be solved by the Lagrange multipliers α_i that transform them to quadratic programming problems.

For the applications, linear SVM does not meet satisfactory performance, non-linear SVM is more often applied. The basic idea of designing a non-linear SVM model is to map the input vector $x \in R^n$ into a high-dimensional feature space to solve a non-linear classification problem. Here the mapping function $\varphi(x)$, called kernel function, is selected in advance. The kernel function can perform a non-linear mapping to a high-dimensional feature space by replacing the inner product for non-linear pattern problem, which performs the non-linear mapping. The kernel functions are Mercer functions which meet Mercer condition, and the approximating feature map for the Mercer kernel is $k(x, y) = \varphi(x)^T \varphi(y)$. The main basis kernel functions are listed as follows:

(1) Linear kernel function: $k(x, y) = (x \cdot y)$

(2) Polynomial kernel function: $k(x, y) = (s(x \cdot y) + \gamma)^d$

(3) RBF kernel function: $k(x, y) = \exp(-\frac{\|x - y\|^2}{2\sigma^2})$

(4) Sigmoid kernel function: $k(x, y) = \tanh(s(x \cdot y) + \gamma)$

The learning algorithm for a non-linear classifier SVM follows the design of an optimal separating hyper-plane in a feature space. The procedure is the same as associated with hard and soft margin classifier SVMs in the x-space. Using the chosen kernel function, the Lagrangian is maximized in the corresponding high-dimensional feature space as follows:

$$\begin{aligned} &maximize: L(\alpha) = \sum_{i=1}^{n}\alpha_i - \frac{1}{2}\sum_{i,j=1}^{n}\alpha_i\alpha_j y_i y_j k(x_i, x_j) \\ &subject\ to: \sum_{i=1}^{n}\alpha_i y_i = 0, \qquad \alpha_i \geq 0, \qquad i = 1, 2, ..., n \end{aligned} \tag{3}$$

where the constraints must be revised by a non-linear soft margin classifier SVM. The unique difference between these constraints

and the separable non-linear classifiers is in the upper bound c and the Lagrangian multipliers α_i. The constraints of the optimization problem become as follows:

$$subject\ to: \quad \sum_{i=1}^{n} \alpha_i y_i = 0, \qquad c \geq \alpha_i \geq 0, \qquad i = 1, 2, ..., n \tag{4}$$

This way, the influences of the training data will be limited and remained on the wrong side of a separating non-linear hyper-plane. The non-linear SVM classifier is described below:

$$f(x) = \text{sgn}(\sum_{i=1}^{l} \alpha_i y_i K(x, x_i) + b) \tag{5}$$

where l presents the number of support vectors.

2.2. Stander particles swarm optimization algorithm

Compared with the other optimization algorithms, PSO algorithm is a kind of global search algorithm with many merits, such as simple concept, fast convergence rate, etc. It has been successfully applied in many fields. [6, 28] The stander PSO algorithm was proposed by James Kennedy and Eberhart, which is derived from the simulations of the birds in finding foods [12, 25, 32]. The basic idea of the stander PSO algorithm is to optimize the solution to every problem as a particle which searches the optimal value by sharing the historical information and the social information amount the particle individuals. Each particle flights with a certain speed in the D-dimensional search space, and uses the fitness function to judge the merits of particles, particle flying experience of its own and other particles flying experiences. Then the speeds and best location of the particle group are adjusted dynamically, finally the optimal solution of optimization problems is given.

Assume m particles and form themselves into a particles swarm in a D-dimensional search space, $x_i = (x_{i1}, x_{i2}, ..., x_{iD})$ denotes the position of the i-th particle, and $v_i = (v_{i1}, v_{i2}, ..., v_{iD})$ denotes the velocity of the i-th particle. The best position of a particle is $p_i = (p_{i1}, p_{i2}, ..., p_{iD})$, and the best position of the whole swarm is $p_g = (p_{g1}, p_{g2}, ..., p_{gD})$. Therefore the position and velocity of the particles in the particles swarm can be expressed as follows:

$$\begin{cases} v_{id}(k+1) = \mathrm{w} \cdot v_{id}(k) + rand(0, c1) \cdot [p_{id}(k) - x_{id}(k)] + rand(0, c2) \cdot [p_{gd}(k) - x_{id}(k)] \\ x_{id}(k+1) = x_{id}(k) + v_{id}(k+1) \qquad d = 1, 2, ..., D \end{cases} \tag{6}$$

where $c1$ and $c2$ are acceleration constants which, respectively, stand for the weights of the accelerations, and by which, a particle flies towards the individual local best position or the best global position; $rand(0, c1)$ and $rand(0, c2)$ are the random numbers evenly distributed in $[0, c1]$ and $[0, c2]$ respectively. If $c1 = 0$, the particle only has self-experience which means that its convergence rate may be fast, and it is easy to fall into the local optimum. If $c2 = 0$, the particle only has social experience which means that all particles in a swarm become moving by themselves without interaction, and the probability of finding a solution is very low. The velocity v_{id} is generally condition by $v_{id} \in [-v_{\max}, v_{\max}]$ to prevent the particles from flying out of the solution area. ω is an inertial weight which denotes the influence of the previous velocity of a particle upon its current velocity. The bigger ω means the bigger velocity v_{id} and search space for the particles, which helps to find the new solution space. The smaller ω means the smaller velocity v_{id}, which helps to find a better solution in the current solution space. ω is always defined as follows [35]:

$$\omega = \omega_{\max} - \frac{\omega_{\max} - \omega_{\min}}{Iter_{\max}} \times Iter \tag{7}$$

where ω_{max} is the initial inertia weight factor, ω_{min} is the final inertia weight factor, $Iter$ is the current iteration number, and $Iter_{\max}$ is the maximum iteration number.

3. Optimization multi-kernel SVM by improved CPSO

For SVM, the penalization parameter c, kernel function and its parameters are the main factors which influence the classification performance [3, 29]. Therefore, in order to obtain good generalization capability of SVM, one of the main issues is to select the appropriate c, kernel function and its parameters. In this section, aiming at the characters of electronic fault diagnosis, we apply multi-kernel SVM to enhance the generalization capability and exploit more discriminative information in sample data. In addition, we propose an improved CPSO, called ICPSO, to jointly optimize the parameters of multi-kernel SVM.

3.1. Improved CPSO algorithm

According to Ref. [7], the performance of standard PSO algorithm mainly depends on the number of particles and initial parameters. We can see from Eq.(6) that current individual local position is attracted not only by its own current local best position but also by the best global position. If both of the local best position and the best global position are local optima, the particles will repeat the same search path, called premature stagnation. The Eq. (6) doesn't offer a method of jumping out of the premature stagnation. In this paper, an improved CPSO (ICPSO) algorithm is proposed to enhance the search diversity and to overcome the premature stagnation.

3.1.1. Initialization of particles

The initialization of the particles of stander PSO algorithm always adopts a random distribution strategy, but it is difficult to ensure better ergodicity of the initial particles swarm. Chaos is an universal phenomenon of non-linear systems [18]. In general, chaotic motion is not haphazard, and the chaotic variable has three main properties, such as ergodicity, randomness and sensitivity to initial conditions. Using these characteristics, the chaos optimization algorithm is utilized to solve the problem of the particles initialization.

Different chaos map functions have great different influences on chaotic optimization search. Logistic map is more often used in research and application currently. Ref. [2, 19, 20, 24] point out that Tent map has better ergodic homogeneity and higher iterative evolution velocity than Logistic map via mathematical analysis and simulation verification. In this paper, we modify stander Tent map function and use it for the chaotic search. The stander equations of Tent map function are shown as follows:

$$x_{n+1} = \begin{cases} 2(x_n + 0.1 \times rand(0,1)) & 0 \le x_n \le 0.5 \\ 2(1 - x_n + 0.1 \times rand(0,1)) & 0.5 < x_n \le 1 \end{cases} \quad (8)$$

Here we modify Eq.(8) with the following constrained condition. If $x_n = \{0, 0.25, 0.5, 0.75\}$ or $x_n = x_{n-m}$, $m = \{0,1,2,3,4\}$, then $x_n \to x_n + 0.1 \times rand(0,1)$. In practice, because the optimization ranges of every parameters are different, we will carry interval [0, 1] of the chaotic variables to define the rang of the particles swarm solution vectors.

3.1.2. Judgment of premature stagnation

In the iteration process of each particle, if the premature stagnation happens, i.e., the best global position of the whole swarm p_g is unchanged within N times iterations, which means that the particles swarm has already or will be fall into local optima. Here, the value of N can be set in advance according to the scale of the problem or the experimental results. Generally, the bigger N means the standard of the judgment of premature stagnation is more lax. Base on this idea, some researchers[8] applied to embed a premature stagnation counter , called K, into the PSO algorithm, K is used to count the number of stagnation. If p_g is same as the previous value, then K adds 1, otherwise K is cleared to zero. When K is up to the limit time N, a mechanism will run to help the particles to jump out of the local optimum. Obviously, this process will consume more computation time in practice, thus we propose to leave this judgment process out, this means that p_g will be replaced by a new value at each iteration process step.

According to the Eq.(6), the next location of particles depends on the current position and speed. The current speed is the key of the particles swarm optimization since it makes the particles to have better movement and enhance the diversity of the particles swarm. The current speed depends on three main factors, called previous speed, the best position of each particle p_i and the global best position p_g. It is obvious that p_g plays a vital role in information exchange among the particles and the convergence rate increase. With the pulling of p_g, the stander PSO algorithm may lose their diversity of the particles swarm and the premature convergence is more likely to happen during the evolutionary process. In order to enhance the diversity of the particles swarm and avoid premature convergence. We develop p_g as follows at each evolution step.

$$p_g \to \overline{p}_g = \frac{1}{m}\sum_{i=1}^{m} p_i \quad (9)$$

Eq.(9) indicates that the global best place p_g will be replaced by the center of all individual best places $\overline{p}_g$. Then the new equations of the position and velocity of the particles in the swarm are shown as follows:

$$\begin{cases} v_{id}(k+1) = \omega \cdot v_{id}(k) + rand(0,c1) \cdot [p_{id}(k) - x_{id}(k)] + rand(0,c2) \cdot [\overline{p}_{gd}(k) - x_{id}(k)] \\ x_{id}(k+1) = x_{id}(k) + v_{id}(k+1) \qquad d = 1,2,...,D \end{cases} \quad (10)$$

From Eq.(10), we can see that the new improved algorithm not only remains the simplicity of the standard PSO algorithm, but also makes the particles to have the capability of jumping out of local optimal position. $\overline{p}_g$ improves the diversity of the particles swarm, and it plays the same effect as the p_g. In fact, this scheme is also accordance with the social and psychological habits, that is, particles not only want to move closer to the best but also hope to be the "majority". Here the "majority" is $\overline{p}_g$, the center of all individual best places. This way, the new ICPSO algorithm can reduce the invalid iteration effectively and improve the convergence rate greatly as well as the optimization accuracy.

3.2. Optimization of multi-kernel SVM

3.2.1. Multi-kernel SVM

The kernel function and corresponding kernel parameters are the key issue affecting the model prediction accuracy. An efficient kernel function should represent sample data adaptively. General kernel methods use a single kernel function and choose consistent parameters for the whole sample data sets. In reality, the distributions of the sample data in the different mapping space are different. So MKL was proposed by Lanckriet et al. [13]

MKL is an active research topic in the field of machine learning and it provides a more flexible framework than a single kernel. MKL mines information in data more adaptively and effectively, especially in enhancing the interpretability of the classification function and improving its performance.

In the MKL framework, a combined kernel function is defined as the weighted sum of the individual basis kernels. MKL aims to optimize combining weights while training the SVM-based methods [11, 31]. Though researchers proposed a variety of methods of integrate multiple kernels, linear convex combination of basis kernels is still one of the most frequently used approaches. With this method, each basis kernel can exploit the full set of features, or use a subset of features. So, using the equations described by Sonnenburg et al. [26], we consider the combined kernel as follows:

$$k(x_p, x_q) = \sum_{j=1}^{m} \mu_j k_j(x_p, x_q)$$

$$subject\ to: \quad \begin{cases} \sum_{j=1}^{m} \mu_j = 1 \\ \mu_j \ge 0 \qquad j = 1,2,...,m \end{cases} \quad (11)$$

where m is the number of basis kernels, μ_j is the combining weight of the j-th basis kernel. According to the properties of kernel function[22], k is Symmetric Positive Semidefinite Matrix, i.e., $k \ge 0$. Afterward, all kernel matrices k_j are normalized by replacing $k_j(x_p, x_q)$ by the following equation to get unit diagonal matrices:

$$k_j(x_p, x_q) \to k_j(x_p, x_q) \Big/ \sqrt{k_j(x_p, x_p) k_j(x_q, x_q)} \quad (12)$$

Based on MKL and Schur complement lemma [11, 27], the solution problem of μ_j can be cast to the form of quadratically constrained

quadratic program (QCQP). The objective of QCQP is convex in μ_j and Lagrange multipliers α_i. Such a QCQP problem can be solved efficiently by the interior point methods. The obtained dual variables can be used to solve the optimal kernel coefficients.

Although some reported optimization software packages, such as MOSEK [1], can solve the primal and dual problems simultaneously, it is also complex and not unfit for application. In this paper, because the combination of several basis kernels is a linear combination, we propose to use joint optimization method to determine the combining weights of the new multi-kernel. This way can not only reduce the computation complexity comparing with MOSEK, but also obtain the best parameters' values combination.

3.2.2. Optimization steps of multi-kernel SVM

In the ICPSO algorithm, the chaotic sequence is used to initiate individual position, which strengthens the diversity of search, and the stander PSO algorithm with new global best place is mainly used to perform a global search. The process of ICPSO is given below.

Step 1: Initialize each parameter, such as population size m, the stopping criterion (maximum number of iterations) $Iter_{\max}$, displacement genes $c1$ and $c2$, weight ω_{max} and ω_{min}, maximum velocity $v_{\max}$. Let the maximum iteration counter $J=0$;

Step 2: Assign the initial location and velocity with the Eq. (8) randomly;

Step 3: Evaluate the fitting degree of each particle, and let initial individual best position to be p_i and let initial global best position to be p_g;

Step 4: Update the position and speed of each particle based on Eq.(6) and Eq.(7);

Step 5: Calculate the new fitting degree of each particle and replace p_g by $\overline{p}_g$ according to Eq. (9);

Step 6: The maximum iteration counter J plus one, and if $J < Iter_{\max}$, return to step 4. Otherwise end the iteration computation and out put the current p_g.

4. Application experiments of electronic system fault diagnosis

4.1. Case representation

Electronic system faults always exist multiple fault modes simultaneously. A local circuit of a certain electronic system is shown in Fig.1. In order to obtain the sample data for information fusion, we measure 7 voltage values with many times at the measuring points called A, B, C, D, E, F and G (with pentagrams representation). In this case, F1 indicates normal mode, F2, F3, and F4 indicate three fault modes respectively: circuit board damaged mode, chip burned mode and pins broken mode.

4.2. Design and optimization of multi-classification SVMs

Because the extension of SVM to multi-classification problems is not straightforward, multi-classification SVMs should be designed in this case. Ref. [37] addressed the existing representative multi-class classification methods with SVM and compared their merits and defects systematically. The popular methods applying SVMs to multi-class classification problems decompose the multi-class classification problems into many binary-class classification problems and incorporate many binary-class SVM [14, 23, 33]. For example, an N-class classification problem needs $N(N-1)/2$ binary-class classification SVMs with the "one-against-one" approach, while N SVMs

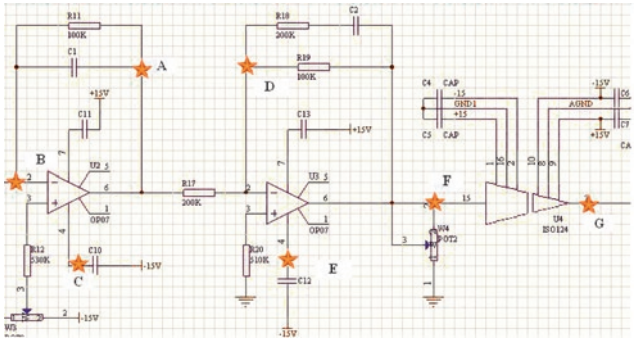

Fig. 1. Local circuit with faults of certain electronic system

for the "one-against-Rest" approach. Although the "one-against-one" approach demonstrates superior performance, it may require prohibitively-expensive computing resources in many real-world problems. The "one-against-rest" approach shows less accuracy, and demands heavy computing resources, especially for the real-time applications.

Based the conclusions of Ref. [37], we establish a multilayered classification structure in this paper. Firstly, we classify the normal mode and fault modes using SVM1 to achieve the purpose of fault detection, and then we use the "DDAG" approach to execute fault pattern recognition, such as recognizing circuit board damaged mode and chip burned mode via SVM2, recognizing chip burned mode and pins broken mode via SVM3, recognizing circuit board damaged mode and pins broken mode via SVM4. The multi-classification SVMs model is shown in Fig. 2.

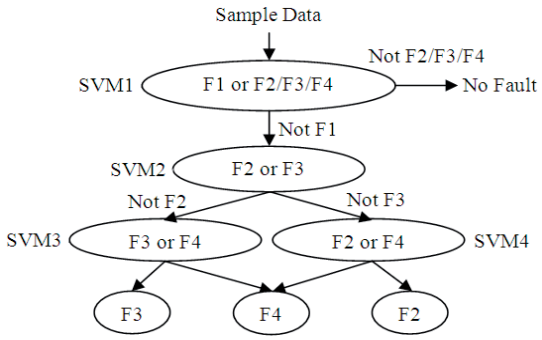

Fig. 2. Fault class flow chart with multi-classification SVMs

Based on Fig.2, we choose appropriate basis kernel functions firstly, and then use the proposed ICPSO algorithm to achieve the optimal parameters' values combination of the multi-kernel SVM. Here we choose the average test set accuracy (TSA) [11] for the sample data as evaluation criteria (fitting function). The TSA is defined as follows:

$$\sigma = \frac{y_t}{y_t + y_f} \tag{13}$$

where y_t and y_f represent the number of true and false classification respectively. That SVM has higher TSA means the model is a better model. The main steps of fault diagnosis are shown as follows

Step 1: Choose sample data via unitary processing and divide them into two parts: training set and testing set;

Step 2: Jointly optimize the parameters of each multi-kernel SVM using the ICPSO algorithm and establish the multi-classification multi-kernel SVMs;

Step 3: Train each multi-kernel SVM of multi-classification SVMs;

Step 4: Verify fault diagnosis accuracy of the multi-classification multi-kernel SVMs using the testing set.

4.3. Experiments and discussion

We collect 1000 voltage values as the sample data from the seven test points (see Fig.1). After unitary processing, we divide them into two parts: 500 data as training set and 500 data as testing set. The number of each fault mode is shown in Tab.1.

Table 1. Number of the fault modes in the sample data

Type	Normal	Fault Mode		
		Circuit Board Damaged	Chip Burned	Pins Broken
Training Set	112	138	150	100
Testing Set	146	121	113	120

In this study, we perform two experiments. Experiment I compares the multi-classification multi-kernel SVMs on fault detection rate (FDR) and fault detection accuracy (FDA) using ICPSO, CPSO and GA respectively. Here we choose one linear kernel function which represents global information and one RBF function which represent local information [36] as basis kernel functions. Experiment II compares single RBF SVM with multi-kernel SVM on FDR and FDA. The multi-kernel SVM has same basis kernel functions as experiment I. Their parameters are optimized by ICPSO in experiment II.

The same set of parameters is assigned for the two experiments: m=20, D=4 (represent the two combination coefficients of the Multi-kernel, the penalization parameter c and the width of RBF σ respectively), ω_{max}=1.2, ω_{min}=0.2, $c1 = c2$=2, $v_{\max}$=15 and $Iter_{\max}$=300. The results are reported in Tab. 2 and Tab. 3.

Table 2. Results of fault diagnosis experiment I (compare with ICPSO, CPSO and GA)

Algorithm	Fault Detection Rate (FDR)	Fault Detection accuracy (FDA)		
		Circuit Board Damaged	Chip Burned	Pins Broken
ICPSO	93.2%	94.2%	95.6%	92.5%
PSO	90.4%	89.3%	92.9%	90.8%
GA	90.0%	89.3%	91.2%	91.7%

Table 3. Results of fault diagnosis experiment II (compare with RBF and multi-kernel)

Algorithm	Fault Detection Rate (FDR)	Fault Detection Accuracy (FDA)		
		Circuit Board Damaged	Chip Burned	Pins Broken
Method with Multi-kernel	93.2%	94.2%	95.6%	92.5%
Method with RBF	87.2%	86.8%	91.2%	83.3%

Tab. 2 and Tab. 3 show that the multi-classification multi-kernel SVMs with optimization parameters by ICPSO have better FDR and FDA. This indicates that the proposed ICPSO algorithm is a better optimization method. Moreover, multi-kernel learning method can enhance the interpretability of the classification function and it is an effective approach to improve performance of SVM-based classifier considerably.

5. Conclusions

The reliability of electronic system has attracted more attention, and SVM is widely applied in the electronic system fault diagnosis. In many reality cases, the parameters of SVM and its kernel function have great impact with the classification accuracy and generalization capabilities. In order to attain satisfactory fault diagnosis results of electronic system, we design a multi-classification multi-kernel SVMs model to perform classification. We propose an improved CPSO algorithm to achieve the optimal parameters' values combination of the electronic fault diagnosis model. In the ICPSO algorithm, a modified Tent map chaotic sequence is used to initiate individual position, and a new scheme is embedded into the stander PSO algorithm to avoid premature stagnation. The feasibility and efficiency of the proposed scheme have been verified via the application experiments.

***Acknowledgments**: The authors would like to thank Prof. Ming J. Zuo, the Director of Reliability Research Laboratory at University of Alberta, for his helpful comments. This work is supported by the National Basic Research Program of China (973 Program), the National Natural Science Foundation of China (No. 61001023 and No. 61371024), Chinese Astronautics Support Technology Foundation, Aviation Science Foundation of China (No.2013ZD53051) and Xi'an Technology Plan Projects 2013.*

References

1. Andersen ED, Andersen AD. The MOSEK interior point optimizer for linear programming: an implementation of the homogeneous algorithm. High performance optimization. Norewll, USA: Kluwer Academic Publishers, 2000.
2. Brian R, Sonja S. Structure of inverse limit spaces of Tent maps with nonrecurrent critical points. Glasnik matematickl 2007; 42(62):43–56.
3. Chapelle O, Vapnik V, Bousquet O, et al. Choosing kernel parameters for support verctor machines. Machine Learning 2002; 46(1):131–159.
4. Diao ZH, Zhao CJ, Guo XY, Lu SL. A new SVM multi-class classification algorithm based on balance decision tree. Control and Decision 2011; 26(1):149-152,156.
5. Drucker H, Wu D, Vapnik V. Support verctor machines for spam categorization. IEEE Transactions on Neural Networks 1999; 10(5):1048–1054.
6. Gaing ZL. Discrete particles swarm optimization algorithm for unit commitment. Power Engineering Society General Meeting, July, 2003.
7. Guo JQ, Li Y, Wang HS. Application of particles swarm optimization algorithms to determination of water quality parameters of river streams. Advances in science and technology of water resources 2007; 27(6):5.
8. Guo YM, Ma JZ, Xiao F, Tian T. SVM with optimized parameters and its application to electronic system fault diagnosis. 2012 IEEE International Conference on Prognostics and Health Management, June, 2012.
9. Hao Y, Sun JG, Yang GQ, Bai J. The application of support vector machines to gas turbine performance diagnosis. Chinese Journal of Aeronautics 2005; 18(1):15-19.
10. He Y, Ding Y, Sun Y. Fault diagnosis of analog circuitswith tolerances using artificial neural networks. IEEE Asia-Pacific Conference on Circuits and Systems, October, 2002.
11. Jian L, Xia ZH, Liang XJ, Gao CH. Design of a multiple kernel learning algorithm for LS-SVM by convex programming. Neural Networks 2011; 24: 476–483.

12. Kennedy J, Eberhart R. Particle swarm optimization. IEEE International Conference on Neural Networks, December, 1995.
13. Shen LC, Huo XH, Niu YF. Survey of discrete particles swarm optimization algorithm. Systems Engineering and Electronics 2008; 30(10): 1986–1990.
14. Lee Yoonkyung. Multicategory support vector machines, theory, and application to the classification of microarray data and satellite radiance data. Technical Report No.1063, 15 Sept. 2002.
15. Li H, Zhang YX. An algorithm of soft fault diagnosis for analog circuit based on the optimized SVM by GA. The Ninth International Conference on Electronic Measurement & Instruments (ICEMI'2009), August, 2009.
16. Li Q, Dong CL, Chen ZZ, He XL. Improved algorithm for kernel-based SVM. Computer Engineering and Application 2010; 46(10): 150–152.
17. Lian GY, Wang WG, Huang KL, Guo R. Research of optimization method for test selection based on particles swarm optimization algorithm. Computer Measurement & Control 2008; 16(10):1387–1389.
18. Liu B, Wang L, Jin YH, Tang F, Huang DX. Improved particles swarm optimization combined with chaos. Chaos, Solitons and Fractals 2005; 25: 1261–1271.
19. Liu JD. A spatiotemporal chaotic sequence based on coupled chaotic Tent map lattices system with uniform distribution. Journal of computers 2011; 6(2): 190–199.
20. Meng LQ, Guo JQ. Application of chaos particles swarm optimization algorithm to determination of water quality parameter of river steam. Journal of earth sciences and environment 2009; 31(2): 169–172.
21. Michael P, Rubyca J. A prognostics and health management roadmap for information and electronics-rich systems. IEICE Fundamentals Review 2010; 3(4): 25–32.
22. Scholkopf B, Smola A,Learning with Kernels. Cambridgeshire MIT Press, 2002.
23. Schwenker F. Hierarchical support vector machines for Multi-class pattern recognition. The fourth international conference on knowledge-based intelligent engineering systems & allied technologies, Augest, 2000.
24. Shan L, Qiang H, Li J, Wang ZQ. Chaotic optimization algorithm based on Tent map. Control and Decision 2005; 20(2): 179–182.
25. Shen LC, Huo XH, Niu YF. Survey of discrete particles swarm optimization algorithm. Systems Engineering and Electronics 2008; 30(10): 1986–1990.
26. Sonnenburg S, Räosch G, Schäer C, Schökopf B. Large scale multiple kernel learning. Journal of Machine Learning Research 2006; 7: 1531–1565.
27. Vandenberghe L, Boyd S, Semidefinite programming. SIAM Review 1996; 38: 49–95.
28. Van B, Engelbrecht A. A new locally convergent particles swarm optimizer. IEEE International Conference on Systems, Man and Cybernetics, October, 2002.
29. Vapnik V. An overview of statistical learning theory. IEEE Transactions on Neural Networks 1999; 10(5): 988–999.
30. Vapnik V. Statistical learning theory. New York: John Wily and Sons, 1998.
31. Wang HQ, Sun FC, Cai YN, Chen N. Ding LG, On multiple kernel learning methods. Acta Automatica Sinica 2010; 36(8): 1037–1050.
32. Wang M, Zhu YL. He XX. A survey of swarm intelligence. Computer Engineering 2005; 31(22):194–196.
33. Weston J, Watkins C. Multi-class support vector machines. Technical Report CSD-TR-98-04, Department of Computer Science, Royal Holloway, University of London, Egham, UK, 1998.
34. Xu QH, Shi J. Fault diagnosis for aero-engine applying a new multi-class support vector algorithm. Chinese Journal of Aeronautics 2006; 19(1): 175–182.
35. Yang CS, Chuang LY , Ke CH , Yang CH. Comparative particles swarm optimization (CPSO) for solving optimization problems. IEEE International Conference on Research, Innovation and Vision for the Future, July, 2008.
36. Zhang JF, Hu SS. Chaotic time series prediction based on multi-kernel learning support vector regression. Acta Physica Sinica (Chinese Physics) 2008; 57(5): 2708–2713.
37. Zhang M Zhang DX. Research on text categorization based on M-SVMs. Computer Technology and Development 2008; 28(3): 139–141, 156.

Yang-Ming GUO
Xiang-Tao WANG
Chong LIU
Ya-Fei ZHENG
Xiao-Bin CAI
Reliability and Maintenance Research Laboratory
School of Computer Science and Technology
Northwestern Polytechnical University
Youyi West Road 127, Xi'an Shaanxi, 710072
P. R. China
E-mail: yangming_g@nwpu.edu.cn (Y. M. Guo)

Article citation info:
GLOWACZ A, GLOWACZ A, GLOWACZ Z. Recognition of monochrome thermal images of synchronous motor with the application of quadtree decomposition and backpropagation neural network. Eksploatacja i Niezawodnosc – Maintenance and Reliability 2014; 16 (1): 92–96.

Adam GLOWACZ
Andrzej GLOWACZ
Zygfryd GLOWACZ

RECOGNITION OF MONOCHROME THERMAL IMAGES OF SYNCHRONOUS MOTOR WITH THE APPLICATION OF QUADTREE DECOMPOSITION AND BACKPROPAGATION NEURAL NETWORK

ROZPOZNAWANIE MONOCHROMATYCZNYCH OBRAZÓW CIEPLNYCH SILNIKA SYNCHRONICZNEGO Z ZASTOSOWANIEM KWADRATOWO-DRZEWOWEJ DEKOMPOZYCJI I SIECI NEURONOWEJ*

Technological progress and decreasing prices of thermographic cameras make their application to monitoring and assessing a technical state of machines is profitable. In article is described the recognition method of imminent failure conditions of synchronous motor. The proposed approach is based on a study of thermal images of the rotor. Extraction of relevant diagnostic information coded in thermal images is important for diagnosing of machine. It can be performed with the use of selected methods of analysis and recognition of images. Studies were carried out for two conditions of motor with the application of quadtree decomposition and backpropagation neural network. The experiments show that the method can be useful for protection of synchronous motor. Moreover, this method can be used to diagnose equipments in steelworks and other industrial plants.

***Keywords**: Maintenance, recognition, thermal images, synchronous motor, neural network.*

Postęp techniczny i malejące ceny kamer termowizyjnych sprawiają, że ich zastosowanie do monitorowania i oceny stanu technicznego maszyn jest opłacalne. W artykule opisano metodę rozpoznawania stanów przedawaryjnych silnika synchronicznego. Proponowane podejście jest oparte na badaniu obrazów cieplnych wirnika. Ekstrakcja istotnej informacji diagnostycznej zakodowanej w obrazach cieplnych jest ważna dla diagnozowania maszyny. Zabieg taki może być wykonany z użyciem wybranych metod analizy i rozpoznawania obrazów. Przeprowadzono badania dla dwóch stanów silnika z zastosowaniem kwadratowo-drzewowej dekompozycji i sieci neuronowej z algorytmem wstecznej propagacji błędów. Eksperymenty pokazują, że metoda może być przydatna do zabezpieczania silników synchronicznych. Ponadto metoda może być stosowana do diagnozowania urządzeń w hutach i innych zakładach przemysłowych.

***Słowa kluczowe**: Eksploatacja, rozpoznawanie, obrazy cieplne, silnik synchroniczny, sieć neuronowa.*

1. Introduction

Thermography is a non-invasive, safe and modern technique of thermal visualisation. Every object on the earth generates infrared radiation. The intensity and spectrum distribution of this radiation depends on the temperature of the mass and the radiation properties of its surface layer. Thermographic camera is able to detect this type of radiation, even small changes in temperature can be accurately monitored. Afterwards recorded data are computer-processed and shown in the form of temperature maps that provide for a detailed analysis of the temperature field. Thermographic camera measures the infrared radiation emitted from an object. This camera shows an image of these temperature differences. The darker areas are those that radiate less thermal radiation. Radiation is emitted from the surroundings and is reflected by the object. To measure temperature accurately, it is necessary to compensate for the effects of a number of the different radiation sources. This is done automatically by the thermographic camera. The thermographic techniques have found many applications, for example in industry, building, energetics, veterinary medicine.

In animals or humans, changes in vascular circulation result in an increase or decrease in their tissue temperature. Thermographic process can be used to evaluate the situation in that area of the body. For example, heat generated by inflammation is transmitted to the overlying skin. After that this energy is dissipated as internal energy. Next thermographic camera and special software can measure thermal radiation.

Advantage of this technique is that it does not require physical contact with the object. It enables measuring temperature distribution of surface. There are also some limitations for thermography. Thermal images should be taken for the clear object (free of dirt and moisture). The investigated object should be out of direct sunlight and wind currents [16].

Studies of infrared thermography have been conducted for numerous applications [16]. Infrared thermography is also used in diagnostics of electrical machines. These machines are constructed of steel elements. Thermal and mechanical properties of steel elements were investigated in the literature [12-15, 17, 21, 23, 24, 27, 28, 30-33, 36, 37]. The article describes the method of diagnosis of a synchronous motor. This technique is based on recognition of thermal

(*) Tekst artykułu w polskiej wersji językowej dostępny w elektronicznym wydaniu kwartalnika na stronie ***www.ein.org.pl***

images of the rotor with the application of quadtree decomposition and backpropagation neural network.

2. Process of recognition of thermal images of synchronous motor

The process of recognition of thermal images contains two phases. First of them is patterns creation process (fig. 1).

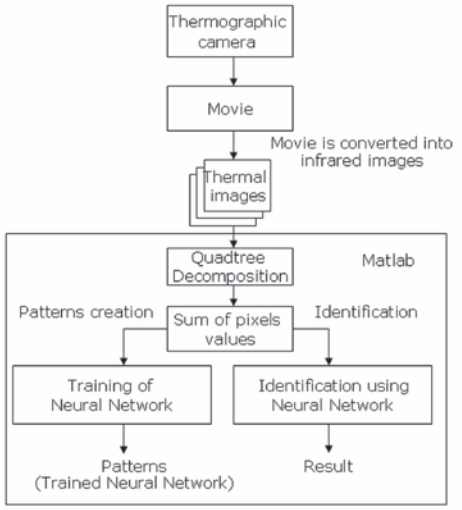

Fig. 1. Process of recognition of thermal image of synchronous motor with the use of quadtree decomposition and neural network

Second phase is identification process. These phases include methods used in image processing. At the beginning of patterns creation process movie is recorded in the computer memory. After that movie is converted into thermal images. These images create training set. Next quadtree decomposition of the image is used. In next step sum of pixels values is calculated. Each sample which is used in patterns creation process gives us one sum of pixels values. This sum of pixels creates feature vector. Next all vectors are used to training of neural network. Steps of identification process are the same as for pattern creation process. Significant change occurs in the classification. In this step neural network is used to identify sample from test set.

2.1. Video recording

All objects emit a certain amount of infrared radiation as a function of their temperatures. Generally the higher an object's temperature is, the more thermal energy this object emits. Thermographic camera can detect this radiation in a way similar to a video camera recording visible light. Thermographic camera can work in darkness because it does not need an external light. Thermographic camera used in experiments was installed 0.25m above rotor of synchronous motor. It recorded images at a resolution of PAL D-1 (640 × 460 pixels) in grayscale with a resolution of 8 bits (values 0–255). Next recorded movie is transferred to a PC. It is stored in permanent memory in AVI format (Audio Video Interleave).

2.2. Acquisition of thermal images

Film with a duration of 1 second has 25 monochrome thermal images. To extract a single thermal image from the movie, a program in a Perl scripting language was implemented. This program uses *mplayer* library. As a result, monochrome thermal images are obtained. Each monochrome image has resolution 256 × 256 pixels.

2.3. Quadtree decomposition of monochrome image

Quadtree decomposition divides a square image into four equal-sized square blocks. Next it analyzes each block to see if it meets criterion of homogeneity [19]. In the event that a square block meets the criterion, it is not divided any further. If it does not meet the criterion, it is subdivided again into four blocks and the criterion is used to those blocks. This process is repeated iteratively until each block meets the criterion. The result can have blocks of several different sizes.

Moreover quadtree decomposition is appropriate primarily for square images whose dimensions are a power of 2, such as 128 × 128, 256 × 256 or 512 × 512. These images can be divided until the blocks are 1 × 1 [19].

Monochrome thermal images of rotor of synchronous motor were presented in figures 2–3.

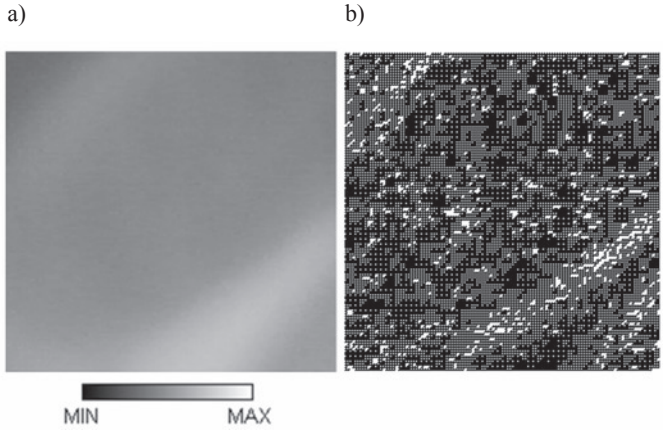

Fig. 2. a) Monochrome thermal image of rotor of faultless synchronous motor, b) Thermal image of rotor of faultless synchronous motor after quadtree decomposition

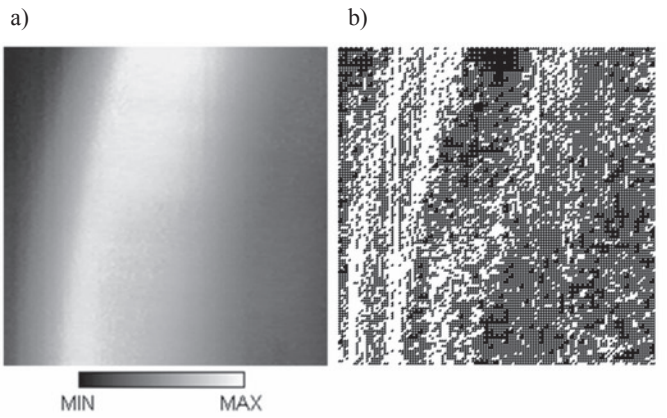

Fig. 3. a) Monochrome thermal image of rotor of synchronous motor with faulty ring of squirrel-cage, b) Thermal image of rotor of synchronous motor with faulty ring of squirrel-cage after quadtree decomposition

2.4. Selection of features

Thermal image contains 256 × 256 pixels. Each pixel has a value from range 1–16 (1 – black pixel, 16 – white pixel). The sum of all pixels values of the image is a feature. This feature creates a feature vector (fig. 4).

Feature vector will be used in classification step.

2.5. Backpropagation neural network

In the literature there are many methods of analysis and recognition [1–11, 18, 20, 22, 25, 26, 29, 35, 38]. The patterns creation process uses feature vectors and backpropagation neural network. Neural

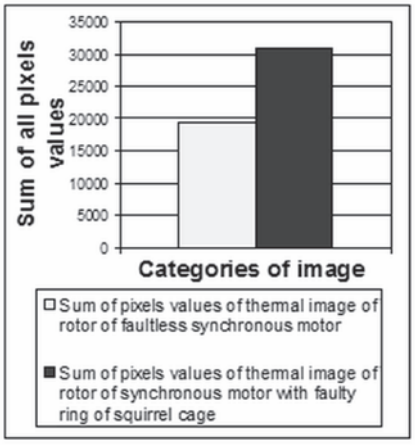

Fig. 4. Sums of pixels values for two categories of thermal images

network consists of many neurons connected by synapses. The learning process of a back-propagation neural network takes place in two phases. In the forward phase, the output of each neuron in each layer and the errors between the actual outputs from the output layer and the target outputs are computed, in the backward phase, weights are modified by the back-propagation errors that occurred in each layer of the network [34]. Structure of backpropagation neural network is shown in figure 5.

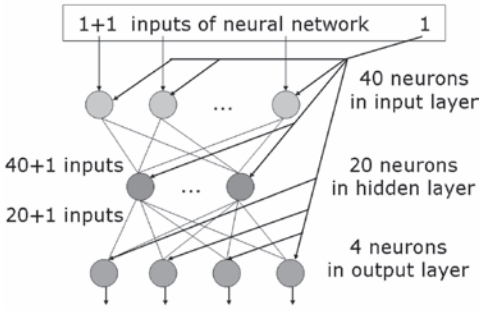

Fig. 5. Structure of backpropagation neural network used in proposed method

During the training of neural network patterns are stored in the form of floating point numbers. System uses character encoding. It converts name of category into the floating-point numbers (ASCII code divided by 128 – vector **a**). Neural network collects the values from all of its input connections (1 feature). After the training of neural network it is necessary to perform the identification process. During identification process floating point values are obtained on the output of neural network (vector **c**).

These four values are converted to ASCII characters. In the identification process the value of the output neuron in the output layer is not equal to the exact value of the character in ASCII code divided by 128. One of the two characters is selected with the help of Manhattan metric (1). This metric calculates the distance defined as:

$$d(\mathbf{c},\mathbf{a}) = \sum_{i=1}^{n} (|\, c_i - a_i \,|) \tag{1}$$

where **c** and **a** are vectors with the same lengths, $\mathbf{c} = [c_1, c_2, \ldots, c_n]$, $\mathbf{a} = [a_1, a_2, \ldots, a_n]$.

For example, for the category of recognition "ring" (image of rotor of synchronous motor with faulty ring of squirrel-cage) the following values should be obtained:

ASCII_CODE (r) / 128 = 114 / 128 = 0.890625,
ASCII_CODE (i) / 128 = 105 / 128 = 0.8203125,
ASCII_CODE (n) / 128 = 110 / 128 = 0.859375,
ASCII_CODE (g) / 128 = 103 / 128 = 0.8046875.

New feature vector **y** is assigned to the class w_j when:

$$d(\mathbf{c},\mathbf{a_j}) = \min_i (d(\mathbf{c},\mathbf{a_i})) \Rightarrow \mathbf{y} \rightarrow w_j \tag{2}$$

where i=1, 2,…, M, j=1, 2,…, M,
$\mathbf{a_i}$, $\mathbf{a_j}$ are vectors containing floating point numbers, **y** is a new feature vector, **c** is a new vector, obtained in the identification process (in output layer), M is the number of classes.

3. Results of thermal image recognition of synchronous motor

Investigations were carried out for two different categories of thermal image of synchronous motor. They are defined as follows: faultless synchronous motor, synchronous motor with faulty ring of squirrel-cage (fig. 6).

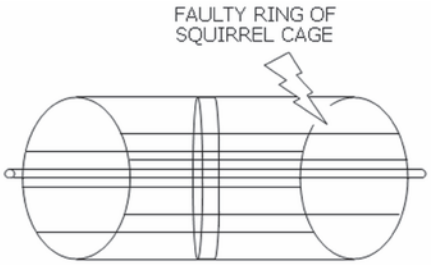

Fig. 6. Faulty ring of squirrel-cage of synchronous motor

Synchronous motor had following operational parameters: faultless synchronous motor, U = 300 V, I = 21.5 A, synchronous motor with faulty ring of squirrel-cage, U = 300 V, I = 77 A,
where: U – supply voltage, I – current of one motor phase.

Thermographic camera recorded two movies. These movies contained thermal images of faultless synchronous motor and synchronous motor with failure.

The process of patterns creation was carried out for 20 monochrome thermal images. Identification process was carried out for 80 monochrome thermal images. Efficiency of recognition of thermal image is defined as:

$$T = \frac{K_1}{K} \tag{3}$$

where: T – efficiency of recognition of thermal image, K_1 – number of correctly identified samples, K – number of all samples.

Efficiency of recognition of thermal image of synchronous motor was presented (tab. 1).

Table 1. Results of recognition of thermal images

Kind of thermal image	Efficiency of recognition of thermal image
Faultless synchronous motor	100%
Synchronous motor with faulty ring of squirrel-cage	100%

4. Conclusion

Thermography can generate important information when the possibilities of conventional diagnostic techniques have been exhausted. In this paper authors proposed a method and a system of recognition of thermal images of synchronous motor. Researches involving the use of image processing methods to thermal diagnostics has been carried out for synchronous motor without faults and motor with faulty ring. Results of recognition of thermal images were good for quadtree decomposition and backpropagation neural network. Efficiency of recognition of thermal images of synchronous motor was 100%. The experiments show that the method can be useful for protection of synchronous motor in steelworks and other industrial plants. A limitation of the method was that the thermographic camera recorded the image of temperature of the surface of the rotor. Further researches should be continued to examine other failures of electrical machines.

***Acknowledgments**: This work has been partly supported by AGH University of Science and Technology, grant nr 11.11.120.612 (Adam Glowacz). This work has been partly financed under AGH researcher grant in 2013 (Andrzej Glowacz). This work has been partly supported by AGH University of Science and Technology, grant nr 11.11.120.354 (Zygfryd Glowacz).*

References

1. Akinci TC, Nogay HS, Yilmaz O. Application of Artificial Neural Networks for Defect Detection in Ceramic Materials. Archives of Acoustics 2012, 37 (3): 279–286.
2. Barbato G, Genta G, Germak A, Levi R, Vicario G. Treatment of Experimental Data with Discordant Observations: Issues in Empirical Identification of Distribution. Measurement Science Review 2012; 12 (4): 133–140.
3. Dudek-Dyduch E, Tadeusiewicz R, Horzyk A. Neural network adaptation process effectiveness dependent of constant training data availability. Neurocomputing 2009; 72 (13–15): 3138–3149.
4. Dudzikowski I, Ciurys M. Analysis of operation of a car starter with BLDC motor. Przeglad Elektrotechniczny 2010; 86 (4): 166–169.
5. Glowacz A, Glowacz Z. Diagnostics of induction motor based on analysis of acoustic signals with application of FFT and classifier based on words, Archives of Metallurgy and Materials 2010; 55 (3): 707–712.
6. Glowacz A, Glowacz Z. Diagnostics of DC machine based on analysis of acoustic signals with application of MFCC and classifier based on words. Archives of Metallurgy and Materials 2012; 57 (1): 179–183.
7. Glowacz A, Glowacz A, Korohoda P. Recognition of Color Thermograms of Synchronous Motor with the Application of Image Cross-Section and Linear Perceptron Classifier. Przeglad Elektrotechniczny 2012; 88 (10a): 87–89.
8. Glowacz A, Glowacz A, Glowacz Z. Diagnostics of Direct Current generator based on analysis of monochrome infrared images with the application of cross-sectional image and nearest neighbor classifier with Euclidean distance. Przeglad Elektrotechniczny 2012; 88 (6): 154–157.
9. Glowacz W. Diagnostics of Induction motor based on Spectral Analysis of Stator Current with Application of Backpropagation Neural Network. Archives of Metallurgy and Materials 2013; 58 (2): 559–562.
10. Glowacz Z, Kozik J. Feature selection of the armature winding broken coils in synchronous motor using genetic algorithm and Mahalanobis distance. Archives of Metallurgy and Materials 2012; 57 (3): 829–835.
11. Glowacz Z, Kozik J. Detection of synchronous motor inter-turn faults based on spectral analysis of park's vector. Archives of Metallurgy and Materials 2013; 58 (1): 19–23.
12. Godlewski S, Szymonski M. Adsorption and Self-Assembly of Large Polycyclic Molecules on the Surfaces of TiO2 Single Crystals. International Journal of Molecular Sciences 2013; 14 (2): 2946–2966.
13. Golanski G, Slania J. Effect of Different Heat Treatments on Microstructure and Mechanical Properties of the Martensitic GX12CrMoVNbN91 Cast Steel. Archives of Metallurgy and Materials 2013; 58 (1): 25–30.
14. Gwozdziewicz M, Zawilak J. Influence of the rotor construction on the single-phase line start permanent magnet synchronous motor performances. Przeglad Elektrotechniczny 2011; 87 (11): 135–138.
15. Kogtenkova O A, Protasova S G, Mazilkin A A, Straumal B B, Zieba P, Czeppe T, Baretzky B. Heat effect of grain boundary wetting in Al-Mg alloys. Journal of Materials Science 2012; 47 (24): 8367–8371.
16. Kunc P, Knizkova I, Prikryl M, Maloun J. Infrared Thermography as a Tool to Study the Milking Process: A Review. Agricultura Tropica et Subtropica 2007; 40 (1): 29–32.
17. Kulesza G, Panek P, Zieba P. Silicon Solar Cells Efficiency Improvement by the Wet Chemical Texturization in the HF/HNO3. Archives of Metallurgy and Materials 2013; 58 (1): 291–295.
18. Markiewicz M, Skomorowski M. Public Transport Information System for Visually Impaired and Blind People. 10th Conference on Transport Systems Telematics 2010; Katowice; Poland: 271–277.
19. MathWorks – MATLAB and SimuLink for Technical Computing 2013; www.mathworks.com.
20. Mazurkiewicz D. Problems of identification of strength properties of rubber materials for purposes of numerical analysis: a review. Archives of Civil and Mechanical Engineering 2010; 10 (1): 69–84.
21. Musial D. Numerical Analysis of the Process of Heating of a Bed of Steel Bars. Archives of Metallurgy and Materials 2013; 58 (1): 63–66.
22. Olszewski R, Trawinski Z, Wojcik J, Nowicki A. Mathematical and Ultrasonographic Model of the Left Ventricle: in Vitro Studies. Archives of Acoustics 2012; 37 (4): 583–595.
23. Orlewski W, Siwek A. Hydroelectric power plant using dump industrial water. Rynek Energii 2010; 6: 87–91.
24. Parzych S, Krawczyk J. The Influence of heat treatment on microstructure and tribological properties of resistance butt welds made of a cast bainitic steel. Archives of Metallurgy and Materials 2012; 57 (1): 261–264.
25. Pinheiro E, Postolache O, Girao P. Contactless Impedance Cardiography Using Embedded Sensors. Measurement Science Review 2013; 13 (3): 157–164.
26. Pribil J, Gogola D, Dermek T, Frollo I. Design, Realization and Experiments with a new RF Head Probe Coil for Human Vocal Tract Imaging in an NMR device. Measurement Science Review 2012; 12 (3): 98–103.

27. Romelczyk B, Kulczyk M, Pakiela Z. Microstructure and mechanical properties of fine-grained iron processed by hydroextrusion. Archives of Metallurgy and Materials 2012; 57 (3): 883–887.
28. Smalcerz A. Aspects of Application of Industrial Robots in Metallurgical Processes. Archives of Metallurgy and Materials 2013; 58 (1): 203–209.
29. Sobieszczyk S. Fuzzy reasoning system design and assessment of load-bearing endoprostheses and their fabrication processes. Archives of Metallurgy and Materials 2012; 57 (3): 759–766.
30. Solek K, Trebacz L. Thermo-Mechanical model of steel continuous casting process. Archives of Metallurgy and Materials 2012; 57 (1): 355–361.
31. Sudhakar K V, Konen K, Floreen K. Beta-Titanium biomedical alloy: Effect of thermal processing on mechanical properties. Archives of Metallurgy and Materials 2012; 57 (3): 753–757.
32. Szymanski Z. Application of the Magnetic Field Distribution in Diagnostic Method of Special Construction Wheel Traction Motors. Studies in Applied Electromagnetics and Mechanics, Advanced Computer Techniques in Applied Electromagnetics 2007; 30: 449–456.
33. Szyszkiewicz K, Dziembaj P, Filipek R. Heat Transfer and Inverse Problems; Selected Cases in 1D and 3D Geometries. Archives of Metallurgy and Materials 2013; 58 (1): 9–18.
34. Tadeusiewicz R. Sieci Neuronowe 1993; Akademicka Oficyna Wydawnicza. Warszawa.
35. Tasinkevych Y, Trots I, Nowicki A, Lewandowski M. Optimization of the Multi-element Synthetic Transmit Aperture Method for Medical Ultrasound Imaging Applications. Archives of Acoustics 2012; 37 (1): 47–55.
36. Tkadleckova M, Machovcak P, Gryc K, Michalek K, Socha L, Klus P. Numerical Modelling of Macrosegregation in Heavy Steel Ingot. Archives of Metallurgy and Materials 2013; 58 (1): 171–177.
37. Wlodarczyk R, Wronska A. Effect of pH on Corrosion of Sintered Stainless Steels Used for Bipolar Plates in Polymer Exchange Membrane Fuel Cells. Archives of Metallurgy and Materials 2013; 58 (1): 89–93.
38. Zawilak T. Investigation of higher harmonics in a Line-Start Permanent Magnet Synchronous Motor. Przeglad Elektrotechniczny 2008; 84 (12): 122–125.

Adam GLOWACZ
AGH University of Science and Technology,
Faculty of Electrical Engineering, Automatics, Computer Science and Biomedical Engineering,
Department of Automatics and Biomedical Engineering
al. A. Mickiewicza 30, 30-059 Krakow, Poland
e-mail: adglow@agh.edu.pl

Andrzej GLOWACZ
AGH University of Science and Technology,
Faculty of Computer Science, Electronics and Telecommunications,
Department of Telecommunications
al. A. Mickiewicza 30, 30-059 Krakow, Poland
e-mail: aglowacz@agh.edu.pl

Zygfryd GLOWACZ
AGH University of Science and Technology,
Faculty of Electrical Engineering, Automatics, Computer Science and Biomedical Engineering,
Department of Power Electronics and Energy Control Systems,
al. A. Mickiewicza 30, 30-059 Krakow, Poland
e-mail: glowacz@agh.edu.pl

Article citation info:
LIU Y, FAN J, LI Y. One system reliability assessment method for cnc grinder. Eksploatacja i Niezawodnosc – Maintenance and Reliability 2014; 16 (1): 97–104.

Yongjun LIU
Jinwei FAN
Yun LI

ONE SYSTEM RELIABILITY ASSESSMENT METHOD FOR CNC GRINDER

METODA OCENY NIEZAWODNOŚCI SYSTEMUSZLIFIERKI CNC

The reliability level of CNC (Computer Numerical Control) grinder is usually assessed by fault data counted in laboratory or in field, which needs the grinder to be assembled and it is one afterwards estimation method. To evaluate the reliability level of CNC grinder in design phrase, one system reliability assessment method and algorithm was put forward by subsystem's reliability in this article, which needs subsystem classification, reliability test, distribution function fitting, parameters estimation and reliability assessment. The calculation result showed that the method was feasible and accurate compared with the traditional way. The method is one contribution to reliability design for CNC grinder and is one reference to other mechatronic products.

***Keywords**: system reliability, assessment method, MTBF, CNC grinder.*

Poziom niezawodności szlifierki CNC (sterowanej numerycznie) zazwyczaj ocenia się na podstawie danych o uszkodzeniach liczonych w laboratorium lub w terenie, co wymaga zmontowania szlifierki i jest metodą oceny post-factum. Aby umożliwić ocenę poziomu niezawodności szlifierki CNC na etapie projektowania, w niniejszym artykule zaproponowano metodę oceny niezawodności systemu oraz odpowiedni algorytm wykorzystujące dane dotyczące niezawodności podsystemów. Model ten wymaga klasyfikacji podsystemów, badań niezawodności, dopasowania funkcji rozkładu, oceny parametrów oraz oceny niezawodności. Wyniki obliczeń wykazały, że omawiana metoda sprawdza się i jest dokładna w porównaniu z metodą tradycyjną. Przedstawiona metoda stanowi wkład do procesu projektowania niezawodności szlifierki CNC i znajduje odniesienie do innych produktów mechatronicznych.

***Słowa kluczowe**: niezawodność systemu, metoda oceny, MTBF, szlifierka CNC.*

1. Introduction

CNC grinder is one machine tool which uses the grinding tools to grind or polish the parts' surface and it is widely applied in the fields of mechanical manufacturing industry, such as aviation and spaceflight, vehicles, ship, etc. Because CNC grinder is the last equipment in manufacturing process usually, its stability and reliability is very important. The critical of reliability enhancement of CNC grinder is design and manufacturing, which needs to evaluate current reliability level and find the weak link to redesign. The reliability assessment, estimation or prediction is the important reference to reliability design and the article aims at the reliability assessment method and algorithm for CNC grinder.

Some approaches for reliability assessment have been proposed and a few achievements have been gained. Young KS proposed one method of reliability prediction of engineering system which the system functionality and system performance are considered [19]. Mohammed TL presented one simple reliability-oriented method to calculate complex distribution system reliability, which is one simplified method [10]. Nathan G developed one method to predict the reliability of electronic packages by expert system [13]. Wei-jenn K proposed one reliability evaluation algorithm countering for imperfect nodes in distributed computing networks [8].

Copal C proposed one system reliability calculation algorithm illustrated through some well-known structures, such as series, parallel, k-out-of-n:G and a fire detector system. The algorithm has been programmed [3]. The difficulty of the algorithm is to solve the structure function. Donald SJ proposed one method to estimate the field-reliability for field-replaceable unit [5]. The estimation model of the method has the merit that the effects of special causes are considered, in addition to the wear of components.

Zunino JL developed the reliability assessment program for MEMS which includes the reliability assessing models and test methodologies [20]. Reliability assessment program is described of aerospace electronic equipment by Condra L [4]. Although the program is standardized, the method is not uniform, instead, it is flexible.

Lu H proposed the reliability sensitivity analysis of mechanical parts with failure modes and Guo J proposed one reliability sensitivity analysis method to identify which variable has the highest contribution to system reliability [11, 7].

The traditional estimation or prediction methods have some shortcomings as follows. 1) The fault distribution function principle of subsystems can not be explored and the distribution function of system is random. 2) Reliability estimation for new product needs to be assembled, which needs high cost and long period. 3) The fact that one product is composed of some universal subsystems whose distributions are known by accumulated reliability data was ignored. For the above, one subsystem distribution function fitting and system MTBF solution method was proposed and the reliability of CNC grinder was assessed by the method.

2. Subsystem distribution function

2.1. Fault data statistic

To find the subsystem's fault time distribution regularity and then evaluate the subsystem's reliability level, the reliability experiments and fault data acquisition are necessary, which are the basis of fault time distribution function fitting of subsystems. Enough fault data must be collected for confidence level and the usual method is time curtailed test. The test time is chosen as the maximal of subsystem's

MTBF (Mean Time Between Failures). Fault data acquisition should meet the conditions as follows [1].

1) Only the relevant fault should be counted and the fault caused by experiment condition or human factor should be ignored.
2) The faults caused by one relevant fault should be combined into one fault with the relevant fault.
3) The fault happened at intermitted period and end of experiment should be counted.

The fault data should be divided into groups by time and the number of groups should be not too big that the probability density will be anamorphic or too small that the calculation load will be heavy and the fitting will be difficult. The number of groups can be calculated by Equation (1) [18].

$$\hat{k} = 1 + 3.3\ln\left(\sum n_i\right) \tag{1}$$

The number of group k can be gained by rounding of $\hat{k}$ and the fault data statistics table should be drawn as table 1. In table 1, Δt_{i-} is the left terminal, Δt_{i+} is the right terminal and $\bar{\Delta} t_i$ is the middle of the time group. n_i is the fault number of the ith group and t_{test} is the test time.

Table 1. Fault data grouping

No.	Δt_{i-}	Δt_{i+}	$\bar{\Delta} t_i$	n_i
1	0	t_{test}/k	$t_{test}/2k$	n_1
2	t_{test}/k	$2t_{test}/k$	$3t_{test}/2k$	n_2
…	…	…	…	…
k	$(k\text{-}1)t_{test}/k$	t_{test}	$(2k\text{-}1)t_{test}/2k$	n_k

2.2. Distribution type identification

After the fault numbers of every interval were counted, the observed value of fault probability density can be calculated by Equation (2). In Equation (2), Δt is the time of each group.

$$\hat{f}(t_i) = \frac{n_i}{\Delta t \sum n_i} \tag{2}$$

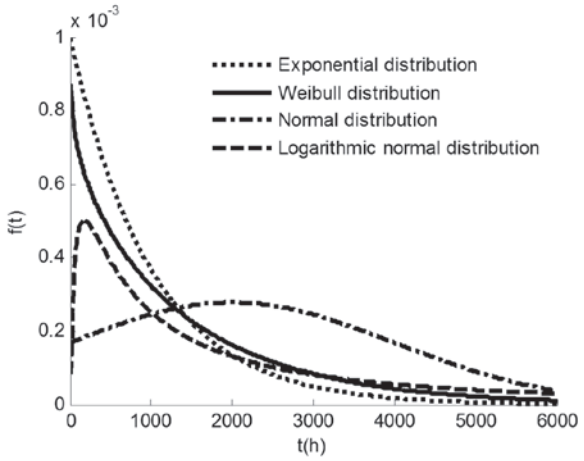

Fig. 1. Common probability distribution

The common probability distributions of mechatronic product are exponential, weibull, normal and logarithmic normal distribution as shown in Fig.1[15]. CNC grinder is one typical mechatronic product and the probability of its subsystem can be confirmed by plotting the scatter points and identifying which distribution curve is the most similar.

2.3. Parameters estimation

2.3.1. Least square method [6, 14]

Least square method is the most common method for parameters estimation as its convenience and practicality. Supposing that there are n values $\{x_i, y_i\}$(i=1, 2, … , n), if the relation of x and y is linear and their relation can be fitted by one equation as shown in Equation (3). The parameters a and b can be estimated by Equation (4) using least square method:

$$\hat{y} = a\hat{x} + b \tag{3}$$

So, when using the least square method for parameters estimation, the linear equation should be created firstly and the parameters in probability density function can be solved by inverse-solving after a and b being calculated by Equation (3). The linear equation creation methods of common distributions are introduced as follows:

$$\begin{cases} a = \dfrac{1}{n}\sum_{i=1}^{n} y_i - \dfrac{b}{n}\sum_{i=1}^{n} x_i \\ b = \dfrac{\sum_{i=1}^{n}\left(x_i - \dfrac{1}{n}\sum_{i=1}^{n} x_i\right)\left(y_i - \dfrac{1}{n}\sum_{i=1}^{n} y_i\right)}{\sum_{i=1}^{n}\left(x_i - \dfrac{1}{n}\sum_{i=1}^{n} x_i\right)^2} \end{cases} \tag{4}$$

2.3.2. Normal distribution

Probability density function of normal distribution is shown in Equation (5) and it has two parameters μ and σ [12]:

$$f(t) = \frac{1}{\sigma\sqrt{2\pi}}\exp\left(-\frac{(t-\mu)^2}{2\sigma^2}\right) \tag{5}$$

The accumulative distribution function meets the relation as shown in Equation (6) if the function is converted to standard normal distribution. The value of $F(t_i)$ can be calculated by Equation (7):

$$F(t_i) = \Phi\left(\frac{t_i - \mu}{\sigma}\right) = \Phi(z_i) \tag{6}$$

$$F(t_i) = \sum_{k=0}^{i} f(t_k) \tag{7}$$

The linear equation can be constructed for normal distribution as shown in Equation (8):

$$t_i = \sigma z_i + \mu \tag{8}$$

In Equation (8), z_i is the lower fractile of standard normal distribution and can be calculated by inverse function of standard normal distribution. If the sample data meet normal distribution, z_i and t_i are linear and the observed value of parameters μ and σ can be calculated by Equation (9).

$$\begin{cases} \hat{\mu} = b \\ \hat{\sigma} = a \end{cases} \tag{9}$$

2.3.3. Logarithmic normal distribution

Probability density function of logarithmic normal distribution is shown in Equation (10) [2] and it has two parameters μ and σ. The accumulative distribution function meets the relation as shown in Equation (11) if the function is converted to standard normal distribution:

$$f(t) = \frac{1}{\sigma t\sqrt{2\pi}} \exp\left(-\frac{(\ln t - \mu)^2}{2\sigma^2}\right) \tag{10}$$

$$F(\ln t_i) = \Phi\left(\frac{\ln t_i - \mu}{\sigma}\right) = \Phi(z_i) \tag{11}$$

The linear equation can be constructed for logarithmic normal distribution as shown in Equation (12):

$$\ln t_i = \sigma z_i + \mu \tag{12}$$

If the sample data meet logarithmic normal distribution, z_i and $\ln t_i$ are linear and the observed value of parameters μ and σ can be calculated by Equation (13):

$$\begin{cases} \hat{\mu} = b \\ \hat{\sigma} = a \end{cases} \tag{13}$$

2.3.4. Exponential distribution

Probability density function of exponential distribution is shown in Equation (14) and it has one parameter λ. The accumulative distribution function of exponential distribution is shown in Equation (15):

$$f(t) = \lambda e^{-\lambda t} \tag{14}$$

$$F(t_i) = 1 - e^{-\lambda t i} \tag{15}$$

Taking the logarithm on both sides of the Equation (15) and Equation (16) can be gained. Supposing $y = \ln[1 - F(t_i)]$ and $x = t_i$, the linear equation can be created as Equation (17):

$$\ln[1 - F(t_i)] = -\lambda t_i \tag{16}$$

$$y = -\lambda x \tag{17}$$

So, if the sample data meet exponential distribution, t_i and $\ln[1 - F(t_i)]$ are linear and the observed value of parameters λ can be calculated by Equation (18).

$$\hat{\lambda} = -a \tag{18}$$

2.3.5. Weibull distribution

Probability density function of weibull distribution is shown in Equation (19) [9] and it has three parameters m, η and γ. Normally, it is considered that the product has the probability of fault when the product starts to run. So, parameter γ equals to zero. The accumulative distribution function of two-parameter weibull distribution is shown in Equation (20):

$$f(t) = \frac{m}{\eta}\left(\frac{t-\gamma}{\eta}\right)^{m-1} \exp\left(-\left(\frac{t-\gamma}{\eta}\right)^{m}\right) \tag{19}$$

$$F(t_i) = 1 - \exp[-(t_i/\eta)^m] \tag{20}$$

Taking the logarithm twice on both sides of the Equation (20) and Equation (21) can be gained. Supposing $y = \ln\ln\frac{1}{1-F(t_i)}$ and $x = \ln t_i$, the linear equation can be created as Equation (22):

$$\ln\left(\ln\frac{1}{1-F(t_i)}\right) = m\ln t_i - m\ln\eta \tag{21}$$

$$y = mx - m\ln\eta \tag{22}$$

If the sample data meet weibull distribution, $\ln\ln\frac{1}{1-F(t_i)}$ and $\ln t_i$ are linear and the observed value of parameters m and η can be calculated by Equation (23):

$$\begin{cases} \hat{\mu} = b \\ \hat{\eta} = \exp\left(-\frac{a}{b}\right) \end{cases} \tag{23}$$

2.4. Goodness of fit test

To find the difference of the fitted values and the real values, the fitting effect should be test after the parameters were estimated, and it is called goodness-of-fit test. The aim of goodness of fit test is to test the quality of fitting and it can be marked by R called goodness of fit coefficient which can be solved by Equation (24) [16]:

$$R^2 = \frac{\sum_{i=1}^{n}(y_i - \overline{y})^2}{\sum_{i=1}^{n}(\hat{y}_i - \overline{y})^2} \tag{24}$$

In Equation (24), y_i is the fitted value, $\hat{y}_i$ is the observed value and $\overline{y}$ is the average of y_i. The bigger R is, the better the goodness of fit is. Goodness of fit not only can evaluate the quality of fitting, but also can find the best distribution type when some distributions are meet one sample at the same time.

3. Algorithms

Reliability grade, failure rate and MTBF are the common index for reliability level and MTBF is the most universal. The system MTBF assessment method of CNC grinder was proposed as follow after the subsystem's distribution functions were fitted.

3.1. Subsystem reliability assessment method

Supposing that the *MTBF* of exponential distribution, weibull distribution, normal distribution, logarithmic normal distribution are $MTBF_{ex}$, $MTBF_{wb}$, $MTBF_{nm}$, $MTBF_{ln}$. *MTBF* of different distribution can be calculated by its definition (Equation (25)) as shown in Equation (26), Equation (27), Equation (28) and Equation (29). So, the subsystem's *MTBF* of CNC grinder can be gained after its probability density function being fitted:

$$MTBF=\int_0^\infty tf(t)dt \tag{25}$$

$$MTBF_{ex}=\frac{1}{\lambda} \tag{26}$$

$$MTBF_{wb}=\gamma+\eta\Gamma(1+\frac{1}{m}) \tag{27}$$

$$MTBF_{nm}=\mu \tag{28}$$

$$MTBF_{ln}=e^{(\mu+\sigma^2)/2} \tag{29}$$

3.2. System MTBF solution algorithm

Supposing that there are n subsystems of the CNC grinder and their reliability are signed as MT_1, MT_2, … , MT_n. The system *MTBF* solution algorithm is proposed as follows.

1) Sort the subsystem's *MTBF*. Vector T is the sorted *MTBF* of subsystem as shown in Equation (30):

$$\mathrm{T}=\mathrm{sort}(MT_1,MT_2,\cdots,MT_n) \tag{30}$$

2) Calculate the fault number during truncated time. The truncated time is the maximum *MTBF* of subsystem and k_i is the rounding value of T_n/T_i as shown in Equation (31):

$$k_i=\left[\frac{T_n}{T_i}\right]\ (1\le i\le n) \tag{31}$$

3) Calculate summary of fault number. θ is the summary of all subsystems' fault number during truncated time as shown in Equation (32):

$$\theta=\sum_{i=1}^{n}k_i \tag{32}$$

4) Calculate the fault time points. $\boldsymbol{tb}$ is the faults time points matrix ($n\times k_1$) and tb_{ij} is the jth fault time point of the ith subsystem as shown in Equation (33).

$$\boldsymbol{tb}=\begin{bmatrix} T_1 & 2T_1 & \cdots & k_1T_1 \\ T_2 & 2T_2 & \cdots & 0 \\ \vdots & \vdots & \ddots & \vdots \\ T_\mathrm{n} & 0 & \cdots & 0 \end{bmatrix}_{n\times k_1} \tag{33}$$

5) Calculate system fault time points. System fault time points are the combination of all subsystems' fault time points. So, if $\boldsymbol{tb}=[\boldsymbol{tb}_1\ \boldsymbol{tb}_2\cdots\boldsymbol{tb}_\mathrm{n}]^T$ (tb_i is one row vector), the system fault time points vector (t_s) can be gained by Equation (34):

$$\boldsymbol{t}_s=[\boldsymbol{tb}_1\ \boldsymbol{tb}_2\cdots\boldsymbol{tb}_n] \tag{34}$$

6) Combine all zeros to one. Many zeros exist in $\boldsymbol{t}_s$. Combine all zeros to one and the pure fault time points vector can be got as shown in Equation (35):

$$\boldsymbol{t}_{sp}=[t_\lambda]\ (0\le\lambda\le\theta) \tag{35}$$

7) Sort $\boldsymbol{t}_{sp}$. Sort the vector $\boldsymbol{t}_{sp}$ and the vector $\boldsymbol{t}$ is got as shown in Equation (36) and some critical point can be gained as shown in Equation (37):

$$\boldsymbol{t}=[t_m]\ (0\le m\le\theta, t_m<t_{m+1}) \tag{36}$$

$$\begin{cases} t_0=0 \\ t_1=T_1 \\ t_\theta=T_n \end{cases} \tag{37}$$

8) Solve system *MTBF*. System *MTBF* signed as *MTBFs* can be solved by Equation (38) based on its definition:

$$MTBF_s=\frac{\sum_{i=0}^{\theta}(t_{i+1}-t_i)}{\theta} \tag{38}$$

The flow chart of system *MTBF* solution is shown in Fig. 2 and the total solution can be programmed easily.

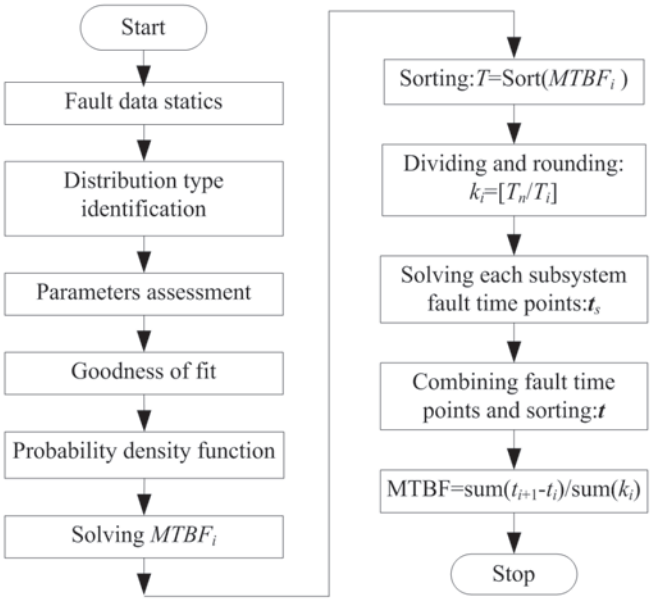

Fig. 2. Flow chart of system MTBF solution

3.3. Considering maintenance time

The maintenance time is ignored of system *MTBF* solution algorithm proposed in section 3.2. If the maintenance time is very small compared to subsystem's *MTBF*, the ignoring is feasible. Otherwise, the maintenance time must be considered [17]. Supposing that the average maintenance time of subsystem i is t_{ri}. Step 1) of section 3.2 should be modified by Equation (39) and the other steps are same:

$$\boldsymbol{T}=\mathrm{sort}(MT_1+t_{r1},MT_2+t_{r2},\cdots,MT_n+t_{rn}) \tag{39}$$

3.4. Considering variety of subsystem's MTBF

The subsystem's *MTBF* variety is not considered in section 3.2. Actually, the subsystem's *MTBF* will be decreased along with the in-

creasing of fault number because of wear, deformation, aging and other factors. If the distribution of subsystem is exponential distribution, its *MTBF* is constant and the subsystem's *MTBF* of other distribution type will be varied after maintenance. In earlier time, the difference of *MTBF* between two maintenances is small and it will become bigger by the increasing of maintenance number. The subsystem's *MTBF* is exponential to the number of maintenance. Supposing that the coefficient is α, the relation between MT_{ij} and MT_{i1} meets Equation (40):

$$MT_{ij} = MT_{i1}(1 - e^{-\alpha(j-1)}) \tag{40}$$

In Equation (40), MT_{ij} is the *MTBF* after j times maintenance of subsystem i. If the subsystem's distribution is exponential, α is zero. The system *MTBF* solution method is as follows.

1) Calculate the fault number. The value of MT_{ij} is one geometric progression when i is one fixed value and the fault number j can be solved by Equation (41). k_i is the rounded of j:

$$MTBF_{i1}(2j - 1 - e^{-\alpha(j-1)}) + jt_{ri} \le T_n \tag{41}$$

2) Calculate the faults time points. Considering the subsystem's *MTBF* variety and maintenance time, the faults time points matrix can be solved as shown in Equation (42).

$$\boldsymbol{tb} = \begin{bmatrix} MT_{11} + t_{r1} & MT_{12} + t_{r1} & \cdots & MT_{1k_1} + t_{r1} \\ MT_{21} + t_{r2} & MT_{22} + t_{r2} & \cdots & 0 \\ \vdots & \vdots & \ddots & \vdots \\ MT_{\mathrm{n}1} & 0 & \cdots & 0 \end{bmatrix}_{n \times k_1} \tag{42}$$

After ***tb*** is solved, other calculation steps are same as the above.

4. Reliability assessment

4.1. Subsystems Partition

The first step of reliability assessment is subsystem partition. The schematic diagram of one type CNC grinder is illustrated in Fig. 3. The part is clamped between headstock and tail bracket. The part can be rotated around axis of headstock and the grinding wheel can be rotated around axis of spindle. The part's surface can be grinded as required by the rectilinear motion and rotatory motion of the headstock and the reciprocating motion of the grinding wheel.

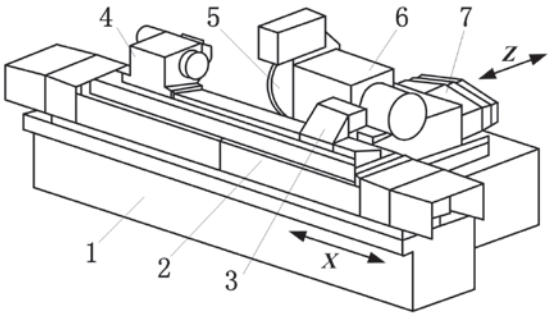

Fig. 3. Schematic diagram of CNC grinder. 1-base, 2- slide carriage of axis Z, 3-tail bracket, 4-headstock, 5-grinding wheel, 6- spindle box, 7-slide carriage of axis X

CNC grinder can be divided into 15 subsystems based its structure feature (in Fig. 3) as shown in table 2.

Table 2. Subsystems partition of CNC grinder

NO.	Subsystem	Abbreviation
1	Base	BS
2	CNC	CNC
3	Spindle	SD
4	Feeder	FD
5	CBN grinding wheel	GW
6	Servo	SV
7	Electrical	EC
8	Hydraulic	HY
9	Cooling	CL
10	Lubrication	LB
11	Safe guard	SG
12	Headstock	HS
13	Measure Instruments	MI
14	Wheel dresser	WD
15	Chip removal	CR

4.2. Subsystem's MTBF solution

The probability density function curves fitted by the fault data are shown in Fig. 4 and there is no fault data of BS in test time and its curve is not illustrated. The subsystems' *MTBF* of CNC grinder are shown in Table 3 solved by the method proposed above.

4.3. MTBF calculation and comparison

System MTBF of CNC grinder can be solved by the algorithm proposed in this paper and the result is 769 h.

If the CNC grinder is seen as one whole and all fault data belong to the whole machine, the probability density function of CNC grinder can be solved as shown in Equation (43) and the fitted curve is shown in Fig. 5, which meets weibull distribution. The system *MTBF* can be calculated by Equation (22) and its value is 785 h.

The design of CNC grinder starts at subsystems and reliability test also starts at subsystems. At this point, the system *MTBF* solution method by subsystems' *MTBF* proposed in this paper has more significance than the traditional method which the product is viewed as one whole:

$$f(t) = \frac{0.915}{753}\left(\frac{t}{753}\right)^{-0.085} \exp\left(\frac{t}{753}\right)^{0.915} \tag{43}$$

4.4. Sensitiveness analysis

Sensitiveness is defined as the increasing ratio of system *MTBF* by one subsystem's *MTBF* being increased a certain extent and other subsystems' *MTBF* maintaining no variety. The aim of sensitiveness analysis is to find that which subsystem has the most contribution to the increasing of system *MTBF*. The analysis result is shown in Fig. 6 by 10% increased of each subsystem.

The system *MTBF* will be enhanced by reliability increasing of SV, EC, HY, LB and CR whose *MTBF* is low relatively. The system *MTBF* will fall conversely when the reliability of BS increases because the fault number will increase during truncated time. Other subsystems' *MTBF* increasing has no influence to system *MTBF*. So, enhancing the *MTBF* of subsystems whose *MTBF* are lower is effective to the increasing of system *MTBF*.

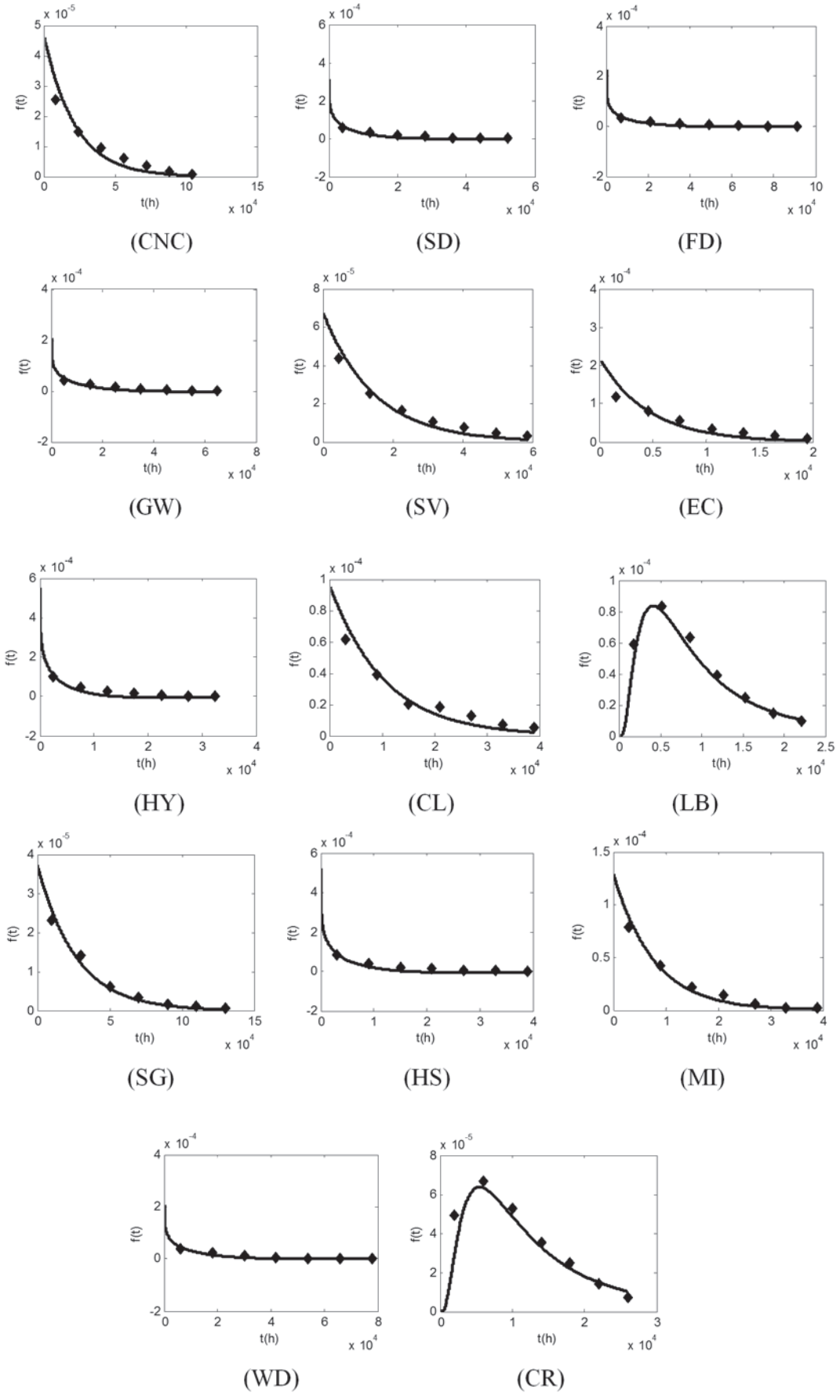

Fig. 4. Probability density function fitting

Table 3. Probability density function and MTBF solution of subsystem

NO.	Subsystem	Probability density function	$MTBF_i$(h)
1	CNC	$f(t)=\lambda e^{-\lambda t}$ ($\lambda=4.5968\times10^{-5}$)	21754
2	SD	$f(t)=\frac{\beta}{\eta}\left(\frac{t}{\eta}\right)^{\beta-1}\exp\left(-\left(\frac{t}{\eta}\right)^{\beta}\right)$ ($\beta=0.8166$, $\eta=7.7875\times10^{3}$)	8698
3	GW	$f(t)=\frac{\beta}{\eta}\left(\frac{t}{\eta}\right)^{\beta-1}\exp\left(-\left(\frac{t}{\eta}\right)^{\beta}\right)$ ($\beta=0.8373$, $\eta=1.1239\times10^{4}$)	12346
4	FD	$f(t)=\frac{\beta}{\eta}\left(\frac{t}{\eta}\right)^{\beta-1}\exp\left(-\left(\frac{t}{\eta}\right)^{\beta}\right)$ ($\beta=0.7938$, $\eta=1.3174\times10^{4}$)	15010
5	SV	$f(t)=\lambda e^{-\lambda t}$ ($\lambda=6.7513\times10^{-5}$)	14812
6	EC	$f(t)=\lambda e^{-\lambda t}$ ($\lambda=2.1604\times10^{-4}$)	4628
7	HD	$f(t)=\frac{\beta}{\eta}\left(\frac{t}{\eta}\right)^{\beta-1}\exp\left(-\left(\frac{t}{\eta}\right)^{\beta}\right)$ ($\beta=0.7849$, $\eta=4.4913\times10^{3}$)	5160
8	CL	$f(t)=\lambda e^{-\lambda t}$ ($\lambda=9.5243\times10^{-4}$)	10499
9	LB	$f(t)=\frac{1}{\sigma t\sqrt{2\pi}}\exp\left(-\frac{(\ln t-\mu)^2}{2\sigma^2}\right)$ ($\mu=9.0009$, $\sigma=0.8282$)	11429
10	SG	$\lambda=3.7371\times1$($\lambda=3.7371\times10^{-5}$)	26759
11	HS	$f(t)=\frac{\beta}{\eta}\left(\frac{t}{\eta}\right)^{\beta-1}\exp\left(-\left(\frac{t}{\eta}\right)^{\beta}\right)$ ($\beta=0.7557$, $\eta=5.6728\times10^{3}$)	6712
12	MI	$f(t)=\lambda e^{-\lambda t}$ ($\lambda=1.2916\times10^{-4}$)	7742
13	WD	$f(t)=\frac{\beta}{\eta}\left(\frac{t}{\eta}\right)^{\beta-1}\exp\left(-\left(\frac{t}{\eta}\right)^{\beta}\right)$ ($\beta=0.8292$, $\eta=1.1830\times10^{4}$)	13077
14	CR	$f(t)=\frac{1}{\sigma t\sqrt{2\pi}}\exp\left(-\frac{(\ln t-\mu)^2}{2\sigma^2}\right)$ ($\mu=9.2772$, $\sigma=0.8165$)	14921

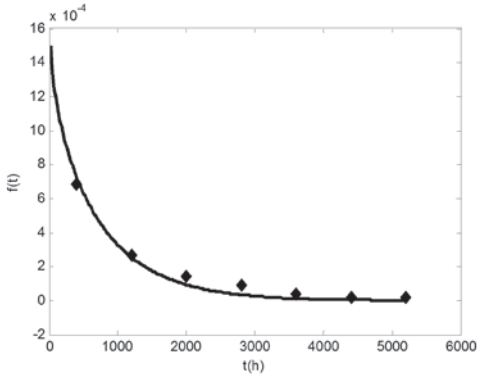

Fig. 5. Curve of probability density function

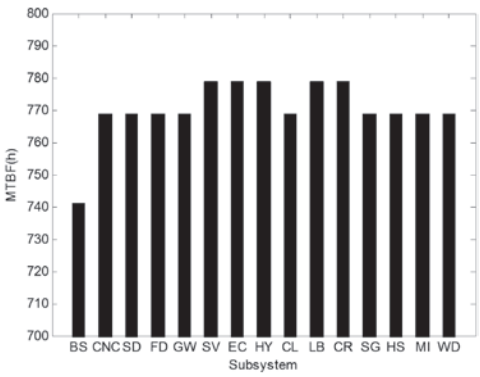

Fig. 6. Reliability sensitiveness analysis

5. Conclusion

Reliability assessment is one important link of product reliability design. The method of fault data processing and distribution type identifying were introduced and the linear equations were constructed for parameters estimation of common distribution. System *MTBF* solving method by subsystems' *MTBF* was proposed for CNC grinder. The reliability sensitiveness analysis method was introduced.

The probability density function of each subsystem was fitted and the *MTBF* of each subsystem was calculated of CNC grinder. The system *MTBF* of CNC grinder was solved by the subsystem's *MTBF*. The reliability sensitivity of subsystem of CNC grinder was analyzed. The result showed that the system *MTBF* calculated by the method proposed in the paper is close to the result calculated by the traditional way. The system *MTBF* solution method is easy and effective and it can be extended for other products.

***Acknowledgement**: The research was sponsored by the National Science and Technology Major Project of China under grant no. 2013ZX04011013 and the National Natural Science Foundation of China under grant no. 51275014.*

References

1. Batson RG, Jeong Y, Fonseca DJ. Control charts for monitoring field failure data. Quality and Reliability Engineering International 2006; 22: 733–755.
2. Bergmann RB, Bill A. On the origin of logarithmic-normal distributions: An analytical derivation, and its application to nucleation and growth processes. Journal of Crystal Growth 2008; 310: 3135–3138.
3. Chaudhuri G, Hu KL, Afshar N. A new approach to system reliability. IEEE Transactions on Reliability 2001; 50: 75–84.
4. Condra L, Bosco C, Deppe R. Reliability assessment of aerospace electronic equipment. Quality and Reliability Engineering International 1999; 15: 253–260.
5. Donald SJ, Himanshu P, Michael T. Improved reliability-prediction and field–reliability–data analysis for field-replaceable units. IEEE Transactions on Reliability 2002; 51: 8–16.
6. Giordano, Arthur A. Least square estimation with applications to digital signal processing, John-wiley, Hoboken, the United States of America, 1985.
7. Guo J, Du XP. Reliability sensitivity analysis with random and interval variables. International Journal for Numerical Methods in Engineering 2009; 78: 1585–1617.
8. Ke WJ, Wang SD. Reliability evaluation for distributed computing networks with imperfect nodes. IEEE Transactions on Reliability 1997; 46: 342–349.
9. Khalili A, Kromp K. Statistical properties of weibull estimators. Journal of Materials Science 1991; 26: 6741–6752.
10. Lazim MT, Zeidan M. Reliability evaluation of ring and triple-bus distribution systems – General solution for n-feeder configurations. International Journal of Electrical Power & Energy Systems 2013; 47: 78–84.
11. Lu H, Zhang YM, Lv H, "Reliability sensitivity analysis of mechanical parts with multiple failure modes," International Conference on Quality, Reliability, Risk, Maintenance and Safety Engineering (QR2MSE) 2012; 1175–1177.
12. Morris HD, Mark JS. Probability and statistics. China Machine Press, Beijing, China, 2012.
13. Nathan G, Anthony P, Srihari K. The reliability prediction of electronic packages – an expert systems approach. International Journal of Advanced Manufacturing Technology 2005; 27: 381–391.
14. Payette GS, Reddy JN. On the roles of minimization and linearization in least-squares finite element models of nonlinear boundary-value problems. Journal of Computational Physics 2011; 230: 3589–3613.
15. Schladitz K, Engelbert HJ. On probability density functions which are their own characteristic functions. Theory of Probability and Its Applications 1996; 40: 577–581.
16. Voinov V, Pya N, Shapakov N. Goodness-of-fit tests for the power-generalized weibull probability distribution. Communications in Statistics-Simulation and Computation 2013; 42: 1003–1012.
17. Wang ZM, Yu X. Log-linear process modeling for repairable systems with time trends and its applications in reliability assessment of numerically controlled machine tools. Proceedings of the Institution of Mechanical Engineers Part O-Journal of Risk and Reliability 2013; 227: 55–65.
18. Yang ZJ, Chen CH, Chen F. Reliability analysis of machining center based on the field data. Eksploatacja i Niezawodnosc – Maintaince and Reliability 2013; 2: 147–155.
19. Young KS. Reliability prediction of engineering systems with competing failure modes due to component degradation. Journal of Mechanical Science and Technology 2011; 25: 1717–1725.
20. Zunino JL, Skelton DR. MEMS reliability assessment program. Conference on Reliability, Packaging, Testing, and Characterization of MEMS/MOEMS VI 2007; D4630–D4630.

Yongjun LIU
Jinwei FAN
Yun LI
College of Mechanical Engineering and Applied Electronics Technology
Beijing University of Technology
Jidian buliding, Room 304, Pingleyuan 100, Chaoyang district, 100124, Beijing, China
E-mails: chengquan33@126.com; jwfan@bjut.edu.cn; handanliyun@126.com

Article citation info:
JAROSIŃSKI W. Periodic technical inspections of vehicles and road traffic safety with the number of road accidents involving fatalities. Eksploatacja i Niezawodnosc – Maintenance and Reliability 2014; 16 (1): 105–111.

Wojciech JAROSIŃSKI

PERIODIC TECHNICAL INSPECTIONS OF VEHICLES AND ROAD TRAFFIC SAFETY WITH THE NUMBER OF ROAD ACCIDENTS INVOLVING FATALITIES

SYSTEM OKRESOWYCH BADAŃ TECHNICZNYCH POJAZDÓW A BEZPIECZEŃSTWO RUCHU DROGOWEGO I LICZBA ZDARZEŃ DROGOWYCH Z UDZIAŁEM OFIAR ŚMIERTELNYCH*

The article is an attempt to find relationship between the implemented system of periodic technical inspections of vehicles and the number of road accidents, reliability of vehicles and road safety. The study utilises results of comparative tests, where the relationships and parameters could be directly observed for the cases with the system implemented and some without periodic technical inspections at all (for example: between the states of the USA, Australia and the research work conducted in Norway in the 90's). The analysis of results leads to unexpected conclusion that system of periodic technical inspections of vehicles does not have statistically significant effect on the number of accidents, including the number of road accidents involving fatalities.

Keywords: *vehicles periodic technical inspections, road traffic safety, road accidents, technical condition of vehicles.*

Artykuł jest próbą znalezienia relacji pomiędzy wdrożonym systemem okresowych badań technicznych pojazdów, a liczbą zdarzeń drogowych i szerzej niezawodnością pojazdów i bezpieczeństwem ruchu drogowego. W pracy między innymi wykorzystano wyniki badań porównawczych, dla których można było wprost obserwować zależność i parametry dla przypadków z wdrożonym systemem okresowych badań technicznych i bez niego (na przykładzie Stanów Zjednoczonych, Australii i Norwegii). Analiza wyników prowadzi do zaskakującego wniosku, że wyżej wymieniony system nie ma statystycznie istotnego wpływu na liczbę wypadków, w tym liczbę zdarzeń drogowych z udziałem ofiar śmiertelnych.

Słowa kluczowe*: okresowe badania techniczne pojazdów, bezpieczeństwo ruchu drogowego, zdarzenia drogowe – wypadki, stan techniczny pojazdów.*

1. Introduction

There is a common, rather obvious opinion that the system of technical inspections of vehicles and the number of defects occurring in the vehicles affect the road safety and the number of road accidents involving fatalities. However, assessment of the magnitude of this effect turns out to be difficult to estimate and the data depending on its source can significantly differ from each other. The problem should be considered in two stages. The first step is a relationship between of the system of periodic roadworthiness inspections and the current technical condition of vehicles on the public roads, while the second is the proportion of the number of road accidents with fatalities, due to technical reasons, to the total number of such road accidents.

Another aspect that has an effect on reducing the number of accidents is a development of automotive technology, the use of ever more sophisticated passive and active safety systems, manufacturing of increasingly sophisticated cars that meet more and more stringent type-approval requirements.

There are two trends that have opposite impact on the road safety: an increasing number of vehicles and ever more perfect vehicles designs. The quality and organization of road infrastructure has also substantial impact .

Both the police as well as scientists involved in road safety issues, as the main causes of road accidents perceive the two factors, which are: man and road infrastructure.

The purpose of this article is to find the answers, to the question, what impact the vehicle's technical defects and the organization of the roadworthiness inspections system have on the road safety.

This article contains an analysis of several studies on this subject. The papers [3] and [7] contain a number of interesting statistics, but are based on unverifiable assumption of proportional impact of periodic technical inspections of vehicles on the reduction of the number of road accidents by limiting the share of vehicles with defects in the road traffic. The papers [2], [5] and [9] attempted to compare the impact of the roadworthiness tests system on the road safety in the United States, where in some states the roadworthiness tests system is in place and functioning properly and in some there is no technical inspection of vehicles at all. The similar situation is in Australia [6], but the paper from Norway [4] made use of the data from before the date of implementation of the vehicles technical inspection and after the implementation, with the turning point date in this case being 1995. Unfortunately, the investigations [2, 4, 5] were carried out in the 70s, up to the beginning of this century, and therefore one can claim that they are not fully up to date nevertheless the empirical character of the data and its direct use, without making a priori assumptions, are worth noting.

(*) Tekst artykułu w polskiej wersji językowej dostępny w elektronicznym wydaniu kwartalnika na stronie ***www.ein.org.pl***

2. Impact of periodic technical inspections of vehicles on the road safety.

"Effect of Vehicles Defects in Road Accidents" by R. W. Cuerden, M. J. Edwards and M. B. Pittman was published in March 2011 and represents relatively new investigation for the UK market [3].

In the UK the roadworthiness inspection system in its current shape was established by the Road Traffic Low in 1988. It is worth noting that according to the regulations, the certificate of roadworthiness test refers to the vehicle's condition during the test and should not be treated as evidence of:

– technical condition of the vehicle at a different time,
– the overall condition of the vehicle
– the vehicle meeting all requirements of construction and use.

These provisions mean that the inspector is responsible for testing vehicle within a scope in which the vehicle is being checked, and that inspection does not guarantee roadworthiness in the period between the tests.

The inspection stations are run either by private entities or the local authorities. These stations are authorized and supervised as far as the personnel and equipment is concerned, by a specialized agency "Vehicle and Operator Services Agency" – VOSA. The authorization specifies which type of vehicle the test centre may examine depending on the equipment and personnel possessed. Test centre sends the findings to a national database, and they include the time, place and the final result of the inspection, data of the vehicle and a separate panel containing information about detected defects with their descriptions. Full computerization of the system took place on the 1st April 2006 and since then it is complete, and contains data from the whole of the country. The study [3] was based on data from 2008-2009. For the purpose of the analysis there was all the data used which allowed to evaluate the share of vehicles defects in the periodic technical inspections.

Accidents are the events that occur seldom, and those for technical reason are even less frequent. Overall, the sensitivity of the databases to the technical factor is limited. While the databases point to a certain contribution of technical factors to the accidents, usually an accident is a conglomerate of a number of factors and circumstances and the exact separation of causes requires to conduct of a thorough investigation. Currently available accident databases are not focused primarily on finding roadworthiness of the vehicle during the accident.

The analysis [3] used four databases. The first is STATS19, which is a national database of reported accidents where at least one person suffered injuries. It should be noted that not all such accidents are reported to the police and, therefore not all are in the database. The database collects about 50 different pieces of information on the time and place of the accident through to the details of the vehicle and the nature and extent of injury. Wounds are classified as slight, not requiring hospitalization, serious requiring hospitalization and fatal, as the result of which the victim dies within 30 days of the event.

The VOSA organization mentioned earlier, being an instrument of the Department of Transport, is responsible for the vehicles roadworthiness system and its supervision. Its competences include also cooperation with the police in the area of analysis of the technical condition of vehicles taking part in accidents. In particular, the VOSA needs to determine if the technical condition of the vehicle was the cause or had an impact on the accident, verify the driver's version of,events, check if the mechanical or structural defects did not occurre prior to the accident and whether there were any penalties for other offences committed by the driver. As part of VOSA's cooperation with the police there is a second database being created.

The third database registers fatalities and is created by TRL (Transport Research Laboratory) based on data delivered by the police.

The fourth and the last database was linked with the research project carried out in 2000–2010 and founded jointly by the Department of Transport and Roads Agency. The project collected information on the causes and consequences of accidents which could provide a basis for the assessment factors: driver, road and vehicle. The data was collected by sending teams of experienced researchers to the accident site and at the same time to the emergency services and the police. Details of the event were the subject of analysis in all cases, however they were limited to the territory of the two regions: Thames Valley and Nottingham and included a total number of 4744 accidents investigations, while the approach to the problem guaranteed recording all accidents reported to the police.

It should be remembered that the researchers did not have such powers as the police and, therefore, their actions were limited and largely confined to observation. Based on the data from 2005 there was a chart created showing the causes of accidents taking into account the most important factors like the man, the road and the vehicle. It should be noted also that that this data is also estimated.

The following distribution of the factors causing accidents was established:

– 96,6% belonged to the human factor (74,4% only human),
– at least one factor associated with the road – environment – 19,9% with for only 1,1% it was the only factor,
– the factor associated with the vehicle – 4,7% where at least one of the factors was connected with the technical defect, but only for 0,6% it was the only the only factor.

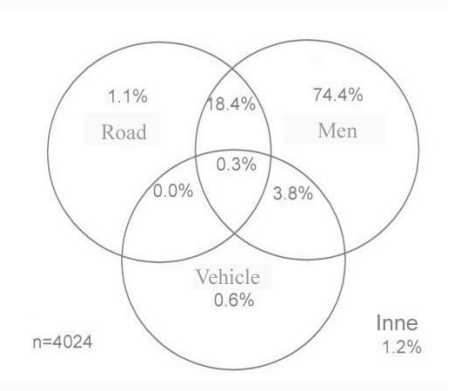

Fig. 1. Distribution of the factors affecting the traffic accident, the data relates to 2005 [3]

In the study [3] Cuerden and Edwards have analyzed the results of technical inspection of vehicles carried out in 2008 when 34 million of periodic technical inspections were done and in 2009 with more than 35 million inspections. Rejection ratio was 29.2% of the population of vehicles in 2008 and 30.3% in 2009 while the minor defects were reported in 9.5% of all vehicles both in 2008 and 2009. Minor defect is one that has no significant effect on the safety and re-examination is not necessarily required, while the car after a quick repair at the inspection station or somewhere else, the same day obtains a positive result of the inspection. Database ignores the fact that some vehicles were tested more than once. The share of positive findings is 60.5% in 2008 and 59.4% in 2009. Statistics also confirmed that newer vehicles have fewer defects than older ones. For the three years old passenger cars (from the date of the first registration in 2006) rejection ratio was 21% while for the thirteen years old (from the date of the first registration in 1996) it increased to 56%. For all negative results the defects were identified and reported. This group of tests was accompanied by an instruction which indicated what should be urgently repaired or serviced.

The distribution of defects reported in 2009 for passenger cars was as follows:

– lighting and signalling equipment 18%
– steering system 3%,
– suspension system 18.9%,

– braking system 25.3,
– tires 14.8%,
– wheels 0.6%,
– safety belts 1.8%,
– body and chassis 1.8%,
– exhaust and fuel system 7.5%,
– field of vision 6.9%.

The data analysis also shows that minor defects concentrated on the braking system, tires and suspension system for all vehicle categories. It has been observed that the number of failures increases for vehicles with their age, but only up to a point, beyond which clearly starts to decrease.

Negative result of the test depending on the defect in decreasing order:
– lighting and signalling equipment 28%,
– braking system 19%,
– suspension system 17%,
– tires and wheels 10%.

Other parts and assemblies constitute a total of less than 10%.

The above data concerns passenger cars, and it differs for other vehicle categories, with every category having own specifics.

Further on the study attempts to predict the likely impact on the road the safety of the changes in the frequency of periodic roadworthiness tests, and to find hypothetical relationship between defects detected in the periodic inspections and accident victims. It is assumed that the number of cases where the technical failure factor had a direct impact on the occurrence of the accident is proportional to the number of vehicles with technical defects in the road traffic. However, due to the uncertainty associated with the quantitative assessment of the share of vehicles with defects in traffic, when the roadworthiness system is in use, the analysis allows only to understand better the mechanism, for the most hazardous defects that can serve as substitute indicators of the vehicle's technical condition. Assuming that 3% of accidents are due to technical reasons about 52 deaths were caused by such accidents in the UK in 2009. For the adopted model it was found that the change of the frequency of the tests from 3-1-1-1 to 4-2-2-2 would cause increase the number of fatal victims by 16-30 and 180-330 of serious injuries.

The model used assumed a hypothetical relationship between the number of defects detected during tests and the number of road accidents victims. However, the authors cautioned that the relationship between the type of defects and their number related to the time when the last periodic technical inspection was carried out is not known. The approach of the driver may also be different in the absence of stress caused by the lack of the periodic technical inspection time approaching.

Conclusions of the study are as follows:
– it is not precisely known how many accidents occurred in Great Britain for technical reasons,
– it was estimated that probably for 3% of the accidents the main reason was the technical defect,
– about 40% of the vehicles failed the test in 2009,
– the age of the vehicle increases the likelihood of a defect occurring (60% of the 13 years old vehicles had a major defect),
– the higher the mileage, the greater probability of a defect occurring (50% of the vehicles with the mileage of more than 90000 miles had major defect),
– there is no direct relation established between the system of periodic technical inspection and the number of accidents due to technical reasons and one can only presume that greater number of technical defects that occur on the road, especially those relevant to road safety, increases the likelihood of an accident involving technical reasons,
– the work involved the analysis of the impact of the frequency of periodic technical inspections on accidents due to technical reasons, and the study used axiomatic assumptions model and found that reducing frequency of testing will increase the number of accidents down to technical reasons,
– the authors believe that factor more susceptible to the probability of failure is the age of the vehicle rather than the mileage, newer vehicles of high mileage are serviced more often and checked and for this reason are less prone to defects,
– the authors stated the need for further research, of an experimental nature aimed at more precisely determining the examined relationships.

The Road Safety Report 2007 by DEKRA [7] has been divided into several parts according to the main factors affecting road safety, one of which being "safe driving in a safe car", which contains a number of interesting statistics and useful analyses. It provides, inter alia, the average age of the vehicles, which for Germany is 8.1 years, 7.9 years for France, 8.4, for Italy and almost 14 years for the Czech Republic. It was also found that in Germany the 12 years old vehicle on average is being removed from use.

In Table 1 presented are statistics that contain the number of victims of road accidents in the current European Union (27 countries), the data is from the years 1991 to 2006.

The study [7] confirmed that technical defects occur more often in older vehicles. The diagram showing the relationship between the number of defects detected, and the age of the vehicle. The report states that with the increase of the vehicles age the probability of the defect occurring, increases while the willingness of some owners to take the vehicle to the garage for repair and maintenance, decreases. This results in a rise of the number of defects and thus creating a potential danger.

Often, in order to reduce expenses, repairs are done by the owners themselves and are of questionable quality.

According to accidents statistics it was discovered that 26.5% of vehicles taking part in accidents had some defect and 6% of them had serious affect on an accident.

Comparative studies from U.S. in the states where the system exists and the states where there is no such system of periodic technical inspection at all, are presented in the paper [2] written by Crain where accidents rates were compared as well.

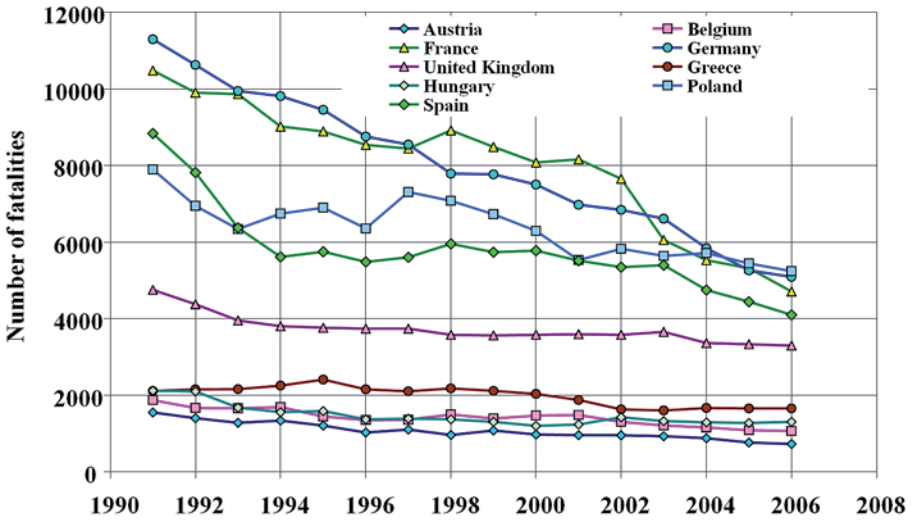

Fig. 1. Number of fatalities in road accidents in selected EU countries for the period 1991 – 2006 [7]

Table 1. The number of fatalities of road accidents in the EU in the years 1991-2006 [7]

	1991	1992	1993	1994	1995	1996	1997	1998	1999	2000	2001	2002	2003	2004	2005	2006
Austria	1551	1403	1283	1338	1210	1027	1105	963	1079	976	958	956	931	878	768	730
Belgium	1873	1671	1660	1692	1449	1356	1364	1500	1397	1470	1486	1306	1214	1162	1089	1069
Bulgaria	1114	1299	1307	1390	1264	1014	915	1003	1047	1012	1011	959	960	943	957	1043
Cyprus	103	132	115	133	118	128	115	111	113	111	98	94	97	117	102	86
Czech R.	1331	1571	1524	1637	1588	1562	1597	1360	1455	1486	1334	1431	1447	1382	1286	1063
Dania	606	577	559	546	582	514	489	499	414	498	431	463	432	369	331	306
Estonia	490	287	321	364	332	213	280	284	232	204	199	223	164	170	169	204
France	10483	9902	9865	9019	8892	8540	8445	8920	8486	8079	8162	7655	6058	5530	5318	4709
Germany	11300	10631	9949	9814	9454	8758	8549	7792	7772	7503	6977	6842	6613	5842	5261	5091
UK	4753	4379	3957	3807	3765	3740	3743	3581	3564	3580	3598	3581	3658	3368	3336	3297
Greece	2112	2158	2160	2253	2412	2157	2105	2182	2116	2037	1880	1634	1605	1670	1658	1657
Hungary	2120	2101	1678	1562	1589	1370	1391	1371	1306	1200	1239	1429	1326	1296	1278	1305
Ireland	445	415	431	404	437	453	473	458	414	418	412	376	337	374	399	368
Italy	8109	8053	7187	7091	7020	6676	6714	6313	6688	6649	6691	6739	6065	5692	5818	5669
Latria	923	729	670	717	611	550	525	627	604	588	558	559	532	516	442	407
Lithuania	1193	779	893	765	672	667	752	829	748	641	706	697	709	752	760	759
Luxem-bourg	83	69	78	65	70	71	60	57	58	76	70	62	53	49	46	36
Malta	16	11	14	6	14	19	18	17	4	15	16	16	16	13	17	10
Poland	7901	6946	6341	6744	6900	6359	7310	7080	6730	6294	5534	5827	5640	5712	5444	5243
Portugal	3217	3086	2701	2505	2711	2730	2521	2126	2028	1877	1670	1655	1542	1294	1247	969
Romania	3782	3304	2826	2877	2845	2845	2863	2778	2505	2499	2461	2398	2235	2418	2641	2478
Slovakia	614	677	584	633	660	616	788	819	647	628	614	610	645	603	560	579
Slovenia	462	493	493	505	415	389	357	309	334	313	278	269	242	274	258	262
Spain	8837	7818	6375	5612	5749	5482	5604	5956	5738	5777	5517	5347	5400	4749	4442	4102
Finland	632	601	484	480	441	404	438	400	431	396	433	415	379	375	379	336
Sweden	745	759	632	589	572	537	541	531	580	591	583	560	529	480	440	445
Nether-lands	1281	1253	1235	1298	1334	1180	1163	1066	1090	1082	993	987	1028	804	750	730
Σ	76076	71104	65322	63846	63106	59357	60225	58932	57680	56000	53909	53090	49857	46832	45296	42953

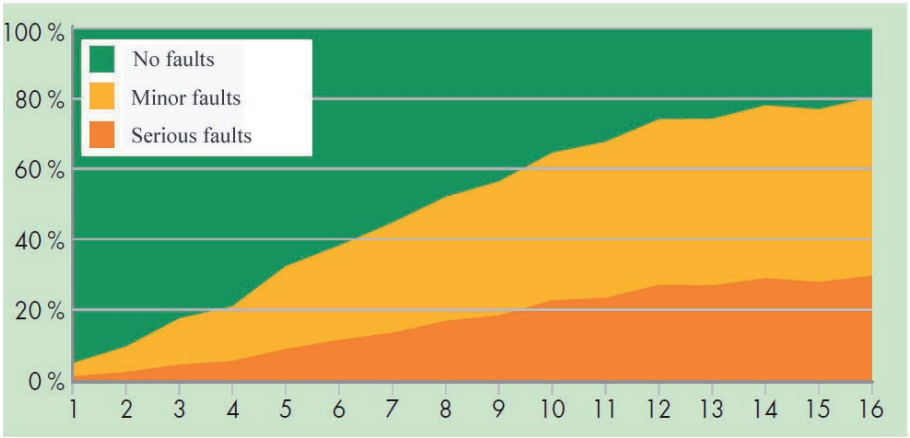

Fig. 2. The share of minor and serious defects depending on the vehicle's age [7]

All data, from 1974, consisted of:
– death rates (number of highway deaths per year per registered vehicle, obtained from the National Safety Council),
– injury rate (number of individuals injured per year per 1,000 vehicle-miles, obtained from the US Federal Highway Administration), and
– accident rate (number of non-fatal accidents per year per 1,000 vehicle-miles, obtained from the US Federal Highway Administration).

The analysis involved the use of statistical model taking into account such basic variables as: the implemented technical inspection program and its scope, procedures for the driving license renewal, and minimum damage required for reporting an accident. In addition, in order to equalize the states on all measures, the following independent variables were incorporated into the statistical equations: population density, median of the family income, fuel consumption, share of federal highways, the percentage of the population between 18 and 24 years of age, and alcohol consumption.

Statistical comparisons were undertaken on data from selected states. The comparisons included:

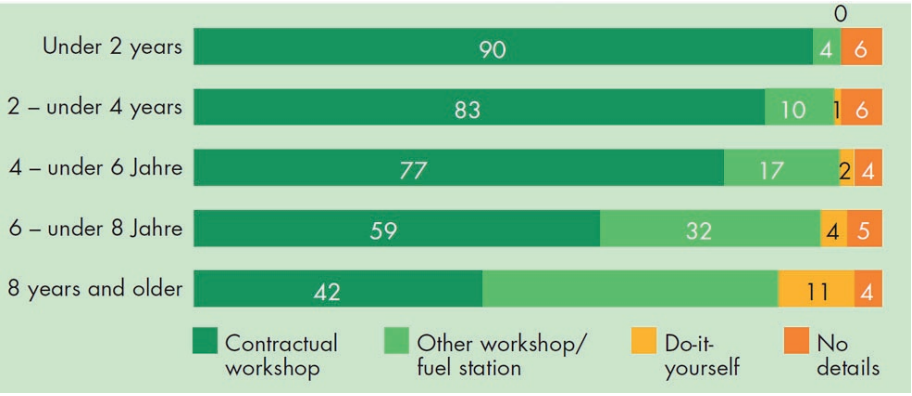

Fig. 3. The type of garage conducting servicing depending on the vehicle's age [7]

– the accident rate of states with *periodic motor vehicle inspection* (PMVI) compared with those states with no PMVI (including those with random inspections),
– states requiring annual inspections compared with the states requiring biannual inspections, and
– states employing random inspection procedures compared with those that employ compulsory periodic inspections and those with no inspection programs.

The results of the analyses showed no statistically significant differences in the accident and injury rates for the states with PMVI compared to the states without PMVI. There was no statistically significant difference in accident rates between the states with biannual PMVI and states with annual PMVI. Crain (1981) has noted that "… vehicle technical inspection programs do not have the expected effect of reducing accident rates" and that "…more frequent inspections do not result in the reduction of the accident rates".

In addition, there were two unexpected findings of this study. The first was that there was a tendency for states with PMVI programs to have higher death rates than those without PMVI, although this was not a statistically significant difference. The second was that states that conduct random vehicle inspections were found to be those with the lowest accident rates.

Crain (1981) suggested two reasons why PMVI programs may have failed to reduce crash rates. Firstly, additional resources devoted to vehicle maintenance as a result of periodic inspection may not affect the vehicle's safety systems, and secondly, even if they do, it is. dissipated by adjustments in drivers behaviour who convinced about their vehicles reliability adopt more risky behaviour.

In the National Highway Traffic Safety Administration (NHTSA) study [5] (1989), data was analyzed to determine whether PMVI system was having an impact on reducing the accident rates of passenger cars.

Three series of analyses were carried out. The method for all three series involved analyzing the crash rate proportion of old to new cars in each state and comparing the results for the states with PMVI system with the results for non-PMVI states. The rationale for this is as follows. As vehicles age, the condition of components critical to safety deteriorates and therefore the likelihood of accident involvement as a result of mechanical failure increases. If PMVI is successful in maintaining the mechanical condition of cars, then there will be less difference in the accident involvement rates of old to new vehicles in PMVI states than in non-PMVI states. Differences just in the accident involvement rate of newer cars in PMVI states as compared to non-PMVI states may discount the effects of PMVI, as new cars would have not been in service long enough for significant wear of mechanical components to occur.

Of all the states in the USA, 22 had PMVI and 29 did not at the time of this study.

Three main data sources were used in the NHTSA analyses:

– Fatal data. This was obtained through the Fatal Accident Research System (FARS). This is a census of all fatal motor vehicle crashes in the US occurring on a public roads in which a death occurs within 30 days of the crash. A limitation of FARS data is that it only contains data for fatal crashes, which make up less than 1% of all crashes. The advantage of this data is that it is available for all states within the US, so valuable comparisons between the states can be made.
– State accident data. State accident file data, obtained from each US state, was also used. Limitations of this data include the fact that only a small number of states were included, and that there may be differences in accident reporting styles between states. The advantage is that this data includes all types of accidents. This data was used for 10 states; four PMVI states and six non-PMVI states.
– Component failure data. CARD file data (Crash Avoidance Research Data) supplied information on component failure. This data identifies vehicles coded by police officers as having a component failure that was suspected of contributing to the crash, as well as coding for all other causes of accidents. Thus, the proportion of vehicles believed to have a component failure contributing to the crash can be identified. Component failures that were identified were categorized into defective brakes, defective steering, defective or improper lights, worn or defective tires and all other defects.

The author has commented on two factors that may be influencing the data. Firstly, 19 out of the 29 non-PMVI states conduct random inspections of passenger vehicles (roadside inspections). Secondly, within the PMVI states there is considerable variation in the equipment items inspected and the procedures, rules and regulations for inspections.

Two comparisons were carried out as part of the first series of analyses. The first comparison was between crash rates of cars ranging from one year to three years old over a single 12 month crash period between July 1 1985 and June 30 1986. FARS and state accident data were used for this comparison. The FARS data showed that fatal crash rates are higher in PMVI states for some model years and lower for others. There is no clear indication that crash involvement rates across vehicle model years are consistently different in non-PMVI, compared to PMVI states. The state accident data showed that the overall accident rate was always higher in states without PMVI, regardless of the age of the vehicle (a 10% difference overall). The fact that this finding was for vehicles of all ages makes the analysis of the effectiveness of PMVI, confusing. If PMVI was having an effect, then there should be no difference in the crash rates of new cars in PMVI states when compared to non-PMVI as they would not yet have had a chance to deteriorate and therefore be able to benefit from inspections. These findings give "…no evidence that PMVI programs affect the crash involvement rates of older vehicles compared to newer vehicles".

The second comparison was for crash rates of 1975 model year cars over the years 1976 to 1986, using the FARS data. It was found that there was a decrease in the relative fatal crash rates as vehicles aged for both PMVI and non-PMVI states. There was no difference between PMVI and non-PMVI states for an older car to have a crash. Thus, there "…is no trend supportive of a PMVI effect".

A second series of analyses used Crash Avoidance Research Data from 1984 to 1986 for four states, Maryland and Washington, which are non-PMVI states, and Pennsylvania and Texas, which are PMVI states. Only passenger cars 10 years or younger were included in the analysis.

The proportion of crashed vehicles with a component failure that was reported to have contributed to the crash was found to be signifi-

cantly greater in the states without PMVI for cars of all ages. This difference ranged from less than 0.25% to a 2.5% difference, depending on the age of the car. Older cars experienced a greater difference.

In a follow up analysis, using FARS data, it was found that the proportion of vehicles involved in a fatal crash with defects reported as having contributed to the crash is consistently higher in non PMVI states than in PMVI states. There was a non statistically significant tendency for this difference to be greater the older the vehicles. The fact that proportion of older crashed vehicles with a component failure reported to have contributed to the crash was found to be greater in the states without PMVI, supports the notion that the difference is due to inspections. However, the author has noted that ".....the differences in defects reported in relatively new vehicles between non-PMVI and PMVI states were most likely due to factors other than the presence or absence of a PMVI program"

Using Crash Avoidance Research Data leads to similar conclusions. Tyre failures were found to be significantly more common (up to 2.5%) in non-PMVI states for almost all vehicle ages, possibly indicating a PMVI effect. However, again, "....the fact that non-PMVI states reported a significantly higher percentage of component failures in relatively new cars suggests that factors other than the presence or absence of PMVI may account for the difference in component failures reported".

An interesting contribution to these considerations makes the study by Christensen and Elvik 2006 "Effects on accidents of periodic motor vehicle inspection in Norway" [1]. System of periodic technical inspection was established in 1995, when Norway signed an agreement with EU in 1994 to ensure access for the Norwegian export to the inner market of the EU. There were negative binomial regression models used in the analysis. Data on the inspections carried out between 1998 to 2002 (5 years) were obtained from the Public Roads Administration. This data contained, for each car, the number of inspections and the outcome (defects coded) of each inspection. Data on the inspections was then forwarded to a major insurance company in Norway and matched with policy holders data (including accidents reported to the insurance company) for cars insured by that company. Data was successfully matched for 253,098 cars. There were the following findings:

1. Technical defects in cars are associated with a small, but statistically significant increase in accident rate.
2. Periodic inspections lead to the repair of technical defects.
3. Following periodic inspections, the accident rate of inspected cars does not decline, but shows a weak tendency to increase.

The third finding was surprising, trying to explain the authors speculated, that after roadworthiness test driver's become convinced that their cars are fully functional and safe, and therefore adopt more risky behaviour.

The next interesting experimental study from Norway [6] was made by Fosser „An experimental evaluation of the effects of periodic motor vehicle inspection on accident rates" several years earlier, when there was no periodic technical inspection. For the purpose of the study there was randomly selected sample of 204000 cars which were divided into three groups. 46000 cars were tested every year, 46000 were tested once every three years and 112000 cars were not tested at all. Accidents involving these vehicles (204000) were recorded in four years. There was no difference in the rate of accidents among groups. The technical condition of tested vehicles was better than those that have not been inspected. The conclusion Fosser reached was: the frequency of periodic technical inspection has no effect on reducing the accident rate, and that periodic technical inspection has no effect on reducing the accident rate if there is roadside inspection system implemented.

3. Conclusions and evaluation of the literature data

Polish statistics are consistent with the results of studies [1, 2, 4, 5]. In Poland there were 3571 fatalities, according to the data of Traffic Department of the Police Headquarters in 2012, out of which six people died due to technical causes, which represents 0.17%. It means that six people died in accidents that occurred for the reasons caused by technical defect, but this number is underestimated, as in other cases, the technical problems causes may also have a significant impact, which, however has not been clearly proven.

It is unquestionable that as a result of periodic roadworthiness tests, the defective cars are repaired and their share in road traffic is decreasing, but on the other hand periodic technical inspection does not guarantee proper technical condition of the vehicle in the period between the tests. During that time the user is responsible for the technical condition of the car. Inspection centre only helps to diagnose defects and forces the user to make a repair. Caring for the condition, attitude, state of mind of the average citizen, as well as his material status is crucial for the proper condition of the vehicle. Test centre disciplines citizens in that matter.

The problem of estimating the exact percentage of the number of road accidents involving fatalities due to technical reasons results from the fact that only the competent authority, which is police, has access to the critical data and cases and the data is only in their discretion and judgment as well as the insurer. Thus the access to this legal sensitive data is difficult for researchers dealing with road traffic safety. The cause of accident is often complex and it may be dependent on the combination of factors and circumstances. It is believed that the number of road accidents that occurred for technical reasons is underestimated relative to the real number of such events [5]. Many publications [3, 6, 7, 9] as an axiom assume that the implemented roadworthiness system reduces the number of road accidents that occurred for technical reasons. In the paper [8], the authors estimate that the implementation of roadworthiness system reduces the number of accidents due to technical reasons by a half. On the other hand comparative studies [1, 2, 4], where the direct comparison was carried out, showed no statistically significant difference between the number of road accidents that occurred for technical reasons for the territories with implemented and not implemented system of periodic technical inspection. There are many publications where the authors take axiomatic assumptions and on its basis build theory of quantifying impact of the roadworthiness system on the number of road accidents due to technical defects. A strong counter-argument to this approach is represented by the results of [1, 2, 4, 5] papers, where they deny correctness of the accepted axioms. It is difficult to solve who is right, because of the difficulties associated with the correct assessment of the methodology adopted, however the author of this paper is inclined to the view that one should not overestimate the impact of the system of periodic technical inspections on the road traffic safety. The system performs the task of reducing the share of vehicles with defects on the road, but it should not be overrated, and its impact on the road safety and the number of accidents due to technical reasons is limited. In the U.S., where there is highly developed automotive industry, in the times of crisis, many states abandoned the system of technical inspection of vehicles [9]. In 2011, only 18 states had the system contrary to the maximum number of 31 states before the crisis. In the states that have moved away from the system of technical inspections there does not seem to be any significant negative impact observed on the indicators related to the road safety. Therefore, when designing new regulation in this area, in the current economic situation, authorities should pay particular attention to the effects of new solutions in conjunction with the burdens for citizens and investments on the side of entities performing technical inspections. Already functioning system should be rationalized so that the changes resulted in the desired high quality of inspections without increasing the burden to the citizens and the

economy. Our Polish solutions should not go beyond the requirements which are set out in the draft Directive on roadworthiness tests for motor traffic, in July 2012.

4. Final conclusions

Review of the literature indicates that the spread of the results of the effects of periodic roadworthiness tests system on the road traffic safety is quite significant. Depending on the methodology adopted it produces result of several percent, but also some empirical studies found no such effect at all, as was the case in the previously cited Fosser's work [4] and Christensen and Elvik [1] who found that the ratio of defects among tested vehicles markedly decreased, but contrary to expectations it had not a significant impact on reducing the number of accidents involving technical causes.

The number of accidents involving also technical causes (failure) is usually estimated at (2–6) %, while for the accidents, where the technical defect was identified as the only cause, the rate is below 1%. All this allows to formulate the thesis that the impact of periodic roadworthiness tests on the road safety should not be seen as a big value, but rather as being too small to be measurable. It is usually estimated at a few tenths of a percent, as for example in the above cited work by Cuerden [3] where for technical reasons there were only 28 cases out of the analyzed sample of 4744 recorded cases, which is equal to about 0.6%.

Above findings lead to a question about the rationality of drastically increasing requirements for roadworthiness inspection system. The European Commission has published a draft "Package on roadworthiness – more stringent checks of vehicles in order to save lives", which began a hot discussion about the need to improve system and inspect the vehicles to a greater extent than before. This discussion was the inspiration for this article. It should also be noted that at the time of work on a draft package a significant number of stringent regulations was dropped and the current version is much less restrictive than the original version.

References

1. Christensen P, Elvik R. Effects on accidents of periodic motor vehicle inspection in Norway. Accident Analysis and Prevention 2007; 39: 47–52.
2. Crain W M. Vehicle Safety Inspection Systems, How Effective? American Enterprise Institute. Washington D.C. 1980.
3. Cuerden R W, Edwards M J, Pittman M B. Effect of Vehicle Defects in The Road Accidents. Transport Research Laboratory Published Project Report (2011).
4. Fosser S. An experimental evaluation of the effects of periodic motor vehicle inspection on accident rates. Accident Analysis and Prevention 1992; 24: 599–612.
5. National Highway Traffic Safety Administration (NHTSA) USA Impact of PMVI on Reducing Crash Rates of Passenger Cars. (1989).
6. Rechnitzer G, Haworth N, Kowadlo N. The effect of vehicle Roadworthiness on crash incidence and severity Report No. 164 Monash University Accident Research Centre.
7. Road Safety Report Dekra. 2007
8. Rompe K, Seul E. Advantages and disadvantages of conducting roadworthiness tests to monitor the mechanical condition for private cars, the impact of such tests on road safety, environmental protection and for the renewal of the vehicle fleet and the scope introducing roadworthiness testing throughout the European community. Final Report commissioned by the Directorate-General for Transport, VII/G-2 of the Commission of the European Communities. Drawn up by the TUV Rheinland (1985).
9. Shuster N. Safety and Emissions Inspections in the U.S. CITA Conference Berlin (May 2011).

Wojciech JAROSIŃSKI
Motor Transport Institute
ul. Jagiellońska 80, 03-301 Warsaw, Poland
E-mail: wojciech.jarosinski@its.waw.pl

Article citation info:
ANTOSZ K, STADNICKA D. The results of the study concerning the identification of the activities realized in the management of the technical infrastructure in large enterprises. Eksploatacja i Niezawodnosc – Maintenance and Reliability 2014; 16 (1): 112–119.

Katarzyna ANTOSZ
Dorota STADNICKA

THE RESULTS OF THE STUDY CONCERNING THE IDENTIFICATION OF THE ACTIVITIES REALIZED IN THE MANAGEMENT OF THE TECHNICAL INFRASTRUCTURE IN LARGE ENTERPRISES

WYNIKI BADAŃ DOTYCZĄCYCH IDENTYFIKACJI DZIAŁAŃ REALIZOWANYCH W ZARZĄDZANIU INFRASTRUKTURĄ TECHNICZNĄ W DUŻYCH PRZEDSIĘBIORSTWACH*

The activities realized within the technical infrastructure supervision are particularly important for large enterprises. It's commonly believed that in large enterprises there is a wide range of tasks realized within the technical infrastructure supervision. The studies done so far indicate only the machine supervision strategies used in enterprises, yet it doesn't indicate what activities are specifically realized. In fact, in spite of the rules adopted for each strategy, they are not used entirely in practice. The aim of the survey, of which the results are presented in this paper, was to identify the real activities conducted in enterprises within the technical infrastructure supervision in large enterprises. The survey concerned production enterprises functioning in different industries on a specified area. The results were drawn up and presented graphically. The results indicate both the activities which are commonly realized and those which are rare in this group of enterprises.

***Keywords**: large enterprises, machines, maintenance, management, survey.*

Działania realizowane w zakresie nadzoru nad infrastrukturą techniczną są szczególnie istotne dla dużych przedsiębiorstw. Powszechnie panuje przekonanie, że w dużych przedsiębiorstwach istnieje duży zakres zadań realizowanych w ramach nadzoru nad infrastrukturą techniczną. Dotychczas przeprowadzone badania wskazują jedynie na stosowane w przedsiębiorstwach strategie nadzoru nad maszynami, jednakże nie wskazuje się, jakie działania są konkretnie realizowane. W rzeczywistości mimo zasad przyjętych dla każdej strategii w praktyce nie są one tak do końca stosowane. Celem badań, których wyniki przedstawiono w niniejszej pracy, było zidentyfikowanie rzeczywistych działań, które są prowadzone w przedsiębiorstwach w zakresie nadzoru nad infrastrukturą techniczną w dużych przedsiębiorstwach. Badania dotyczyły przedsiębiorstw produkcyjnych funkcjonujących w różnych branżach przemysłu na określonym obszarze. Wyniki badań opracowano i przedstawiono w postaci graficznej. Wyniki badań wskazują zarówno na te działania, które są powszechnie realizowane, jak i na te, które rzadko występują w tej grupie przedsiębiorstw.

***Słowa kluczowe**: ankietyzacja, duże przedsiębiorstwa, maszyny, utrzymanie ruchu, zarządzanie.*

1. Introduction

The technical condition of the technical infrastructure owned influences substantially the quality level of the product and the final competitiveness of the enterprise. This issue is particularly important in large enterprises where the sudden production interruptions caused by unexpected failures incur huge financial losses of the enterprises [21, 25]. The failures may cause sudden changes of the processing parameters, and, in consequence, in the production of the parts that don't meet the quality requirements, what increases the production costs. Additionally, it may generate costs connected with the failure to meet the deadlines of the contracts concluded. There are also obviously repair costs. That is why an important task of the managers of these enterprises is forming a proper level of exploitation efficiency of the technical infrastructure owned through the realization of the proper activities.

The research done so far is limited to the identification or indication of the machine supervision strategies [28, 33]. The way of their matching and incorporating into an organization's strategies was analysed [3, 24]. The research related to the identification and assessment of policy used by the enterprises on the technical infrastructure supervision was carried out [31, 34], and in the paper [30] the examples of the development of the strategies used were presented.

Whereas, in the paper [4] the authors point to the necessity of the personnel participation in the maintenance program. In another, paper [22] the framework for using the modern strategy of RBM (risk-based maintenance) is presented. The suggestions of the application of new approaches into the technical infrastructure supervision [5], as well as models of decision processes support in using particular strategies [1, 10] also appear.

Different models of the optimization of activities related to the machine maintenance [23] and also indicators for the machine supervision assessment [16] were demonstrated, or the ones used in practice were identified by means of a questionnaire [18]. In the paper [26] a literature review for the indicators used in the machine efficiency assessment in the industrial sector was presented.

However, it is difficult to find any study indicating what activities are realized by enterprises in reality. E.g. in the paper [12] the results of the study ran in the Czech agro-industrial enterprises were shown, but the emphasis was put on the IT systems used. Likewise, in the

(*) Tekst artykułu w polskiej wersji językowej dostępny w elektronicznym wydaniu kwartalnika na stronie ***www.ein.org.pl***

paper [11] computer systems supporting machine supervision strategies were described.

The authors found the study of which the results were presented in the paper [29]. The authors of this paper analysed five large companies but only for the applied condition-based maintenance strategy. Then, in paper [2] the results of the study ran in the Swedish enterprises were presented. Among others, the most willingly used strategies were indicated.

The results of the research conducted in small and medium enterprises are available. They aimed at identifying the factors which influence taking decisions on the maintenance strategy improvement [7]. And the paper [8] classifies the tools used in the machine supervision with regard to the quantitative and qualitative division.

The known strategies of the technical infrastructure management point to the activities which should be performed, however the reality may differ.

In this article, the typical machine supervision strategies were reviewed and the actions that should be realized within the particular strategies were indicated, and then, it was checked if these actions are actually realized in practice.

Next, the results of the survey conducted in the chosen large enterprises located in the limited geographical area (Poland, podkarpackie province) were presented. The survey concerned the identification of actions realized in the technical infrastructure management, with a particular focus on the organization and realization of the preventive activities of the maintenance services.

2. A review of the machine supervision strategies and the actions performed within them

2.1. Development of the machine supervision strategies

Organizing a production system, particularly a set of machines and appliances, its usage and reorganization or liquidation is connected to a specific exploitation strategy and with the implementation of the appropriate management methods.

The analysis of the approaches to the machine and appliances performance maintenance, done in a period of time, allows distinguishing three periods which evolve into one another [15, 17, 19, 20]:

I The period of reactive maintenance – the repairs are done after the failure appears (Corrective Maintenance), in other words, it is emergency maintenance. It means that the employees wait till the failure appears and then they attempt to remove it.

II The period of preventive maintenance – planned preventive repairs – a strategy according to the exploitation potential (Scheduled Maintenance).

III The period of the predictive (proactive) maintenance – preventive inspections, technical condition monitoring, participation of the machine and appliances operators in the maintenance (a strategy according to the condition - Condition Based Maintenance, according to reliability – Reliability Centered Maintenance and TPM – Total Productive Maintenance).

In an enterprise, several of them are used at the same time; however one dominant can often be distinguished.

2.2. Corrective Maintenance

The approach to failures is a typical example of a reactive approach in the machine maintenance. Running machines till the moment of the increased intensity of the machine or appliance's failures is the characteristic of this strategy. The most often used within this strategy is a method of corrective maintenance which means that maintenance is carried out only after the failure, that causes a loss of operational condition, occurred. The scope of corrective maintenance is determined on the basis of the inspection done after the failure occurred, and it includes the measures and activities which assure the object's restoration to its operational condition. This method is used only for the machines and appliances where the failure aftereffects don't cause risks, don't violate the rules of work safety and don't increase the exploitation costs [9, 13].

2.3. Scheduled Maintenance

This approach, often called a system of preventive and repair works, is one of the most efficient methods of technological machines park management. The main determinant of its use is the exploitation life (a resource set). It is one of the important determinants of the exploitation quality of mechanical objects in exploitation theory and practice. A service life is a measure of the object's ability to perform its distinguished kinds of usage. For every mechanical object such a work life may be determined and expressed by e.g. a number of working hours after which it requires specific technical service (TS1, TS2,…) or replacement. For the proper (optimal) work of the object, it is crucial to determine the values of inter-service life, or periodical service and its extent [6, 9, 13].

2.4. Condition Based Maintenance

The condition based approach involves the control of the machines technical condition as well as formulating diagnostic information on that basis, what enables taking effective decisions in the exploitation system and its environment. We can distinguish two ways of the technical condition assessment: continuous (monitoring the system) or periodic, in the chosen periods of time, with different periods between the subsequent assessments [13, 14]. Due to this approach, it is possible to run a machine almost to the very moment of its failure. This solution is economically beneficial as well [15, 32].

The process of continuous monitoring has a lot of advantages: extended service intervals (increased performance and lower repair costs), real increased elimination of unexpected failures (increased reliability, and, consequently, performance as well), elimination of consequent damages (e.g. a simple bearing damage ends with a transmission gear damage), elimination of component losses (irreparable parts don't have to be replaced), reduction of a spare part warehouse (the method indicates the required spare parts), shortening of the repair time (planning the necessary operations) [6].

2.5. Mixed approach

In practice, it is common to comprise a partially fixed schedule and a continuous or periodic diagnostics [27, 32].

2.6. Actions taken within particular strategies of the machine supervision

Table 1 shows actions imposed by applying a particular strategy of the machine supervision. These actions have been divided into the ones performed by maintenance services, an operator or automatically. Additionally, tools supporting the proper strategy have been determined.

The actions presented should be performed while applying a particular strategy. However, based on the authors' experience, it is not always the case. Therefore, the decision to carry out the survey presented in this paper.

3. Survey subject and methodology

The actions identified and presented in Table 1 were verified by the survey on the technical infrastructure supervision carried out in large enterprises. The survey regarded production enterprises from different industries on a specified area. As a detailed subject of the

Table 1. Actions taken for the particular strategies of technical infrastructure management

Supervision strategy	Actions performed by maintenance services	Actions performed by an operator	Actions performed automatically	Use of additional tools
Exploitation potential based (Scheduled Maintenance, Preventive Maintenance) **PM**	Machine maintenance, inspections and repairs according to the number of the hours worked	Reporting the machine incorrect operation	Recording the machine working time	Machine work schedule
Potential condition based (Condition Based Maintenance) **CBM**	Analysis of the machines technical condition and continuous monitoring of their condition	Regular analysis of the technical condition, reporting the machine incorrect operation	Collection and analysis of the data considering technical parameters of the machine (e.g. vibrations, noise, processing accuracy)	Analysis of vibrations noise, temperature, vibrations, etc.
Efficiency based (Corrective Maintenance) **CM**	Regular failure removal, identification of the failure causes and its maintenance	Reporting the machine incorrect operation	Recording irregularities	-
Mixed Strategy **MS**	Machine maintenance, inspections and repairs according to the number of the hours worked, machines technical condition analysis, continuous monitoring of the machines condition	Regular analysis of the technical condition, reporting the machine incorrect operation	Recording the machine working time, collection and analysis of the data considering technical parameters of the machine (e.g. vibrations, noise, processing accuracy)	Machine work schedule. Analysis of vibrations noise, temperature, vibrations, etc.
Outsourcing **O**	None – performed by external services	Regular analysis of the technical condition	-	-

Table 2. The areas of the infrastructure management covered by the survey

It. No.	Area of infrastructure management	Element of infrastructure management being studied
1.	Ways of technological machines supervision	• The kind and scope of the tasks performed • The responsible for the machine supervision
2.	Kinds of information regarding the machines collected in enterprises	• Kinds of downtime present in a company • Information collected • People responsible for collecting information • The way of recording information
3.	Actions taken in order to minimize unexpected machine downtimes	• The kind of action undertaken

survey, the areas of the enterprise infrastructure management described in the Table 2 were analysed.

In the area surveyed (podkarpackie province), in 2010 when the research started, there were 152 618 enterprises registered, including 202 large ones (data from the Marshal's Office of podkarpackie province, Department of Strategy and Planning). During the survey of the enterprises, the following categories for population identification were adopted: business and production types. 150 enterprises were invited to take part in the survey. Any enterprise, plant or its department that had its own strategy and accounted of its accomplishments could be the object of the survey. 46 questionnaires were obtained as a feedback.

The survey took the form of interviews. The subjects of the survey were the representatives of a medium and top level management as well as the employees directly responsible for the process of technological machines and appliances supervision in a company, and also chosen machine operators. The surveys were conducted in a conjunctive multiple choice format, and included a list of prepared, provided in advance options presented to a respondent with a multiple response item in which more than one answer might be chosen. Additionally, one could give other answers if they were not among the provided options.

4. The structure of the surveyed enterprises

During the survey, the enterprises were classified according to the following criteria: business type, production type, ownership (type of capital) and technical infrastructure organization.

Most companies, as many as 42% (Fig. 1), were aviation companies and 34% were automotive companies. The remaining business types included among others metal processing, chemical, wood and paper, and food industry.

Figure 2 shows the structure of the enterprises surveyed according to the production type. Among the surveyed enterprises most were the organizations with

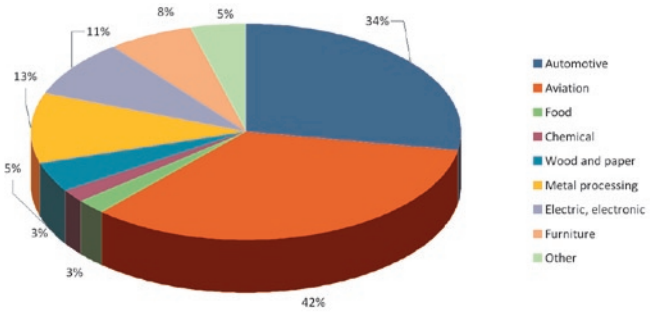

Fig. 1. Enterprises structure based on a business type

big-batch production as a dominant type of production – 27%. In the 6% of the surveyed companies, there are a few types of production combined at the same time.

Most of the surveyed companies (91%) are privately owned, the rest (9%) are state-owned (Fig. 3). 68% of them possess foreign majority capital, 15% domestic majority capital, whereas 17% possess entirely Polish capital (Fig. 4). In most of the companies mainly CNC machines are used.

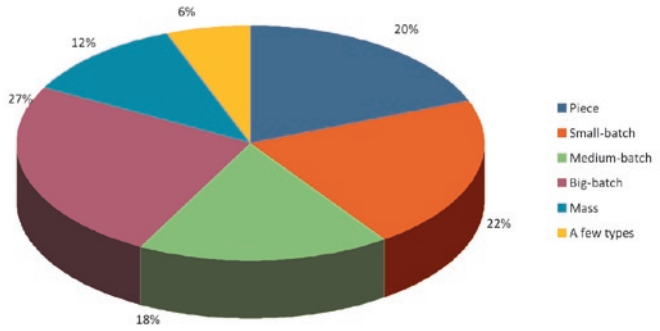

Fig. 2. Enterprises structure based on a production type

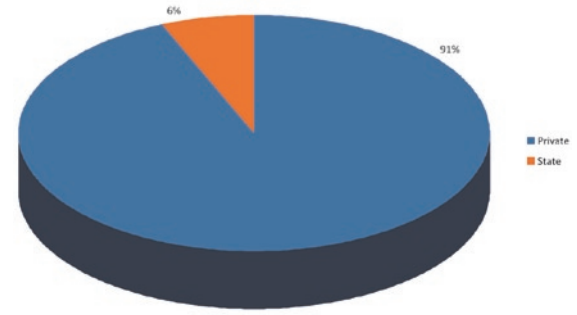

Fig. 3. Ownership type of the surveyed enterprises

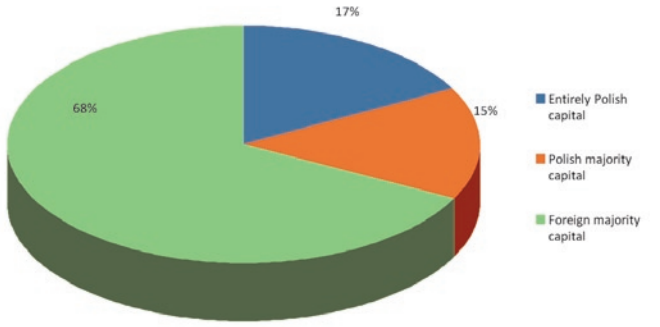

Fig. 4. Type of capital in the surveyed enterprises

In most of the surveyed enterprises, numerically controlled machines prevailed (74%). Among other technical machines, automats were mentioned.

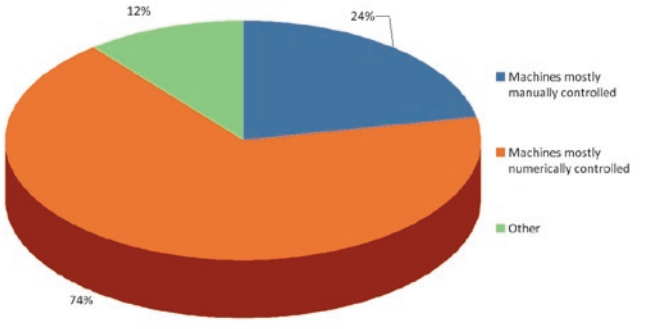

Fig. 5. Kind of machines in the surveyed enterprises

Most of the surveyed enterprises, because 72%, describe their situation as developing, and 28% of the enterprises as stable. None of the companies described their situation as difficult.

5. Survey results

5.1. Ways of technological machines supervision

The survey shows that merely one of the surveyed company uses only the strategy based on a failure removal (Fig. 6). Yet, performing planned inspections by maintenance services is the most commonly used strategy as 65% of the surveyed companies employ it. 63% of the companies implemented a technical condition assessment by an operator before taking up work. Additional data show that e.g. monthly machines cleaning and their general inspections are also performed.

In most of the companies (77%), the actions connected to machines are partly conducted by external companies; however none of the companies commissions all the technological machine park supervision tasks to an external company on the basis of outsourcing (Fig. 7).

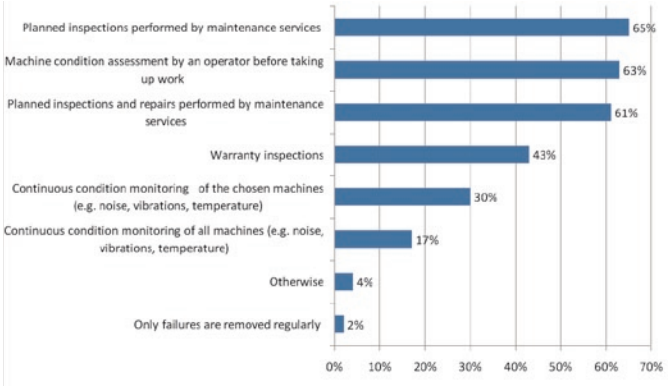

Fig. 6. Ways of the technological machines supervision

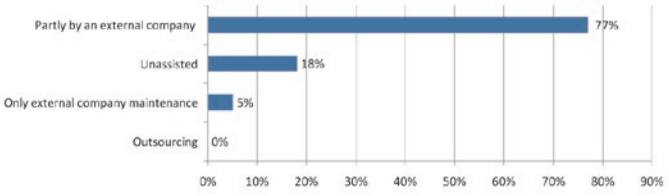

Fig. 7. Realization of the technological infrastructure maintenance tasks

18% of the companies implement the process of the machines supervision independently, and in 5% of the cases machine supervision tasks are performed within external companies maintenance.

5.2. Types of machine-related information recorded in enterprises

The decisions on the actions within the technological machines park supervision should be based on facts. It can be said that efficiency of the technical infrastructure management depends largely on the kind and amount of information on machines that is gathered. Since we don't know if there are any problems and where they are, we are not able to either eliminate or prevent them.

As the author points out in paper [13] collecting the necessary information, taking right decisions at the right time as well as providing intended actions and reactions are an on-going challenge for an organization's information system.

One of the groups of information which should be recorded in companies is the information on downtimes. The surveys show that the most commonly recorded kinds of downtimes are machine failures (Fig.8), what was indicated by 93% of the surveyed enterprises. In 71% of the companies, the recorded downtimes are caused by changeovers.

The kinds of information on machines gathered in companies are diverse. They regard both single workstations and production lines

or production departments. They concern machine uptimes, waiting time for service, machine spare parts, efficiency as well as machines capacity. The studies showed that the information which was most commonly gathered in companies in order to facilitate machine-related actions is the information on a number of failures of individual machines (72%). Picture 9 shows other collected information and the percentage of the enterprises that record this information.

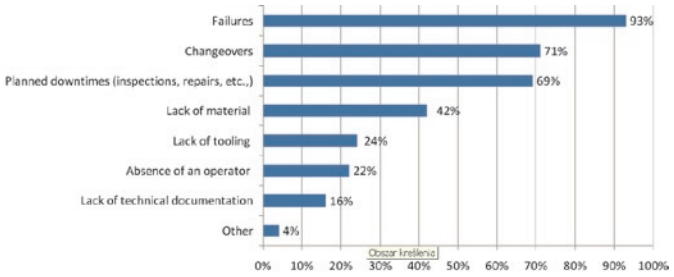

Fig. 8. Types of downtimes recorded in enterprises

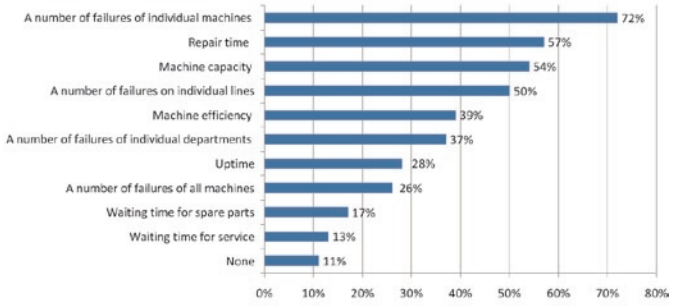

Fig. 9. Kinds of machine-related information gathered in enterprises

An important element of the completeness and credibility of the data obtained is to determine the appropriate and effective way of their collecting and recording. In most of the companies (81%) a maintenance employee is responsible for collecting information on machines (Fig. 10). It is worth pointing out that in 52% of the companies, a number of people collect and record information. A question may arise if the same pieces of information are recorded by different people and if the data overlap. However, it wasn't checked in the survey. Among other people engaged in collecting information, a continuous improvement specialist and a technologist were mentioned.

In 65% of the cases, the place of recording the information regarding machines is the maintenance department (Fig. 11). In 42% of the companies the information is directly entered into IT system e.g. information kiosk located in a production hall.

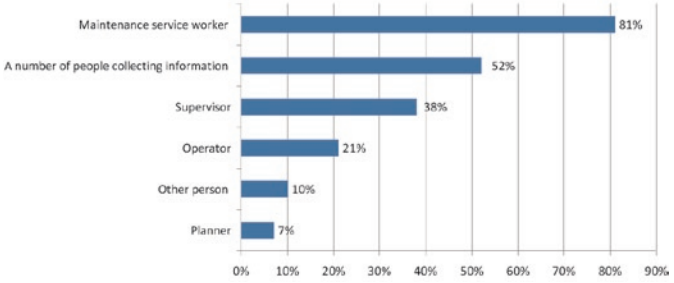

Fig. 10. People responsible for collecting information regarding machines in enterprises

Only in 16% of the companies machine-related information is recorded in the planning department.

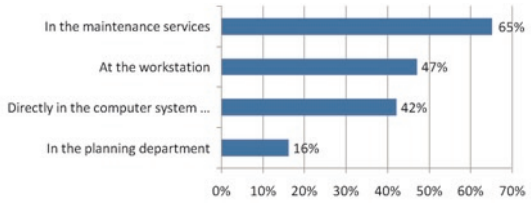

Fig. 11. The place of collecting information regarding machines in enterprises

5.3. Actions taken in order to minimize unplanned downtimes

It is important in minimizing downtimes to perform the appropriate tasks. These actions can be performed both by an operator directly on the machine as well as by the services established in an enterprise for this purpose.

The surveys show that in order to minimize machine unplanned downtimes the most commonly taken actions are (Fig. 12) machine modernization (69%), preventive maintenance (64%) and autonomous maintenance by an operator (64%).

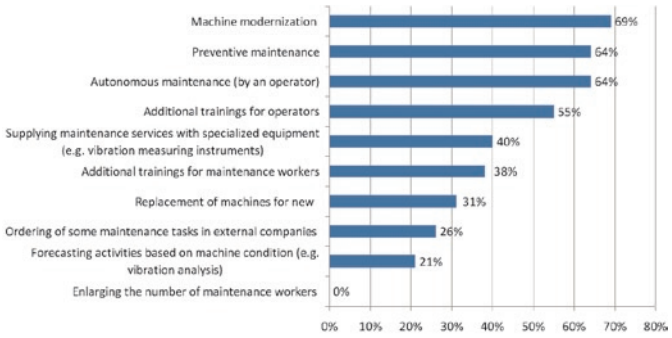

Fig. 12. Actions taken in order to minimize unplanned machine downtimes

Only 31% of the companies showed that they decide to replace machines and none of the surveyed enterprises increase employment of maintenance workers to prevent unplanned downtimes.

5.4. Data analysis

In the further analyses, the authors looked for similarities between:

- the type of capital and the form of actions taken (Fig. 13),
- the business type of a company and the form of actions taken (Fig. 14),
- the production volume and the form of actions taken (Fig. 15),
- the type of capital and the information on infrastructure gathered in an organization (Fig. 16),
- the business type of a company and the information on infrastructure gathered in an organization (Fig. 17),
- the production volume and the information on infrastructure gathered in an organization (Fig. 18).

For the data presented, Chi² analyses were conducted to evaluate if there is a statistically justified influence of a business type, type of the possessed capital, or a production volume on the actions regarding infrastructure supervision or on the information collected. The analyses were conducted using Minitab 16 program, and their results are presented in Table 3.

The analyses conducted show that neither the sort of actions taken within the technological machines park supervision, nor the kind of information collected is conditioned by the type of capital, or business type, or production volume in large enterprises.

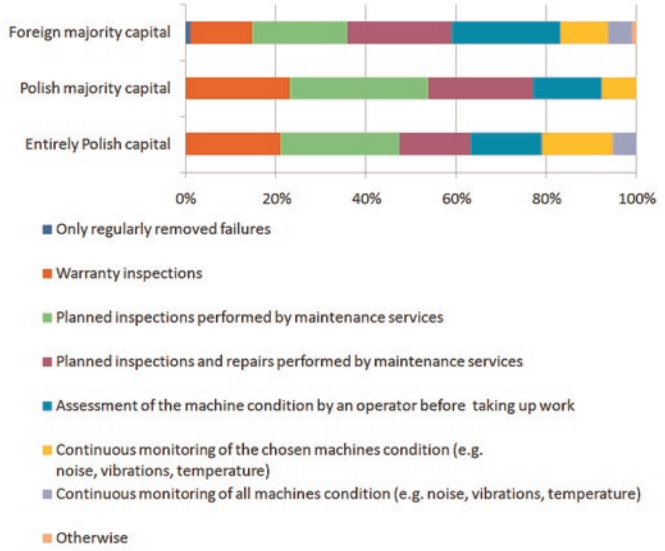

Fig. 13. Actions taken in order to minimize unplanned downtimes dependent on the type of company capital

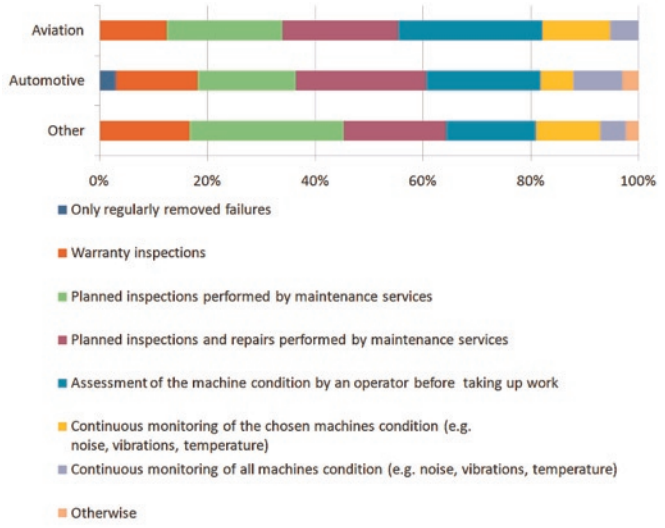

Fig. 14. Actions taken in order to minimize unplanned downtimes dependent on a business type

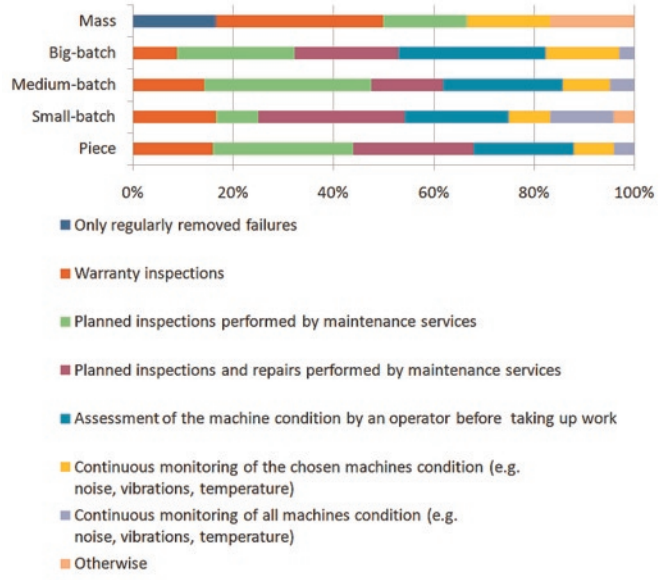

Fig. 15. Actions taken in order to minimize unplanned machine downtimes dependent on the production volume

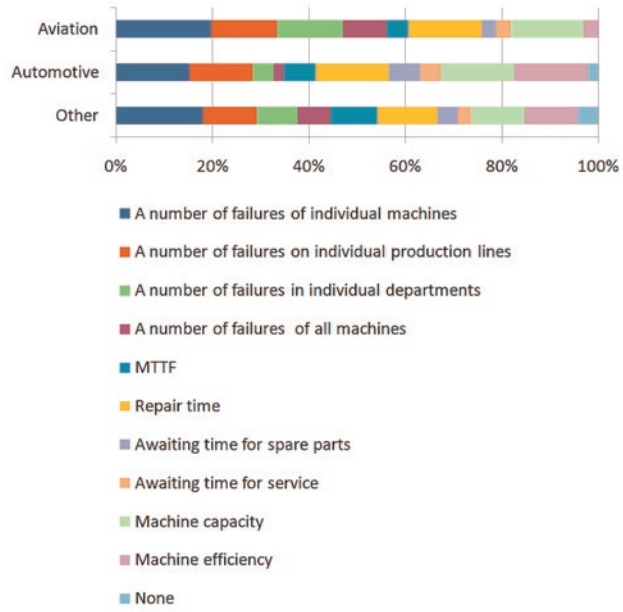

Fig. 16. Information regarding infrastructure recorded in enterprises dependent on the type of the company capital

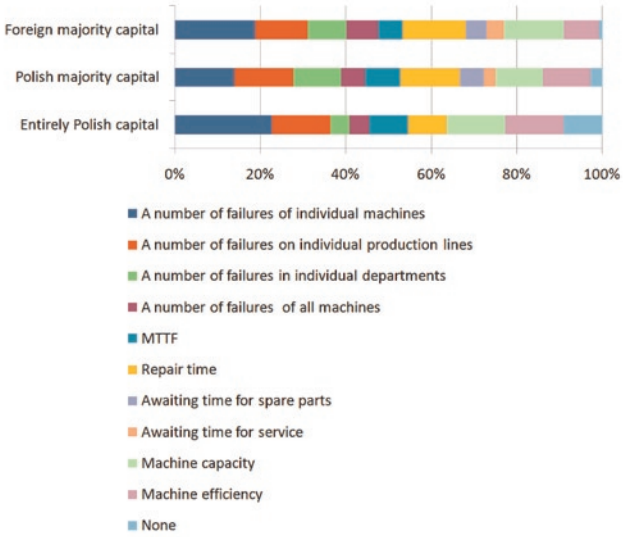

Fig. 17. Information regarding infrastructure recorded in enterprises dependent on a business type

Table 3. Hypotheses made and P-values obtained

It. No.	Hypothesis	*P-value*
1.	There is no difference in actions taken between the enterprises with Polish capital or Polish majority capital and the enterprises with foreign capital	0,726
2.	There is no difference in actions taken among enterprises of different business types	0,941
3.	There is no difference in actions taken among enterprises with different production volume	0,755
4.	There is no difference in the information recorded between the enterprises with Polish capital or Polish majority capital and the enterprises with foreign capital	0,811
5.	There is no difference in the information recorded among enterprises of different business types	0,798
6.	There is no difference in the information recorded among enterprises with different production volume	0,940

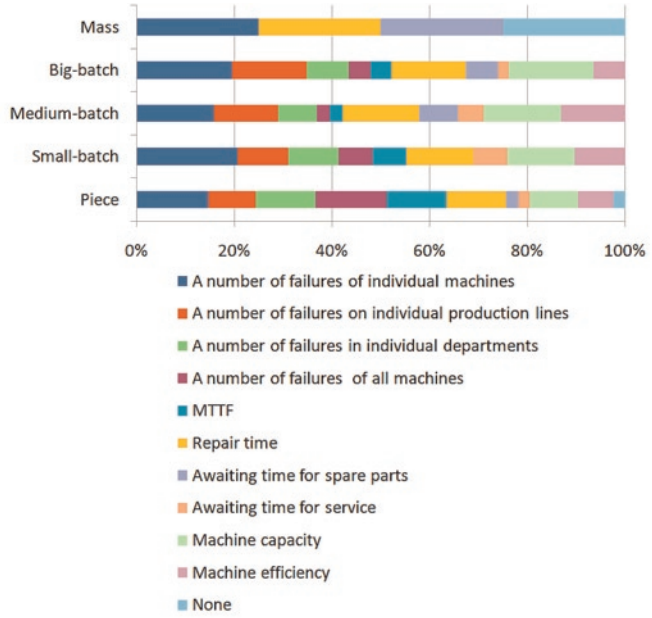

Fig. 18. Information regarding infrastructure recorded in enterprises dependent on a production volume

5.5. Evaluation of the actions performed within technological machines park supervision in comparison to the theoretical assumptions

The main aim of the study was the identification of the real actions that are performed in large enterprises within the technical infrastructure supervision. Table 4 shows the actions related to the machine supervision recommended by the theory within defined strategies and these which were identified as used in practice. It also presents the percentage of the enterprises which perform specified tasks.

Based on the analyses of the data from table 4, it may be concluded that the most commonly used approach in enterprises is preventive maintenance (PM): warranty inspections, planned inspections performed by maintenance services, planned inspections and repairs performed by maintenance services. Occasionally, the activities recommended in condition based maintenance (CBM) are realized. Fortunately, the less frequently used approach is the corrective maintenance approach (CM), which is directed only to the actions related to removing already arisen failures and undertaking inspections required in the warranty period. A mixed approach is also frequently used, and only 26% of the surveyed claimed the use of outsourcing (O).

6. Summary and conclusions

The proper performance of the technical infrastructure management in an enterprise requires regular, planned and economically justified actions. The surveys conducted show that managers of large enterprises, being aware of the technical infrastructure influence on the final quality of products and on the enterprise competitiveness, take up various actions in order to improve the efficiency of machines and appliances operation.

In a number of companies, regular inspections are conducted as well as different actions are undertaken in order to eliminate unplanned downtimes and failures. The survey results show that preventive maintenance (PM) is the most preferably used approach. However, companies are more willing to use the continuous monitoring as well. 30% of the surveyed indicated that they use continuous monitoring in reference to the chosen machines.

However, there is still the need of performing the tasks connected with both the development of the technical infrastructure supervision strategy as well as promoting the knowledge of the current and applied strategies.

Table 4. The actions related to the machine supervision recommended by the theory in realization of the technical infrastructure supervision strategies defined and used in practice together with the assessment of their practical use

Supervision strategy					Actions related to machine supervision recommended by the theory within the defined supervision strategies	Recommended by theory	Used in practice	Percentage of the companies where the actions are applied in practice [%]
PM	CBM	CM	MS	O				
■					Machine modernization	+	+	69
■					Planned inspections by the maintenance services	+	+	65
■	■		■		Technical condition analysis by an operator	+	+	64
■			■		Preventive maintenance	+	+	64
■	■				Assessment of the machine condition by an operator before taking up work	+	+	63
■			■		Planned inspections and repairs realized by maintenance services	+	+	61
			■		Additional trainings for operators	+	+	55
■	■	■	■		Warranty inspections	+	+	43
	■				Supplying maintenance services with specialized equipment (e.g. vibration, noise measuring instruments)	+	+	40
■	■		■		Additional trainings for maintenance services workers	+	+	38
	■				Replacement of machines	+	+	31
	■				Continuous monitoring of the chosen machines condition (e.g. noise, vibrations, temperature)	+	+	30
				■	Ordering some maintenance tasks to external companies	+	+	26
	■				Forecasting activities based on the machine condition (e.g. vibration analysis)	+	+	21
	■				Continuous condition monitoring of all machines (e.g. noise, vibrations, temperature)	+	+	17
		■			Only failure removal	-	+	2

References:

1. Ahmad R, Kamaruddin S, Azid I, Almanar I. Maintenance management decision model for preventive maintenance strategy on production equipment. J. Ind. Eng. Int. 2011; 7(13): 22–34.
2. Alsyouf I. Maintenance practices in Swedish industries: Survey results. International Journal of Production Economics 2009; 121(1): 212–23.
3. Al-Turki U. A framework for strategic planning in maintenance. Journal of Quality in Maintenance Engineering 2011; 17(2): 150–162.
4. Arca JC, Prado JCP. Reflective practice; personnel participation as a factor for success in maintenance program implementation. International Journal of Productivity and Performance Management 2008; 57(3): 247–258.
5. Baglee D, Knowles M. Maintenance strategy development within SMEs: the development of an integrated approach. Control and Cybernetics 2010; 39 (1): 275–303.
6. Będkowski L. Elementy diagnostyki technicznej. Warszawa: WAT, 1992.
7. Burhanuddin M A, Ahmed A R, Desa M I. An application of decision making grid to improve maintenance strategies in small and medium industries. Second IEEE Conference on Industrial Electronics and Applications 2007; 455–460.
8. Crespo Márquez A, Moreu de León P, Gómez Fernández J F, Parra Márquez C, López Campos M. The maintenance management framework: A practical view to maintenance management. Journal of Quality in Maintenance Engineering 2009; 15(2): 167–178.
9. Downarowicz O. Systemy eksploatacji. Zarządzanie zasobami techniki. Radom: ITE, 2000.
10. Fatemeh H, Sha'ri M Y. Continuous improvement through an integrated maintenance model. Contemporary Engineering Sciences 2011; 4(8); 353–362.
11. Hao Q, Xue Y, Shen W, Jones B, Zhu J. A Decision support system for integrating Corrective Maintenance, Preventive Maintenance, and Condition-Based Maintenance. Construction Research Congress 2010: 470–479.
12. Jurca V, Ales Z. Maintenance management systems in agricultural companies in the Czech Republic. Eksploatacja i Niezawodnosc – Maintenance and Reliability 2012; 14(3): 233–238.
13. Kaźmierczak J. Eksploatacja systemów technicznych. Gliwice: Wydawnictwo Politechniki Śląskiej, 2000.
14. Kwiotkowska A. Zagadnienia działalności remontowej w przedsiębiorstwie produkcyjnym w ujęciu logistycznym. Gliwice: Wydawnictwo Politechniki Śląskiej, 2006.
15. Legutko S. Trendy rozwoju utrzymania ruchu urządzeń i maszyn. Eksploatacja i Niezawodnosc – Maintenance and Reliability 2009; 42(2): 8–16.
16. Muchiria P, Pintelona L, Geldersa L, Martinb H. Development of maintenance function performance measurement framework and indicators. International Journal of Production Economics 2011; 131(1): 295–302.
17. Muther R, Wheeler JD. Simplified systematic layout planning. Management and Industrial Research Publications, USA 1994.
18. Muchiria PN, Pintelona L, Martinb H, De Meyerc A. Empirical analysis of maintenance performance measurement in Belgian industries. International Journal of Production Research 2010; 48(20): 5905–5924.
19. Piersiala S, Trzcieliński S. Systemy utrzymania ruchu. Koncepcje zarządzania systemami wytwórczymi. Poznań: Instytut Inżynierii Zarządzania Politechniki Poznańskiej, 2005.
20. Pruszkowski L. Zarządzanie obsługą eksploatacyjną nieruchomości i obiektów technicznych. Płock: K&K, 2010.
21. Salonen A, Deleryd M. Cost of poor maintenance: A concept for maintenance performance improvement. Journal of Quality in Maintenance Engineering 2011; 17(1): 63–73.
22. Selvika JT, Avenb T. A framework for reliability and risk centered maintenance. Reliability Engineering & System Safety 2011; 96(2): 324–331.
23. Sharma A, Yadava GS, Deshmukh SG. A literature review and future perspectives on maintenance optimization. Journal of Quality in Maintenance Engineering 2011; 17(1): 5–25.
24. Sherwin DJ. A review of overall models for maintenance management. Journal of Quality in Maintenance Engineering 2000; 1(1): 15–19.
25. Shingo S. Study of "Toyota" Production system from industrial engineering viewpoint. Tokyo: Japan Management Association, 1981.
26. Simões JM, Gomes CF, Yasin MM. A literature review of maintenance performance measurement: A conceptual framework and directions for future research. Journal of Quality in Maintenance Engineering 2011; 17(2): 116–137.
27. Słowiński B, Podstawy badań i oceny niezawodności obiektów technicznych. Koszalin: WU WSI, 1992.
28. Tan CM, Raghavan N. A framework to practical predictive maintenance modeling for multi-state systems. Reliability Engineering and System Safety 2008; 93(8): 1138–1150.
29. Veldman J, Klingenberg W, Wortmann H. Managing condition-based maintenance technology: A multiple case study in the process industry. Journal of Quality in Maintenance Engineering 2011; 17(1): 40–62.
30. Waeyenberg G, Pintelon L. Maintenance concept development: A case study. International Journal Production Economics 2004; 89: 395–405.
31. Wang H. A survey of maintenance policies of deteriorating systems. European Journal of Operational Research 2002; 139(3): 469–489.
32. Ważyńska-Fiok K, Jaźwiński J. Niezawodność systemów technicznych. Warszawa: PWN, 1990.
33. Zhaoyang T, Jianfeng L, Zongzhi W, Jianhu Z, Weifeng H. An evaluation of maintenance strategy using risk based inspection. Safety Science 2011; 49(6): 852–860.
34. Zhu G, Gelders L, Pintelon L. Object/ Objective oriented maintenance management. Journal of Quality in Maintenance Engineering 2002; 8(4): 306–318.

Katarzyna ANTOSZ
Dorota STADNICKA
The Faculty of Mechanical Engineering and Aeronautics
Rzeszow University of Technology
Al. Powstańców Warszawy 12, 35-959 Rzeszów, Poland
E-mails: katarzyna.antosz@prz.edu.pl , dorota.stadnicka@prz.edu.pl

Article citation info:
GALAR D, BERGES L, SANDBORN P, KUMAR U. The need for aggregated indicators in performance asset management. Eksploatacja i Niezawodnosc – Maintenance and Reliability 2014; 16 (1): 120–127.

Diego GALAR
Luis BERGES
Peter SANDBORN
Uday KUMAR

THE NEED FOR AGGREGATED INDICATORS IN PERFORMANCE ASSET MANAGEMENT

POTRZEBA ZAGREGOWANYCH WSKAŹNIKÓWWYDAJNOŚCI W ZARZĄDZANIUAKTYWAMI

Composite indicators formed when individual Indicators are compiled into a single index. A composite indicator should ideally measure multidimensional concepts that cannot be captured by a single index. Since asset management is multidisciplinary, composite indicators would be helpful. This paper describes a method of monitoring a complex entity in a processing plant. In this scenario, a composite use index from a combination of lower level use indices and weighting values. Each use index contains status information on one aspect of the lower level entities, and each weighting value corresponds to one lower level entity. The resulting composite indicator can be a decision-making tool for asset managers.

Keywords: *Indicator, aggregation, KPI (key performance indicator), performance, hierarchy, DSS (Decision Support Systems).*

Wskaźniki złożone tworzy się poprzez zebranie pojedynczych wskaźników w jeden indeks. Idealnie, wskaźnik złożony powinien mierzyć pojęcia wielowymiarowe, których nie da się uchwycić przy pomocy pojedynczego indeksu. Ponieważzarządzanie aktywami jest dziedziną wielodyscyplinarną, przydatne byłoby wykorzystanie w niejwskaźników złożonych. W przedstawionej pracyopisano metodęmonitorowania złożonej jednostki w zakładzie przetwórczym. W podanym scenariuszu, złożony wskaźnik wykorzystania powstał z połączenia wskaźników wykorzystania niższego rzędu z wartościami ważonymi. Każdy wskaźnik wykorzystania zawiera informacje na temat statusu jednego aspektu jednostek niższego rzędu, a każda wartość ważona odpowiada jednej jednostce niższego rzędu.

Słowa kluczowe*:Wskaźnik, agregacja, KPI(kluczowy wskaźnik wydajności), wydajność, hierarchia, DSS (systemy wspomagania decyzji).*

1. Introduction

Companies aim to get maximum return on their investments, i.e. assets. Therefore, a proper asset management policy is essential. A good asset management policy requires that asset managers receive accurate information. Indicators have become a popular decision-making support tool for engineering asset management, especially in the maintenance field [13].

However, the recent flurry of indicator related activity has led some to argue that there is a danger of information overload. In this case, one way to assist asset managers is to develop composite indices that summarise the information contained in the many maintenance indicators. To date, little work has been done on developing composite maintenance indicators that take into consideration more than two information sources. Only the OEE (overall equipment effectiveness) uses maintenance indicators. Many authors suggest further research into indicators focusing on the development of highly aggregated indicators is required.

Others are not so sanguine about the appropriateness of composite indicators [3]. The purpose of this paper is to address the debate surrounding composite maintenance indices. The paper first highlights the strengths and weaknesses of composite indices. It then presents a framework to guide the development of composite asset indices. This framework provides insight into several methodological issues that must be addressed when calculating composite indices for a complex function like maintenance.

2. Why Composite indices?

It is often argued that those making decisions about maintenance have specific requirements of indicators. References [13] and [2] summarise the decision-makers' demands as follows:

- Only a limited number of indicators should be used to convey the performance of assets. Too many indicators can compromise the legibility of the information.
- Information should be presented in a format tailored to decision-making. This requires the construction of indicators that reduce the number of parameters needed to only those necessary to give a precise account of a situation.
- In the context of global business competition, decision-makers are interested in the relationship between asset management and company profitability. Indicators should, therefore, concentrate on the interaction, rather than on just the asset management itself.

In the production of accurate performance indicators, maintenance managers face a problem of data quality. Information is not easily accessible and sometimes even not collected, so decision-makers cannot rely on scientific data as it stands. The challenge is to transform existing data into condensed, or aggregate, information for decision-makers [9]. An alternative to a matrix of indicators is a aggregate index or indices. A single index may be easier for decision-makers to use because it summarises important information in one or a few numbers.

Preferences for scalars (composite indices like OEE) or matrices (indicator 'profiles' configured as scorecards, for instance) triggers a controversial and long-standing methodological debate. Essentially the debate centres on the amount of information that is lost in the simplification made possible by the index proposed by defenders of balance Scorecard and other groupings of indicators.

In an indicators' matrix, the observer's eye scans the individual indicators; he/she is implicitly asked to aggregate the indicators to form an overall impression of the issue of interest. Because the mathematical aggregation of different variables to form a single number does not occur, proponents of profiles argue that they have 'less chance for misinterpretation or misunderstanding than composite indices' [15].

On the one hand, people who are familiar with the complexities of monitoring interactions generally prefer profiles and view the potential distortion occurring in an index as unacceptable.

Also, people who are removed from the measurement process have a greater willingness to accept the simplification, and potential distortion of information for the sake of obtaining an easy-to-understand, albeit crude, picture of the environment.

This paper uses the terms 'composite/grand index' and 'composite/grand indices' to refer to composite indicators. When calculating an index, the aggregation process is carried out using a mathematical equation; it is not necessarily done by the observer. This method necessarily simplifies the information in the matrix of indicators.

Asset managers have shown considerable interest in developing composite indices, including financial ones. The quantity of data describing maintenance that has to be handled by the top management must be reduced, i.e., no large sets, but the data should contribute excellent information to facilitate good decision-making. The maintenance budget that concerns the replacement value of the assets is an indispensable element in decisions associated with renovation of equipment and plant delocalisation. Equally, the relationship of maintenance to the manufactured product(s) or to the cost of that manufacture, they will present/display all the scenarios in which present maintenance occurs.

The following indicators measure the costs of maintenance incurred in the process of manufacturing the end item, relative to the secured availability or the value of the machinery. These corporate numbers are used at the highest levels of management to guide overall changes in manufacturing policies and, by extension, in maintenance policies. These figures are the most rudimentary composite indicators widely used in asset management:

$$E1 = \frac{\text{Total Maintenance Cost}}{\text{Assets Replacement Value}} \tag{1}$$

$$E4 = \frac{\text{Total Maintenance Cost}}{\text{Production transformation Cost}} \tag{2}$$

$$E3 = \frac{\text{Total Maintenance Cost}}{\text{Quantity of Output}} \tag{3}$$

For the directors of factories or operations departments, excellent composite indices refer to availability with respect to production.

$$E5 = \frac{\text{Total Maintenance Cost} \ + \ \text{unavailability costs related to maintenance}}{\text{Quantify of output}} \tag{4}$$

$$E6 = \frac{\text{Availability related to maintenance}}{\text{Total Maintenance Cost}} \tag{5}$$

The indicators mentioned above and proposed by UNITE 15341 [8], are examples of costs aggregated with other parameters. This aggregation is produced by forming a ratio of two magnitudes. Three or more maintenance indicators are seldom involved in the production of composites. In maintenance, and beyond, there is an ongoing debate on the appropriateness of aggregating indicators.

3. Issues and challenges of aggregation.

A. Strengths of composite indices

Proponents of indices argue that there are several reasons for aggregation. One obvious benefit of a composite index is its production of a single or a few numbers, making the use of indices for decision-making relatively straightforward. Composite indices assist decision-makers by reducing the clutter of too much information, thereby helping to communicate information succinctly and efficiently [1, 4, 17].

As [14] states, 'aggregation is necessary to keep from overwhelming the system at the higher levels of the hierarchy.' Heycox [12] adds that 'a complex, information-rich world requires frameworks that organise data to reveal succinct views and interrelationships.'

An aggregation function formalises what is often done implicitly. Ultimately, when making a decision, the decision-maker must go through a process of condensing information to make simple comparisons. Proponents of composite indices argue that it is better to make this process explicit through an aggregation function.

B. Weaknesses of composite indices

Critics of composite indices proffer equally persuasive arguments. They argue that composite indices can lead to incorrect conclusions about policy performance. Development of the aggregation equation almost always requires more assumptions and arbitrary decisions than the design of a profile warrants. Thus, composite indices are frequently criticised by scientists familiar with the data; they feel that assumptions can lead to a loss of information and introduce serious distortions [14]. Critics caution that the distortions can lead the observer to misinterpret the data. As [14] states, 'if too many things are lumped together, their combined message may be indecipherable.' However, it is important to note that 'it is not that more detailed information is lost – usually it is possible to look at the details of how any composite indicator has been constructed – but rather that decision-makers are too busy to deal with these details' [5].

If users are not careful and informed, they can be ignorant of the source of the numbers, how the numbers were aggregated, and the uncertainties, weights, and assumptions involved, etc. This can also lead to spurious conclusions. A major limitation of composite indices is the manner in which the constituent variables to be included in the index are determined. Generally, the parameters are chosen on the basis of expert opinion. Critics argue that there is no single satisfactory method of selecting parameters. Therefore, an index is always in danger of missing important parameters. However, it is generally not feasible or practical to monitor the hundreds of potential variables.

Another problem with composite indices is that it is difficult to capture the interrelationships between individual variables. Gustafsson [10] warns against the reductionist views encouraged by composite indices. Physical processes that occur in the assets producing degradation are complex and interdependent. And a stress on one part of the system affects other system elements as well. It is unrealistic to expect composite indices or a single index to capture this complexity.

In reality, the two views of composite indices are not so black and white. In fact, they are necessarily complementary. A high level of indicator aggregation is necessary to increase the awareness of economy-environment interaction problems. But even given the advantages of composite indices, no single index can possibly answer all questions. Multiple indicators will always be needed, as will intelligent and informed use of the ones we have [5]. Nevertheless, it can be argued that composite indices have a role in assisting policy development and evaluation.

4. Methodological considerations for aggregating asset management indicators

Given that composite indices have a role in informing policy makers, the question remains, what can be done to ensure that high quality composite indices are produced?

A. The aggregation process

A significant gap in theory relating to composite indices is the lack of a framework to guide aggregation. A generic framework is shown below (see Figure 1). This framework can be applied to the estimation of composite asset management indices. Several of the steps are described in more detail below.

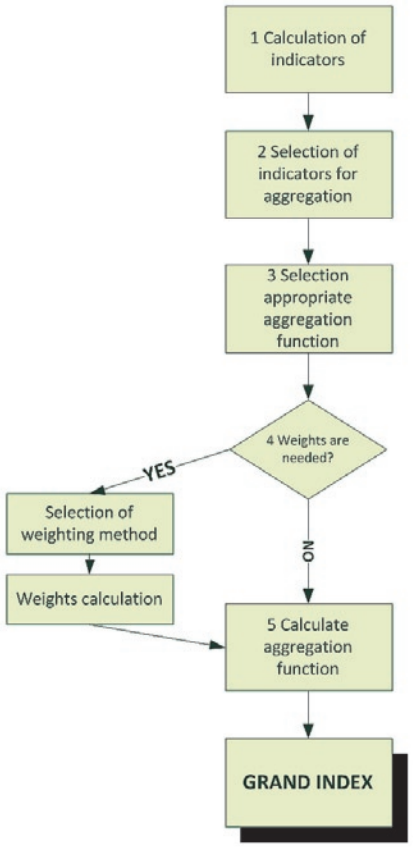

Fig. 1. A generic process for calculating composite indices

B. Selection subindices for inclusion in aggregation

After the indicators are calculated, the second step is to select variables for inclusion in the aggregation function. The selection of the variables is a contentious issue and must be approached with caution. First, the range of the indicators should provide an overarching representation of the principal factors of interest. In the context of asset indicators, this suggests a need for a representative coverage of functions or services for which data are available [18].

Second, the problem of 'multicolinearity' should be addressed by eliminating any correlated variables [18]. A standard test is the correlation coefficient. For example, variables that are highly correlated can be considered substitutes. By including only one indicator from a highly correlated set and excluding the others, we not only account for the trend in the variables, but also achieve parsimony in the data matrix.

Finally, and perhaps most importantly, there is a need to weigh data parsimony against the purpose. For example, often there is policy interest in both maintenance efficiency and effectiveness. Obviously, these are correlated. However, if decision-makers require an aggregate that reports both, the analyst (often implicitly) considers the balance between policy relevance and statistical integrity.

C. Selection of appropriate aggregation function

There is considerable debate over the most appropriate method for aggregating subindices. Aggregation functions usually comprise one of the following:

- Summation operation, in which individual indicators are added together;
- Multiplication operation, in which a product is formed of some or all of the indicators;
- Maximum or minimum operation, in which just the maximum indicator or minimum indicator is reported, algebraically shown as $I = \max\{\varepsilon 1, \varepsilon 2, \ldots \varepsilon i, \ldots \varepsilon n\}$ or $I = \min\{\varepsilon 1, \varepsilon 2, \ldots \varepsilon i, \ldots \varepsilon n\}$ respectively.

Several aspects must be considered when choosing the most appropriate aggregation function. First, the functional form of the indicator is important. Indicators can take the form of an increasing or a decreasing scale. In increasing-scale indicators, higher values are regarded as a 'worse' state than lower values. In decreasing-scale indicators, the reverse is true: higher values are associated with 'better' states than lower values.

The second consideration is the strengths and weaknesses of the aggregation function itself. Ott [15] identifies two potential problems with aggregation functions:

- An overestimation problem, where the composite index exceeds a critical level without any subindex exceeding that critical level.
- An underestimation problem, where an index does not exceed a critical level, despite one or more of its indicators exceeding that critical level.

The above are particularly problematic with dichotomous indicators (where they take on just two values, such as acceptable or unacceptable). An appropriate aggregation function will minimise the risk of both of the overestimation and underestimation problems.

A third aspect to consider when selecting the most appropriate aggregation function is the parsimony principle. That is, when competing aggregation functions produce similar results with respect to overestimation and underestimation, the most appropriate function will be the 'simplest' mathematically. In other words, simple mathematical functions are preferred over complex functions.

Finally, an aggregation approach will succeed if all assumptions and sources of data are clearly identified, the methodology is transparent and publicly reported, the index can readily be disaggregated to the separate components and no information is lost.

D. The challenge of setting the weights

The most popular aggregation function is the weighted summation given as:

$$ai = \frac{\sum_{i=1}^{n} w_i \cdot p_i}{\sum_{i=1}^{n} w_i} \tag{6}$$

where w_i is the weight, p_i denotes the selected performance indicators to be aggregated (individual assets or asset groups), n is the number of asset considered for study and ai is the grand index.

As can be seen in the above equation, the composite index for a group can be created as a normalized expression in which the range of the composite index is within the range of the indices used to create it. This allows the equation to be used with various index ranges and allows the composite index to be used for various asset groups with assets of differing importance. In particular, the index value for each asset in the group is within a common range of index values and the

weighting value for each asset in the group is within a common range of weighting values. As a result, the composite index for the group will be within the same range and the range used for the indices of the assets within the group.

A significant challenge is the selection of appropriate weights. Methods like public polls or expert assessment are based on the knowledge and criteria of the people working with the assets, as their opinions on performance are relevant. However, this is a subjective (i.e., qualitative) approach, strongly dependant on humans, and quantitative methods, mostly statistical, are becoming more popular in assessments of performance. Statistical methods offer an alternative to 'subjective' systems of setting weights. Statistics provides a multivariate technique, namely, principal component analysis (PCA), that is useful for setting weights in the context of multi-dimensional data.

There is still considerable debate among experts about which weighting system to use. While each approach has merits, one advantage of PCA is its relative 'objectivity'. Unfortunately, PCA has received little attention in indicator aggregation literature in general and asset management literature specifically. Possible reasons include a lack of statistical skills among researchers and/or little linking of PCA with the need for composite indices. For a detailed discussion of these techniques, refer to [16].

5. Index aggregation in asset management

A. Asset information sources in plants

Process control systems, like those used in chemical, paper mills, etc., typically include one or more centralized or decentralized process controllers communicatively coupled to at least one host or operator workstation and to one or more process control and instrumentation devices which perform functions within the process such as opening or closing valves and measuring process parameters.

Process controllers receive thousands of signals indicative of process measurements or process variables made by or associated with the field devices and/or other information pertaining to the field devices; they use this information to implement a control routine and then generate control signals which are sent over one or more of the buses to the field devices to control the process. This information from the field devices and the controller is typically made available to one or more applications executed by an operator workstation; this enables an operator to perform functions related to the process, such as viewing its current state, modifying its operation, etc. All of this data contains performance information that is rarely extracted and sent to the proper decision-makers.

A typical processing plant has many hierarchical levels because of the interconnected assets, and a business enterprise may include interconnected processing plants. Assets related to a processing plant or processing plants themselves may be grouped together to form assets at higher levels; the complexity increases when decision-makers and information are found on different hierarchical levels and in different functional units.

In a typical plant, people have a number of different functions. For example, process control activities, device and equipment maintenance and monitoring activities, and business activities such as process performance monitoring all play a unique role. Process control operators generally oversee the day-to-day operation and are primarily responsible for assuring the quality and continuity of the operation; they typically set and change certain points within the process, scheduling processes like batch operations, etc. As a result, process control operators may be most interested in the status of process loops, sub-unit, units and areas. Of course, this is not always the case, and process control operators may also be interested in the status of devices that may have an effect on the loops, sub-units, unit, areas, etc.

B. Maintenance related information in processing plants

Maintenance personnel are also responsible for assuring that equipment is operating efficiently, repairing and replacing malfunctioning equipment and using tools such as maintenance interfaces and other diagnostic tools which provide information on the operating states of the various devices, Figure 2. As such, maintenance personnel will be interested in the status of devices and control loops, though they may also be interested in the status of sub-units, units, etc. [7].

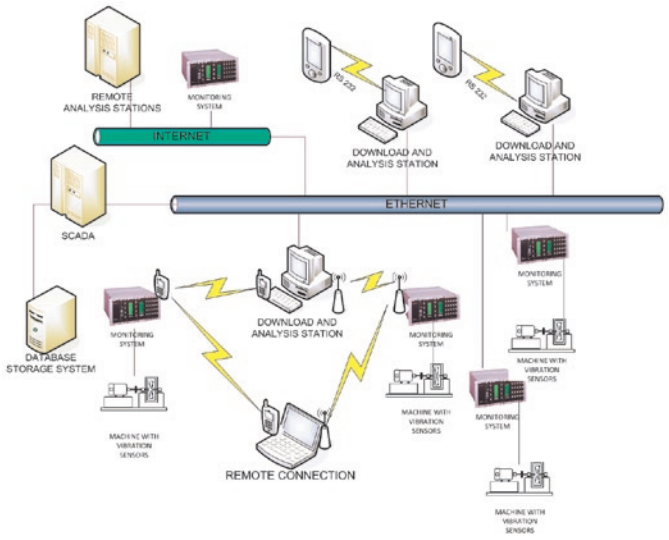

Fig. 2. Typical maintenance data architecture within a plant

Others may be responsible for business applications, such as ordering parts, supplies, raw materials, etc., making strategic business decisions such as choosing which products to manufacture, what variables to optimize within the plant, etc., based on process performance measures. Likewise, managers or other persons may want to have access to certain information within the processing plant or from other computer systems associated with the processing plant to oversee the plant operation and to make long-term strategic decisions. Such persons may be interested in status information pertaining to areas within a processing plant, the processing plant itself and/or all processing plants that make up a business enterprise.

As a result, a processing plant may have several persons (at different hierarchical levels) interested in the status of devices, loops, sub-units, units, etc. To meet their often quite different needs, a variety of systems monitor and report the status of various devices, including health, performance, utilization, and variability [11]. The problem with this approach is that there are thousands of devices in a typical plant and the status of any single device generally cannot be used to determine the overall status of the loop, sub-unit, unit, area or process plant where the device is found.

Some solutions already exist for determining the status of devices, sub-units, units, areas and/or plants. Several Computer Maintenance Management System (CMMS) applications provide asset utilization indexes that include index generation routines related to the health, performance, utilization and variability of various assets at different levels of the plant's hierarchy.

C. The need for aggregation in process plants

An index can be generated by interconnecting various models representing, sub-units, units, areas, etc., within the plant to produce information on the operation of each loop, sub-unit, unit, area, etc., [6]. Alternatively, an indicator can be defined for each device to create a composite index at each level in the system hierarchy.

The composite index could be a weighted average or a weighted combination of the indices of the assets that make up the larger asset.

However, within a typical processing plant, some assets are considered more important than others within a group of assets. Some devices are considered more critical to the larger loop, or to the sub-unit, unit, area, etc., of which they are a part. If such a device were to fail, it would have a greater impact on the loop, sub-unit, unit, area, etc., than if others were to fail and should therefore be prioritised. Likewise, some loops are more important than others among a group of loops interconnected to form a sub-unit, unit, area, etc. In short, the importance of an asset among a group of assets may greatly affect the overall status of the group. However, in the past, varying degrees of importance were not necessarily considered.

In this paper, we propose a way to monitor an entity with a plurality of lower level entities and accounting for varying degrees of importance among the lower level entities. We acquire use indices pertaining to status information of the lower level entities, as well as weighting values. Generally, the weighting value indicates the importance of a lower level entity among a plurality of lower level entities. The weighting values may be based on the impact and frequency of failure. The impact and/or frequency of failure may, in turn, be based on maintenance information, process data, diagnostic data, on-line monitoring data and/or heuristic data. A composite use index representing status information on the entity can be created from a combination of the lower level use indices and weighting values. It may be a composite health index, a composite performance index, an aggregate variability index (indicating the deviation of a parameter of the entity) or a composite utilization index (indicating a degree of exploitation of the entity). The combination of the lower level use indices and weighting values may be a normalized expression, such that the range of values for the use indices is the same among the lower level entities. The combination may involve creating a weighted average of the use indices of the lower level entities.

D. The aggregation process

A processing plant can include a number of business and computer systems interconnected with a number of control and maintenance systems by one or more communication networks as shown in Figure 2. The plant can also include one or more process control systems. Maintenance systems, such as computers or any other device monitoring and communication applications may be connected to the process control systems or to the individual devices therein to perform maintenance and monitoring activities. Similarly, maintenance applications may be installed in and executed by one or more of the user interfaces associated with the distributed process control system to perform maintenance and monitoring functions, including data collection related to the operating status of the devices.

As mentioned above, the index aggregation methodology will receive information from various data sources, such as data collectors, data generators or data tools including index generation routines, model generation routines, control routines, maintenance system applications, data historians, diagnostic routines, etc. This application may receive information from performance systems embedded in CMMS, SCADA (Supervisory Control and Data Acquisition) etc. This information may include indices related to the health, performance, utilization and variability of a particular device, loop, unit, area, etc. This data can take any desired form based on how the data are generated or used by other functional systems. Finally, these data may be sent to the index aggregation using any desired or appropriate data communication protocol.

Information received from the index generation, control routines, maintenance system applications, data historians, diagnostic routines, etc., may be used to create and assign a weighting value to each of the devices within a logical and/or physical group of devices. Further, weighting values may be created and assigned to logical and/or physical groups including a logical process, a subunit, an area or a plant.

The weighting value generally indicates the importance or priority of a device, loop, sub-unit, etc., among the corresponding devices, loops, sub-units, etc. within the same physical and/or logical grouping. In other words, each asset within a group is ranked according to system criticality, operational criticality, asset criticality, etc. based on an assessment of each asset within the group, and a weighting value is assigned based upon its importance. For example, within a sub-unit that includes a plurality of devices and/or loops, a particular piece of rotating equipment may be considered more critical to the operation of the overall sub-unit than a field device. If both the rotating equipment and the field device require maintenance, the rotating equipment may receive priority over the field device in terms of resources allocated to maintenance. As a result, the rotating equipment is assigned a greater weighting value greater than the field device.

Similarly, among the subunits and/or units within an area, a particular sub-unit may be considered more important than another sub-unit, and is weighted accordingly. Areas within a plant may be weighted according to importance, and plants within a business enterprise may likewise be weighted. It should further be recognized that assets within a grouping need not be limited to an immediately preceding level. For example, weighting values may be assigned to each device, loop, sub-unit and/or unit within an area, rather than just each unit within an area. Likewise, weighting values may be assigned to each device, loop, sub-unit, unit and/or area in a plant. A user may define the groupings in a manner most helpful him/her, and weighting values may be assigned accordingly. As a result, each device, loop, sub-unit, unit, area, plant, etc. may be weighted according to its importance within a particular grouping. Generally, the importance of a device, loop, sub-unit, unit, area, etc., and its corresponding weighting value is based on two contributing factors: the impact on the group when the asset fails and the frequency of failure.

In fact, a device that has little impact on an area when it fails may be weighted lower than a device that has a high impact on an area during failure. Likewise, a device with a low frequency of failure may be weighted lower than a device with a high frequency of failure. The impact and the frequency of failure may be quantified, with the product of the impact and frequency of failure resulting in the weighting value. The evaluation of impact and frequency of failure may be based on a variety of factors, including, but not limited to, process information, on-line monitoring information, historical information, maintenance information, diagnostic intonation, and heuristic information based on the experience of plant personnel.

The index aggregation process may acquire weighting values related to each device, loop, sub-unit, unit, area, plant, etc., within a group by receiving each weighting value from another source or by creating each weighting value based on information from a variety of sources. For example, it may receive data relating to the impact and frequency of failure of each device, loop, sub-unit, unit, area, plant, etc. within a group and create each weighting value based on the impact and frequency of failure, (e.g., the product of the impact and frequency of failure).

The aggregation process may also receive information relating to each device, loop, sub-unit, unit, area, plant, etc., within a group to evaluate the impact and frequency of failure of each asset within the group, and to create a weighting value for each asset within the group. The information may include process information, on-line monitoring information, historical information, maintenance information, diagnostic information, and heuristic information as described above.

Accordingly, this process should be communicatively coupled with control routines, maintenance system applications, data historians, diagnostic routines, or other data. Each of the various types of information may be used to evaluate the impact and/or frequency of failure of an asset within a group of assets. For example, historical information, diagnostic information and maintenance information may provide information on previous failures of a device, while historical informa-

tion, process information, on-line monitoring information and heuristic information may provide information on the impact of past failures on the group or the predicted impact of a failure on the group.

Of course, it should be recognized that the weighting values may be created in a similar manner using other routines or systems within the processing plant or created outside it. In addition to acquiring weighting values pertaining to each device, loop, sub-unit, unit, area, plant, etc., within a group, the index aggregation application acquires indices pertaining to their status within the group. The indices may be acquired from the application and each aggregated index may include a health index, a utilization index, a performance index or a variability index as described above.

Accordingly, weighting values may be acquired by receiving impact and frequency of failure information or by receiving information from the model generators, control routines, maintenance system applications, data historians, diagnostic routines, etc., to create a weighting value for each of the devices, loops, sub-unit, units, areas and/or plants, etc. within a logical and/or physical group. Further, indices pertaining to each devices loop, sub-unit, unit, area and/or plant, etc., within the logical and/or physical group may be acquired by the aggregation process. Using the weighting values and indices, the aggregation process may create an index pertaining to the overall status of the group, such as an aggregate health index, an aggregate utilization index, an aggregate performance index or an aggregate variability index.

6. Case study: aggregation of qualitative and quantitative maintenance data

Traditional models advocate audit to measure maintenance performance through surveys of various aspects of the maintenance function. The model considers the information from those involved in maintenance function as very important if it is duly validated by objective numerical indicators. Validation by objective indicators reduces part of the human factor inherent to surveys and interviews.

The case study combines the results of maintenance KPIs (Key Performance Indicators) wit questionnaires, both strongly correlated in terms of content and information to be achieved. The resulting model is shown in the figure below:

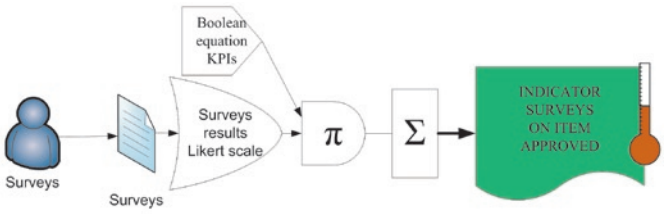

Fig. 3. Model validation surveys through equations based on efficiency KPIs

$$Validated\_surveys\_results = \\ = \sum_{i=1}^{n} Raw\_survey\_results \bullet KPI\_efficiency\_equation \quad (7)$$

Where n is the total number of questions performed in the survey and the KPI equation is as follows:

$$KPI\_efficiency\_equation = \prod_{i=1}^{n} KPI_1 \cdots KPI_n \quad (8)$$

Where n is the total number of normalized KPIs selected because of their strong correlation with the audited item in the figure.

It can be observed how the results obtained from questionaries are multiplied (block π) by the results of the efficiency equation proposed as a combination of one or more KPIs. Two aggregation functions have been explored. In one case, normalised KPIs (between 0 and 1) are multiplied to get a combined grand index related to some specific topic where the lowering effect of the product will be visible and will produce a final value that is less than one (the goal of efficiency or effectiveness in such aggregation function).

Afterwards, this grand index is multiplied by the indicators resulted from questionaries. This last stage aggregation reduces the numerical value in function of the value of the KPI grand index. In this case study, survey results from two paper mills are presented to compare traditional and the proposed methods of aggregating maintenance data.

This case considers data collected from the information systems of the companies and questionaries filled out by three different levels: Level 3 maintenance manager, level 4 maintenance supervisors and finally level 5 technicians. The topic of the questions was the quality and performance of "Maintenance Scheduling". For this purpose, thirteen questions were formulated:

1. Are there work requests to the department from other areas such as production, quality and prevention labor risks?
2. Are there priorities between jobs?
3. Is there a workload known as outstanding work?
4. Are these tasks scheduled?
5. Are these tasks planned?
6. Is the duration of the planned and scheduled work known with any degree of accuracy?
7. Is there a checking on both the work performance and the results obtained?
8. Are 95% of maintenance works scheduled and planned at the latest 1 day before being made?
9. Are spare parts, tools, equipment needed and appropriate documentation ready for the completion of this work?
10. Do planners clearly suggest the tools to use and the components to replace?
11. Are there instructions or procedures for carrying out the work?
12. Do maintenance people know tasks previously to be performed?
13. Is the role of planner defined?

The values received from questionaries are shown in Figures 4 and 5. These questionaries were made following Likert scale, ranked from 1 to 5, as shown in Table I for paper industry 1.

Figure 5 shows the responses of the three organisational levels surveyed: maintenance manager, supervisors and technicians, for paper industry 2. Table II shows the number of questionaries collected from each level for paper industry 1 and 2.

It can be seen that the work planning indicators are generally given high values by the three hierarchical levels and at the two plants audited. In fact most of the values and averages are above 4. This fact indicates that according to questionaries, i.e., human perception, the planning work is being carried out in a successful way.

These values are the result of aggregation, i.e. average of different questions and different hierarchies. However an aggregation with a different indicator is proposed. This index can be part of a grand index if multiplied by the maintenance KPI that are strongly correlated with the goals of the questionaries. In the studied case of questionaries about work planning, the numerical indicator that resulted from filling the forms can be the result of the product with O5, as seen in Figure 7.

O5 is an indicator proposed by EN 15341 that represents the volume of the total planning:

$$O5 = \frac{\text{Planned and scheduled maintenance man hours}}{\text{Total maintenance man hours available}} \quad (9)$$

Table I. Results of questionaries on work planning. Paper industry 1

	Planned maintenance							
	Level 3 Maintenance Manager	Level 4 Supervisor			Level 5 Technician			
		1	2	Avg	1	2	3	Avg
1	4	5	5	5	4	5	4	4,333
2	3	5	4	4,5	5	5	5	5,000
3	5	5	4	4,5	5	5	3	4,333
4	4	5	4	4,5	5	5	5	5,000
5	4	4	4	4	5	5	4	4,667
6	4	4	3	3,5	4	5	3	4,000
7	3	4	4	4	5	5	4	4,667
8	4	5	4	4,5	5		4	4,667
9	3	4	4	4	4	5	4	4,333
10	4	3	2	2,5	4	4	4	4,000
11	3	4	4	4	5	5	4	4,667
12	4	3	3	3	5	5	3	4,333
13	4	5	4	4,5	5	5	5	5,000

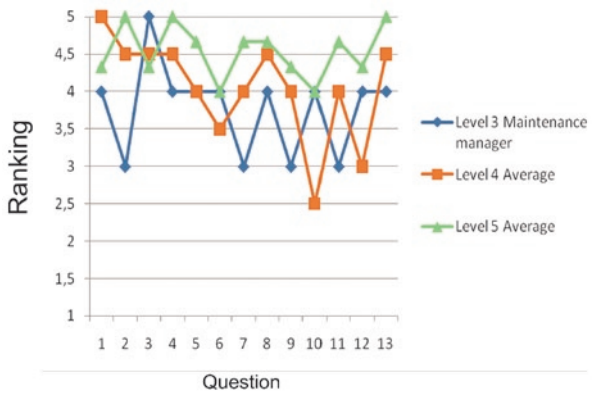

Fig. 4. Results of surveys on maintenance planning. Paper Industry 1

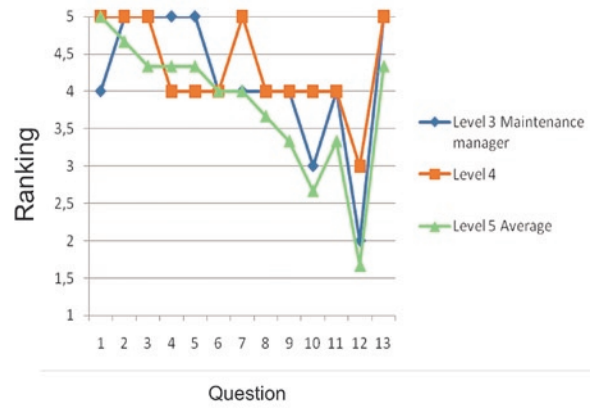

Fig. 5. Results of surveys on maintenance planning. Paper Industry 2

There are many theories and proposals on this indicator, 'World Class' perspective being adopted by the company. According to the current one the majority, around 95% of labor available hours, must be occupied in planned maintenance. Thereby, the problem of hypothetical lack of contingency workforce is solved by hiring overtime associated with outside companies.

This strategy stems from an aversion to the waste caused by idle resources and requires a comprehensive work planning and control,

Table II. Results according to hierarchical levels in industry surveys evaluated

Results Paper Industry 1	Planning work	
	Level 3	3,769
	Level 4	4,038
	Level 5	4,538
Average result		4,115

Results Paper industry 2	Planning work	
	Level 3	4,154
	Level 4	4,308
	Level 5	3,821
Average result		4,094

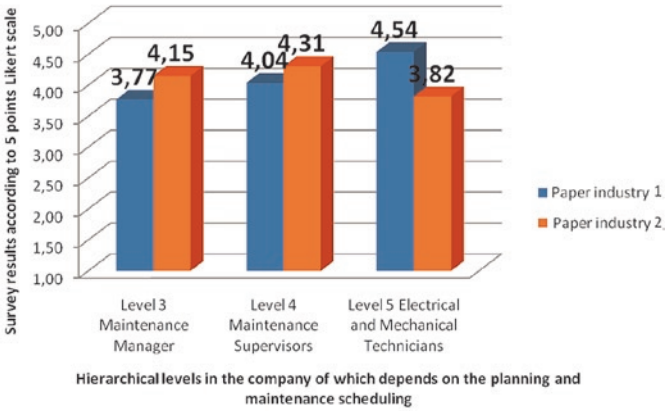

Fig. 6. Result of the survey planning work. Paper industry 1 versus Paper industry 2

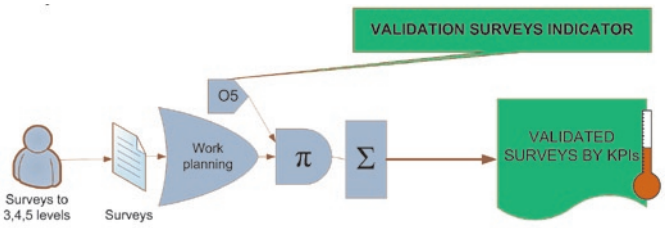

Fig. 7. Variation of classical model validated by KPIs. Calculation mode

i.e., an indicator close to unity, like the previous one, which is true. The companies in the past three years have come and gone into the range of 95% in compliance with the mark of World Class Maintenance (WCM). As for the industry 1, IO5 value is 96.96% while the second industry value is 28.32%, being these quantitative figures extracted from the CMMS.

Results of aggregation can be seen in Table III and compared with questionaries results in figure 6. Aggregating the values derived from surveys with the KPis, very high values around 4 are obtained again for industry 1, which means that the findings of the surveys are reliable and perform a work schedule maintenance work. Therefore the human per-

Table III. Validated indicator

COMPANY	Survey results	O5	Validated surveys
Paper Industry 1	4,115	96,96%	3,9899
Paper industry 2	4,094	28,32%	1,159

ception matches with the audit results. It is not like that for the second industry, since we see a significant reduction between the grand index and the one obtained from the surveys, reflecting the feeling timidly expressed in the responses regarding knowledge of the planned activity.

This aggregation process shows a failure of the traditional model based on questionaries that only take the human perception into consideration. Therefore corrective actions should be taken address the situation where the performance is low but people perceive that they are being successful.

7. Conclusions.

Composite indices are a useful communication tool for conveying performance information in a relatively simple way and to signal policy priorities. They are used widely in many sectors, but rarely in asset management. Composite performance indicators have a number of advantages, such as focusing attention on important policy issues, offering a more rounded assessment of performance and presenting the 'big picture' in a way the public can understand. It is likely, therefore, that they will be used in the future in many policy areas.

However, it is important to recognize that the construction of composite indicators is not straightforward; many methodological issues must be addressed if the results are not to be misinterpreted. Some pragmatism in the approach to composites may be appropriate.

Technical and analytical issues in the design of composite indicators clearly have important implications. This paper highlights some considerations in the construction of robust asset management composite indicators. For example, if the potential for producing misleading information is not addressed, composite measures may fail to deliver the expected improvements in performance or may even induce unwanted side-effects.

References

1. Alfsen KH, Saebo HV. Environmental quality indicators: background, principles and examples from Norway. Environmental and Resource Economics 1993; 3: 415–435.
2. Boisevert V, Holec N et al. Economic and Environmental Information for Sustainability. Valuation for sustainable development: methods and policy indicators. S. Faucheux and M. O'Connor. Edward Elgar Publishing Ltd, Cheltenham 1998: 99–119.
3. Bradbury R. Are indicators yesterday's news? Proceedings of the Fenner Conference 'Tracking Progress: Linking Environment and Economy through Indicators and Accounting Systems, University of New South Wales, Sydney 1996.
4. Callens I, Tyteca D. Towards indicators of sustainable development for firms. Ecological Economics 1999; 28(1): 41–53.
5. Costanza R. The dynamics of the ecological footprint concept. Ecological Economics 2000; 32: 341–345.
6. Dasarathy BV. Information Fusion. What, Where, Why, When, and How? Information Fusion 2001; 2: 75–76.
7. Davies C. Greenough RM. The use of information systems in fault diagnosis, in : Proceedings of the 16th National Conference on Manufacturing Research, University of East London 2000.
8. EN 15341:2007 Maintenance – Maintenance Key Performance Indicators, CEN – European Committee for Standardization.
9. Galar D, Gustafson A, Tormos B, Berges L. Maintenance Decision Making based on different types of data fusion. Eksploatacja i Niezawodnosc – Maintenance and Reliability 2012; 14(2): 135–144.
10. Gustafsson B. Scope and limits of the market mechanism in environmental management. Ecological Economics 1998; 24(2–3): 259–274.
11. Hall DL, Llinas J. An introduction to multisensor data fusion. Proceedings of the IEEE 1997; 85(1): 6–23.
12. Heycox J. Integrating data for sustainable development: introducing the distribution of resources framework. Novartis Foundation Symposium 220: Environmental statistics – analysing data for environmental policy, John Wiley & Sons London 1999.
13. Kumar U, Galar D, Aditya Parida, Stenström C, Berges-Muro L. "Maintenance Performance Metrics: a State-of-the-Art Review", Journal of Quality in Maintenance Engineering 2013; 19(3).
14. Meadows D. Indicators and information for sustainable development. USA, The Sustainability Institute 1998.
15. Ott WR. Environmental Indices: Theory and Practice. Ann Arbor Science, Ann Arbor1978.
16. Sharma S. Applied Multivariate Techniques. John Wiley & Sons, New York 1996.
17. Williams MR. Use of principal component biplots to detect environmental impact. Statistics in Ecology and Environmental Monitoring, University of Otago, University of Otago Press 1994.
18. Yu C, Quinn JT et al. Effective dimensionality of environmental indicators: a principal component analysis with bootstrap confidence intervals. Journal of Environmental Management 1998; 53: 101–119.

Diego GALAR
Division of Operation and Maintenance Engineering
Luleå University of Technology
Luleå, 97187 Sweden
E-mail: diego.galar@ltu.se

Peter SANDBORN
CALCE Center for Advanced Life Cycle Engineering
University of Maryland
College Park, MD USA
E-mail: sandborn@calce.umd.edu

Luis BERGES
Department Design Engineering and Manufacturing
University of Zaragoza
Zaragoza. 50018 Spain
E-mail: bergesl@unizar.es

Uday KUMAR
Division of Operation and Maintenance Engineering
Luleå University of Technology
Luleå, 97187 Sweden
E-mail: uday.kumar@ltu.se

Article citation info:
TAO J, YU Z, REN Z, YI X. Study of an adaptive accelerated model and a data transfer method based on a reliability enhancement test. Eksploatacja i Niezawodnosc – Maintenance and Reliability 2014; 16 (1): 128–132.

Junyong TAO
Zongyue YU
Zhiqian REN
Xiaoshan YI

STUDY OF AN ADAPTIVE ACCELERATED MODEL AND A DATA TRANSFER METHOD BASED ON A RELIABILITY ENHANCEMENT TEST

BADANIA ADAPTACYJNEGO MODELU PRZYSPIESZONEGO ORAZ METODY TRANSFERU DANYCH W OPARCIU O TEST POPRAWY NIEZAWODNOŚCI

To assess the reliability of a product using a Reliability Enhancement Test (RET), this study first considers the change process of the Arrhenius model parameters by combining the Arrhenius model with the Duane model and gives an adaptive accelerated model and a parameter estimation method. Then, the data transfer method from the RET to normal test stress are described based on the adaptive accelerated model. Finally, the differences observed when the RET is used for a reliability identity test or a reliability growth test are discussed, and an engineering case demonstrates a method for obtaining the reliability index of a product using the RET.

***Keywords**: reliability enhancement test, Arrhenius model, Duane model, adaptive accelerated model, acceleration factor.*

Aby ocenić niezawodność produktu za pomocą testu poprawy niezawodności (Reliability Enhancement Test, RET), w badaniach najpierw rozważano proces zmiany parametrów modelu Arrheniusa poprzez połączenie modelu Arrheniusa z modelem Duane'a oraz przedstawiono adaptacyjny model przyspieszony i metodę oceny parametrów. Następnie, na podstawie adaptacyjnego modelu przyspieszonego opisano metodę transferu danych z RET do badań przy normalnym oddziaływaniu czynników zewnętrznych. Wreszcie, omówiono różnice obserwowane przy zastosowaniu RET do badań identyfikacyjnych niezawodności i badań wzrostu niezawodności. Na przykładzie zagadnienia inżynierskiego przedstawiono także metodę obliczania wskaźnika niezawodności produktu za pomocą RET.

***Słowa kluczowe**: test poprawy niezawodności, model Arrheniusa, model Duane'a, adaptacyjny model przyspieszony, współczynnik przyspieszenia.*

1. Introduction

Reliability enhancement tests (RETs) can quickly stimulate the latent defects of a product by using the accelerated test stress in the product development stage, which is an effective approach for improving product reliability [2, 6, 14].

Since 1988, many researchers have studied this area, and RETs have been used in engineering. For instance, a RET was used in a Sidewinder development stage [7] and in a radar development stage [16]. Although RETs can effectively improve product reliability, the product reliability index cannot be quantitatively given. The development of methods for assessing product reliability have been the focus of RET research. Determining how to set up an accelerated model, and understanding how to transfer data from a RET to a normal stress test through an accelerated model, are the core problems of RET research. Mike Silverman [8, 9], Harry Mclean [4] and Pascal Lantieri [13] have done some researches on assessment of products in the RET.

In the process of conducting a RET, the design defects of a simulated product are improved to rapidly increase the product reliability. Thus, the parameters of the accelerated model also change as the product reliability increases. In focusing on the adaptive accelerated model of a RET, this study first considers the change process of the Arrhenius parameters and obtains an adaptive accelerated model by combining the Arrhenius model with the Duane model. Then, the parameter estimation and the data transfer method of the RET data are given based on the new model, and the difference observed when the RET is used for reliability assessment and reliability growth is analyzed. Finally, an engineering case verifies that the accelerated model is correct and useable.

This study first presents the adaptive accelerated model of a RET, by combining the Arrhenius accelerated model and the Duane increase model, examining the change process of the Arrhenius accelerated model parameters, and setting up the adaptive accelerated model. Next, it presents the estimated measure of the adaptive accelerated model parameter, and the enhancement step in the test data transfer of the adaptive accelerated model. Finally, analyses are presented of the differences observed due to RET technology used in a reliability identity test and a reliability growth test.

2. Model hypotheses

(1) Product life is assumed to follow an exponential distribution for each stress level, and after the product is improved, the parameters of the product life distribution change, but the distribution function type does not change.

(2) Product life and the accelerated test stress follow the Arrhenius model, and the test data transferred from the RET test stress to the normal test stress follow the Duane model.
(3) The residual life of the product only depends on the current accumulated failure and the current stress value and is not dependent on the cumulative method.

For most electronic and mechatronical products, the life distribution follows an exponential distribution. Product improvements are generally only partially carried out so that the basic attributes of the product are not changed, i.e., after the improvement, they are still mechatronical products, so hypothesis 1 is satisfied.

The Arrhenius model is generally used in accelerated life tests of products. Generally, for product failure under different stress test levels, the same corrective measures are employed, so data transferred to the normal stress test will follow the Duane model, i.e., hypothesis 2 is satisfied.

Hypothesis 3 was proposed by Nelson based on the physics-of-failure (POF), and for the data transfer problem in the step stress test, hypothesis 3 is satisfied.

3. Adaptive accelerated model

the product life varies under different temperature stresses. For a product whose life follows an exponential distribution, the characteristics of the product life can be described by the Arrhenius accelerated model [10, 15]:

$$L=\mathrm{A}e^{\frac{Ea}{kT}} \tag{1}$$

Here, A is a constant that depends on the product geometry, the specimen size and fabrication, the test method, and other factors. E_a is the activation energy of the reaction, usually in electron-volts. k is Boltzmann's constant, 8.6171×10^{-5} electron-volts per °C. T is the absolute temperature in Kelvin, which is equivalent to the Centigrade temperature plus 273.16 degrees.

Obviously, according to Equation (1), the relation of the product life under different temperature stresses is expressed as follows:

$$A_F=\frac{L_0}{L_1}=\frac{A\,e^{\frac{Ea}{kT_0}}}{A\,e^{\frac{Ea}{kT_1}}}=e^{\frac{Ea}{K}(\frac{1}{T_0}-\frac{1}{T_1})} \tag{2}$$

Here, L_1 is the product life under the accelerated test stress, L_0 is the product life under the normal test stress, T_0 is the normal test temperature stress, and T_1 is the accelerated test temperature stress.

A_F is generally called the acceleration factor [5] and is used in the transfer of failure data for a product at two stress levels. After obtaining failure data for a product in an accelerated test, the test data for normal stress can be transferred through the acceleration factor using the following equation:

$$L_{0i}=L_{1i}e^{\frac{Ea}{K}(\frac{1}{T_0}-\frac{1}{T_1})} \tag{3}$$

When carrying out the RET, the product should be continuously improved to determine its reliability growth. This process causes the activation energy E_a of failure due to the stimulated latent defects to grow as the product reliability increases. Thus, it is necessary to ensure that the evolution of the activation energy E_a of the acceleration factor during the test time allows the RET data to be transferred to normal test stress data; such a change process can be obtained by combining the Arrhenius model with the Duane model.

In a traditional reliability growth test that simulates the practical stress of a product, the Duane growth model [1, 11] has shown that the cumulative failure rate plotted against the cumulative test time in a log-log space exhibits an almost linear relationship and can give the instantaneous MTBF of the product because the mean life of the product can be expressed by the MTBF for an exponential product, namely, the instantaneous MTBF of the product is equal to the product mean life at the current moment. Therefore, based on the Arrhenius accelerated model and the Duane growth model, the following equation can be found:

$$\hat{MTBF}=\frac{{t_0}^m}{a(1-m)}=L_0=Ae^{\frac{E_a(t)}{kT_0}} \tag{4}$$

Here, a is a scale parameter, m is the growth rate($0<m<1$), t_0 is the cumulative test time for the normal stress, $\hat{MTBF}$ is the instantaneous MTBF at t_0, and L_0 is the mean life at t_0.

According to Equation (4), the activation energy E_a can be expressed as a function of the cumulative test time under the normal test stress,

$$E_a(t_0)=kT_0\times Ln\frac{{t_0}^m}{B(1-m)} \tag{5}$$

where $B=A\times a$.

In the RET, the reliability of the product increases at each stress level with product improvement, and thus, the activation energy E_a will increase as well. Obviously, the activation energies of the RET for the time interval $(t_{1i},\ t_{1(i+1)})$, from the i^{th} to the $(i+1)^{\text{th}}$ failure, and that for the time interval $(t_{0i},\ t_{0(i+1)})$ transferred to the normal stress test E_{ai} are equal. Therefore, the activation energy at any moment t_1 under the accelerated stress test is equivalent to that at t_0 under the normal stress test. The data transfer process from the RET to the normal test is shown in Figure 1.

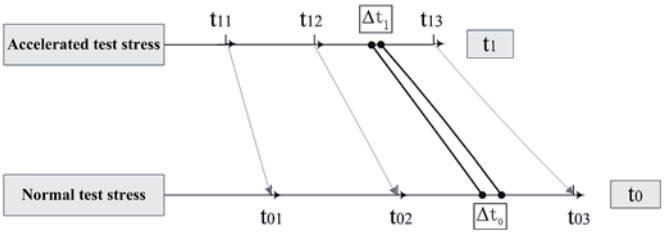

Fig. 1. The data transfer process

Figure 1 shows that the activation energy E_a is constant in the minimal interval $\Delta t_1\to 0$ and $\Delta t_0\to 0$. Assuming that the value of E_a is $E_a(t_0)$, then Δt_1 and Δt_0 follow Equation (3):

$$\Delta t_0=\Delta t_1\times e^{\frac{E_a(t_0)}{K}(\frac{1}{T_0}-\frac{1}{T_1})} \tag{6}$$

According to Equation (6), can be expressed by Equation (7).

$$t_1 = \int_0^{t_0} e^{\frac{Ea(t_0)}{K}(\frac{1}{T_1}-\frac{1}{T_0})} dt_0 \tag{7}$$

Based on Equations (7) and (5), the relation between the cumulative time t_1 of the accelerated stress test and the cumulative time t_0 of the normal stress test is described by the following expression:

$$t_0 = \left\{ t_1 \left[(\frac{1}{T_1}-\frac{1}{T_0})T_0 m + 1 \right] \times \left[B(1-m) \right]^{(\frac{1}{T_1}-\frac{1}{T_0})T_0} \right\}^{\frac{1}{(\frac{1}{T_1}-\frac{1}{T_0})T_0 m+1}} \tag{8}$$

Equation (8) is obtained by replacing t_0 in Equation (5), and the activation energy E_a for the cumulative test time of the RET is expressed as Equation (9):

$$E_a(t_1) = kT_0 \times Ln \frac{\left\{ t_1 \left[(\frac{1}{T_1}-\frac{1}{T_0})T_0 m + 1 \right] \times \left[B(1-m) \right]^{(\frac{1}{T_1}-\frac{1}{T_0})T_0} \right\}^{\frac{m}{(\frac{1}{T_1}-\frac{1}{T_0})T_0 m+1}}}{B(1-m)} \tag{9}$$

After finding the expression for $E_a(t_1)$, the Arrhenius model can be rewritten as follows for the RET:

$$L = Ae^{\frac{Ea(t_1)}{kT}} \tag{10}$$

Moreover, the acceleration factor of the RET is expressed by Equation (11):

$$A_{Fi} = \frac{L_{0i}}{L_{1i}} = e^{\frac{E_a(t_1)}{k}(\frac{1}{T_0}-\frac{1}{T_1})} \tag{11}$$

4. RET data transfer method

4.1. Parameter estimation of the acceleration factor

based on the accelerated model assumption and assuming that the RET is conducted under different accelerated stresses, the parameters of the adaptive accelerated model can easily be estimated by Equation (11), i.e., the conversion factor for any two accelerated stress data sets is described as follows:

$$A_{F12i} = \frac{L_{1i}}{L_{2i}} = e^{\frac{E_a(t_1)}{k}(\frac{1}{T_1}-\frac{1}{T_2})} \tag{12}$$

Using Equation (9), we can rewrite Equation (12) in logarithmic form,

$$\ln \frac{L_{1i}}{L_{2i}} = \frac{Dm}{Cm+1}\ln t_{1i} + \frac{Dm}{Cm+1}\ln(Cm+1) - \frac{D}{Cm+1}\ln B - \frac{D}{Cm+1}\ln(1-m) \tag{13}$$

where $C = (\frac{1}{T_1}-\frac{1}{T_0})T_0$, $D = \left(\frac{1}{T_1}-\frac{1}{T_2}\right)T_0$.

Obviously, by using Equation (13), the acceleration factor can be estimated by the least squares method.

4.2. RET test data transfer method

obviously, the product reliability is improved step by step in the RET, and the activation energy E_a increases as well. When transferring the RET data to normal test data for the time interval between the i^{th} failure and the $i+1^{th}$ failure, the cumulative time for Equation (9), t_1, should be the total test time before the i^{th} failure.

The Duane model makes the activation energy infinitesimal when the initial time is zero[11]. Therefore, when we first transfer the failure data for each stress level, the activation energy E_a is the value of the last stress level at the last time step. For the first test stress level, the first failure data point will be used to calculate the E_a of the second failure data point. Thus, the data transfer process will begin from the second failure data point.

Through the above analysis, the steps of transferring the RET test data to normal test stress data based on the adaptive accelerated model (10) are described as follows:

$$L_{0j} = L_{ij} A_{Fij} \tag{14}$$

where $L_{ij} = t_{ij} - t_{i(j-1)}$ is the time interval from the $j-1^{th}$ failure to the j^{th} failure at the i^{th} stress level. $L_{0j} = t_{0j} - t_{0(j-1)}$ is the time interval from the j-1^{th} failure to the j^{th} failure after the RET data are transferred to the normal test stress. A_{Fij} is the acceleration factor for the translation of L_{ij} to L_{0j}.

When j>1, Equation (11) is used by replacing the cumulative time of the $j-1^{th}$ failure under this test stress, and the acceleration factor is given by Equation (15):

$$A_{Fij} = e^{\frac{E_a(t_i)_{j-1}}{k}(\frac{1}{T_0}-\frac{1}{T_i})} \tag{15}$$

When j=1, Equation (11) is used by replacing E_a for the final time step of the previous test level, and the acceleration factor is given by Equation (16):

$$A_{Fi1} = e^{\frac{Ea'}{K}(\frac{1}{T_0}-\frac{1}{T_i})} \tag{16}$$

For the first accelerated stress, Equation (9) is used by replacing the first failure data set, and then the activation energy $E_a''(t)$ is found, which is used for the second failure data transfer. Equation (11) is used by replacing $E_a''(t)$, and then A_{F11} is found by Equation (17):

$$A_{F11} = e^{\frac{Ea''}{K}(\frac{1}{T_0}-\frac{1}{T_i})} \tag{17}$$

Therefore, the RET failure data can be transferred to the normal test failure data using the data transfer method, the transferred failure data can be used as the reliability growth test (RGT) failure data, and the product reliability value can be given by the RGT assessment method.

5. Illustrative example

5.1. Design of the RET Project

The traditional RET focuses on how to stimulate product defects, which cannot give the reliability index of a product. If we wish to obtain the reliability index by RET, it is necessary to modify the traditional RET [3,17] project based on the adaptive accelerated model.

(1) For a traditional RET, one or two samples is sufficient. If the RET is used for product reliability assessment, the number of samples is usually three to five, which allows one to obtain more accurate parameter estimate values of the adaptive accelerated model.

(2) There are several temperature stress levels in a RET, such as $S_1 < S_2 < \cdots < S_K$. Here, S_1 is the initial temperature. When a RET is used for reliability assessment, the number of stress levels is smaller, and the stress step is larger.

(3) In the parameter estimating process for the adaptive accelerated model, the RET must be conducted under two accelerated stresses at the same time, and the same corrective measures should be applied to the products.

Based on the above analyses, the adaptive accelerated model is suitable for a step-up-stress temperature test for samples under different accelerated stresses at the same time, and the test profile is shown in Figure 2.

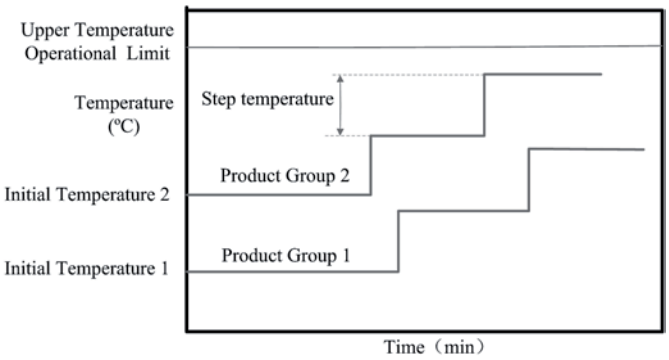

Fig. 2. Test profile sketch map

5.2. Case Analyses

Consider a special case, i.e., where the acceleration factor is equal to 1, so the accelerated test stress is equal to the normal test stress, namely $T_1 = T_0$. According to Equation (8), $t_1 = t_0$. Therefore, the data transfer method is correct when the acceleration factor is 1.

When the acceleration factor is greater than 1, the following case demonstrates the analysis process.

Table 1. RET failure data

Stress level	RET failure data
S_1=1.2S_0	12.5, 39.4, 92.3, 170.2, 289.4, 454.8, 679.3, 952.6, 1311.4
S_2=1.3S_0	5.6, 17.4, 39.9, 71.6, 117.8, 178.8, 257.3, 350.9, 470.1

Table 2. Estimation of parameters and transferred data

M	B	Transferred data
0.13	4.02×10^{-4}	110.4, 332.9, 667.3, 1185.4, 1912.5, 2909.9, 4135, 5755.3

In the development process of a new product, a RET was conducted in which the accelerated stress levels were *S1*=1.2*S0* and *S2*=1.3*S0* and the number of samples was 3 for each level. For failures in the RET, the same improvement measure was used for each product failure, and the test was stopped once the product had failed 9 times.

To improve the precision of the parameter estimate, the average of the failure data for three products under the same stress level was used as the final analysis data, as shown in Table 1.

Based on the failure data given in Table 1, the parameter estimate of the adaptive accelerated model and the transferred data were determined, as shown in Table 2.

In the data transfer process employed in this study, the first failure data point of both accelerated stresses is used to calculate the acceleration factor, so the data transfer process begins from the second failure data point. Therefore, we can obtain eight transferred failure data points.

Treating the transferred failure data as a set of RGT data, the MTBF of the product is 2004.3 (h) based on the Duane model. This case shows that the adaptive accelerated model given by this study can realize RET data transfer, and that the MTBF of a product can be calculated by the RET.

6. Conclusion

By focusing on the reliability assessment of a RET, the change process of the Arrhenius model parameters was examined, an adaptive accelerated model was developed by combining the Arrhenius model with the Duane model, and the RET data transfer method was described. Through an engineering case, this study showed that the adaptive accelerated model is correct and useable in practice. A new assessment method is given for the reliability index based on a RET.

Acknowledgement:
This study was supported by National Advanced Research Project of China.

References

1. Duane JT. Learning Curve Approach to Reliability Monitoring . IEEE Trans Aerospace.1964.
2. Hobbs GK. Accelerated Reliability Engineering HALT and HASS. John Wiley & Sons Ltd, New York 2000.
3. HALT Guideline. QualMark Corporation. 2003
4. Mclean H, Silverman M. From HALT Results to an Accurate Field MTBF Estimate. Proceeding Annual Reliability and Maintainability Symposium;2010 Jan 25–28;San Jose, CA.2010.
5. Xie J. Determination of Acceleration Factor in Predicting the Field Life of Plated Through Holes From Thermal Stress Data. IEEE TRANSACTIONS AND PACKAGING TECHNOLOGIES, 2008.
6. Silverman M. Summary of HALT and HASS Results at an Accelerated Reliability Test Center. Proceeding Annual Reliability and Maintainability Symposium. CA, USA 1998: 30–36.

7. Connolly MP, Kenneth R. Can HALT and HAST Replace Some U.S. MIL-STD-331 Climatic Tests for Electronic Fuzes . NDIA 47th Annual Fuze Conference. NDIA, USA. 2000.
8. Silverman M, Why HALT Cannot Produce a Meaningful MTBF Number and Why This Should not Be A Concern. 2009. Available from: http://http//www.opsalacarte.com
9. Silverman M. Field Failure Rate Estimate from HALT Results. 2009. Available from: http://http//www.opsalacarte.com
10. Celina M. Accelerated Aging and Lifetine Prediction: Review of Non-Arrhenius Behaviour due to Competing Processes. Degrad Stab. 2005; 90: 395–404.
11. MIL-HDBK-189. Reliability Growth Management, 1981.
12. MEI Wenhua. Reliability Growth Test. Beijing: National Defense Industry Press, 2003.
13. Lantieri P, Dumon B. Applying Accelerated Life Models to HALT Testing. 9th ISSTIA International Conference on Reliability and Quality Design, 2003.
14. Robert WD, Edward OM. Reliability Enhancement testing. Proceeding Annual Reliability and Maintainability Symposium. Anaheim, CA, USA.1994: 91–98.
15. Schuller S. Determination of the Degradationg Constant of Bulk Heterojunction Solar Cells by Accelerated Lifetime Measurements. Appl. Phys. 2004; 79: 37–40.
16. WANG Hong. Reliability Enhancement Testing and Its Application in Design and Production Phases of Radar . Modern Radar. 2008; 30: 26–28.
17. Wei Li. Highly Accelerated Life Test for the Reliability Assessment of the Lead-Free SMT Mainboard. Microsystems, Packaging, Assembly Conference; 2006 Oct 18-20; Taiwan. 2006.

Junyong TAO
Zongyue YU
Zhiqian REN
Xiaoshan YI
Science and Technology on Integrated Logistics Support Laboratory,National University of Defense Technology
Yanwachi str., 47 Changsha, 410073, P.R.China
E-mails: taojunyong@nudt.edu.cn, yuzongyue1986@126.com, renzhiqian@nudt.edu.cn yixiaoshan@nudt.edu.cn

Article citation info:
KOSZAŁKA G. Model of operational changes in the combustion chamber tightness of a diesel engine. Eksploatacja i Niezawodnosc – Maintenance and Reliability 2014; 16 (1): 133–139.

Grzegorz KOSZAŁKA

MODEL OF OPERATIONAL CHANGES IN THE COMBUSTION CHAMBER TIGHTNESS OF A DIESEL ENGINE

MODEL EKSPLOATACYJNYCH ZMIAN SZCZELNOŚCI PRZESTRZENI NADTŁOKOWEJ SILNIKA O ZAPŁONIE SAMOCZYNNYM*

The paper presents the results of tightness testing of an internal combustion engine combustion chamber during long-term operation. The tests were conducted on 5 six-cylinder diesel engines used in motor trucks. Changes in tightness for the distance range 0–500,000 km were determined based on the measurement results of the following: pressure drop measured using a cylinder leakdown tester, maximum compression pressure in the cylinders, and the blow-by flow rate at different engine operating conditions. The obtained test results were analyzed statistically. Stochastic models of changes in engine combustion chamber tightness versus distance traveled were developed. Each model describes the time history of the mean value of a selected diagnostic parameter and the limits of probable changes in this parameter. The test results have shown that both the rate and character of changes as a function of engine operation time differed depending on a parameter. The maximum compression pressure was characterized by the lowest dynamics of changes (a decrease by less than 20% for the distance range 0–500,000 km), the cylinder leakage was characterized by a moderate change dynamics, while the blow-by flow rate exhibited the highest dynamics of changes (a threefold increase at 2200 rpm). It should also be mentioned that in the case of the first two parameters, the rate of changes increased with the distance traveled, whereas in the case of the blow-by the observed changes were linear. Also, dispersion fields (i.e. changes in standard deviations) were calculated for the tested diagnostic parameters.

***Keywords**: internal combustion engine, ring pack, diagnostics, stochastic model, compression pressure, blow-by, wear.*

W artykule przedstawiono wyniki badań szczelności komory spalania silnika o zapłonie samoczynnym w czasie długotrwałej eksploatacji. Badania przeprowadzono na 5 egzemplarzach sześciocylindrowego silnika wykorzystywanego do napędu samochodów ciężarowych. Zmiany szczelności w zakresie przebiegów 0–500 tys. km określono na podstawie wyników pomiarów: spadku ciśnienia z wykorzystaniem próbnika szczelności komory spalania, maksymalnego ciśnienie sprężania w cylindrach oraz natężenia przedmuchów spalin do skrzyni korbowej w różnych warunkach pracy silnika. Wyniki badań poddano analizie statystycznej. Opracowano stochastyczne modele zmian szczelności komory spalania silnika w funkcji przebiegu samochodu. Model opisuje przebieg wartości średniej wybranego parametru diagnostycznego w czasie oraz granic obszaru prawdopodobnych zmian tego parametru.Wyniki badań wykazały, że zarówno prędkość jak i charakter zmian w funkcji czasu eksploatacji były różne dla różnych parametrów. Najmniejszą dynamiką zmian wyróżniało się maksymalne ciśnienie sprężania (spadek o mniej niż 20% w zakresie przebiegów samochodu: 0–500 tys. km), średnią dynamiką – wskaźnik szczelności, a największą – natężenie przedmuchów spalin (3-krotny wzrost przy 2200 obr/min), przy czym dla dwóch pierwszych parametrów szybkość zmian zwiększała się wraz z przebiegiem samochodu, natomiast w przypadku przedmuchów spalin zmiany miały charakter liniowy. Wyznaczono również pola rozproszeń (zmian odchyleń standardowych) dla badanych parametrów diagnostycznych.

***Słowa kluczowe**: silnik spalinowy, uszczelnienie pierścieniowe, diagnostyka, model stochastyczny,ciśnienie sprężania, przedmuchy spalin, zużycie.*

1. Introduction

Combustion chamber tightness is one of the most important features affecting the technical condition of an internal combustion engine. Due to the wear of a cylinder liner, piston rings and piston ring grooves during operation, the clearances in the piston-rings-cylinder pack increase. In effect, the combustion chamber tightness deteriorates. The decrease in tightness leads to lower engine performance, higher fuel and engine oil consumption, increased toxic substance emissions, lower cold start capacity, as well as faster engine oil degradation and piston-rings-cylinder unit wear [2, 3, 5, 12, 13, 14, 16].

The commonly used means of determining combustion chamber tightness include measuring diagnostic parameters such as compression pressure in the cylinder, sub-atmospheric pressure in the inlet duct or blow-by flow rate [12]. It is important to know operational changes in these parameters, including their rate and character of changes (linear or non-linear), as well as the scatter of measurement results, due to their importance in diagnosing the technical condition of an engine as well as predicting its durability and evaluating its reliability [1, 4, 8, 9, 10, 17]. These parameters can also be useful for the modeling of an engine ring-pack [7, 15, 18]. The relevant studies offer numerous general descriptions of various models of changes in the technical condition of objects [11]. However, there is scarce quantitative information on real changes in parameters characterizing the technical condition of the piston-rings-cylinder unit in real engine operation. [14].

The changes in tightness of the combustion chamber from the moment of production to the serviceability limit of objects operated in

(*) Tekst artykułu w polskiej wersji językowej dostępny w elektronicznym wydaniu kwartalnika na stronie ***www.ein.org.pl***

normal conditions is very seldom studied due to the long time and high costs of conducting such research. Such results can be obtained in a shorter time by means of curtailed studies using the layer test method [13]. The curtailed studies consist in performing tests on statistical samples of vehicles with different distances traveled. The test results are analyzed as a whole to determine a model of changes in a given parameter for the whole service life of a vehicle. A shortcoming of this method lies in the uncertainty of the assumption made, which says that there are no systematic differences between the studied layers – objects with different kilometrage values.

The aim of the tests described in the paper was to develop stochastic models of changes in diagnostic parameters that characterize the combustion chamber tightness of a high-speed diesel engine versus distance traveled based on long-term observations of the homogenous sample of objects, as opposed to the layer test method. Such models should allow for determining both mean value changing tendencies and a dispersion field of the investigated parameters versus engine operation time.

2. Test object and method

The test object was a six-cylinder compression-ignition engine with a displacement of 6.8 dm^3, maximum torque of 432 Nm in the range of 1800-2200 rpm, and a rated power of 110 kW at a speed of 2800 rpm. The engine was equipped with wet, cast iron cylinder liners with a nominal internal diameter of 110 mm. The aluminum piston was equipped with a toroidal combustion chamber and a cast-iron carrier for the top ring groove. The top ring was a keystone type, the second one was rectangular, and the twin-land oil ring was equipped with a spiral spring. The piston stroke was 120 mm. The engine had two cylinder valves powered by the camshaft mounted in the engine block and actuated by valve rods and valve arms.

The tests were performed on 5 engines mounted in trucks of a medium load capacity and gross weight of 12 tons. The tests were performed in normal operating conditions. All the vehicles were the property of one transport service provider and they were all used in similar conditions. The vehicle engines were all lubricated with CE/SF SAE 15W/40 oil. An average monthly distance traveled by the vehicles was 10,000 km.

The engines were periodically subjected to measurements, including diagnostic tests that allow for the evaluation of combustion chamber tightness. The frequency of the conducted measurements resulted from the frequencies of periodical technical inspections of the engines. By combining the measurements, the number of servicing activities and vehicle operation disturbances could be reduced to the minimum. Until the distance traveled by the vehicle was below 100,000 km, the measurements were performed approximately every 15,000 km, and when the distance traveled exceeded 100,000 km – they were taken approximately every 50,000 km. In addition to that, the tests were conducted at the same stand by the same individuals, using the same instruments, which allowed for reducing the error connected with the non-repeatability of measurement conditions.

In order to evaluate the combustion chamber tightness, the following were measured:

– cylinder leakage,
– compression pressure in the cylinder,
– blow-by flow rate.

The cylinder leakage was determined by measuring the relative pressure drop of compressed air that was led into the combustion chamber through the injector hole at the TDC piston position after the compression stroke. The measurement was conducted using a PSC-2M cylinder leak-down tester. The compression pressure, i.e. the maximum pressure in the combustion chamber at the end of a compression stroke, was measured by means of an SPCS-50 controlled compression pressure tester. The compression pressure and cylinder leakage were successively measured in the 6 cylinders of the warmed-up engine. The blow-by flow rate was measured for both idle run (approx. 600 rpm) and full load (the maximum position of the accelerator pedal) of the engine at the following speeds: 1570, 1880, 2200 and 2800 rpm.

3. Results

The diagnostic parameter values obtained in the operational tests for particular cylinders, i.e. the results of the cylinder leakage and compression pressure measurements, are shown in Figs. 1-2, while the measurement results of the blow-by flow rate for particular engines at various crankshaft speeds are illustrated in Figs. 3-7. The obtained results are characterized by a considerable scatter. What is more, the

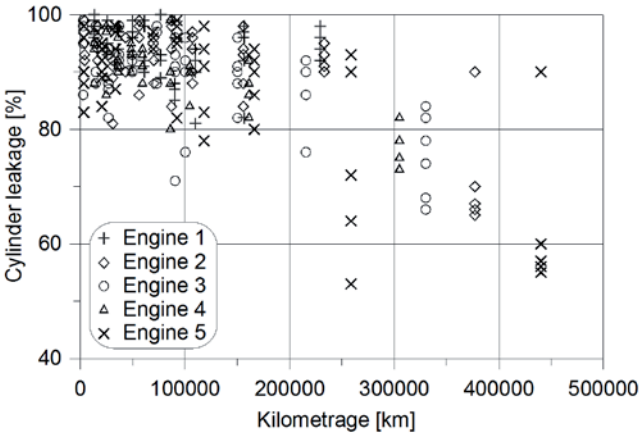

Fig. 1. Measurement results of cylinder leakage

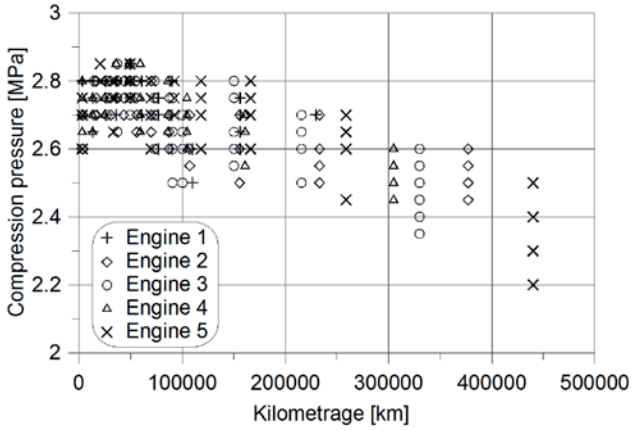

Fig. 2. Measurement results of compression pressure

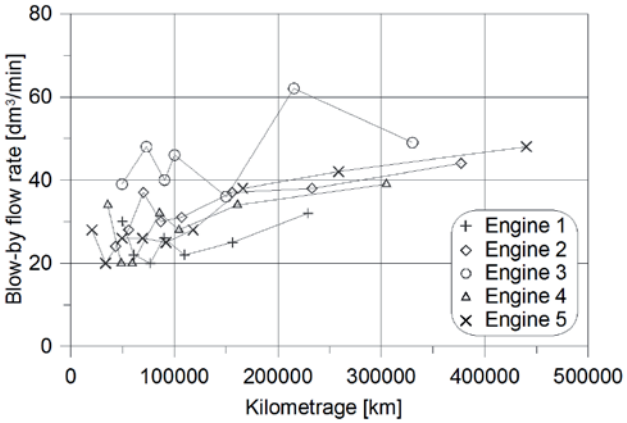

Fig. 3. Measurement results of the blow-by flow rate at idle run

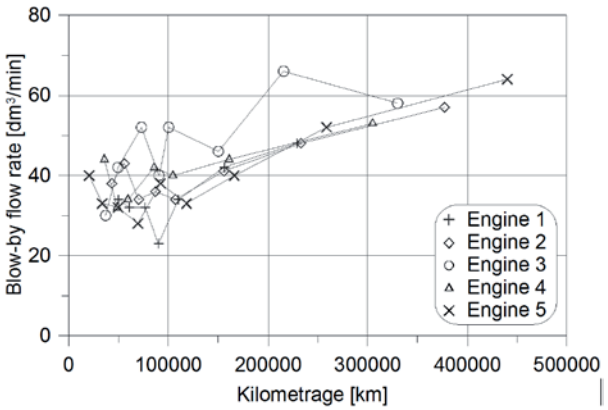

Fig. 4. Measurement results of the blow-by flow rate at full load and a speed of 1570 rpm

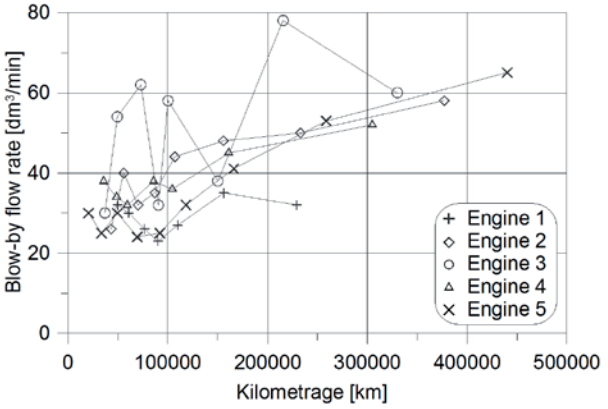

Fig. 5. Measurement results of the blow-by flow rate at full load and a speed of 1880 rpm

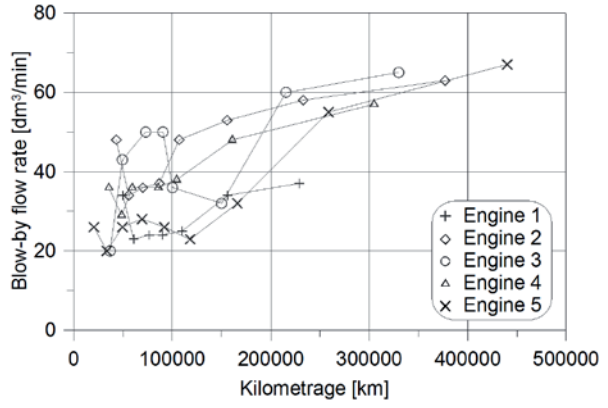

Fig. 6. Measurement results of the blow-by flow rate at full load and a speed of 2200 rpm

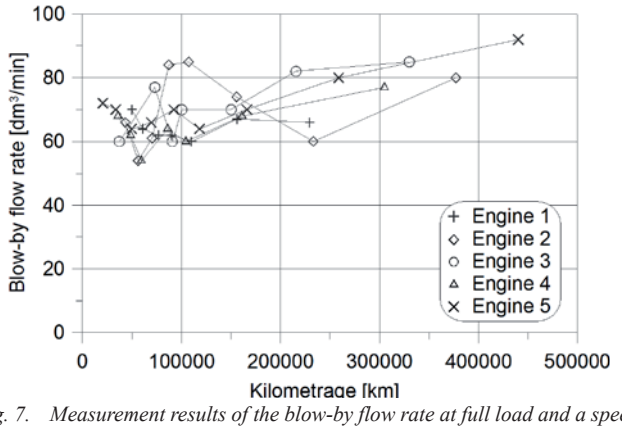

Fig. 7. Measurement results of the blow-by flow rate at full load and a speed of 2800 rpm

changes in a selected diagnostic parameter versus distance traveled were not always monotonic, even in the case of the same object. For that reason, the measurement results were analyzed as a whole for all the investigated cylinders and engines, using statistical methods.

4. Empirical model

The developed models should provide information on the mean value of a selected parameter in time $P(t)$ and the ranges of the parameter P with an assumed probability p. The range can be described by means of the following equations:

$$P_d(t) = P(t) - \Delta P(t)\,, \tag{1}$$

$$P_g(t) = P(t) + \Delta P(t)\,, \tag{2}$$

where: $P(t)$ is the mean value of the diagnostic parameter, $P_d(t)$ and $P_g(t)$ are the lower and upper limits of the confidence interval, respectively, $\Delta P(t)$ is a width of the confidence interval for the assumed significance level, while t is the distance traveled (Figs. 8).

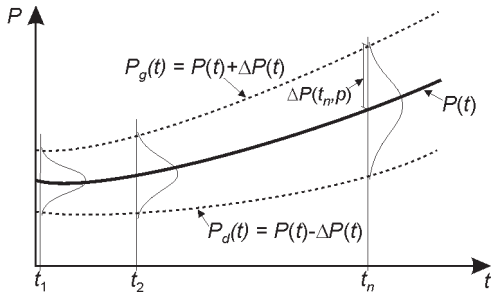

Fig. 8. Stochastic model of changes in the diagnostic parameter P during operation

It was assumed that mean changes in a given diagnostic parameter $P(t)$ will be best illustrated by a regression curve determined based on all measurement results. The analyzed regression curves included linear and exponential functions, as well as a second order polynomial. To describe the mean changes in a given parameter, the function with the highest coefficient of determination R^2 was selected. Table 1 lists the linear regression equations and selected curvilinear regression equations, as well as determination coefficient values.

In order to determine the scatter of the results around the mean value, standard deviations of the results obtained for different ranges of distances traveled were calculated. Determining the kilometrage ranges, the number of available measurements was taken into account – there were more measurements taken for low kilometrage. The following kilometrage ranges were adopted: 0-30,000, 30,000-70,000, 70,000-120,000, 120,000-200,000, 200,000-300,000, 300,000-400,000 and over 400,000 km, yet it should be noted that in the case of the blow-by flow rate the last two ranges were combined due to the small number of available measurement results. Figs. 9 and 10 illustrate the basic descriptive statistics for particular kilometrage ranges for cylinder leakage and compression pressure.

The standard deviation values changed with the distance traveled in an irregular manner (Figs. 9–11). In order to determine the limits of confidence intervals, it was assumed that the standard deviation would change linearly with the distance traveled. Using the least squares method, relevant regression lines were determined. Fig. 11 shows the standard deviation values for particular ranges and regression lines for compression pressure and cylinder leakage. The regression line equations of the standard deviations calculated in this way for all the investigated diagnostic parameters are listed in Table 1.

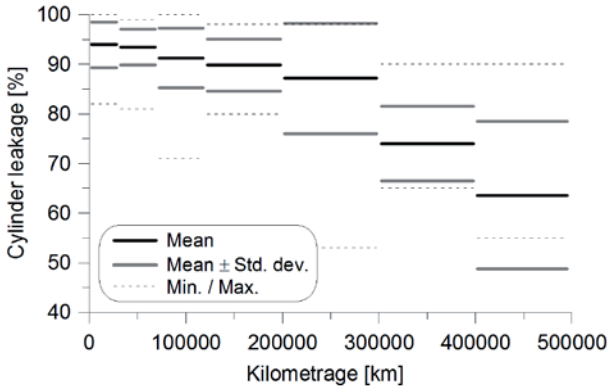

Fig. 9. Cylinder leakage versus kilometrage

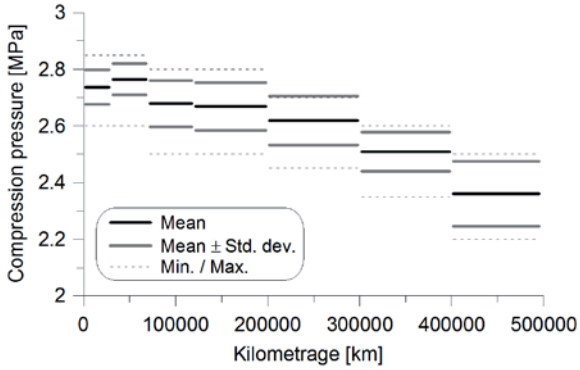

Fig. 10. Compression pressure versus kilometrage

It was assumed that the mean value of a given parameter is:

$$P(t) = y(t) \tag{3}$$

where $y(t)$ is the regression equation from column 2 in Table 1, for which the determination coefficient R^2 reached the highest value.

Based on the Kolmogorov-Smirnov tests for a confidence level of 0.99, it can be stated that the measurement results of compression pressure and cylinder leakage in particular kilometrage ranges corresponded to the normal distribution. Assuming that the measurement results have normal distributions, the confidence interval limits at a significance level of 0.05 are determined by the following functions:

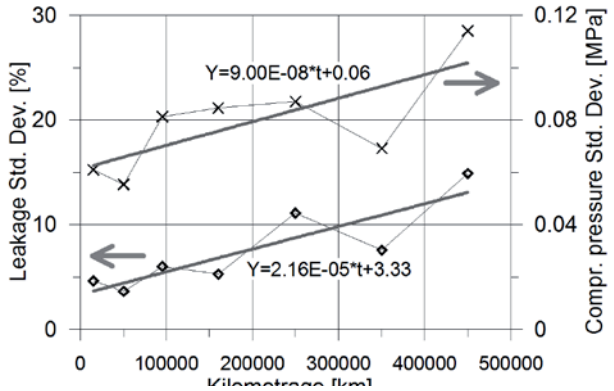

Fig. 11. Standard deviations of cylinder leakage and compression pressure

$$P_d(t) = P(t) - \Delta P(t) = y(t) - 2 \cdot Y(t)\,, \tag{4}$$

$$P_g(t) = P(t) + \Delta P(t) = y(t) + 2 \cdot Y(t)\,, \tag{5}$$

where $Y(t)$ is the regression equation of the standard deviation listed in Table 1.

The models of changes in the diagnostic parameters characterizing the combustion chamber tightness determined thereby and the marked limits of the confidence intervals at a level of 95% are shown in Figs. 12-18 (continuous lines). The thin dotted lines in Figs. 12-18 mark the rival models of changes in the diagnostic parameters versus kilometrage: the linear models for the cases when the curvilinear models were selected and the curvilinear models when the linear models were selected.

5. Discussion

The mean values of all the analyzed parameters were changing with the distance traveled, thus indicating the deterioration of the engine technical condition. Nevertheless, the dynamics and character of these changes differed for every parameter. In order to characterize the parameter change dynamics depending on the distance traveled, the following coefficient was employed:

$$x_d = \frac{P(t_2) - P(t_1)}{P(t_1)} \cdot 100\%\,, \tag{6}$$

where $P(t_2)$ is the value of a given diagnostic parameter calculated from the equation (3) for the distance traveled t_2 that is the section end where the parameter change dynamics is evaluated, while $P(t_1)$ is the parameter value for t_1 which is the beginning of this section.

The mean value of the compression pressure after 500,000 km decreased only by 16% compared to its value at zero kilometrage. The mean value of the cylinder leakage for the same traveled distance decreased by 42%, while the blow-by flow rates increased significantly, i.e. by 116% at idle run, whereas the increase at full load was as follows: 117% at 1570 rpm, 149% at 1880 rpm, 194% at 2200 rpm and 51% at 2800 rpm. A much lower relative increase in the blow-by flow rate at full load and a crankshaft speed of 2800 rpm

Tab. 1. Results of regression analysis for particular diagnostic parameters

Diagnostic parameter	Regression equation	Coefficient of determination R^2	Regression equation for standard deviation
1	2	3	4
Cylinder leakage	y = -1,58E-10t² - 5,09E-07t + 93,7 y = -5,75E-05t + 96,3	0,516 0,463	Y = 2,16E-05t + 3,33
Compression pressure	y = -8,41E-13t² - 4,60E-07t + 2,76 y = -7,56E-07t + 2,77	0,502 0,493	Y = 9,00E-08t + 0,06
Blow-by flow rate at idle run	y = 5,88E-05t + 25,3 y = 2,53E+01e$^{1,72E-06t}$	0,372 0,366	Y = -9,12E-07t + 7,70
Blow-by flow rate at 1570 rpm	y = 7,41E-05t + 31,8 y = 3,25E+01e$^{1,65E-06t}$	0,574 0,512	Y = -2,65E-06t + 6,15
Blow-by flow rate at 1880 rpm	y = 8,57E-05t + 28,8 y = 2,93E+01e$^{2,00E-06t}$	0,421 0,409	Y = -1,50E-06t + 10,2
Blow-by flow rate at 2200 rpm	y = 1,01E-04t + 26,0 y = 3,99E-12x² + 1,00E-04x + 26,0	0,567 0,566	Y = -1,30E-05t + 11,1
Blow-by flow rate at 2800 rpm	y = 1,17E-10x² + 7,49E-06x + 64,8 y = 5,47E-05t + 61,8	0,397 0,374	Y = 4,21E-06t + 6,13

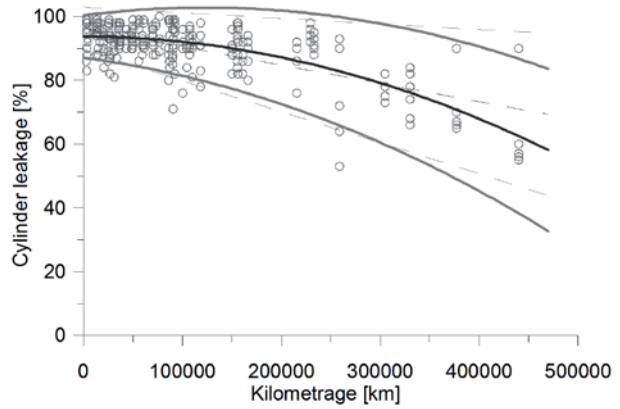

Fig. 12. Changes in cylinder leakage versus kilometrage

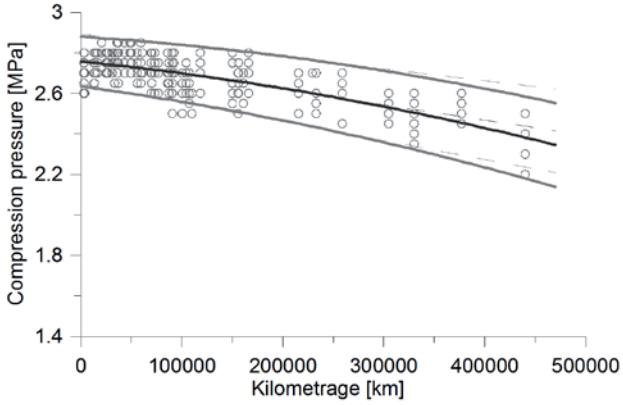

Fig. 13. Changes in compression pressure versus kilometrage

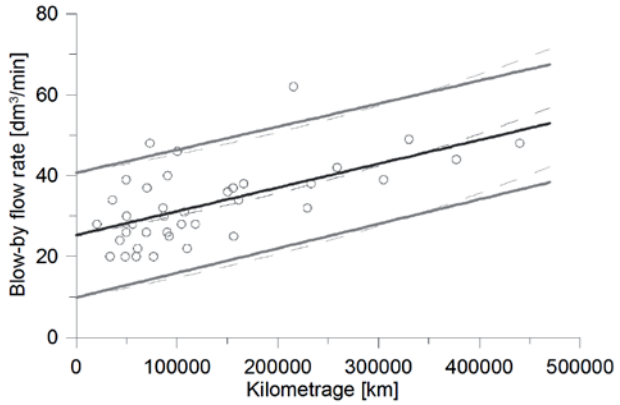

Fig. 14. Changes in the blow-by flow rate at idle run versus kilometrage

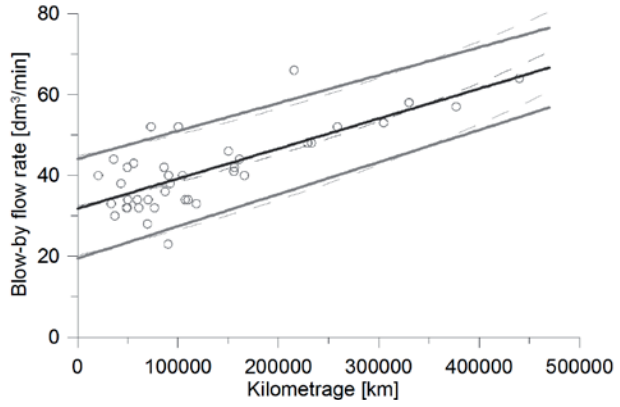

Fig. 15. Changes in the blow-by flow rate at full load and a speed of 1570 rpm versus kilometrage

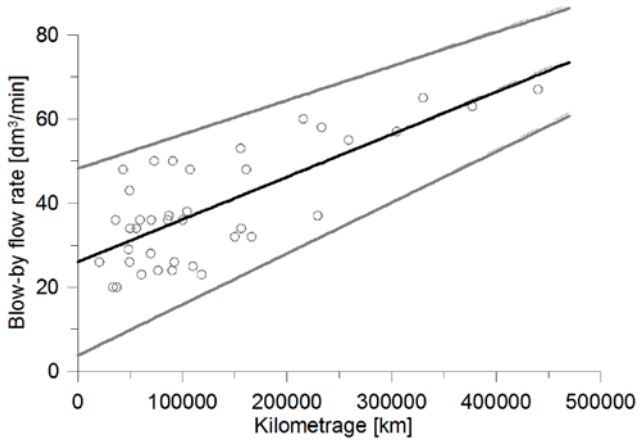

Fig. 16. Changes in the blow-by rate at full load and a speed of 1880 rpm versus kilometrage

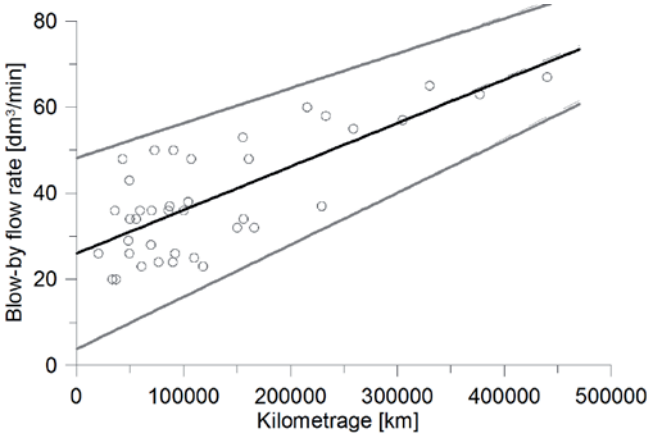

Fig. 17. Changes in the blow-by flow rate at full load and a speed of 2200 rpm versus kilometrage

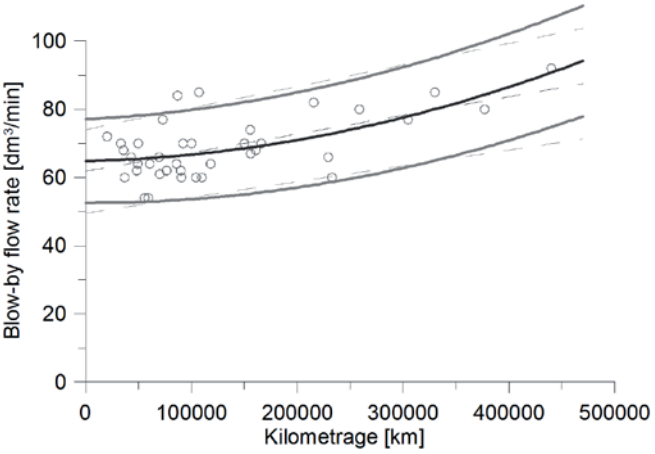

Fig. 18. Changes in the blow-by flow rate at full load and a speed of 2800 rpm versus kilometrage

resulted from approximately two-times higher absolute values of the blow-by in these engine operating conditions, compared to the blow-by flow rate in other measurement conditions.

In four cases, the obtained models are linear, while in three cases – they are non-linear. However, it is only in the case of the cylinder leakage and blow-by flow rate at a speed of 1570 rpm that the differences between the determination coefficients for the linear and curvilinear regression are significant, which proves that the selected regression curve was much better fitted. In other cases, the differences are smaller, which does not allow for a definite selection of

Table 2. Values of dynamics coefficient and coefficient of variation

	x_d calculated based on mean values from the first and last kilometrage range, [%]	x_d calculated based on curvilinear regression equation, [%] **	x_d calculated based on linear regression equation, [%] **	Coefficient of variation V, [%] (calculated for 250000 km)
Cylinder leakage	–32,3	–32,9	–25,6	10,4
Compression pressure	–14,6	–13,0	–11,6	3,18
Blow-by at idle run	71,3 *	73,4	66,6	18,7
Blow-by at 1570 rpm	64,9 *	69,6	66,8	10,9
Blow-by at 1880 rpm	78,5 *	89,6	82,9	19,6
Blow-by at 2200 rpm	100,5 *	104,9	104,1	15,3
Blow-by at 2800 rpm	31,6 *	27,7	27,1	9,71

* *for the blow-by flow rate the first range is 30000-70000 km*

** *for the tightness ratio and compression pressure, x_d was calculated for t_1 = 15000 and t_2 = 440000, while the blow-by for t_1 = 50000 and t_2 = 370000*

the parameter change character as a function of kilometrage. Owing to this, increases in the mean parameter values for successive kilometrage ranges were additionally evaluated. The changes in the cylinder leakage and compression pressure in the first period of engine operation were smaller than in the second one – exceeding 300,000 km (Figs. 9 and 10). Moreover, in the case of the compression pressure, an improvement in the initial period of operation could be observed. Also, the values of the coefficient (6) that were calculated based on the mean values of the first and last kilometrage ranges and the values of this coefficient calculated based on the linear and curvilinear regression equations were compared (Table 2).

Based on the results of the above analysis, it can be stated that the changes in the cylinder leakage and compression pressure with the distance traveled were non-linear – their rate was increasing with the kilometrage. In the case of the blow-by at the speeds of 1570 rpm and 1880 rpm, the changes were however linear. In the remaining cases, the models selected due to the determination coefficients should be adopted; yet the rival models also seem acceptable.

The scatter of the results of particular diagnostic parameters differed both in terms of their values and character of changes versus kilometrage.

The standard deviation of the cylinder leakage in the range of 0-500,000 km increased by more than three times, while in the case of the compression pressure – by 75%. The changes were smaller in the case of the blow-by, yet it should be mentioned that an increase with the distance traveled (by 34%) was observed only at a speed of 2800 rpm, whereas in the other engine operation conditions a decrease was observed, ranging from 6% to 58%. It should however be remembered that the standard deviations of the blow-by were calculated based on six times smaller number of measurements than in the case of the cylinder leakage and compression pressure, and the last two kilometrage ranges contained only four measurement results each. Taking the above into consideration, it should be stated that based on the available results it cannot be unanimously claimed whether and to what extent the scatter of the results changes with the distance traveled in the case of the blow-by flow rate. The obtained results do not undermine the hypothesis that the standard deviations of the blow-by flow rates are constant and do not depend on the distance traveled.

In order to perform the quantitative evaluation of the scatter of the results of particular diagnostic parameters, the coefficient of variation was applied:

$$V = \frac{S}{P} \cdot 100\% , \tag{7}$$

where S is the standard deviation and P is the mean value.

The values of coefficient of variation significantly changed with the distance traveled only in the case of the cylinder leakage: from 3.6% at zero kilometrage to 26% at 500,000 km – which is a sevenfold increase (a significant increase in S and a decrease in P, simultaneously). As for the remaining parameters these changes were much smaller, the mean values of V – calculated for the traveled distance of 250,000 km – can be used to evaluate the scatter of the results. Comparing the coefficient of variation of particular diagnostic parameters at 250,000 km, it should be observed that compression pressure results varied the least – by approx. 3%, while the blow-by flow rates were characterized by the highest variations – by 10-20% depending on the engine speed (Table 2).

The rates and character of changes of the analyzed diagnostic parameters as a function of distance traveled were different, despite the fact that they all characterized the combustion chamber tightness. The variations resulted from different conditions in which the engine was operating when the measurements were taken: the cylinder leakage was measured when the engine was at a standstill, the compression pressure was measured when the engine was being rotated by the starter, whereas the blow-by flow rate was measured when the engine was operating.

6. Conclusion

Based on the tests conducted on 5 trucks, the changes in combustion chamber tightness of a diesel engine during long-term operation were analyzed. The stochastic models of changes in the diagnostic parameters versus the distance traveled were determined. The mean values and standard deviations – two parameters of the instantaneous distribution of the measurement results, were calculated based on the regression analysis.

It was found that the cylinder leakage and compression pressure changed in a non-linear manner, i.e. their change rates increased with the distance traveled. The rate of change of the cylinder leakage was three times higher than that of the compression pressure – they decreased by 42% and 16% for the distance range 0–500,000 km, respectively. The standard deviation values for these diagnostic parameters also increased as a function of distance traveled – but in the case of the cylinder leakage the increase was 4 times higher than in the case of the compression pressure.

The blow-by flow rate exhibited a considerably higher dynamics of changes – it increased by three times for the distance range 0–500,000 km (at an engine speed of 2200 rpm). The changes in the blow-by flow rate as a function of the distance traveled were linear (with the exception of the blow-by flow rate at 2800 rpm). The dispersion of the results for the blow-by flow rate was higher than in the

case of the cylinder leakage and compression pressure; yet it did not increase with the distance traveled.

The determined models of changes in the diagnostic parameters characterizing the combustion chamber tightness, correlated with the data on engine wear [6], will be used as the point of reference to verify the results of the blow-by flow rate simulations based on the analytical model of the ring pack.

Acknowledgments*:*

The work was financed by the National Research Center as a research project in the years 2010-2012.

References

1. Giorgio M, Guida M, Pulcini G. A state-dependent wear process with an application to marine engine cylinder liners. Technometrics 2010; 52 (2): 172–187.
2. Jones NB, Li Y-H. A review of condition monitoring and fault diagnosis for diesel engines. Tribotest 2000; 6 (3): 267–291.
3. Kazmierczak A. Computer simulation of the new ring seal coaction in combustion engine. Industrial Lubrication and Tribology 2004; 56 (4): 210–216.
4. Kaźmierczak A. Tarcie i zużycie zespołu tłok-pierścienie-cylinder [Friction and wear of the piston-rings-cylinder unit]. Wrocław: Prace Naukowe Instytutu Konstrukcji i Eksploatacji Maszyn Politechniki Wroclawskiej [Scientific Papers of the Institute of Machine Design and Operation of the Technical University of Wroclaw] 2005, 89 (32).
5. Kazmierczak A. Physical aspects of wear of the piston-ring-cylinder set of combustion engines. Proceedings of the Institution of Mechanical Engineers, Part D: Journal of Automobile Engineering 2008; 222: 2103–2119.
6. Koszałka G, Niewczas A. Wear profile of the cylinder liner in a motor truck diesel engine. Journal of KONES Powertrain and Transport, 2007; 14 (4): 183–190.
7. Koszalka G. Application of the piston-rings-cylinder kit model in the evaluation of operational changes in blowby flow rate. Eksploatacja i Niezawodnosc – Maintenance and Reliability 2010; 4: 72–81.
8. Koszalka G, Niewczas A, Pieniak D. Reliability assessment of a truck engine based on measurements of combustion chamber tightness. Quality, Reliability, Risk, Maintenance, and Safety Engineering 2012 Conference Proceedings, IEEE 2012, pp. 995–999.
9. Kouremenos DA, Rakopoulos CD, Hountalas DT, Kouremenos AD. The maximum compression pressure position relative to top dead centre as an indication of engine cylinder condition and blowby. Energy Conversion and Management 1994; 35 (10): 857–870.
10. Lamaris VT, Hountalas DT. Validation of a diagnostic method for estimating the compression condition of direct injection diesel engines. Proceedings of the Institution of Mechanical Engineers, Part A: Journal of Power and Energy 2010; 224 (4): 517–532.
11. Lemski J. Modele zmian stanu technicznego [Models of technical state changes of objects]. Zagadnienia Eksploatacji Maszyn 2001; 1 (125): 193–210.
12. Merkisz J, Tomaszewski F, Ignatow O. Trwałość i diagnostyka węzła tłokowego silników spalinowych. Poznań: Wydawnictwo Politechniki Poznańskiej, 1995.
13. Niewczas A. Trwałość zespołu tłok-pierścienie tłokowe-cylinder silnika spalinowego. Warszawa: WNT, 1998.
14. Piekarski W. Wybrane problemy diagnostyki ciągników rolniczych w aspekcie doskonalenia ich eksploatacji. Lublin: Wydawnictwo Akademii Rolniczej, 1994.
15. Rakopoulos CD, Kosmadakis GM, Dimaratos AM, Pariotis EG. Investigating the effect of crevice flow on internal combustion engines using a new simple crevice model implemented in a CFD code. Applied Energy 2011; 88 (1): 111–126.
16. Serdecki W, Krzymień P. How the wear of cylinder liner affects the cooperation of piston-cylinder assembly of IC engine. Journal of KONES Powertrain and Transport 2012; 19 (1): 357–363.
17. Watzenig D, Steiner G, Sommer MS. Robust estimation of blow-by and compression ratio for large diesel engines based on cylinder pressure traces. Instrumentation and Measurement Technology 2008 Conference Proceedings, IEEE 2008, pp. 974–978.
18. Wolff A. Numerical analysis of piston ring pack operation. Combustion Engines 2009; 2: 128–141.

Grzegorz KOSZAŁKA
Institute of Transport, Combustion Engines and Ecology
Lublin University of Technology
ul. Nadbystrzycka 36, 20-618 Lublin, Poland
E-mail: g.koszalka@pollub.pl

Article citation info:
GAN S, SHI J. Maintenance optimization for a production system with intermediate buffer and replacement part order considered. Eksploatacja i Niezawodnosc – Maintenance and Reliability 2014; 16 (1): 140–149.

Shuyuan GAN
Jinfei SHI

MAINTENANCE OPTIMIZATION FOR A PRODUCTION SYSTEM WITH INTERMEDIATE BUFFER AND REPLACEMENT PART ORDER CONSIDERED

OPTYMALIZACJA KONSERWACJI SYSTEMU PRODUKCYJNEGO UWZGLĘDNIAJĄCA BUFOR POŚREDNI I ZAMÓWIENIA CZĘŚCI ZAMIENNYCH

Existing research on maintenance is mostly devoted to maintenance planning without considering other related issues. However, optimizing maintenance separately may lead to unexpected system cost, due to the interaction between maintenance, buffer, and replacement parts. In this paper, a production system consisting of two serial machines and an intermediate buffer is studied. The upstream machine deteriorates with time, and the deterioration degrees are classified into different working conditions and represented by ascendant states. During the maintenance optimization for the upstream machine, the replacement part order and buffer inventory are both considered. Therefore, the system state is complex with the buffer level, machine working condition, and replacement parts taken into account together. One type of control-limit policy is applied based on system state, and then the system and decision process are modeled by discrete Markov method. Through policy-iteration algorithm, the control-limit policy is optimized for the minimal long-term expected cost rate. Numerical examples are delivered to illustrate the proposed method and for the parameter sensitivity analysis.

Keywords*: maintenance, replacement part, buffer, production system, Markov model.*

Prowadzone dotychczas badania nad konserwacją poświęcone są głównie harmonogramowi konserwacji, nie przywiązując uwagi do innych wiążących się z nią zagadnień. Jednakże, prowadzona niezależnie optymalizacja konserwacji może prowadzić do nieplanowanych kosztów z uwagi na powiązania między konserwacją, buforem i częściami zamiennymi. Niniejszy artykuł analizuje system produkcyjny składający się z dwóch urządzeń szeregowych oraz bufora pośredniego. Urządzenie na początku linii z czasem się zużywa, a stopień zużycia sklasyfikowano z uwagi na różne warunki pracy i przedstawiono za pomocą stanów wstępujących. W ramach optymalizacji konserwacji urządzenia na początku linii, rozważono zarówno zamówienia części zamiennych jak i zapasy bufora. Tak więc, na kompletny obraz stanu systemu składają się poziom bufora, warunki pracy urządzenia, oraz części zamienne. Jeden z rodzajów strategii poziomu kontroli oparty jest o stan systemu, następnie system i proces decyzyjny są modelowane przy wykorzystaniu ukrytych modeli Markowa. Strategia poziomu kontroli została zoptymalizowana dla minimalnego długofalowego i prognozowanego poziomu kosztu za pomocą algorytmu iteracji strategii. Przedstawiono również przykłady liczbowe aby zilustrować proponowaną metodę a także przeprowadzić analizę wrażliwości na zmiany parametrów.

Słowa kluczowe*: konserwacja, części zamienne, bufor, system produkcyjny, model Markowa.*

1. Introduction

In a production system, maintenance is very important for keeping machine availability and production line stability. Since the middle of last century, many categories of maintenance model have been studied [23]. However, maintenance activity is usually related to other issues in a production system, and the interaction between them may cause unexpected system cost, which makes the maintenance optimization complex [15].

Firstly, replacement part (or spare part) shortage will make the maintenance activity couldn't be implemented in time, and long-term storage of spare parts is also not suitable for the consideration of cost saving. Hence, some research was focused on maintenance optimization considering spare parts. Continuous review (s, S) policy for spare parts associated with certain maintenance strategy was studied in Zohrul Kabir and Al-Olayan [28], Vaughan [22], and Ling Wang [17]. De Smidt-Destombes et al. took into account repair capacity, spare numbers, and maintenance frequency together, to investigate availability function of k-out-of-N systems, and achieved joint optimization [4–7]. Other examples for joint optimization of maintenance and spare parts can be seen in Brezavšček and Hudoklin [1], Ilgin and Tunali [11], Huang et al. [10], and Chien [3]. Secondly, buffer capacity is usually built to cope with unexpected interruptions due to preventive maintenance or failure. Therefore, some papers were devoted to joint optimization of maintenance and buffer size [2, 14, 19, 20, 24]). Some other studies were presented for one type of control-limit policy, which initiates the preventive maintenance based on the buffer level and the deterioration degree of machine, with the buffer size predetermined [8, 12, 13, 16, 18, 21].

However, there is no research presented to optimize the maintenance strategy with the replacement part (or spare part) order and intermediate buffer simultaneously considered. It can be understood

that in a production system with the replacement parts needed to be ordered, the buffer inventory is built not only for meeting the need of the downstream machine during the maintenance duration time, but also for that during the replacement part shortage time (or the waiting time for ordered replacement part), when the upstream machine is down. Therefore, the joint consideration of replacement part (or spare part) order and buffer inventory when optimizing maintenance is necessary. This study is aimed to fill this gap, and obtain a balance between maintenance cost, inventory cost, replacement part order cost, and production cost.

In this paper, a production system containing two serial machines is considered, and an intermediate buffer is built for coping with unexpected disruptions. The upstream machine deteriorates in time, and the increasing degrees of deterioration are classified into different states. The system studied is similar to that studied by Dimitrakos and Kyriakidis [8], but differs from Dimitrakos and Kyriakidis' paper in taking into account replacement part order. For two-unit series system, the condition-based maintenance optimization without a predetermined strategy structure has been studied by our group in an early paper [26]. Some other research on machine deterioration and maintenance optimization by our group can be seen in Zhou et al.[27] and Zhang et al. [25]. Then in a recent study, we has analyzed the intermediate buffer under an age-based maintenance policy[9]. In this paper, the replacement part order and buffer inventory are both considered during the condition-based maintenance optimization for the upstream machine. Two types of replacement part order, general order and urgent order, can be chosen according to the present system state. If the machine is found at a failure state, an urgent order is carried out immediately. Otherwise, a general order is carried out when the machine state equals to or is higher than the critical state corresponding to the current buffer level. As long as the ordered replacement parts arrive, the maintenance is initiated. The maintenance may be a preventive maintenance or a corrective maintenance, which depends on the present state of the upstream machine. Therefore, the purpose of this paper can be described as finding the conditions under which to place a general order for replacement parts, with the intent of doing preventive maintenance when the replacement parts arrive, and with the corrective maintenance and urgent order for replacement parts taken into account.

In this paper, the maintenance, replacement part order and buffer inventory are all considered, therefore, the system state contains three kinds of information, and the analysis of system action and incurred cost is very complex. For this problem, the system and decision process are described by discrete Markov model, in which the replacement part state is divided into several states to represent different situations. Then based on policy-iteration algorithm, the minimal long-term expected cost rate is achieved, and the critical machine states corresponding to different buffer levels, i.e. the control parameters for judging whether or not carrying out a general replacement part order, are also determined.

The rest of this paper is organized as following. In section 2, the system is described. In section 3, the mathematic formulation is presented. The policy-iteration algorithm in this paper is introduced in section 4. Then in section 5, some numerical examples are delivered for illustrating the proposed method and analyzing parameter sensitivity. Finally the conclusion is given in section 6.

2. System descriptions

In the production system, two serial machines and an intermediate buffer are involved. The downstream machine A_2 operates at a constant rate p_2. The upstream machine A_1 operates at a rate $p_1 + p_2$ if the buffer is not full. As long as the buffer is full, the operation rate of A_1 is decreased to p_2. A practical example of the production system may be a work center consisting of an automated part feeder, an automated drilling machine, and an intermediate buffer, or be an assembly work shop consisting of a semi-finished good feeder, an assembly machine, and an intermediate buffer. In this study, the upstream machine A_1 deteriorates with time, and the maintenance planning and replacement part order are considered for it (see fig. 1).

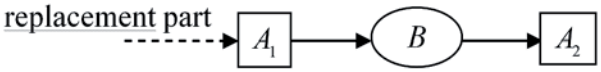

Fig. 1. The production system studied

2.1. Notation

A_1	the upstream machine
A_2	the downstream machine
p_1	the buffer accumulation speed
p_2	the buffer consumption speed or the operation rate of machine A_2
B	the buffer or the buffer size
λ_1/λ_2	the parameter of probability distribution function of preventive maintenance duration time/ corrective maintenance duration time
c_p/c_f	the cost of preventive maintenance / corrective maintenance during a unit time (say one day)
λ_3/λ_4	the parameter of probability distribution function of general replacement part order lead time / urgent replacement part order lead time
c_{go}/c_{uo}	the cost of a general replacement part order/ an urgent replacement part order
h	the inventory holding cost per unit per unit time (say one day)
c_i	the production cost of machine A_1 when it is at state i and operates at a rate of $p_1 + p_2$ during a unit time (say one day)
c_i'	the production cost of machine A_1 when it is at state i and operates at a rate of p_2 during a unit time (say one day)
p_{ij}	the transition probability of the machine state moving from state i to state j during a unit time (say one day)
c	the shortage cost during a unit time (say one day)
W	the state space of the system
w	the system state

2.2. The assumption and policy

In this study, the deterioration and maintenance of the upstream machine is considered, and one type of control-limit policy is implemented, which takes into account maintenance, replacement part order, and intermediate buffer. The purpose of this study is optimizing the control-limit policy to obtain the minimal long-term expected cost rate, which involves the buffer inventory holding cost, replacement part order cost, maintenance cost, production cost, and shortage cost.

At each time epoch, if machine A_1 doesn't fail, and the machine state exceeds the critical value corresponding to the current buffer level, a general replacement part order is carried out. If machine A_1 is found to encounter failure, an urgent replacement part order is carried out. As soon as the ordered replacement parts arrive, the maintenance is initiated. If machine A_1 doesn't fail at the arrival time of the replacement part, a preventive maintenance is implemented. If machine A_1 is found failed at the arrival time of the replacement part, a cor-

rective maintenance is required. Both the preventive maintenance and corrective maintenance can restore machine A_1 to a new state. Additionally, it is supposed that the preventive maintenance and corrective maintenance of machine A_1 are both non-preemptive (i.e. the maintenance can't be interrupted), and the duration time lengths of them follow geometrical distribution with the probability of success as λ_1 and λ_2 respectively. If the maintenance is not finished when the buffer is exhausted, a shortage cost is incurred. Conversely, if the buffer is not empty when the maintenance is finished, machine A_1 is kept idle until the buffer is exhausted rather than being resumed to work immediately. The allowing of idle time of machine A_1 is reasonable for the reduction of production cost [12]. According to the policy applied, it is seen that the interval between the time epochs when the maintenance is finished and the buffer is exhausted is a renewal cycle.

2.3. System state space

It is assumed that the system state is inspected at discrete equidistant time epochs t =0, 1, …(say every day), and a decision is made for machine A_1. The system state contains the information of machine state 'i', buffer level 'b', and replacement parts 's', which is denoted by $w=(i,b,s)$. A decision is selecting an action 'a' from five possible actions $\{0,1,2,3,4\}$, depending on the current system state and the control parameters involved in the control-limit policy. The action $a=0$ represents doing nothing (leaving the machine A_1 working, failure, or idle). The action $a=1$ and action $a=2$ represent carrying out a general replacement part order and carrying out an urgent replacement part order respectively. The action $a=3$ and action $a=4$ represent doing preventive maintenance and doing corrective maintenance respectively.

The states of machine A_1 are classified into M+2 states 0, 1, …, M+1, corresponding to ascending deterioration degrees. State 0 represents a new machine, or the machine operates as new. State M+1 represents a failure machine. The other states represent the intermediate working conditions. If the working condition of machine A_1 is found to be at state i $(0\le i\le M+1)$ at a time epoch, the state j $(0\le j\le M+1)$ can be reached at the next time epoch with the transition probability p_{ij}, which only depends on the state i and state j. It is supposed that the state M+1 can be reached from any state with non-zero probability during a unit time, i.e. $p_{iM+1}>0, 0\le i\le M+1$, and machine A_1 can not improve on its own, i.e. $p_{ij}=0, j<i$. The production cost rate of machine A_1 at state i $(0\le i\le M)$ is assumed to be c_i when it operates at rate p_1+p_2 and assumed to be c_i' when it operates at rate p_2.

The intermediate buffer size is predetermined to be B. If the buffer level is b $(0\le b\le B)$ with the machine state found at i $(0\le i\le M)$ at a time epoch, it will change to $\min(B,b+p_1)$ at the next time epoch. If the buffer level is b $(0\le b\le B)$ with the machine state found at M+1 at a time epoch, it will change to $\max(0,b-p_2)$ at the next time epoch.

It is supposed that two types of replacement part order policy, general order and urgent order, can be chosen for different lead time requirements. It is assumed that only one replacement part is needed for a preventive maintenance or a corrective maintenance, which can easily be released according to practical condition. In a renewal cycle, the replacement part order cost is c_{go} due to general order or c_{uo} due to urgent order. The lead times of the two types of replacement part order both follow geometrical distribution, and the arrival rates of replacement part under general order and urgent order are λ_3 and λ_4 respectively. It is reasonable that the value of c_{uo} is larger than that of c_{go}, and the value of λ_4 is larger than that of λ_3. The replacement part state is described by $s\in\{0,go,uo,1\}$. State '0' represents the situation that the replacement part is not ordered, or the situation that the replacement part has been consumed by the maintenance and machine A_1 is idle waiting for the buffer to be exhausted. State 'go' represents the situation that a general replacement part order is carried out, but the replacement part hasn't arrived. State 'uo' represents the situation that an urgent replacement part order is carried out, but the replacement part hasn't arrived. State 1 represents the situation that the replacement part has arrived, but the maintenance hasn't be finished.

Additionally, state 'PM' and state 'ID' are given to represent the situations that machine A_1 is during a preventive maintenance and during an idle state respectively. Therefore, the state space of the system is as following:

$$W=\{0,...,M+1\}\times\{0,...,B\}\times\{0,go,uo,1\}\cup\{(PM,b,1):0\le b\le B\}\cup\{(ID,b,0):0\le b\le B-p_2\} \quad (1)$$

Notation: because machine A_1 could not improve by itself, some states involved in eq. (1) can't be reached from any other state. The actual system states that can be accessible under a control-limit policy are obtained by eliminating the inaccessible states from state space W, based on the policy and the system parameter setting.

3. The mathematical formulation

Based on the system descriptions in section 2, the mathematic formulation is presented for describing the cost incurred by feasible actions at different system states. When the current system state is found at $w=(i,b,s)$ $(w\in W)$ and certain action is chosen, the expected cost from the current time epoch to the following time when the maintenance is finished and the buffer is exhausted (i.e. to the end of the current renewal cycle) is described by $C(i,b,s)$. Therefore, the mathematic formulation is as following:

$$C(i,b,0)\ (0\le i\le M, 0\le b<B)=\begin{cases} c_i+hb+\sum_{j=i}^{M+1}p_{ij}C(j,\min(b+p_1,B),0), & a=0\\ c_i+hb+c_{go}+\lambda_3\sum_{j=i}^{M+1}p_{ij}C(j,\min(b+p_1,B),1)+(1-\lambda_3)\sum_{j=i}^{M+1}p_{ij}C(j,\min(b+p_1,B),go), & a=1\end{cases} \quad (2)$$

$$C(i,B,0)\ (0\le i\le M)=\begin{cases} c_i'+hB+\sum_{j=i}^{M+1}p_{ij}C(j,B,0), & a=0\\ c_i'+hB+c_{go}+\lambda_3\sum_{j=i}^{M+1}p_{ij}C(j,B,1)+(1-\lambda_3)\sum_{j=i}^{M+1}p_{ij}C(j,B,go), & a=1\end{cases} \quad (3)$$

$$C(M+1,b,0)\ (0\le b\le B)=hB+c_{uo}+c\max(0,p_2-b)/p_2+\lambda_4C(M+1,\max(0,b-p_2),1)+(1-\lambda_4)C(M+1,\max(0,b-p_2),uo),\quad a=2 \quad (4)$$

$$C(i,b,go)\ (0\le i\le M, 0\le b<B)=c_i+hb+\lambda_3\sum_{j=i}^{M+1}p_{ij}C(j,\min(b+p_1,B),1)+(1-\lambda_3)\sum_{j=i}^{M+1}p_{ij}C(j,\min(b+p_1,B),go),\quad a=0$$

$$C(i,B,go)\ (0\le i\le M)=\ c_i'+hB+\lambda_3\sum_{j=i}^{M+1}p_{ij}C(j,B,1)+(1-\lambda_3)\sum_{j=i}^{M+1}p_{ij}C(j,B,go),\qquad a=0$$

$$C(M+1,b,go)\ (0\le b\le B)=\ hb+c\max(0,p_2-b)/\ p_2+\lambda_3C(M+1,\max(0,b-p_2),1)$$
$$+(1-\lambda_3)C(M+1,\max(0,b-p_2),go),\qquad a=0$$

$$C(M+1,b,uo)\ (0\le b\le B)=\ hb+c\max(0,p_2-b)/\ p_2+\lambda_4C(M+1,\max(0,b-p_2),1)$$
$$+(1-\lambda_4)C(M+1,\max(0,b-p_2),uo),\qquad a=0$$

$$C(i,b,1)\ (0\le \mathrm{i}\le M,0\le b\le B)=\ C(PM,b,1),\quad a=3 \tag{5}$$

$$C(M+1,b,1)\ (p_2<b\le B)=\ c_f+hb+\lambda_2C(ID,b-p_2,0)+(1-\lambda_2)C(M+1,b-p_2,1),\qquad a=4$$

$$C(M+1,b,1)\ (0\le b\le p_2)=\ c_p+hb+c(p_2-b)/\ p_2+\lambda_2C(0,0,0)+(1-\lambda_2)C(M+1,0,1),\ a=4$$

$$C(PM,b,1)\ (p_2<b\le B)=\ c_p+hb+\lambda_1C(ID,b-p_2,0)+(1-\lambda_1)C(PM,b-p_2,1),\quad a=3 \tag{6}$$

$$C(PM,b,1)\ (0\le b\le p_2)=\ c_p+hb+c(p_2-b)/\ p_2+\lambda_1C(0,0,0)+(1-\lambda_1)C(PM,0,1),\quad a=3 \tag{7}$$

$$C(ID,b,0)\ (p_2<b\le B)=\ hb+C(ID,b-p_2,0),\quad a=0$$

$$C(ID,b,0)\ (0\le b\le p_2)=\ hb+c(p_2-b)/\ p_2+C(0,0,0),\ a=0$$

In eq. (2) and eq. (3), the upper expression on the right of the equal sign represents that the action 0 (do nothing) is adopted, and the lower expression represents that the action 1 (carrying out a general replacement part order) is adopted, when the current system state is found at state $(i,b,0)\ (0\le i\le M,0\le b<B)$ and state $(i,B,0)\ (0\le i\le M)$ respectively. In eq. (4), the expression on the right of the equal sign represents that the action 2 (carrying out an urgent replacement part order) is adopted when machine A_1 fails and no replacement part is ordered. In eq. (5), the preventive maintenance is initiated, when the ordered replacement part has arrived and the machine state is not at M+1. In eq. (6), the action 3 (carrying out the preventive maintenance) is adopted when the machine state is found during preventive maintenance ($i=PM,s=1$). In eq. (7), the action 3 is adopted, and the shortage cost from the current time epoch to the next is calculated by $c(p_2-b)/p_2$, with the buffer level b is equal to or smaller than the operation rate of machine A_2. Other equations can be explained similar to eq. (2) ~ eq. (7).

4. The policy-iteration algorithm

Based on section 2, the control-limit policy applied is described by B+1 control parameters, respectively corresponding to different buffer levels, i.e. 0, 1, …, B. For clarity, the B+1 control parameters are denoted by $cp_0,cp_1,...,cp_B$. During each renewal cycle, when the machine state i $(i\le M)$ is found to exceed the control parameter corresponding to current buffer level, a general replacement part order is carried out. For example, the interpretation of cp_2=5 is that if the buffer inventory between the machines is equal to 2, a general replacement part order should be carried out only if the current machine state exceeds 5. If the control parameter is set as M+1 for buffer level b, it means that the replacement part order will not be carried out when the buffer level is b, unless machine A_1 encounters failure.

In this paper, the policy-iteration algorithm is applied to obtain the minimal long-term expected cost rate and determine the related B+1 control parameters. The main method of this algorithm is successively generating a new policy with smaller long-term expected cost rate than the current one, until the two neighboring policies is the same, or their long-term expected cost rates are of equal values.

Therefore, the steps of policy-iteration algorithm for the optimal control-limit policy in this paper are as following:

Step 1

Set the system parameters, including the machine parameters ($M,p_1,p_2,p_{ij},c_i,c_i'$), maintenance parameters ($\lambda_1,\lambda_2,c_p,c_f$), buffer parameter ($B,h$), shortage parameter ($c$), and replacement part parameters ($\lambda_3,\lambda_4,c_{go},c_{uo}$). Set the initial policy as $(cp_0,cp_1,...,cp_B)=(M+1,M+1,...,M+1)$.

Step 2

Eliminate the inaccessible system states from state space W in eq. (1), based on the system description and parameter setting. The actual system state space or accessible system state space is denoted as W'.

Step 3

Based on the current policy, determine which action is chosen when the system is found at each accessible state. Then solve the following equations, and obtain the value of g and values of $v(i,b,s)$ for all states in W'. g is the long-term average cost rate for the current policy:

$$v(i,b,0)\ (0\le i\le M,0\le b<B)=$$
$$\begin{cases} v_0(i,b,0)=c_i+hb-g+\sum_{j=i}^{M+1}p_{ij}v(j,\min(b+p_1,B),0), & a=0 \\ v_1(i,b,0)=c_i+hb+c_{go}-g+\lambda_3\sum_{j=i}^{M+1}p_{ij}v(j,\min(b+p_1,B),1)+(1-\lambda_3)\sum_{j=i}^{M+1}p_{ij}v(j,\min(b+p_1,B),go), & a=1 \end{cases} \tag{8}$$

$$v(i,B,0)\ (0\le i\le M)=\begin{cases} v_0(i,B,0)=c_i'+hB-g+\sum_{j=i}^{M+1}p_{ij}V(j,B,0), & a=0 \\ v_1(i,B,0)=c_i'+hB+c_{go}-g+\lambda_3\sum_{j=i}^{M+1}p_{ij}V(j,B,1)+(1-\lambda_3)\sum_{j=i}^{M+1}p_{ij}V(j,B,go), & a=1 \end{cases} \tag{9}$$

$$
\begin{aligned}
v(M+1,b,0)\ (0\le b\le B) &= hB + c_{uo} - g + c\max(0,p_2-b)/p_2 + \lambda_4 v(M+1,\max(0,b-p_2),1)\\
&\quad + (1-\lambda_4)v(M+1,\max(0,b-p_2),uo), \qquad a=2\\
v(i,b,go)\ (0\le i\le M, 0\le b<B) &= c_i + hb - g + \lambda_3\sum_{j=i}^{M+1} p_{ij}V(j,\min(b+p_1,B),1)\\
&\quad + (1-\lambda_3)\sum_{j=i}^{M+1} p_{ij}V(j,\min(b+p_1,B),go), \qquad a=0\\
v(i,B,go)\ (0\le i\le M) &= c_i' + hB - g + \lambda_3\sum_{j=i}^{M+1} p_{ij}V(j,B,1) + (1-\lambda_3)\sum_{j=i}^{M+1} p_{ij}V(j,B,go), \qquad a=0\\
v(M+1,b,go)\ (0\le b\le B) &= hb + c\max(0,p_2-b)/p_2 - g + \lambda_3 v(M+1,\max(0,b-p_2),1)\\
&\quad + (1-\lambda_3)v(M+1,\max(0,b-p_2),go), \qquad a=0\\
v(M+1,b,uo)\ (0\le b\le B) &= hb + c\max(0,p_2-b)/p_2 - g + \lambda_4 v(M+1,\max(0,b-p_2),1)\\
&\quad + (1-\lambda_4)v(M+1,\max(0,b-p_2),uo), \qquad a=0\\
v(i,b,1)\ (0\le i\le M, 0\le b\le B) &= v(PM,b,1), \quad a=3\\
v(M+1,b,1)\ (p_2<b\le B) &= c_f + hb - g + \lambda_2 v(ID,b-p_2,0) + (1-\lambda_2)v(M+1,b-p_2,1), \qquad a=4\\
v(M+1,b,1)\ (0\le b\le p_2) &= c_p + hb - g + c(p_2-b)/p_2 + \lambda_2 v(0,0,0) + (1-\lambda_2)v(M+1,0,1), \quad a=4\\
v(PM,b,1)\ (p_2<b\le B) &= c_p + hb - g + \lambda_1 v(ID,b-p_2,0) + (1-\lambda_1)v(PM,b-p_2,1), \quad a=3\\
v(PM,b,1)\ (0\le b\le p_2) &= c_p + hb - g + c(p_2-b)/p_2 + \lambda_1 v(0,0,0) + (1-\lambda_1)v(PM,0,1), \quad a=3\\
v(ID,b,0)\ (p_2<b\le B) &= hb - g + v(ID,b-p_2,0), \quad a=0\\
v(ID,b,0)\ (0\le b\le p_2) &= hb - g + c(p_2-b)/p_2 + v(0,0,0), \quad a=0\\
v(0,0,0) &= 0
\end{aligned}
\tag{10}
$$

The adding of Eq. (10) makes the number of the equations and that of the unknowns equal. The system state (0, 0, 0) is arbitrary selected.

Step 4

For each $b\ (0\le b\le B)$, calculate the values of $v_0(M,b,0)$ and $v_1(M,b,0)$ according to eq. (8) or eq. (9). If $v_0(M,b,0)<v_1(M,b,0)$, change the value of cp_b to M+1. Otherwise, calculate the values of $v_0(M-1,b,0)$ and $v_1(M-1,b,0)$, and compare them. If $v_0(M-1,b,0)<v_1(M-1,b,0)$, change the value of cp_b to M. Otherwise, calculate the values of $v_0(M-2,b,0)$ and $v_1(M-2,b,0)$, and compare them. Do the calculation and comparison as above until finding $v_0(M-x,b,0)<v_1(M-x,b,0)\ (0\le x\le M)$ and changing the value of cp_b to $M-x+1$.

If the inequality $v_0(M-x,b,0)\ge v_1(M-x,b,0)$ is obtained for all $x\ (0\le x\le M)$, change the value of cp_b to 0. After the above process is repeated for all $b\ (0\le b\le B)$, a new policy is generated.

Step 5

Compare the new policy and the last policy. If the two policies are the same or the long-term expected cost rates of them are of equal values, stop the iteration. Then the optimal policy is the last two policies, and the minimal long-term expected cost rate is the value of g under them. Otherwise, treat the new policy as the current one and return to step 3 to repeat the iteration.

5. Numerical examples

In this paper, the maintenance planning, buffer inventory, and replacement part order are taken into account for optimizing the long-term expected cost rate and control-limit policy. In order to investigate the influence of system parameters on the optimization result, numerical examples are delivered under various situations with different maintenance parameters, replacement part order parameters, buffer inventory parameters, and shortage parameters.

5.1. Sensitivity analysis for maintenance parameter

The system parameters related to maintenance are λ_1, λ_2, c_p, and c_f. The change of them will cause preference variation of the optimal policy. In this section, the minimal long-term expected cost rate and the optimal policy are investigated in different numerical examples with increasing values of c_p and c_f respectively.

Numerical example 1: changing the corrective maintenance cost rate c_f

The system parameters are set as following. M=5, B=4, $\lambda_1=0.7$, $\lambda_2=0.5$, $\lambda_3=0.6$, $\lambda_4=0.9$, $c_p=4$, $c_g=5$, $c_u=8$, $h=0.7$, $c=10$, $c_i=0.6(i+1)\ (0\le i\le M)$, $c_i'=0.2(i+1)\ (0\le i\le M)$, $p_1=1$, $p_2=1$. The transition probability from state i to state j of machine A_1 is described by the element at the crossing of row i+1 and column j+1 in matrix P:

$$
P=\begin{bmatrix}
0.2 & 0.35 & 0.23 & 0.15 & 0.06 & 0.01\\
0 & 0.2 & 0.36 & 0.3 & 0.12 & 0.02\\
0 & 0 & 0.18 & 0.5 & 0.26 & 0.06\\
0 & 0 & 0 & 0.14 & 0.66 & 0.2\\
0 & 0 & 0 & 0 & 0.1 & 0.9\\
0 & 0 & 0 & 0 & 0 & 1
\end{bmatrix}
$$

The corrective maintenance cost rate c_f is changed from 4 to 8 in the increment of 0.5. For each c_f, the optimal control-limit policy is obtained, and the long-term expected cost rate g is minimized, by using the method in section 4. The result is shown in table 1.

Numerical example 2: changing the preventive maintenance cost rate c_p

The system parameters are set as numerical example 1, except that the value of c_f is set as 6, and the value of c_p is changed from 2 to 6 in the increment of 0.5 (it is reasonable to assume that the preventive maintenance cost rate is not higher than the corrective maintenance cost rate). For each c_p, the optimal control-limit policy is obtained, and the long-term expected cost rate g is minimized, by using the method in section 4. The result is shown in table 2.

Table 1. the optimization result of changing the corrective maintenance cost rate c_f

c_f	cp_0	cp_1	cp_2	cp_3	cp_4	min g
4.0	5	2	1	1	0	4.3612
4.5	5	2	1	0	0	4.4273
5.0	5	2	1	0	0	4.4933
5.5	5	2	1	0	0	4.5593
6.0	5	2	1	0	0	4.6253
6.5	5	2	1	0	0	4.6914
7.0	5	2	1	0	0	4.7574
7.5	5	2	1	0	0	4.8234
8.0	5	1	1	0	0	4.8840

Table 2. the optimization result of changing the preventive maintenance cost rate c_p

c_p	cp_0	cp_1	cp_2	cp_3	cp_4	min g
2.0	5	1	0	0	0	4.3011
2.5	5	1	0	0	0	4.3893
3.0	5	1	0	0	0	4.4775
3.5	5	2	1	0	0	4.5564
4.0	5	2	1	0	0	4.6253
4.5	5	2	1	0	0	4.6943
5.0	5	2	1	0	0	4.7632
5.5	5	3	2	1	1	4.8265
6.0	5	3	2	1	1	4.8783

In each optimal policy inside of table 1 and table 2, the control parameters corresponding to higher buffer levels are smaller than or equal to those corresponding to lower buffer levels. It is for the reason that the replacement part order should be carried out when the buffer level is too high or the value of machine state is too large, to prevent too much inventory holding cost or the failure of machine. However, for the same buffer inventory level, the optimal control parameter is gradually decreased when increasing c_f (see table 1), and gradually increased when increasing c_p (see table 2). It can be explained that when the value of c_f becomes larger, the cost incurred by corrective maintenance also becomes larger. Then the replacement part is expected to be ordered earlier for larger possibility to perform preventive maintenance. Similarly, when the value of c_p becomes larger, the cost incurred by preventive maintenance also becomes larger. Then the replacement part is not expected to be ordered too early for frequent preventive maintenance.

The minimal long-term average cost is found becoming larger when increasing c_f or c_p. It can be explained that the long-term expected cost rate is equal to the ratio of the expected total cost in a renewal cycle and the expected time length of the renewal cycle, and the maintenance cost is an important section of the total cost. Additionally, it is seen that the increments between the adjacent minimal long-term expected cost rates are almost to be same values (about 0.066) in table 1. And some increments in table 2 also seem to be stable. In order to investigate the character of the increment of minimal long-term expected cost rate when the value of c_f or c_p is increased by a determined quantity and to be much larger, numerical example 3 and 4 are delivered.

Numerical example 3: The corrective maintenance cost rate c_f is changed from 4 to 20 in the increment of 0.5. Other parameters are set as numerical example 1. For each c_f, the optimal control-limit policy is obtained, and the increments of the adjacent minimal long-term expected cost rates are calculated. The result is depicted in figure 2.

Numerical example 4: The preventive maintenance cost rate c_p is changed from 2 to 18 in the increment of 0.5. The corrective maintenance cost rate c_f is set as 18. Other parameters are set as numerical example 1. For each c_p, the optimal control-limit policy is obtained, and the increments of the adjacent minimal long-term expected cost rates are calculated. The result is depicted in figure 3.

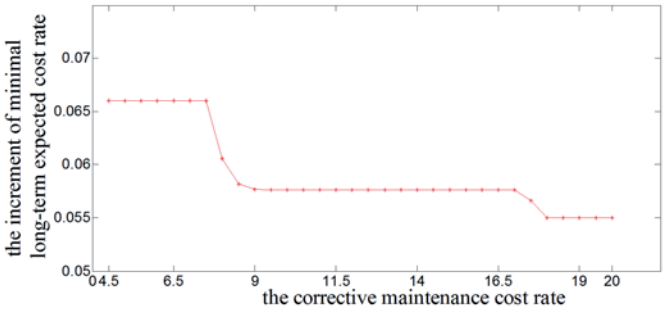

Fig. 2. The increment of minimal long-term expected cost rate when increasing c_f

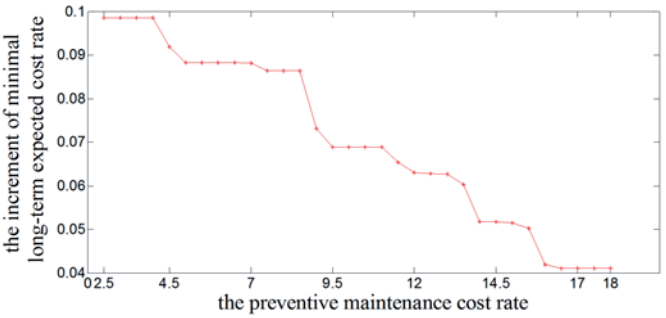

Fig. 3. The increment of minimal long-term expected cost rate when increasing c_p

In Figure 2 and Figure 3, the increment of adjacent minimal long-term expected cost rates appears to be stable in some certain ranges when the value of c_f or c_p is increased by a determined quantity. However, the increment does not always keep unchanged. When c_f or c_p is much larger, the increment gradually becomes smaller.

5.2. Sensitivity analysis for replacement part order parameter

In this section, the minimal long-term expected cost rate and the optimal policy are investigated in different numerical examples with increasing values of c_u and c_g respectively.

Numerical example 5: changing the urgent replacement part order cost c_u

The system parameters are set as numerical example 1, except that the value of c_f is set as 7, and the value of c_u is changed from 6 to 14 in the increment of 1 (it is reasonable that the urgent replacement part order cost is larger than the general replacement part order cost). For each value of c_u, the optimal control-limit policy is obtained, and the long-term expected cost rate g is minimized, by using the method in section 4. The result is shown in table 3.

Numerical example 6: changing the general replacement part order cost c_g

The system parameters are set as numerical example 5, except that the value of c_u is set as 11, and the value of c_g is changed from 2 to 10 in the increment of 1. For each value of c_g, the optimal control-limit policy is obtained, and the long-term expected cost rate g is minimized, by using the method in section 4. The result is shown in Table 4.

Table 3. the optimization result of changing the urgent replacement part order cost c_u

c_u	cp_0	cp_1	cp_2	cp_3	cp_4	min g
6	5	2	1	0	0	4.7511
7	5	2	1	0	0	4.7542
8	5	2	1	0	0	4.7574
9	5	2	1	0	0	4.7605
10	5	2	1	0	0	4.7637
11	5	2	1	0	0	4.7668
12	5	2	1	0	0	4.7700
13	5	2	1	0	0	4.7731
14	5	2	1	0	0	4.7763

Table 4. the optimization result of changing the general replacement part order cost c_g

c_g	cp_0	cp_1	cp_2	cp_3	cp_4	min g
2	5	1	0	0	0	4.2388
3	5	1	0	0	0	4.4178
4	5	1	0	0	0	4.5968
5	5	2	1	0	0	4.7668
6	5	2	1	0	0	4.9262
7	5	2	1	0	0	5.0856
8	5	2	1	0	0	5.2450
9	5	2	2	1	0	5.4017
10	5	2	2	1	0	5.5553

In each optimal policy inside of table 3 and table 4, the control parameters corresponding to higher buffer levels are smaller than or equal to those corresponding to lower buffer levels, which is similar to the situations of table 1 and table 2 for the same reason. As for the same buffer inventory level, the corresponding optimal control parameter is not changed when increasing c_u (see table 3), but gradually gets larger when increasing c_g (see table 4). Additionally, the increment between adjacent minimal long-term expected cost rates with increasing c_g is obviously larger than that with increasing c_u. It means that the optimization result is much more sensitive to c_g than to c_u. It can be explained that the economical way of restoring machine A_1 as new is performing general replacement part order and preventive maintenance, and then much more general replacement part orders should be carried out in a long term under an optimal policy. Note that although the corrective maintenance is not preferred in an optimal policy, the optimization result is still sensitive to c_f (see table 1). It is because that the machine may encounter failure when waiting for a general replacement part order, and the success rate of corrective maintenance is not high.

In order to investigate the character of the increment of minimal long-term expected cost rate when the value of c_u or c_g is increased by a determined quantity and to be much larger, numerical example 7 and 8 are delivered.

Numerical example 7: The system parameters are set as numerical example 1, except that the value of c_f is set as 7, and the value of c_u is changed from 6 to 64 in the increment of 2. For each value of c_u, the optimal control-limit policy is obtained, and the increments of the adjacent minimal long-term expected cost rates are calculated. The result is depicted in Figure 4.

Numerical example 8: the value of c_f is set as 7, and the urgent replacement part order cost is set as 32. The value of c_g is changed from 2 to 31 in the increment of 1. Other parameters are set as numerical example 1. For each value of c_g, the optimal control-limit policy is obtained, and the increments of the adjacent minimal long-term expected cost rates are calculated. The result is depicted in Figure 5.

Both in figure 4 and figure 5, the increments of minimal long-term

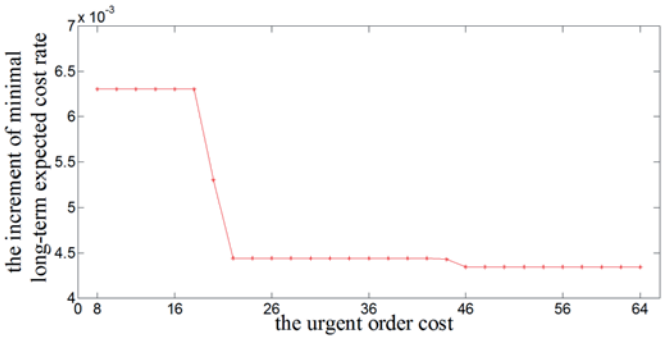

Fig. 4. The increment of minimal long-term expected cost rate when increasing c_u

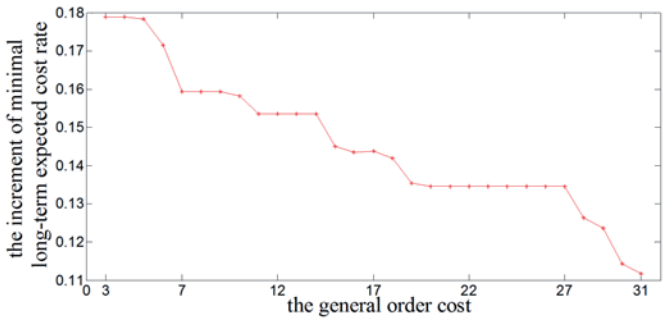

Fig. 5. The increment of minimal long-term expected cost rate when increasing c_g

expected cost rate are decreased, although in some ranges it remains unchanged. It is seen that the increment with increasing c_u is very small (lower that 0.0065, about 0.14% of the minimal long-term expected cost rate). Therefore, the minimal long-term expected cost rate can be considered as stable when the value of c_u is increased.

5.3. Sensitivity analysis for buffer inventory parameter

In this section, the minimal long-term expected cost rate and the optimal policy are investigated in numerical examples with increasing value of h.

Numerical example 9: changing the buffer inventory parameter h

The system parameters are set as numerical example 1, except that the value of c_f is set as 7, and the value of h is changed from 0.1 to 1.7 in the increment of 0.2. For each value of h, the optimal control-limit policy is obtained, and the long-term expected cost rate g is minimized, by using the method in section 4. The result is shown in table 5.

Table 5. The optimization result of changing the inventory holding cost rate h

h	cp_0	cp_1	cp_2	cp_3	cp_4	min g
0.1	5	2	2	1	1	3.8357
0.3	5	2	2	1	1	4.1494
0.5	5	2	1	0	0	4.4568
0.7	5	2	1	0	0	4.7574
0.9	5	1	0	0	0	5.0401
1.1	5	1	0	0	0	5.3110
1.3	5	0	0	0	0	5.5787
1.5	5	0	0	0	0	5.8305
1.7	5	0	0	0	0	6.0824

In each optimal policy inside of table 5, it is seen that the control parameters corresponding to higher buffer levels are smaller than or equal to those corresponding to lower buffer levels, which is similar to the situations of increasing c_f, c_p, c_u, and c_g for the same reason. For the same buffer inventory level, the control parameter is gradually decreased when h is increased. It can be explained that when the buffer inventory holding cost rate is increased, it is preferred to perform the replacement part order and the maintenance earlier under an optimal policy, to prevent too much buffer inventory holding cost.

It is found that the minimal long-term expected cost rate becomes larger with increasing h. In order to investigate the character of the increment of minimal long-term expected cost rate when the value of h is increased by a determined quantity and to be much larger, numerical example 10 is delivered.

Numerical example 10: The system parameters are set as numerical example 1, except that the value of c_f is set as 7, and the value of h is changed from 0.1 to 8.8 in the increment of 0.3. For each value of h, the optimal control-limit policy is obtained, and the increments of the adjacent minimal long-term expected cost rates are calculated. The result is depicted in figure 6.

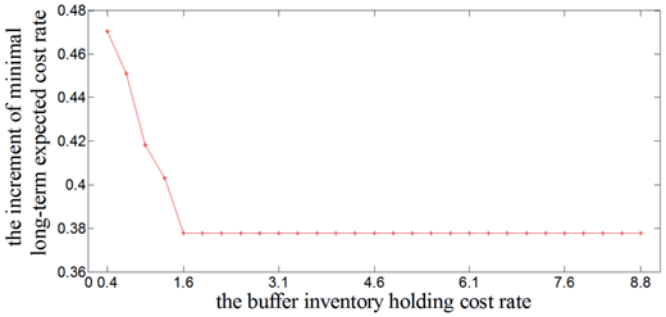

Fig. 6. The increment of minimal long-term expected cost rate when increasing h

In Figure 6, the increment of minimal long-term expected cost rate is continually decreased until the value of h is increased to 1.6. It means that when the value of h is equal to or larger than 1.6, under the parameter setting in the numerical example, the minimal long-term expected cost rate is proportional to h.

5.4. Sensitivity analysis for shortage parameter

In this section, the minimal long-term expected cost rate and the optimal policy are investigated in numerical examples with increasing value of c.

Numerical example 11: changing the shortage cost rate c

The system parameters are set as numerical example 1, except that the value of c_f is set as 7, and the value of c is changed from 3 to 27 in the increment of 3. For each value of c, the optimal control-limit policy is obtained, and the long-term expected cost rate g is minimized, by using the method in section 3. The result is shown in table 6.

Table 6. The optimization result of changing the shortage cost rate c

c	cp_0	cp_1	cp_2	cp_3	cp_4	min g
3	5	1	0	0	0	4.4215
6	5	1	1	0	0	4.5701
9	5	2	1	0	0	4.7106
12	5	2	1	0	0	4.8509
15	5	2	1	0	0	4.9912
18	5	2	1	0	0	5.1315
21	5	2	1	0	0	5.2718
24	5	2	1	0	0	5.4121
27	5	2	1	0	0	5.5523

In table 6, it is seen that in each optimal policy the control parameters corresponding to higher buffer levels are smaller than or equal to those corresponding to lower buffer levels, which is similar to the situations with increasing c_f, c_p, c_u, c_g, and h for the same reason. For certain lower buffer inventory level (b=0, 1, or 2), the corresponding control parameter is gradually increased when c is increased. It can be explained that when the shortage cost rate gets larger, it is more expected in an optimal policy to build higher buffer inventory level preparing for maintenance duration and preventing shortage. However, for certain higher buffer inventory level (b=3 or 4), the corresponding control parameter is not increased when c is increased. It is because that for higher buffer inventory levels, the replacement part order is preferred to be carried out earlier to prevent the shortage caused by machine failure.

The minimal long-term expected cost rate is found to become larger with increasing c. In order to investigate the character of the increment of minimal long-term expected cost rate when the value of c is increased by a determined quantity and to be much larger, numerical example 12 is delivered.

Numerical example 12: The system parameters are set as numerical example 1, except that the value of c_f is set as 7, and the value of c is changed from 3 to 61 in the increment of 2. For each value of c, the optimal control-limit policy is obtained, and the increments of the adjacent minimal long-term expected cost rates are calculated. The result is depicted in figure 7.

In figure 7, it is seen that when the value of c is smaller than 7, the increment is continually decreased with increasing c. It is also seen that in a wide range (the value of c is about 7 ~49), the increment of minimal long-term expected cost rate keeps unchanged (equaling to 0.0935). It means that the minimal long-term expected cost rate

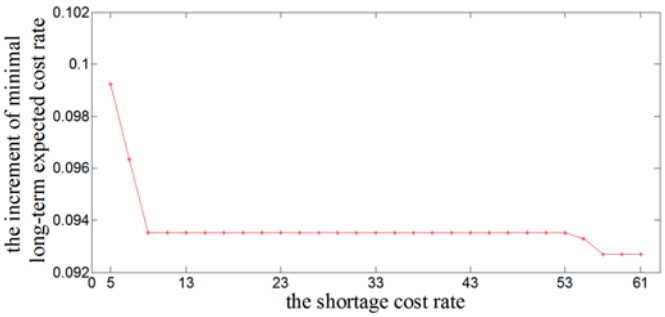

Fig. 7. The increment of minimal long-term expected cost rate when increasing c

is proportional to c in the range and under the parameter setting of numerical example 12.

6. Conclusion

In this paper, a production system consisting of two serial machines and an intermediate buffer is studied. The deterioration of the upstream machine is considered. One type of control-limit policy is applied, which takes into account the maintenance, replacement part order, and buffer level. The system and decision process are modeled by discrete Markov method, and through a policy-iteration algorithm, the long-term expected cost rate and control policy are optimized.

Numerical examples are delivered for parameter sensitive analysis. The result shows that in all cases the optimal control parameters corresponding to higher buffer levels are smaller than or equal to those corresponding to lower buffer levels. It is also shown that the change of urgent replacement part order cost doesn't have obvious effect on the optimal result. However, the increasing of any other parameter (the maintenance cost rate, general replacement part order cost, buffer inventory holding cost rate, or shortage cost rate) makes the minimal long-term expected cost rate become larger, and under some situations, the minimal long-term expected cost rate is proportional to the parameter. For the same buffer inventory level, the optimal control parameter gradually gets larger with increasing preventive maintenance cost rate or general replacement part order cost, and gets smaller with increasing corrective maintenance cost rate or buffer inventory holding cost rate. When the shortage cost rate is increased, the optimal control parameters for lower buffer levels gradually become larger; however, the optimal control parameters for higher buffer levels keep stable.

Additionally, the maintenance time duration and replacement part lead time are both assumed to follow geometric distribution in this paper. If they follow some known continuous distribution, the states of replacement part order and maintenance can be respectively divided into several states, and then the continuous Markov model is transformed into discrete Markov model which can be analyzed by using the method proposed in this paper. However, the system state will be changed to be much larger in the situation. An effect method for solving this problem is needed to be studied in future.

***Acknowledgement**: The research work is supported by National Natural Science Foundation of China (71201025), National Natural Science Foundation of China (51275090), the Foundation of the Key Laboratory of the Measurement and Control of Complex Engineering Systems, Ministry of Education of China (2010B001), and Research Fund for the Doctoral Program of Higher Education of China (20110092120007)*

References

1. Brezavšček A, Hudoklin A. Joint optimization of block-replacement and periodic-review spare-provisioning policy. IEEE Transactions on Reliability, 2003; 52(1): 112–117.
2. Chelbi A, Ait-Kadi D. Analysis of a production/inventory system with randomly failing production unit submitted to regular preventive maintenance. European Journal of Operational Research 2004; 156(3): 712–718.
3. Chien Y-H. Optimal number of minimal repairs before ordering spare for preventive replacement. Applied Mathematical Modelling 2010; 34(11): 3439–3450.
4. De Smidt-Destombes KS, Van der Heijden MC, Van Harten A. Availability of k-out-of-N systems under block replacement sharing limited spares and repair capacity. International journal of Production Economics 2007; 107(2): 404–421.
5. De Smidt-Destombes KS, Van der Heijden MC, Van Harten A. Joint optimisation of spare part inventory, maintenance frequency and repair capacity for k-out-of-N systems. International Journal of Production Economics 2009; 118(1): 260–268.
6. De Smidt-Destombes KS, Van der Heijden MC, Van Harten A. On the availability of a k-out-of-N system given limited spares and repair capacity under a condition based maintenance strategy. Reliability Engineering & System Safety 2004; 83(3): 287–300.
7. De Smidt-Destombes KS, Van der Heijden MC, Van Harten A. On the interaction between maintenance, spare part inventories and repair capacity for a k-out-of-N system with wear-out. European Journal of Operational Research 2006; 174(1): 182–200.
8. Dimitrakos TD, Kyriakidis EG. A semi–Markov decision algorithm for the maintenance of a production system with buffer capacity and continuous repair times. International Journal of Production Economics 2008; 111(2): 752–762.
9. Gan S et al. Intermediate Buffer Analysis for a Production System. Applied Mathematical Modelling 2013; 37(20–21): 8785–8795.
10. Huang R et al. Modeling and Analyzing a Joint Optimization Policy of Block-Replacement and Spare Inventory With Random-Leadtime. IEEE Transactions on Reliability 2008; 57(1): 113–124.
11. Ilgin M, Tunali S. Joint optimization of spare parts inventory and maintenance policies using genetic algorithms. The International Journal of Advanced Manufacturing Technology 2007; 34(5): 594–604.
12. Karamatsoukis CC, Kyriakidis EG. Optimal maintenance of a production-inventory system with idle periods. European Journal of Operational Research 2009; 196(2): 744–751.
13. Karamatsoukis CC, Kyriakidis EG. Optimal maintenance of two stochastically deteriorating machines with an intermediate buffer. European Journal of Operational Research 2010; 207(1): 297–308.
14. Kenné JP, Gharbi A, Beit M. Age-dependent production planning and maintenance strategies in unreliable manufacturing systems with lost sale. European Journal of Operational Research 2007; 178(2): 408–420.
15. Kennedy WJ, Wayne Patterson J, Fredendall LD. An overview of recent literature on spare parts inventories. International Journal of Production Economics 2002; 76(2): 201–215.
16. Kyriakidis EG, Dimitrakos TD. Optimal preventive maintenance of a production system with an intermediate buffer. European Journal of Operational Research 2006; 168(1): 86–99.

17. Ling Wang, JC, Weijie Mao. A condition-based replacement and spare provisioning policy for deteriorating systems with uncertain deterioration to failure. European Journal of Operational Research 2009; 194(1): 184–205.
18. Pavitsos A, Kyriakidis EG. Markov decision models for the optimal maintenance of a production unit with an upstream buffer. Computers & Operations Research 2009; 36(6): 1993–2006.
19. Ribeiro MA, Silveira JL, Qassim RY. Joint optimisation of maintenance and buffer size in a manufacturing system. European Journal of Operational Research 2007; 176(1): 405–413.
20. Teresa Murino ER, Pasquale Zoppoli. Maintenance policies and buffer sizing: an optimization model. Wseas Transactions on Business and Economic 2009; 6(1): 21–30.
21. Van der Duyn Schouten FA, Vanneste SG. Maintenance optimization of a production system with buffer capacity. European Journal of Operational Research 1995; 82(2): 323–338.
22. Vaughan TS. Failure replacement and preventive maintenance spare parts ordering policy. European Journal of Operational Research 2005; 161(1): 183-190.
23. Wang H. A survey of maintenance policies of deteriorating systems. European Journal of Operational Research 2002; 139(3): 469–489.
24. Zequeira RI, Valdes JE, Berenguer C. Optimal buffer inventory and opportunistic preventive maintenance under random production capacity availability. International Journal of Production Economics 2008; 111(2): 686–696.
25. Zhang Z et al. Reliability Modeling and Maintenance Optimization of the Diesel System in Locomotives. Eksploatacja i Niezawodnosc – Maintenance and Reliability 2012; 14(4): 10.
26. Zhang Z et al. Condition-based Maintenance Optimisation without a Predetermined Strategy Structure for a Two-component Series System. Eksploatacja i Niezawodnosc – Maintenance and Reliability 2012; 14(2): 10.
27. Zhou Y et al. Asset life prediction using multiple degradation indicators and failure events: a continuous state space model approach. Eksploatacja i Niezawodnosc – Maintenance and Reliability 2009; 4(44): 10.
28. Zohrul Kabir ABM, Al-Olayan AS. A stocking policy for spare part provisioning under age based preventive replacement. European Journal of Operational Research 1996; 90(1): 171–181.

Shuyuan GAN
Jinfei SHI
School of Mechanical Engineering
Jiulong Lake Campus, Southeast University
Nanjing, 211189, China
Emails: gxganshuyuan@163.com, shijf@seu.edu.cn

Article citation info:
SOWA A. Formal models of generating checkup sets for the technical condition evaluation of compound objects. Eksploatacja i Niezawodnosc – Maintenance and Reliability 2014; 16 (1): 150–157.

Andrzej SOWA

FORMAL MODELS OF GENERATING CHECKUP SETS FOR THE TECHNICAL CONDITION EVALUATION OF COMPOUND OBJECTS

MODELE FORMALNE GENEROWANIA ZBIORÓW SPRAWDZEŃ DLA OCENY STANU TECHNICZNEGO OBIEKTÓW ZŁOŻONYCH*

The paper refers to problems connected with building systems of computer-aided generation of evaluation sets of features necessary for the evaluation of compound objects' ability, and also the localization of imperfections of their component elements. In order to solve these problems, the usefulness of both the matrix method of determining sets of checkups and the cross-out method was analyzed. Binary and three-valued models of technical condition evaluation of the object's elements as well as the object's input and output features were formed. It allows then for the creation of the object matrix model which is used in both analyzed methods. For the matrix method, binary and three-valued evaluation models of distinguishing of the object technical condition were also defined. The binary models were used in a program which generates sets of features of the ability and localizing test. This program was written with the use of a Mathematica package. For a three-valued evaluation model for generating the feature checkup sets, the use of the cross-out method was proposed for both tests, with the technical state distinguishing conditions formed for this method. There was also presented an example of using this method to determine checkup sets of features which allow for the evaluation of the technical condition of part of the carriage brake pneumatic system.

***Keywords**: compound objects, technical condition evaluation, formal models of objects, binary and multiple-valued evaluation, computer aiding.*

Praca dotyczy problemów związanych z budową systemów wspomaganego komputerowo generowania zbiorów sprawdzeń cech niezbędnych do oceny zdatności obiektów złożonych, a także lokalizacji niezdatności ich elementów składowych. Analizowano przydatność do tego celu macierzowej metody określania zbiorów sprawdzeń oraz metody skreśleń. Sformułowano binarne i trójwartościowe modele ocen stanu technicznego elementów obiektu oraz jego cech wejściowych i wyjściowych. Pozwala to wtedy na utworzenie macierzowego modelu obiektu, wykorzystywanego w obu analizowanych metodach. Dla metody macierzowej zdefiniowano także binarne i trójwartościowe modele oceny rozróżnialności stanów technicznych obiektu. Binarne modele wykorzystano w programie generującym zbiory cech testu zdatności i lokalizującego, napisanym przy użyciu pakietu Mathematica. Przy trójwartościowym modelu ocen do generowania zbiorów sprawdzeń cech dla obu testów zaproponowano użycie metody skreśleń i sformułowano dla niej warunki rozróżnialności stanów technicznych. Przedstawiono także przykład użycia tej metody do określenia zbiorów sprawdzeń cech pozwalających na ocenę stanu technicznego części układu pneumatycznego hamulca wagonu.

***Słowa kluczowe**: obiekty złożone, ocena stanu technicznego, modele formalne obiektów, binarna i wielowartościowa ocena, wspomaganie komputerowe.*

1. Introduction

The use of advanced technologies in the construction of modern land vehicles does not give the vehicles' component elements protection against possibilities of wear occurrence and damage. The detection of these imperfections in numerous complex vehicle systems is more than once a difficult task to fulfill without using certain methods of technical condition identification. These methods described, for example, in [1, 3, 5, 6, 13, 15] enable us to choose sets of checkups necessary for the control of the object's proper functioning and for the localization of imperfections of the object's elements. The need for using such two stages of the technical condition examining is distinguished, among others, in [9, 15]. Some methods of the creation of checkup sets use the matrix model of an examined object. It is most frequently a model which is created on the basis of a binary evaluation of the object's features and on the technical condition of its component elements. The methods which are easy to use for a computer-aided generation of the checkup sets of the ability tests and the localization of damage are: a matrix method (Boolean matrices [3]) and a cross-out method (of a characteristic number [11]). The advantage of the latter method is the possibility of its effective application in the case of the multiple-valued evaluation of the object's features and the technical condition of its component elements. The issues connected with objects whose elements may take up a lot of technical conditions are discussed in a number of works [5, 7, 8, 10, 12, 16, 17], especially in reference to looking for optimal strategies of maintenance. For such objects, there is a need for applying a multiple-valued evaluation of the features which identify the objects' technical conditions [2].

This paper presents formal models of the matrix method and the cross-out method which may be used in the case of the binary or three-valued evaluations of input and output features and the technical condition of the object's compound elements. The possibilities of using both methods for a computer-aided generation of check-up sets of the ability test and the localizing test are also compared in the paper.

2. Binary models of evaluation

A technical object may be shown with the use of a functional model [3], which is built up from a certain number of distinguished boxes (rectangles) e_k representing certain sets, subsets, or elements of this

(*) Tekst artykułu w polskiej wersji językowej dostępny w elektronicznym wydaniu kwartalnika na stronie ***www.ein.org.pl***

object. Specified external input features (w_i) or output features from other object's elements (y_{ej}) can act on a single functional box. Specified output features (y_j) are obtained on the output of the box. Every functional box can be shown as this one presented in Figure 1 [13].

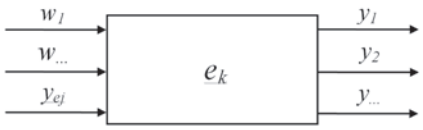

Fig. 1. A functional box as part of a functional model: e_k– element, w_1, $w_.$ – external input features, y_1, y_2, y – output features, y_{ej} – the output feature of the element e_j [13]

Both the element technical condition and the input and output features undergo evaluations in the process of examining of a given technical object. The acceptance of a given model of these evaluations also allows for going from an object's functional model to a matrix model.

For a binary evaluation of the technical condition of each object element, a two-valued characteristic function may be used. This function is used, for example, in [3] and [7] and it can be written in the following form:

$$Q_k = \varphi_2(e_k) = \begin{cases} 1, \ when\ e_k \Leftrightarrow S_0 \\ 0, \ when\ e_k \Leftrightarrow S_1 \end{cases} \tag{1}$$

where: Q_k – the evaluation variable of the technical condition of the element e_k,

$\varphi_2(...)$ – the binary characteristic function,

S_0, S_1 – technical conditions of the element e_k, respectively: ability and imperfection.

A two-valued function (1) assigns the logical value "1" to each variable Q_k which refers to the element e_k if this element is in the ability condition S_0, and "0" in the opposite case.

The basis for a binary evaluation of input and output features is checking whether an examined feature is within a determined range of values. Formally it is formulated by characteristic functions which, in order to unify the notation, can be shown as follows:

$$v_i = \varphi_2(w_i) = \begin{cases} 1, \ when\ \ (w_i)_{\min} \le w_i \le (w_i)_{\max} \\ 0, \ when\ \ w_i < (w_i)_{\min} \vee\ w_i > (w_i)_{\max} \end{cases} \tag{2}$$

$$z_j = \varphi_2(y_j) = \begin{cases} 1, \ when\ \ (y_j)_{\min} \le y_j \le (y_j)_{\max} \\ 0, \ when\ \ y_j < (y_j)_{\min} \vee\ y_j > (y_j)_{\max} \end{cases} \tag{3}$$

where: w_i – the external input feature for the element e_k,

y_j – the evaluated output feature,

v_i – the binary logical value of evaluation of the external input feature,

z_j – the binary logical value of evaluation of the output feature,

$(w_i)_{\min}$, $(w_i)_{\max}$ – boundary values of the input feature,

$(y_j)_{\min}$, $(y_j)_{\max}$ – boundary values of the output feature.

These functions assign the logical value „1" in reference to the situations in which input and output features are within the predicted ranges determined by the values $(w_i)_{\min}$, $(w_i)_{\max}$ and $(y_j)_{\min}$ and $(y_j)_{\max}$, and "0" in the opposite case.

If it is assumed that the values of each external input feature are within the standard range then, with the use of functions (1), (2) and (3), the matrix model of the object can be created [3]. The model shows the relations between the output features of the individual elements and the technical conditions of this object, i.e. the condition of ability and the conditions of imperfections induced by the appearance of imperfect elements in this object. In the case of a binary evaluation, the matrix of such a model is frequently referred to as the truth table.

The truth table is the basis for determining the sets of features which allow for the verification of the object's ability and the localization of the imperfections of its elements. It requires a twofold transformation of the truth table into the matrix of the ability test and the matrix of the localization test in the way described in a written form in [3]. In a formal perspective, these transformations require the use of two characteristic functions: one function evaluates the distinguishing of the ability condition of the examined object from any optional condition of imperfection; the other function allows for distinguishing the individual states of imperfection among themselves.

For the evaluation of the technical condition distinguishing in the first case, a two-valued function in the following form may be used:

$$z_j^{0,i} = \varphi_2(S_0, S_i) = \forall(i, j \in [1,k]): \begin{cases} 1, \ when\ z_j(S_0) = 1 \wedge z_j(S_i) = 0 \\ 0, \ when\ z_j(S_0) = z_j(S_i) \end{cases} \tag{4}$$

where: $z_j^{0,i}$ – the logical variable of the evaluation of the ability and imperfection conditions' distinguishing,

$z_j(S_0)$ – the logical variable of evaluation of the feature y_j in the ability condition S_0,

$z_j(S_i)$ – the logical variable of evaluation of the feature y_j in the imperfection condition S_i.

A two-valued function of the evaluation of imperfection conditions' distinguishing is as follows:

$$z_j^{i,l} = \varphi_2(S_i, S_l) = \forall(i, l, k \in [1,k] \wedge (i \ne l)): \begin{cases} 1, \ when\ \ z_j(S_i) \ne z_j(S_l) \\ 0, \ when\ z_j(S_i) = z_j(S_l) \end{cases} \tag{5}$$

where: $z_j^{i,l}$ – the logical variable of the evaluation of distinguishing imperfection conditions S_i and S_l on the basis of the evaluation of the feature y_j,

$z_j(S_i)$ – the logical variable of the evaluation of the feature y_j in the imperfection condition S_i,

$z_j(S_l)$ – the logical value of the evaluation of the feature y_j in the imperfection condition S_l.

Functions (4) i (5) allow for the transformation of the truth table successively into the matrix of the ability test and the matrix of localization test. Instead of these functions, an operation of adding modulo 2 may be used. This operation has to be applied for appropriate values from a two-valued truth table, i.e. the following formulae:

$$z_j^{0,i} = z_j(S_0) \oplus z_j(S_i) \tag{6}$$

$$z_j^{i,l} = z_j(S_i) \oplus z_j(S_l) \tag{7}$$

where: $\oplus$ – the modulo 2 sum.

The obtained matrices are the basis for determining respectively the sets of features for the object's ability test and for the localization test. Part 4 of this paper contains a description of the mode of generating such sets with the use of the matrix method.

3. Three-valued evaluation models

A binary evaluation model is insufficient in the case of features which have two or more ranges of boundary values, as well as for such object's elements which can take up various forms of imperfection [11, 13]. In the latter case, it refers to some elements of electric, hydraulic or pneumatic systems which constitute a given technical object. For such elements, even with one range of permissible values of the given input or output feature, it is important to have information which boundary value was exceeded: a maximum or minimum one.

In electric systems, for example, the appearance of such basic imperfections like a break in the circuit or the insulation punch-through can significantly influence the values of the object's features, i.e. generate distinct technical conditions [11]. In this case, for each *i* element of the object a set of technical conditions SU_i can be determined. This set contains, for example:

- the ability condition – S_i^0,
- the imperfection condition caused by the insulation punch-through – S_i^n,
- the imperfection condition of the element which results from a break in the circuit – S_i^d,

which is:

$$SU_i = \left\{S_i^0, S_i^n, S_i^d\right\} \tag{8}$$

Figure 2 shows a graph of walks between technical conditions of one such element of the set [11]. In operation it is possible to go from the ability condition to one of the two imperfection conditions and a return to the ability condition takes place after completing appropriate operational activities.

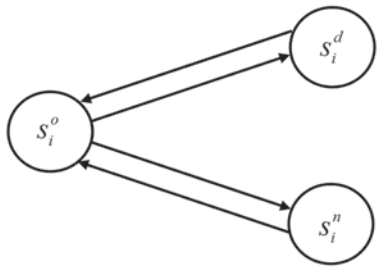

Fig. 2. Graph of walks for the set of the technical conditions of the exemplary element of the system that powers the rail-vehicle brake [11]

After the denotations of the individual technical conditions of a single element have been generalized, the following characteristic function may be proposed for this element's three-valued evaluation:

$$Q3_k = \varphi_3(e_k) = \begin{cases} 2, \ when \ e_k \Leftrightarrow S_2 \\ 1, \ when \ e_k \Leftrightarrow S_0 \\ 0, \ when \ e_k \Leftrightarrow S_1 \end{cases} \tag{9}$$

where: $Q3_k$ – a three-valued variable of the technical condition evaluation of the element e_k,

S_0, S_1, S_2 – technical conditions of the element: the ability, the 1st and 2nd form of the imperfection,

$\varphi_3(...)$ – a three-valued characteristic function.

If the individual elements of the object can take up more than one imperfection form and when there is a possibility of the occurrence of an optional combination of imperfect elements then the size of the technical condition full set of such an object can be determined with the formula [13]:

$$l_m = (m+1)^k \tag{10}$$

where: l_m – the size of the set of the object's technical conditions,

m – the number of imperfection forms of each component element of the object,

k – the number of elements of the object.

For a three-valued evaluation of the external input features and the output features, the following characteristic functions can be applied [13]:

$$v3_i = \varphi_3(w_i) = \begin{cases} 2, \ when \ w_i < (w_i)_{\min} \\ 1, \ when \ (w_i)_{\min} \le w_i \le (w_i)_{\max} \\ 0, \ when \ w_i > (w_i)_{\max} \end{cases} \tag{11}$$

$$z3_j = \varphi_3(y_j) = \begin{cases} 2, \ when \ y_j < (y_j)_{\min} \\ 1, \ when \ (y_j)_{\min} \le y_j \le (y_j)_{\max} \\ 0, \ when \ y_j > (y_j)_{\max} \end{cases} \tag{12}$$

where: $v3_i$ – a three-valued variable of the evaluation of the measured external value of the input feature w_i,

$z3_j$ – a three-valued variable of the evaluation of the measured value of the output feature y_j.

The essence of the three-valued evaluation with the use of functions (11) and (12) is the assigning of various logical values when the upper or lower boundary values of the examined feature are exceeded, which is basically different from the proposition included in [2] in which the evaluation values were assigned in the following way: "2" – for the insignificant changes of the feature's value, "1" – for the significant changes of the feature's value, and "0" – for the unacceptable changes of the feature's value.

Similarly to a binary evaluation, functions (9), (11) i (12) allow for the creation of a three-valued matrix that constitutes the model of an object and which subsequently can be transformed into the matrix of the ability test and the matrix of the localization test.

An essential form of the distinguishing evaluation function of the pairs of the ability and imperfection conditions, i.e. pairs of the type $\langle S_0, S_i \rangle$ can be obtained by the modification of function (4):

$$z3_j^{0,i} = \varphi_2(S_0, S_i) = \forall(i, j \in [1,k]): \begin{cases} 1, \ when \ z3_j(S_0) = 1 \wedge z3_j(S_i) \neq 1 \\ 0, \ when \ z3_j(S_0) = z3_j(S_i) \end{cases} \tag{13}$$

where: $z3_j^{0,i}$ – a three-valued logical variable of the distinguishing evaluation of the ability and imperfection conditions,

$z3_j(S_0)$ – a three-valued logical variable of the evaluation of the feature y_j in the ability condition S_0,

$z3_j(S_i)$ – a three-valued logical variable of the evaluation of the feature y_j in the imperfection condition S_i.

This function assigns the logical value "0" in such a situation when it is impossible to distinguish the ability and imperfection conditions on the basis of the value evaluation of the feature y_j, and "1" in the opposite situation. Since the variables $z3_j(S_0)$ and $z3_j(S_i)$ can take up one of the three logical values from the set $\{0,1,2\}$, the results obtained by using function (13) are impossible to be reached with the use of a two-argument modulo 2 sum operation working on the values of these variables. Moreover, with a three-valued model of the object's feature evaluation, the negation of the values of the variables $z3_j$, i.e. the one-argument operation $\overline{\overline{z3_j}}$ should be defined in the following way:

$$\overline{\overline{z3_j}} = \begin{cases} 0 \vee 2, when\, z3_j = 1 \\ 1, when\, z3_j = (0 \vee 2) \end{cases} \tag{14}$$

If, for the simplification of the notation, it is assumed that:

$$\begin{aligned} z3_j(S_0) &= a \\ z3_j(S_i) &= b \end{aligned} \tag{15}$$

then the form of the two-argument function $\Omega(a,b)$, which allows for the obtaining of the values consistent with those given by the function (13), is as follows:

$$z3_j^{0,i} = \Omega(a,b) = \left[\min(a,b) + a + b\right] \bmod 3 \tag{16}$$

Function (16) may be also used for the creation of the three-valued matrix of the localization test, but then its two arguments refer to the imperfection conditions, i.e. assuming that:

$$z3_j(S_l) = d \tag{17}$$

then $$z3_j^{i,l} = \Omega(b,d) = \left[\min(b,d) + b + d\right] \bmod 3 \tag{18}$$

where: $z3_j^{i,l}(S_l)$ – a three-valued logical variable of the evaluation of the feature y_j in the imperfection condition S_l,

$z3_j^{i,l}$ – a logical variable of the distinguishing evaluation of the pair of the imperfection conditions $\langle S_i, S_l \rangle$.

The values obtained with the use of function (18) correspond with the values of the distinguishing evaluation of the pairs of the imperfection conditions $\langle S_i, S_l \rangle$ obtained with the use of a three-valued characteristic function, whose form may be defined by using the simplifications of notation from the formulae (15) and (17) in the following way:

$$z3_j^{i,l} = \varphi_3(S_i, S_l) = \forall(i,l,k \in [1,k] \wedge (i \neq l)): \begin{cases} 0, when\, b = d \\ 1, when [b = 1 \wedge (d = (0 \vee 2))] \vee \\ \quad [d = 1 \wedge (b = (0 \vee 2))] \\ 2, when\, (b = 0 \wedge d = 2) \vee \\ \quad (d = 0 \wedge b = 2) \end{cases} \tag{19}$$

The matrices obtained with the use of functions: (13) or (16) and: (18) or (19) constitute the basis for further operations in order to distinguish the checkup sets of the ability test and the localization test.

4. An example of using a binary evaluation model for the generation of the checkup sets with the use of a matrix method

The process of selecting features for the checkup set of the object's ability with the use of a matrix method can be performed through indicating the determined columns of features on the basis of a certain criterion. It leads to the minimization of the matrix of the ability test. This criterion is, first of all, the uniqueness of the object's features in the range of the distinguishing of the technical condition pairs. It is expressed through the occurrence of one "1" in the row of this matrix. The column in which this value occurs indicates the feature belonging to the checkup set of the ability test because only this column feature allows for the distinguishing of the pairs of the ability and imperfection conditions assigned to this row. The use of this criterion leads to the choice of the features which are in the columns of the features representing the external outputs from a given object. In the next order, such factors as availability or measurement costs can act as the criteria for choosing the features for the ability test. After marking out the features which create the checkup set of the ability test it has to be controlled whether this set is sufficient to distinguish all pairs of the technical conditions. It is performed through crossing out the column of the selected features and all distinguishable rows from the matrix of the ability test. The crossing out of all the columns and rows allows for the closure of the checkup set of this test.

The method of looking for a set of the object's features necessary for the localization test is similar to that one employed in the ability test. The method is based on a subsequent choosing (for this set), first of all these object's features which, as the only ones, provide the distinguishing of certain pairs of the technical conditions $\langle S_i, S_l \rangle$. Then the ability of the distinguishing of all the remaining pairs of the imperfection conditions is checked. If the result of such a checkup is positive then the set of features can be closed. In the opposite case, one should continue the selection of features in a minimized matrix of the localization test; this matrix is formed after crossing out the columns of the selected features and the rows with the pairs of the technical conditions which can be distinguished on the basis of these features. The selection process is finished by a positive result of checking of the distinguishing abilities of all imperfection conditions' pairs. If, despite using the features which belong to the checkup set of the localization test, there are still undistinguishable pairs of the imperfection conditions then it may mean errors in the constructed model of the object or the need for using a multiple-valued evaluation of the input and output features.

An exemplary form of the truth table created for the railway carriage brake gear is shown in Table 1 [14]. Table 1 was created for a case in which the possibility of occurring at most one imperfect element of the brake gear was assumed. The table contains the evaluation values of the features $y_1 \div y_{21}$, i.e. the forces occurring in the brake gear

Table 1. The truth table for a railway carriage brake gear [14]

SU_k	z_j																				
	y_1	y_2	y_3	y_4	y_5	y_6	y_7	y_8	y_9	y_{10}	y_{11}	y_{12}	y_{13}	y_{14}	y_{15}	y_{16}	y_{17}	y_{18}	y_{19}	y_{20}	y_{21}
S_0	1	1	1	1	1	1	1	1	1	1	1	1	1	1	1	1	1	1	1	1	1
S_1	0	0	0	0	0	0	0	0	0	0	0	0	0	0	0	0	0	0	0	0	0
S_2	1	0	0	0	0	0	0	0	0	0	0	0	0	0	0	0	0	0	0	0	0
S_3	1	1	0	0	0	0	0	0	0	0	0	1	1	1	1	1	1	1	1	1	1
S_4	1	1	1	0	0	0	0	1	1	1	1	1	1	1	1	1	1	1	1	1	1
S_5	1	1	1	1	0	1	1	1	1	1	1	1	1	1	1	1	1	1	1	1	1
S_6	1	1	1	1	1	0	0	1	1	1	1	1	1	1	1	1	1	1	1	1	1
S_7	1	1	1	1	1	1	0	1	1	1	1	1	1	1	1	1	1	1	1	1	1
S_8	1	1	1	1	1	1	1	0	0	0	0	1	1	1	1	1	1	1	1	1	1
S_9	1	1	1	1	1	1	1	1	0	1	1	1	1	1	1	1	1	1	1	1	1
S_{10}	1	1	1	1	1	1	1	1	1	0	0	1	1	1	1	1	1	1	1	1	1
S_{11}	1	1	1	1	1	1	1	1	1	1	0	1	1	1	1	1	1	1	1	1	1
S_{12}	1	1	1	1	1	1	1	1	1	1	1	0	0	0	0	0	0	0	0	0	0
S_{13}	1	1	1	1	1	1	1	1	1	1	1	1	0	0	0	0	0	0	0	0	0
S_{14}	1	1	1	1	1	1	1	1	1	1	1	1	1	0	0	0	0	1	1	1	1
S_{15}	1	1	1	1	1	1	1	1	1	1	1	1	1	1	0	1	1	1	1	1	1
S_{16}	1	1	1	1	1	1	1	1	1	1	1	1	1	1	1	0	0	1	1	1	1
S_{17}	1	1	1	1	1	1	1	1	1	1	1	1	1	1	1	1	0	1	1	1	1
S_{18}	1	1	1	1	1	1	1	1	1	1	1	1	1	1	1	1	1	0	0	0	0
S_{19}	1	1	1	1	1	1	1	1	1	1	1	1	1	1	1	1	1	1	0	1	1
S_{20}	1	1	1	1	1	1	1	1	1	1	1	1	1	1	1	1	1	1	1	0	0
S_{21}	1	1	1	1	1	1	1	1	1	1	1	1	1	1	1	1	1	1	1	1	0

in the particular feasible technical conditions of this system. The set of these technical conditions includes the ability condition of the gear S_0 and the imperfection conditions $S_1 \div S_{21}$ resulting from the imperfection of – respectively – the elements $e_1 \div e_{21}$.

The presented models of binary evaluations and the specified methodology of choosing the evaluation sets of the ability test and the localization test allows for their programmable creation. This type of a program which generates the checkup sets for the evaluation of the object's technical condition and which is written with the use of a Mathematica package is included in [14]. With the use of this program for a matrix model as in Table 1, the following input command should be employed:

```
Tp={{1,1,1,1,1,1,1,1,1,1,1,1,1,1,1,1,1,1,1,1,1},
    {0,0,0,0,0,0,0,0,0,0,0,0,0,0,0,0,0,0,0,0,0},
    {1,0,0,0,0,0,0,0,0,0,0,0,0,0,0,0,0,0,0,0,0},
    {1,1,0,0,0,0,0,0,0,0,0,0,0,0,0,0,0,0,0,0,0},
    {1,1,1,0,0,0,0,1,1,1,1,1,1,1,1,1,1,1,1,1,1},
    {1,1,1,1,0,1,1,1,1,1,1,1,1,1,1,1,1,1,1,1,1},
    {1,1,1,1,1,0,0,1,1,1,1,1,1,1,1,1,1,1,1,1,1},
    {1,1,1,1,1,1,0,1,1,1,1,1,1,1,1,1,1,1,1,1,1},
    {1,1,1,1,1,1,1,0,0,0,0,1,1,1,1,1,1,1,1,1,1},
    {1,1,1,1,1,1,1,1,0,1,1,1,1,1,1,1,1,1,1,1,1},
    {1,1,1,1,1,1,1,1,1,0,0,1,1,1,1,1,1,1,1,1,1},
    {1,1,1,1,1,1,1,1,1,1,0,1,1,1,1,1,1,1,1,1,1},
    {1,1,1,1,1,1,1,1,1,1,1,0,0,0,0,0,0,0,0,0,0},
    {1,1,1,1,1,1,1,1,1,1,1,0,0,0,0,0,0,0,0,0,0},
    {1,1,1,1,1,1,1,1,1,1,1,1,0,0,0,1,1,1,1,1,1},
    {1,1,1,1,1,1,1,1,1,1,1,1,1,0,1,1,1,1,1,1,1},
    {1,1,1,1,1,1,1,1,1,1,1,1,1,1,0,0,1,1,1,1,1},
    {1,1,1,1,1,1,1,1,1,1,1,1,1,1,1,0,1,1,1,1,1},
    {1,1,1,1,1,1,1,1,1,1,1,1,1,1,1,1,0,0,0,0,0},
    {1,1,1,1,1,1,1,1,1,1,1,1,1,1,1,1,1,0,1,1,1},
    {1,1,1,1,1,1,1,1,1,1,1,1,1,1,1,1,1,1,0,0,0},
    {1,1,1,1,1,1,1,1,1,1,1,1,1,1,1,1,1,1,1,1,0}}
```

The checkup set of the ability test obtained due to the operation of the program is as follows:

Tds // question about the checkup set of the ability test

{y5,y7,y9,y11,y15,y17,y19,y21} // response

and the checkup set of the localization test has the form:

Tdl // question about the checkup set of the localization test

{y1,y2,y6,y10,y12,y16,y20,y5,y7,y9,y11,y15, y17,y19} // response

A such obtained solution allows for the localization of any optional imperfect element of the examined carriage brake gear.

5. The application of the cross-out method for generating sets of features for the evaluation of the technical condition of the compound object

A three-valued model of evaluation, described in Entry 3 of this paper, can be used, for example, for distinguishing a break in the electromagnetic circuit of the rail brake from the punch-through of the insulation of the brake's winding [11], i.e. the distinguishing of three classes of the technical condition specified by formula (8). The other example of the three-valued evaluation model application with the use of functions (9), (11) and (12) is a matrix model (Table 2) which can be created for part of the pneumatic system of the carriage brake on the basis of the computing model included in [4] and referring to a phase of filling up the system.

The matrix presented in Table 2 contains the values of evaluations of such features as: $y_0 \div y_4$ – i.e. the pressures in the system, and $y'_0 \div y'_4$ – massive intensity of the air flow in part of the carriage pneumatic system, in the technical conditions that belong to a set:

$$SU_r = \left\{ S_o, S_i^n, S_1^d, S_2^n, S_2^d, S_3^n, S_3^d, S_4^n, S_4^d, S_5^n, S_5^d \right\} \tag{20}$$

where: S_0 – the ability condition of the object,

$S_1^n \div S_5^n$ – technical conditions characteristic of leaks of the object's elements,

$S_1^n \div S_5^n$ – technical conditions characteristic of choking of air flow in the object's elements.

The transformation of a matrix which constitutes a three-valued model of an exemplary object (Table 2) into a matrix of the ability test with the use of functions (13) or (16) allows for the determination of

Table 2. The matrix model of part of the pneumatic system of the carriage brake

Item number	Technical condition	Evaluations of the object's features - $z3_j$											
		y_0	$y_0^{'}$	y_1	$y_1^{'}$	y_2	$y_2^{'}$	y_3	$y_3^{'}$	y_4	$y_4^{'}$	y_5	$y_5^{'}$
1.	S_0	1	1	1	1	1	1	1	1	1	1	1	1
2.	S_1^n	1	0	1	1	1	1	1	1	1	1	1	1
3.	S_1^d	1	2	0	2	0	2	0	2	0	2	0	2
4.	S_2^n	1	0	1	1	2	2	1	1	1	1	1	1
5.	S_2^d	1	2	1	1	1	2	1	1	1	1	1	1
6.	S_3^n	1	0	1	1	1	1	2	0	2	0	2	0
7.	S_3^d	1	2	1	1	1	1	2	2	2	2	2	2
8.	S_4^n	1	0	1	0	1	1	1	0	2	0	1	1
9.	S_4^d	1	2	1	2	1	1	1	2	2	2	1	1
10.	S_5^n	1	0	1	0	1	1	1	0	1	1	2	0
11.	S_5^d	1	2	1	2	1	1	1	2	1	1	2	2

the checkup set of this test in the same way as with a binary evaluation model. Thus the algorithmical generation of the set is possible. In the case of a matrix of the localization test obtained with the use of functions (18) or (19), the previously used methodology of the minimization of the checkup set is ineffective. It is easier to choose a minimal checkup set of the localization test with the use of a cross-out method.

While analyzing the form of the object's matrix model it can be noticed that each row of this matrix constitutes a sequence of the evaluation values. This sequence can be interpreted as a characteristic number written in a binary, ternary or quaternary codes - it depends on the number of values used for the evaluation of the features of this object. If a conversion of this number into a decimal number is performed then it can be used for the evaluation of the uniqueness of the individual rows of this matrix. Such a decimal number d_r can be derived from the formula [13]:

$$d_r = \sum_{j=1}^{j_{\max}} z_j^r \cdot p^{j-1} \tag{21}$$

where: z_j^r – the evaluation value of the feature y_j in the row r of the object's matrix model,

j – the number of the column of the object's feature counting from the right side of this matrix,

p – the number of evaluation values which can be assigned to the individual features.

The condition for the distinguishing of each pair of the technical conditions $\langle S_r, S_s \rangle$ on the basis of the evaluation of all the features of the object (or of only a certain subset of the features) is the requirement that all characteristic numbers in the individual rows of the matrix (which constitutes the object's model) corresponding with the features are different, i.e. [13]:

$$\bigwedge_{r \neq s} S_r \neq S_s \Leftrightarrow d_r \neq d_s \tag{22}$$

where: s – the index of the matrix row different from r.

With a great number of the object's elements and the evaluated values, the conversion of the row of the matrix model is difficult without computer-aided calculations. Besides, the numbers obtained from formula (21) are so big that they only slightly facilitate the evaluation of their uniqueness. As a consequence, the evaluation of the distinguishing of the individual conditions of the analyzed object is also only slightly facilitated. In such a situation, when one decides to use a specialist computer program it is convenient to treat each row of this matrix as a conventional characteristic number represented by a sequence of the symbols c_r obtained in the following way [13]:

$$c_r = \sum_{j=j_{\max}}^{1} Str\left(z_j^r\right) \tag{23}$$

where: $\sum$ – the operator of the connection of symbols,

$Str()$ – the function converting the numerical value of the feature evaluation into a symbol.

By using such sequences, the distinguishing condition of the rows of this matrix can be formulated analogically to formula (22), i.e. [13]:

$$\bigwedge_{r \neq s} S_r \neq S_s \Leftrightarrow c_r \neq c_s \tag{24}$$

The substantial benefit of using symbol sequences is the ability of deploying a great number of the features of an object. It results from the acceptable lengths of the variables of the symbol type. The way of seeking the resulting checkup set of the localization test relies on the removing of the individual columns of the matrix of a given object, beginning from the left or the right side, and checking the distinguishing condition of the technical conditions which is included in formulae (22) or (24). In the case when this condition is fulfilled, one has to go to the next column and remove it. However, if the checkup is not successful, the previously removed column has to be restored and the feature from this restored column should be introduced into the set of the features of the localization test. Such an operation has to be continued until the list of features from the columns of this matrix is emptied. The values from the remaining columns form a minimal

signature of each technical condition which is assigned to each row of the matrix.

In order to check the possibility of generation (with the use of the cross-out method) of the sets of features for the evaluation of the object's ability and for the localization of the imperfections of its elements, a computer program which performs the tasks of creating such sets was worked out. This computer application has a form with a window which is designed for the edition of the binary or multiple-valued matrix of a given object, and the buttons which start the generation of the checkup sets of the ability test and the localization test. Figure 3 contains a view of this form for the object whose three-valued matrix is shown in Table 2.

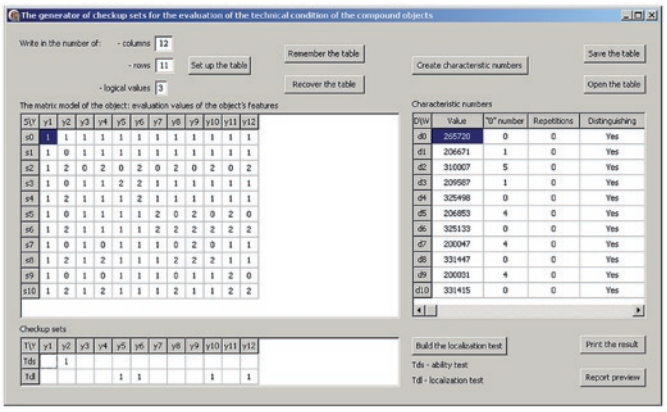

Fig. 3. A view of the form of the ability and localization tests' generator with the data as in Table 2

Before the input data is introduced, the size of a matrix has to be arranged and the number of logical values used for the evaluation of the object's features has to be defined. In evaluations like in Table 2, the application enables the checkup sets of the ability and localization tests to be generated. Thus the following report can be obtained:

A set of checkups of the ability test
Tds = { y2 }

A set of checkups of the localization test
Tdl = { y5,y6,y10,y12 }

The sum of checkup sets
Tdc = { y2,y5,y6,y10,y12 }

This report is a confirmation of the effectiveness of this method for creating feature sets which allow for identification of the technical condition of the compound object.

6. Summary

Binary and three-valued models of evaluations which are shown in this paper can be used for building systems of the computer-aided generation of feature sets whose examining allows for the checkup of the ability of a compound object and the localization of imperfections of its constituent elements. Such systems should choose only the necessary features out of the whole amount of the object's features. It can be done with the use of the matrix method or the cross-out method.

As it is shown in this paper, with the binary evaluation the task of choosing the features can be relatively easily accomplished with the use of a matrix method of creation of the checkup sets of the object's features. In order to achieve this, the functions of distinguishing evaluation of both the ability and imperfection conditions were formulated and an exemplary result of the functions' application in a program written with the use of a Matematica package was given. The matrix method may also be used for determining appropriate checkup sets for a case in which the object's features undergo a three-valued evaluation. Then, it is however necessary to admit other three-valued functions of the technical condition distinguishing evaluation of a compound object. It is also shown that in this case the criteria for the computer-aided selection of features into the checkup sets can't be uniquely distinguished, as it is in the binary evaluation of the object's features.

This fact was an impulse for creating another method of distinguishing checkup sets, i.e. the cross-out method. This method may be applied in both a binary and a multi-valued evaluation of the examined features. The method relies on subsequent attempts of eliminating of individual features and checking the truthfulness of the distinguishing condition of technical conditions of the analyzed object. The efficiency of this method was verified on the example which referred to part of the carriage brake pneumatic system.

The cross-out method can be applied with both the full and limited measurement availability of the features of a given object. By accepting the inability of checking of some features one can, however, obtain information about a possible undistinguishing of the technical conditions of a given object caused by the occurrence of certain imperfections of its constituent elements.

References

1. Chalecki D. Algorytm minimalizacji sygnatur uszkodzeń. Diagnostyka 2006; 3(39): 297–300.
2. Duer S. Creation of the servicing information to support the maintenance of a technical object with the use of three-value logic diagnostic information. Zagadnienia Eksploatacji Maszyn 2009; 3(159): 35–48.
3. Hebda M. i inni. Eksploatacja samochodów. Wydawnictwo Instytutu Technologii Eksploatacji, Radom 2005.
4. Jeleśniański Z, Sowa A, Walczak S. Model analityczny pneumatycznego układu hamulca pojazdu szynowego. Pojazdy Szynowe 2004; 2: 23–27.
5. Kapur KC. Multi-state reliability: models and applications. Eksploatacja i Niezawodnosc – Maintenance and Reliability 2006; 2: 8–10.
6. Kościelny JM, Dziembowski B. Rozróżnialność uszkodzeń w układach liniowych. Diagnostyka 2006; 2(38): 93–100.
7. Liu Y, Huang H-Z. Optimal selective maintenance strategy for multi-state systems under imperfect maintenance. IEEE Transactions on Reliability 2010; 59.2: 356–367.
8. Liu Y, Huang H-Z. Optimal replacement policy for multi-state system under imperfect maintenance. IEEE Transactions on Reliability 2010; 59.3: 483–495.
9. Niziński S, Liger K. Diagnostyka techniczna w systemach działania. Zagadnienia Eksploatacji Maszyn 2001; 3(127): 171–189.
10. Nourelfath M, Fitouhi M, Machani M. An integrated model for production and preventive maintenance planning in multi-state systems. IEEE Transactions on Reliability 2010; 59.3: 496–506.
11. Skowron J, Sowa A. System oceny cech diagnostycznych układu zasilania elektromagnetycznego hamulca szynowego. Czasopismo Techniczne 2012; 7-M: 251–260.

12. Soro I. W, Nourelfath M, Aït-Kadi D. Performance evaluation of multi-state degraded systems with minimal repairs and imperfect preventive maintenance. Reliability Engineering & System Safety 2010, 95.2: 65–69.
13. Sowa A. Distinguishing factor of the technical conditions of a compound object. Monographs of the Maintenance System Unit, Polish Academy of Sciences Committee on Machine Building, Maintenance Fundamentals Section, "Problems of maintenance of sustainable technological systems". Kielce University of Technology, Kielce 2012; V: 154–171.
14. Sowa A. Macierzowa metoda generowania testów diagnostycznych przy użyciu pakietu Mathematica. XIX Konferencja Naukowa „Pojazdy Szynowe", Targanice k. Andrychowa 2010; t. II: 211–221.
15. Tylicki H. Metodyka wyznaczania procedury diagnozowania stanu maszyn. Diagnostyka 2004; 33: 179–185.
16. Zaitseva E, Levashenko V, Matiaško K. Failure analysis of series and parallel multi-state system. Eksploatacja i Niezawodnosc – Maintenance and Reliability 2006; 2: 29–32.
17. Zio E, Podofillini L. The use of importance measures for the optimization of multi-state systems. Eksploatacja i Niezawodnosc – Maintenance and Reliability 2006; 2: 33–36.

Andrzej SOWA
The Institute of Rail Vehicles
Cracow University of Technology
al. Jana Pawła II 37, 31-864 Kraków, Poland
E-mail: andre@mech.pk.edu.pl

Article citation info:
BAJRIĆ R, ZUBER N, ŠOSTAKOV R. Relations between pulverizing process parameters and beater wheel mill vibration for predictive maintenance program setup. Eksploatacja i Niezawodnosc – Maintenance and Reliability 2014; 16 (1): 158–163.

Rusmir BAJRIĆ
Ninoslav ZUBER
Rastislav ŠOSTAKOV

RELATIONS BETWEEN PULVERIZING PROCESS PARAMETERS AND BEATER WHEEL MILL VIBRATION FOR PREDICTIVE MAINTENANCE PROGRAM SETUP

RELACJE MIĘDZY PARAMETRAMI PROCESÓW ROZDRABNIANIA I DRGANIAMI MŁYNA WENTYLATOROWEGO A USTAWIENIA PROGRAMU KONSERWACJI PREDYKCYJNEJ

Beater wheel mills are designed to prepare a coal powder air fuel mixture for combustion in furnace chambers of coal-fired power plants by coal drying, pulverizing, classifying and transport. Their multipurpose function usually results in operation instability accompanied by unacceptable vibration. This usually is a significant problem due to unplanned shutdowns. Beater wheel mill maintenance program requires special attention due to operation under non-stationary conditions. The purpose of this paper was to identify pulverizing process parameter that affect the beater wheel mill vibration level and severity at the same time by using statistical principles under a wide range of operating conditions. This paper intends to establish the foundations to investigate correlation of pulverizing process parameter with beater wheel mill vibration in order to setup a better predictive maintenance program. To achieve this goal, the beater wheel mill vibration under different combinations of selected pulverizing process parameters are analyzed using statistical tools. Experiments were carried out under different conditions for two identical but separated beater wheel mills. The influence of pulverizing process parameter, such as electrical current of the driving motor, mill capacity, boiler production, coal types on mill vibration are investigated to identify the potential malfunction of beater wheel mills and their associated components for predictive maintenance purposes. The results have demonstrated that the selected pulverizing process parameters do not have significant influence on beater wheel mill vibration severity. Unlike most coal mills where pulverizing process parameters must take into account, here with beater wheel impact mills it is not the case and condition monitoring of these mills could be conducted offline or online using standard vibration condition monitoring methods.

***Keywords**: predictive maintenance, multiple regression analyses, non-stationary operational conditions, beater wheel mil.*

Młyny wentylatorowe są urządzeniami, które poprzez suszenie, rozdrabnianie, odsiewanie i transport węgla przygotowują mieszankę pyłowo-gazową przeznaczoną do spalania w komorach paleniskowych elektrowni węglowych. Ich uniwersalność zwykle wiąże się z niestabilną pracą połączoną z niepożądanymi drganiami. Jest to zwykle znaczący problem z uwagi na niezaplanowane przerwy w pracy. Program konserwacji młyna wentylatorowego wymaga szczególnej uwagi ze względu na działanie w niestacjonarnych warunkach pracy. Celem artykułu jest wyznaczenie parametrów procesów rozdrabniania wpływających jednocześnie na poziom i natężenie drgań młyna wentylatorowego przy użyciu reguł statystycznych w zróżnicowanych warunkach pracy. Zamierzeniem pracy jest stworzenie podstaw dla badań nad zależnościami między parametrami procesu rozdrabniania a drganiami młyna wentylatorowego w celu ulepszenia programu konserwacji predykcyjnej. Aby osiągnąć założony cel, przeanalizowano przy użyciu narzędzi statystycznych drgania młyna wentylatorowego przy różnych kombinacjach wybranych parametrów procesu rozdrabniania. Badania przeprowadzono w różnych warunkach na dwóch identycznych, lecz odrębnych młynach wentylatorowych. Wpływ parametrów procesu rozdrabniania, takich jak prąd elektryczny silnika napędowego, pojemność młyna, kotły, czy typ węgla, na drgania młyna zbadano w celu określenia potencjalnych awarii młyna i jego części składowych na potrzeby jego konserwacji predykcyjnej. Wyniki badań pokazały, iż wybrane parametry procesu rozdrabniania nie mają znaczącego wpływu na natężenie drgań młyna wentylatorowego. W przeciwieństwie do większości młynów węglowych, w przypadku których należy brać pod uwagę parametry procesu rozdrabniania, kontrola stanu młynów wentylatorowych może być prowadzona w trybie offline lub online za pomocą standardowych metod monitorowania warunków drgania.

***Słowa kluczowe**: konserwacja predykcyjna, analizy regresji wielorakich, niestacjonarne warunki pracy, młyn wentylatorowy.*

1. Introduction

Typically the lignite fuelled power station is consisted of a number of tangentially fired furnaces with beater wheel arranged mill-duct systems. These mill-ducts systems are responsible for grinding the raw coal and distributing the pulverized fuel to the furnace at appropriate concentrations to provide ideal combustion characteristics within the furnace. Because the power station production is in direct relation with beater wheel mill availability, maintenance of beater wheel mill is very important task. Maintenance is a function that operates in parallel to production and can have a great impact on the capacity of the production and quality of the products produced, and therefore, it deserves continuous improvement [16]. According to the study conducted by Mobley [15], between 15% and 40% of total production cost is attributed to maintenance activities in the factory. Furthermore,

with the energy costs, maintenance costs can be the largest part of any operational budget [14]. Predictive maintenance is a maintenance policy in which selected physical parameters associated with an operating machine are sensored, measured and recorded intermittently or continuously for the purpose of reducing, analyzing, comparing and displaying the data and information obtained for support decisions related to the operation and maintenance of the machine [6]. Predictive maintenance can be disaggregated into two specific sub-categories: statistical-based predictive maintenance - the information generated from all stoppages facilitates development of statistical models for predicting failure and thus enables the developing of a preventive maintenance policy and condition-based predictive maintenance-condition-based monitoring is related to the examination of wear processes in mechanical components [7]. Condition based monitoring (CBM) is one of the maintenance policies that require an intense use of modern technologies. CBM attempts to avoid unnecessary maintenance tasks by taking maintenance actions only when there is an evidence of abnormal behaviors of a physical asset. A CBM program, if properly established and effectively implemented, can significantly reduce maintenance cost by reducing the number of unnecessary scheduled preventive maintenance operations [2]. It is based on the periodical acquisition of data in order to verify the condition of the critical machinery, diagnosis of the faults and evaluation of the remaining life time of the machine [15]. The predictive maintenance through vibration analysis is the best tool for rotating machinery maintenance purpose. The vibration analysis is a technique, which is being used to track machine operating conditions and trend deteriorations in order to reduce maintenance costs and downtime simultaneously [1, 20]. Machine vibration signals often demonstrate a highly non-stationary and transient nature and carry small yet informative components embedded in larger repetitive signals due to external varying operating conditions and internal natural deterioration characteristics of machinery [21]. The traditional vibration-based diagnostic approaches for rotational machines are largely designed for stationary and known operating conditions. The problem of fault detection under fluctuating load and speed has received commendable attention so far. Usually, the information regarding operating conditions is directly used in the process of calculating feature values. On the other hand, there are approaches that exploit the non-stationary character of the vibration signals generated by mechanical drives operating under variable conditions [22]. Additionally, variable operational conditions may cause significant variation of the energy of investigated component. Vibration signals are particularly dependent on variable load and speed fluctuation [13]. However, these parameters cannot be used to precisely detect faults of machinery in unsteady operating conditions; as in the case here, where the rotating speed and load of the machine are always changing [19, 22]. To minimize the cost of power generation in thermal power stations based on CBM philosophy and vibration based diagnostic signature analysis techniques study for bowl-roller coal pulverizes where used [17]. The influence of operating parameters, such as coal flow, primary air flow, and operating temperature, on roller mill vibration are investigated. The experimental results for industrial tubular ball mil show that the operating modes of the mill, such as mill over-load, stable case, etc., can be diagnosed by proper interpretation of vibration characteristics; and also the unmeasured parameters, i.e., level of coal powder filling the mill, can be monitored on line [12]. Most of the researcher focused on ball and bowl mills but interaction of pulverizing process parameters with beater wheel mill overall vibration have not been reported. The objectives of the present study ware (1) to instigate correlation between pulverizing process parameter, such as electrical current of the driving motor, mill capacity, boiler production, coal types on beater wheel mill overall vibration, (2) to use multiple regression analysis to assess the quality of the beater wheel mill overall vibration prediction in regard of selected pulverizing process parameters with intent to gather appropriate information for beater wheel mill predictive maintenance program setup.

2. Beater wheel mill pulverized coal firing supplying system

The circulated flue gas of coal furnace is used to transport the fuel. Flue gas is discharged from the furnace, and then the pre-crushed coal transported by a belt conveyor is fed into the flue gas pipe through a feeder. Afterwards, a heat exchanger considerably decreases the flue gas temperature and the flue gas with the fed and crushed coal gets into the beater wheel mill. The beater wheel mill has two basic roles; it is a ventilator and a mill at the same time. Those two functions cannot be controlled separately which is considerable disadvantage of this technology. The mill is a beating–impacting type of mill. Combination mainly takes place by impacting and by beating in smaller extent. Beater wheel mill concept is shown on Fig. 1.

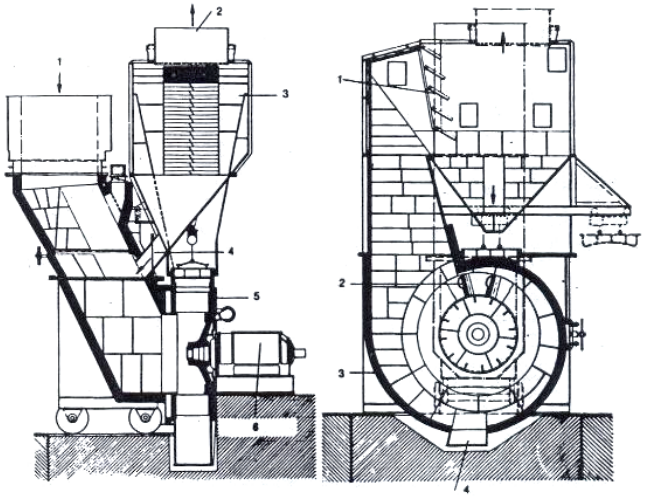

Fig. 1. Beater wheel mill concept; 1-coal and recalculation gasses; 2-mixture; 3-seperation; 4-return of larger coal particles; 5-beater wheel; 6-double bearing; (1)-regulation flap; (2)-beater wheel; (3)-housing armor; (4)-metal bins canal.

The product of the mill–classifier cycle is transported by the flue gas, through a heat isolated pipe into the burner in the furnace [3]. The total power requirement for grinding is dependent on the mill size, the grinding fineness specified and the type and layout of the suction and pressure ducting. The inlet ducting of the mill is mounted on a carriage assembly to facilitate access to the beater wheel. Since the wheel is the principal grinding element it suffers most of the wear. Mill availability is largely determined by the service life of the wheel and the ease with which it can be replaced [8]. It is usual to replace the worn beater wheel with a refurbished wheel and resume the operation. The worn wheel may then be refurbished and rebalanced at leisure [8]. Pulverized coal fuel availability is critical element in achieving an efficient combustion in power plants. To have high availability, maintenance of beater wheel mill is crucial. Failure or high vibration of beater wheel mill require mill shutdown and other fuel usage-like crude oil to maintain furnace production which increase an electricity production costs.

2.1. Beater wheel mill maintenance

Beater wheel mill vibrations influence the durability, operating condition and the product quality of many coal power plants. Vibrations can lead to component failures, speed fluctuations, surface defects and strip thickness undulations. The coal pulverizing process consists of sudden unstable condition and usually leading to high

vibration resulting pulverizing shutdown and economic losses. Beater wheel mills, an important part of steam production process in most of Balkan countries coal-fired power plants have experienced many vibration problems during operation [4]. Therefore, studies of pulverizing process parameters are important and interesting for the determination of the beater wheel mill vibration origin, influence and distribution. While the construction geometry characteristics of beater wheel mill vibration have been studied [4], there is no available data for pulverizing process parameters and beater wheel mill vibration interaction. During operation, conditions are changing all the time and they are stochastic [10]. However, when rotation of the rotor, multiplied by the number of beater plates, approaches a resonant frequency, the vibration could rises well beyond an acceptable limit and resonances can be excited in the pipe, base, valve, pump or other nearby equipment [5]. Quality balance of rotor at the beginning, need for rotor replacement and its unbalance progression during operation could be clearly identified using vibration frequency spectrums at the beginning and end of lifetime of the beater wheel mill, primarily in axial direction [4]. Continuous and quality monitoring of beater wheel mill increases safety and productivities, reducing failure time and provide continuous operation in close optimum conditions [4].

3. Material and methods

To identify the relationship between the selected pulverizing process parameters and beater wheel mill overall vibration, multiple correlation and multiple regression analysis were used. Correlation measures the strength of inter relationship between the selected pulverizing process parameters and overall mill vibration. Multiple regression analysis is used to assess the quality of the prediction of the dependent variable. It corresponds to the squared correlation between the predicted and the actual values of the dependent variable. It can also be interpreted as the proportion of the variance of the dependent variable explained by the independent variables. When the independent variables (used for predicting the dependent variable) are pair wise orthogonal, the multiple correlation coefficient is equal to the sum of the squared coefficients of correlation between each independent variable and the dependent variable. This relation does not hold when the independent variables are not orthogonal [9]. It can be important to determine whether a multiple regression coefficient is statistically significant, because multiple correlations calculated from observed data will always be positive. The multiple regression procedure capitalizes on chance by assigning greatest weight to those variables which have the strongest relationships with the criterion variables in the sample data [18]. The ability of any single variable to predict the criterion is measured by the simple correlation and the statistical significance of the correlation can be tested with the t-test, or with an f-test. Often it is important to determine if a second variable contributes reliably to prediction of the criterion after any redundancy with the first variable has been removed [9]. Regression analysis is not always needed for prediction or explanatory models; sometimes the intention is only to adjust a regression equation to available data. In fact King [11] argues that the objective of a regression analysis is simply to measure the effects of predictors on the dependent variable. The experiments for the study were implemented under practical working conditions at synthetic soda ash producer FSL-Fabrika Sode Lukavac, Tuzla, Bosnia and Herzegovina, at furnace supplied by two fuel preparing systems, each with a beater wheel mill used for drying, pulverizing and conveying coal to furnace. Both beater wheel mills were used in the study. In this research beater mill produced by RGMK Serbia with 2090 mm rotor diameter driven by a three-phase electrical motor (320 kW and 987 min^{-1}) was used. Vibration measurement was carried out on the mill rotor double bearing housing support. In the vibration measurement, a vibration measurement device (Pruftechnik, Vibscanner) was used. The piezoelectric accelerometer (PruftechnikVIB 6.142 R) was mounted on the double bearing housing in axial direction. The accelerometer was connected to the vibration measurement device and vibration amplitudes Va-Root Mean Square were collected. Electrical motor speed was held constant at 987 min^{-1} in the measurements. Selected pulverizing process parameters in the tests were: electrical current of the driving motor Am, mill capacity Tkp, boiler production Qk, coal types St-Stanari, Ba-Banovići, Mr-Mramor. Measurement of mill overall vibration and selected pulverizing process parameters was simultaneously. Mill capacity setting was adjusted by the operator during the tests. Sampling systems were conducted for two fuel supplying systems, separately, followed the practical production needs only sampling time was constant. Eight tests for first and second fuel supplying systems were conducted. This procedure was applied to all test and 7 days was the time between tests. Duration of experiment was limited to 56 days and after this period unacceptable vibration was generated which required mill rotor replacement. The data recorded were statistically analyzed using multiple correlations and multiple regression analysis to study the effects of selected pulverizing process parameters to mill vibration.

4. Results and discussion

Selected pulverizing process parameters and overall mill vibration for the first and second fuel supplying system is shown on Fig. 2. It displays grouped Scatter Plots of overall mill vibration against other selected pulverizing process parameters over the different mill capacity. Correlation coefficient matrix for selected pulverizing process parameters and mill overall vibration is shown in Fig. 3, for first fuel supplying system as model 1, Fig. 4 for second fuel supplying system as model 2 and Fig. 5 considering both fuel supplying systems as model 3. Histograms of the variables appear along the matrix diagonal and scatter plots of variable pairs appear off-diagonal. Relationships provide interesting interaction information of selected pulverizing process parameters and mill vibration. Observing first fuel supplying system boiler production Qk correlation coefficient was highest while the mill capacity Tkp was lowest, presented in Fig. 3. All correlation coefficient was relatively low. Observing second fuel supplying

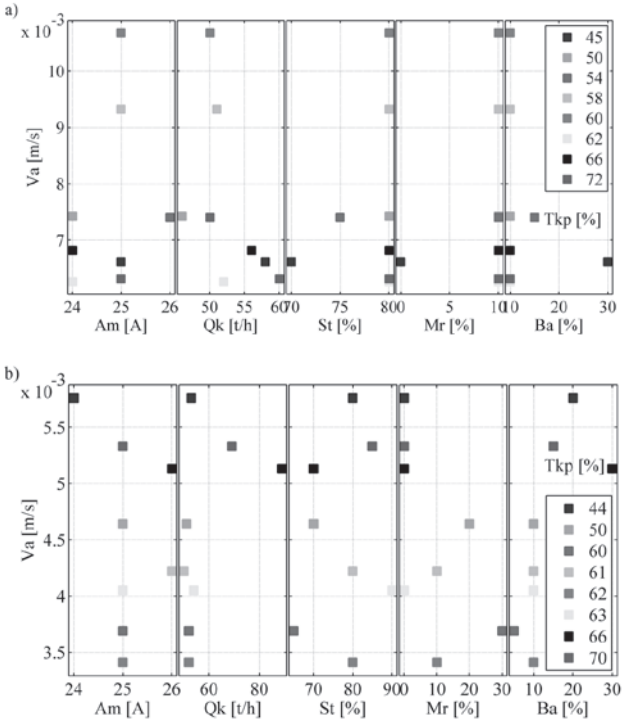

Fig. 2. Scatter plots of selected palavering process parameters and mill overall vibration: (a) First fuel supplying system; (b) Second fuel supplying system

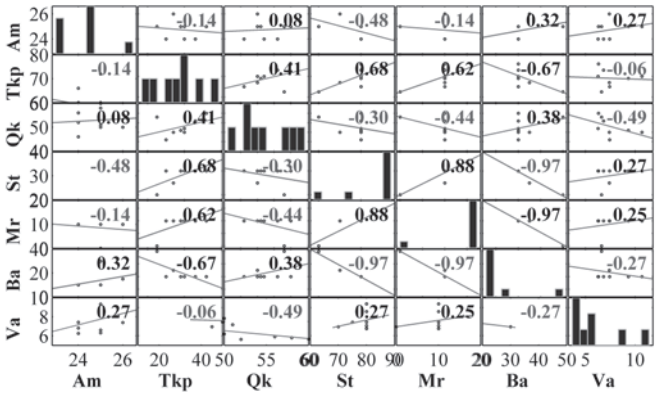

Fig. 3. First beater wheel mill correlation coefficient matrix

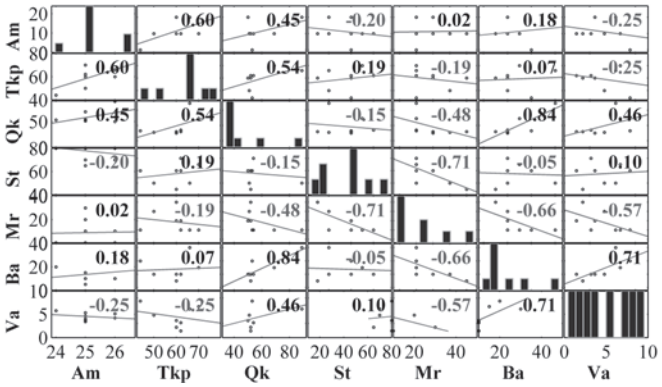

Fig. 4. Second beater wheel mill correlation coefficient matrix

system, coal type Ba had highest correlation coefficient and the coal type St lowest, presented in Fig. 4. All other correlation coefficient was relatively low, too. Taking in to consideration both fuel supplying system and correlating vibration amplitude with selected pulverizing process parameters, it is evident low correlation interaction. In this case, with more data taking in consideration, the highest correlation coefficient had boiler production Qk and the lowest coal type Ba presented in Fig. 5.

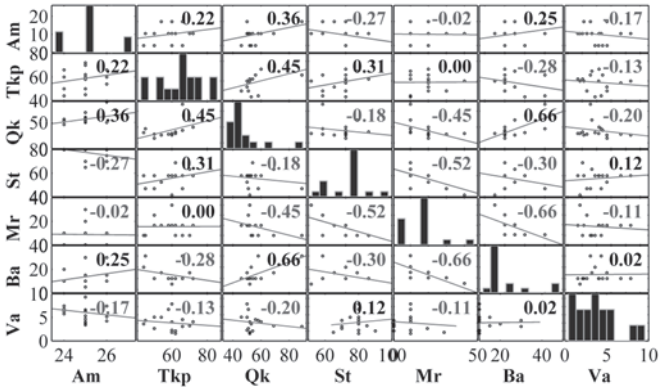

Fig. 5. Combined, first and second beater wheel mill correlation coefficient matrix

Results of correlation coefficient analysis indicate that beater wheel mill overall vibration is not significantly correlated with selected pulverizing process parameters. Values of the correlation coefficient coal type Ba for the second beater wheel mill are relatively high and positive which indicates relation with beater wheel mill vibration in a positive linear sense. This could be explained due the relatively hard coal, much harder than other two types used in pulverizing mixture. Increasing the percentage of coal type Ba it results in increase of beater wheel mill vibration, presented in Fig. 4. Tables 1-3 shows results of analysis of variance for first, second and third model, respectfully.

Multiple regression analysis was used to test possibility of mathematical model development and the analysis of variance method was used to test their adequacy. The goal of the multiple regression analysis was to determine the dependency of selected pulverizing process parameters to beater wheel mill vibration. The input variables for model prediction were: electrical current of the driving motor, mill capacity, boiler production, coal types and output variable was mill overall vibration. The analysis of variance as model was used to test model regression significance. This approach uses the variance of the observed data to determine if a regression model can be applied to the observed data. The analysis of variance calculations for multiple regressions are nearly identical to the calculations for simple linear regression, except that the degrees of freedom are adjusted to reflect the number of explanatory variables included in the model. With this organization of the data sets, the modeling study for the beater wheel mill has been carried out. Model 1 estimating the relationships among selected variables for the first fuel supplying system, model 2 for the second fuel supplying system and model 3 for combined data sets of first and second fuel supplying systems. According to multiple regression analyses, 88 % for model 1, 73 % for model 2 and 15 % for model 3; beater wheel mill vibration variability depends on selected pulverizing process parameters. This analysis was out for a 5% significance level, i.e., for a 95%

Table 1. First wheel regression coefficients

	Coeffi-cients	Standard Error	t Stat	P-value	Lower 95%	Upper 95%	Lower 95%	Upper 95%
Intercept	-192,85	71,410	-2,700	0,1141	-500,1	114,39	-500,1	114,39
Am	1,8933	0,9467	1,9999	0,1835	-2,180	5,9665	-2,180	5,9665
Tkp	0,4949	0,3561	1,3896	0,2991	-1,037	2,0272	-1,037	2,0272
Qk	-0,9712	0,5287	-1,837	0,2076	-3,245	1,3035	-3,245	1,3035
St	1,9943	0,6809	2,9288	0,0995	-0,935	4,9240	-0,935	4,9240
Ba	1,5532	0,6080	2,5545	0,1251	-1,062	4,1693	-1,062	4,1693
Mr	0,0000	0,0000	65535	0,0000	0,0000	0,0000	0,0000	0,0000

Table 2. Second wheel regression coefficients

	Coeffi-cients	Standard Error	t Stat	P-value	Lower 95%	Upper 95%	Lower 95%	Upper 95%
Intercept	-0,2279	32,685	-0,007	0,9951	-140,8	140,40	-140,8	140,40
Am	-0,1393	0,7031	-0,198	0,8612	-3,164	2,8858	-3,164	2,8858
Tkp	-0,1124	0,1403	-0,801	0,5072	-0,716	0,4913	-0,716	0,4913
Qk	0,1014	0,1399	0,7247	0,5439	-0,500	0,7032	-0,500	0,7032
St	0,1090	0,2524	0,4317	0,7080	-0,977	1,1951	-0,977	1,1951
Ba	0,0000	0,0000	65535	0,0000	0,0000	0,0000	0,0000	0,0000
Mr	0,0590	0,1971	0,2992	0,0000	-0,789	0,9071	-0,789	0,9071

Table 3. Both wheels regression coefficients

	Coeffi-cients	Standard Error	t Stat	P-value	Lower 95%	Upper 95%	Lower 95%	Upper 95%
Intercept	17,341	22,2522	0,7793	0,4538	-32,23	66,922	-32,23	66,922
Am	-0,4974	0,9925	-0,501	0,6271	-2,708	1,7140	-2,708	1,7140
Tkp	0,1387	0,1790	0,7745	0,4566	-0,260	0,5376	-0,260	0,5376
Qk	-0,1833	0,1694	-1,082	0,3046	-0,560	0,1941	-0,560	0,1941
St	0,0000	0,0000	65535	0,0000	0,0000	0,0000	0,0000	0,0000
Ba	0,2361	0,2805	0,8417	0,0000	-0,388	0,8612	-0,388	0,8612
Mr	0,0056	0,1162	0,0484	0,9624	-0,253	0,2645	-0,253	0,2645

Table 4. Summary of the multiple linear regression models

Model	RR	R^2	Adjusted R^2	Standard error	Observations	Significance F
1	0.94	0.88	0.11	0.98	8	0,6170
2	0.85	0.73	-0.41	0.79	8	0,4029
3	0.39	0.15	-0.36	2.25	16	0,8825

confidence level. Model summaries in the terms of regression statistics are presented in Table 4.

After the models were obtained, including all variables considered predictors, the statistical significance of the model was tested. In the first place it was necessary to understand whether a mathematical model combining the predictors considered would be able to model the reality found in the field work. The value found for R^2 was 0.88 for model 1, 0.73 for the model 2 and 0.15 for model 3, which shows a poor match between the model and reality. The Significance F was used to evaluate the explanation of the regression model; since the Significance F for all three models is much higher than 0.05 for a confidence level of 95%, then the null hypothesis is accepted, there is no statistically significant association between selected pulverizing process parameters and overall mill vibration, indicate inappropriate multiple regression model build. In all three models, since the t values for all predictor coefficients are lower in absolute value than t-critical, it was considered that the models are not well adjusted. Also, 34% for model 1, 51% for model 2 and 92% for model 3; beater wheel mill vibration cannot be explained by selected pulverizing process parameters. Standard regression error, 0.98 for model 1, 0.79 for model 2 and 2.25 for model 3, indicates poor regression equations for all three models.

5. Conclusions

Linear relationship between the beater wheel mill overall vibration and selected pulverizing process parameters significantly does not exist and creation of mathematical model would not be adequate are major contributions of presented study. Beater wheel mill vibration cannot be fully correlated with the selected pulverizing process parameters and those parameters are not the only parameters that determine the level of mill overall vibration due to low correlation coefficients presented in statistical analysis. To effectively setup predictive maintenance program selected pulverizing process parameters need to be excluded as important factors. Unlike most coal mills where pulverizing process parameters must take into account, here with beater wheel impact mills it is not the case and condition monitoring of these mills could be conducted offline or online using standard vibration condition monitoring methods.

References

1. Alguindigue IE, Buczak LA, Uhrig RE. Monitoring and diagnosis of rolling element bearings using artificial neural networks. IEEE Transactions on Industrial Electronics 1993; 40(2): 209–17.
2. Andrew KS. Jardine, Daming Lin, Dragan Banjevic. A review on machinery diagnostics and prognostics implementing condition-based maintenance. Mechanical Systems and Signal Processing 2006; 20(7): 1483–1510.
3. Csoke JB, Faitli G, Mucsi G, Antal F Bartók. Comminution of forest biomass by modified beater wheel mill in a power plant. International Journal of Mineral Processing 2012; 112-113(10): 13–18.
4. Bajrić R, Zuber N, Karić S. Experimental vibration investigation of an industrial beater wheel mill, Technics Technologies Education Management 2010; 5(4): 688–692.
5. Bajrić R, Baričak V, Delalić S, Muratović P, Zuber N. Investigation of possible resonant problems during beater wheel mill operation, Technics Technologies Education Management 2010; 5(1): 32–37.
6. Carnero MaCarmen. Selection of diagnostic techniques and instrumentation in a predictive maintenance program. A case study. Decision Support System 2005; 38(4): 539–555.
7. Carnero MaCarmen. An evaluation system of the setting up of predictive maintenance programme. Reliability Engineering & System Safety 2006; 91(8): 945–963
8. Christer AH, Wang W, Sharp JM. A state space condition monitoring model for furnace erosion prediction and replacement. European Journal of Operational Research 1997; 101: 1–14.

9. Cohen J, Cohen P. Applied multiple regression/correlation analysis for the behavioral sciences -2nd edition. New York: Erlbaum Hillsdale, 1993.
10. Scott DH. Coal Pulverizes: Performance and Safety, London: IEA Coal Research Report V (79), 1995.
11. King G. How not to lie with statistics: avoiding common mistakes in quantitative political science, American Journal of Political Science 1986; 30: 666–687.
12. Si GQ, Cao H, Zhang YB, Jia LX. Experimental investigation of load behaviour of an industrial scale tumbling mill using noise and vibration signature techniques. Minerals Engineering 2009; 22: 1289–1298.
13. Urbanek J. Application of averaged instantaneous power spectrum for diagnostics of machinery operating under non-stationary operational conditions. Measurement 2012; 45(7): 1782–1791.
14. Lofsten H. Measuring maintenance performance-in search for a maintenance productivity index. International Journal of Production Economics 2000; 63: 47–58.
15. Mobley RK. An introduction to predictive maintenance. 2nd ed., Boston, USA: Butterworth Heinemann; 2003.
16. Moubray J. Reliability-centered maintenance. 2nd ed., Oxford: Butterworth Heinemann; 1997.
17. Nathan RJ, Norton MP. Vibration signature based condition monitoring of bowl-roller coal pulverizers, Journal of Vibration and Acoustics, ASMS Transactions 1993; 115(4): 452–462.
18. Draper NR, Smith H. Applied Regression Analysis, John Wiley and Sons Inc., New York, 1998.
19. Peng Chen, Masatoshi Taniguchi, Toshio Toyota, Zhengja He. Fault diagnosis method for machinery in unsteady operating condition by instantaneous power spectrum and genetic programming. Mechanical Systems and Signal Processing 2005; 19(1): 75–194.
20. Sedat Karabay, Ibrahim Uzman. Importance of early detection of maintenance problems in rotating machines in management of plants: Case studies from wire and tyre plants. Engineering Failure Analysis 2009; 16: 212–224.
21. Tsang AHC. Condition-based maintenance: tools and decision making. Journal of Quality in Maintenance Engineering 1995; 1(3): 3–17.
22. Zhan Y, Makis V, Jardine AKS. Adaptive model for vibration monitoring of rotating machinery subject to random deterioration. Journal of Quality in Maintenance Engineering 2003; 9(4): 351–375.

Rusmir BAJRIĆ
Public enterprise Elektroprivreda BIH
Coal Mine Kreka
Mije Keroševica 1,
Tuzla, Bosnia and Herzegovina
E-mail: rusmir.bajric@kreka.ba

Ninoslav ZUBER
Rastislav ŠOSTAKOV
Faculty of Technical Sciences
University of Novi Sad
Trg Dositeja Obradovica 6, Serbia
E-mails: zuber@uns.ac.rs , sostakov@uns.ac.rs

Article citation info:
KOPECKI T, MAZUREK P. Numerical representation of post-critical deformations in the processes of determining stress distributions in closed multi-segment thin-walled aircraft load-bearing structures. Eksploatacja i Niezawodnosc – Maintenance and Reliability 2014; 16 (1): 163–169.

Tomasz KOPECKI
Przemysław MAZUREK

NUMERICAL REPRESENTATION OF POST-CRITICAL DEFORMATIONS IN THE PROCESSES OF DETERMINING STRESS DISTRIBUTIONS INCLOSED MULTI-SEGMENT THIN-WALLED AIRCRAFT LOAD-BEARING STRUCTURES

NUMERYCZNE ODWZOROWANIE DEFORMACJI ZAKRYTYCZNYCH W PROCESACH OKREŚLANIA ROZKŁADÓW NAPRĘŻEŃ W ZAMKNIĘTYCH WIELOSEGMENTOWYCH CIENKOŚCIENNYCH LOTNICZYCH STRUKTURACH NOŚNYCH*

The study presents results of a research work on the problem of obtaining reliable results of nonlinear FEM analyses of thin-walled load-bearing structures subjected to post-critical loads. Consistency of numerical simulations results and actual stress distribution states depends on the correct numerical reproduction of bifurcations that occur during advanced deformations processes.

***Keywords**: shell, torsion, bifurcation, experiment, load-bearing structures, nonlinear numerical analysis.*

Opracowanie przedstawia wyniki badań związanych z problemem uzyskiwania wiarygodnych wyników nieliniowych analiz numerycznych, w ujęciu metody elementów skończonych, cienkościennych struktur nośnych poddawanych obciążeniom zakrytycznym. Zgodność wyników numerycznych symulacji z rzeczywistymi dystrybucjami naprężeń uzależniona jest od poprawnego numerycznego odwzorowania bifurkacji zachodzących w procesach zaawansowanych deformacji.

***Słowa kluczowe**: powłoka, skręcanie, bifurkacja, eksperyment, struktury nośne, nieliniowa analiza numeryczna.*

Introduction

Thin-walled load-bearing systems are widely applied in modern aviation structures. The strict requirements with regard to the levels of transferred loads and the need to minimise the total mass of the structure is often the cause for which it becomes necessary to accept occurrence of physical phenomena that in case of other structures are considered as inadmissible. An example of such a phenomenon is the loss of stability of shells that are parts of load-bearing structures within the range of admissible operating loads [13].

Thus, an important stage in the design work on an aircraft load-bearing structure is to determine the stress distribution in post-critical deformation state [12]. One of the numerical tools used to obtain actual displacement distributions and the resulting stress distributions is the nonlinear finite elements analysis. The assessment of the reliability of the results thus obtained is based on the solution uniqueness rule according to which a specific deformation pattern can correspond to one and only one stress state. In order to apply this rule it is necessary to obtain such displacement distributions of the numerical model that fully corresponding to actual deformations of the analysed structure.

An element decisive for a structure's deformation state is the effect of a rapid change of the structure's shape occurring when the critical load levels are exceeded [2]. From the numerical point of view, this phenomenon is interpreted as a change of the relationship between state parameters corresponding to specific degrees of freedom of the system and the control parameter related to the load [3]. This relationship, defined as the equilibrium path, in the case of occurrence of the above-mentioned phenomenon, has an alternative nature usually called bifurcation. Therefore, the fact of taking a new deformation pattern by the structure corresponds to a sudden change to an alternative branch of the equilibrium path [4].

Therefore, a prerequisite for obtaining a proper form of the numerical model deformation is to retain the conformity between numerical bifurcations and those occurring in the actual structure. In order to determine such conformity it is necessary to verify the results obtained by an appropriate model experiment or by using the data obtained during the tests of the actual object [9]. Obtaining reliable results of nonlinear numerical analyses is often troublesome and it requires an appropriate selection of numerical methods depending on the type of the analysed structure and the degree of precision to which the parameters controlling the course of procedures were determined [14].

In view of the number of state parameters, the full equilibrium path should be interpreted as a hyper-surface in hyperspace of states satisfying the matrix equation for residual forces:

$$\mathbf{r}(\mathbf{u}, \Lambda) = \mathbf{0}, \tag{1}$$

where $\mathbf{u}$ is the state vector composed of structure nodes' displacement components corresponding to current geometrical configuration, Λ is a matrix composed of control parameters corresponding to the current load state, and $\mathbf{r}$ is the residual vector composed of uncompensated force components related to the current system deformation state. The

(*) Tekst artykułu w polskiej wersji językowej dostępny w elektronicznym wydaniu kwartalnika na stronie ***www.ein.org.pl***

set of control parameters can be represented by a single parameter that is a function of the load. Equation (1) takes then the form

$$\mathbf{r}(\mathbf{u}, \lambda) = \mathbf{0}, \tag{2}$$

called a monoparametric equation of residual forces.
The prediction-correction methods of determining the consecutive points of the equilibrium path used in contemporary software routines contain also a correction phase based on the requirement that the system satisfies an additional equation called the increment control equation or the constraints equation [5]:

$$c(\Delta\mathbf{u}_n, \Delta\lambda_n) = 0, \tag{3}$$

where the increments

$$\Delta\mathbf{u}_n = \mathbf{u}_{n+1} - \mathbf{u}_n \qquad \text{and} \qquad \Delta\lambda_n = \lambda_{n+1} - \lambda_n \tag{4}$$

correspond to the transition from n-th state to n+1-th state.

Graphical interpretation of the increment control equation is shown in Figure 1.

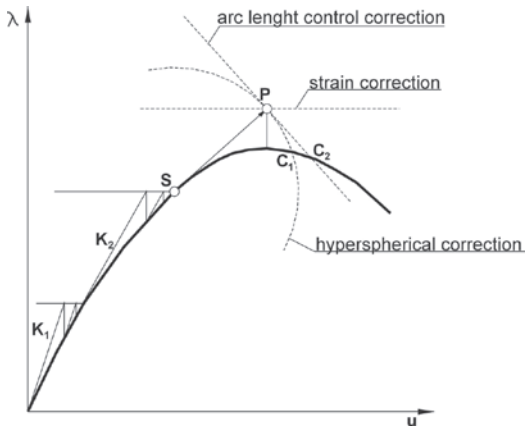

Fig. 1. Graphical representation of various correction strategies for the representative system with one degree of freedom

Because of the large number of degrees of freedom and state parameters corresponding to them, the deformation processes are represented in practice by applying substitute characteristics called the representative equilibrium paths [8]. They define relationships between a control parameter related to the load and a selected characteristic geometric value related to deformation of the structure.

2. Subject and scope of research

Bifurcation changes of forms observed in load-bearing structures containing shells with considerable curvature occur the more violently the higher is the ratio of the square of the smaller of dimensions of the shell segment area limited by the adjacent member frames to the value of the local radius of its curvature [6]. Semi-monocoque structures with relatively low number of the framing elements are therefore especially difficult as far as their nonlinear numerical representations are considered [7].

An example of such a structure is a closed cylindrical thin-walled shell reinforced with frames and stringers. The type of the structure itself corresponds to solutions commonly used in the aviation technology, e.g. the construction of an aircraft fuselage tail beam (Figure 2). The subject of the present research were structures a general schematic diagram of which is presented in Figure 3.

Several variants of them were analysed, differing in the number of stringers and frames. The first variant was considered a fundamental

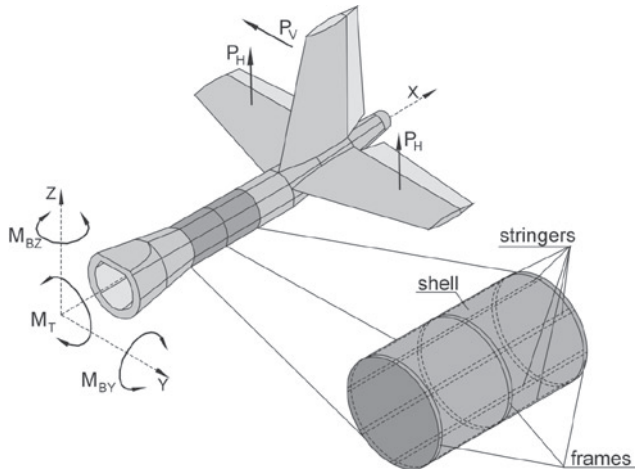

Fig. 2. Application of the examined structure in the airframe structure

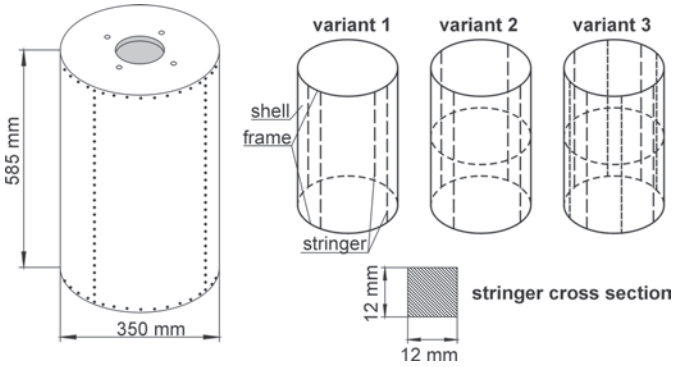

Fig. 3. Schematic drawing of the examined structure

one, with the skeleton consisting of two frames and four stringers. The second variant represented a structure with four stringers reinforced with additional frame placed in the middle of the shell length. The third variant was the structure reinforced with eight evenly distributed stringers. Models of all variants of the structure were made out of polycarbonate for which the tensile strength test was carried out and the material constants determined, yielding the Young's modulus E = 3000 MPa and the Poisson ratio v = 0.36.

Figure 4 shows the characteristic of the above-mentioned material corresponding to one-dimensional tensile stress. The clearly visible elastic and inelastic deformation zones suggest the possibility to approximate the actual material characteristic by the ideal elastic-plastic model. However, due to fact that only a local elastic loss of stability of the structure is acceptable, the elastic material model was adopted in all numerical models. Moreover, because of its low elasticity modulus value (by two orders of magnitude less than this of steel) it was possible to carry out experiments at low values of external loads.

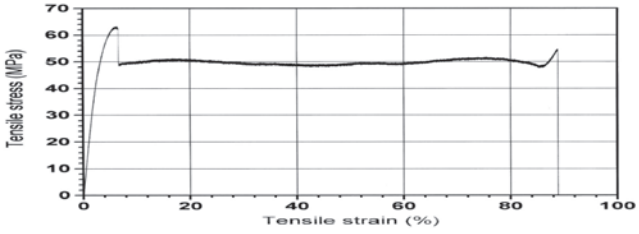

Fig. 4. The tensile stress plot for a polycarbonate sample

The choice of the material, apart from the above-mentioned physical characteristics, was also justified by its high optical activity thanks to which it became possible to obtain qualitative information about optical effect distribution in circular polarisation conditions [1]. Joints

Fig. 5. Distribution of isochromatic fringe patterns in vicinity of bolts subject to control during the assembly

between the shell and the stringers were realised by means of steel bolts spaced 20 mm apart. In order to avoid possible assembly stress at bolt joints, continuous observation of isochromatic fringe pattern fields in the vicinity of each bolt was carried out throughout the whole assembly work (Figure 5).

3. Experimental research

The first variant of the structure's framing comprises a minimum number of crosswise elements, i.e. two closing frames and four longitudinal members. It should be emphasised, however, that the model subjected to examinations constituted a special instance of a structure of purposefully minimised number of longitudinal members. The actual solutions are usually based on more extended framings corresponding to the consecutive two variants.

The examined structure was subjected to constrained torsion using the experimental set-up depicted in Figure 6.

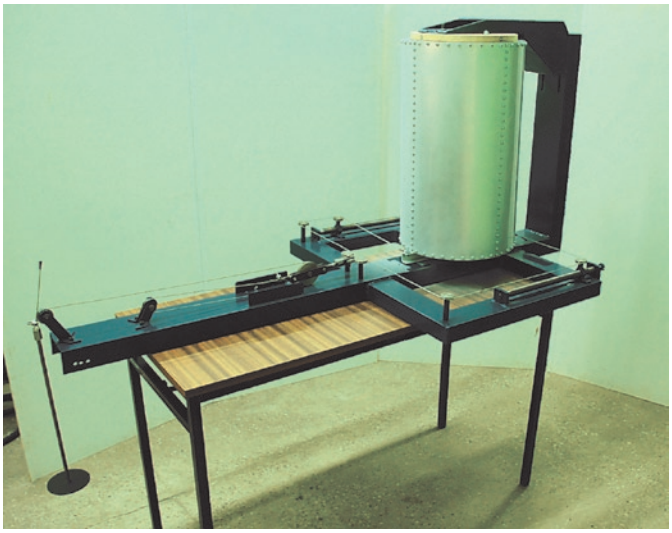

Fig. 6. Experimental set-up

According to the expectations, post-critical deformations occurred in a violent way. Due to application of gravitational load, the measurement of the relationship between the torsion angle and the torque moment, assumed to be the representative equilibrium path, corresponded to the steady states [9] (Figure 16).

With this measurement method, the representative characteristics does not reflect bifurcation points in an apparent way, but attention should be drawn to the occurrence of its horizontal section. It corresponds to the phase of the experiment in which a sudden change occurred in the structure state while the load level remained constant. The nature of the equilibrium path curve corresponds to the unstable bifurcation type typical for shell structures.

With regard to the symmetry, the deformed structure revealed four characteristic wrinkles in all the shell segments (Figure 7). During the experiment, the surface geometry was registered using the projection moiré method. Atos scanner by German company GOM Optical Measuring Techniques was used for this purpose.

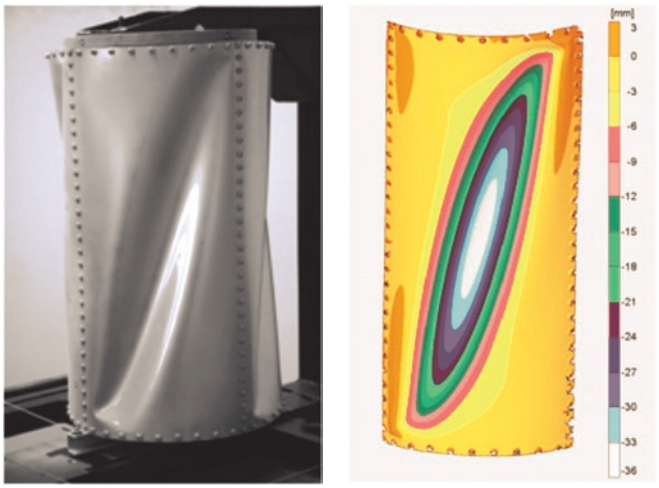

Fig. 7. Advanced post-critical deformation of the examined structure (left) and the distribution of contour lines representing magnitude of deformation with the use of the projection moiré method (right) – variant 1

Due to large dimensions of the shell segments, the loss of stability resulted in this case in an abrupt significant change of the total torsion angle of examined structure. As it has been already mentioned above, such a property makes it impossible to apply such technical solution in actual aircraft structures [13]. However, analyses of similar special cases allow to elaborate FEM numerical models and represent a significant research potential.

In the next step, another variant of the structure (Figure 3, variant 2) with an additional frame was examined. The change of dimension ratios characterising shell segments limited with skeleton components of the structure did not result in any significant change of the critical load value. However, the loss of stability revealed a more gentle nature in this case manifesting with a lack of a sudden change on the representative equilibrium path shown in Figure 17.

A large decrease of the total torsion angle value was also observed compared to the first variant. Therefore, this kind of technical solution seems to be much more useful from the practical point of view. Thanks to the lack of rapid deformation increases, there is no considerable risk that an aircraft will lose its essential aerodynamic characteristics (for instance, effectiveness of its flight control surfaces).

Figure 8 presents distribution of deformations in an isolated shell segment of the examined structure and the related displacement distribution obtained by means of the optical scanner.

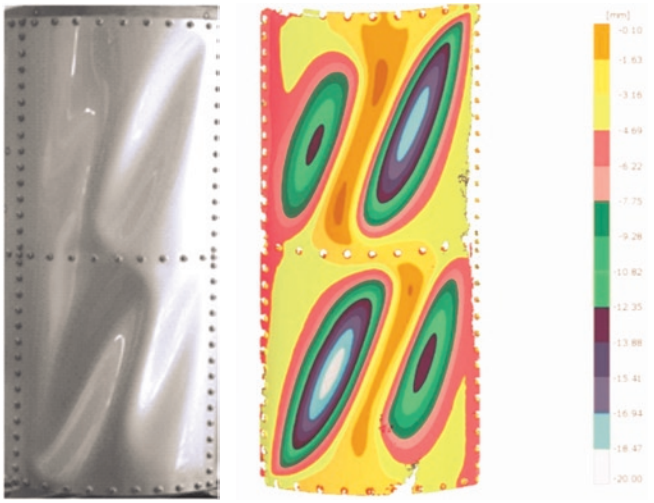

Fig. 8. Advanced post-critical deformation of the examined structure (left) and the distribution of contour lines representing magnitude of deformation with the use of the projection moiré method (right) – variant 2

In the last version of the examined structure, four additional stringers were applied (Figure 3, variant 3). Distribution of post-critical deformations presented in Figure 9 and the representative equilibrium path plotted in Figure 18 allow to conclude that the observed phenomena had in this case significantly different nature then in the two previous models. First of all, the loss of stability occurred at much lower level of the load. It seems to be a result of change of the ratio of shell segments dimensions to their curvature radii [6]. Decrease of the critical load value, however, does not mean necessarily the lessening of practical value of the structure. It should be emphasised that its torsional stiffness significantly increased. Therefore, the loss of stability results in occurrence of small geometrical imperfections on the fuselage skin and the related increase of the drag coefficient, but higher stiffness guarantees that essential aerodynamic characteristics of the aircraft are maintained.

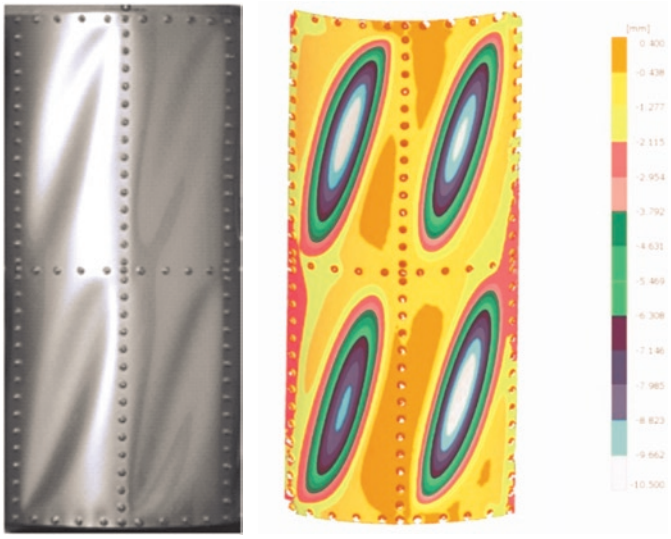

Fig. 9. Advanced post-critical deformation of the examined structure (left) and the distribution of contour lines representing magnitude of deformation with the use of the projection moiré method (right) – variant 3

4. Numerical FEM analysis

The first variant of the examined structure turned out to be one of the most troublesome from the point of view of a FEM-based nonlinear numerical simulation. A number of tests performed with the use of MSC MARC software revealed the lack of effectiveness of its procedures in case of this problem, with regard to determining the appropriate post-buckling state of the structure. The algorithms used in these procedures are characterised by inability to represent the symmetry of the phenomenon. With the idealised geometric form of the model, the obtaining of the new form of the structure after crossing the critical load value occurs only in one of the segments, despite the apparently correct symmetrical initiation of the loss of stability [11]. This indicates existence of errors in algorithms used for choosing appropriate variants of the equilibrium path in case of the appearance of changes in the state parameters combinations in several of their independent subsets [8].

The situation improved when the shell imperfections were implemented by introducing forces normal to the skin and applied to central points of individual skin segments (Figure 10). The values of the forces in all cases corresponded to their highest values applied during the experiment.

However, even in the case of using this type forcing a change in the fuselage shape, it was still very difficult to obtain results fully consistent with the experiment. Assuming the use of shell elements with linear shape functions, the appropriate density of the mesh turned out

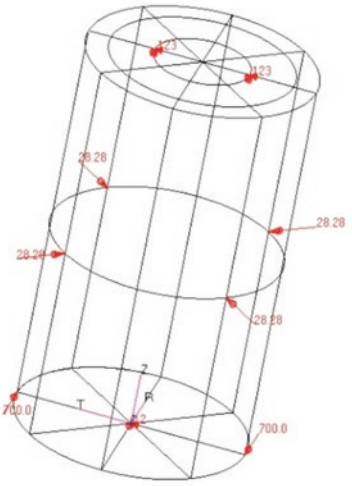

Fig. 10.A geometrical model of a structure defined in MSC PATRAN environment with boundary conditions and load (in N)

to be the key factor, but excessive density resulted in appearance of incorrect forms of post-critical deformations [14] (Figure 11).

A better result, in the case of beam elements representing stringers, was obtained with the use of a relatively low density of FE mesh. This speaks for correctness of the argument, confirmed many times in the course of numerous studies, that the decrease of the overall number of degrees of freedom corresponding to the number of state parameters, in case of nonlinear procedures used in the available commercial programs, often brings benefits that considerably exceed the deficiencies of mathematical description related to reduced number of elements [5].

Fig. 11. An incorrect form of deformation obtained in case of too many elements

The best result was obtained only after the fundamental change of FEM model concept, when a different type of finite element was applied to represent stringers (thick shell element instead of the usually recommended beam element). Although this solution is considered less correct from the point of view of mathematical description, it turned out to be much more effective in the case of relatively low value of the structure's total torsion angle The results of analysis of this FEM model version obtained using the secant prediction method and the strain correction strategy [10] (Figure1) are presented in Figure 12.

The strain-correction strategy turned out to be most effective in case of significant violent change of the deformation pattern when the representative equilibrium path comprised a relatively long "horizontal section".

Modelling stringers with thick-shell elements turned out to be effective also when applied to the other two variants of the model. In order to obtain the symmetry of deformations, small forces normal to the skin surface representing geometrical imperfections were applied

in all cases at central points of each of the shell segments. The way in which variants 2 and 3 of the structure were modelled is shown in Figure 13.

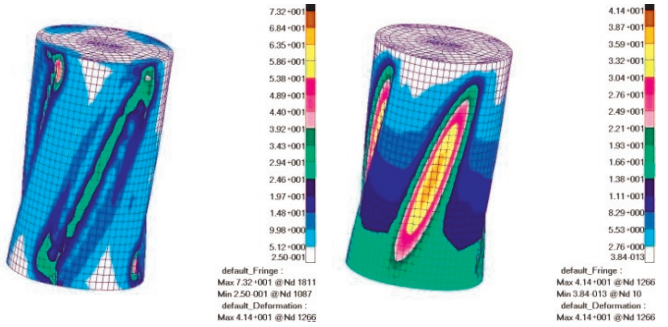

Fig. 12. Distribution of displacement (left) and reduced stress according to Huber-Mises hypothesis (right) for 100% of the maximum load (stringers modelled with thick-shell bilinear elements)

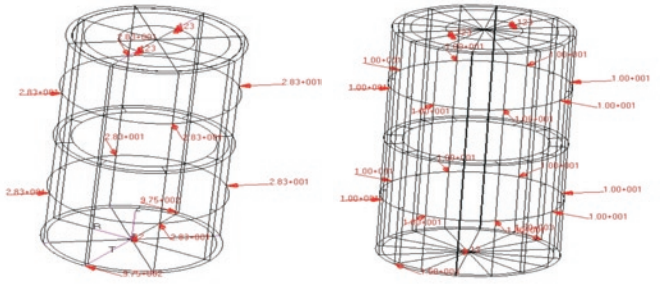

Fig. 13. Geometrical models of the 2-nd (left) and 3-rd (right) variant of a structure created in MSC PATRAN environment with boundary conditions and loads (in N)

Results of FEM-based nonlinear analyses of the above-discussed structure variants are presented in Figures 14 and 15. The representative equilibrium paths are compared in Figures 16–18.

The deformation distributions obtained numerically reveal satisfactory consistence with the above-presented results of experiments, both quantitatively and qualitatively. Plots of representative equilib-

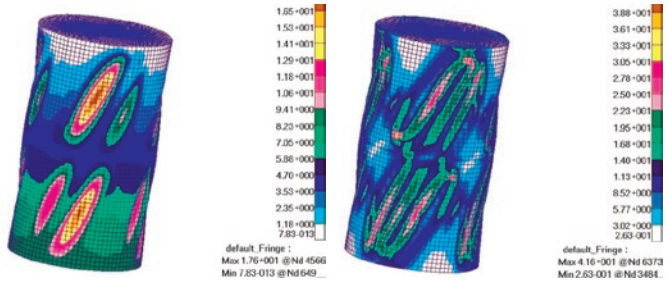

Fig. 14. Distribution of displacement (left) and reduced stress according to Huber-Mises hypothesis (right) for 100% of the maximum load (variant 2)

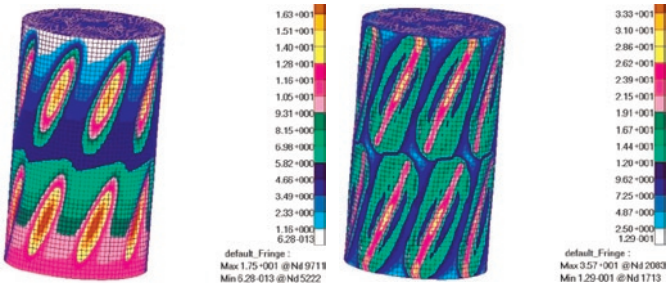

Fig. 15. Distribution of displacement (left) and reduced stress according to Huber-Mises hypothesis (right) for 100% of the maximum load (variant 3)

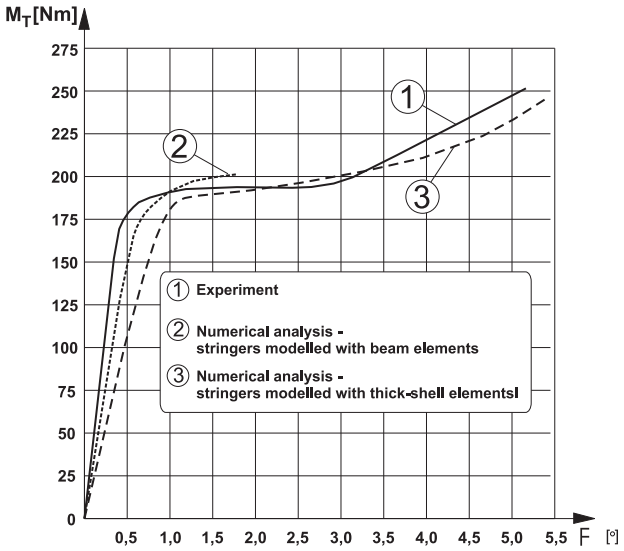

Fig. 16. A comparison of representative equilibrium paths – variant 1

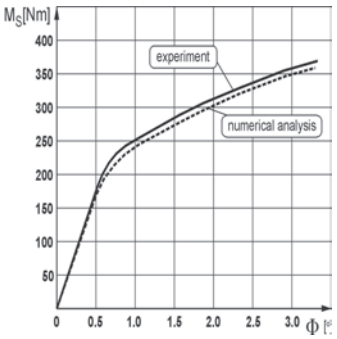

Fig. 17. A comparison of representative equilibrium paths – variant 2

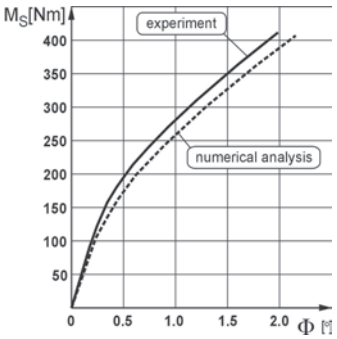

Fig. 18. A comparison of representative equilibrium paths – variant 3

rium paths are characterised by much better conformity with results of the experiment than those obtained for variant 1. This compliance is almost perfect in the subcritical range, whereas for the maximum load, the error of reproduction of the total torsion angle value does not exceed 10%. It allows to conclude that the adopted modelling method and the choice of the numerical procedures turned out to be satisfactory.

More gentle nature of equilibrium paths compared to those observed for variant 1 allows for a greater deal of freedom in selection of nonlinear procedures, e.g. application of Newton-Raphson's method or Crisfield's hyperspherical correction [8].

5. Conclusions

The results of numerical analyses presented above prove that thanks to the use of contemporary engineering tools, it is possible to analyse in detail both values and gradients of effective stress in thin-

walled structures subjected to complex post-critical deformations. However, to be able to accept the obtained results as reliable ones, correct numerical reproduction of bifurcations occurring in the actual hyperspace of states is necessary.

The fundamental conclusion that can be drawn from the presented research results is the absolute need for using experimental verifications with regard to FEM nonlinear numerical analyses concerning structures if this type. In fact, even in the cases where correctness of the results obtained seems to be unquestionable, they may be burdened with errors resulting from the very limited reliability of the numerical procedures used in commercial programs.

Results of the studies on certain variants of a closed, thin-walled cylindrical shell, constituting typical example of the design solution used in aviation, can be recognised as a structural standard, in qualitative meaning, in view of the fact that qualitative nature of post-critical deformations, in case of maintaining geometrical ratios and proportions of stiffness between components of the structure, will not change after applying other isotropic materials and different load values. It is confirmed by numerical tests carried out with the presented models.

Based on the nonlinear numerical analyses concerning the presented structures, and in many instances repeated a number times, a general recommendation can be also formulated as for the maximum possible limitation of the size of a task. Striving for improving accuracy of calculations by increasing the density of finite elements mesh, applied successfully in linear analyses, may turn out to be ineffective in case of a nonlinear analysis and lead to incorrect results or the lack of convergence of calculations.

Detailed analysis of the presented research results allows to formulate design recommendations concerning selection of most effective number of structure skeleton components and most effective ways of their arrangement. As it has been proven, by increasing number of stringers and applying additional frames which results in reducing the size of shell segments, improves stiffness of the structure. However, it is necessary to remember that this means also an increase of mass of the design solution. Comparison of representative equilibrium paths obtained for separate variants of the examined structure allows to claim that applying another stringers or frames may not bring the benefit in the form of increase of the stiffness in view of the related increase of the mass. The detailed determination of this relationship requires further experiments with the use of larger models and appropriate experimental set-up.

References

1. Aben H. Integrated photoelasticity. Mc Graw-Hill Book Co., London 1979.
2. Andrianov J, Awrejcewicz J, Manewitch LI. Asymptotical Mechanics of thin-walled structures. Springer, Berlin 2004.
3. Andrianov J, Verbonol VM, Awrejcewicz J. Buckling analysis of discretely stringer-stiffened cylindrical shells, International Journal of Mechanical Sciences 2006; 48: 1505–1515.
4. Arborcz J. Post-buckling behavior of structures. Numerical techniques for more complicated structures. Lecture Notes In Physics 1986; 228.
5. Bathe KJ. Finite element procedures. Prentice Hall, USA 1996.
6. Brzoska Z. Statics and stability of bar and thin-walled structures. PWN, Warszawa 1965.
7. Doyle JF. Nonlinear analysis of thin-walled structures. Springer-Verlag, Berlin 2001.
8. Felippa CA. Procedures for computer analysis of large nonlinear structural system in large engineering systems. Pergamon Press, London 1976.
9. Kopecki T. Advanced deformation states in thin-walled load-bearing structure design work. Publishing House of Rzeszów University of Technology, Rzeszów 2010.
10. Marcinowski J. Nonlinear stability of elastic shells. Publishing House of Technical University of Wrocław, Wrocław 1999.
11. Mohri F, Azrar L, Potier-Ferry M. Lateral post buckling analysis of thin-walled open section beams. Thin-Walled Structures 2002; 40: 1013–1036.
12. Niu MC. Airframe structural design. Conmilit Press Ltd., Hong Kong 1988.
13. Rakowski G, Kacprzyk Z. Finite elements method in structure mechanics. Publishing House of Technical University of Warszawa, Warszawa 2005.
14. Ramm E. The Riks/Wempner Approach – An extension of the displacement control method in nonlinear analysis. Pineridge Press, Swensea 1987.

Tomasz KOPECKI
Przemysław MAZUREK
Faculty of Mechanical Engineering and Aeronautics
Rzeszów University of Technology
Al. Powstańców Warszawy 12
39-959 Rzeszów, Poland
E-mail: tkopecki@prz.edu.pl

INFORMATION FOR AUTHORS

Terms and Conditions of Publication:

- The quarterly „Maintenance and Reliability" publishes original papers written in Polish with an English translation.
- Translation into English is done by the Authors after they have received information from the Editorial Office about the outcome of the review process and have introduced the necessary modifications in accordance with the suggestions of the referees!
- Acceptance of papers for publication is based on two independent reviews commissioned by the Editor.

Fees:

- Pursuant to a resolution of the Board of PNTTE, as of 2009 the publication fee for one text is 600 zloty + VAT.
- Coloured graphical elements in the submitted text require agreement from the Editor and are charged extra.

Technical requirements:

- After receiving positive reviews and after acceptance of the paper for publication, the text must be submitted in a Microsoft Word document format.
- Drawings and photos should be additionally submitted in the form of graphical files in the *.tif, *.jpg or *.cdr (v. X3) formats.
- A manuscript should include (in accordance with the enclosed correct manuscript format: *.pdf, *.doc):
- names of authors, title, abstract, and key words that should complement the title and abstract (in Polish and in English)
- the text in Polish and in English with a clear division into sections (please, do not divide words in the text);
- tables, drawings, graphs, and photos included in the text should have descriptive two-language captions,
- if this can be avoided, no formulae and symbols should be inserted into text paragraphs by means of a formula editor
- references (written in accordance with the required reference format)
- author data – first names and surnames along with scientific titles, affiliation, address, phone number, fax, and e-mail address
- The Editor reserves the right to abridge and adjust the manuscripts.
- All submissions should be accompanied by a submission form.

Editor contact info: (Submissions should be sent to the Editor's address)

Editorial Office of „Eksploatacja i Niezawodność - Maintenance and Reliability"
Nadbystrzycka 36, 20-618 Lublin, Poland
e-mail: office@ein.org.pl

INFORMATION FOR SUBSCRIBERS

Fees

Yearly subscription fee (four issues) is 100 zloty and includes delivery costs.
Subscribers receive any additional special issues published during their year of subscription free of charge.

Orders

Subscription orders along with authorization to issue a VAT invoice without receiver's signature should be sent to the Editor's address.

Note

In accordance with the requirements of citation databases, proper citation of publications appearing in our Quarterly should include the full name of the journal in Polish and English without Polish diacritical marks, i.e.,

Eksploatacja i Niezawodnosc – Maintenance and Reliability.